

JOURNAL OF AGRICULTURAL SCIENCES

TARIM BİLİMLERİ DERGİSİ

ANKARA UNIVERSITY FACULTY OF AGRICULTURE

e-ISSN 2148-9297

JIAS



Year 24

Volume 30

Issue 01

Ankara University
Faculty of Agriculture

JOURNAL OF AGRICULTURAL SCIENCES

**TARIM BİLİMLERİ
DERGİSİ**

e-ISSN: 2148-9297

Ankara - TÜRKİYE



JOURNAL OF
AGRICULTURAL SCIENCES

TARIM BİLİMLERİ DERGİSİ
ANKARA UNIVERSITY FACULTY OF AGRICULTURE

e-ISSN 2148-9297

Product Information

Publisher	Ankara University, Faculty of Agriculture
Owner (On Behalf of Faculty)	Prof. Dr. Hasan Huseyin ATAR
Editor-in-Chief	Prof. Dr. Halit APAYDIN
Journal Administrator	Salih OZAYDIN
Library Coordinator	Dr. Can BESIMOGLU
IT Coordinator	Lecturer Murat KOSECAVUS
Graphic Design	Ismet KARAASLAN & Ayda ALACA
Date of Online Publication	09.01.2024
Frequency	Published four times a year
Type of Publication	Double-blind peer-reviewed, widely distributed periodical
Aims and Scope	JAS publishes high quality original research articles that contain innovation or emerging technology in all fields of agricultural sciences for the development of agriculture.
Indexed and Abstracted in	Clarivate Science Citation Index Expanded (SCIE) Elsevier-Scopus TUBITAK-ULAKBIM-TRDizin CAB International EBSCO FAO-AGRIS SOBIAD OpenAire BASE IFIS CNKI

Management Address

Journal of Agricultural Sciences - Tarım Bilimleri Dergisi
Ankara University Faculty of Agriculture Publication Department 06110
Diskapi/Ankara-Türkiye
Telephone : +90 312 596 14 24 | Fax : +90 312 317 67 24
E-mail: tbdeditor@ankara.edu.tr | <http://jas.ankara.edu.tr/>



e-ISSN 2148-9297

JOURNAL OF
AGRICULTURAL SCIENCES

TARIM BİLİMLERİ DERGİSİ
ANKARA UNIVERSITY FACULTY OF AGRICULTURE

Editor-in-Chief Halit APAYDIN, Ankara University, Ankara, TÜRKİYE

Managing Editor Muhittin Onur AKCA, Ankara University, Ankara, TÜRKİYE

Ahmet ULUDAG, Canakkale Onsekiz Mart University, TÜRKİYE

Akasya TOPCU, Ankara University, TÜRKİYE

Ali Adnan HAYALOĞLU, Inonu University, TÜRKİYE

Ali UNLUKARA, Erciyes University, TÜRKİYE

Anna Maria DE GIROLAMO, Italian National Research
Council, ITALY

Belgin COSGE ŞENKAL, Yozgat Bozok University, TÜRKİYE

Bilal RASOOL, Government College University Faisalabad,
Punjab, PAKISTAN

Burhan OZKAN, Akdeniz University, TÜRKİYE

Claudia Di BENE, Research Centre for Agriculture and
Environment, ITALY

Duygu SEMİZ, Ankara University, TÜRKİYE

Engin YENICE, Ankara University, TÜRKİYE

Erhan MUTLU, Akdeniz University, TÜRKİYE

Farhat JABEEN, Government College University, PAKISTAN

Fatma Sezer ŞENOL DENİZ, Gazi University, TÜRKİYE

Fazıl SEN, Van Yuzuncu Yil University, TÜRKİYE

Filiz ERTUNC, Ankara University, TÜRKİYE

Giuseppe BADAGLIACCA, Mediterranean University of
Reggio Calabria, ITALY

Giuseppe GAVAZZI, University of Milan, ITALY

Giuseppe PULIGHE, CREA Research Centre for Agricultural
Policies and Bioeconomy, ITALY

Gunars LACIS, Latvia University of Life Sciences and Techn.,
Dobele, LATVIA

Habib ALI, Khwaja Fareed University of Eng. and Inf., Rahim Yar
Khan, PAKISTAN

Hasan YETİM, Istanbul Sebahattin Zaim University, TÜRKİYE

Ismail KARACA, Isparta University of Applied Sciences,
TÜRKİYE

Isil CAKCI, Ankara University, TÜRKİYE

Julia MALYSH, All-Russian Institute for Plant Protection,
RUSSIA

Karina BATISTA, Instituto de Zootecnia, BRAZIL

Mahmut ELP, Kastamonu University, TÜRKİYE

Mine TURKTAS, Gazi University, TÜRKİYE

Mehmet Emin CALISKAN, Nigde Omer Halisdemir University,
TÜRKİYE

Muhammad SULTAN, Bahauddin Zakariya University, Multan,
PAKISTAN

Panagiotis SIMITZIS, Agricultural University of Athens,
GREECE

Peter SCHAUSBERGER, University of Vienna, AUSTRIA

Renata BAZOK, University of Zagreb, CROATIA

Sefa TARHAN, Tokat Gaziosmanpaşa University, TÜRKİYE

Selen SAYGIN, Ankara University, TÜRKİYE

Semra DEMİR, Van Yuzuncu Yil University, TÜRKİYE

Serpil SAHİN, Middle East Technical University,
TÜRKİYE

Stanislav TRDAN, University of Ljubljana, SLOVENIA

Tuba SANLI, Ankara University, TÜRKİYE

Turkan AKTAS, Namık Kemal University, TÜRKİYE

Umut TOPRAK, Ankara University, TÜRKİYE

Yang LI, Shihezi University, CHINA

Yonca YUCEER, Canakkale Onsekiz Mart University,
TÜRKİYE

Advisory Board

Cengiz SAYIN, Akdeniz University, Antalya, TÜRKİYE

Fahrettin GÖĞÜŞ, Gaziantep University, Gaziantep, TÜRKİYE

Fazlı OZTURK, Ankara University (Em.), Ankara, TÜRKİYE

Ensar BASPINAR, Ankara University, Ankara, TÜRKİYE

Sultan COBANOGLU, Ankara University (Em.), Ankara, TÜRKİYE



e-ISSN 2148-9297

JOURNAL OF
AGRICULTURAL SCIENCES

TARIM BİLİMLERİ DERGİSİ
ANKARA UNIVERSITY FACULTY OF AGRICULTURE

CONTENTS

2024, 30(1)

Invited reviews:

- 1 **A Quantitative and Qualitative Assessment of Turkey's Water Resources Potential**
Ahmet ÖZTÜRK, Müslüme Sevba ÇOLAK
- 35 **Evaluation of Water Sources and Animal Species in Terms of Scarcity, Rights and Welfare**
Bahattin ÇAK

Research articles:

- 47 **Determination of Van Basin Groundwater Potential by GIS Based, AHP and Fuzzy-AHP Methods**
Veysel ASLAN
- 61 **Meteorological Drought Assessment and Prediction in Association with Combination of Atmospheric Circulations and Meteorological Parameters via Rule Based Models**
Fatemeh Shaker SUREH, Mohammad TAGHI SATTARI, Hashem ROSTAMZADEH, Ercan KAHYA
- 79 **A Study on Recognizing the Value of Chestnut (*Castanea sativa*) Blossom Waste**
Huseyin SAHIN, Sevgi KOLAYLI, Yakup KARA, Zehra CAN, Halil Ibrahim GULER, Asli OZKOK, Umit SERDAR
- 90 **Environmental Factors and Semiarid Plants Species on Eroded Marly Soils in Southwest Anatolia (Eskişehir/Türkiye)**
Münevver ARSLAN, Neslihan BALPINAR, Mesrur Ümit BİNGÖL, Nejat ÇELİK
- 99 **Enhancing Pest Detection: Assessing *Tuta absoluta* (Lepidoptera: Gelechiidae) Damage Intensity in Field Images through Advanced Machine Learning**
Alperen Kaan BÜTÜNER, Yavuz Selim ŞAHİN, Atilla ERDİNÇ, Hilal ERDOĞAN, Edwin LEWIS
- 108 **A Determination of the Change in Variance Components due to Heat Stress in Dairy Cattle Using a Random Regression Model**
Ayşe PINARBAŞI, Kemal YAZGAN
- 118 **A Meta-Heuristic Algorithm-Based Feature Selection Approach to Improve Prediction Success for *Salmonella* Occurrence in Agricultural Waters**
Murat DEMİR, Murat CANAYAZ, Zeynal TOPALCENGİZ
- 131 **The Public Sector's Role Towards Sustainable Agricultural Economy and Rural Development: Techno-economic Feasibility Analysis of Hybrid Paddy Production**
Sheer ABBAS, Waqar AHMED, Rana Shahzad NOOR, Sidra FATİMA, Muhammad Aali MİSAA
- 145 **Parasitism (*Flamingolepis liguloides* Gervais, 1847) with High Prevalence in Brine Shrimp Population from Çamaltı Saltworks**
Edis KORU
- 153 **Potato Plant Leaf Disease Detection Using Deep Learning Method**
Cemal İhsan SOFUOĞLU, Derya BİRANT
- 166 **Optimization of Inulin Extraction from Chicory Roots and an Ultrafiltration Application to Obtain Purified Inulin and Hydrolyzed Fructooligosaccharides**
Nihan SAGCAN, Hasan SAGCAN, Fatih BOZKURT, Ayse Nur BULUT GUNES, Huseyin FAKIR, Enes DERTLİ, Osman SAGDIC

- 179 Organic Water-Soluble Fertilizers Enhance Pesticide Degradation: Towards Reduced Residues**
Dongsheng LIU, Weizhen LI, Haixiang GAO, Changsheng HUANG, Shihong XU, Wenqi LIU
- 193 An Analysis of Factors Influencing African Indigenous Vegetable Farmers' Bargaining Power: A Case Study from Zambia**
Zhigang YU, Huiping XU, Ramu GOVINDASAMY, Emmanuel Van WYK, Burhan OZKAN, James E. SIMON



A Quantitative and Qualitative Assessment of Turkey's Water Resources Potential

Ahmet ÖZTÜRK^{a*} , Müslüme Sevba ÇOLAK^a 

^aAnkara University, Faculty of Agriculture, Department of Agricultural Structures and Irrigation, TURKIYE

ARTICLE INFO

Review Article

Corresponding Author: Ahmet ÖZTÜRK, E-mail: aozturk@ankara.edu.tr

Received: 24 March 2023 / Revised: 19 July 2023 / Accepted: 25 August 2023 / Online: 09 January 2024

Cite this article

Öztürk A, Çolak M S (2024). A Quantitative and Qualitative Assessment of Turkey's Water Resources Potential. *Journal of Agricultural Sciences (Tarım Bilimleri Dergisi)*, 30(1): 1-34. DOI: 10.15832/ankutbd.1270229

ABSTRACT

One of the most basic human needs is water, which is also needed to create all the nutrients required for nutrition. For this reason, water is the basic element of life. While the presence of underground mines and oil is an indicator of the wealth of a country, the existence of water resources is now considered a part of this group.

A hundred years ago, the existing water availability in a country was a direct indicator of the water wealth of that country. However, as a result of the increase in industrialization and the rapid pollution of water resources, it has become a necessity to evaluate water not only in terms of quantity but also in terms of quality. Because the unit water value of a source is related to the number of different purposes that source can be used for, the more varied a water resource's application, the more valuable it is. Sometimes one unit of very clean water is more valuable than a hundred units of dirty water. For this reason, the value of a country's water resources should be evaluated not only in terms of quantity but also in terms of quality.

In this study, the total surface water as rivers and lakes and groundwater of Turkey were examined in terms of quantity and quality on a basin basis, and assessments were made about the basin water potentials.

Keywords: Water resources, Irrigation water quality, Watershed, Turkey

While the amount of water in 25 water basins in Turkey does not show a significant change over time, a serious changing draws attention in terms of quality, especially in the last 50 years. The change in the amount of water in the basin primarily manifests itself in the form of a decrease in the water levels of rivers, lakes and groundwater. This process arises due to the effects of global warming and climate change, which is a global problem that concerns the whole world. However, pollution in water resources and making the water resource unusable are all related to the fact that the regulations on the protection of water are not adequately implemented and people do not act consciously. In other words, although quantitative reduction is a global problem, the quality problem is related to the polluting factors in the region of that resource.

In a country with a very high population growth rate, the decrease in the per capita water potential and the rapid increase in the pollution in the existing resources leads to a steady decline in the availability of usable water resources. In this study, attention was drawn to point and diffuse pollution on the basis of water presence and water source on the basis of basin, and an evaluation of Turkey's water resources in terms of quantity and quality was made.

1. Introduction

The greatest absolute needs of people are drinking water and nutrition. Nearly 1 billion people in the world suffer from drinking water shortages while 2 billion people live with insufficient access to quality water. In addition, half of the world's population is struggling with water scarcity. Water is a vital resource not only for drinking but also in the production of nutrients (Öztürk & Çolak 2021).

While water is an absolute necessity in the lives of all living things, it is also used wastefully and carelessly. Water, which has not only an economic aspect, is also a natural resource that should be considered as a social asset, political and strategic power related to the right to life of humans and nature (Sevindi 2005).

Meeting the ever growing demands for the world growing population in terms of food and water continues to be a global concern. A large part of the efforts to feed the world is made through agricultural production. There are three main inputs of agricultural production. These are soil, water and sunlight. Although there may be enough agricultural land, a lack of water and sunlight in many areas are the main issues that limit production. While there is usually sufficient water at high latitudes, temperature and sunlight are the limiting factors for agriculture. At lower latitudes, which are typically semi-arid and arid, water is usually the main factor limiting agricultural production. The amount of evaporation from the earth has increased due to climate change and related global warming. Excessive evaporation causes a decrease in the water on the earth and an increase in the

water in the atmosphere. With excessive evaporation, there is not only a decrease in the water on the earth, but also a deterioration in water quality. Because evaporation takes place as pure water, the salt concentration of the remaining water rises even more and the water becomes of increasingly poor quality. The quality of most water sources in summer is often lower than in winter. One reason for this is evaporation with the other being the increase in microbial activities in hot conditions.

Although the total amount of water on earth shows no change, the distribution of this water is disordered and shows significant variation. More than half of the world's fresh water is found in Canada. The potential of water resources is evaluated in two different ways. While one of them is the total fresh water availability, the other is the per capita water potential. Since the population of the countries interact in terms of these two parameters, the ranking can vary significantly in the population-based assessment. For example, Iceland, with a population of 357 thousand, is 5 times better than Canada, which has half of the world's fresh water in terms of water potential per capita. Therefore, the total water potential and the per capita potential lead to different conclusions.

36% of the water used in the world is distributed in Asia, 25% in South America, 15% in North America, 11% in Africa, 8% in Europe and 5% in Oceania. An examination of this distribution shows that the water potential per capita is insufficient since Asia has 60% of the world's population. There is 5 000–6 000 m³ of water per person per year in the world (UN 2007). Falkenmark et al. (1989) developed an indicator called the “Falkenmark water stress indicator” to define the water scarcity threshold. According to this indicator, if the annual water potential per capita in a country is below 1700 m³, then that country suffers from water scarcity. A water-scarce country faces seasonal or continuous water stress. If the water potential falls below 1 000 m³, problems arise in human living conditions and water stress is experienced. If the water potential falls below 500 m³, serious problems emerge in basic human life, which is defined as absolute water scarcity. This classification is common in many studies due to the ease of its calculations (UNDP 2006).

If the world population continues to increase in this way, the proportion of people experiencing water shortages will increase to 36% in 2025 and 42% in 2050. Today, 700 million people in 43 countries suffer from water stress and water scarcity. In the Middle East, which is one of the regions where water stress is most apparent in the world, the annual water potential per person is 1200 m³ on average. The only countries in the region where the per capita water availability exceeds this value are Iran, Iraq, Lebanon and Turkey. Palestine, especially Gaza, suffers from the most severe water shortage in the Middle East with 320 m³ per capita per year (UNDP 2006).

The quality of the water is also important as well as the amount of water available, since the quality of water is the most important feature that limits its use. The existence of a water source that cannot be used for any purpose can be taken as the equivalent of not having that water source at all. In many regions, a small amount of good quality water is preferred over a large amount of poor quality water. Today, if there is water of different qualities in the same area, a quality-based water pricing is applied. For example, when it comes to using poor quality groundwater cheaply in an agricultural area, the farmer may prefer to use higher quality but more expensive surface water. In fact, in the near future, considering the reaction of the crops to the water quality, it is possible to implement planned agricultural practices such as using quality water in sensitive periods and using low-quality water in non-sensitive periods.

In arid and semi-arid areas, irrigation has become even more dependent on poorer quality and deficit quantity water. Moreover, differences in resistance to drought and salinity between varieties, which were not covered extensively before, have become more important than before (Semiz et al. 2023). Both irrigation water pollution and increasing soil salinity in agricultural lands are the most important limiting factors for cultivation of culture crops. To meet increasing needs, marginal waters should be used and agricultural lands should be used for production. Saline lands could also be used in production through the use of salt-resistant plants (Taş et al. 2022).

While there is vast quantities of water in the seas and oceans what makes water scarce is its quality. The problem is not one of water scarcity in the world, but a problem of quality water scarcity. It is still not considered economical to treat sea water into good quality water. The cheapening of treatment technologies will significantly affect the availability of quality water. Transferring water to where it is needed is not an economical solution at present due to the high energy cost. The development of inexpensive methods of conveying water is vital in wider efforts towards eliminating water scarcity.

In low latitudes where arid and semi-arid climatic zones are located, it is almost impossible to carry out crop production without irrigation. The presence of water resources required for plant production in these latitudes, including Turkey, directly affects the agricultural production potential. The significant increase in the yield of some products with irrigation, or the fact that many products cannot be grown in dry farming is an indicator of how important irrigated agriculture is.

In this study, Turkey's water resources potential was examined in terms of its quantity and quality and evaluated on a basin basis. The evaluation on the basis of basin was made quantitatively and qualitatively in the form of rivers, lakes and groundwater.

2. Turkey's Water Availability

Turkey consists of 25 river basins (Figure 1). Most of the rivers in the country originate within the borders of the country and reach the sea. The most important rivers in the country are the Kızılırmak (1 355 km), Sakarya (824 km), Meander (548 km), Seyhan (560 km), Yeşilirmak (519 km), Ceyhan (509 km), Gediz (401 km), and Little Meander (114 km) rivers. The rivers that originate within the country borders and flow into the sea from the shores of other countries are the Euphrates (1 263 km in Turkey), Tigris (512 km in Turkey), Chorokhi (354 km in Turkey), Kura (189 km in Turkey) and Aras (548 km in Turkey) rivers. The Orontes (98 km in Turkey) and Meriç (187 km in Turkey) rivers originate in the lands of other countries and flow into the sea on the shores of Turkey (SHW 2022).



Figure 1- Turkish water basins

As a result of the topography of Turkey, which is quite young in terms of geological age and due to the high slope of the land, the regimes of the rivers are generally irregular and wild stream. Therefore, it is often not possible to use water directly without taking the necessary regulations and precautions. While it may appear that Turkey has vast quantities of water, the needs cannot always be met due to different levels of precipitation in the basins and precipitation at different times of the year (Burak et al. 1997).

The water availability of a country is directly related to the levels of rainfall that occur in that country. Precipitation varies depending on the country's precipitation regime, geographical location, topography, climatic conditions and season. In Turkey, which has continental and semi-arid climate characteristics, although there are regional differences depending on these characteristics, the annual average precipitation amount is 574 mm, which corresponds to an average precipitation volume of 450 billion m³ per year. According to the basin master plans, it is calculated that 185 billion m³ of this water flows into the seas and lakes through streams of various sizes. The groundwater reserve determined through Turkey's hydrogeological studies has been calculated as 23 billion m³, and the safe usable groundwater reserve has been calculated as 18 billion m³. Within the framework of today's technical and economic conditions, the surface water potential that can be used for various purposes is 94 billion m³ annually, and the groundwater potential that can be safely used is 18 billion m³ annually. Thus, the total consumable surface and groundwater potential of Turkey can be calculated as 112 billion m³ per year (Anonymous 2018).

According to the 2021 realization values of Turkey's total water potential, it was determined that 58.41 billion m³ of water was used for various purposes (45.05 billion m³ (77%) for irrigation water, 13.36 billion m³ (23%) for drinking, domestic and industrial water) (Figure 2) (SHW 2022).

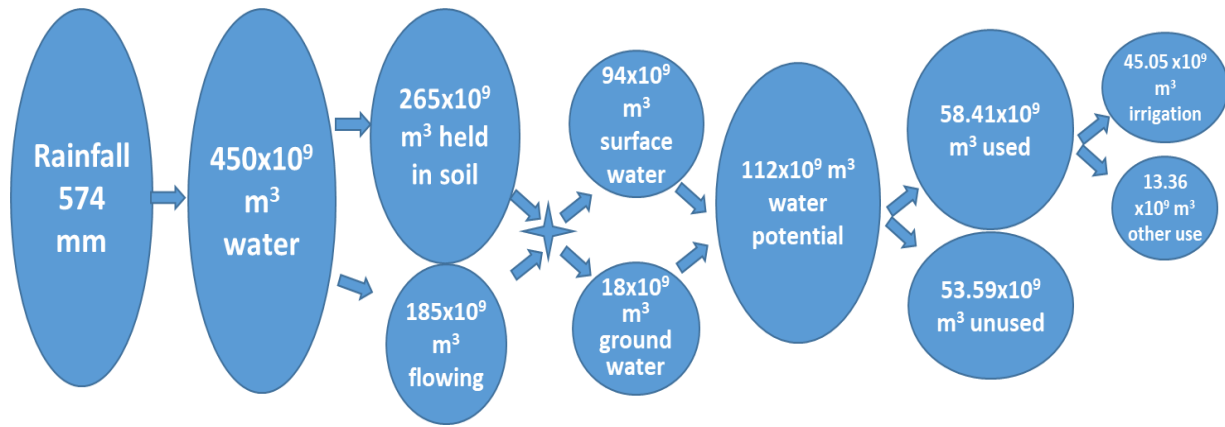


Figure 2- Turkey's water availability and use

According to the data of the Turkish Statistical Institute, the population of Turkey is 84 680 273 as of 2021. The annual amount of usable water per capita in the country is 1 323 m³ in 2021. Considering the usable water potential per capita, Turkey is among a wider group of countries experiencing water stress. The population of Turkey in 2050 is predicted to be 96 498 000, which means that even if the amount of water in the country does not decrease, the water potential per capita will decrease to 1 161 m³/year and Turkey will become a water-poor country (SHW 2019, TUIK 2019). Due to the drought in Turkey, especially in recent years, significant problems have been experienced in both the agriculture and domestic use of water and economic losses have occurred. It is estimated that the social and economic problems in the country will grow exponentially, as climate instabilities to be experienced due to global climate change will cause water shortage. For this reason, an accurate monitoring of Turkey's water potential and appropriate use of water will be vital in planning the future.

In Turkey, it is important to use water economically and in an optimum way, and studies have been carried out to evaluate the potential of water resources and to use it in a multi-purpose way through the construction of storage facilities. The use of water in a multi purpose way is aimed to prevent water losses in the irrigation projects under operation and to use water more effectively and efficiently. In addition, it is aimed to give importance to renovation works in order to prevent drainage problems affecting soil quality and to expand the use of closed irrigation systems instead of classical open system irrigation networks (SHW 2021).

3. Water Resources Status in Quantitative and Qualitative Aspects in Turkey's Water Basins

The flow regimes of the rivers in Turkey vary throughout the year due to variables in precipitation levels according to the regions and seasons as well as differences in the bed slopes of the rivers. The high slopes of the rivers does provide the potential to generate hydroelectric energy from the rivers. However, the fact that the rivers have different bed morphology and high bed slopes does create certain obstacles for transportation (SHW 2019).

13 of the 25 basins (the Euphrates and Tigris, Seyhan, Ceyhan, Kızılırmak, Sakarya, Chorokhi, Yeşilirmak, Susurluk, Aras, Orontes, Meander, Gediz and Little Meander) can be considered as individual river basins. The other 12 basins (the Eastern Mediterranean, Eastern Black Sea, Antalya, Western Black Sea, Western mediterranean, Marmara, Konya Closed, Van Lake, North Egean, Meriç-Ergene, Burdur Closed and Akarçay) cover large and small discrete streams and lakes. Of these 12 basins, 4 (Konya Closed, Van Lake, Burdur Closed and Akarçay) are closed basins that are not in contact with the seas (SHW 2022).

Lakes; It has attracted the attention of human beings for centuries, both in terms of supply of fresh water, which is inevitable for living life, and with its unique resources. From the perspective of the historical process of humanity, many important civilizations were established and rooted in areas where fresh water resources were found.

As a result of the studies carried out by the General Directorate of Nature Conservation and National Parks, there are 320 natural lakes in Turkey. Some of these lakes are seasonal and are filled through winter precipitation and then dry up due to a lack of precipitation in the summer. Of the lakes in Turkey, Lake Van (3 713 km²), Salt Lake (1 300 km²), Beyşehir Lake (656 km²), Eğirdir Lake (482 km²) are the largest lakes in size (SHW 2022).

There are 861 dams in operation in Turkey. Of the dams in Turkey, the Atatürk Dam has a surface area of 817 km², Keban Dam 675 km², Ilısu Dam 313 km², Karakaya Dam 268 km², Hirfanlı Dam 263 km² (SHW 2022).

Groundwater sources are water reserves that have been formed by accumulating underground for many years, show small changes with annual consumption and re-feeding, and constitute a country's safe water resources. It is important to protect groundwater both quantitatively and qualitatively. Groundwater polluting factors are restricted by law. Excessive use of groundwater may cause the source to dry out completely through these sources inability to renew themselves. Overuse can also

cause seawater to enter the freshwater aquifer at seaside. For this reason, in terms of resource conservation, the annual use of underground reserves should never exceed the average recharge rate. The water reserve in underground aquifers should not be allowed to decrease over time. Groundwater sources protected in terms of quantity and quality by regulations. On the other hand, in many areas monitored by observation wells, excessive water use occurs during dry periods.

In this study, the rivers, lakes and groundwater resources of Turkey's basins have been analyzed on a basin basis in terms of both quantity and quality and evaluated according to the basin numbers provided below.

3.1. Meriç-ergene basin

The precipitation area of the Meriç-Ergene Basin, which is one of the smaller basins, is 14 486 km². The basin has an annual precipitation average of 665 mm. The estimated total water potential of the basin is approximately 2 billion m³ per year. A total of 1.235x10⁹ m³ of water is consumed in the basin, 970x10⁶ m³ for irrigation, 112x10⁶ m³ for domestic use and 153x10⁶ m³ for industrial use. This figure constitutes 61.8% of the total water potential of the basin (Anonymous 2018a).

The main rivers in the Meriç-Ergene Basin are the Ergene River and its tributaries. The Ergene River originates from the Ergene springs in the Istranca Mountains in the northeast of Thrace and flows in a northeast-southwest direction under the name of Ergene Creek. Later on, it merges with the Çorlu Stream coming from the east near the village of İnanlı and takes the name of the Ergene River. The Ergene River flows in an east-west direction, taking the Ana Stream, Soğucak Stream, Lüleburgaz Stream, Şeytan Stream, Çimenli Stream and Süloğlu Stream from the north, and the Çengelli Stream, Beşiktepe Stream, Hayrabolu Stream and Bayramlı Stream tributaries from the south. It then joins with the Meriç River in the south of Adasarhanlı village (Anonymous 2018a).

Water pollution is the biggest problem facing the Meriç-Ergene Basin. The waters of the Ergene River are in the low irrigation water quality class due to uncontrolled industrialization, failures in waste water management and incorrect agricultural practices. Due to the overflow of the stream, particularly after rainfall, the plain is polluted with flood waters and soil pollution arises from the polluted waters. In recent years in particular, through excessive industrialization in the Tekirdağ region, an excessive pollution load has been observed in the Çorlu Stream owing to waste discharge from industrial facilities.

The electrical conductivity (EC) values of the basin waters show significant regional differences. With the exception of the Çorlu Stream, the tributaries of the Ergene River and the Meriç River are in the 2nd class in terms of EC values. The Ergene River has 3rd class water quality, excluding the source area and its tributaries, and Çorlu Stream has 4th class water quality (WPCR 2015).

The lakes found in the basin are the Çeltik (Gala) and the Pamuklu Lakes. The Gala Lake has a total area of 601 hectares and is divided into the Grand Gala (Çeltik) and Small Gala (Pamuklu). The Grand Gala has a large water area. Some parts of the lakes are in the form of reed beds (Small Gala), seasonal marshes and wetlands consisting of salty lakes containing salt water. Rice is cultivated extensively in the region. The lakes in this basin are under the threat of pollution coming from the Meriç River, agricultural activity wastes and the sediment created by the floods. Especially in dry periods, the salinity value of the lake water tends to increase (Anonymous 2015). The Gala Lake has an EC 2.5 dS/m salinity in terms of irrigation water quality and an irrigation water class of 4 (Tokatlı et al. 2014).

Along the river route, which is 283 km in total from its source to the point where it reaches the sea, the stream flow gradually increases as a result of the industrial and domestic wastes absorbed by the river.

When the basin is evaluated in terms of groundwater. The groundwater recharge quantity is 507.7x10⁶ m³/year with an operating reserve is 498.2x10⁶ m³/year. Three-quarters of the total annual operating reserve of the groundwater potential of the basin is allocated to domestic and industrial water. In addition, an area of 15 585 ha is irrigated from 347 wells belonging to 46 irrigation cooperatives. The effect of the climate on groundwater is most apparent through precipitation levels. While the amount of water in the aquifers increases with the effect of precipitation, precipitation does not affect the deep wells. In recent years, it has been observed that there has been a decrease in groundwater levels and a decrease in groundwater quality (Anonymous 2015).

3.2. Marmara basin

The precipitation area of the Marmara Basin is 23 074 km². The Marmara Basin is the most populated basin in Turkey, and İstanbul, the most populated city of Turkey, is located in this basin. The average annual precipitation of the basin is 685 mm. The annual average flow value of the Marmara Basin is 5.08x10⁹ m³ (6.69 L/s/km²) and constitutes 2.77% of Turkey's surface water potential. Considering the 5.08x10⁹ m³/year surface and 396x10⁶ m³/year groundwater potential in the basin, the total water potential is 5.476x10⁹ m³/year. Of the total water potential, the usable water potential of the basin is stated as 2.54x10⁹ m³/year surface water and 297x10⁶ m³/year groundwater, totalling 2.837x10⁹ m³/year. 11% of the total water potential of the Marmara Basin is used for irrigation and 89% for domestic water (drinking, using, industry, etc.) activities (Anonymous 2010).

Since the Marmara Basin is not a large river basin, it has many large and small streams. The streams in the basin demonstrate very different water quality characteristics from each other as they are exposed to domestic and industrial wastewater discharges (Anonymous 2010).

Natural lakes in the basin are İznik, Küçükçekmece and Dalyan lakes. The main water source in the basin is Lake İznik, which is predominantly used for drinking water and irrigation water. A total of 7036 ha of agricultural land is irrigated by the irrigation facilities built by DSI in İznik, Boyalıca and Orhangazi (Anonymous 2015). Lake İznik is the largest and deepest natural lake in the Marmara and the fifth largest natural lake in Turkey (Anonymous 2022). In terms of the irrigation water quality of the lake, the electrical conductivity values vary between 0.68-1.10 dS/m (Anonymous 2022a).

The surface area of Lake Küçükçekmece is 1956 ha, its length in the north-south direction is 10 km and its widest part is approximately 6 km. Although Küçükçekmece Lake is not very deep, its depth reaches up to 20 m near the southern shore. The lake contains brackish water and has a lagoon type character (Anonymous 2015). The water of the lake is salty because of the transfer of seawater from the Marmara Sea into the lake when it swells (Okumuş 2007).

The other lake in the Marmara Basin is Dalyan Lake with an approximate size of 400 ha. The depth, which is about 10-20 cm on the shores of the lake, increases up to 1.5 meters towards the centre of the lake. The lake waters are not used because they are alkaline and salty. Since the lake surroundings are sandy, it lacks any natural vegetation. The groundwater recharge quantity of the Marmara Basin is 241.7×10^6 m³/year, and the operating reserve is 210.7×10^6 m³/year (Anonymous 2015).

3.3. Susurluk basin

The precipitation area of the Susurluk Basin is 24 319 km² while the population numbers 3 139 112. The average annual precipitation in the Susurluk River Basin is approximately 662 mm/year. The total water potential of the Basin, including surface and groundwater, is approximately 5.81×10^9 m³/year. Within the basin potential, it is estimated that 1.18×10^9 m³/year for irrigation, 200×10^6 m³/year for domestic use and 234×10^6 m³/year for industrial use, a total of 1.614×10^9 m³/year water is used (Anonymous 2018b).

Many small and large rivers discharge the rainfall of the Susurluk Basin into the Marmara Sea and Lakes Uluabat and Manyas. There are many large and small rivers in the basin flowing continuously throughout the year or for a short time.

- The Simav Stream (Susurluk Stream): The most important stream of the Susurluk Basin, the Simav Stream originates in Kütahya. The length of the Simav Stream, which enters Balıkesir from the Sındırgı district and disembogues into the Marmara Sea, is 175 km. It is also fed by many streams in the basin. High boron concentration waters discharged from Bigadiç Borax plants to Simav Stream, which adversely affect the irrigations in Balıkesir, Susurluk, Kemalpaşa, Karacabey plains located in the Susurluk Basin.

- The Dursunbey Stream (Balat Stream): The Dursunbey Stream, which originates in the Alaçam Mountains and merges with the Simav Stream and disembogues into the Marmara Sea, has a length of 65 km.

- The Kille Stream: The length of the Kille Stream, which originates from the Dursunbey district and joins with the Simav Stream and disembogues into Marmara Sea is 97 km.

- Yağcılar Creek: It originates in the Bigadiç district and merges with Simav Creek in Kepsut and disembogues into the Marmara Sea. The length of the stream is 30 km.

- The Atnos Stream: The river originates in Kütahya, joins with the Simav Stream in Sındırgı and disembogues into the Marmara Sea.

- The Üzümcü Stream: Originating in the İvrindi district of Balıkesir, the stream merges with the Simav Stream and disembogues into the Marmara Sea. The Üzümcü Stream is approximately 56 km long.

- The Dombay Stream: The stream originating from Bigadiç district merges with the Simav Stream and disembogues into the Marmara Sea.

- The Kocaçay: The Kocaçay, one of the important rivers of the basin, arises from the foothills of the Madra Mountain and flows 140 km from south to north and disembogues into Lake Manyas. It is the most important river source feeding the lake.

- The Nilüfer Stream: It is the most important stream of Bursa province and one of the characteristics of Bursa city. The stream originates around Keles and merges with the Susurluk Stream and disembogues into the Marmara Sea around Karacabey Boğaz district.

- The Deliçay: It arises from the northern slopes of Uludağ and brings vast quantities of sediment as a result of the melting of snow in spring due to the very steep slope. The Deliçay joins the Nilüfer Stream and disembogues into the Marmara Sea.
- Aksu Creek: This streams descends from the northern slopes of Uludağ. It reaches to Gölbaşı Pond.
- The Kaplıkaya Stream: It arises from the northern slopes of Uludağ, after entering the Bursa Plain, it merges with the Deliçay and joins the Nilüfer Stream.
- The Ayvalı Stream: It joins the Nilüfer Stream by passing through the Çayırköy Plain.
- The Hasanağa Stream: It joins with the Nilüfer Stream about 7 km west of the Ayvalı Stream.
- The Orhaneli Stream (Kocasu Stream): The Orhaneli Stream, which is 104 km long within the provincial borders, arises in the Gediz district of Kütahya Province. 20 km from Mustafakemalpaşa district, in Çamandar Village, it merges with the Emet Stream, which is the branch of the Mustafakemalpaşa Stream coming from the west, and takes the name Mustafakemalpaşa Stream and disembogues into Lake Uluabat.
- The Emet Stream: It originates at 1100 meters on the Şaphane Mountain in the Gediz region and merges with the Orhaneli Stream in the north and forms the Mustafakemalpaşa Stream. Its length within the provincial borders is 44 km.
- The Mustafakemalpaşa Stream: The Mustafakemalpaşa Stream, which is 134 km long within the provincial borders and formed by the merging of Orhaneli and Emet Streams in Çamandar Village, flows into Uluabat Lake 40 km from here.
- The Sultaniye: The length of this stream, which is a branch of the Nilüfer Stream, within the provincial borders is 11 km.
- The Kurtkaya Stream: The length of the Kurtkaya Stream, which is a branch of the Nilüfer Stream, within the provincial borders is 20 km.
- The Değirmendere: The length of this stream, which is a branch of the Nilüfer Stream, within the provincial borders is 16 km.
- The Yaylacıkdere: The length of this stream, which is a branch of the Nilüfer Stream, within the provincial borders is 22 km.
- The Emet Stream: The 90 km long brook consists of springs near the Saruhanlar and Aşıkpaşa villages, and merges first with the Kocadere, then the Doğanakası Stream and the Kayaköy, and takes the name of the Emet Stream.
- The Bedir Stream: Flowing in the southwest-northeast direction, the stream passes through Çavdarhisar and merges with the Barağı Stream, İmam Stream and Çat Stream. Its average flow is 0.178 m³/s.
- The Tavşanlı Stream: The brook, which is 65 km long within the provincial borders, originates in Esatlar Village. It merges with the Bedir Creek, and flows northward from here to the Tavşanlı Plain.
- The Simav Stream: The length of the brook, which starts from the point where Kalkan Stream ends and leaves the provincial borders after Beciler Village, is 40 km.
- The Hamzabey Stream (Kocaçay): The length of the stream, which originates from the town of Naşa and then reaches the Emet Stream, is 45 km (Anonymous 2018c).

There are 2 natural lakes in the Susurluk Basin, which is located in the west of the country and has a population density of more than 100 people per km².

Lake Manyas is located within the borders of the Manyas district of Balıkesir province and covers an area of approximately 16 069 ha. Since Lake Manyas has shallow waters, the water temperature varies depending on the atmospheric conditions. Lake Manyas, which hosts a bird paradise and is a RAMSAR area, is one of the important of Turkey's wetlands. With the water of the lake having high turbidity, it almost exclusively used for irrigation purposes and the area around the lake has a high number of agricultural fields and factories (Anonymous 2017). The increase in the regions in the region's population as well as growing industrial use and domestic waste has led to a deterioration in the water quality Lake Manyas (Gürlük & Rehber 2009).

Lake Uluabat, located within the borders of the Karacabey and Mustafakemalpaşa districts of Bursa province, covers an area of approximately 15 409 ha and has been included in the List of Ramsar Wetlands as of 1998. The lake, with a maximum depth of 6 m is a shallow, turbid, eutrophic freshwater lake. The most important water source feeding the lake is the Mustafakemalpaşa Stream. In addition, the drainage waters of the surrounding agricultural areas are also discharged into the lake. The quantity of

water entering the lake varies greatly according to the seasons and years. The excess water of the lake flow into the Uluabat Stream and the Susurluk Stream to the west of the lake and then into the Marmara Sea. However, when the water level of the lake falls below that of the Uluabat Stream, the stream flows towards the lake and feeds the lake. With the water pumped from the lake, 6 350 ha of land around the lake is irrigated (Anonymous 2017).

A high number of settlements, factories, workplaces, agricultural lands and mines can be found around Lake Uluabat, which is located in the Marmara Region, where the population and industry are dense. This leads to the deterioration of the water quality and an increase in the lake's pollution levels (Akdeniz 2005).

There are over 30 lakes in the Living Lakes network. Lake Uluabat is among these globally important lakes and is recognized and supported internationally (Karaer et al. 2009) Lake Uluabat is in the 4th class according to the irrigation water criteria (Katip & Karaer 2011). The groundwater operation reserve of the Susurluk Basin varies in the range of 503×10^6 - 671×10^6 m³/year (Anonymous 2015).

3.4. North Aegean basin

The precipitation area of this basin is 9 861 km² while the population living within the borders of the basin is approximately 800 000 people. Many rivers of different sizes in the North Aegean Basin that disembogue their waters into the Aegean Sea including the Bakırçay River, Karamenderes Stream, Madra Stream, Güzelhisar Stream, Tuzla Stream, Havran Stream and Black Stream. The flow rates of the rivers in the basin vary most of the year depending on precipitation and discharges (Anonymous 2019).

In the North Aegean Basin, the annual average precipitation value is around 672 mm. The annual average flow amount is 1.39×10^9 m³ (4.86 L/s/km²) and constitutes 0.75% of Turkey's surface water potential. The usable part of this water is estimated to be 695×10^6 m³/year. The groundwater operating reserve of the North Aegean Basin is 187×10^6 m³/year and the groundwater potential is estimated to be around 249×10^6 m³/year. Considering the 1.39×10^9 m³/year surface and 249×10^6 m³/year groundwater potential in the basin, the total water potential is calculated as 1.639×10^9 m³/year. The usable water potential of the basin is stated as 882×10^6 m³/year in total, of which 695×10^6 m³/year is surface water and 187×10^6 m³/year is groundwater operating reserves (Anonymous 2015).

While there is no significant lake in the North Aegean Basin, there are still many dams in operation, under construction and planned. The important dams in the basin and their features are given in Table 1.

Table 1- Important dams in the North Aegean Basin (Anonymous 2019)

<i>Dam name</i>	<i>Surface area km²</i>	<i>Storage volume $\times 10^6$ m³</i>
Güzelhisar Dam	5.80	158.0
Sevişler Dam	6.05	127.0
Bayramiç Dam	5.85	86.5
Madra Dam	2.68	79.4
Yortanlı Dam	4.25	67.3
Havran Dam	3.15	66.5
Çaltıkoru Dam	1.90	46.0
Kestel Dam	2.40	37.4
Ayvacık Dam	3.42	30.0
Sarıbeyler Dam	1.37	15.6
Akçin Pond	0.70	9.0

Within the scope of the North Aegean River Basin Management Plan, monitoring was carried out at 101 points in the basin according to the Surface Water Quality Regulation. According to the monitoring results, the water quality status of the basin has been determined.

As a result of surface water quality evaluation; 2 water sources “bad” (3%), 11 water sources “poor” (16%), 34 water sources “moderate” (49%), 4 water sources “good” (6%), 2 water sources “very good” (3%), and there is no monitoring in the remaining 16 water bodies (23%) (Anonymous 2019)

When the Bakırçay River is evaluated in terms of all parameters in general, it is reported to be in class 4 water quality. Olives, vegetables and fruit cultivation is widely practiced in the basin. There are stone quarries and tomato paste factories in Bergama. There is a Thermal Power Plant in Manisa Soma and it is important in terms of environmental pollution (Anonymous 2014).

The potential for groundwater in the basin to be affected by climate changes will not be as high as other basins in the region (eg Gediz, Meander and Little Meander). According to the results of the examinations made in terms of groundwater quality, 11 aquifers were determined as "good" and 20 aquifers were determined as "poor" in groundwater.

The main problems identified in the North Aegean Basin include domestic and industrial wastewater discharged without treatment, septic tank water from rural areas, leakages from irregular solid waste landfills to water resources, fertilizers and pesticides used in agricultural activities, pollutants originating from livestock activities, mining and hydro morphological changes. In addition, in the olive growing facilities located in the basin the coal mining enterprises located around Manisa Soma cause significant environmental pressures (Anonymous 2019).

3.5. Gediz basin

The precipitation area of the Gediz Basin is 17 145 km² with an annual average rainfall of 585 mm. The basin receives a significant amount of precipitation, and most of this precipitation disembogues into the sea (Anonymous 2018d). The population of the basin is just over 2 million.

The annual average flow amount of the Gediz Basin is 1.09×10^9 m³ (2.01 L/s/km²) and covers 0.59% of Turkey's surface water potential. The usable water potential of the basin is determined as 545×10^6 m³/year; the groundwater potential of the Gediz Basin is 555×10^6 m³/year, and the groundwater operating reserve is 248×10^6 m³/year. Considering the 1.09×10^9 m³/year surface and 555×10^6 m³/year groundwater potential in the basin, the total water potential is 1.645×10^9 m³/year. The total usable water potential of the basin has been determined as 793×10^6 m³/year considering the groundwater operation reserve (Anonymous 2015).

The main water source of the Gediz Basin is the Gediz River. In addition, the Alaşehir Stream, Gürduk Stream, Kemalpaşa (Nif) Stream, Kum (Gördes) Stream, Kurşunlu Stream, Kokarazmak Stream, Gümüş Stream, Irlamaz Stream, Ağlı Stream, Doğucan Stream, Karacalı Stream, Zeytin Stream, Sart Stream, Ahmetli Stream, Tabakçayı Stream, Şahyar Stream, Kısık Stream, Medet Stream, Üçgöz Stream, Merdiven Stream, Aşağıkoçak Stream, Göbekli Stream, Gökçay, Değirmendere and Derbent Stream are the other most important water resources of this basin (Anonymous 2019a).

The flow values measured in the basin are quite high. It has been stated that the long-term annual total flow in the Muradiye Bridge of the Gediz River is 1.228×10^9 m³, and the annual average flow is 39.134 m³/s. The annual flow of the Alaşehir Stream, which is one of the tributaries feeding the Gediz River, is 106×10^6 m³, and the annual average flow is 3.379 m³/s. The annual total flow of the Gördes Stream, one of the rivers feeding the Gördes Dam, is 113×10^6 m³ and its annual average flow is 3.61 m³/s. When the Nif Stream, which is the most important stream of the Kemalpaşa sub-basin, is examined, the annual average total flow is recorded as 73.5×10^6 m³ with an annual average flow of 2.749 m³/s (Anonymous 2019a).

The Gediz river faces a growing pollution threat resulting from industrial waste, domestic waste and also pesticides and artificial fertilizers from agricultural areas in the region. It is in the 4th class in terms of irrigation water quality (Öner & Çelik 2011).

The number of natural lakes in the Gediz Basin is almost non-existent. The most important natural lake in the basin is the Marmara, near the Marmara town of Akhisar. The storage volume of Lake Marmara is 320×10^6 m³. Apart from Marmara Lake, there are Gölcük and Sazlı Lakes as natural lakes in the basin (Anonymous 2019a).

The surface area of Lake Marmara varies between 3400-6800 hectares (Girgin 2000). Pollution found in the lake originates from the sewage in the Gölarmara district. Fertilizers and pesticides used in agricultural areas around the lake are transported to the area by surface runoff and drainage waters (Anonymous 2017). The lake water is recorded as medium salty, and of a low sodium irrigation water class with a pH value of 8 (Ünlü 2013).

Lake Gölcük, one of the natural lakes of the Gediz Basin, is located in the middle of Bozdağlar, 22 km southwest of Salihli. The deepest area of the lake is 8.5 meters. Its surface area is 0.8 km² and its volume is approximately 4×10^6 m³ (Ünlü 2013). Agricultural activities are carried out on the lands on the shores of the streams feeding the lake, and as a result of these activities, both the lake water level decreases and fertilizers and pesticides used for agricultural purposes pollute the lake (Anonymous 2017).

Demir (2020) in his study; By taking groundwater samples from 392 points in the Gediz Basin, irrigation water classification was made according to the Technical Principles of the Water Pollution Control Regulation (1999). The SAR (Sodium Adsorption Ratio) parameter value was found between 0-10 in 383 of the total 392 points in the basin. According to the SAR parameter, the groundwater in the basin are largely suitable for agricultural irrigation. The SO₄ parameter recorded a value between 0-192 mg/L at 364 points and was included in the 1st class waters, 15 points in the 2nd class waters, and 7 points in the 3rd class waters. It has been determined that it is within the scope of 4th class waters at 5 points and cannot be used as 5th class waters at 1 point. In terms of Cl parameter; Waters are classified as 1st class waters at 378 points, 2nd class waters at 4 points, 3rd class waters at 4 points,

4th class waters at 3 points, and 5th class waters at 3 points. According to these results, it has been stated that the groundwaters of Gediz Basin are in the appropriate class in terms of agricultural irrigation, except for a few regions.

3.6. Little meander basin

The Little Meander Basin is the smallest basin in Turkey with a surface area of 6 963 km². The population of the basin is 3 793 321 (Anonymous 2018e).

The annual average flow in the Little Meander Basin is 540x10⁶ m³ (2.40 L/s/km²), constituting 0.29% of Turkey's surface water potential. The usable part of this water is estimated to be 270x10⁶ m³/year. The groundwater operating reserve of the Little Meander Basin is 185x10⁶ m³/year and the groundwater potential is estimated to be 247x10⁶ m³/year. Considering the 540x10⁶ m³/year surface and 247x10⁶ m³/year groundwater potential in the basin, the total water potential was to be calculated as 787x10⁶ m³/year. The usable water potential of the basin has been determined as 455x10⁶ m³/year, taking into account 270x10⁶ m³/year usable surface water and 185x10⁶ m³ year groundwater operating reserves (Anonymous 2015).

The most important stream of the Little Meander Basin, the Little Meander River, is 129.1 km long. Other important rivers include the Çevlik Stream (12 km), Deveçukuru Stream (10.7 km), Keleş Stream (11.6 km), Kemer Stream (6.7 km), Kervan Stream (4.2 km), Kocaçay Stream (5.4 km), Manda Stream (7.7 km), Rahmanlar Menderes Stream (13.3 km), Tahtalı Stream (12.7 km), Udi Stream (4.7 km), Yassı Stream (11.9 km), Boğaz Stream (16.6 km), Çay Stream (Değirmen Stream) (10.8 km), Değirmen Stream (10.3 km), Döşeme Stream (11.3 km), Gök Stream (22.9 km), Ilıca Stream (14.2 km), Kızılkaya Stream (10.3 km), Koca Stream (11.7 km), Fetrek (Vişneli) Stream (13.8 km) and Aktaş Stream (8.9 km). The average annual precipitation in the basin is 622 mm with an average annual flow of 11.45 m³/s (Anonymous 2018e).

The basin is home to both large and small lakes. The main lakes include Lake Gölcük in the west of Bozdağ, Karagöl, which is a typical crater lake on Yamanlar Mountain, Lake Belevi, a shallow lake between Torbalı and Selçuk, and Lake Çakal and Lake Gebekirse, which are made up of alluvium brought by the Little Meander River. The most important lakes in the basin and their characteristics are given in Table 2 (Anonymous 2017).

Table 2- The important lakes of the Little Meander Basin and some of their characteristics

Lake name	Surface area (ha)	Maximum depth (m)	Storage volume (10 ⁶ m ³)
Gölcük Lake	94.1	7	1.81
Karagöl Lake	3.1	23	0.70
Belevi Lake	192.0	3	1.50
Çakal Lake	78.0	4	0.90
Gebekirse Lake	96.0	5	1.50

Among the lakes of the Little Meander Basin, Lake Karagöl is a popular natural park and recreation area, while other lakes are used specifically for providing irrigation water. It is known that the Çakal and Gebekirse lakes are considered to be second quality water (slightly contaminated water) in terms of ortho phosphate phosphorus and nitrite parameters. In terms of the electrical conductivity parameter, it has been determined that Lake Çakal is deemed to be of the second quality (slightly contaminated) water class, and Lake Gebekirse third quality (contaminated) water class. In addition, Lake Gebekirse is of the second quality (slightly contaminated) water class in terms of its anionic detergent parameter. According to the irrigation water criteria, the average concentrations of temperature, pH, boron, nitrate and ammonium are below the limit values and both lake waters can be used for irrigation water. The electrical conductivity of the water of Lake Çakal are recorded as 925 µS/cm, and that of the water of Lake Gebekirse as 1 025 µS/cm (Minareci & Sungur 2019).

The waters of the (Vişneli) Stream and Gelinbözü Stream, which feed the Little Meander River, are in the 4th class according to the chemical oxygen demand (COD) and ammonium nitrogen (NH₄-N) parameters. In terms of COD, the Ilıca Stream waters is class 3, whereas other streams are typically classes 1-2. It is stated that all the rivers in the basin are in the 4th class in terms of nitrite nitrogen (NO₂-N) and in the 1st class in terms of nitrate nitrogen (NO₃-N). According to group A (physical and inorganic pollutants) parameters, the water quality was found to be in the 4th class due to nitrite nitrogen (NO₂-N). In the evaluation made in terms of Biochemical Oxygen Demand (BOD) for group B (organic) parameters, the Little Meander River, Fetrek Stream, Gelinbözü Stream were in the 4th class, and the other creeks (with the exception of the Aktaş Stream, which was in the 2nd class) were in the 3rd class. In the evaluation of group C (inorganic pollution) parameters of all streams and creeks in the basin, it was observed that the waters were generally in the 3rd and 4th classes. There is very important organic and inorganic pollution in the Little Meander River after Beydağ district. For COD, BOD, NH₄-N, dissolved oxygen, color and boron parameters, the river is in the 4th class, that is, very polluted category. In addition, it is recorded as in the 3rd class in terms of iron, manganese and fluoride. In summary, in the evaluation made in terms of water quality in the rivers in the basin, the Little Meander River can be described as in the very polluted water category in terms of its organic matter, nitrogen, color, dissolved oxygen and salinity values. This situation is one of the most serious problems seen in the basin. In the Fetrek (Vişneli) Stream, after the Torbalı district, there are extreme values in terms of many parameters such as organic matter, nitrogen, color, dissolved oxygen, salinity,

fluoride, manganese and boron. The Fetrek Stream is in the category of highly polluted water and is the most problematic stream in the basin, thus increasing the pollution in the Little Meander River. The Gelinbözü Stream is in the very polluted water category in terms of organic matter, nitrogen and color parameters, and in the polluted or very polluted category in terms of dissolved oxygen, total coliform, color and iron parameters (Anonymous 2015).

Since the surface water potential is insufficient in the Little Meander Basin, the sustainability of agricultural production depends entirely on the use of groundwater. Reducing this dependence on groundwater in agricultural production may be possible by expanding the use of pressurized irrigation systems in agriculture.

In the Little Meander Basin, groundwater is widely used for drinking, irrigation and industrial purposes. The distribution of total groundwater use in the basin by sectors is 78% irrigation, 20% drinking and utilization and 2% industry (Tol 2021).

The wastes of surface and groundwaters used for irrigation, urban and industrial purposes in the basin are returned to the environment as wastewater. In particular, in this basin, which suffers from water shortage, the possibility of reusing the wastewater for certain purposes after treatment is of great importance in terms of the sustainability of the basin's water resources.

The groundwater resources of the Little Meander Basin face not only the problem of overexploitation but also pollution. Urban and industrial wastewater discharged to surface water resources without treatment, drainage waters containing fertilizer and pesticide residues returning from agricultural activities, animal wastes from livestock facilities, irregular dumping sites, wastes from olive processing and mining facilities, waste geothermal fluid discharge in geothermal fields, are sources of pollution which impact groundwater.

3.7. Meander basin

The precipitation area of the Meander Basin is 25 960 km². The average annual precipitation in the Meander Basin is about 637 mm. Estimated total runoff of the Meander Basin, including surface and groundwater bodies, is 2.673x10⁹ m³ per year. Almost all of this amount is used. On average, 2.414x10⁹ m³ is used for irrigation, 184x10⁶ m³ for residential use and 72x10⁶ m³ for industrial purposes per year (Anonymous 2018f). The population living in the basin is recorded as 2 283 812 people.

The groundwater operating reserve of the Meander Basin is 700x10⁶ m³/year and the groundwater potential is estimated to be around 933x10⁶ m³/year. Considering the 2x10⁹ m³/year surface and 933x10⁶ m³/year groundwater potential in the basin, the total basin water potential was calculated as 2.933x10⁹ m³/year (Anonymous 2015).

The Meander River is both the main river in the basin and the longest river in the Aegean Region. This river originates from springs flowing from the plains between Sandıklı, Dinar, Çivril and Honaz in Western Anatolia. The Meander River is fed by the waters that fill Lake Işıklı. The river is fed by many tributaries (Anonymous 2018f). It takes the Banaz Stream from Uşak and the Çine Stream from Muğla and flows into the Aegean Sea. The average flow of the river is approximately 110 m³/s. Since the river is mostly fed by winter precipitation, the highest flow rate is determined in January and February (average 164 m³/s). In summer, the quantity of water that makes up the natural flow of the stream is very low (Yenici 2010).

The Banaz, Akçay, Kufi, Dokuzsele, Geyre (Dandalaz), Dipsiz, Çine and Hamam rivers can be listed as the most important rivers of the basin (Anonymous 2018f).

The natural lakes in the basin are Lake Bafa, Lake Işıklı and Lake Azap (Anonymous 2017).

Lake Bafa is a lagoon lake and is located in the southeast of the Meander Delta. The total area of the lake is 7 088 ha, its altitude is 10 m from the sea level, its circumference is 50 km and its distance to the sea is 17 km. The lake is characterised by its large and small island found within the waters of the lake. The main source feeding the lake is the Meander River (Anonymous 2017).

Lake Işıklı (Çivril Lake) is a 4 976 ha lake located in the south of Akdağ within the borders of the Çivril district of Denizli. In 1968, the western, southern and eastern shores of the lake were surrounded by a set; later, the lake became a dam lake. Lake Çivril is today used as a reservoir for large-scale irrigation in the surrounding plains (Anonymous 2017).

Lake Azap is popular destination for many domestic and foreign bird watchers, especially in the winter months, as it has a rich ecosystem where aquatic creatures such as the reed rat and the whitetail eagle inhabit. Although the total area covered by the lake is 166 ha, almost all of the lake had dried up by 2007; however, in 2008 the lake began to slowly fill up again (Anonymous 2017).

Yenici (2010) evaluated the measurement results at State Hydraulic Works (SHW) stations between 2003 and 2008 and determined the water quality of the basin according to the classes defined in the Water Pollution Control Regulation. When the

analysis results of the samples taken from the stations in the Meander River Basin are evaluated; It has been stated that there is no class 1, that is, high quality water in the basin. It has been determined that the water quality in the basin is generally class 4.

One of the most significant problems faced in terms of water quality in the basin's rivers is the excessive organic matter, nitrogen, pH and heavy metal pollution and oxygen deficiency in the Gökpınar Stream originating from Denizli. An additional problem is the salinity added to the organic matter and nitrogen pollution in the Çürüksu Stream and the Meander River on the Denizli-Sarayköy-Kuyucak line. In addition, excessive organic matter and nitrogen pollution, salinity and oxygen deficiency originating from Uşak in the Dokuzsele Creek (before Banaz Stream) and significant salinity, organic matter and boron pollution in Gümüşçay (around Ortaklar-Söke) can be listed as significant issues faced (Anonymous 2015).

3.8. Western Mediterranean basin

The precipitation area of this basin is 20 956 km². The surface water resources of the Western Mediterranean Basin are largely composed of rivers including the Alakır Stream, Akçay, Demre Stream, Eşen Stream, Kargıcak Stream, Dalaman Stream, Yuvarlakçay Stream, Namnam Stream, Kazandere Stream, Kocaalan Stream, Değirmendere Stream, Kocaçay Stream, Gerin Stream, Batış Stream, Koca Stream, Sarıçay Stream, Hamzabey Stream, Kurbanlı Stream, Kandak Stream and Derince Stream (Anonymous 2018g). The population living in the basin is around 1.25 million.

Natural lakes in the Western Mediterranean Basin include Lake Köyceğiz, Lake Gölhisar, Lake Avlan, Lake Girdev, Kocagöl and Lake Yazır (Anonymous 2017).

Lake Köyceğiz is Turkey's 16th largest lake with an area of 52 km². It is situated 8 meters above sea level. The sulphur content of the lake water is high. The lake water, which is polluted by mixing with domestic wastewater, is also polluted by agricultural pollutants from the agricultural areas found around the lake. The salinity in the lake, which is connected to the sea, is very high in places, and the electrical conductivity varies between 4 dS/m and 65 dS/m (Ceviz 2020).

Lake Avlan, which serves as an important station on bird migration routes and has international importance, was completely dried in the 1970s in order to expand on the region's agricultural land. Agricultural activities were carried out in the lake area for a while, but as of 2001, water was started to be kept in the lake again in order to re-create the lake. Around 2004, the lake started to dry up again. It may even become impossible for fish to survive in the lake, which tends to dry out especially in summer. The area of the lake, which is one of the few reclaimed wetlands in the world, is currently 797 ha (Anonymous 2018h).

Lake Gölhisar has an area of 459 ha and is located in the Gölhisar District of Burdur Province. There is plenty of catfish fishing in the lake. The lake is situated 1000 meters above sea level and has a maximum depth of 10 meters and is surrounded by reeds. The lake is eutrophic and under the threat of drought (Anonymous 2017). The lake waters have C₂S₁ quality class and can be used for the irrigation of all cultivated plants with the exception of salinity sensitive plants (Anonymous 2018h).

Mumcular Dam is a dam built between 1986 and 1989 on Kocadere in Muğla for irrigation and drinking water purposes. The body volume of the earthfill dam is 986 000 m³, its height from the river bed is 32 m, the lake volume at a normal water level is 19.04x10⁶ m³, and the lake area at a normal water level is 1.42 km². While the dam provides irrigation water to an area of 1 365 hectares, it also provides drinking water at 10x10⁶ m³ per year.

Alakır Dam is a dam built between 1967 and 1971 for irrigation and flood control purposes on the Alakır Stream in Antalya. The body volume of the dam, which is a rock body fill type, is 1.6x10⁶ m³, its height from the river bed is 44.5 m, the lake volume at a normal water level is 91.75x10⁶ m³, and the lake surface area at a normal water level is 4.28 km². It provides irrigation water to an area of 3 262 hectares.

Çayboğazı Dam is a dam built between 1996 and 2000 for irrigation purposes on the Çayboğazı Stream in Antalya. The body volume of the dam, which is an earth body fill type, is 10.7x10⁶ m³, its height from the river bed is 79 m, the lake volume at a normal water level is 56x10⁶ m³, and the lake area at a normal water level is 2.25 km². The dam provides irrigation water to an area of 13 848 hectares.

Yapraklı Dam is a dam built between 1985 and 1991 for irrigation purposes on Horzum Stream in Burdur. The body volume of the dam, which is an earth body fill type, is 1.6x10⁶ m³, its height from the river bed is 70 m, the lake volume at a normal water level is 113x10⁶ m³, and the lake area at a normal water level is 6.5 km². The dam provides irrigation water to an area of 19 576 hectares.

Çavdır Dam is a dam built between 1993 and 1996 for irrigation purposes on the Bayır Stream in Burdur. The body volume of the dam, which is a rock body fill type, is 2.6x10⁶ m³, its height from the river bed is 60 m, the lake volume at a normal water level is 36.42x10⁶ m³, and the lake area at a normal water level is 1.94 km². The dam provides irrigation water to an area of 4 254 hectares.

Belkaya Dam is a dam built between 1993 and 2003 for irrigation purposes on the Aksu Stream in Burdur. The body volume of the dam, which is an earth body fill type, is 1.4×10^6 m³, its height from the river bed is 68 m, the lake volume at a normal water level is 56×10^6 m³, and the lake area at normal water level is 5.2 km². The dam provides irrigation water to an area of 4 545 hectares. The dam water is in the C₂S₁ class in terms of quality.

Geyik Dam in the same basin is a dam built for the purposes of drinking water between 1986 and 1988 the Sarıçay in Milas district of Muğla. The body volume of the dam, which is a rock body fill type, is 260 000 m³, its height from the river bed is 41 m, the lake volume at a normal water level is 40.8×10^6 m³, and the lake area at a normal water level is 3.74 km². The dam provides 38×10^6 m³ of drinking water per year and serves the Yeniköy Thermal Power Plant between Milas and Ören.

Akgedik Dam is a dam constructed for irrigation purposes on the Sarıçay in Muğla. The dam has a rock body filling type with a height of 51 m above the river bed and a lake volume of 31 hm³ at a normal water level. The drainage area is approximately 93 km² (Aydın & Aydın 2006).

The annual average flow amount in the Western Mediterranean Basin is 7.11×10^9 m³ (9.97 L/s/km²), constituting 3.87% of Turkey's surface water potential. The usable part of this water is estimated to be 3.555×10^9 m³/year. The groundwater operating reserve of the Western Mediterranean Basin is 317×10^6 m³/year, and the groundwater potential is 473×10^6 m³/year. Considering the 7.11×10^9 m³/year surface and 473×10^6 m³/year groundwater potential in the basin, the total water potential was calculated as 7.583×10^9 m³/year. The usable water potential of the basin is calculated as 3.872×10^9 m³/year, considering 3.555×10^9 m³/year usable surface water and 317×10^6 m³/year groundwater operating reserves (Anonymous 2015).

The waters of the Western Mediterranean Basin are in the 1st and 2nd classes in terms of COD and BOD. However, it is designated as class 3 in terms of COD and BOD at the Mumcular and Geyik Dam outlets, and class 3 in terms of BOD at the Akgedik Dam outlet. In terms of ammonium nitrogen (NH₄-N), the waters in the basin are in the 1st and 2nd class quality, while in terms of nitrate nitrogen (NO₃-N), the waters in the basin are in the 1st class. In terms of nitrite nitrogen (NO₂-N), although most station values are in the 1st or 2nd class, this parameter is in the 3rd and 4th class levels in the Çavdır Stream, Dalaman Stream, Namnam Stream, Sarıçay Stream, Kocadere Stream, Esen Stream and Hamzabey Stream. The total phosphorus (TP) parameter is not measured at most stations, but is at the 2nd class level in the Çavdır and Dalaman Streams and Başpınar springs (Anonymous 2015).

3.9. Antalya basin

The precipitation area of the Antalya Basin is 20 249 km² with an average precipitation value of the basin is 973.7 mm. The total annual average water potential of the Antalya Basin is over 10×10^9 m³. This potential is approximately 30% higher than the water potential of the Seyhan Basin, which is approximately 22 000 km², and the Yeşilirmak Basin, which is approximately 38 000 km². These data are indicative of the high water yield of the Antalya Basin (Anonymous 2016). The population of the basin area is recorded to be more than 2 million.

The annual average flow for Antalya Basin is 13×10^9 m³ (27.96 L/s/km²), constituting 6.97% of the total runoff in the basins. The usable quantity of this water is estimated as 6.5×10^9 m³/year. The groundwater potential of Antalya Basin is 1.1×10^9 m³/year, and the groundwater operating reserve is 526×10^6 m³/year. Considering the 13×10^9 m³/year surface and 1.1×10^9 m³/year groundwater potential in the basin, the total water potential is calculated as 14.1×10^9 m³/year. The usable water potential of the basin is expressed as 7.03×10^9 m³/year, taking into account 6.5×10^9 m³/year usable surface water and 526×10^6 m³/year groundwater operating reserves (Anonymous 2015).

The most important rivers of the region are the Köprüçay River, Manavgat River, Aksu Stream, Alara Stream, Kargı Stream, Dim Stream, Karpuz Stream, Acısu Stream, Sarısu Stream, Kömürcüler and Ilıca streams.

The largest and most important lake of the basin is Lake Eğirdir, followed by Lakes Kovada, İlvat and Dipsiz.

Lake Eğirdir is in the Western Mediterranean part of Turkey, within the borders of the province of Isparta, surrounded by the districts of Eğirdir, Senirkent, Yalvaç and Gelendost. Lake Eğirdir has an area of 45 633 ha of tectonic origin extending in the north-south direction, in the north of the Eğirdir district. Lake Eğirdir is considered as a hot spot because it is used as a drinking water source.

The surface area of Kovada Lake is 929 hectares. The water entering Lake Kovada through a channel is taken through a bypass channel and given to the hydroelectric power plant channel. For this reason, when the water input to the lake decreased, the lake level decreased.

Oruçoğlu & Beyhan (2019) evaluated the water samples taken monthly in 2016 in the Lakes Region of Turkey and located within the borders of the 18th Regional Directorate of State Hydraulic Works, in accordance with the Water Pollution Control

Regulation in force. In the results of working, it has been reported that Lakes Eğirdir and Kovada have 1st class water quality in terms of their freshwater characteristics.

When the Antalya Basin is evaluated in terms of its water quality in general, the quality of the water resources in the basin is predominantly less polluted water quality (Anonymous 2015).

The most important factor in the decrease in the water quality of the basin is the wastewater discharged without domestic treatment. Activities such as nitrogen and phosphorus fertilizer applications used for agricultural activities and cage fishing in the lakes negatively affect the water quality in the basin (Anonymous 2018i).

Within the scope of the Antalya Basin Drought Management Plan, 1 of the 46 stations evaluated in the basin in terms of irrigation water quality is 1st class, 4 of them are 3rd class, and the remaining 41 stations have been designated 2nd class. Since two of the four stations designated as 3rd class irrigation water are found to be effluent downstream of the wastewater treatment plant, the other two stations are of low quality because of their high electrical conductivity values due to their being fed from karstic sources and coastal water intrusion.

Half of the Antalya Basin groundwater reserve has been determined as the safe groundwater reserve for the entire basin. Groundwater use in the basin is produced through wells. In places where there is no surface water source, agricultural irrigation is completely dependent on groundwater (SHW 2016).

The groundwater recharge of basins occurs in three basic ways: by direct infiltration from the surface during and after precipitation, by infiltration from water transmission and distribution lines, and by groundwater from neighboring basins. In this case, the total groundwater reserve in the Antalya Basin can reach 4.3×10^9 m³/year, which is higher than the known the operable amount (SHW 2016).

3.10. Burdur closed basin

The Burdur Closed Basin is the second smallest basin in Turkey comprising 6 294 km². The annual precipitation of the basin is 508.7 mm (Anonymous 2019b). In terms of population, it is the lowest recorded population area with 214 715 inhabitants.

The annual average flow for the Burdur Closed Basin is 250×10^6 m³ (0.91 L/s/km²), constituting 0.14% of Turkey's surface water potential. The usable part of this water is 125×10^6 m³/year. The groundwater operating reserve of Burdur Closed Basin is 43×10^6 m³/year and its groundwater potential is 57×10^6 m³/year. Considering the 250×10^6 m³/year surface and 57×10^6 m³/year groundwater potential in the basin, the total water potential was calculated as 307×10^6 m³/year. The usable water potential of the basin is determined as 168×10^6 m³/year considering 125×10^6 m³/year usable surface water and 43×10^6 m³/year groundwater operating reserves (Anonymous 2015).

The regimes of the streams in the basin are quite irregular; streams in the basin include the Bozçay (Eren) Stream, Değirmen Stream, Sarı Stream, Yayla Stream, Domuz (Elmacık) Stream, Menevşeli (Kent) Stream, Özdere Stream, Karapınar Stream, Ulupınar Stream, and Çolakboğazı Stream (Anonymous 2019b).

The lakes in the Burdur Closed Basin include Lake Burdur, Lake Salda, Lake Acıgöl, Lake Sıralı and Lake Karataş.

Lake Burdur is one of the important lakes of the basin and is located between the provinces of Burdur and Isparta. The average lake area is 20 311 ha with an altitude of 857 meters. Lake Burdur is structurally tectonic and mesotrophic - eutrophic in terms of eutrophication. The water of Lake Burdur is insuitable for drinking, domestic, industrial and agricultural use. Due to the high sodium, sulfate and chloride content in its water, plant species diversity is low and only a few species of fish inhabit the lakes waters. The salinity rate is high and the Burdur toothed carp has adapted to it.

Lake Salda is a slightly salty tectonic lake surrounded by forest-covered hills, rocky lands and small alluvial plains, with a surface area of 4 451 ha. The waters of the streams feeding the lake are used for the irrigation of agricultural lands in the basin.

Acıgöl, located in the Çardak district of Denizli province. Acıgöl is the second saltiest lake in Turkey after Lake Salt. Intensive agriculture is conducted on the plain in the Başmakçı region. The lands around the lake, especially the eastern and northeastern shores, are used as pasture.

Lake Yarıklı is a shallow lake with high sodium phosphate, sodium chloride and sodium sulfate concentrations. The lake is surrounded by agricultural areas where cereals and poppies are cultivated in the west and north. The natural vegetation around the lake has been removed by converting it into agricultural land. Wind and water erosion have become a significant problem in the agricultural lands around the lake, and have been caused by inappropriate agricultural practices. Fresh water resources feeding the lake are used in agricultural irrigation.

Lake Karataş is located in the south of Burdur province and northeast of Tefenni Plain. The lake is a shallow freshwater lake with a surface area of 526 ha. In addition to agriculture, commercial fishing is practiced on the lake. The most significant problem of the lake is its insufficient water level due to the lack of precipitation and the drying up of the sources feeding the lake (Anonymous 2017).

3.11. Akarçay basin

The Akarçay Basin is the 4th smallest basin constituting 7 995 km², and the 3rd least populated basin with a population of 725 568 (Tüik 2019).

The average precipitation value of the Akarçay Basin is 436.1 mm/year. The Akarçay Basin is a very poor basin in terms of surface and groundwater resources. It is important to know the characteristics of the sub-basins for both water management and land use. The Akarçay Basin is studied as two sub-basins. The area where the Akarçay river starts from the point where it originates and flows into the Eber Lake is defined as the Upper Akarçay (Eber) Sub-Basin. This upper basin (Lake Eber Basin) covers an area of 5 660.5 km². The second sub-basin located further down is the Lower Akarçay (Akşehir) Basin, which can be defined as the branches feeding Lake Akşehir and the area surrounded by these branches. This sub-basin area is approximately 2 334.5 km² (Anonymous 2019c).

The annual average flow in the Akarçay Basin is $260 \times 10^6 \text{ m}^3$ (0.97 L/s/km^2), constituting 0.14% of Turkey's surface water potential. The usable part of this water is estimated as $130 \times 10^6 \text{ m}^3/\text{year}$. The groundwater potential of the Akarçay Basin is $188 \times 10^6 \text{ m}^3/\text{year}$, and the groundwater operating reserve is $182 \times 10^6 \text{ m}^3/\text{year}$. Considering the $260 \times 10^6 \text{ m}^3/\text{year}$ surface and $188 \times 10^6 \text{ m}^3/\text{year}$ groundwater potential in the basin, the total water potential is calculated as $448 \times 10^6 \text{ m}^3/\text{year}$. Considering the $130 \times 10^6 \text{ m}^3/\text{year}$ usable surface water and $182 \times 10^6 \text{ m}^3/\text{year}$ groundwater operating reserves, it has been recorded that the usable water potential of the basin is $312 \times 10^6 \text{ m}^3/\text{year}$ (Anonymous 2015).

The important streams of the basin are the Akarçay River, Aksu (Araplı) Stream, Seydiler (Kuruçay) Stream, Çayözü Stream and Kali Stream (Anonymous 2019c).

The main source of the Akarçay River is the Aksu (Araplı) Stream. The waters of the Seydiler (Kuruçay) Stream originating from the north, the Çayözü Stream waters originating from the north and the Kali Stream waters originating from the south join the Akarçay River and disemboque into Lake Eber (Anonymous 2019c).

Kıvrak et al. (2012) took water samples every month from March to December 2008 at four different stations to determine the water quality of the Akarçay. Their analyses of the water samples found that the pH of the river was between 7.4 and 8.7. They stated that this fluctuation in pH values was caused by the effect of pollution rather than the geological structure. The electrical conductivity values of the samples were found to be generally high in all stations during the summer months. In particular, the electrical conductivity and water temperature were recorded at a record level at the 2nd station. In this station, their research found that the thermal facilities' discharge of waste water to the Akarçay River had a significant effect on the increase in the electrical conductivity and temperature of the river water at this station. They found that the high EC values at other stations were closely related to the levels of pollution in the river by domestic and industrial waste.

The natural lakes in the basin are Lakes Eber and Akşehir. Lake Eber is an important source of irrigation and drinking water in the southwest of Turkey and is also a 1st Degree Natural Protected Area. It is a tectonic lake with an altitude of 966 m, located 65 km from the city center of Afyonkarahisar. The most important source feeding Lake Eber is the Akarçay River. Gümüş et al. (2020), determined the average conductivity value of the lake to be 1.740 (0.697-2.590 dS/m).

While Lake Eber used to be a single large lake that included the waters of Lake Akşehir; with the decrease of water resources over time, Lake Akşehir was separated from Lake Eber and formed a separate lake. It still transfers water from Lake Eber to Akşehir Lake through a channel. Today, with the effect of global warming and especially the unconscious use of water resources, the lake has begun to shrink in size. For this reason, the water flowing into Lake Akşehir was stopped, which caused the waters of Lake Akşehir to be withdrawn. For this reason, the lake, which is one of the most beautiful lakes in Turkey, is in danger of drying out.

Lake Akşehir, like Lake Eber, is located in the depression area between the Sultan Mountains and Mount Emir. It is located 10.2 km away from the Akşehir District and is the fifth largest lake in Turkey. Administratively, it is located within the borders of Konya and Afyonkarahisar provinces. Since it is in a closed basin, it has no outflow (Elmacı & Obalı 1998).

Lakes Eber and Akşehir, which form the downstream of the Afyonkarahisar-Akarçay Basin, which is a bowl basin, are not suitable for drinking and domestic use of water quality. COD and BOD values, which are important parameters indicating organic pollution in the Akarçay Basin, are predominantly of class 4 quality. When the basin is evaluated in terms of water quality in general, it is deemed to be dirty or very polluted (Anonymous 2015).

3.12. Sakarya basin

The Sakarya Basin is the third largest basin constituting 6 3303 km². Ankara, the second most populous city of Turkey, is located in this basin, and the total municipal population in the basin is 7 034 906. The annual average precipitation value of the basin is 850.2 mm (Anonymous 2019d).

The average annual flow value of the Sakarya Basin is 5.02×10^9 m³ (2.82 L/s/km²), which corresponds to 2.73% of Turkey's surface water potential. The usable part of this water is estimated to be 2.51×10^9 m³/year. The groundwater potential of the Sakarya Basin is recorded as 2.192×10^9 m³/year, with a groundwater operating reserve of 1.519×10^9 m³/year. Considering the 5.02×10^9 m³/year surface and 2.192×10^9 m³/year groundwater potential in the basin, the total water potential has been calculated as 7.21×10^9 m³/year. The usable water potential of the basin has been determined to be 4.03×10^9 m³/year considering 2.51×10^9 m³/year usable surface water and 1.519×10^9 m³/year groundwater operating reserves (Anonymous 2015).

There are many streams in the Sakarya Basin. The waters of these streams flow into the Black Sea via the Sakarya River. Important streams feeding the Sakarya River include the Porsuk Stream, Kirmir Stream, Ankara Stream, Mudurnu Stream, Seydi Stream, Göksu Stream, Gökınar Stream, Aladağ Stream, Karasu Stream, Göynük Stream, Çark Stream, Bardakçı Stream, Ilcaözü Stream, Nallidere Stream, Çatak Stream and Değirmendere Stream (Anonymous 2019d).

Lakes in the Sakarya Basin include Lake Mogan, Lake Poyrazlar, Lake Ilgın, Lake Eymir, Lake Taşkısığı, Lake Balıkdanı, Lake Çubuk, Lake Sünnet, Lake Uyuz, Lake Sapanca, Lake Akgöl, Lake Küçük Akgöl and Lake Acarlar (Anonymous 2017).

Lake Mogan is situated 17 km south of Ankara. The altitude of the lake is 972 m above sea level, the lake area at a normal water level is 6.64 km², the average depth of the lake is 3-5 m, and the lake volume at a normal water level is 13.34×10^6 m³. The groundwater recharge of Lake Mogan is quite low, and the water inflow is through streams with an irregular regime, which typically dry up in the summer months. Lake Mogan is situated within the Gölbaşı Special Environmental Protection Area and is also one of the important bird areas in the country nominated for Ramsar (Anonymous 2017).

Lake Sapanca takes its name from Sapanca, the town of Sakarya in the south. Lake Sapanca, one of the few lakes in the world with high quality drinkable features, is the only source of drinking and domestic water for Sakarya Province and an important source for Kocaeli Province. The surface area of the lake is 4 771 ha, the surface altitude is 31 m above sea level, and the deepest point is 61 m. Lake Sapanca, which has a precipitation area of 252 km², has an average of 75 cm level change per year. During the rainy months of the year, the covers of the Çark Creek are opened and the level of the lake is kept in balance. Sapanca Lake is an important wetland where tens of thousands of migratory birds stay migrate to every year, as well as being a source of drinking and utility water (Anonymous 2017).

In terms of COD and BOD, which are important parameters that show organic pollution in the Sakarya Basin, the waters of the Porsuk Stream, Karasu Stream and Çarksuyu Stream and Kalburt Göksu Stream are predominantly of the 4th class (highly polluted water), while the waters of the Sakarya River and its other branches are deemed 2nd class (less polluted water) or 3rd class (dirty water). In terms of NH₄-N, which is one of the important nitrogen parameters, the waters of the Porsuk Stream, Karasu Stream and Çarksuyu Stream are in the 4th class, and the water of the Kalburt Göksu Stream and the creeks feeding it varies between 2nd and 4th class. In the Sakarya River and its other branches, the pollution level is predominantly at a 2nd class level. In terms of NO₃-N parameter, the basin in general is predominantly class 1 (clean water) quality. However, nitrate pollution at the 3rd and 4th class levels was determined at the stations in the Çubuk Stream, Sukesen Stream, Kadıköy Stream and Bayındır Stream. In terms of total phosphorus parameter, while the waters in the Sakarya River were 1st and 2nd class before the addition of the Porsuk Stream, it turns becomes 3rd class water after the addition of the Porsuk Stream. After the addition of the Ankara Stream, the waters become more polluted and take the 4th class feature. After the addition of Karasu and Kalburt Göksu Streams, it was determined that the water quality improved slightly and turned could be deemed to be of a 3rd class level.

In terms of total phosphorus, the Porsuk Stream shows grades ranging from 2 to 4, but before the Porsuk Dam and before the Sakarya River, the quality completely turns into 4th class pollution. The total phosphorus was determined to be class 4 in the Ankara Stream, Karasu Stream, Kalburt Göksu Stream and Çarksuyu Stream. In other branches, it is typically at the 1st and 2nd class levels. When the basin is evaluated in terms of water quality in general, it can be said that the Sakarya River and the important streams that feed it, the Porsuk Stream, Karasu Stream, Çarksuyu Stream, Kalburt Göksu Stream, Ankara Stream and Çubuk Stream have polluted or very polluted water quality in terms of different parameters. The Sakarya River, especially after the addition of the Porsuk and Ankara Streams, shows dirty or very polluted features in terms of organic matter, ammonium nitrogen, total phosphorus as well as conductivity, inorganic parameters, boron and certain metals (Anonymous 2015).

3.13. Western black sea basin

The Western Black Sea Basin has a precipitation area of 28 855 km² and an annual precipitation level of 774.05 mm (Anonymous 2019e). The basin is the 5th most populated basin in Turkey with a population of approximately 3.8 million.

The annual average flow value of the Western Black Sea Basin is 9.36×10^9 m³ (9.99 L/s/km²), constituting 5.09% of Turkey's surface water potential. The usable part of this water is estimated to be 4.68×10^9 m³/year. The groundwater operating reserve of the Western Black Sea Basin is recorded as 412×10^6 m³/year, with a groundwater potential of 416×10^6 m³/year. Considering the 9.36×10^9 m³/year surface and 416×10^6 m³/year groundwater potential in the basin, the total water potential is 9.78×10^9 m³/year. Considering the 4.68×10^9 m³/year usable surface water and 412×10^6 m³/year groundwater operating reserves, usable water was determined as 5.09×10^9 m³/year (Anonymous 2015).

The streams in the Western Black Sea Basin include the Filyos Stream, Bartın River, Ovaçayı and İnönü Streams, Küçük Melen Stream, Asar Stream, Uğur Stream, Aksu Stream, Büyük Melen Stream, Güllüç Stream, Devrek River, Alaplı River, Üzülmez Stream and Kozlu Stream (Anonymous 2019e).

The natural lakes in the basin include Lake Abant, Lake Sarıkum, Lake Yeniçağa and Lake Efteni.

Lake Abant, located 30 km southwest of Bolu in the Western Black Sea region, is a landslide set lake in terms of formation. The lake is located at an altitude of 1 345 m above sea level, its maximum depth is 18 m and its surface area is 125 ha. Lake Abant was taken under protection on October 21, 1988 by the National Parks Law No. 2873 dated 9 August 1983 and declared a "Nature Park" (Atıcı & Obalı 2002; Müderrisoğlu et al. 2005).

Lake Sarıkum is located between Sinop and Ayancık. The lake is a lagoon lake and its depth varies between 0.5-1 m. The entire area of the lake comprises 785 ha, and the lake surface area, which is especially important as a habitat for waterbirds, is 102 ha, as well as a swamp area of 82 ha. The lake was declared a 1st Degree Natural Protected Area in 1991 (Yılmaz 2005). The Black Sea climate effect is observed in the region (Özkoç et al. 2019).

Hasançavuşoğlu & Gündoğdu (2021) reported that the physico-chemical structure of Lake Sarıkum deteriorated due to the discharge of domestic wastewater into the lake and the natural and artificial fertilizers used in the agricultural areas around the lake entering the lake. In addition, they stated that there was an increase in the level of salinity due to the mixing of sea water with lake water from the connection channel of the lake and the sea.

Lake Yeniçağa is located in the Yeniçağa district of Bolu. The lake is of great economic importance because of fishery. Tunca et al. (2012) measured the EC value of the lake as 0.439 dS/m in their study.

Lake Efteni, located in the southwest of Düzce city center and 14 km away from the center, is located at 40°45' N latitude – 31° 03' E longitude. Lake Efteni wetland is within the drainage area of the Düzce plain formed by the Melen Stream and many surface waters of the Melen Sub-basin within the Western Black Sea Basin. The elevation of the area above sea level is approximately 115 m. The lake area decreases to 5 km² when the waters recedes, and it can reach up to 25 km² in times of flooding. The lakes water is recorded as being in the "medium saline waters" class and can be used for irrigation puposes, and are of the "C2S1" class (Şener & Kırilangıç 2014).

Many water sources in the Western Black Sea Basin are classified as either 1st (clean) or 2nd (less polluted) in terms of COD and BOD, which are important parameters indicating organic pollution. In terms of COD parameter, the Gerede Stream is in the 3rd class (dirty water) in the Bahçedere region. However, in terms of BOD parameter, the Gerede Stream, Büyüksu Stream, Devrek Stream, Markusa Stream, Mudurnu Stream, Ulusu Stream and Zonguldak Acılık Stream are in the 3rd or 4th Class, that is, in the polluted or highly polluted water class. When the basin is evaluated in terms of water quality in general the water resources in the basin consist of 4th class, 3rd class and 2nd class waters. However, due to parameters such as iron, ammonium nitrogen, nitrite, total phosphorus, dissolved oxygen, sodium, chloride and sulfate, the water quality in some of the above-mentioned streams is classified as contaminated or very polluted (Anonymous 2015).

3.14. Yeşilirmak basin

The Yeşilirmak catchment area is 39 595 km² with a population of around 3 million. The rivers in the region include the Yeşilirmak River, Çekerek River, Tersakan Stream, Kelkit Stream, Abdal River, Kürtün River, Engiz Stream and Derinöz Stream (Anonymous 2015a).

According to the data from the General Directorate of Meteorology, the Yeşilirmak Basin has an annual precipitation value of 646 mm (Kale 2018). The annual average flow in the Yeşilirmak Basin is 5.28×10^9 m³ (4.63 L/s/km²), constituting 2.87% of Turkey's surface water potential. The usable part of this water is 2.64×10^9 m³/year. The groundwater potential of the Yeşilirmak Basin is 609×10^6 m³/year and the groundwater operating reserve is 456×10^6 m³/year. Considering the 5.28×10^9 m³/year surface and 609×10^6 m³/year groundwater potential in the basin, the total water potential is 5.9×10^9 m³/year. The usable water potential of the basin is calculated as 3.1×10^9 m³/year considering the 2.64×10^9 m³/year usable surface water and 456×10^6 m³/year groundwater operating reserves (Anonymous 2015).

The number of dam lakes in the Yeşilırmak Basin is high. The most important of these are the Hasan Uğurlu, Almus, Çakmak, Kılıçkaya, Süreyyabey and Koçhisar dam lakes. These dam lakes meet the demand for irrigation, drinking, industrial and utility water in addition to hydroelectric power generation.

The natural lakes in the basin are Lakes Ladik and Simenli. Winter precipitation waters stored in lake Ladik are left to the Tersakan River from the regulator on the outlet side in summer and used in Amasya-Suluova irrigation project area. The water altitude of the lake varies between 861 m and 867 m. The lake waters are fed by waters flowing from Akdağ, which is located at an elevation of 2 050 m, and by side streams.

One of the most significant problems in terms of surface water pollution in the Yeşilırmak Basin is that the Tersakan and Çorum Streams are highly polluted in terms of organic matter and ammonium nitrogen due to the wastewater discharges they are exposed to. There is significant organic matter pollution in the Boğazköy area, which is close to the downstream of Tersakan Stream, especially before it confluence with Yeşilırmak. Pollution load concentration becomes even more evident during dry periods. In addition, dissolved oxygen, sulfate, total dissolved matter, sodium, chloride, nitrate and phosphate pollutants are also present in the Çorum Stream (Anonymous 2015).

3.15. Kızılırmak basin

The Kızılırmak Basin is the second largest basin with an area of 82 181 km². With a population of 4 million inhabitants, it is the 4th most populated basin in Turkey (Anonymous 2010a).

More than one climate is effective in the basin due to its coverage and location over a wide area. The average annual precipitation of the basin is 435.6 mm with an average annual flow of 6.12 km³. The circumference of the basin is 3 546 km and the length recorded as 293 km (Anonymous 2019f).

The annual average flow value of the Kızılırmak Basin is 5.18x10⁹ m³ (2.09 L/s/km²) and constitutes 2.82% of Turkey's surface water potential. The usable part of this water is 2.59x10⁹ m³/year. The groundwater operating reserve of the Kızılırmak Basin is 1.02x10⁹ m³/year and the groundwater potential is 1.36x10⁹ m³/year. Considering the 5.18x10⁹ m³/year surface and 1.36x10⁹ m³/year groundwater potential in the basin, the total water potential becomes 6.54x10⁹ m³/year. The usable water potential of the basin is 3.61x10⁹ m³/year considering the 2.59x10⁹ m³/year usable surface water and 1.02x10⁹ m³/year groundwater operating reserves (Anonymous 2015).

The longest of the Turkey's rivers, the Kızılırmak River has a length of 1 151 km and discharges the waters of an area of 78 180 km² into the Black Sea (Anonymous 2010a). There is no known issues with the chemical properties of the waters from the İmranlı district, where the Kızılırmak originates, to the borders of Zara district. However, after Hafik, due to the presence of gypsum and salt minerals and the addition of its southern branches (Tuzlasuyu Stream, Yavşanlı Stream, İslim Stream and Fadlum River), the chemical structure of the water changes and becomes quite salty. The waters of the Kızılırmak River is generally in the 3rd and 4th classes in terms of irrigation water quality (Koç et al. 2018).

The most important streams of the Kızılırmak Basin are the Delice River, Gökırmak Stream and Devres Stream, which collects the waters of the mountainous northern part (Anonymous 2010a).

There are a large number of rivers and streams in the Kızılırmak Basin: those with a than 20 km in the basin include the Gökırmak River, Kanak Stream, Karasu Stream, Acısu Stream, Delice Stream, Devrez Stream, Mısmıl Stream and Tecer Stream.

Important lakes in the Kızılırmak Basin include the Sultansazlığı Marshes and Lake Tuzla (Palas). Sultansazlığı is one of the 14 wetlands of the country; in 1994 it was declared a Ramsar Site and later registered as a National Park on 17/03/2006 and taken under protection (Anonymous 2017).

Lake Tuzla (Palas) is covers an area of 2 387 ha in the Palas Plain, 40 km northeast of Kayseri. The important water resources of this lake include the Değirmen, Yertaşpınar, Körpınar, Başpınar and Soğukpınar streams. The lake was declared a first degree natural protected area in 1993 and has also been registered as a wetland of national importance (Anonymous 2017).

The most important source of pollution in the Kızılırmak Basin are natural resources. Due to the geological factors arising from the source of the river and the land it passes through, there is a high amount of salt and sulfate in the Kızılırmak River water. The Kızılırmak River water is unsuitable for use as drinking and irrigation water or for industrial use, with the exception of the upstream section, which does not have a gypsum area. In addition, arsenic found in the territory of the region where the river passes through is also carried into the river, negatively affecting the water quality. In addition to Kızılırmak, the water sources of Seyfe and Göydün in the Sivas region and Lakes Hafik, Tödürge and Lota are also exposed to salt and sulfate pollution by natural means (Anonymous 2017).

The Kızılırmak River is in the 1st or 2nd class in terms of COD, which is one of the organic parameters. The waters along the main river are in the 2nd and 4th class for nitrogen parameters (NH₄-N), 3rd and 4th classes in terms of NO₂-N, and 1st and 2nd classes in terms of NO₃-N. The river waters are between 2nd and 4th classes in terms of total phosphorus parameter. In terms of sodium, chloride, nitrite and sulfate, which are salinity factors, it ranks 3rd 4th class and is in the 2nd or 3rd class in terms of total dissolved matter (Anonymous 2015).

3.16. Konya closed basin

The Konya Closed Basin is the fifth largest basin with an area of 49 930 km². The annual precipitation average in Konya Closed Basin is recorded as 454 mm. The estimated total surface flow of Konya Closed Basin is 4.9×10^9 m³ per year, including surface and groundwater bodies. A very large part of this water (4.7×10^9 m³) is used in the basin. Of the used part, 4.43×10^9 m³ is used for irrigation, 0.2×10^9 m³ for residential use and 0.07×10^9 m³ for industry (Anonymous 2018j). As can be seen, the amount of irrigation water used in the basin corresponds to 94% of the total usable water. The population of the Konya Closed Basin is about 2.6 million people.

Located in the southwest of the Konya Closed Basin, in the province of Konya, the Çarşamba Stream is one of the most important streams in the basin. The Çarşamba Stream joins the Beyşehir Canal near Pınarcık village on the east side and flows into Lake Beyşehir. The Melendiz Stream, originating from the Melendiz Mountains in Aksaray, is another important stream of the Konya Closed Basin. After merging with the Belisırma and Ilısu streams, it pours into Lake Salt. The Mamasın Dam Lake, which is the most important water source of Aksaray and meets the drinking water and irrigation water needs of the province, was built on the Melendiz Stream (Anonymous 2018j).

Lakes in the Konya Closed Basin include Lake Salt, Lake Beyşehir, Lake Hotamış, Lake Uyuz, Lake Tersakan, Lake Kozanlı, Lake Samsam, Lake Meke, Lake Akgöl, Lake Bolluk and Lake Düden (Anonymous 2017).

Lake Salt, which is the second largest lake in Turkey, is 940 m above sea level, 80-100 km long, 20-25 km wide, and covers an area of 193 946 ha. The waters that feed the lake are streams whose waters decrease or completely dry up in the summer months. Lake Salt, which is a class A wetland according to international criteria, is fed by the Peçeneksu Stream passing through Şereflikoçhisar in the east, the Bağlıca and Kırkdelik streams entering the lake from Eskişehir in the south, the Tersakan Stream in the southwest and the İnsuyu Stream coming from Cihanbeyli in the west. The growing population in Konya and its vicinity, industrial facilities established without wider considerations of the environmental impact, direct discharge of sewage wastes into Lake Salt and pollution from agricultural lands are the main factors threatening the future of the lake (Anonymous 2017).

Lake Beyşehir is the third largest lake in Turkey. It is the largest natural lake in terms of fresh water reserve and is 69 086 hectares wide. In addition, it is a tectonic depression lake and was formed in the northern part of the Beyşehir, Seydişehir and Bozkır depression basin. The lake, which was formed between two fault breaks of the Taurus Mountains, is located in the depression area of the earth's crust in the third geological time. Its average altitude above sea level is around 1 124 m. This height rises to a maximum of 1 126 m in a periodic time frame, and decreases to a minimum of 1 121 m, resulting in a level difference of 5 m in the lake. The 88 750 ha area in and around Beyşehir Lake has been taken under protection as a National Park with the decision of the Council of Ministers dated 11/01/1993. It was also approved as a wetland protection zone in 2007 and entered into force. The water level of the lake has been gradually decreasing due to insufficient rainfall and excessive water withdrawal from the lake. As a freshwater lake, Lake Beyşehir is used as a source of drinking and irrigation water. Agricultural water is drawn from the lake through the Çarşamba Canal, which was built to irrigate the Konya Plain, and other irrigation canals and wells. The drinking water needs of 19.6% of the basin's population are met by the lake (Anonymous 2017). Şener and Taştekin, in their 2019 study, stated that the electrical conductivity (EC) values of Lake Beyşehir varied between 0.388-0.868 dS/m, and the SAR values calculated using the results of the analysis of the waters in the study area were generally between 0.04-0.29 and % Na values between 1.14-9.09.

While Lake Hotamış was a 13 615 ha wide and dense reed-covered lake located between Karapınar and Çumra counties in Konya Province, it started to dry up in the early 2000s when the water channels coming to the lake were directed to Lake Salt. Today, the lake has completely dried up and the lake area has been opened to agriculture. During the rainy seasons, only a small area between Adakale and Sürgüç villages accumulates water, and this place dries up during the summer months (Anonymous 2017).

Lake Meke is another lake that has since dried up. Lake Acı, on the other hand, is a lake with a significant decrease in water level, although it is a very deep lake. The lake waters contain high levels of magnesium and sulfate and the salinity is considered to be very high. No fish inhabit the lake water, but the lake is a wetland for birds.

The Peçenek Stream one of the streams feeding the Konya Closed Basin and Lake Salt subbasin, carries domestic pollution originating from the district of Şereflikoçhisar. The Peçenek dam lake waters are in the 2nd Class in terms of NH₄-N and NO₃-N. According to group A parameters (physical and inorganic pollutants), the lake waters are in the 4th class in terms of NO₂-N, in

the 3rd class in terms of group B parameters (organic) and in the 2nd class in terms of group C parameters (inorganic pollution). The Pınarbaşıözü (İnsuyu) Stream waters passing through the Cihanbeyli district are in the 3rd class in terms of NH₄-N and in the 2nd class in terms of NO₃-N. Stream waters are in the 4th class in terms of A parameters (NO₂-N), 4th class in terms of B parameters (COD-BOD), and 4th class in terms of C parameters (Boron class determining parameter) (Anonymous 2015).

3.17. Eastern mediterranean basin

The Eastern Mediterranean Basin covers the area between the Antalya, Seyhan and Closed Konya Basins in the south of Turkey, which disembogues its waters into the Mediterranean along with the Göksu River and some other streams. The Eastern Mediterranean Basin consists of the area between the Sedir Stream in the east of Alanya and the Tarsus River in the East (Anonymous 2017).

The Eastern Mediterranean Basin has an area of 21 150 km². The annual average flow in the Eastern Mediterranean Basin is 9.46x10⁹ m³ (13.34 L/s/km²) and covers 5.15% of Turkey's surface runoff potential. The usable part of this water is estimated to be 4.73x10⁹ m³/year. The groundwater operating reserve of the Eastern Mediterranean Basin is 70.5x10⁶ m³/year, and the groundwater potential is 96.5x10⁶ m³/year. Considering the 9.46x10⁹ m³/year surface and 96.5x10⁶ m³/year groundwater potential in the basin, the total water potential is 9.56x10⁹ m³/year. The usable water potential of the basin is 4.8x10⁹ m³/year considering the 4.73x10⁹ m³/year usable surface water and 70.5x10⁶ m³/year groundwater operating reserves (Anonymous 2015). The population of the basin is recorded as around 1.5 million people (Anonymous 2016a).

The Göksu River is the main stream of the Eastern Mediterranean Basin. The Eastern Mediterranean Basin includes the sub-basins that discharge their waters into the Mediterranean via the Göksu River and its tributaries, the Berdan Stream, Anamur Stream, Limonlu Stream, Efenk Stream, Alata Stream, Çubuk Stream, Kirmir Stream, Ova Stream and Seydi Stream (Anonymous 2016a). Kılıç conducted a study in 2020 to determine the water quality of the Göksu River and to examine the flow change over the years. In the study, some seasonal measurements made by the State Hydraulic Works in the downstream of the Göksu River between 1992 and 2017 were evaluated. The study evaluated the temperature (°C), nitrite (NO₂⁻), nitrate (NO₃⁻), ammonium (NH₄⁺), biological oxygen demand (BOD), chemical oxygen demand (COD), dissolved oxygen (DO), pH, sulfate (SO₄⁻²), sodium (Na⁺), total dissolved solids (TDS) parameters. When the annual average concentration values of the parameters were compared with the Water Pollution Control Regulation, the water quality was deemed to be 1st class in terms of pH, DO, COD, SO₄⁻², Na⁺, TDS, NO₃ parameters. It has been determined that the waters vary between 1st class and 2nd class in terms of BOD parameter and between 1st class and 4th class in terms of NO₂, NH₄ parameters. Kilic found that there are changes in water quality depending on the seasons, and that there is a significant decrease in water quality as a result of increased evaporation in summer (Kılıç 2020).

The natural lakes in the Eastern Mediterranean Basin are Lakes Akgöl and Eğrigöl (Anonymous 2017).

Lake Akgöl covers an area of 1 200 hectares. Since Lake Akgöl is fed by the water coming from the drainage channels in the delta, the salt rate is around 1 g/l. The water level in Lake Akgöl is at its highest level and quite stable during the peak irrigation period (June-October). During the winter, the water level changes by 0.4 m depending on the precipitation (Anonymous 2013).

The Eastern Mediterranean Basin waters are in the first class, that is, clean water category, in terms of COD and BOD, which are important parameters indicating quality class organic pollution. When the nitrogen parameters are evaluated, the quality class is 1st or 2nd in terms of NH₄-N parameter, and 1st 2nd or 3rd class in terms of NO₂-N. In terms of NO₃-N, it was determined that the waters were 1st class throughout the basin. When the basin is evaluated in terms of water quality in general, it can be said that the water quality is at the 2nd class level, in other words, it has the characteristic of less polluted water quality (Anonymous 2015).

3.18. Seyhan basin

The Seyhan Basin area is 22 035 km² with a population of around 2 million people (Anonymous 2016b).

When the precipitation data of the meteorological stations in the Seyhan Basin are examined, winter and spring months are rainy, summer months and the beginning of autumn are dry months. The driest month is August (7.8 mm), while the wettest month is December (77.4 mm). Considering the average of the annual total precipitation of the stations, the highest precipitation was seen at the Karaisali station with an average of 860.3 mm, while the lowest precipitation was seen at the Ulukışla station with 317.1 mm. The long-term annual total precipitation average of the stations in the basin is 531.4 mm (Anonymous 2019g).

The annual average flow for the Seyhan Basin is 6.66x10⁹ m³ (10.18 L/s/km²), corresponding to 3.62% of Turkey's surface water potential. The usable part of this water is estimated to be around 3.3x10⁹ m³/year. The total groundwater potential in the Seyhan Basin is around 300x10⁶ m³/year, and the associated operating reserve is 200x10⁶ m³/year. Considering the 6.66x10⁹ m³/year surface and 300x10⁶ m³/year groundwater potential in the basin, the total water potential is 6.96x10⁹ m³/year. The usable

water potential of the basin is found as 3.5×10^9 m³/year considering the 3.3×10^9 m³/year usable surface water and 200×10^6 m³/year groundwater operating reserves (Anonymous 2015).

The longest of the two important tributaries of the Seyhan River is the Zamantı River, which originates from the Long Plateau at an altitude of 1 500 m in the Kayseri-Pınarbaşı district and passes through the Pınarbaşı, Tomarza, Develi and Yahyalı districts of Kayseri. Before descending to Çukurova, the Zamantı branch passes through Adana, merging with another important branch, Göksu, on the slopes of Mount Akinek of the Aladağ district, 80 km north of Adana, and disembogues into the Mediterranean Sea from the Deli Burnu point on the Adana-Mersin border, at the westernmost part of Çukurova. The length of the main tributary of the Seyhan River with its tributaries is 560 km, and the length from the junction point of the Zamantı and Göksu tributaries to the Mediterranean Sea is 137 km (Anonymous 2016b).

The Seyhan Basin is not rich in natural lakes, but is richer in terms of its dam lakes. The only natural lakes in the basin are Lakes Akyatan and Tuzla.

Lake Akyatan is Turkey's largest lagoon lake. Demir and Selek, in their study in 2009, defined the electrical conductivity value of the Akyatan Lagoon as 0.65-105.7 dS/m, and defined the lagoon as extremely salty because it has values of 1.5-2 times higher than sea water (Demir & Selek 2009). The main reason why the salinity is so variable in the lagoon is because the lagoon is fed by both waters returning from irrigation and by the waters originating from the sea. Salinity is lower in the regions where the drainage channels are discharged into the lagoon, and quite high in parts in close proximity to the sea.

Lake Tuzla, with its 808 ha area, forms a part of the Çukurova Delta wetlands system (Gençoğlu 2019). Tuzla Lagoon has a channel connected to the sea and the water quality of the lagoon is characterized as slightly salty throughout the year. The water quality improves due to winter precipitation but salinity of water increases due to excessive evaporation in summer. The lagoon is also used for irrigation purposes from time to time, from the regions of the lagoon where the water quality is good.

When the Seyhan Basin was evaluated in terms of surface water quality, it was determined that it was of 3rd class water quality in the Zamantı sub-basin, 3rd class water quality in the Göksu sub-basin, and 4th class water quality in the Seyhan sub-basin. In terms of groundwater quality, the Seyhan Basin was found unsuitable for domestic use in accordance with the relevant regulation.

3.19. Orontes basin

The precipitation area of the Orontes Basin is 7 886 km² and the basin has a population of just over 3 million inhabitants (Anonymous 2019h).

The annual average rainfall of the basin is 816 mm, the annual total flow is 1.17 km³/year, and the average basin yield is 2.60 L/s/km². Of the annual 2.8×10^9 m³ water potential of the basin, 300×10^6 m³ originates in Lebanon, 1.2×10^9 m³ originates in Syria, while 1.3×10^9 m³ originates in Turkey. The important tributaries of the Orontes River are the Karasu Stream, which comes from the Kahramanmaraş direction and is used as a flood protection channel, the Afrin Stream coming from the Gaziantep direction, and the Little Orontes, which is the part after the junction of the Karasu and Afrin Streams. In addition, in the downstream, Defne Stream, Big Karaçay and some other streams flow into the Orontes River (Anonymous 2015).

The Orontes River, the most important river of the Orontes Basin, was formed by the merging of the rivers originating in the Bekaa Valley between the Lebanon Mountains and the Anti-Lebanon Mountains. The total length of the Orontes River is 386 km, and most of the river is situated in Syrian territory. Its length in the territory of Turkey is 88 km. Many floods occur in the winter and spring seasons. The Orontes River forms wide valleys in the form of plains and bowls along its bed, and sometimes narrow and deep gorges. A large delta was formed where the river disembogues into the sea. The Orontes River is the only river whose source is not in Turkey but where it spills out. The flow of the river, which has a precipitation area of 1 800 km² in Turkey, is very irregular. This current overflows in winter and spring, crossing the river bed and causing damage to its surroundings. The annual average flow of the river, which is 8 m³/s, approaches 20-40 m³/s in winter and spring, and may even rise to 100 m³/s from time to time. The Orontes River is also important in that its most important tributaries including the Karasu Stream, Afrin Stream, Little Orontes and Karadere Stream are located in Turkish territory. Since the river disembogues into the sea by crossing three different countries, it is necessary to determine the annual average water volume, but there are very different measurements of the average water volume. In some sources published in Turkey, the annual water volume of the Orontes River is given as 1.2×10^9 m³ (Anonymous 2019h). The quality of the Orontes River water has been determined as C₃S₁ (Ağca & Doğan 2020).

The only natural lake in the basin is Gölbaşı (Fish). Lake Fish, which does not have a natural wetland protection status, is actually the remnant of the dried up Lake Amik. The lake serves as an important stop for migratory birds, especially during the migration season, and has a rich aquatic life. The area of the lake is 55 ha. Gölbaşı Lake, below the Kurt Mountains, in the northeast of the Amik Plain, is 11 km from Kırıkhan. It is fed by spring waters arising from the base of the Kurt Mountains. The lake is very similar to Lake Amik in terms of its flora and fauna features and richness (Anonymous 2017).

The Orontes Basin is in the 1st or 2nd class in terms of COD and BOD, which are important parameters that show organic pollution, that is, clean and less polluted water. However, in the Orontes River, Afrin Stream and Muratpaşa Stream, the BOD parameter is in the 3rd class, that is, the polluted water level. Among the important nitrogen parameters, NH₄-N is at the 4th class, that is, very polluted water, in the Orontes River, Afrin Stream, Belen Stream, Beyazçay (Bohşin Stream) and Muratpaşa Stream, and at the 3rd class, that is, polluted water level, in the Karasu Stream, Büyük Karaçay Stream and Tahtaköprü Dam Lake. Throughout the basin, the NO₂-N parameter was determined as 4th class and NO₃-N as 1st class. When the water quality is evaluated in general, the water quality in the stations in the basin is at the 4th class level, in other words, it has the characteristics of highly polluted water quality (Anonymous 2015).

3.20. Ceyhan basin

The Ceyhan Basin area is 21 391 km² with approximately 2 million people living in this area (Anonymous 2010b).

The average annual total precipitation in the Ceyhan Basin is 727.3 mm (Anonymous 2019i) while the annual average flow value of the is 6.5x10⁹ m³ (9.72 L/s/km²), corresponding to 3.54% of Turkey's surface water potential. The usable part of this flow is 3.25x10⁹ m³/year. The groundwater operating reserve of the Ceyhan Basin is 559x10⁶ m³/year and the groundwater potential is 745x10⁶ m³/year. Considering the 6.5x10⁹ m³/year surface and 745x10⁶ m³/year groundwater potential in the basin, the total water potential becomes 7.25x10⁹ m³/year. The usable water potential of the basin has been determined as 3.81x10⁹ m³/year considering the 3.25x10⁹ m³/year usable surface water and 559x10⁶ m³/year groundwater operating reserves (Anonymous 2015). 38% of the total water potential of the Ceyhan Basin is used for irrigation, and 62% is used for non-irrigation (drinking, using, industry, etc.) activities (Anonymous 2010b).

The important streams in the Ceyhan Basin include the Ceyhan River, Aksu Stream, Göksun Stream, Söğütlü Stream, Hurman Stream, Körsulu Stream, Savrun Stream, Deli Stream, Karanlık Stream, Ördeközü Stream and Bertiz Stream (Anonymous 2010b).

Streams and dams in the Ceyhan Basin are generally classified as 1st class in terms of COD parameter indicating organic matter pollution. The water quality of the Ceyhan River, which is the main stream of the basin, and the large streams feeding it and the dams on it, is generally classified as high quality water or less polluted water in terms of organic substances, nitrate nitrogen and inorganic parameters. However, in terms of ammonium nitrogen, the Ceyhan River water is in the polluted water class after Kahramanmaraş. Dissolved matter, chloride, sulfate and sodium values are high in terms of surface water pollution (Anonymous 2015).

When the Ceyhan Basin is evaluated in terms of water quality in general; As a result of the discharge of industrial wastewater into streams in Kahramanmaraş, the water quality in the region is reduced to the 4th class. It is known that the water quality is better around Adana due to the added clean water. While the Ceyhan River is in the 4th class in terms of pollution in Kahramanmaraş, the water quality in Adana improves and rises to the 2nd class (Anonymous 2016c).

3.21. Euphrates and Tigris basin

In the "International River Basins" list published by the UN, the water catchment basin of the Euphrates and Tigris (Turkey, Syria, Iraq, Iran, Saudi Arabia) is given as 895 628 km². The population of the Euphrates-Tigris Basin, which is the second most populated basin in terms of population, is approximately 7.7 million people. The Euphrates and Tigris Basin is largely fed by snow falling on the mountainous areas of northern and eastern Turkey, Iran and Iraq. The basin has the largest drainage area of Western Asia and Turkey. The Euphrates, the longest of the rivers in Western Asia, flows in this basin (Yıldırım 2006).

The total precipitation area of the Euphrates-Tigris Basin is 182 614 km² (Al-Ansari et al. 2019) and the annual average flow rate of the basin is 52.94 km³ (8.29 L/s/km² in the Euphrates part and 14.44 L/s/km² in the Tigris part). The annual average precipitation level is 540 mm for the Euphrates section and 807 mm for the Tigris section, while the annual average flow rate is 1002 m³/s in the Euphrates section and 744 m³/s in the Tigris section (Anonymous 2015).

The Euphrates Basin consists of basins and low hills. The basin extending to the Persian Gulf has the appearance of a high plateau (Atuk 2005). The distribution of the Euphrates River basin area and long-term average water potential by countries is summarized below. In Table 3, catchment areas (Al-Ansari et al. 2019) and flow amounts (Onüçyıldız et al. 2016) are given on a country basis.

Table 3- The area and flow rate of the Euphrates Basin

Country	Catchment area (km ²)	Catchment area (%)	Annual km ³ /year	Flow	Flow Rate %
Turkey	125000	28.1	33.1		98.5
Syria	76000	17.1	0.5		1.5
Iraq	177000	39.9	0		0
Saudi Arabia	66000	14.9	0		0
Total	444000	100	33.6		100

Considering the water potential of the Euphrates in Turkey, it is at a level that can easily meet the water needs of the region. With the waters of the Euphrates, 1.6 million hectares of agricultural land in Turkey and 800 thousand hectares in Syria can be irrigated. If Turkey and Syria irrigate in this level, it is estimated that there will not be much irrigation water left for Iraq. For this reason, it will be necessary to meet the irrigation water needs of the agricultural lands on the Euphrates river route, with the waters to be transferred from the Tigris River, which has a lot of water in Iraq (Özdemir et al. 2002).

The distribution of the Tigris River basin area and long-term average water potential by countries is summarized below. In Table 4, catchment areas (Al-Ansari et al. 2019) and flow amounts (Onüçyıldız et al. 2016) are given on a country basis.

Table 4- The area and flow rate of the Tigris Basin

Country	Catchment area (km ²)	Catchment area (%)	Annual km ³ /year	Flow	Flow Rate %
Turkey	57 614	12.2	27.2		53.4
Syria	834	0.2	0		0
Iraq	253 000	58	3		5.9
Iran	140 180	29.6	20.7		40.7
Total	451 628	100	50.9		100

Considering the water potential of the Tigris, it is predicted that 650 thousand hectares of agricultural land in Turkey and 3.5 million hectares in Iraq (partly along the Euphrates) could be irrigated beyond the water needs of the settlements and industry in the region.

Turkey has initiated the Southeastern Anatolia Project (GAP), a multi-sectoral regional development project located in the Southeastern Anatolia Region around the Euphrates and Tigris rivers. The project area covers 45% of the Euphrates-Tigris Basins within the borders of Turkey (Onüçyıldız et al. 2016).

The Murat River, which is the most important first-degree tributary of the Euphrates, arises from the skirts of Mount Ararat and flows approximately 500 km to the southwest, and joins the Karasu River coming from the north (Erzurum) 10 km north of the Keban Dam. The river, named the Euphrates River after this confluence point, reaches a length of approximately 3 000 km, 1 230 km in Turkey, 710 km in Syria, 1 060 km in Iraq, from this point until it merges with the Tigris River (Kaya 2007).

Lakes in the Euphrates-Tigris Basin include Lake Hazar, Lake Akdoğan, Lake Haçlı, Lake Ekşisu and Lake Gaz.

Lake Hazar is situated 22 km away from Elazığ, on the Elazığ-Diyarbakır highway route, and is a tectonic lake between the Hazar Baba and Mastar Mountains. It has a length of 22 km and width of 5-6 km. The lake basin constitutes 8 166 ha with a water surface of 78.8 km². It was registered as a wetland of national importance in 2015.

The COD of Euphrates-Tigris Basin is predominantly at the level of 1st class (clean water) or 2nd class (less polluted water). In terms of this parameter, the Nizip Stream, Samözü Stream, Şehir Stream, Eğriçay Stream, Haringet Stream and Lülük Stream are 4th class, while Sacır Stream, Akdere Stream and Sitalce Stream are 3rd class quality. NH₄-N, one of the important nitrogen parameters, is largely in the 1st and 2nd class quality throughout the basin. In the Euphrates River basin, the Haringet Stream, Lülük Stream, Karakoyun Stream, Habur Stream, Çatak Stream, Nizip Stream, Sacır Stream, Sitalce Stream, Şehir Stream, Eğriçay Stream, Samözü Stream and Hancağız Dam water were evaluated as 4th class. When the Tigris River basin is examined in terms of NH₄-N, at some points in the Tigris River, it is classed 3 to 4. While Kulp Stream, Batman Stream, Çavuşbayırı Station of Garzan Stream and before the Tigris River joint in Devegeçidi Stream and Beyhan Stream in 3rd class quality, and it is 4th class in Sarge Stream after Ergani (Anonymous 2015).

3.22. Eastern black sea basin

The area of the Eastern Black Sea Basin is 22 846 km² with an average precipitation value of just over 1 000 mm (Anonymous 2016d). Its population is recorded as more than 2 million.

The annual average flow amount of the Eastern Black Sea Basin is $17.85 \times 10^9 \text{ m}^3$ (23.57 L/s/km^2) and covers 9.72% of Turkey's surface water potential. The usable part of this water is $8.9 \times 10^9 \text{ m}^3/\text{year}$. The groundwater potential of the Eastern Black Sea Basin is $0.44 \times 10^9 \text{ m}^3/\text{year}$ and all of them constitute the operational reserve. Considering the $17.85 \times 10^9 \text{ m}^3/\text{year}$ surface and $0.44 \times 10^9 \text{ m}^3/\text{year}$ groundwater potential in the basin, the total water potential becomes $18.29 \times 10^9 \text{ m}^3/\text{year}$. The usable water potential of the basin has been determined as $9.34 \times 10^9 \text{ m}^3/\text{year}$ considering the $8.9 \times 10^9 \text{ m}^3/\text{year}$ usable surface water and $0.44 \times 10^9 \text{ m}^3/\text{year}$ groundwater operating reserves (Anonymous 2015).

Almost all the rivers of the Eastern Black Sea Basin obtain their sources from the peaks of the mountains that run parallel to the coast. Streams descending rapidly from the slopes are short rivers and overflow frequently after heavy rains; the most important stream being the 160 km long Harşit Stream. Other water sources include the Gelevera, Yağlıdere, Aksu, Batlama, Pazar, Turnasuyu, Melet, Civil, Akçaova, Bolaman, Elekçi, Cevizdere, Lahna, Curi and Akçay rivers. Since these waters overflow from their beds following heavy precipitation, they show an irregular flood regime (Anonymous 2016d).

The physical structure of the basin, especially the topography, prevents the formation of a large lake. There are small crater lakes of touristic importance in the İkizdere and Çamlıhemşin districts of the Kaçkars in Rize. In Trabzon, are are found Lakes Uzungöl and Sera.

COD, which is one of the important parameters showing organic pollution in the Eastern Black Sea Basin, is in the 1st class (clean water) in all water quality monitoring stations. In the evaluation made in terms of BOD, the majority of the water is in the 1st class and less in the 2nd class (less polluted water). In terms of $\text{NH}_4\text{-N}$ and $\text{NO}_3\text{-N}$, which are important nitrogen parameters, most of the waters are in the 1st class. When the basin is evaluated in terms of water quality in general, many streams can be considered as clean or less polluted in terms of organic substances, ammonium, nitrate and microbiology (Anonymous 2015).

3.23. Chorokhi basin

The area of the Chorokhi Basin amounts to 20 248 km^2 with an average annual precipitation of approximately 560 mm. The annual average of the basin water potential is 6.5 billion m^3 (Anonymous 2020) while the annual average flow of the Chorokhi Basin is 201.81 m^3/s (9.97 L/s/km^2). The contribution of the Chorokhi Basin to the total water potential of Turkey is approximately 3.47% (Anonymous 2015). The population of the basin is around 300 thousand people (Fakioğlu ve Kağncıoğlu 2009).

The Chorokhi River is one of the largest rivers in the Northeast Anatolia. The three largest tributaries joining the Chorokhi River include Oltu Stream, Berta Stream and Barhal Stream, respectively. Of these, the Oltu Stream, which originates in Erzurum province, has a precipitation area of approximately 4 900 km^2 and 25% of the Chorokhi Basin. The Chorokhi River is fed from many tributaries in Erzurum and Artvin, especially after it enters Erzurum province; the most important of these are the Aralık Stream, Deviskel Stream, Murgul Stream, Hatila Stream, Çamlıkaya Stream, Aksu Stream, Cala Stream, Karataş (Engücek) Stream, Çapan Stream, Anuri Stream, Sırakonaklar Stream and Cihala Stream (Fakioğlu & Kağncıoğlu 2009).

The Deriner Dam, which was started to be built in 1998 in order to generate energy on the Chorokhi River, is the second highest dam in Turkey in terms of body height and the 13th tallest dam in the world. At the average water level of the dam, which is a concrete arch body fill type, the lake volume is recorded as $1.97 \times 10^9 \text{ m}^3$, and the lake area as 26.4 km^2 .

The Yusufeli Dam, which is located in the basin, started to be built in 2013 and water was started to be retained in 2022, is in the 1st place in Turkey and 3rd in the world in terms of body height. The body height of Yusufeli dam is 275 m and the lake volume will be $2.2 \times 10^9 \text{ m}^3$ at normal water level. When Yusufeli Dam is full, it will be one of the most important water resources of the basin.

The lakes in the Chorokhi Basin include Lakes Tortum and Karagöl. Lake Tortum, located within the borders of Erzurum Province, covers an area of 615 ha. The lake has a maximum water level elevation of 1014 m, and a minimum water level elevation of 1 005 m. Lake Tortum is a risk of drying up due to the sediment problem. In their 2018 study, Fakioğlu and Nuhoğlu determined that Lake Tortum is in the 2nd class according to the dissolved oxygen value and in the hard water class according to the total hardness, Ca hardness and Mg hardness values (Fakioğlu & Nuhoğlu 2018).

Karagöl-Sahara National Park, located within the boundaries of the district of Şavşat, consists of two separate parts. The Sahara is located 25 km north of the town of Şavşat. Lake Karagöl is a landslide lake formed by water accumulating in the basin behind the rationally sliding mass (Anonymous 2020). Şener & Kibar in their study in 2017; by examining the geological and hydrogeological features of Karagöl Lake and its surroundings, they evaluated the hydrogeochemical properties, use cases and pollution of the water resources in the region. At the end of the study; they determined that all of the waters in the study area are in the 1st class in terms of water quality, are in the C1S1 class according to SAR and EC values, and are suitable for use as drinking and irrigation water. When the Chorokhi Basin is evaluated in general, it is less polluted in terms of water quality (Anonymous 2015).

3.24. Aras basin

The area of the Aras Basin, which has a population of around 800 thousand, is 27 775 km². The Aras Basin has a semi-arid and arid climate type. Iğdır, one of the provinces with the least rainfall in Turkey, is located in this basin. The average annual precipitation in Ardahan is recorded as 550.8 mm, in Kars 486.9 mm, in Iğdır 258.8 mm, and in Erzurum 405.3 mm. The level of snowfall is one of the factors affecting the occurrence of floods. Heavy snowfall occurs in the upper basins. The highest recorded snowfall is 110 cm in Ardahan, 88 cm in Kars, 38 cm in Iğdır and 110 cm in Erzurum (Anonymous 2019j).

The annual average flow of the Aras Basin is 4.63x10⁹ m³. In terms of runoff levels, the share of Aras Basin water potential in Turkey's wider water potential is 2.5% (Anonymous 2015).

The Aras River is the main stream of the Aras Basin. Originating from the northwestern piedmonts of the Bingöl Mountains, the Aras River flows to the north and enters the Erzurum-Pasinler Plain, and after receives the Zivin Stream from the north and the Velibaba Stream from the south. In Kağızman, it passes through deep valleys between the mountains and flows in the plain formed at the bottom of the 10 km wide valley. After leaving this narrow valley, known as Buğum Boğazı, The Aras River takes the Arpaçay Stream coming from the north in Aşağı Çıyıklı. After crossing the Iğdır Plain, it leaves from Turkey to Nakhchivan. The total length of the river is 920 km, and its length within the borders of Turkey is 411 km. The average flow rate at the junction of the Aras River with the Arpaçay branch is 56.7 m³/s.

The most important water resources of the Aras Basin can be listed as the Aras River, Kura River, Kars Stream, Arpaçay Stream, Lake Balık, Lake Çıldır, Lake Aktaş and the Arpaçay Dam Lake. The largest lake in the Aras Basin is Lake Çıldır in Ardahan. There are many HEPPs in operation and under construction in the basin. In addition, there are four ponds built by SHW (Anonymous 2015).

Lake Çıldır is located at an altitude of 1 959 m above sea level and amounts to a surface area of 126 km² (Anonymous 2015). In their study, conducted between 1991-93, Yerli et al. (1996) recorded the EC value of the lake as ranging between 60-155 µS/cm.

Lake Aktaş, shared by Turkey and Georgia, is a tectonic lake located in the Aras Basin. The water of the lake, which has a surface area of 27 km², is soda (Yerli & Zengin 2019) BOD and nitrogen measurements are made at some stations in the Aras Basin, and the waters are classified as 1st and 2nd in this respect. When the basin is evaluated in general, it shows less polluted or clean water characteristics in terms of water quality (Anonymous 2015).

3.25. Van lake basin

The Van Lake Basin has an area of 17 861 km² and is home to 730 000 people. The annual average rainfall of the basin is 474 mm with an annual water potential of approximately 3.5x10⁹ m³ (annual average flow is 95.32 m³/s) (Anonymous 2019k).

The groundwater potential of the Van Lake Basin is 180x10⁶ m³/year, and the groundwater operating reserve is 148x10⁶ m³/year. Considering the 3x10⁹ m³/year surface and 180x10⁶ m³/year groundwater potential in the basin, the total water potential is 3.18x10⁹ m³/year (Anonymous 2015).

Most of the rivers in the basin flow into Lake Van. The rivers, which are considered relatively large in terms of the water they carry and the distance they cover, are located in the east of Lake Van. The main streams in the Van Lake Basin include the Zilan and Deliçay Streams in the north, the Bendimahi Stream in the northeast, the Karasu Stream in the east, Engil Stream in the southeast, the Gevaş Stream in the south, the Kotum Stream in the southwest and the Sufesor-Ahlat creeks in the west. The Özalp and Büyükçaylak Streams, which flow from east to west, are located within the closed basin Lake of Erçek.

Natural lakes in the basin include Lakes Van, Nemrut, Erçek, Nazik, Turna and Gövelek (Ermenis).

Lake Van is Turkey's largest lake with an area of 357 269 ha. It is ranked 15th among the largest closed lakes in the world and is the largest soda lake on earth. The waters of Lake Van are brackish and salty. The salt concentration of water is 0.224%. Chemical composition of the salts in water is 42% NaCl, 34% NaCO₃, 16% Na₂SO₄, 3% KSO₄ and 2.5% MgCO₃. As a result of this feature, the lake has a large reserve as a soda production source. The water level of the Lake Van fluctuates by 50-60 cm between the summer and winter months. However, in recent years, these fluctuations have reached several meters (Anonymous 2017).

Nemrut is a crater lake located on the lands belonging to Tatvan, Ahlat and Güroymak districts to the west of Lake Van, spread over an area of 1 266 ha. The average depth of the half-moon shaped Lake Nemrut is around 100 m. The water of the lake is colorless, odorless and tastes like drinking water (Anonymous 2017).

Lake Erçek is located 30 km east of Lake Van, in a collapse of basin. The water of the lake, which has an area of 9904 ha, is salty and soda (Anonymous 2017).

Lake Nazik is a freshwater lake with an area of 46 km² located on The Van Lake Basin. (Bozaoğlu & Akkuş 2019). The lake waters are used for the irrigation of Adabağ and Sarıkum villages lands (Anonymous 2017).

Lake Van is highly polluted in terms of pH, salinity and total phosphorus parameters, and in the polluted water class in terms of organic matter and ammonium nitrogen. In particular, the fact that the total phosphorus parameter is at the level of dirty or highly polluted water in many stations indicates diffuse phosphorus pollution caused by fertilizers. In the streams flowing into Lake Van, the BOD parameter value varies between 3rd class and the NH₄-N parameter value varies between 2nd and 3rd class. In many water sources flowing into Lake Van, the NO₂-N parameter is at the 4th class level (Anonymous 2017).

4. Conclusions and Recommendations

Although there are still thoughts that reject global warming today; the claim that the consumption of fossil fuels would cause global warming existed even 100 years ago. However, the measures taken on this issue were so delayed that although global warming was known, it took more than 45 years to reveal its causes. Average global temperatures today are estimated to have risen by about 1.1 °C in 2021 compared to pre-industrialization. It is stated that as the temperature rises above 1.5 °C, climate-related disasters will become increasingly more common (Anonymous 2022b). With the effect of global warming, significant climate changes have already been seen in many parts of the world. The most important effect of climate change is the decrease in water resources and the change of habitats of many species. For many creatures living in extreme conditions, these effects have reached critical points. It has become almost impossible for polar bears, especially those living in the Arctic, to sustain their generation. If the polar bears that reach the continents cannot adapt to a terrestrial life, it seems unlikely that they can continue their generation. Moreover, the fact that sea creatures living in the equatorial region have started to be seen in more northern and more southerly seas due to the warming of the seas reveals the importance of climate change.

The effects of climate change are particularly apparent in the decrease in water resources on a global scale, the threat of desertification over large areas, the shrinking of forest areas, the decrease in stream flows, the decrease in water levels in lakes and the drying up of some lakes.

The effects of climate change are also seen in Turkey to a great extent and manifests itself in the form of the deterioration in the distribution of precipitation levels throughout the year. Instead of raining at a constant rate over a regular period of time, rapid precipitation in intense form causes a decrease in the amount of water held by the soil and an increase in the amount of surface runoff. This leads to a significant deterioration in the balance between retained water and flowing water.

The total annual average flow of the basins in Turkey is 185.37 billion m³. Since the annual precipitation is not the same in each of the hydrological water basins, their yields and water potentials also differ from one another. While the Euphrates-Tigris Basin has the highest water yield with 56.3 km³, the Burdur Closed Basin has the lowest water potential with 0.2 km³, while the Akarçay Basin has 0.4 km³. In addition, the Euphrates-Tigris Basin constitutes approximately 30.3% of the total country's water potential. Annual average runoff and water potential values by basins are given in Table 5 for 2019.

About half of the total annual water flow in the country is located in four of the 25 basins (Euphrates and Tigris, Eastern Black Sea, Eastern Mediterranean and Antalya). Apart from these four basins, the remaining 21 share the remaining half of the total water flow. This shows the imbalance in the distribution of waters according to the basins. On the other hand, there are also imbalances between the flow rates of the basins and the population they serve. For example, the Marmara Basin, where 28% of the total population lives, has only 4% of the total flow. Similarly, in basins such as Sakarya, Little Meander, Meander, Kızılırmak and Konya Closed Basin, significant differences exist in the proportion between the flow amounts and the population served. This further affects the water use in the basins and causes water shortages (Aküzüm et al. 2010).

Turkey is a country with a high probability of encountering serious water problems in the near future. For this reason, Turkey needs to protect its resources and use them more effectively in order to maintain sufficient quality water for future generations (Aküzüm et al. 2010).

Table 5- Annual Average Surface Water Potential by Basins, 2019 (SHW 2019)

<i>Basin No</i>	<i>Name of the Basin</i>	<i>2019</i>		
		<i>Basin Precipitation area (km²)</i>	<i>Average Annual Flow (km³)(*)</i>	<i>Potential Affiliate Rate (%)</i>
01	Meriç-Ergene Basin	14486	1.7	0.9
02	Marmara Basin	23074	7.4	4.0
03	Susurluk Basin	24319	5.0	2.7
04	North Egean Basin	9861	2.0	1.1
05	Gediz Basin	17145	1.8	1.0
06	Little Meander Basin	6963	0.6	0.3
07	Meander Basin	25960	3.0	1.6
08	Western Mediterranean Basin	20956	6.5	3.5
09	Antalya Basin	20249	12.9	7.0
10	Burdur Closed Basin	6294	0.2	0.1
11	Akarçay Basin	7995	0.4	0.2
12	Sakarya Basin	63303	6.5	3.5
13	Western Black Sea Basin	28855	10.8	5.8
14	Yeşilirmak Basin	39595	7.0	3.8
15	Kızılırmak Basin	82181	7.0	3.8
16	Konya Closed Basin	49930	2.4	1.3
17	Eastern Mediterranean Basin	21150	7.6	4.1
18	Seyhan Basin	22035	6.2	3.3
19	Orontes Basin	7886	1.8	1.0
20	Ceyhan Basin	21391	7.7	4.2
21	Euphrates and Tigris Basin	181204	56.3	30.3
22	Eastern Black Sea Basin	22846	16.4	8.9
23	Chorokhi Basin	20248	7.0	3.8
24	Aras Basin	27775	4.5	2.4
25	Van Lake Basin	17861	2.6	1.4
Total		783562	185.37	100

*: These values were obtained from the base station flows at the most downstream of the basins in the country

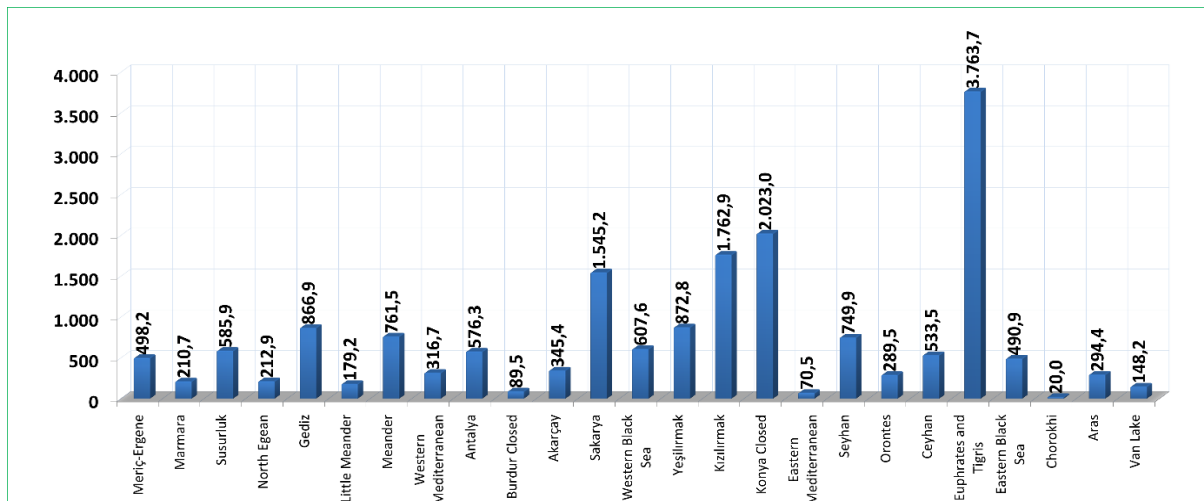
About 54 billion m³ of Turkey's annual potential of 112 billion m³ is in use. Of this 54 billion, 40 billion m³ (74%) is used in irrigation (Table 7), 7 billion m³ (13%) in domestic use and 7 billion m³ (13%) in industry (SHW 2017). These rates are respectively 70%, 22%, 8% in the world, and 33%, 51% and 16% in Europe (Anonymous 2018). The fact that the irrigation water for agricultural use is so high in Turkey makes the agricultural sector the focal point in terms of water saving. Because a 10% savings to be made in domestic use or industry corresponds to a small rate of only 1.75% in agriculture. In other words, saving that can be made by forcing people for domestic use is a goal that can be achieved very easily in agriculture. So that; It is possible to save at least 25% of water in a certain area, even by switching from the surface irrigation method to the pressurized irrigation methods. The water obtained with a 25% savings in agricultural irrigation corresponds to more water than all domestic use at the whole country level. It can be clearly observed how important water conservation is in agriculture. The water savings that can be achieved by the use of advanced technologies in agriculture are far more than the total use of the domestic and industrial sectors, and it is enough to irrigate more areas than the existing irrigated areas.

The amount of surface water used in irrigation throughout Turkey between 2000 and 2019 is given in Table 6.

Table 6- Amount of Surface Water Used in Irrigation in Turkey, 2000-2019 (SHW 2019)

<i>Year</i>	<i>Amount of Irrigation Water Used in SHW Irrigation (km³/year)</i>	<i>Estimated Amount of Irrigation Water Used in Other Irrigations (km³/year)</i>	<i>Total Amount of Surface Water Used in Irrigation (km³/year)</i>
2000	12839	14398	27237
2001	10964	12477	23441
2002	12214	14707	26921
2003	13442	14029	27471
2004	14487	16543	31030
2005	13231	17491	30722
2006	13847	15567	29414
2007	11756	13420	25176
2008	12182	14814	26996
2009	13566	16306	29872
2010	14396	16553	30949
2011	14764	18335	33099
2012	15831	18172	34003
2013	15373	19326	34699
2014	14285	12383	26668
2015	16727	14699	31426
2016	17694	15530	33224
2017	17425	14771	32197
2018	18693	14796	33490
2019	20450	14912	35363

In Turkey, there are serious imbalances between the water needed for irrigation according to the regions and the amount of water in that region. For this reason, in many regions of the country, groundwater is used as a supplement to irrigation, since the available surface waters are not sufficient for irrigation. Almost all of the existing groundwater reserves in almost every basin are drawn through wells and used for irrigation purposes. In some regions, groundwater is used for domestic and industrial purposes due to a regional lack of water. The groundwater reserve status according to the basins in Turkey is shown in Figure 3.

**Figure 3- Annual Groundwater Reserve by Basin (10⁶ m³/year, SHW 2019)**

Freshwater lakes in Turkey are mostly used intensively for irrigation purposes. However, the withdrawal of water for different purposes from many lakes, whose levels are already decreasing under the influence of global warming, jeopardizes the future of the lake. In particular, Lakes Eğirdir and Burdur are used intensively for irrigation and utility water, and face the risk of drying up in the near future. Unfortunately, regulations regarding the use of lakes in Turkey are insufficient and only one third of Turkey's lakes and wetlands have water management plans. The unauthorized use of lakes for different purposes is in question without a water management plan. For this reason, it is crucial to prepare water management plans for all water resources as soon as possible to better existing water sources.

Meeting the water needs of the growing world population is becoming more difficult not only due to the gradual decrease in water resources, but also because of the pollution of existing water resources. Even the supply of drinking water is a critical problem for many countries of the world. Today, the presence of water in countries has begun to be perceived as an indicator of the wealth of that country. However, it should not be forgotten that the most important parameter besides the presence of water is the presence of uncontaminated water. The real wealth is to have water that can be used for a specific purpose without undergoing any procedure or treatment. There is enough water in the seas and oceans for all humanity in the world for all purposes. However, seawater can be used directly in a few processes such as cooling without purification. Very high treatment costs may limit the evaluation of many waters even as water assets. Many countries have taken serious measures through legislation to protect their existing water resources not only in quantity but also against quality deterioration. The loss of a water source does not mean its disappearance, but it becoming unusable. In this respect the pollution of water resources is equivalent to the destruction of that resource.

An awareness of water quality is now growing in Turkey and monitoring of the quality of water sources is being carried out in many locations. In addition, studies for the preparation of quality maps of water resources are being conducted. All water resources are threatened by point and diffuse pollutants. Even the causes of pollution in water resources can sometimes be revealed as a result of analyses made on the waters. For this reason, periodic analyses must be made in both surface and groundwater sources and pollution must be kept under control.

Even if there is no pollutant discharge, it should not be ignored that the quality of the remaining water source will decrease slightly, even with evaporation due to extreme temperatures, so a quality difference will occur between early spring and early autumn in the same source. Since water quality is a parameter that directly affects the purpose of use, it is as important as the quantity of water today.

In the near future, water used for different purposes may be priced according to its quality, and the cost of obtaining better quality water will continue to grow. In terms of water quality, Turkey's basins show different values from each other. Generally, the effect of industrial pollutants in places where industrial activities are intense and the effects of agricultural pollutants in agricultural regions are observable in water resources.

Since there are intense industrial areas in the Meriç-Ergene Basin, the waters of the basin show industrial pollution, and many sources used in irrigation are of the 2nd and 3rd classes.

Since the Marmara Basin has the densest population of the country, the pollution caused by domestic wastes is observable in the water resources. At the same time, industrial waste is evident in the waters as the region is industry intense.

The Susurluk Basin is also a densely populated region, domestic waste load in water resources is quite high and this pollution is seen especially in the lakes in the basin. In Lake Uluabat, the lake waters are in the class of very polluted waters (4th class) due to intense domestic and industrial waste.

The waters of the North Aegean Basin are relatively high quality waters, and $\frac{3}{4}$ of the basin waters consist of waters that can be called clean. Since agriculture is intensive in the basin, $\frac{1}{3}$ of the groundwater is clean and the rest is of medium quality.

The Gediz Basin contains intensive agricultural regions, agricultural pollution is the leading cause of water pollution. Fertilizer and pesticide pollution can be found in the surface water resources and a diffuse pollution problem in the area that is difficult to control. However, groundwater is in a slightly better condition than surface waters.

Since The Little Meander Basin contains both industrial and residential areas, domestic wastes and industrial wastes are also polluting factors in the waters. Most of the basin waters consist of polluted and very polluted waters (3rd and 4th class).

The Meander Basin is a basin that hosts important industrial facilities. The waste from industrial facilities in the Denizli and Uşak provinces, in particular, adversely affect the water resources of the basin. Most of the basin waters consist of very polluted waters.

Agricultural contamination is common in surface waters as there are intensive agricultural areas in the Western Mediterranean Basin. Industrial waste in the region also pollutes rivers. For this reason, rivers generally consist of polluted and very polluted

(3rd and 4th class) waters. However, the lakes in the basin are cleaner and generally consist of clean or less polluted (1st and 2nd class) waters.

Although there are intensive agricultural regions in the Antalya Basin, the region receives a lot of orographic precipitation due to the Taurus Mountains. For this reason, many streams flowing from the mountains to the sea have very clean waters. However, depending on the heavy use of fertilizers, there is pollution in groundwater coming from agricultural pollutants.

The main water sources in the Burdur Closed Basin are Lake Burdur and Lake Acı Göl. However, both sources are extremely salty and have high values of sodium, sulfate, and chlorine.

The Akarçay Basin is a basin exposed to multi-directional pollution and agricultural, domestic and industrial pollution is found in the waters. Salinity is high in the Akarçay River, which is the main stream of the basin, due to pollutant discharges.

Lake Sapanca has remained relatively clean within the waters of the Sakarya Basin. However, rivers in the basin, especially the Sakarya, Porsuk, Ankara Brook, and Çark Brook, are in the category of very polluted waters (4th class) due to the discharge of intense industrial and domestic wastes.

The lakes in the Western Black Sea Basin remained relatively clean, while the streams have been polluted by industrial wastes, particularly by iron, ammonium, nitrite, phosphorus, sodium and chlorine.

While only partial agricultural pollution is observed in the groundwaters of the Yeşilirmak Basin, there is intense biological pollution in the surface waters due to the wastewater discharges to the surface waters, especially to the Tersakan and Çorum streams. The pollution of these streams is more evident in dry periods.

A feature that distinguishes the Kızılırmak Basin from other basins is related to the rock structure in the river bed. In some regions along the bed where the Kızılırmak River flows, there are salt minerals in the mineral structure of the soil, referred to as primary salinity. During the flow of the river and its tributaries, salt mixes with the stream from the eroded soils, thus increasing the sodium, chlorine and sulfate salts in the water content. Especially the waters of Hirfanlı dam and afterwards are in the 3rd and 4th class values in terms of irrigation water quality.

Since the Konya Closed Basin has the characteristics of a closed basin, the pollution of the rivers in the region directly affects the lakes where those rivers flow. Therefore, besides Lake Beyşehir, there are significant lake pollutions in the basin. In addition, groundwater is saltier than other basins due to the intense use of groundwater in the region.

Although the streams in the Eastern Mediterranean Basin are relatively less polluted, both high salinity and agricultural pollution are observed, especially in streams where drainage waters are discharged. During the dry summer seasons, a significant decrease in quality is observed in the streams.

The salinity in the sea-connected lagoons in the Seyhan Basin is very high and the surface water quality is quite low throughout the basin. Generally, irrigation water consists of 3rd or 4th class waters.

The water resources in the Orontes Basin are generally clean or slightly polluted waters and are in the 1st and 2nd classes in terms of COD and BOD. However, due to the high level of agricultural pollution, nitrogen-based pollutants rank first among the parameters that cause the main pollution. Most of the basin waters are in the 4th class in this respect.

Ceyhan Basin also shows a different situation compared to other basins. Although the water quality in the part of the Ceyhan River up to Kahramanmaraş is quite good and is first class in most places, the wastes of Kahramanmaraş province pollute the river to such an extent that from that point on, the Ceyhan River quickly becomes 4th class water in its quality.

Most of the Euphrates and Tigris Basin is clean in terms of BOD and COD and has 1st and 2nd class waters. Although the higher parts of the basin contain relatively clean waters, the wastes from the cities pollute the waters significantly. Industrial wastes are mixed into the Euphrates River near Gaziantep and the water quality becomes 3rd and 4th class. Similarly, when the Tigris River passes through Diyarbakır, it turns into 3rd and 4th class water with a significant amount of domestic waste discharge.

The Eastern Black Sea Basin is one of the country's cleanest watersheds. In terms of most parameters, the waters are first class. Only a significant part of it is in the 2nd class in terms of the COD parameter.

The waters of the Chorokhi Basin contain Class 1 waters for all parameters at almost every point. In the basin, which has clean waters enough to be called the basin where the cleanest waters in Turkey are found, the waters have remained cleaner because of a lack of industrial development and a geographical structure that prevents crowded settlements.

The Aras Basin has both rivers and lakes and is a basin where all water resources are clean. Only in terms of BOD, some sources show 2nd class characteristics.

The largest water source of the Lake Van Basin is Lake Van, the soda water of which limits its potential uses. The lake waters are considered polluted in terms of salinity, phosphorus, organic matter and ammonium nitrogen. The lake is exposed to diffuse pollution and is classified as 2nd class water in terms of ammonium nitrogen, 3rd class in terms of BOD, and 4th class water in terms of salinity.

In Turkey, adequate control is not provided for water use and allocations. In particular, groundwater is used far above the operable reserves through illegal wells. Therefore, laws and sanctions regarding the protection of water resources must be determined and introduced. In addition, basin-based water management should be institutionalized and the relevant structures be established as soon as possible. Since the characteristics of basins are different from each other, management plans to be implemented for each basin should be put into effect. In many basins, it is not possible to meet the allocations due to insufficient water. Therefore, the usage habits of users in such basins should be changed and water should be used sparingly.

Care should be taken to ensure that any water management plans to be carried out on a basin basis in Turkey are carried out in the form of real evaluations in the field. The management organizations to be established on basin basis should be in a manner that can carry out all kinds of inspections regarding the use of water in the field. It is of great importance to implement the prepared basin water management plans and basin water allocation plans in the field in accordance with the reality and to minimize water loss.

It is necessary to give the authority to influence both the plant pattern and the irrigation method to be applied in the relevant region to the organizations that have undertaken the management of water. In addition, activities that raise awareness should be carried out to ensure that water is used in the most efficient and responsible way at this stage.

References

- Ağca N & Doğan K (2020). Asi Nehrinin su kalite parametre düzeylerinin belirlenmesi. MKU. Tar. Bil. Derg. 25(1): 1-9.DOI: 10.37908/mkutbd.585057
- Akdeniz S (2005). Uluabat Gölü Su Kalitesinin Değerlendirilmesi ve Coğrafi Bilgi Sistemi Ortamında Analizi, U.Ü. Fen Bilimleri Enstitüsü, Yüksek Lisans Tezi, Bursa. 126 pp. <http://dx.doi.org/10.18016/ksujns.08103>.
- Aküzüm T, Çakmak B & Gökalp Z (2010). Türkiye’de su kaynakları yönetiminin değerlendirilmesi. Tarım Bilimleri Araştırma Dergisi 3(1): 67–74. <http://ijans.org/index.php/ijans/article/view/86>
- Al-Ansari N, Nasrat Adamo & Varoujan K. Sissakian (2019). Hydrological Characteristics of the Tigris and Euphrates Rivers., Journal of Earth Sciences and Geotechnical Engineering, Vol.9, No. 4, 1-26 ISSN: 1792-9040 (print version), 1792-9660. <http://dx.doi.org/10.47260/jesge/1111>
- Anonymous (2010). Marmara Basin Action Plan Report (Marmara Havzası Eylem Planı Raporu). <https://www.tarimorman.gov.tr/Sygm/Sayfalar/Detay.aspx?SayfaId=6>. Project Name: Preparation of Basin Protection Action Plans-Marmara Basin Page/Total Page: 18/466. Ankara
- Anonymous (2010a). Kızılırmak Basin Protection Action Plan (Kızılırmak Havzası Koruma Eylem Planı). Republic of Turkey Ministry of Agriculture and Forestry General Directorate of Water Management. Ankara
- Anonymous (2010b). Ceyhan Basin Protection Action Plan (Ceyhan Havzası Koruma Eylem Planı). Ministry of Forestry and Water Affairs, General Directorate of Water Management
- Anonymous (2013). Eastern Mediterranean Basin Protection Action Plan (Doğu Akdeniz Havzası Koruma Eylem Planı). Ministry of Forestry and Water Affairs, General Directorate of Water Management
- Anonymous (2014). North Aegean Basin Water Quality Monitoring Report (Kuzey Ege Havzası Su Kalitesi İzleme Raporu). Ministry of Environment and Urbanization. Ankara
- Anonymous (2015). Wastewater Treatment Action Plan (Atıksu Arıtım Eylem Planı), 2015-2013. Republic of Türkiye Ministry of Environment and Urbanization. 2015. Ankara
- Anonymous (2015a). Yeşilirmak Basin Flood Management Plan (Yeşilirmak Havzası Taşkın Yönetim Planı). Ministry of Forestry and Water Affairs, General Directorate of Water Management. Ankara
- Anonymous (2016). Antalya Basin Flood Management Plan (Antalya Havzası Taşkın Yönetim Planı). Ministry of Forestry and Water Affairs, General Directorate of Water Management. Ankara
- Anonymous (2016a). Evaluation Report on Pollution Prevention Studies in the Eastern Mediterranean Basin (Doğu Akdeniz Havzasında Kirliliği Önleme Çalışmaları Değerlendirme Raporu). Ministry of Environment and Urbanization General Directorate of Environmental Management. Ankara
- Anonymous (2016b). Seyhan Basin Pollution Prevention Action Plan (Seyhan Havzası Kirlilik Önleme Eylem Planı). Ministry of Environment and Urbanization General Directorate of Environmental Management. Ankara
- Anonymous (2016c). Ceyhan Basin Pollution Prevention Action Plan (Ceyhan Havzası Kirlilik Önleme Eylem Planı). Ministry of Environment and Urbanization General Directorate of Environmental Management. Ankara
- Anonymous (2016d). Eastern Black Sea Basin Master Plan (Final) Report (Doğu Karadeniz Havzası Master Plan (Nihai) Raporu). Republic of Turkey Ministry of Environment and Urbanization. Ankara
- Anonymous (2017). Lakes and Wetlands Action Plan (Göllere Ve Sulak Alanlar Eylem Planı) 2017-2023. Republic of Turkey Ministry of Forestry and Water Affairs General Directorate of Water Management. Ankara
- Anonymous (2018). Report of the Special Specialized Commission on Water Resources Management and Security (Su Kaynakları Yönetimi Ve Güvenliği Özel İhtisas Komisyonu Raporu). Eleventh Development Plan (2019-2023)

- Anonymous (2018a). Meriç-Ergene River Basin Management Plan (Meriç-Ergene Nehir Havzası Yönetim Planı). TR2011/0327.21-05-01-001. November. Ankara
- Anonymous (2018b). Susurluk River Basin Management Plan (Susurluk Nehir Havzası Yönetim Planı). Tr2011/0327.21-05-01-001. (Europeaid/134561/D/Ser/Tr). Ankara
- Anonymous (2018c). Susurluk Basin Flood Management Plan Executive Summary (Susurluk Havzası Taşkın Yönetim Planı Yönetici Özeti). Ministry of Forestry and Water Affairs, General Directorate of Water Management. Ankara
- Anonymous (2018d). Gediz River Basin Management Plan (Gediz Nehir Havzası Yönetim Planı). Ministry of Agriculture and Forestry General Directorate of Water Management. Ankara
- Anonymous (2018e). Little Meander River Basin Management Plan Strategic Environmental Assessment Scoping Report (Küçük Menderes Nehir Havzası Yönetim Planı Stratejik Çevresel Değerlendirme Kapsam Belirleme Raporu). Republic of Turkey Ministry of Agriculture and Forestry General Directorate of Water Management. Ankara
- Anonymous (2018f). Meander River Basin Management Plan (Büyük Menderes Nehir Havzası Yönetim Planı). TR2011/0327.21-05-01-001. Ministry of Agriculture and Forestry General Directorate Of Water Management. Ankara
- Anonymous (2018g). Western Mediterranean Basin Drought Management Plan (Batı Akdeniz Havzası Kuraklık Yönetim Planı). Republic of Turkey Ministry of Agriculture and Forestry General Directorate of Water Management Flood and Drought Management Department. Ankara
- Anonymous (2018h). Burdur Province 2017 Environmental Status Report (Burdur İli 2017 Yılı Çevre Durum Raporu) (2018). Burdur Provincial Directorate of Environment and Urbanization. Access address: https://webdosya.csb.gov.tr/db/ced/icerikler/burdur-cdr-2017_son20180810152249.pdf.
- Anonymous (2018i). Antalya Basin Drought Management Plan (Antalya Havzası Kuraklık Yönetim Planı). Ministry of Agriculture and Forestry General Directorate of Water Management Department of Flood and Drought Management. Ankara
- Anonymous (2018j). Konya Closed Basin Management Plan (Konya Kapalı Havzası Yönetim Planı). TR2011/0327.21-05-01-001. Ankara
- Anonymous (2019). North Aegean River Basin Management Plan Preparation Project Scoping Report (Kuzey Ege Nehir Havzası Yönetim Planının Hazırlanması Projesi Kapsamlaştırma Raporu). Ministry of Agriculture and Forestry General Directorate of Water Management. Ankara
- Anonymous (2019a). Gediz Basin Flood Management Plan (Gediz Havzası Taşkın Yönetim Planı). Ministry of Agriculture and Forestry General Directorate of Water Management. Ankara
- Anonymous (2019b). Burdur Basin River Basin Management Plan (Burdur Havzası Nehir Havzası Yönetim Planı). Republic of Turkey Ministry of Agriculture and Forestry General Directorate of Water Management. Ankara
- Anonymous (2019c). Akarçay Basin Flood Management Plan (Akarçay Havzası Taşkın Yönetim Planı). Republic of Turkey Ministry of Agriculture and Forestry General Directorate of Water Management. Ankara
- Anonymous (2019d). Sakarya Basin Flood Management Plan (Sakarya Havzası Taşkın Yönetim Planı). Republic of Turkey Ministry of Agriculture and Forestry General Directorate of Water Management. Ankara
- Anonymous (2019e). Western Black Sea Basin Flood Management Plan (Batı Karadeniz Havzası Taşkın Yönetim Planı). Ministry of Forestry and Water Affairs, General Directorate of Water Management. Ankara
- Anonymous (2019f). Kızılırmak Basin Flood Management Plan Executive Summary (Kızılırmak Havzası Taşkın Yönetim Planı Yönetici Özeti). Republic of Turkey Ministry of Agriculture and Forestry General Directorate of Water Management. Ankara
- Anonymous (2019g). Seyhan Basin Drought Management Plan (Seyhan Havzası Kuraklık Yönetim Planı). Republic of Turkey Ministry of Agriculture and Forestry General Directorate of Water Management Flood and Drought Management Department. Ankara
- Anonymous (2019h). Orantes and Seyhan Basins Flood Management Plan Preparation Project (Asi ve Seyhan Havzaları Taşkın Yönetim Planının Hazırlanması Projesi). Ministry of Agriculture and Forestry General Directorate of Water Management Department of Flood and Drought Management. Ankara
- Anonymous (2019i). Ceyhan Basin Drought Management Plan (Ceyhan Havzası Kuraklık Yönetim Planı). Republic of Turkey Ministry of Agriculture and Forestry General Directorate of Water Management Flood and Drought Management Department. Ankara.
- Anonymous (2019j). Aras Basin Flood Management Plan (Aras Havzası Taşkın Yönetim Planı). Ministry of Forestry and Water Affairs, General Directorate of Water Management. Ankara
- Anonymous (2019k). Van Lake Basin Flood Management Plan Strategic Environmental Assessment Draft Scoping Report (Van Gölü Havzası Taşkın Yönetim Planı Stratejik Çevresel Değerlendirme Taslak Kapsam Belirleme Raporu). Ministry of Agriculture and Forestry General Directorate of Water Management. Ankara
- Anonymous (2020). Chorokhi Basin Flood Management Plan Draft Strategic Environmental Assessment Report (Çoruh Havzası Taşkın Yönetim Planı Taslak Stratejik Çevresel Değerlendirme Raporu). Ministry of Agriculture and Forestry General Directorate of Water Management. Ankara
- Anonymous (2022). <http://www.cevreorman.gov.tr>. Date of access: 04.01.2022
- Anonymous (2022a). <https://docplayer.biz.tr/17047395-Iznik-golu-su-kalitesinin-fitoplankton-gruplarina-gore-belirlenmesi.html>. Date of access: 04.01.2022
- Anonymous (2022b). <https://tr.euronews.com/green/2022/05/10/dunya-meteoroloji-orgutu-kuresel-s-nmada-1-5-derece-esigini-asma-olas-l-g-yar-yar-ya>. Date of access: 08.08.2022
- Atıcı T & Obalı O (2002). Yedigöller ve Abant (Bolu) fitoplanktonunun mevsimsel değişimi ve klorofil a değerlerinin karşılaştırılması. Ege Üniversitesi Su Ürünleri Dergisi, 19(3/4): 281-289.
- Atuk N (2005). Türkiye'den Suriye'ye Akan Yerüstü ve Yer Altı Suyu Miktarı ve Bunların Ekonomik Değerleri. Devlet Planlama Teşkilatı Yayın No: DPT: 2422
- Aydın M C & Aydın S (2006). Dolusavaklarda Hidrolik Karakteristiklerin Sayısal Analiz Yöntemi ile Belirlenmesi. Fırat Üniv. Fen ve Müh. Bil. Dergisi Science and Eng. J of Fırat Univ. 18(4): 521-533
- Burak S, Duranyıldız İ & Yetiş Ü (1997). Su Kaynaklarının Yönetimi, Ulusal Çevre Eylem Planı, DPT
- Bozaoğlu A S & Akkuş M (2019). Nazik Gölü Balıkçılığı Üzerine Bir Araştırma. Journal of Anatolian Environmental and Animal Sciences. Year: 4, No: 3, 2019 (380-386). <http://dx.doi.org/10.35229/jaes.605597>
- Ceviz N A (2020). Sülüngür Gölü'nün (Köyceğiz-Dalyan Lagün Havzası) Limnolojik Ve Su Kalitesi Yönünden İncelenmesi, Yüksek Lisans Tezi, Ocak. Muğla

- Demir A & Selek Z (2009). Akyatan Lagününde Tuzluluk Ve Bazı Kirlilik Düzeylerinin Saptanarak Coğrafi Bilgi Sistemi Destekli Dağılımlarının Belirlenmesi. Ç.Ü Fen Bilimleri Enstitüsü. Cilt: 20-1
- Demir H K (2020). Yeraltı Su Kalitesinin Tahmin Modelleri Kullanılarak Değerlendirilmesi; Gediz Havzası Örneği. Yüksek Lisans Tezi. İstanbul Teknik Üniversitesi. FBE. İstanbul
- Elmacı A & Obalı O (1998). Akşehir Gölü Kıyı Bölgesi Alp Florası. *Journal of Biology* 22: 81- 98
- Fakıoğlu S & Kağncıoğlu N (2009). Doğu Karadeniz ve Çoruh Havzalarının Hidroelektrik Enerji Üretimi Açısından Değerlendirilmesi, FORUM 2009, Doğu Karadeniz Bölgesi Hidroelektrik Enerji Potansiyeli ve Bunun Ülke Enerji Politikalarındaki Yeri, Trabzon. <http://dx.doi.org/10.28948/ngumuh.598239>
- Fakıoğlu Ö & Nuhoglu A (2018). Derin Heyelan Set Gölü (Tortum Gölü)nde Biyolojik ve Kimyasal Değişimlere Neden Olan Etkilerin Belirlenmesi. Tübitak Çaydag Sayfa Sayısı: 68. Proje No: 116Y261. Proje Bitiş Tarihi: 01.04.2018
- Falkenmark M, Lundqvist J & Widstrand C (1989). "Macro-scale water scarcity requires micro-scale approaches: Aspects of vulnerability in semi-arid development". *Natural Resources Forum* 13(4): 258–267. <http://dx.doi.org/10.1111/j.1477-8947.1989.tb00348.x>
- Gençoğlu M (2019). Tuzla Lagününün (Karataş) Mikrobiyal Kalitesinin Belirlenmesi, Antibiyotik Dirençlilik Frekansının Tespiti. Çukurova Üniversitesi Fen Bilimleri Enstitüsü Biyoloji Anabilim Dalı. Yüksek Lisans Tezi. Basılmış.
- Girgin M (2000). Marmara Gölü. *Doğu Coğrafya Dergisi*. Cilt: 6 Sayı: 3
- Gümüş N E & Akkız C (2020). Eber Gölü (Afyonkarahisar) Su Kalitesinin Araştırılması. *LIMNOFISH-Journal of Limnology and Freshwater Fisheries Research* 6(2): 153-163. <http://dx.doi.org/10.17216/limnofish.638567>
- Gürlük S & Rehber E (2009). Manyas Gölü'nün Çevresel Değerleme Üzerine Bir Araştırma. *Tarım Ekonomisi Dergisi* 15(1): 9 – 15
- Hasançavuşoğlu Z & Gündoğdu A (2021). Sarıkum Gölü'nde (Sinop) Ötrofikasyona Neden Olan Bazı Besin Tuzlarının ve Fizikokimyasal Parametrelerin İncelenmesi. *Sinopfbd*; 6(2): 115-129. ISSN: 2536-4383. <http://dx.doi.org/10.33484/sinopfbd.912499>
- Kale M M (2018). Determination of Changing Spatial Distribution of Precipitation with Deterministic and Stochastic Methods in Yeşilirmak Basın. *Yerbilimleri*, 39(3): 263-276
- Karaer F, Katip A, Aksoy E, İleri S & Sarmaşık S (2009). Sulak Alanların Önemi, Sorunları ve Uluabat Gölü, Türkiye Sulakalanlar Kongresi, 81-87, 22-23 Mayıs, Bursa
- Katip A & Karaer F (2011). Uluabat Gölü Su Kalitesinin Türk Mevzuatına Ve Uluslararası Kriterlere Göre Değerlendirilmesi-Uluabat Üniversitesi Mühendislik-Mimarlık Fakültesi Dergisi Cilt 16, Sayı 2. <http://dx.doi.org/10.17341/gazimmfd.406790>
- Kaya I (2007) "Avrupa Birliği Sürecinin Türkiye'nin Sınıraşan Sular Politikasına Olası Etkileri" TÜBİTAK Proje No: 105K272, Çanakkale.
- Kılıç E (2020). Evaluation of water quality by water quality index method using long time monitoring data in Gökusu River. *Marine and Life Sciences* 2(1): 5-12
- Kıvrak E, Uygun A & Kalyoncu A (2012). Akarçay'ın (Afyonkarahisar, Türkiye) Su Kalitesini Değerlendirmek İçin Diyatome İndekslerinin Kullanılması. *Akı Febid* 12 021003 (27-38)
- Koç H, Doğru D & Han E (2018). Yukarı Kızılırmak Havzası'nda ırmak sularının tarımda sulama amaçlı kullanım özelliklerinin belirlenmesi üzerine bir araştırma. *Türk Coğrafya Dergisi* 70: 57-70. <http://dx.doi.org/10.17211/tcd.321037>
- Minareci O & Sungur Ö (2019). Akgöl ve Gebekirse Göllerinde (Selçuk, İzmir, Türkiye) Bazı Fiziko-Kimyasal Parametrelerin Mevsimsel Değişimi- 2019-GÜFBED/GUSTIJ, 9(4): 751-758 DOI: 10.17714/gumusfenbil.528798. <http://dx.doi.org/10.17714/gumusfenbil.528798>.
- Müderrişoğlu H, Yerli Ö, Turan A A & Duru N (2005). ROS (Rekreasyonel Fırsat Dağılımı) Yöntemi ile Abant Tabiat Parkı'nda kullanıcı memnuniyetinin belirlenmesi. *Tarım Bilimleri Dergisi* 11(4): 397-405. http://dx.doi.org/10.1501/tarimbil_0000000555
- Okumuş E (2007). Küçükçekmece Gölü Sedimentinde Ağır Metal (Zn²⁺, Fe²⁺, Cu²⁺) Adsorpsiyonu. Yüksek Lisans Tezi. Yıldız Teknik Üniversitesi, Fen Bilimleri Enstitüsü. İstanbul
- Onüçyıldız M, Abdulmohsin M S, Büyükkaracıoğlu N (2016). Fırat-Dicle Havzası Ve Irak Su Yapıları. *Selçuk University Journal Of Social And Technical Researches* Volume:12, pp. 118-151
- Oruçoğlu K & Beyhan M (2019). Göller Bölgesi Göllerinde Ağır Metal Kirliliğinin Değerlendirilmesi. *Bilge International Journal of Science and Technology Research* 3(1): 10-20. <http://dx.doi.org/10.30516/bilgesci.449984>
- Öner Ö & Çelik A (2011). Gediz Nehri Aşağı Gediz Havzası'ndan Alınan Su ve Sediment Örneklerinde Bazı Kirlilik Parametrelerinin İncelenmesi. *Ekoloji* 20, 78: 48-52, doi: 10.5053/ekoloji.2011.788. <http://dx.doi.org/10.5053/ekoloji.2011.788>
- Özdemir Y, Öziş Ü, Baran T, Demirci N, Fıstıkoğlu O & Çanga R (2002). "Fırat-Dicle Havzasının Türkiye, Suriye, Irak, İran'daki Su Potansiyeli". *Türkiye Mühendislik Haberleri*, Y.47, N.420-421-422, pp.27-34
- Özkoç Ö Ü, Yavuz N & Yavuz K E (2019). Sarıkum Gölü'nde Kışlayan Sukuşları. *KSÜ Tarım ve Doğa Derg* 22(4): 631-640, 2019 KSU J. Agric Nat 22(4): 631-640, 2019 DOI:10.18016/ksutarimdogu.vi.505706. <http://dx.doi.org/10.18016/ksutarimdogu.vi.505706>
- Öztürk A & Çolak M S (2021). The Effects Of Different Irrigation Water Quality And Irrigation Methods On Salt Accumulation In The Soil. *Middle East International Conference On Contemporary Scientific Studies-V1* September 20-22, Beirut, Lebanon. Isbn - 978-625-7464-25-3
- Semiz G D, Şentürk C, Yıldırım A C, Torun E (2023). Modelling Yield Response and Water Use to Salinity and Water Relations of Six Pepper Varieties. *Journal of Agricultural Sciences (Tarım Bilimleri Dergisi)*, 29(1):188-199. DOI: 10.15832/ankutbd.1017255
- Sevindi N (2005). "Kazakistan ve Su Kaynakları Yönetimi", *Zaman Gazetesi* Cumartesi Eki, 17 Ağustos 2005
- SHW (2016). Antalya Havzası Master Plan Ara Raporu. Ankara: DSİ Genel Müdürlüğü
- SHW (2017). Devlet Su İşleri (DSİ) Genel Müdürlüğü. Erişim adresi <https://www.dsi.gov.tr>
- SHW (2019). DSİ 2019 Yılı Resmi Su Kaynakları İstatistikleri. <https://www.dsi.gov.tr/Sayfa/Detay/1344>
- SHW (2021). DSİ 2021 Yılı Faaliyet Raporu. Pdf. Access date: 12.10.2022
- SHW (2022). Devlet Su İşleri (DSİ) Genel Müdürlüğü. Erişim adresi <https://www.dsi.gov.tr>. Date of access: 06.02.2022.
- Şener Ş & Kırilangıç E (2014). Efteni Gölü (Düzce) Sulak Alanı ve Çevresinin Hidrojeoloji İncelemesi. *AKÜ FEMÜBİD* 14. 025802 (13-25). DOI:10.5578/fmbd.7768. <http://dx.doi.org/10.5578/fmbd.7768>
- Şener Ş & Kibar H (2017). Karagöl (Borçka-Artvin) Gölü ve Çevresinin Hidrojeokimyasal İncelemesi. *Jeoloji Mühendisliği Dergisi / Journal of Geological Engineering* 41: 101-116. <http://dx.doi.org/10.24232/jmd.334464>
- Şener Ş & Taştekin N (2019). Beyşehir (Konya) Ovasının Hidrojeolojik Ve Hidrojeokimyasal İncelemesi. *Mühendislik Bilimleri Ve Tasarım Dergisi* 7(3), 647 – 661, E-Issn: 1308-6693. <http://dx.doi.org/10.21923/jesd.541781>
- Tas I, Tutenocaklı T, Coskun Y, Akcura M (2022). Determination of Germination Threshold Value of Chickpea Varieties with GGE Biplot Method Under Different Irrigation Water Salinity Conditions. *Journal of Agricultural Sciences (Tarım Bilimleri Dergisi)*, 28(4):711-722. DOI: 10.15832/ankutbd.876362

- Tokatlı C, Çiçek A, Emiroğlu Ö, Arslan N, Köse E & Dayıoğlu H (2014). Statistical Approaches to Evaluate the Aquatic Ecosystem Qualities of a Significant Mining Area: Emet Stream Basin (Turkey). *Environmental Earth Sciences*, 71, (5), 2185. <http://dx.doi.org/10.1007/s12665-013-2624-4>
- Tol T (2021). <https://kalkinmaguncesi.izka.org.tr/index.php/2021/08/24/kucuk-menderes-havzasinda-yeralti-su-kaynaklarinin-surdurulebilirliigi/>.
- The Water Pollution Control Regulations (1999). <https://faolex.fao.org/docs/pdf/swa142028.pdf>
- Tunca E, Atasagun S & Saygı Y (2012). Yeniçağa Gölü'nde (Bolu-TÜRKİYE) Su, Sediment ve Kerevitteki (*Astacus leptodactylus*) Bazı Ağır Metallerin Birikimi Üzerine Bir Ön Çalışma. *Ekoloji* 21, 83, 68-76. Doi: 10.5053/ekoloji.2012.838. <http://dx.doi.org/10.5053/ekoloji.2012.838>
- TUIK (2019). <https://data.tuik.gov.tr/Kategori/GetKategori?p=nufus-ve-demografi-109&dil=1>
- UN (United Nations) (2007). Coping with water scarcity-challenge of the twenty centur World water day 22 March 2007 United Nations – Food and Agricultural Organization
- UNDP (United Nations Development Programme) (2006). Human Development Report 2006 Beyond scarcity: Power, poverty, and the global water crisis. <https://hdr.undp.org/content/human-development-report-2006>. Access date: 05.01.2023. <http://dx.doi.org/10.18356/334c604b-en>
- Ünlü M (2013). Gediz Akarsuyu Havzası'nın Biyolojik Özellikleri ve Balıkçılık. *Marmara Coğrafya Dergisi*, (1), 309-323. Retrieved from <https://dergipark.org.tr/tr/pub/marucog/issue/448/560500>
- WPCR (2015). Water Pollution Control Regulation (Su Kirliliği Kontrol Yönetmeliği). Resmi Gazete: Tarih 15 Nisan Çarşamba, Sayı:259327.
- Yenici E. (2010). Havza Ölçeğinde Su Kalite Yönetimi: Büyük Menderes Nehir Havzası Örnek Çalışması. Yüksek Lisans Tezi, İstanbul Teknik Üniversitesi, Fen Bilimleri Enstitüsü
- Yerli V S, Zengin M, Günüz E, Çalışkan M, Canbolat A F, Akbulut A, Emir N & Ataç Ü (1996). Çıldır Gölü stok tayini, TÜBİTAK, DEBAG 17/G No'lu proje, Ankara, 95 pp
- Yerli S V & Zengin M (2019). Aktaş Gölü ile İlgili Bir Değerlendirme. Aktaş Gölü Biyoçeşitliliğin Korunması ve Sürdürülebilir Gelişme Çalıştayı 27 Eylül 2019 – Ardahan. ISBN: 978-605-68045-9-5. pp. 19-28
- Yıldırım A (2006). Karakaya Barajı ve Doğal Çevre Etkileri, D.Ü. Ziya Gökalp Eğitim Fakültesi 6: 32–39
- Yılmaz C (2005). Sarıkum Gölü Ekosistemi (Sinop). Türkiye Kuvaterner Sempozyumu V, 02-03 Haziran, Bildiriler Kitabı, (Editörler: O. Tüysüz-M. K. Erturaç), İstanbul Teknik Üniversitesi, Avrasya Yerbilimleri Enstitüsü Yayını pp. 219–226, İstanbul



Copyright © 2024 The Author(s). This is an open-access article published by Faculty of Agriculture, Ankara University under the terms of the [Creative Commons Attribution License](https://creativecommons.org/licenses/by/4.0/) which permits unrestricted use, distribution, and reproduction in any medium or format, provided the original work is properly cited.



Evaluation of Water Sources and Animal Species in Terms of Scarcity, Rights and Welfare

Bahattin ÇAK^a

^aVan Yüzüncü Yıl Üniversitesi, Veteriner Fakültesi, Zootekni ABD, Kampüs-VAN, TÜRKİYE

ARTICLE INFO

Review Article

Corresponding Author: Bahattin ÇAK, E-mail: bahattincak@yyu.edu.tr

Received: 13 March 2023 / Revised: 27 September 2023 / Accepted: 21 October 2023 / Online: 09 January 2024

Cite this article

Çak B (2024). Evaluation of Water Sources and Animal Species in Terms of Scarcity, Rights and Welfare. *Journal of Agricultural Sciences (Tarim Bilimleri Dergisi)*, 30(1):35-46. DOI: 10.15832/ankutbd.1264536

ABSTRACT

Problems such as global warming, climate change, water, and food availability have been some of the most important issues on the world agenda in recent years. For sustainable welfare, the concepts of equality, justice, and rights are indispensable for the ecosystem. At present, the adoption of legal regulations on water scarcity, the right to water, animal welfare, and animal rights as well as the awareness of conscientious responsibility for the individual and wider society has been an important development for the future. With this in mind, this article is aimed at contributing to the objective questioning of the concepts of rights and welfare with their emotional, legal, and scientific aspects by removing our

presuppositions about life, and abandoning the distinction between living and non-living things. The study consists of two parts. In the first part, water scarcity and the right to water, and in the second part, evaluations are made in terms of animal welfare and rights. The general acceptance of water consumption as a need rather than a right has turned it into a commodity that can be bought and sold with the use of money. Although there is enough water in the world, the perception of scarcity consciousness arising from the possible inadequacy of the amount of consumable water needs to be re-questioned at the intellectual level by considering it from the perspective of a biological transformation.

Keywords: Water, Animal, Scarcity, Right, Welfare

1. Introduction

1.1. Water scarcity

Şahin (2016), while explaining water scarcity in her thesis, evaluated its conceptual definition in terms of economic science. Accordingly, a hotly debated topic in economics is the concept of scarcity. In economic terms, scarce resources are expressed as meeting infinite needs. The fact that needs are infinite and resources are limited means that individuals are confronted with a problem of choice.

Classical and neo-classical economics literature refers to individuals who act rationally and in line with their interests when deciding between options as "*Homo economicus*". The fact that individuals behave like homo economicus in decision-making processes is usually explained by Adam Smith's "diamond-water paradox". In simple terms, the diamond-water paradox is based on a choice that a person in the desert has to make between diamonds and water, and the choice between diamonds, a luxury good, and water, of seemingly lesser value, favors water under the extreme conditions of the desert. The change in the value attributed to water and the characterisation of water as an economic commodity covers a certain process (Şahin 2016). It can be stated that this has become more evident in the changing world economic understanding.

Water scarcity is one of the most important global environmental problems. Water scarcity, which is measured by the amount of water per capita and evaluated with the help of various indices, shows its effects in many regions of the world. The main causes of water scarcity are global climate change, drought, deforestation, the increase in fossil fuel use, change in consumption habits, economic growth, the increase in the global population and urbanization rates, pollution, lack of personal water use awareness, and water management policies that are not suitable for resources and shaped according to political understandings (Şahin 2016).

In the water cycle (hydrological cycle), the basic dynamics of which is formed by solar energy, the water in the oceans first turns into vapour with solar energy, and the water that rises to the atmosphere by evaporation is carried over land. The water in

the clouds encountering cold air condenses and descends to the earth in the form of rain or snow. Some of the precipitation falling on the land returns to the atmosphere by evaporation and transpiration through soil and vegetation (Bilen 2008).

The fact that water resources are facing the danger of extinction makes the problem of water scarcity the most important issue of the 21st century. For this reason, water resources have been a subject on the agenda on international platforms since the late 1990s (Şahin 2016).

It has been observed that average temperatures on land and in seas have increased by 0.85 °C in the last 100 years. As a result of increasing greenhouse gas emissions in the world and increasing global warming, it is estimated that the global temperature will increase by 1 - 3.5 °C over the next 100 years (Aksoy & Çabuk 2015).

By 2050, the world population is expected to increase by 33% to 9.3 billion and accordingly, the demand for food is expected to increase by 60% in the same period. It is also estimated that the population living in urban areas will reach 6.3 billion in 2050, almost two-fold greater than the current population. In the Baseline Scenario of the Global Environmental Outlook prepared by the OECD, an upward trend in the strain on access to freshwater is projected by 2050, with an additional 2.3 billion people in addition to the current population living in regions subject to severe water stress, particularly in Northern and Southern Africa and South and Central Asia. Another report, BAU (a business-as-usual) scenario, estimates a 40% global water deficit by 2030 (Küçükşakarya & Göçmen 2019).

The decrease in water resources as a result of global warming is expected to cause a decrease in agricultural and forestry products, energy shortages, and population movement from coastal to inland areas. In order to protect the ecological balance and ensure the sustainable development of urban and rural communities, water resources should be used in the most rational way to meet current and future needs (Karaman & Gökcalp 2010).

In general, the water potential of a country is evaluated according to the amount of water per capita in that country. According to a widely used international criterion, countries with a water potential of 10,000 m³ per capita per year are called water-rich countries; countries with a water potential between 10,000 m³ and 3000 m³ per capita per year are called self-sufficient countries and countries with a water potential between 3000 m³ and 1000 m³ per capita per year are called water-scarce countries. Countries with less than 1000 m³ per capita per year are classified as water-poor countries (Uluirmak 2014).

Another measure used to indicate water scarcity or water stress is the 'Falkenmark Index'. According to this index, scarcity or stress is determined in line with the annual per capita water amount in a region or country as follows

- No water problem above 1.700 m³
- Water shortage between 1.700-1.000 m³
- Water scarcity between 1,000-500 m³ and
- Below 500 m³ is considered as a region or country with absolute water scarcity (Muluk et al. 2013).

Whether water is an economic or public good is a long-debated issue. However, the water policies implemented by countries today demonstrate that water is considered as an economic good. Economic science categorizes goods into different groups. One of these distinctions is free goods, which are abundant in nature according to human desires; the other is economic goods, which are scarce according to human desires. Beyond these goods, water is a geo-strategic and geo-political resource. It is not like other goods, it has a special position, strategy and policy. Namely (Savenije 2002);

- a. Water is mandatory.
- b. Water is limited.
- c. Water is fluid.
- d. Water is a system, the existence and continuation of the natural system depends on water.
- e. Water is difficult to transport.
- f. Water has no substitutes and its area of use is extensive.
- g. Water cannot be treated freely.
- h. Water is complex and cannot be subject to free trade.

According to Küçüksakarya & Göçmen (2019), if we need to emphasize the seriousness of the issue in our country, according to the State Hydraulic Works (DSİ) data, Turkey's per capita water potential is 1422 m³. In terms of both classifications, it is observed that Turkey is facing a water shortage. Based on the estimation of the Turkish Statistical Institute (TurkStat) that the population of Turkey will reach 88 million in 2030, it is thought that the annual per capita water level will be around 1 200 m³ by 2030. However, these assessments are based on the assumption that Turkey, which is not a water-rich country, will transfer its current water resources to 2030 without depleting them, and it is estimated that Turkey, like many countries around the world, will experience water scarcity in the near future.

According to a report published by the United Nations World Water Assessment Programme (DSDP 2015), 663 million people do not have access to drinking water. Similarly, according to the World Resources Institute, more than one billion people are facing water scarcity today and this number is expected to reach 3.5 billion by 2025. Considering these reports and the findings of various studies, water is fast becoming a scarce resource day by day and needs to be managed carefully and wisely.

The agriculture sector is the field in which water resources are most extensively used. Worldwide, 70% of the fresh water extracted is used in agricultural activities and this rate reaches 90% in less developed countries (DSDP 2015). The rapid consumption and pollution of water resources by agricultural activities in order to meet the food demands of the growing global population and national populations increases the already existing scarcity and pressure on these resources. The fact that agricultural activities are carried out globally with inefficient irrigation systems further amplifies the problems. Considering the predictions that by 2050 there will be 60% more agricultural production in the world and 100% more in developing countries (DSDP 2015), it appears inevitable that many wetlands and river basins will face water scarcity in the near future.

With climate change and human activities expected to increase, the increasing trend in conflict events could persist, with water resources becoming a more frequent cause of future conflict. Identifying these complex cooperation-conflict changes is vital in determining future actions required to reduce conflict events and promote cooperation on the subject of water (Kåresdotter et al. 2023).

Water scarcity affects more than 40% of people worldwide, an alarming figure that is projected to rise as temperatures do. Although 2.1 billion people have improved water sanitation since 1990, dwindling drinking water supplies are affecting every continent. More and more countries are experiencing water stress, and increasing drought and desertification is already worsening these trends. By 2050, it is projected that at least one in four people will suffer recurring water shortages. Safe and affordable drinking water for all by 2030 requires investment in adequate infrastructure, the provision of sanitation facilities, and high hygiene levels. Protecting and restoring water-related ecosystems is essential. Ensuring universal safe and affordable drinking water involves accounting for over 800 million people who lack basic services and improving accessibility and safety of services for over two billion people (UNDP Turkey 2023).

With this progress, per capita water use has reached unprecedented levels. A hundred years ago, even in the most developed societies, the services provided by these infrastructures, which were accessible to a limited number of people, were regarded as a fundamental right of citizenship, and for this reason, governments have made great efforts to rectify the deficiencies in these infrastructures, regardless of the costs. As a result, water use in the world in the 20th century increased at twice the rate of the global population growth (WHO 2021). However, this increase, together with the new problems of the modern age, has seen water shortages around the world reach unprecedented historic levels. Billions of people around the world face problems such as excessively polluted water; extreme climate events linked to global climate change, manifested by severe droughts or floods; and a lack of access to safe and affordable drinking water. These water challenges lead to increased insecurity, migration and the risk of violent conflict, especially in developing countries that lack the financial, technical and governance capacities to address these problems.

Water is of great importance in all areas of agriculture, including crop farming, animal husbandry and aquaculture. The amount of water used in agriculture varies according to the method used. While soil moisture is sufficient for agriculture in some regions, rainwater-based agriculture is practiced in many regions, and irrigated agriculture can be practiced in suitable regions. Rainfed agriculture is practiced in 80% of the cultivated areas in the world and 60% of food production is provided from these areas. Although irrigated agriculture is practiced in about 20% of cultivated areas in the world, it accounts for 40% of food production (FAO 2020). Water withdrawals from surface and groundwater sources for irrigation are 2,797 km³ per year by 2020, accounting for 70% of all water withdrawals worldwide. In drier regions, this rate rises to over 90%. Irrigated agriculture accounts for more than 70% of global water use (FAO 2020).

Excessive groundwater abstraction, inefficient irrigation methods, salination of groundwater reserves and excessive use of fertilizers have become major threats to water resources. Water is mobile, it does not disappear. The amount of water on earth remains constant over the years. The water cycle is the most important assurance of the renewal of water resources. Every year, a volume more than the water mass in the Black Sea, i.e. 577,000 km³ of water, is recirculated in this cycle (TEMA 2021).

According to the UN, a "water shortage" occurs when a region withdraws 25% or more of its renewable freshwater resources (United Nations Water 2021). Today, one of the main factors for the current water crisis is global climate change. Due to global

warming, rainfall irregularity as well as widespread and prolonged drought, on the other hand, are becoming frequent occurrences (UNDRR 2021). The UN defines water scarcity as "the point at which the demands of all water users for water supply or quality cannot be fully met within the framework of the institutional arrangements in place" (United Nations Water 2021). Mathematically, water scarcity is defined as "the ratio of human water consumption to available water supply in a given area". Hydrologists generally assess and rate water scarcity in a region according to this population/water ratio.

The National Water Policy (Ulusal Su Planı 2019-2023) sets out the general outlines of our national water policy with the goal of "A Turkey with a National Water Policy" in the vision of 2023. In this context, in the publication prepared by the Turkish Ministry of Agriculture and Forestry; i.e. the Special Expertise Commission Report on Water Resources Management and Security prepared within the scope of the 10th Development Plan, water security is defined as 'the ability of a society to maintain its access to the water it needs for purposes such as drinking, using, irrigation water supply and energy production and to protect itself from the possible damages of water' (Ulusal Su Planı 2019-2023).

According to the proceedings (DSİ 2017), 51 decisions on water were reached at the 2nd Forestry and Water Council. Among these decisions, the decision on water law is provided below; Decision 34. Institutions and organizations working in the field of water law and policies should be supported and the development of their institutional capacity on these issues should be encouraged.

The establishment of a healthy supply-demand balance depends on the correct determination of inter-sectoral water use needs. In Turkey, a total of 54 billion m³ of water are used annually, of which 7 billion m³ (13%) are used in industry, 7 billion m³ (13%) as drinking and potable water and 40 billion m³ (74%) in irrigation. This amount corresponds to 48.2% of the technically and economically available 112 billion m³ water potential. In the last 20 years, there has been a 40% increase in the total amount of water consumed in Turkey. Considering the population growth rate and the growth in the drinking-utilization, agriculture, industry and energy sectors, it is predicted that the amount of water that will be needed in the next 25 years will reach three times the current water consumption. (Ulusal Su Planı 2019-2023).

According to the Ulusal Su Planı (2019-2023), it is clear that the increasing water demand will gradually increase the pressure on existing resources. Within the scope of the use of 112 billion m³ of water, which is among our 2030 targets, which is the current technically and economically usable potential, and the development and utilization of irrigated agricultural areas, sectoral water use is planned to be 64% for agriculture, 20% for industry and 16% for domestic use (DSİ 2017). The distribution of population, industrial activities and other sectoral activities in Turkey does not exhibit a balanced and homogenous structure. As of 2017, the total gross irrigated land area reached 6.5 million hectares, which corresponds to 72% of the total economically irrigable land (DSİ 2017).

In 2016, the net irrigation area in Turkey was 3 million hectares (DSİ 2017). Most of the irrigable agricultural land (about 75-80%) is irrigated with surface water and the rest with groundwater. In 2016, 77% of the 43 billion m³ of water used for irrigation in Turkey was surface water and 23% was groundwater (DSİ 2017). In water distribution systems, traditional systems with high leakages and evaporation losses account for the majority.

1.2. Right to water

The right to water is the right of people to have access to healthy and economically viable water. What is meant by this right is that it is not only a right specific to humans, but also covers all living beings (Firdin 2015).

Water is a fundamental element of vital importance not only for humans but also for all living things in nature. Due to the vital importance of water, it is a fundamental right for humans and this right must be evaluated within the scope of human rights. Human rights include the fundamental rights and freedoms recognized as possessed by all human beings. These rights are the rights that every human being can enjoy regardless of race, language, religion and gender (Özsoy 2009).

According to the neo-liberal approach, the right to education, health and water are not rights but needs and the state should intervene and meet these needs (Çulhaoğlu 2001).

The basic view of neo-classical economics is based on the assumption that human needs are diverse and infinite, whereas the means and earth resources that can fulfil human needs are limited. For this reason, every object intended to fulfil these needs is considered as a "commodity" whose value must be determined. This presupposition tries to transform water, which is indispensable for all living beings and cannot be substituted, into a commodity in today's conditions; the privatization of water is brought to the agenda in the global stage of capitalism due to the excessive profit ambition of capital, and with commercialization, water is offered to the market as a commodity that can be bought and sold, accessible only to those with money (Özsoy 2009).

In discussions on the relationship between neoliberal policies and health, health is frequently reduced to health policies and the effect of neoliberal policies are generally assessed only in the frame of global transformation of health systems. However, health is being shaped not only by biological factors and health systems, but also by economic, social and political factors like

living, working, housing conditions and nutrition. The rise in unemployment; worsening of working conditions; increased flexibility of legislations regarding the security of the environment, agriculture and food, urbanization and nutrition; weakening of state supervision on capitalist enterprises which harm public health and the deepening of social inequalities are the other dimensions of the impact of neoliberal policies on public health (Temmuz 2017).

The greatest threat to nature is the transformation of technological progress into a mechanism that is deeply connected to the capitalist system and operates only by the rules of the market. Since the capitalist system, which recognizes nature as a tool, tries to dominate nature, the results that have emerged today have been constantly ignored. As Marx stated in his 1844 Political Economy and Philosophical Writings, "Man lives in dependence on nature. Nature is man's body. Man must be in a good and constant dialogue with nature in order not to die. To say that man's physical and cerebral life depends on nature is to say that man depends on nature itself. Because man is a part of nature with his whole being." The capitalist system, which worships overproductionism with the greed for profit, uses nature irreversibly. The exploitation of all elements of human and nature for capital accumulation is perceived as the natural dynamics of the system and these conditions pave the way for ecological destruction. The process transforms natural relations into commodity relations (Özsoy 2009).

According to Minibaş (2008) quoted by Özsoy (2009) in his article, water is one of the most indispensable requirements for the life of other living creatures as well as humans. Therefore, its demand is continuous. Due to its non-substitutable feature, its use value is very high. Since it is an indispensable requirement of life, it is a compulsory complement in agriculture and animal husbandry. It is used as input in various stages of production from the manufacturing industry to construction, from mining to health, from transport to energy production. It is an energy source used in transport and lighting as well as irrigation.

The following first three articles of the Universal Declaration of Human Rights and articles 11 and 12 of part III of the International Covenant on Economic, Social and Cultural Rights and are of a nature that can be a source for recognizing water as a fundamental human right:

Article 1) All human beings are born free and equal in dignity and rights, are endowed with reason and conscience, and should act towards one another in a spirit of brotherhood.

Article 2) Everyone is entitled to all the rights and freedoms set forth in this Declaration without distinction of any kind, such as race, colour, sex, language, religion, political or other opinion, national or social origin, wealth, birth or other status.

Article 3) Every individual has the right to life, liberty and security (Anonymous 2023a).

International Covenant on Economic, Social and Cultural Rights (PART III):

Article 11

1. The States Parties to the present Covenant recognize the right of everyone to an adequate standard of living for himself and his family, including adequate food, clothing and housing, and to the continuous improvement of living conditions. The States Parties will take appropriate steps to ensure the realization of this right, recognizing to this effect the essential importance of international cooperation based on free consent.

2. The States Parties to the present Covenant, recognizing the fundamental right of everyone to be free from hunger, it shall take, individually and through international co-operation, the measures, including specific programmes, which are needed:

(a) To improve methods of production, conservation and distribution of food by making full use of technical and scientific knowledge, by disseminating knowledge of the principles of nutrition and by developing or reforming agrarian systems in such a way as to achieve the most efficient development and utilization of natural resources;

(b) Taking into account the problems of both food-importing and food-exporting countries, to ensure an equitable distribution of world food supplies in relation to need.

Article 12

1. The States Parties to the present Covenant recognize the right of everyone to the enjoyment of the highest attainable standard of physical and mental health.

2. The steps to be taken by the States Parties to the present Covenant to achieve the full realization of this right shall include those necessary for:

(a) The provision for the reduction of the stillbirth-rate and of infant mortality and for the healthy development of the child;

(b) The improvement of all aspects of environmental and industrial hygiene;

(c) The prevention, treatment and control of epidemic, endemic, occupational and other diseases;

(d) The creation of conditions which would assure to all medical service and medical attention in the event of sickness (Anonymous 2023b).

Every human being deserves to have the means to meet his/her most basic needs such as food, shelter and water. Although there is no article on water in the Universal Declaration of Human Rights, it can be argued that the right to life stated in the third article includes water. Many people interested in the subject have also emphasized the third article and expressed a similar opinion.

Many international treaties and conventions define a wide range of human rights. The 1966 "International Covenant on Economic, Social and Cultural Rights", the 1966 "International Covenant on Civil and Political Rights", the "Declaration on the Right to Development" and the "European Convention on Human Rights" being the most notable ones (Tomanbay 2008). All other fundamental rights included in the scope of human rights in such agreements and conventions are rights related to the "right to water". These conventions, which include provisions on issues such as food, health and housing, both directly and indirectly refer to the right to water. Because water, as the basic building block of life, is directly linked to many issues such as clean and sufficient food, health and medical care.

Ünlü (2017) in his article, Right to Water, stated that water resources are adversely affected as a result of the harmful activities of people. These negative developments cause people to be more sensitive to water policies and even the right to water. The right to water is the right of people to access healthy and affordable water (Firdin 2015). In the third article of the Universal Declaration of Human Rights, it is stated that the individual has the right to life. The individual's right to life is directly proportional to the water he/she needs to consume daily. Since humans cannot live without water, the right to water becomes a fundamental human right. In 1994, the Programme of Action of the Conference on Population and Development clearly states that the right to water and the right to protect one's health are included in the right to life (İlhan 2011). Five years after this programme, according to Article 175, paragraph 53 of the General Assembly Resolution 175, clean water is one of the fundamental human rights. According to General Statement 15, the international document was published by the United Nations Committee on Economic, Social and Cultural Rights in 2002. The Committee's report states that "Every individual living in the community has the right to adequate, safe, physically accessible and affordable water for personal and domestic use". However, the right to water cannot be demanded directly from the state. The state is obliged to provide clean and safe drinking water in a way that the society will pay for it (Kartal 2009).

UNDP also defines water as a human right in international treaties. International human rights laws includes specific obligations regarding access to safe drinking water. These obligations require access to clean drinking water in quantities necessary for personal and living space uses, defined as drinking water, sanitation, food and personal; water for household hygiene. These obligations require states to maintain the quality of sanitation to ensure access to adequate sanitation (OHCHR 2010).

Narin (2016) discusses the right to water as a human right and the privatization of water. Water was recognized as a human right by the UN Committee on Economic, Social and Cultural Rights in 2002 with General Comment 15. In the following years, the right to water has been the subject of many international conferences as well as constitutionally recognized in national law. Today, the right to water has been recognized by more than 160 countries and constitutionally protected by 28 countries. Since water is essential for life, the demand for the right to water in terms of access to sufficient water is not so different from the demand for the right to life. For this reason, it is crucial that the regulations of the right demand, which have started in national-international law, are reflected in constitutional and legal regulations.

In Narin's (2016) article, the right to water was included in human rights law with General Comment No. 15, which was introduced at the 29th session of the UN Committee on Economic, Social and Cultural Rights in Geneva (Topçu 2009). Accordingly, the right to water is an integral part of the right to adequate housing and adequate nutrition under Article 11 and the right to health under Article 12. In General Comment No. 15, it is stated that water is a basic public good for life and health, a prerequisite for the realization of other rights, and the right to water is defined as follows: "The right to water as a human right stipulates that everyone has the right to adequate, safe, acceptable, physically accessible and affordable water." It is expressed as follows.

The right, which is expressed as the embodied form of freedom, is the means of realizing freedom (Kaboğlu 1993). The powers recognized as "rights" in the Constitution and laws bring with them the "power to demand", which means that the person can demand the fulfilment of his/her rights by the state or individuals. In terms of the right to water as a human right, individuals can undoubtedly make some demands. However, for this, the basis of this "power to demand" of the person must be established.

In Narin's (2016) article, although it is a generally accepted thesis that international law norms are superior to all domestic law rules, including the constitution (Gözler 2010), some authors distinguish international law from domestic law and argue that the rules in international law cannot be directly applicable in domestic law. Therefore, in order for the right to water, which is widely recognized in international texts, to be claimable, its place in domestic law is important. Turkey has ratified the conventions and directives mentioned in this study. While some of these conventions directly include the right to water, in some texts it is considered among the obligations of the state. Aside from this, the right to water is also considered as a part of the right to life. Therefore, a normative justification can be made in terms of the right to water in all cases; however, what is important here is the impact of these international texts on Turkish law. According to Article 90 of the Turkish Constitution, international treaties have at least the force of law in domestic law. In this respect, the right to water as a human right is not a foreign concept to Turkish law (Şirin 2010). Moreover, when water is considered within the right to life, it imposes both positive and negative obligations on the state. In this case, the state is obliged to fulfil the acts necessary to ensure the use of the right to water as well as eliminating the factors that prevent the use of the right to water (Çiçek 2009).

Constitutions are the fundamental texts that provide the strongest protection for fundamental rights and freedoms. If a guarantee is to be mentioned in terms of the right to water, constitutional protection must be provided first and foremost. Although it is stated that there are many constitutions that include provisions on the right to water in their constitutions, it is stated that the Uruguayan Constitution is the first constitution that recognizes water and sanitation as a human right and explicitly guarantees it (Narin 2016).

2. Animal welfare and rights

2.1. Animal welfare

Animal welfare discipline originates from animal rights and animal protection philosophy. It was only in the later period of time that the subject was handled within the scope of positive animal sciences (Fraser 1999).

Today, many factors play a role in the adoption of legal regulations on animal welfare as a social consensus text. Animal welfare or welfare is a field that has been carried out as a task by practitioners in line with social needs. On the other hand, animal welfare is an issue that concerns all areas and persons related to animals. All kinds of studies on the subject will continue as long as people "need" animals. Considering that the needs of humans and other animal species for each other as parts of the world ecosystem (although the contribution of humans to the functioning of the world ecosystem is not known) will not end, it is clear that studies on the subject will not end (Savaş et al. 2009).

The concept of animal welfare is defined in various ways by many people and organizations. The first official definition of animal welfare was defined as the physical and emotional well-being of the animal by the Brambell Committee (Thorpe 1965) established by the British government in 1965. In another definition, welfare includes not only the physical conditions of the animal but also its emotional state (Duncan 2002; Fidan 2012).

If we look at animal welfare from a more general perspective, it can be said that it is a complex definition that includes all components of animal life.

In Bilgili's (2021) article, the Animal Welfare Committee established in 1993 within the UK government listed the 5 freedoms that should be given to animals as follows (FAWC 1993):

- 1- Animals should not be deprived of their needs in the form of hunger, thirst, etc.,
- 2- Animals should not be disturbed by the environmental conditions they are in,
- 3- Protection of animals from bumps, injuries and diseases that cause pain and suffering,
- 4- The ability of animals to exhibit normal behavior and
- 5- Protection of animals from activities or situations that cause fear and stress

As can be concluded all animals should have access to the appropriate water source and feed at intervals appropriate to their physiological needs. The water to be consumed should be clean and of good quality, and animals should be able to access the water source at liberty.

Similarly, there are provisions regarding access to water in the existing laws in Turkey. For example; as can be observed in Article 13 of the "Regulation on the Welfare of Farm Animals" prepared on the basis of Article 9 of the Veterinary Services, Plant Health, Food and Feed Law No. 5996 dated 11/6/2010 and numbered 5996, "All animals are provided with access to fresh water in sufficient quantities and their daily fluid intake needs are met" (Anonymous 2010).

Regulation on the Welfare of Farm Animals

(This Regulation has been prepared based on Article 9 of the Veterinary Services, Plant Health, Food and Feed Law No. 5996 dated 11/6/2010).

Feed, water and other substances

ARTICLE 13

(1) Farm animals are fed in sufficient quantities to maintain their health and meet their nutritional needs and with a suitable feed adapted to their age, weight, behaviour and physiological needs. No animals shall be given food or liquids containing any substance which may cause unnecessary suffering or injury.

(2) All animals are given access to feed at intervals appropriate to their physiological needs.

(3) All animals are provided with access to fresh water in sufficient quantities to meet their daily fluid intake needs.

(4) Feeding and drinking water equipment is designed, constructed and installed in such a way as to prevent contamination of food and water and to minimize the harmful effects of competition between animals.

(5) Except for substances authorized for use by the Ministry for treatment, protection or zootechnical treatment, no other substance shall be administered to animals unless it is shown by scientific studies or experience that the effect of the substance in question is not harmful to the health or welfare of the animal (Anonymous 2010).

Human beings have different abilities to understand, interpret and question the universe and life. This situation causes perceptual differences in analyzing, thinking and reasoning in mental activities. Therefore, scientific approaches are also affected.

2.2. *Animal rights*

According to Arslan & İlgili (2022), the concept of animal rights is defined in a wide range of ways, from views that oppose the use of animals in any way to approaches that approve their use with certain limitations. The main arguments are shaped in contexts such as animals' ability to feel, to feel pain and pleasure, to have interests, to be subjects of life, their moral status and speciesism. Based on these contexts, rights such as the right to life, to be respected, not to be exploited, to be well cared for, to be looked after, to be protected, to benefit from the knowledge of humanity, not to be mistreated, not to be made to suffer, to be killed painlessly and without fear when death is mandatory, to live and reproduce in an environment suitable for its nature, to complete its natural life, not to be abandoned, rest, nutrition, limitation of workload for animals used in various jobs, not to be made the subject of human entertainment, protection of honour and protection of habitats are mentioned (Neumann 2012; Phillips & Kluss 2018).

Sinmez (2022), in his article entitled "The Current Constitutional Position of Animal Rights in the World and Turkey", analyzed the constitutional texts and identified a total of 15 countries (Germany, Austria, Bolivia, Brazil, Gambia, South Sudan, India, Switzerland, Iceland, Libya, Malaysia, Mexico, Egypt, Papua New Guinea, Slovenia) that protect animal rights and include articles that protect these rights in principle.

It is only possible for people to protect and develop their material and spiritual assets by ensuring that they live in a healthy and balanced environment with all other living and non-living things. In this context, the most fundamental duty of humans is to leave a habitable world for future generations by protecting nature and all living and non-living things that are part of it from existing dangers (Akbulut & Çobanoğlu 2020).

Among legal systems, there are three main views on whether animals should be accepted as a subject of law, and these are listed as follows (Koçhisarlıoğlu & Erişgin 2013);

- The view that animals are recognized as property (object),
- The view that animals are recognized as person-like,
- The view that animals are recognized as persons.

The view that accepts animals as things (objects) positions animals within the human-centered understanding of environmentalism. In anthropocentric environmentalism, humans are placed at the center of the environment and everything in nature is positioned according to humans. In this understanding, the human being is considered as an entity that is at the top of

the species in a hierarchy, separate from nature, and independent from the natural relations to which other species are connected (Keleş et al. 2012).

The human-centered understanding of environmentalism reveals the justification for the protection of the environment based on human beings. Although the necessity of protecting the environment is emphasized in this understanding, this necessity is not based on a conception of nature that deserves to be protected for its own sake, apart from human purposes. As such, environmental policy based on anthropocentric environmentalism aims to protect only those assets that need to be protected in terms of instrumental values corresponding to human goals. An ecological problem is considered as a policy problem to the extent of the negativities, threats and dangers it poses for human beings. In cases where there is no benefit for human beings, such an environmental policy neither identifies an ecological problem nor resorts to any protective measures (Keleş et al. 2012).

According to those who proceed from this idea, animals should be accepted as goods by legal systems and there is no concept of animal rights. Therefore, it is impossible for animals to be subjects of law (Akbulut & Çobanoğlu 2020).

Today, it is frequently stated that the legal status of animals is not property, in other words, they should not be subject to similar provisions as tables, clothes, automobiles. It is even argued that animals can also have rights within the framework of certain principles (Akbulut & Çobanoğlu 2020).

This view proposes to create a special legal personality for animals instead of recognizing a personality by likening animals to humans as a method to be applied. This is because the characterizations based on the concept of person refer to the animal being the subject of rights, while the characterizations based on the concept of property refer to the animal being the object of rights. In attempts to define animals based on the concepts of "person" and "thing", which are two important concepts of law, animals are referred to with terms such as "person-like" or "atypical thing" (Cumalıoğlu 2017).

The view that recognizes animals as persons is based on theories based on the animal rights approach. It can be said that the animal rights movement emerged as a result of sensitivity towards the suffering of animals. The living conditions imposed on cattle, sheep and poultry in order to obtain more meat, more milk and more eggs in animal farms, the slaughter of lambs in the early period, and the use of animals for sports purposes causing pain to humans (Ünder 1996).

The proponents of this view proceed from the criterion of "suffering" and state that all living beings with a nervous system and a brain can suffer. Since animals, just like human beings, have an interest in not suffering, it is stated that humans and animals have equal rights. According to this understanding, every living being that can enjoy pleasure and feel pain should be recognized as a subject of law, without any distinction between human or animal. Otherwise, if the interests of animals are ignored or deemed insignificant just because they are not of the same species as humans, a racist and sexist logic is adopted (Özgür 2010).

In Turkey, efforts to make a law on the protection of animals were first initiated in the 1980s, and it was not until 2004 that the idea in question was realized. When the historical process is analyzed, while the activities related to stray animals were within the duties and responsibilities of municipalities until 1991, with the establishment of the Ministry of Environment, the responsibility was divided between these two institutions. While the Ministry of Environment was tasked with the preparation of the legal framework, making strategies and plans related to stray animals and supervision issues, the responsibility for the implementation of the law to be enacted was left to the municipalities. In 1995, two separate draft laws of the protection of animals were prepared, one by the General Directorate of Environmental Protection and the other by the State Ministry responsible for human rights, but neither of these two drafts was enacted (Menteş & Osmanağaoğlu 2009). This objective could only be realized with the adoption of the Animal Protection Law No. 5199 on 24.06.2004.

Article 4/1-(a) of the Law states that "All animals are born equal and have the right to live within the framework of the provisions of this Law" and Article 4/1-(b) states that "domestic animals have the freedom to live in the living conditions specific to their species. The lives of stray animals should be supported just like owned animals", and in Article 4/1-(c); "Necessary measures should be taken for the protection, care and care of animals and to keep them away from maltreatment" (Cumalıoğlu 2017). Article 14 of the Law titled "Prohibitions" regulates the acts considered as misdemeanors within the scope of the Law, and these acts include; intentionally mistreating animals, cruel treatment, beating, starving, exposing to extreme heat and cold, neglecting their care, causing physical and psychological pain, forcing animals to perform acts that are clearly beyond their strength, giving animals addictive food or drinks such as alcohol, cigarettes, drugs, distributing animals other than animals raised for slaughter as prizes, bonuses or premiums, and torturing animals.

When evaluated in general, it can be said that in addition to the results that can be perceived as animal rights in Law No. 5199, there are approaches to the continuity of biological and physical phenomena specific to the species of animals in the ecosystem

Similarly, Law No. 5996 on Veterinary Services, Plant Health, Food and Feed published in the Official Gazette No. 27610 dated 13 June 2010 sets out the provisions on the protection and welfare of animals. Article 9 of the Law No. 5996 contains the

following provisions (Anonymous 2010);

(1) Animal owners or persons responsible for animal care are obliged to meet the shelter, care, nutrition, health and other needs of animals in order to ensure animal welfare, and to take the necessary measures against the negative effects that the animals under their responsibility may have on human, animal and environmental health.

Environmental Law (Anonymous, 1983) No. 2872 contains some provisions protecting endangered species. In Article 9/1-(f) of the Environmental Law titled "Protection of the Environment"; "f) In order to ensure the sustainability of biological diversity, it is essential to protect threatened or endangered species and rare plant and animal species and it is forbidden to trade them in violation of the legislation".

Article 181 of the Turkish Penal Code regulates the act of polluting the environment intentionally, in other words, knowingly and willingly, while Article 182 of the Turkish Penal Code regulates the act of polluting the environment negligently. The aforementioned article is as follows (Anonymous 2004);

(1) A person who negligently causes waste or residues to be discharged into the soil, water or air in such a way as to damage the environment shall be punished with a judicial fine. If these wastes or residues leave a permanent effect on soil, water or air, imprisonment from two months to one year shall be imposed.

In the Turkish legal system, it should not be forgotten that it is necessary to develop laws on the protection and rights of animals, to revise the current situation according to new needs and to raise awareness in individuals and wider society within a hierarchical and systematic scientific discipline.

The lexical meaning of the concept of animal;

Şengül (2019) made the definition of the word animal in his thesis as follows; Sahihi is in the meter of "halecân" with the conquest of ya. It belongs to the classification of words in which a vowel drop is seen as the reason for falling into a galat state. Today it is used as an "animal".

Kamus-ı Türkî gives the meaning of "vitality, life, vitality, ab-1 animal, ab-1 hayat".

In the Ottoman-Turkish Encyclopaedic Dictionary, it has four meanings: The first meaning is "vitality". This meaning almost matches the meaning in Kamus-ı Türkî. The second meaning is "living thing" and the third meaning is "all living things, including human beings". These meanings evoke the concept of human being, which is a part of life, and the meaning event of name transfer is experienced with the part-whole relationship. In the fourth meaning, it is clear that the word has expanded its meaning by adding a semantic element in the form of "foolish man".

There are four meanings of the word in the Grand Turkish Dictionary: The first meaning is explained as "a living creature with the ability of feeling and movement, acting with instincts", the second meaning is "mindless, emotionless, rude, harsh (person)", and there is a transition to grammatical meaning by giving the meaning of "mindless, emotionless, rude, harsh (person)". (noun→adjective) by changing the word type (noun→adjective), meaning expansion occurred in the lexeme with the change of live→mindless. The third meaning is "a word said to someone who is angry", which can be considered as an insult. Although slang generally covers the uses of a language outside the written language, we can observe this meaning in the dictionary since these uses are one of the sources that dictionaries feed on in terms of words and meaning. The fourth meaning is stated to mean "a creature used in various services such as horse, donkey, mule".

While scientists have made many definitions concerning animal welfare, it has been emphasized that animals have emotions and the importance of both physical health and mental health.

In the Protocol on the Protection and Welfare of Animals (Amsterdam Treaty 1997), animals are recognized as "sentient beings" (Antalyalı 2007; Ünal 2007).

In an article entitled "An evaluation on the protection and welfare of animals in hadiths" published by Sinmez et al. (2015); there are provisions (albeit in small numbers) about animals in the Torah, Psalms and the Bible that animals have rights as living beings (Armutak 2008a). The fact that seven sūrahs in the Qur'an, which consists of one hundred and fourteen sūrahs, have animal names and deal with animals, and that this constitutes 6.14% of the total of the holy book, is considered among the reasons for the importance given to animals and the compassion shown towards them in the Islamic religion and Islamic societies (Armutak 2008b). According to the above, it is concluded that there are provisions about animals in all divine religions, but more importance is given in Islam and the Qur'an.

Körbalta (2019) in his article, in terms of Turkey's national security, food, environment, economic and social security in the future may threaten this process can be reversed by stopping. Ensuring that water resources are more usable and sustainable in terms of quality is possible through effective environmental management. Within the scope of the presentation of water resources,

which are conserved in terms of quantity and quality, to users, water should be presented as a "human right" without forgetting that water is a basic requirement for life. Therefore, it can be said that water is a fundamental right and need for all living things.

3. Conclusions

In recent years, environmental problems have become one of the most discussed issues in public opinion as the effects of natural events, which are estimated to threaten humanity, are observed. The life of all living things is also endangered in nature whose balance is disturbed. If necessary, precautions are not taken, it is inevitable that water resources will also be affected.

Considering that the majority of people in many countries today face water shortage, it can be observed how important the dimensions of the danger are. Failure to take action and plan accordingly in terms of the efficient use of water as well as ensuring easy access to water now will ensure that we lack the necessary water sources and water availability for the continually growing global population. Therefore, people should be made aware of the importance of protecting the ecological balance with all stakeholders, the necessity of the rights of all living beings to access and use water without discrimination, the necessity of protecting existing water resources, and the understanding of animal welfare and animal rights.

From the point of view of the responsibility and competence of the universe, it should never be forgotten that the rights of each of the living species sharing the world with all their formations should be respected in accordance with their own biological characteristics - balanced - understanding behaviour. We have to be more careful about the cosmos to be bequeathed to future generations. For this reason, the concepts of the right to water, animal welfare, and animal rights should be evaluated in a multidimensional manner with a holistic approach within the framework of equality and respect.

References

- Anonymous (1983). 2872 Sayılı Çevre Kanunu. Retrieved in February, 28, 2023 from <https://www.mevzuat.gov.tr/mevzuatmetin/1.5.2872.pdf>.
- Anonymous (2004). Türk Ceza Kanunu. 181. ve 182. Maddeleri. Retrieved in February, 28, 2023 from <https://www.mevzuat.gov.tr/MevzuatMetin/1.5.5237.pdf>.
- Anonymous (2010). Veteriner Hizmetleri, Bitki Sağlığı, Gıda ve Yem Kanunu (2010):11 Haziran 2010 tarih, 5996 Kanun Numarası ve 27610 Sayılı Resmî Gazete, Tertip: 5, Cilt: 49
- Anonymous (2023a). The Universal Declaration of Human Rights. Retrieved in March, 13, 2023 from <https://www.un.org/en/about-us/universal-declaration-of-human-rights>.
- Anonymous (2023b). United Nations, "International Covenant on Economic, Social and Cultural Rights (PART III)", Retrieved in July, 03, 2023 from <https://www.ohchr.org/en/instruments-mechanisms/instruments/international-covenant-economic-social-and-cultural-rights>.
- Akbulut O & Çobanoğlu N (2020). Türk Hukukunda Hayvanların Korunmasına İlişkin Yasal Mevzuat ve Bu Mevzuata Göre Hayvanların Hukuki Durumları. *Süleyman Demirel Üniversitesi Sosyal Bilimler Enstitüsü Dergisi*, (36): 1-37
- Aksoy T & Çabuk A (2015). Coğrafi bilgi sistemleri kullanılarak küresel ölçekte su kıtlığı yaşanan bölgelerin tespiti. XVII. Akademik Bilişim Konferansları, 4 - 6 Şubat, Eskişehir, pp. 4-6
- Antalyalı A (2007). Avrupa Birliği ve Türkiye’de Hayvan Refahı Uygulamaları. AB Uzmanlık Tezi, T.C. Tarım ve Köyişleri Bakanlığı Dış İlişkiler ve Avrupa Birliği Koordinasyon Dairesi Başkanlığı, Ankara.
- Armutak A (2008a). Yahudi ve Hristiyan dini kutsal kitaplarında hayvan hakları. *İstanbul Üniversitesi Veteriner Fakültesi Dergisi*, 2008a; 34(1): 39-55
- Armutak A (2008b). İslam dini kutsal kitabında hayvan hakları. *İstanbul Üniversitesi Veteriner Fakültesi Dergisi*, 2008b; 34(1): 57-66
- Arslan M & İlgili Ö (2022). Türkiye’de hayvan hakları ve refahı kavramlarının biyoetik yönüne değinen lisansüstü tezler: Nitel araştırma. *Veteriner Hekimler Derneği Dergisi*, 93(2): 133-150
- Şahin B (2016). Küresel Bir Sorun: Su Kıtlığı ve Sanal Su Ticareti. Hitit Üniversitesi, Sosyal Bilimler Enstitüsü İktisat Anabilim Dalı Yüksek Lisans Tezi (Basılı), Çorum.
- Bilen Ö (2008). Türkiye’nin Su Gündemi Su Yönetimi ve AB Su Politikaları, Ankara: DSİ.
- Bilgili A (2021). Sahipsiz Hayvanların Şehir, Çevre ve Halk Sağlığı, Hayvan Sağlığı ve Hayvan Refahı Yönünden Kontrolünde Bakanlıklar Arası İşbirliğinde Karşılaşılan Aksaklıklar ve Çözüm Önerileri. *Icontech International Journal of Surveys, Engineering, Technology. Journal Homepage: Http://icontechjournal.com/Index.Php/İj*
- Birleşmiş Milletler Dünya Su Değerlendirme Programı (DSDP). (2015). The United Nations world water development report: Water for a sustainable world. Paris, UNESCO.
- Çiçek E (2009). Kar mı insan hakkı mı" Bir insan hakkı olarak su hakkının dava edilebilirliği". *Türkiye Barolar Birliği Dergisi* (80): 182-228
- Cumalioglu E (2017). Medeni Hukukta Hayvan Hakları ve Hayvanlar Üzerindeki Hak. *Dokuz Eylül Üniversitesi Hukuk Fakültesi Dergisi*, 19(3): 573-610
- Çulhaoğlu M (2001). Kapitalist Özel Mülkiyetin Karşısında Kamusal Mülkiyetin Temelleri, *Toplum ve Hekim Dergisi*, Cilt 16, Sayı 1, İstanbul, 2001
- DSİ (2017). 2. Ormancılık ve Su Şurası - DSİ Barajlar ve HES Dairesi Raporu. Afyonkarahisar: OSİB. <https://www.hidropolitikakademi.org/uploads/wp/2017/11/ORMANCILIK-VE-SU-%C5%9EURASI-KARARLARI-20173.pdf>.
- Duncan IJH (2002). Poultry welfare: science or subjectivity. *Br Poult Sci* 43: 643-652
- FAO, Food and Agriculture Organization of the United Nations, (2020), "The State of Food and Agriculture", Retrieved in October, 14, 2021 from <http://www.fao.org/3/cb1447en/cb1447en.pdf>.
- Farm Animal Welfare Council (FAWC). 1993. Second Report on Priorities for Research and Development in Farm Animal Welfare. MAFF Tolworth, United Kingdom.
- Fidan E D (2012). Türkiye’de çiftlik hayvanları ile ilgili refah uygulamaları. *Animal Health Production and Hygiene*, 1(1): 39-46.

- Firidin E (2015). Su Sorununun, Su Hakkı ve Su Etiği Çerçevesinde Değerlendirilmesi. *Aksaray Üniversitesi İktisadi ve İdari Bilimler Fakültesi Dergisi*, 7 (2),43-55.
- Fraser D (1999). Animal ethics and animal welfare science: bridging the two cultures. *Applied Animal Behavioural Science* 65: 171–189.
- Gözler K (2010). Anayasa Hukukunun Genel Esasları, Ekin, 2010, s. 77.
- İlhan A (2011). Yeni Bir Su Politikasına Doğru, Türkiye’de Su Yönetimi, Alternatifler ve Öneriler, Sosyal Değişim Derneği, 1. Baskı, Eylül Ofset, İstanbul, 2011.
- Kaboğlu İ (1993). Özgürlükler Hukuku, Alfa, 1993, İstanbul, s.12.
- Karaman S & Gökalp Z (2010). Küresel Isınma ve İklim Değişikliğinin Su Kaynakları Üzerine Etkileri. *Tarım Bilimleri Araştırma Dergisi*, (1): 59-66.
- Kåresdotter E, Skoog G, Pan H & Kalantari Z (2023). Water-related conflict and cooperation events worldwide: A new dataset on historical and change trends with potential drivers. *Science of the Total Environment*, 868: 161555
- Kartal F (2009). Suyun Metalaşması, Suya Erişim Hakkı ve Sosyal Adalet, TMMOB Su Politikaları Kongresi, Ankara, 2009
- Koçhisarlıoğlu C & Erişgin Ö S (2013). Hayvanın hukuki konumu. *Journal of Yasar University* 8: 1691-1723
- Keleş R, Hamamcı C, Çoban A (2012). Çevre Politikası (7. baskı), Ankara: İmge Kitabevi.
- Körbalta H (2019). Türkiye’de yerel su güvenliği. *Güvenlik Bilimleri Dergisi*, 8(1): 55-84
- Küçüksakarya S & Göçmen A H (2019). Suyun ekonomik değeri üzerine bir inceleme. *Anadolu Üniversitesi İktisadi ve İdari Bilimler Fakültesi Dergisi* 20(2): 44-62
- Menteş G A & Osmanağaoğlu Ş (2009). Türkiye’de Hayvanları Koruma Kanununun Tarihsel Gelişimi, *Kafkas Üniversitesi Veteriner Fakültesi Dergisi*, C. 15, S. 3, (s. 325-330), http://vetdergikafkas.org/uploads/pdf/pdf_KVFD_478.pdf, 19.11.2018.
- Muluk Ç B, Kurt B, Turak A, Türker A, Çalışkan M A, Balkız Ö, Gümrükçü S, Sarıgül G & Zeydanlı U (2013). Türkiye’de suyun durumu ve su yönetiminde yeni yaklaşımlar: çevresel perspektif. Ankara: İş Dünyası ve Sürdürülebilir Kalkınma Derneği– Doğa Koruma Merkezi.
- Narin A (2016). Su Hakkı ve Bir Müdahale Aracı Olarak Suyun Özelleştirilmesi. *Türkiye Adalet Akademisi Dergisi*, (27): 729-756
- Neumann J M (2012). The universal declaration of animal rights or the creation of a new equilibrium between species. *Animal L Rev* 2012; 19(91): 91-109
- OECD (Organisation for Economic Co-operation and Development). OECD Environmental Outlook to 2050: The Consequences of Inaction. Paris, OECD Publishing. <http://dx.doi.org/10.1787/9789264122246-en>
- OHCHR, The Right to Water, The Human Rights Fact Sheet no.35, UN High Commissioner for Human Rights (2010). Retrieved in April, 12, 2017 from <http://www.ohchr.org/Documents/Publications/FactSheet35en.pdf>.
- Özgür A (2010). Hayvanlarla Yaşamı Paylaşmak, Veteriner Hekimler Derneği Dergisi, C. 81, S. 2, s. (9-13)
- Özsoy S (2009). Su ve yaşam: suyun toplumsal önemi. Yüksek Lisans Tezi, Ankara Üniversitesi, Ankara.
- Phillips C J C & Kluss K (2018). Chapter 20-animal welfare and animal rights. In: Scanes CG, Toukhsati SR, editors. *Animals and human society*. 1st ed. Amsterdam: Academic Press. Elsevier Inc; 2018. pp. 483-497
- Savaş T, Yurtman İ Y & Cemil T (2009). Hayvan hakları ve hayvan refahı: Felsefi bakış-nesnel arayışlar. *Hayvansal Üretim*, 50 (1)
- Savenije H H G (2002). “Why Water Is Not An Ordinary Economic Good, Or Why The Girl Is Special”, *Physics And Chemistry Of The Earth*, S.27, ss.741-744
- Sinmez Ç Ç, Arıcan M K & Yaşar A (2015). Hadislerde hayvanları koruma ve gönenci (refahı) üzerine bir değerlendirme. *Erciyes Üniversitesi Veteriner Fakültesi Dergisi*, 12(2): 115-121
- Sinmez Ç Ç (2022). Dünyada ve Türkiye’de Hayvan Haklarının Anayasal Konumu. *Harran Üniversitesi Veteriner Fakültesi Dergisi*, 11(1):51-57.
- Şengül İ (2019). Sırrı Paşa'nın Galatat adlı eseriyle İbn-i Kemal'in Galatatü'l-Avam adlı eserinin tercümesinin anlamsal bakımdan karşılaştırılması. Yüksek lisans tezi, İstanbul Üniversitesi, İstanbul.
- Şirin T (2010). Suyun İnsan Hakkı Olarak Değeri. *Marmara Üniversitesi Hukuk Fakültesi Hukuk Araştırmaları Dergisi*, 16(3-4): 85-168
- TEMA (2021). “Su Bütçesi”. Retrieved in October, 14, 2021 from <https://sutema.org/mavi-gezegen/su-butcesi.3.aspx>.
- Temmuz G (2017). Neoliberal Politikaların Küresel Düzeyde Sağlık Üzerindeki Etkileri. *Anadolu Üniversitesi Sosyal Bilimler Dergisi*, 17(1): 159-178
- Thorpe W H (1965). The assessment of pain and distress in animals. Appendix III in report of the technical committee to enquire into the welfare of animals kept under intensive husbandry conditions, F.W.R. Brambell (chairman). H.M.S.O., London.
- Tomanbay M (2008). Dünyada Su ve Küresel Isınma Sorunu, Phoenix Yayınları, Ankara.
- Topçu E (2009). “Bir İnsan Hakkı Olarak Su Hakkı”, 2009, Ankara, s. 9.
- Ulunmak A (2014). Türkiye’de su yönetimi. Yüksek Lisans Tezi, Ankara Üniversitesi, Ankara.
- Ulusal Su Planı, (2019-2023). T.C. Tarım ve Orman Bakanlığı Ulusal Su Planı (2019-2023). <https://www.tarimorman.gov.tr/SYGM/Belgeler/NHYP%20DEN%C4%B0Z/ULUSAL%20SU%20PLANI.pdf>.
- UNDP Turkey (2023). “Clean Water and Sanitation”, Retrieved in July, 06, 2023 from. <https://www.undp.org/sustainable-development-goals/clean-water-and-sanitation>.
- UNDRR (United Nations Office for Disaster Risk Reduction) (2021). “Special Report on Drought 2021”. Retrieved in October, 14, 2021 from <https://www.undrr.org/media/49386/download>.
- United Nations Water (2021). “Summary Progress Update 2021: SDG 6 — water and sanitation for all”. Retrieved in October, 14, 2021 from <https://www.unwater.org/publications/summary-progress-update-2021-sdg-6-water-and-sanitation-for-all/>.
- Ünal N (2007). Hayvan Refahı Ders Notları. Ankara Üniversitesi Veteriner Fakültesi Zootekni Anabilim Dalı, Ankara.
- Ünder H (1996). Çevre Felsefesi, Ankara: Doruk Yayınları.
- Ünlü E (2017). Avrupa Birliği müzakere sürecinde Türkiyede içilebilir su yönetimi politika analizi. Master's thesis, İzmir Katip Çelebi Üniversitesi, İzmir.
- WHO (World Health Organization) (2021). “Water, health and ecosystems”. Retrieved in October, 14, 2021 from <https://www.who.int/heli/risks/water/water/en/>.





Determination of Van Basin Groundwater Potential by GIS Based, AHP and Fuzzy-AHP Methods

Veysel ASLAN^a 

^aHilvan Vocational High School, Department of Construction Technology, Harran University, Sanliurfa, TURKIYE

ARTICLE INFO

Research Article

Corresponding Author: Veysel ASLAN, E-mail: vaslan@harran.edu.tr

Received: 05 January 2023 / Revised: 05 June 2023 / Accepted: 15 July 2023 / Online: 09 January 2024

Cite this article

Aslan V (2024). Determination of Van Basin Groundwater Potential by GIS Based, AHP and Fuzzy-AHP Methods. *Journal of Agricultural Sciences (Tarim Bilimleri Dergisi)*, 30(1):47-60. DOI: 10.15832/ankutbd.1229799

ABSTRACT

Global warming and climate change put excessive pressure on the use of groundwater resources. As the demand for water consumption in fields such as agriculture and industry increases worldwide, the need for the modeling and evaluation of groundwater potential and quality efficiency increases accordingly. Nowadays, methods based on multi-criteria decision-making techniques such as geographic information systems (GIS), analytical hierarchy process (AHP), fuzzy analytical hierarchy process (F-AHP) and ELECTRE have begun to be used rapidly in the field of groundwater. These methods are of great importance because they reveal information faster. They are also a tool for the communication and meaning of information. In the light of this information, this study was carried out in order to model and evaluate the groundwater potential and quality of Van, Türkiye. In order to evaluate the groundwater potential of the Van province basin, remote sensing data with AHP and Fuzzy AHP methods, which are GIS-based MCDM programs, were used. Eight

thematic maps such as precipitation, slope, soil texture, land use/land cover, geology, geomorphology, drainage density, drainage density and fault density were created. These thematic parameters were graded and weighted in the AHP method according to their effects on the groundwater potential. Then, five different groundwater recharge potential regions were classified as very good (8%), good (17%), moderate (43.37%), poor (23.03%) and very poor (9.6%). The evidence obtained by validating the results is in line with flow calculation studies showing that groundwater flows from the south to the northeast, middle and north to the southwest of the basin. The evidence obtained by validating the results is consistent with the flow calculation values showing that the groundwater basin flows from south to northeast, center and north to southwest of the study area. The validation shows that the method applied for the study area gives a meaningful and reliable result.

Keywords: AHP, Fuzzy-AHP, GIS, Groundwater Potential, MCDM

1. Introduction

Groundwater, one of nature's most valuable resources, is found in underground rocks, sediments, cracks and pore spaces. This groundwater plays an important role in economic growth as well as human welfare and maintaining the ecological balance (Zekai 2008; Naghibi et al. 2015). About 30% of the fresh water in the world is groundwater, of which only 0.3% is surface water, lakes, marshes, reservoirs and rivers (Senanayake et al. 2016). Rainwater seeping into the aquifer through soil pores and snowmelt are the two main sources of groundwater. The consumption of groundwater is more dependable and fresher than that of surface waters since it is more practical and less prone to pollution. Groundwater, which is more reliable and pure than surface water, has emerged as a global concern in the last century as the demand for fresh water increased with rapid industrialization and population growth (Manap et al. 2014). For this reason, groundwater extraction is crucial for water management and planning, particularly in rural areas (Das & Pardeshi 2018). In order to build a large irrigation system that uses sustainable resources, it is crucial to identify any possible groundwater locations. Groundwater formation in the region might be referred to as prospective groundwater in terms of groundwater exploration (Pathak 2017).

Although there is not enough groundwater in the world, excessive consumption and uncontrolled water use cause a further decrease in groundwater. Remedial procedures at the national, regional, and local levels should therefore be identified in advance and then used in order to ensure the sustainability and protection of groundwater and surface waters.

Groundwater movement; Lithological variation is defined by topographic condition, slope, geology, precipitation patterns, soil texture, etc., through soil pores (Mallick et al. 2014). This knowledge is an important link between the conservation and management of regional, national and international biodiversity, and the extensive exploration of local water resources. The use of Remote Sensing (RS) and Geographical Information System (GIS), which are powerful tools, is very valuable in determining possible groundwater potential regions of arid and semi-arid regions (Rahmati et al. 2015). Analytical Hierarchy Process (AHP),

which is one of the multi-criteria decision-making methods in various fields such as water, natural resources method, environmental impact analysis and regional planning, is widely used as well as being applied effectively (Rahaman et al. 2015).

In multiple data set analysis, the geometric mean of the parameters and the comparison matrix AHP technique is used in normalized weight calculation (Chowdhury et al. 2010).

The Van basin depends on groundwater, which is a reliable and vital natural water source. Currently, groundwater constitutes the majority of the city's annual water demand for agricultural, domestic and industrial needs. In addition to the rapid population growth, the excessive water demand of sectors such as agriculture, industry, and tourism poses a significant problem for the city of Van (DSI (State Hydraulic Works) 2015).

There are not many studies on the determination of potential groundwater resources in Van province. Therefore, this study provides a broader view of the potential groundwater distribution of the basin by using multi-criteria decision analysis (MCDA) and other variables in the evaluation of groundwater potential regions (Aslan & Celik 2021).

AHP, one of the multi-criteria decision making techniques, has been widely used by Saaty in the field of water resources engineering. In various water resource management studies, the AHP method has been successfully applied by integrating it with MCDA, RS and GIS techniques (Machiwal et al. 2011; Pinto et al. 2017).

For this reason, GIS supported AHP and Fuzzy-AHP methods were used to evaluate the groundwater potential resources of the Van basin and to integrate parameters such as hydrogeology, geology, geomorphology, soil texture, drainage density, and LU/LC. In addition to ensuring optimum and sustainable development and management of this critical groundwater resource, the purpose of designing potential sites is to develop a guide map for prospective groundwater exploration/operation (Das & Pardeshi 2018). Technologies such as remote sensing and GIS supported, AHP, TOPSIS, Fuzzy - AHP methods can be used with relatively accurate results in determining groundwater regions to solve the problems (whether there is groundwater or not). With these methods, it is possible to determine the boundaries of high potential regions in accessible areas.

2. Material and Methodology

2.1 Location and hydro-meteorology of the study area

The drainage area (17861.2 km²) of Lake Van basin (The study area is located between 42° 40' and 44° 30' East longitudes and 37° 43' and 39° 26' North latitudes) was calculated using GIS. The land surface area of the basin excluding the lakes is 14101.4 km² (Ozler 2005). In the Van basin, transitional climate characteristics are observed between the continental climate of the Central Anatolia and Southeastern Anatolia regions and the Mediterranean climate. In terms of temperature, the degraded type of the Mediterranean climate is dominant. The main factor of this climate change (humidity and precipitation) is Lake Van. According to the Thiessen Polygons Method, the annual average precipitation in the basin is 447.29 mm (Konyar et al. 2019). Van basin location map is shown in Figure 1.

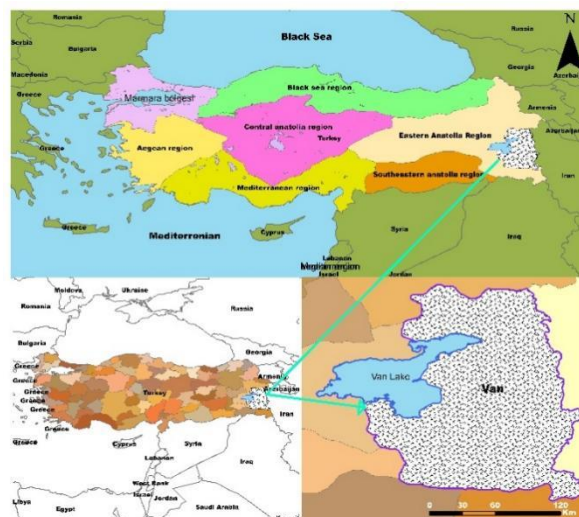


Figure 1- Van Basin Location Map

There are sedimentary, magmatic and metamorphic rocks formed from the earliest times to the present in the study area. Generally, metamorphic rocks belonging to the Bitlis Massif in the south of the basin, volcanic and volcanic rubber rocks that

are the products of the young Nemrut and Suphan Mountains in the west and north, volcanic rocks belonging to the Yuksekova Complex and ophiolite components, current fluvial and lacustrine fragments and carbonates crop out in the east (Erdogan 2017).

2.2 Establishment of geographical data for the groundwater potential assessment of the basin

In the study, the Fuzzy Analytical Hierarchy Process (F-AHP) and Remote Sensing supported GWPI region mapping method were used along with ArcMap 10.2 program software (Jesiya & Gopinath 2020).

In the Van basin study, hydrological, anthropogenic and geological factors were taken into account, as well as expert opinions, field observations and literature reviews in evaluating the groundwater potential. Factors such as slope, geology, and geomorphology are considered geological elements. Data such as fault density, drainage density, land use/land cover, topographic class, current aquifer status and proximity to water bodies were evaluated as anthropogenic features (Akter et al. 2020; Jesiya & Gopinath 2020). Thematic data such as geology, aquifer (hydrogeology) and soil type were obtained by digitizing in Arcmap 10.2 software. The 1:50,000 scale drainage density map of the Van Basin was taken from the 17th Regional Directorate of State Hydraulic Works. Linear density analysis was performed to prepare the lineament and drainage density in km² (Kumar et al. 2016; Akter et al. 2020; Jesiya & Gopinath 2020). The map in Figure 2 was produced by Aslan & Çelik (2021), inspired by the groundwater potential mapping study with geographical information techniques for a sustainable environment in the Haliliye basin (Aslan & Çelik 2021). These 8 parameters considered in the ArcMap environment were first converted into raster thematic maps and then into reclassified maps. Finally, the groundwater potential index distribution map was produced (Figure 2).

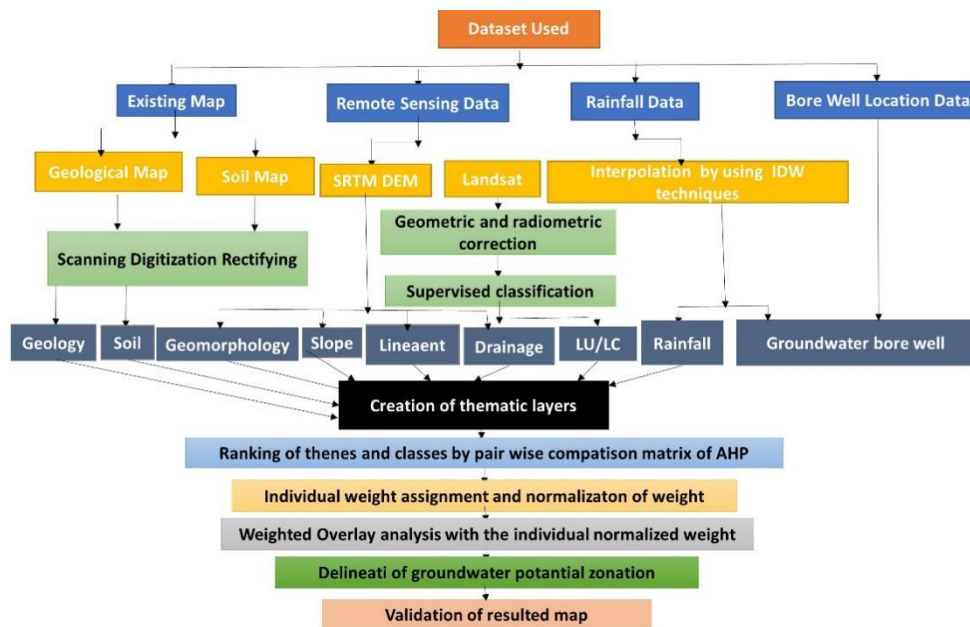


Figure 2- Hierarchical flow chart for groundwater potential area mapping of Van basin (Aslan & Celik 2021)

2.3 AHP method

The AHP method is an approach that evaluates Saaty's criteria in a certain order (according to the effects of parameters on groundwater), evaluates the weights of these criteria, compares the alternatives according to the criteria and provides ranking (Ozder et al. 2021; Munier & Hontoria 2021). The AHP method, which is based on three basic principles such as problem solving process decomposition, comparative judgments and synthesis of priorities, is a systematic approach that determines and represents the priority status of its multi-criteria elements in an order (Parameters or criteria) (Fedrizzi et al. 2018; Ly et al. 2018). Based on expert opinion through pairwise comparisons, the AHP method is widely used in situations such as setting priorities, reducing problem complexity, simplifying and planning decisions, choosing the best alternative, allocating resources, and conflict resolution (Samuel et al. 2017; Fattahi & Khalilzadeh 2018; Ozder et al. 2021). In pairwise comparison matrices, when comparing two criteria in relation to each other and each binary alternative according to any criteria, questions such as which one is more important and how important it is are asked (Di Bona et al. 2017). The implementation stages of AHP can be listed as follows (Pinto et al. 2017; Xingfeng 2017; Patra et al. 2018; Wang 2020);

Stage 1: Establishment of the Model and Formation of the Problem: In the AHP approach, quantitative and qualitative factors affecting the decision process are determined by conducting a survey or consulting expert opinions. As a result of the information obtained, a hierarchical structure is created by determining the criteria, sub-criteria and alternatives (Ozder et al. 2021).

Stage 2: Creating the Pairwise Comparisons Matrix: After the hierarchical structure is created, the data are collected using the pairwise comparisons scale in Table 1 and the paired comparisons matrix is obtained (Ozder et al. 2021).

Table 1- Importance level scale (Ozder et al. 2021)

<i>Importance level</i>	<i>Definition</i>
1	Equally important
3	Moderately important
5	Strongly important
7	Very strongly important
9	Definitely important

Stage 3: Determination of Criterion Weights and Scores of Alternatives: using pairwise comparison matrices, the weight of each decision alternative is calculated and accordingly, the matrix is normalized by dividing each column in the comparison matrix by the total column with its value. In the normalized matrix, the total value of each column is 1 and the eigen vectors are obtained by finding the average of the values in the row (Table 1).

Stage 4: Calculating Consistency Ratio: The following formulas were used to calculate the Eligibility Ratio (CI).

$$CI = \frac{\lambda_{\max} - n}{n-1} \quad (1)$$

In the formula, the CI Conformity Index is the largest eigenvalue in the λ_{\max} matrix, where n is the number of elements in each matrix.

The Conformity Ratio (CR) is obtained by dividing the consistency index by the Random Index (RI) corresponding to the matrix of the same size;

$$CR = \frac{CI}{RI} \quad (2)$$

The random index table made for matrices of different sizes is in Table 2 (Saaty 2000).

Table 2- Randomness indexes (Saaty 2000)

<i>N</i>	<i>1</i>	<i>2</i>	<i>3</i>	<i>4</i>	<i>5</i>	<i>6</i>	<i>7</i>	<i>8</i>	<i>9</i>	<i>10</i>	<i>11</i>	<i>12</i>	<i>13</i>	<i>14</i>	<i>15</i>
RI	0.00	0.00	0.60	1.00	1.10	1.20	1.30	1.40	1.50	1.50	1.50	1.60	1.60	1.60	1.59

2.4 Fuzzy AHP

The Fuzzy AHP method is an effective tool that combines the fuzzy logic approach with the AHP method, and with this aspect, it cannot be digitized with precise data, and is an effective tool in decision-making processes where uncertainty and relativity are high. The decision maker is asked to verbalize his personal evaluation while determining of criterion weights. With this aspect, it is a more realistic evaluation method (Tu et al. 2020; Chaudhry et al. 2021). The ranking of alternatives is accomplished by means of linguistic variables. Each linguistic variable has a corresponding fuzzy logic. Equivalents of these expressions are triangular membership functions. There are 3 parameters that define the triangular membership function. If these parameters are taken as l, m, u, the components and shape of the triangular membership function are given below (Figure 1);

$$\mu_a(x; l, m, u) = \begin{cases} 1 \leq x \leq m & \text{if } \frac{(x-l)}{(m-l)} \\ m \leq x \leq u & \text{if } \frac{(u-x)}{(u-m)} \\ x > u \text{ or } x < l & \text{if } 0 \end{cases} \quad (3)$$

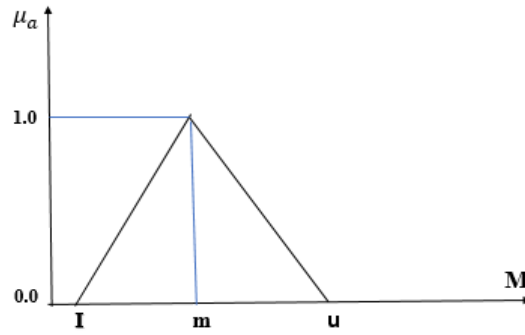


Figure 1- Triangle Membership Function (Ahirwar et al. 2021)

A triangular fuzzy number with A=1 is defined as the vertex m, and m need not be the midpoint between l and u (Mallick et al. 2019; Ahirwar et al. 2021; Singh et al. 2021). Fuzzy AHP steps (Sener et al. 2018; Tiri at al. 2018);

Step 1: The verbal comparison matrix between the criteria is obtained by using the fuzzy numbers given in Table 3 (Equation 4). At this stage, for a problem where k decision makers evaluate n criteria, the fuzzy comparison matrix for each k decision maker is defined as follows (Chai & Wei 2001).

Table 3- Verbal expressions and fuzzy triangular number equivalents in fuzzy AHP (Kaplan & Arikan 2012)

Language scale in order of importance	Triangular fuzzy scale	Triangle fuzzy mutual scale
Just equal	(1, 1, 1)	(1, 1, 1)
Equally important	(1/2, 1, 3/2)	(2/3, 1, 2)
Weakly more important	(1, 3/2, 2)	(1/2, 2/3, 1)
Strongly more important	(3/2, 2, 5/2)	(2/5, 1/2, 2/3)
Much more strongly important	(2, 5/2, 3)	(1/3, 2/5, 1/2)
Very much more strongly important	(5/2, 3, 7/2)	(2/7, 1/3, 2/5)
Definitely more important	(3, 7/2, 9/2)	(2/9, 1/5, 1/3)

In this comparison matrix, the expression d_{ij}^k is the i of the decision maker k . criterion j . is the fuzzy triangular number corresponding to the verbal pairwise comparison with the criterion.

$$A^k = \begin{bmatrix} \tilde{d}_{11}^k & \tilde{d}_{12}^k & \dots & \tilde{d}_{1n}^k \\ \tilde{d}_{21}^k & \dots & \dots & \tilde{d}_{2n}^k \\ \dots & \dots & \dots & \dots \\ \tilde{d}_{n1}^k & \tilde{d}_{n2}^k & \dots & \tilde{d}_{nn}^k \end{bmatrix} \tag{4}$$

Step 2: If the number of decision makers is K, these values are averaged. According to this;

$$d_{ij}^{\sim} = \frac{\sum_{k=1}^K d_{ij}^k}{K} \tag{5}$$

The averaged matching matrix can be represented as follows.

$$A = \begin{bmatrix} d_{11}^{\sim} & \dots & d_{1n}^{\sim} \\ \vdots & \ddots & \vdots \\ d_{n1}^{\sim} & \dots & d_{nn}^{\sim} \end{bmatrix} \tag{6}$$

Step 3: The geometric mean of the fuzzy triangle numbers given for each criterion is found (Li, & Li 2009; Das 2017).

$$r_i^{\sim} = \left(\prod_{j=1}^n d_{ij}^{\sim} \right)^{\frac{1}{n}}, \quad i = 1, 2, 3, \dots, n \tag{7}$$

Step 4: The value of each criterion, whose fuzzy weights are given, is calculated as follows (Senko 2018).

$$W_i \sim = \oplus (r_1 \sim \oplus r_2 \sim \oplus r_n \sim)^{-1} = (lw_i, mw_i, uw_i) \quad (8)$$

Step 5: The fuzzy \tilde{w}_i values are clarified with the help of the formula below.

$$M_i = \frac{lw_i + mw_i + uw_i}{3} \quad (9)$$

Step 6: In the last step, the M_i value is normalized (Hossain & Thakur 2020).

$$N_i = \frac{M_i}{\sum_{i=1}^n M_i} \quad (10)$$

3. Results

3.1 Generating Raster and Classification Lines with GIS Program

Firstly, raster maps of the parameters of precipitation, slope, soil texture, land use/land cover, geology, geomorphology, drainage density, drainage density and fault density to be used in the study were produced. Later these maps have been reclassified.

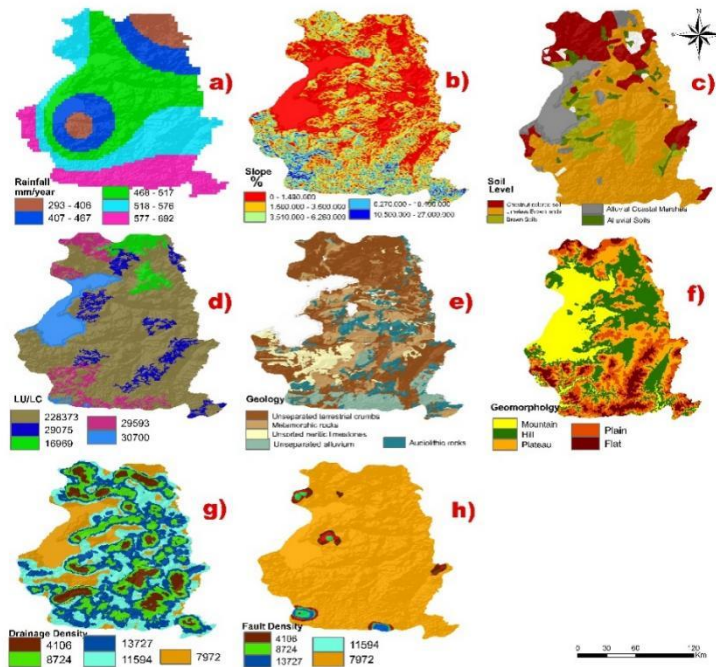


Figure 3- Groundwater thematic (a. Rainfall, b. Slope, c. Soil, d. Land Use/Land Cover, e. Geology, f. Geomorphology, g. Drainage Density, h. Fault Density) maps of the Van province basin

Rainfall: the most important parameter that ensures groundwater formation by filtration of the soil. As seen in Figure 3a, 41.23% of the Van basin has a maximum precipitation rate of 468-517 mm/year and approximately 21% has a maximum precipitation rate of 577-698 mm/year. Only 6% of the area has a precipitation rate of 293-408 mm/year (Figure 3a).

Slope: an effective parameter in obtaining the groundwater potential. In the parts where the slope is low, the flow of precipitation waters to the surface will be low and the underground infiltration will be high. This is an effective parameter in obtaining the groundwater potential. In places where the slope is low, the flow of precipitation waters to the surface will be low and underground infiltration will be high. Figure 3b shows that in about 35% of the basin the slope is 15% and close to 30% is above 30% (Figure 3b)(Batelaan & De Smedt 2001).

Soil Texture: like other parameters, soil also allows precipitation to infiltrate underground, and the rate and amount of infiltration varies according to the grain structure (groundwater infiltration is more in coarse-grained porous structures, infiltration is slower and less in fine-grained soils such as clay), and porosity in groundwater movement and recovery. The parameter in which permeability plays an important role is soil. Approximately 10% of the Van basin is chestnut colored soil, 52% limesless brown lands, 9% brown lands, 12% alluvial coastal marshes and 3% alluvial soils soil (Figure 3c).

Land Use: an important parameter for groundwater formation and is directly related to the infiltration of precipitation into the soil. Due to urbanization, low leakage and high surface flow rate, and wetlands and water bodies are considered to have the highest evaluation scores. Irrigated farmland also has high infiltration of water into the soil, and there is a high rate of seepage in plant areas, partly in the form of land, because the runoff is blocked by the fields.

Geology: an important parameter and seen in Figure 3e, is important in terms of reflecting the aquifer status showing the storage of groundwater. The proportion of unweathered terrestrial clastics in the basin is approximately 41%, and metamorphic rocks are at the highest level with 24%. The water holding capacity in these formations is not very high. Unsorted neritic limestones in the region are 21% and their water holding capacity is quite high (Figure 3e).

Geomorphology: (Figure 3f) the geomorphology map is the map describing the mountains, hills, plateaus, plains and plains in the basin. It states that the flat part of the basin has the highest groundwater potential and the lowest part of the groundwater is in the mountainous areas. The flat part of the field is approximately 39%, the plain 30%, the plateau 17%, the hill 10%, and the mountainous area 4% (Figure 3f) (Celik 2019).

Drainage Density: Affects groundwater potential and quality. It is also the reason for the decrease in the flow rate of water (Singh et al. 2018). For this reason, the performance coefficient of the ratios with low drainage density was taken as a higher value and the drainage density is mostly seen as low in the Van province basin (Figure 3g).

Fault Density: has a geological feature that shows the effect of precipitation on the ground. Feeding is more common in underground fractured areas. Although the cracked areas create discontinuity between the regions, they allow the precipitation to be fed to the underground aquifers in a shorter time. In areas with high lineament density, groundwater recharge is greater; in regions with low density, groundwater recharge is low (Magowe 1999). There is fault density in almost all of Van province (Figure 3h).

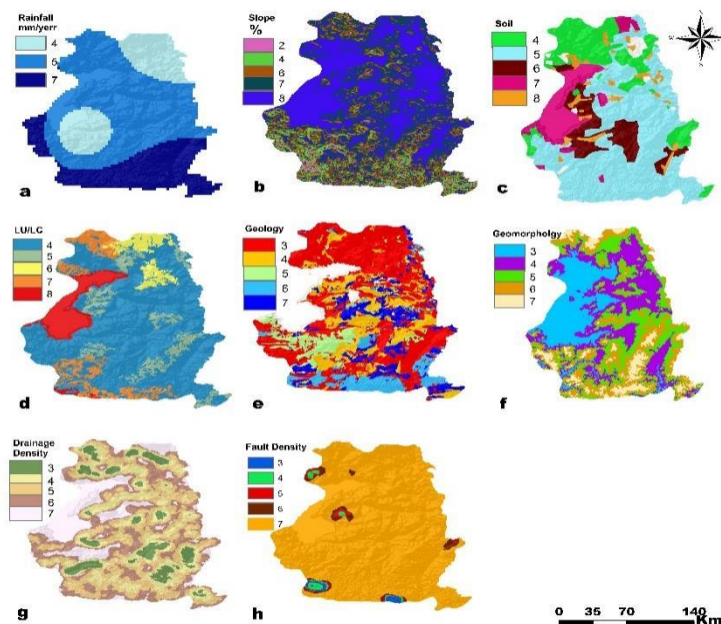


Figure 4- Van province basin groundwater classified (a. Rainfall, b. Slope, c. Soil, d. Land Use/Land Cover, e. Geology, f. Geomorphology, g. Drainage Density, h. Fault Density) maps

Rainfall (precipitation): in the Reclassify environment, the precipitation parameter is divided into 3 classes. Here, the best region is the area that scored 7 points and covers the south of the basin. The weakest part of the basin, rated as 4, is the north-eastern part of the city, which corresponds to the Siverek district (Figure 4a).

Slope: slope data is divided into 5 classes in ArcToolbox → Spatial Analyst Tools → Reclass → Reclassify table due to both visibility and ease of calculation. The lowest value obtained in this table received 1 point and the highest value received 5 points (Figure 4b).

Soil Texture: in this classification, the best area of the basin in terms of soil is the orange- colored areas (5), the weakest region of the basin, which was evaluated with 8 points, was the northern part, which received 4 points (Figure 4c).

Land Use/Land Cover: This parameter is divided into 5 classes in the reclassification table. According to the result in the basin, it is the red colored area in the western region, which received 8 points. The weakest area is the 4-dot blue areas (Figure 4d).

Geology: this parameter is also divided into 5 classes, and the parts evaluated with dark blue and evaluated with 7 points. The weakest part is the red area, which is evaluated with 3 points (Figure 4e).

Geomorphology: is divided into 5 classes in Spatial Analyst Tools → Reclassify → Reclassify environment. In the classification, burgundy-colored (4) and almost the middle part of the basin is the most productive (in terms of groundwater) area. The yellow-colored (7) is weak in the southern parts of the basin, and the weakest part is the blue part in the west of the basin (Figure 4f).

Drainage Density: This parameter is divided into 5 classes. The most valuable part of the basin in terms of drainage density receives 7 points, while the weakest part is the region with 3 points (Figure 4f).

Fault Density: Like other parameters, this parameter is divided into 5 classes. While the yellow area in the basin, which has 7 points and covers almost the entire region, is the weakest region, the region with 3 points is the best region in terms of high groundwater potential (Figure 4h).

3.2 Application of the AHP method

After these 8 parameters used in the AHP method were graded according to their effects on the groundwater potential and quality, the application of the AHP method could begin.

The precipitation used in the study was accepted as the most important parameter and was weighted with 9 points from the values from 1 to 9 in Table 1. When the slope is low, it is easier and more for precipitation waters to seep into the ground (In other words, in areas with low slope, the soil allows rainwater to seep underground). The higher the slope, the easier it is for precipitation water to disperse and the harder it is for the water to seep into the ground. Therefore, the slope parameter was scored as 7 (at 1-9) from the values given in Table 1. The remaining 5 parameters were graded according to their impact on groundwater and used in the AHP method (Saaty 2000).

In line with Saaty's suggestions in the AHP method, 8 parameters to be used in the study were graded according to their effects on groundwater potential and quality and implemented (Table 4).

Table 4- Pairwise comparison matrix table of eight thematic data selected in the study

Criteria	Assigned Weight	Rainfall	Slope	Soil Type	LU/LC	Geology	Geomorphology	Drainage Density	Fault Density
k ₁	9	1.000	1.125	1.286	1.286	1.600	1.600	1.800	2.250
k ₂	8	0.940	1.000	1.143	1.143	1.333	1.333	1.600	2.000
k ₃	7	0.880	0.875	1.000	1.000	1.167	1.167	1.400	1.750
k ₄	7	0.760	0.875	1.143	1.000	1.167	1.167	1.400	1.750
k ₅	6	0.710	0.750	0.857	0.857	1.000	1.000	1.200	1.200
k ₆	6	0.650	0.750	0.857	0.857	1.000	1.000	1.200	1.200
k ₇	5	0.530	0.625	0.714	0.714	0.833	0.833	1.000	1.000
8 ₈	4	0.410	0.500	0.571	0.571	0.667	0.667	0.800	1.000
Total		5.880	6.500	7.571	7.428	8.867	8.867	10.40	12.40

Table 5 contains the criteria ranges according to Table 4. For example; In the process performed here, the first and second... eighth columns are completed by dividing the first weight by the total weight, then dividing the second weight by the total weight, starting from the first column.

"Then the values in the rows are summed to calculate the normalized weight. The Geometric Average is also obtained by dividing each of these summed values by eight (total number of parameters)."

Table 5- Normalizing and geometric averaging of selected layers

Criteria	Rainfall	Slope	Soil Type	LU/LC	Geology	Geomorphology	Drainage Density	Fault Density	Geometric Mean	Normalized weight
k ₁	0.170	0.154	0.169	0.173	0.180	0.180	0.173	0.181	0.1725	1.380
k ₂	0.159	0.145	0.151	0.154	0.150	0.150	0.154	0.162	0.1531	1.223
k ₃	0.149	0.135	0.132	0.135	0.132	0.132	0.135	0.141	0.1364	1.091
k ₄	0.129	0.117	0.151	0.135	0.132	0.132	0.135	0.141	0.1340	1.072
k ₅	0.121	0.109	0.113	0.115	0.113	0.113	0.115	0.097	0.1120	0.896
k ₆	0.111	0.100	0.113	0.115	0.113	0.113	0.115	0.097	0.1096	0.877
k ₇	0.090	0.092	0.094	0.096	0.094	0.094	0.096	0.081	0.0921	0.737
8 ₈	0.069	0.077	0.075	0.077	0.075	0.075	0.077	0.081	0.0664	0.531

Finally, the following values are obtained by following the formulas in the AHP method.

$$\text{Average } \lambda_{\max} = \frac{\sum(\text{Normalized weight})/(\text{Geometric Mean})}{8} = 8.12$$

In the last step, the CR value is calculated as follows. The fact that the value of CR is less than 0.1 in AHP applications shows that the application is consistent, otherwise the process should be reviewed again (Saaty 2000).

$$\text{Consistency Index (CI)} = \frac{8.12 - 8}{7} = 0.01714$$

$$\text{CR} = \frac{\text{CI (Consistency Index)}}{\text{Randomness Indicator}} = \frac{0.01714}{7} = 0.01224 < 0.1$$

Since the result is < 0.1 , it is within the limits of agreement.

Table 6 was created after the raster thematic map of eight parameters was created in the GIS environment. Aslan and Celik (2021) examined the groundwater of the Harran Plain basin and mapped their modeling with the GIS supported AHP method. In addition, they created a groundwater database with the maps they obtained. Table 6 was created by considering this study (Aslan & Celik 2021).

Table 6- Details of layer properties and ordering properties and normalized weights

Sequence	Layer	Weighting	Normalized total weight	Sub-Feature	Field Cover	Groundwater Potential zone	Evaluation	Sum of normalized weight of soil is not 100
1	Rainfall	9	3411	Brown field	257	Very very poor	3	%08
				Dark blue field	577	Very poor	4	%17
				Green field	1139	Very poor	4	%33
				Blue field	846	Poor	5	%24
				Purple field	592	Moderate	6	%18
2	Slope	8	129795	The slope is too low	1931	Very good	7	%01
				The slope is low	8557	Good	6	%07
				Moderate slope	21525	Moderate	5	%17
				High slope	42802	Poor	4	%33
				The slope is too high	54980	Very poor	2	%42
3	Soil	7	120442	Chestnut colored soil	60297	Very poor	3	%5
				Limeless Brown lands	5097	Poor	4	%04
				Brown Soils	35934	Poor	5	%30
				Alluvial Coastal Marshes	228	Moderate	6	%02
				Alluvial Soils	18886	Good	7	%16
4	LU/LC	7	334710	Blue field	228373	Good	7	%68
				Green field	29075	Good	6	%8
				Red field	16969	Moderate	5	%5
				Purple field	29593	Poor	4	%9
				Brown field	30700	Very poor	3	%10
5	Geology	6	38652	Unseparated terrestrial crumbs	519	Poor	2	%1
				Metamorphic rocks	4698	Poor	3	%12
				Unsorted neritic limestones	6954	Moderate	5	%18
				Unseparated alluvium	7080	Good	7	%19
				Audiolithic rocks	19401	Very good	9	%50
6	Geomorphology	6	129765	Mountain	26742	Poor	3	%21
				Hill	36088	Poor	4	%28
				Plate	32908	Moderate	5	%25
				Plain	23057	Good	6	%18
				Flat	10970	Good	6	%8
7	Drainage Density	5	46123	Brown area	4106	Very poor	3	%9
				Green area	8724	Poor	4	%19
				Blue area	13727	Moderate	5	%30
				Turquoise area	11594	Good	6	%25
				Light brown area	7972	Very good	7	%17
8	Fault Density	4	42468	Blue area	455	Poor	7	%1
				Green area	447	Poor	6	%1
				Red area	794	Moderate	5	%2
				Brown area	2788	Very good	4	%7
				Orange area	37984	Good	3	%89

3.3 Distribution of the groundwater potential evaluation map of the region

Groundwater potential index distribution map was produced in the ArcMap environment with 8 parameters (precipitation, slope, soil, land use/land cover, geology, geomorphology, drainage density, fault density). As seen in Figure 5, these data were classified

and weighted according to the values obtained in the AHP method and a precise map of the groundwater potential zone (GWPZ) was created (Dilekoglu & Aslan 2022).

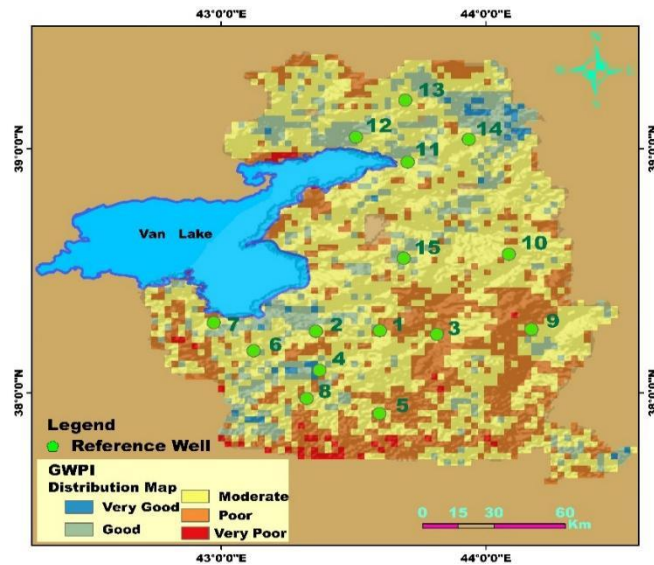


Figure 5- Groundwater Potential Area Distribution Map (GWPI_Zone)

As seen in Figure 5, the distribution values of the Groundwater Potential are between 406 and 683. According to the figure, it can be said that the groundwater potential is at a good level towards the center and partly to the south of the basin. The classification ranges of these GWPZ values and the total ratio of the basin are shown in table 7 (Aslan & Celik 2021).

Table 7- Classification of Van Basin according to Groundwater Potential GWPI Values

GWPI value	Explanation	Rate (%)	Covered area (km ²)
406 - 461	Very Good	8.000	1128.08
462 - 517	Good	17.00	2397.17
518 - 572	Moderate	43.37	6115.37
573 - 628	Poor	22.03	3102.22
629 - 683	Very Poor	9.600	1353.70

3.4 Validity (Verification)

The Groundwater Potential Index map obtained from 15 observation water wells in Figure 5 represents both the water well locations and the groundwater study area. The groundwater potential of the pump wells drilled for irrigation purposes was evaluated with the degrees of very good, good, moderate, poor, very poor. Only one of the reference wells is partially compatible, and 14 of the data are compatible (Table 8).

Table 8- Groundwater Potential Index and Well Data

R.N.	Town	X	Y	Depth (m)	SWL (m)	DWL (m)	Yield m ³ /day	GWPI	Evaluation	Notifications
0	Kavuncular	383685	4265203	80	13.21	41.14	0.00	406	Poor	Compatible
1	Ercek	386375	4279150	75	8.95	32.73	0.00	417	Poor	Compatible
2	Cedel-ova	368366	4273846	100	15.92	68.00	0.42	420	Good	Compatible
3	Mollahasan	404724	4279217	178.2	1	8.15	1.40	426	Poor	Compatible
4	Taskonak	366200	4249080	132	13.13	51.08	0.85	428	Good	Compatible
5	S. Cavus hamlet	383875	4216966	100	60	90.00	0.05	430	Poor	P.Compatible
6	Elmalik	353125	4253075	56	49	54.00	0.32	438	Poor	Compatible
7	UI. Tunal	330892	4241674	77	6.57	38.12	0.22	509	Good	Compatible
8	Kusdagi Koyu	362500	4234750	141	56.13	51.00	0.00	515	Good	Compatible
9	Saray	427683	4279296	136	11.53	17.01	9.35	577	Good	Compatible
10	Kilimli K.	413243	4317686	119.5	4.7	15.29	3.27	419	Poor	Compatible
11	Kosk Koyu	389414	4310080	36.5	12.25	12.42	0.19	556	Good	Compatible
12	Unseli	379250	4316000	90	0.91	46.47	0.17	586	Poor	Compatible
13	Partak yolu	349570	4318439	200	30	37.0	0.20	622	Moderate	Compatible
14	Kockopru	355882	4331627	70	23.68	40.68	0.59	683	Moderate	Compatible

*: Where, Partially Compatible is P. Compatible, References Number are R.N., Urpinar Irrigation Tunnel is UI. Tunal

3.5 Fuzzy AHP

In this method, named Chang's Fuzzy AHP Method, each object is taken and a degree analysis is applied for each purpose in order.

Table 9- Comparison matrix and significance weighting values of eight parameters

Criteria	Rainfall	Slope	Soil Type	LU/LC	Geology	Geomorphology	Drainage Density	Fault Density	Fuzzy Geometric mean value
ST	(1, 1, 1)	(1, 3/2, 2)	(3/2,2,5/2)	(3/2,2,5/2)	(2,5/2,3)	(5/2,3,7/2)	(5/2,3,7/2)	(3,7/2,9/2)	1.56,1.85,2.06
R	(1/2,2/3,1)	(1, 1, 1)	(1,3/2,2)	(3/2,2,5/2)	(3/2,2,5/2)	(2, 5/2, 3)	(5/2,3,7/2)	(3,7/2,9/2)	1.33,1.59,1.89
ST	(2/5,1/2,2/3)	(1/3,2/3, 1)	(1, 1, 1)	(1,3/2,2)	(3/2,2,5/2)	(3/2,2,5/2)	(2,5/2,3)	(5/2,3,7/2)	1.04,1.31,1.56
LU/LC	(2/5,1/2,2/3)	(2/5,1/2,2/3)	(1/2,2/3,1)	(1, 1, 1)	(1,3/2,2)	3/2,2,5/2)	(3/2,2,5/2)	(2,5/2,3)	0.90,1.10,1.32
G	(1/3,2/5,1/2)	(2/5,1/2,2/3)	(2/5,1/2,2/3)	(1/2,2/3,1)	(1, 1, 1)	(1, 3/2, 2)	(3/2,2,5/2)	(2,5/2,3)	0.78,0.85,1.13
GM	(2/7,1/3,2/5)	(1/3,2/5,1/2)	(2/5,1/2,2/3)	(2/5,1/2,2/3)	(1/2,2/3,1)	(1, 1, 1)	(1, 3/2, 2)	(3/2,2,5/2)	0.64,0.76,0.92
DD	(2/7,1/3,2/5)	(2/7,1/3,2/5)	(1/3,2/5,1/2)	(2/5,1/2,2/3)	(2/5,1/2,2/3)	(1/2,2/3,1)	(1, 1, 1)	(1, 3/2, 2)	0.63,0.64,0.90
FD	(1/3,2/5,1/2)	(1/3,2/5,1/2)	(2/5,1/2,2/3)	(2/5,1/2,2/3)	(2/3, 1, 2)	(1/2,2/3,1)	(1/2,2/3,1)	(1, 1, 1)	0.62,0.67,0.86

Note; Abbreviations used in Table 9 and Table 10 GWPI: Groundwater Potential Index, R: Precipitation, S: Slope, ST: Soil Type, LU/LC: Land Use and Land Cover, G: Geology, GM: Geomorphology, DD: Drainage Density and FD: Fault Density, FGM: Fuzzy is the geometric mean value. In addition, FwW_i: W_i are fuzzy weights, and the subscripts r and w: denote the degree and weight of the parameter, respectively. In addition, Weights are indicated by W_i, W_i and Normalized weight NW

$$r_1 = (1 * 1 * 3/2 * 3/2 * 2 * 5/2 * 5/2 * 3)^{\frac{1}{10}}, (1 * 3/2 * 2 * 2 * 5/2 * 3 * 3 * 7/2)^{\frac{1}{10}}, (1 * 2 * 5/2 * 5/2 * 3 * 7/2 * 7/2 * 9/2)^{\frac{1}{10}} = (2.08, 2.38, 2.89)$$

Table 10- Weighting of thematic layers using the fuzzy-AHP method

	R	S	ST	LU/LC	G	GM
R	(1, 1, 1)	(1, 3/2, 2)	(3/2,2,5/2)	(3/2,2,5/2)	(2,5/2,3)	(5/2,3,7/2)
S	(1/2,2/3,1)	(1, 1, 1)	(1,3/2,2)	(3/2,2,5/2)	(3/2,2,5/2)	(2, 5/2, 3)
ST	(2/5,1/2,2/3)	(1/3,2/3, 1)	(1, 1, 1)	(1,3/2,2)	(3/2,2,5/2)	(3/2,2,5/2)
LU/LC	(2/5,1/2,2/3)	(2/5,1/2,2/3)	(1/2,2/3,1)	(1, 1, 1)	(1,3/2,2)	3/2,2,5/2)
G	(1/3,2/5,1/2)	(2/5,1/2,2/3)	(2/5,1/2,2/3)	(1/2,2/3,1)	(1, 1, 1)	(1, 3/2, 2)
GM	(2/7,1/3,2/5)	(1/3,2/5,1/2)	(2/5,1/2,2/3)	(2/5,1/2,2/3)	(1/2,2/3,1)	(1, 1, 1)
DD	(2/7,1/3,2/5)	(2/7,1/3,2/5)	(1/3,2/5,1/2)	(2/5,1/2,2/3)	(2/5,1/2,2/3)	(1/2,2/3,1)
FD	(1/3,2/5,1/2)	(1/3,2/5,1/2)	(2/5,1/2,2/3)	(2/5,1/2,2/3)	(2/3, 1, 2)	(1/2,2/3,1)

Table 10 (Continue)- Weighting of thematic layers using the fuzzy-AHP method

	DD	FD	FGM	FwW ₁	W _i	NW
R	(5/2,3,7/2)	(3,7/2,9/2)	1.56,1.85,2.06	0.20,0.21,0.19	0.200	0.204
S	(5/2,3,7/2)	(3,7/2,9/2)	1.33,1.59,1.89	0.18,0.18,0.18	0.180	0.184
ST	(2,5/2,3)	(5/2,3,7/2)	1.04,1.31,1.56	0.14,0.15,0.15	0.146	0.149
LU/LC	(3/2,2,5/2)	(2,5/2,3)	0.90,1.10,1.32	0.12,0.13,0.12	0.123	0.126
G	(3/2,2,5/2)	(2,5/2,3)	0.78,0.85,1.13	0.10,0.10,0.11	0.103	0.105
GM	(1, 3/2, 2)	(3/2,2,5/2)	0.64,0.76,0.92	0.11,0.09,0.09	0.097	0.099
DD	(1, 1, 1)	(1, 3/2, 2)	0.63,0.64,0.90	0.06,0.07,0.08	0.063	0.064
FD	(1/2,2/3,1)	(1, 1, 1)	0.62,0.67,0.86	0.05,0.08,0.07	0.067	0.068
Total					0.979	0.999

Weights are indicated by W_i and Normalized weight NW.

Kaplan & Arikan (2012) studied the subject of Evaluation of Equipment Investment Projects in the Air Defense Sector with Fuzzy Analytical Hierarchy Process and Fuzzy AHP method (Kaplan & Arikan 2012). Table 10 was produced by making use of the literature and the studies of experts.

4. Conclusions and Recommendation

In this produced map, very weak areas (GWPZ value: 629 - 683) are found in clayey, calcareous soils, and rocky areas. Areas classified as moderate in terms of GWPZ (518 and 572) constitute a significant portion of the basin, approximately 43.37% of the total basin area (as it includes some agricultural and barren lands, it has a wide catchment area). The improvement of this area classified as moderate offers broader opportunities for the implementation of groundwater resources development programs compared to the weak GWPZ category. Improvement in this moderately moderate category requires less effort compared to the weak GWPZ category.

Areas identified as good level (462 – 517), corresponding to about 17% of the basin, not only offer productivity from an agricultural perspective but also present good opportunities for the improvement of irrigation facilities. Furthermore, this region, which is at a good level in terms of groundwater potential, provides a great opportunity for current research efforts, irrigation possibilities, and increased agricultural productivity.

The part of the basin with the best GWPZ level (629 – 683) provides the best opportunities for research activities, irrigation and increasing agricultural productivity. In short, for the groundwater potential of the Van Basin, there is a need for rigorous and appropriate planning and management studies by state institutions, albeit partially.

The well data obtained in order to determine the groundwater potential and quality of Van province with geographic information system supported AHP and Fuzzy AHP methods were updated in accordance with the purpose of the study. In this study, maps of selected wells representing the border regions of the basin and data on well yields were used and classifications were made accordingly. Then, thematic maps were created using GIS, IDW methods and other techniques in order to determine the formation of groundwater in the basin boundaries, where and in what proportion the groundwater is located, and usage possibilities. The thematic maps produced were applied by making the ratings suggested by Thomas L. Saaty to be used in AHP and Fuzzy AHP methods according to the potential effects of groundwater. The values obtained as a result of the application are given to the parameters suggested by Thomas L. Saaty (1, 2, 3, 4, 5, 6, 7, 8, 9). Since the result obtained in Table 9 is smaller than the value of 0.1 suggested by Saaty, a suitable solution was obtained according to the AHP method. Then, groundwater potential and quality analysis distribution map were created in ArcMap 10.2 environment. As a result of the application of the F-AHP method, the ideal order of the parameters was found.

The thematic maps created with the aim of understanding the groundwater potential of the Van basin, and the possibilities of using groundwater effectively and the selection of the well location to be drilled can be used to give a better idea for those who work in related fields of study. In the future, if water needs cannot be met from alternative water sources, the need for the drilling of new wells may emerge. In this eventuality, the thematic maps created will be useful in determining suitable well locations.

Limited surface and underground fresh water resources should be effectively protected with long-term programs for rapidly increasing urban drinking water, industrial and agricultural water needs. In order to protect and develop groundwater in accordance with different usage purposes, information about its potential status should be obtained from reliable units, institutions and organizations in a timely manner. Necessary plans should be made and implemented for the measures to be taken in case of negative effects on the work (such as excessive water withdrawal, illegal use, drought).

References

- Ahirwar R, Malik M S, Ahirwar S, & Shukla J P (2021). Groundwater potential zone mapping of Hoshangabad and Budhni industrial area, Madhya Pradesh, India. *Groundwater for Sustainable Development*, 14, 100631. <https://doi.org/10.1016/j.gsd.2021.100631>
- Akter A, Uddin A M H, Wahid K B & Ahmed S (2020). Predicting groundwater recharge potential zones using geospatial technique. *Sustainable Water Resources Management*, 6(2): 1-13. <https://doi.org/10.1007/s40899-020-00384-w>
- Aslan V & Celik R (2021). Integrated gis-based multi-criteria analysis for groundwater potential mapping in the euphrates's sub-basin, harran basin, turkey. *Sustainability*, 13(13): 7375. <https://doi.org/10.3390/su13137375>
- Chai W Y & Wei B C (2001). Compactness measurement using fuzzy multicriteria decision making for redistricting. In *Proceedings of IEEE Region 10 International Conference on Electrical and Electronic Technology. TENCON 2001 (Cat. No. 01CH37239) (Vol. 1, pp. 459-465)*. IEEE. doi: 10.1109/Tencon.2001.949635
- Chaudhry A K, Kumar K & Alam M A (2021). Mapping of groundwater potential zones using the fuzzy analytic hierarchy process and geospatial technique. *Geocarto International* 36(20): 2323-2344. <https://doi.org/10.1080/10106049.2019.1695959>
- Chowdhury A, Jha M K & Chowdary V M (2010). Delineation of groundwater recharge zones and identification of artificial recharge sites in West Medinipur district, West Bengal, using RS, GIS and MCDM techniques. *Environmental Earth Sciences*, 59(6): 1209-1222. <https://doi.org/10.1007/s12665-009-0110-9>
- Das S & Pardeshi S D (2018). Morphometric analysis of Vaitarna and Ulhas river basins, Maharashtra, India: using geospatial techniques. *Applied Water Science*, 8(6): 1-11. <https://doi.org/10.1007/s13201-018-0801-z>
- Di Bona G, Silvestri A, Forcina A & Falcone D (2017). AHP-IFM target: an innovative method to define reliability target in an aerospace prototype based on analytic hierarchy process. *Quality and Reliability Engineering International* 33(8): 1731-1751. <https://doi.org/10.1002/qre.2140>

- Dilekoglu M F & Aslan V (2022). Determination of groundwater potential distribution of Ceylanpinar Plain (Turkey) in Upper Mesopotamia by using geographical information techniques and Fuzzy-AHP with MCDM. *Water Supply* 22(1): 372-390. <https://doi.org/10.2166/ws.2021.268>
- DSI (State Hydraulic Works) (2015). 17. Regional Directorate Activity Report. Ankara: Ministry of Forestry and Water Affairs.
- Erdogan S (2017). An Evaluation on the Relationship between the Menua (Samram) Canal and the Garden of Tariria. *Yuzuncu Yil University Journal of Social Sciences Institute* 36: 11-24. <https://dergipark.org.tr>
- Fattahi R & Khalilzadeh M (2018). Risk evaluation using a novel hybrid method based on FMEA, extended MULTIMOORA, and AHP methods under fuzzy environment. *Safety science*, 102: 290-300. <https://doi.org/10.1016/j.ssci.2017.10.018>
- Fedrizzi M, Giove S & Predella N (2018). Rank reversal in the AHP with consistent judgements: A numerical study in single and group decision making. In *Soft Computing Applications for Group Decision-making and Consensus Modeling* (pp. 213-225). Springer, Cham. Doi:10.1007/978-3-319-60207-3_14
- Hossain M K & Thakur V (2020). Benchmarking health-care supply chain by implementing Industry 4.0: a fuzzy-AHP-DEMATEL approach. *Benchmarking: An International Journal*. <https://doi.org/10.1108/bij-05-2020-0268>
- Jesiyi N P & Gopinath G (2020). A fuzzy based MCDM-GIS framework to evaluate groundwater potential index for sustainable groundwater management-A case study in an urban-periurban ensemble, southern India. *Groundwater for Sustainable Development*, 11: 100466. <https://doi.org/10.1016/j.gsd.2020.100466>
- Kaplan S & Arikian F (2012). Evaluation Of Equipment Investment Projects In Air Defence Sector By Fuzzy Analytic Hierarchy Process. *Journal of Aeronautics and Space Technologies*, 5(3): 23-33. <https://search.trdizin.gov.tr>
- Konyar E, Genç B, Avci C & Tan A (2019). Excavations at the Old City, Fortress, and Mound of Van: Work in 2018. *Anatolia Antiqua*. *International Journal of Anatolian Archeology*, (XXVII), 169-183. DOI: 10.4000/anatoliaantiqua.1076
- Kumar P, Herath S, Avtar R & Takeuchi K (2016). Mapping of groundwater potential zones in Killinochi area, Sri Lanka, using GIS and remote sensing techniques. *Sustainable Water Resources Management*, 2(4): 419-430. <https://doi.org/10.1007/s40899-016-0072-5>
- Li C H & Li H M (2009). Developing a model to evaluate the safety management performance of construction projects. In *2009 International Conference on Management and Service Science* (pp. 1-5). IEEE. doi: 10.1109/ICMSS.2009.5304613.
- Ly P T M, Lai W H, Hsu C W & Shih F Y (2018). Fuzzy AHP analysis of Internet of Things (IoT) in enterprises. *Technological Forecasting and Social Change*, 136, 1-13. <https://doi.org/10.1016/j.techfore.2018.08.016>
- Machiwal D, Jha M K & Mal B C (2011). Assessment of groundwater potential in a semi-arid region of India using remote sensing, GIS and MCDM techniques. *Water resources management* 25(5): 1359-1386. <https://doi.org/10.1007/s11269-010-9749-y>
- Mallick J, Al-Wadi H, Rahman A & Ahmed M (2014). Landscape dynamic characteristics using satellite data for a mountainous watershed of Abha, Kingdom of Saudi Arabia. *Environmental earth sciences*, 72(12): 4973-4984. <https://doi.org/10.1007/s12665-014-3408-1>
- Mallick J, Khan R A, Ahmed M, Alqadhi S D, Alsubih M, Falqi I & Hasan M A (2019). Modeling groundwater potential zone in a semi-arid region of Aseer using fuzzy-AHP and geoinformation techniques. *Water* 11(12): 2656. <https://doi.org/10.3390/w11122656>
- Manap M A, Nampak H, Pradhan B, Lee S, Sulaiman W N A & Ramli M F (2014). Application of probabilistic-based frequency ratio model in groundwater potential mapping using remote sensing data and GIS. *Arabian Journal of Geosciences* 7(2): 711-724. <https://doi.org/10.1007/s12517-012-0795-z>
- Munier N & Hontoria E (2021). *Uses and Limitations of the AHP Method*. Springer International Publishing.
- Naghibi S A, Pourghasemi H R, Pourtaghi Z S & Rezaei A (2015). Groundwater qanat potential mapping using frequency ratio and Shannon's entropy models in the Moghan watershed, Iran. *Earth Science Informatics* 8(1): 171-186. <https://doi.org/10.1007/s10661-015-5049-6>
- Ozder E H, Alakas H M, Ozcan E & Eren T (2021). Shift scheduling solution with hybrid approach in a power plant. *Alexandria Engineering Journal* 60(6): 5687-5701. <https://doi.org/10.1016/j.aej.2021.03.076>
- Ozler H M (2005). Hydrogeology of Van aquifer and causes of salinization. <https://dergipark.org.tr>
- Pathak D (2017). Delineation of groundwater potential zone in the Indo-gangetic plain through GIS analysis. *Journal of Institute of Science and Technology*, 22(1): 104-109. <https://doi.org/10.3126/jist.v22i1.17760>
- Patra S, Pulak M & Subhash CM (2018). Delineation of groundwater potential zone for sustainable development: A case study from Ganga Alluvial Plain covering Hooghly district of India using remote sensing, geographic information system and analytic hierarchy process. *Journal of Cleaner Production* 172: 2485-2502. <https://doi.org/10.1016/j.jclepro.2017.11.161>
- Pinto D, Shrestha S, Babel M S & Ninsawat S (2017). Delineation of groundwater potential zones in the Comoro watershed, Timor Leste using GIS, remote sensing and analytic hierarchy process (AHP) technique. *Applied Water Science* 7(1): 503-519. <https://doi.org/10.1007/s13201-015-0270-6>
- Rahaman S A, Ajeez S A, Aruchamy S & Jegankumar R (2015). Prioritization of sub watershed based on morphometric characteristics using fuzzy analytical hierarchy process and geographical information system-A study of Kallar Watershed, Tamil Nadu. *Aquatic Procedia*, 4: 1322-1330. <https://doi.org/10.1016/j.aqpro.2015.02.172>
- Rahmati O, Nazari Samani A, Mahdavi M, Pourghasemi H R & Zeinivand H (2015). Groundwater potential mapping at Kurdistan region of Iran using analytic hierarchy process and GIS. *Arabian Journal of Geosciences* 8(9): 7059-7071. <https://doi.org/10.1007/s12517-014-1668-4>
- Saaty T L (2000). *Fundamentals of decision making and priority theory with the analytic hierarchy process* (Vol. 6). RWS publications. [https://Saaty TL \(2000\)](https://Saaty TL (2000))
- Senanayake I P, Dissanayake D M D O K, Mayadunna B B & Weerasekera W L (2016). An approach to delineate groundwater recharge potential sites in Ambalantota, Sri Lanka using GIS techniques. *Geoscience Frontiers*, 7(1), 115-124. <https://doi.org/10.1016/j.gsf.2015.03.002>
- Sener E, Sener Ş & Davraz A (2018). Groundwater potential mapping by combining fuzzy-analytic hierarchy process and GIS in Beyşehir Lake Basin, Turkey. *Arabian Journal of Geosciences* 11(8): 1-21. <https://doi.org/10.1007/s12517-018-3510-x>
- Senko S, Kurttila M & Karjalainen T (2018). Prospects for Nordic intensive forest management solutions in the Republic of Karelia. <https://erepo.uef.fi/handle/123456789/7429>
- Shekhar S & Pandey A C (2015). Delineation of groundwater potential zone in hard rock terrain of India using remote sensing, geographical information system (GIS) and analytic hierarchy process (AHP) techniques. *Geocar Int* 30(4): 402-421. <https://doi.org/10.1080/10106049.2014.894584>
- Singh V K, Kumar D, Singh S K, Pham Q B, Linh N T T, Mohammed S & Anh D T (2021). Development of fuzzy analytic hierarchy process based water quality model of Upper Ganga river basin, India. *Journal of Environmental Management*, 284, 111985. <https://doi.org/10.1016/j.jenvman.2021.111985>

- Tiri A, Belkhir L & Mouni L (2018). Evaluation of surface water quality for drinking purposes using fuzzy inference system. *Groundwater for Sustainable Development*, 6: 235-244. <https://doi.org/10.1016/j.gsd.2018.01.006>Get rights and content
- Tu Y, Chen K, Wang H & Li Z (2020). Regional water resources security evaluation based on a hybrid fuzzy BWM-TOPSIS method. *International Journal of Environmental Research and Public Health* 17(14): 4987. <https://doi.org/10.3390/ijerph17144987>
- Wang Z, Ran Y, Chen Y, Yu H & Zhang G (2020). Failure mode and effects analysis using extended matter-element model and AHP. *Computers & Industrial Engineering* 140: 106233. <https://doi.org/10.1016/j.cie.2019.106233>
- Xingfeng L I U (2017). Performance evaluation of engineering teachers in universities based AHP and fuzzy mathematical methods. *Revista de la Facultad de Ingeniería*, 32(5): 141-149. <https://doi.org/10.2991/meici-16.2016.25>
- Yang W Z, Ge Y H, Xiong B & Wang X B (2011). Petroleum Contaminated Site Remedial Countermeasures Selection Using Fuzzy ANP Model. In *International Workshop on Computer Science for Environmental Engineering and EcoInformatics* (pp. 224-229). Springer, Berlin, Heidelberg. https://doi.org/10.1007/978-3-642-22691-5_39
- Zekai S E N (2008). The flow of groundwater from a fissured medium to a porous medium of variable diameter and impermeable wall. *Water resources*, 1(1): 39-55. <https://dergipark.org.tr/techniques> and Fuzzy-AHP with MCDM. *Water Supply*, 22(1): 372-390. <https://doi.org/10.2166/ws.2021.268>



Copyright © 2024 The Author(s). This is an open-access article published by Faculty of Agriculture, Ankara University under the terms of the [Creative Commons Attribution License](https://creativecommons.org/licenses/by/4.0/) which permits unrestricted use, distribution, and reproduction in any medium or format, provided the original work is properly cited.



Meteorological Drought Assessment and Prediction in Association with Combination of Atmospheric Circulations and Meteorological Parameters via Rule Based Models

Fatemeh Shaker SUREH^a , Mohammad TAGHI SATTARI^{b,c*} , Hashem ROSTAMZADEH^d , Ercan KAHYA^e 

^aWater Resources Engineering, Faculty of Agriculture, Tarbiat Modares University, IRAN

^bDepartment of Water Engineering, Faculty of Agriculture, University of Tabriz, IRAN

^cDepartment of Agricultural Engineering, Faculty of Agriculture, Ankara University, TURKEY

^dDepartment of Climatology, Geography and planning Faculty, University of Tabriz, Tabriz, IRAN

^eWater Resources, Hydrology Civil Engineering Department, Istanbul Technical University, Istanbul, TURKEY

ARTICLE INFO

Research Article

Corresponding Author: Mohammad TAGHI SATTARI, E-mail: mtsattar@gmail.com

Received: 03 February 2022 / Revised: 13 July 2023 / Accepted: 22 July 2023 / Online: 09 January 2024

Cite this article

Sureh F S, Sattari Taghi M, Rostamzadeh H, Kahya E (2024). Meteorological Drought Assessment and Prediction in Association with Combination of Atmospheric Circulations and Meteorological Parameters via Rule Based Models. Journal of Agricultural Sciences (Tarim Bilimleri Dergisi), 30(1): 61-78. DOI: 10.15832/ankutbd.1067486

ABSTRACT

The development of data-driven models in conjunction with the advances in technologies regarded as remote sensing in generating recorded data from satellites has guided water management studies towards using these technologies, especially in the regions dealing with drought, like the Lake Urmia basin, Iran. In this basin, the agricultural sector has been exposed to dryness due to a decrease in rainfall and uncontrolled water consumption. In the last decade, many studies have tried to brighten this arena of water knowledge. However, the relationship between meteorological variables and atmospheric circulation with the meteorological drought of Lake Urmia had never been determined. The relationship between meteorological variables and atmospheric circulation with Lake Urmia's meteorological drought has been determined. This study calculated Standardized Precipitation Evapotranspiration Index (SPEI) values based on meteorological variables. Then a combination of the meteorological variables and atmospheric circulation values was considered a data mining model input for estimating the droughts. The series of the SPEI values for 3-, 6-, 9-, 12-, 24-, and 48-month time scales were obtained during 1988-2016. In

this study, both the M5 Tree model and Associate Rules were used to predict and analyze the meteorological drought at six synoptic stations in the basin, considering both the atmospheric circulations (North Atlantic Oscillation (NAO), Southern Oscillation Index (SOI), Mediterranean Oscillation Index of Gibraltar-Israel (Mogi), Mediterranean Oscillation Index of Algiers-Cairo (MOac), Western Mediterranean Oscillation Index (WEMO), Mediterranean, Red, Black, Caspian, and Persian Gulf SSTs) and the meteorological variables (lagged relative humidity, evapotranspiration, average temperature, minimum-maximum temperature, and pressure). The results showed that using a combination of the atmospheric circulation indices and meteorological variables in the models increases the model's accuracy and improves the results in a long-term period. The best result in the study of drought in the Lake Urmia basin is related to SPEI48 ($R = 0.85$, $RMSE = 0.08$, $MAE = 0.11$), and in the association rules, the value of the lifting index of the best rule is 1.32. Although both approaches provided acceptable results, the M5 Tree model had a comparative advantage due to simple and practical linear relationships.

Keywords: SPEI, Associate Rules, M5 Tree Model, The Urmia Lake basin, Iran

1. Introduction

Drought, as a natural disaster, is one of the main aspects of the climate in Iran. There are a number of research studies involving atmospheric circulations in drought prediction potentials. The teleconnections between El-Niño Southern Oscillation (ENSO) and critical flood and drought events have been reported all over the world (i.e., Barlow et al. 2001; Kahya & Karabörk 2001; Lee & Julien 2017; Kuzay et al. 2022). The most frequently used drought indexes are Palmer Drought Severity Index (PDSI) (Palmer 1965), Standardized Precipitation Index (SPI) (McKee et al. 1993) and Standardized Precipitation Evapotranspiration Index (SPEI) (Stagge et al. 2015; Wang et al. 2015).

In fact, various analysis methods have been proposed to monitor drought in two main categories: (i) statistical analysis (e.g., non-linear regression (Masocha et al. 2017), Geostatistical approach (Buttafuoco et al. 2018), log-linear (Moreira 2016) and Markov chain (Alam et al. 2017)) and (ii) data mining, which were developed to make a predictive decision based on the obtained knowledge. Data mining methods facilitate access to a large data set (Indurkha & Weiss 1998), and allow the extraction of rules through pattern recognition technologies (e.g., neural networks, machine learning, and genetic programming).

Dracup & Kahya (1994) have examined the four regions for a relationship between streamflow and the cold (La Niña) phase of the Southern Oscillation (SO). They pointed out a strong and significant connection between streamflow and La Niña in southwestern US. The results of this study show significant midlatitude streamflow responses to the tropical SO phenomenon but major limitation to this study is the limited length of records, which shows only nine El Niño and La Niña episodes occurring in the 41 years of streamflow data. Tadesse et al. (2004), who used data based approaches in drought analysis in the Nebraska for improve understanding of the characteristics and relationships of atmospheric and oceanic parameters that cause drought, examined a group of large-scale circulation the Results showed that the three indices have a stronger relationship with drought in the study area. The study suggests that data mining techniques can help us to monitor drought using oceanic indices as a precursor of drought but they did not investigate meteorological variables. Le et al. (2016) aims examining the lagged climate signals to predict SPEI at Khanhhoa province, using artificial neural network. They surveyed atmospheric circulations to predict SPEI using an artificial neural network method. Their results showed that adding more atmospheric circulations in the analysis could lead to better forecasting. The developed model can benefit developing long-term policies for reservoir and irrigation regulation and plant alternation schemes in the context of drought hazard. Nourani et al. (2017) proposed a hybrid application of Decision Tree and Associate Rule in SPI data in Tabriz and Kermanshah synoptic stations in Iran and de-trend SST data in the Black Sea, the Mediterranean Sea, and the Red Sea. They used classification, selection, and extraction to provide decision rules to monitor drought. Confidence and Heidke Skill Score (HSS) were used to evaluate the performance of the hybrid data mining methods, and thus, high Confidence was demonstrated between the monthly SPI values and the de-trend SST. This has resulted from the existence of a relative correlation between the three seas' de-trend SSTs and drought in Tabriz but they only used two station in Iran and can be used other ocean-atmospheric climate phenomena as predictors to predict maximum MP of station through the proposed method. The purpose of the study by Sezen & Partal (2017) is determining the effects of NAO and NCP on the temperature and precipitation regime of Mediterranean region in Turkey. As a result, NAO and NCP have remarkable influences on temperature and precipitation regime of Mediterranean region of Turkey for either seasonal or annual. It can be concluded that when the value of aforementioned teleconnection rises, the temperature value reduces. Nam et al. (2018) developed a satellite-based hybrid drought index called the vegetation drought response index for South Korea (VegDRI-SKorea) that could improve the spatial resolution of agricultural drought monitoring on a national scale. Their results showed that the hybrid drought index put forwarded spatially more improved drought patterns as opposed to that of station-based drought indices. Meteorological droughts threaten human societies in many parts of the world that are struggling with the water crisis.

Sattari et al. (2020) successfully predicted monthly precipitations at six meteorological stations in the Urmia Lake basin situated in north western Iran. They proved increased accuracy rate of models when using atmospheric circulation indices together with meteorological variables. Uzun & Ustaoglu (2022) examining current climatic conditions and atmospheric indices together on the Mediterranean crop yield. Hence, extreme weather conditions affect the yield of crops with high economic value in the Mediterranean Basin. Hosseini et al. (2022) determine the relationship between the NAO index and the precipitation of the APHRODITE base in Iran, to besides investigating the effect of these two phenomena in the country, the zones with positive, negative and no correlation to be identified with accuracy. The results in an analysis of North Atlantic Oscillation and monthly precipitation in Iran during the Last Half Century show that significant correlation is different between these two variables in time and space scale. In general, in more than 90% of Iran's area, there is no direct correlation between rainfall and NAO. In 9%, the correlation is negative and in only 1% of the Iranian zone, the correlation is positive.

In this study, we aimed to explore the linkage between atmospheric circulations and meteorological variables in the Urmia Lake basin for the purpose of drought assessment and prediction. The mergences of meteorological variables and atmospheric circulations using the Association Rules and M5 model has important implications in analysing drought prediction in the study area. This study has, therefore, special relevance to the understanding of drought patterns within the Urmia Lake basin. For this purpose, it used two M5 tree and Association Rules models, one of them evaluates the data numerically and the other after the discrete data examines the relationship variables. Both of them identify effective variables on the SPEI of the area.

2. Material and Methods

2.1. Study area

According to the Ramsar Convention, in 1971, Urmia Lake was declared an important international wetland. Urmia Lake, once the second largest saline lake in the world, is on the verge of complete desiccation. It has been suggested that the desiccation is caused by intensified human activities, and prolonged droughts in the lake basin. Finding the factors affecting the drought in this region is very important. In this study, we used from atmospheric circulations and meteorological parameters and data mining methods to investigate drought of Urmia lake basin. The closed catchment basin of Urmia Lake, which is considered as the main basin in the watershed division in Iran, has an area of 51 801 km² (Figure 1). Urmia Lake, situated in northwestern Iran, is one of the largest hypersaline lakes all over the world. Mediterranean air mass provides the main source of rainfall to the Urmia Lake. In our study area, there are six meteorological stations (Table 1) having an observation period spanning from January 1988 to December 2016; namely, Urmia, Tabriz, Sarab, Takab, Mahabad, and Maragheh. In this study, we used the meteorological station's local meteorological data in study area. The maximum statistical period was 28 (1988-2016) years and was available only for these six stations, which were provided to us by the Weather bureau. Only this number of stations were available in the area for the parameters of calculating evapotranspiration.

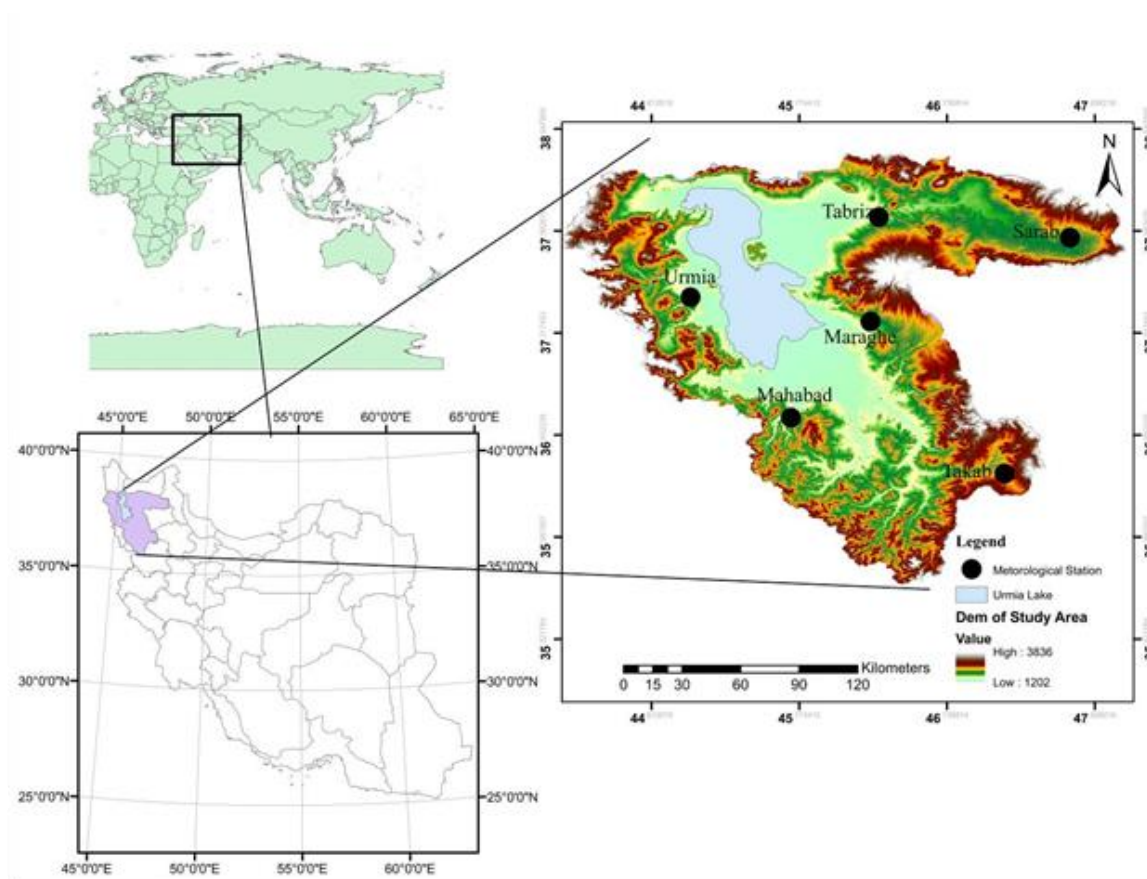


Figure 1- The geographic location of The Urmia Lake basin

Table 1- The statistical characteristics of the meteorological variables of six meteorological stations used in the Urmia Lake basin

Station		Mahabad	Maragheh	Sarab	Tabriz	Takab	Urmia
R (mm)	min	0.00	0.00	0.00	0.00	0.00	0.00
	max	155.92	114.81	102.24	114.84	165.72	147.54
	mean	33.19	23.67	20.29	20.57	26.85	25.54
	SD	34.06	25.89	19.10	19.95	27.77	27.48
ET (mm)	min	19.50	17.91	-30.00	21.35	19.51	16.21
	max	235.14	271.08	10.40	272.30	276.52	233.87
	mean	118.56	123.12	-5.67	126.05	117.15	109.77
	SD	61.93	71.61	9.97	72.25	69.55	62.536

In this research, the input variables in the models including meteorological variables and atmospheric circulation indices are described in Table 2.

Table 2- The Input variables used

Atmospheric circulations	Meteorological variables
Mediterranean sea surface temperature (MSST)	Minimum Temperature (Tmin)
Black Sea surface temperature (BSST)	Maximum Temperature (Tmax)
Red Sea surface temperature (RSST)	Rainfall (R)
Persian Gulf surface temperature (PSST)	Average Temperature (Tmean)
SOI	Average Relative Humidity (RH)
NAO	Average Wind speed (W)
MOac	Evapotranspiration (ET)
MOgi	-----
WEMO	-----

In recent decades, drought has been affecting the Urmia Lake basin which can be seen in the average annual rainfall distribution (Figure 2). The Urmia Lake, which is the largest territorial lake in Iran and the second largest lake in the world, drying at an alarming rate. Therefore, various drought factors were studied to determine the causes of drought in the region in this study.

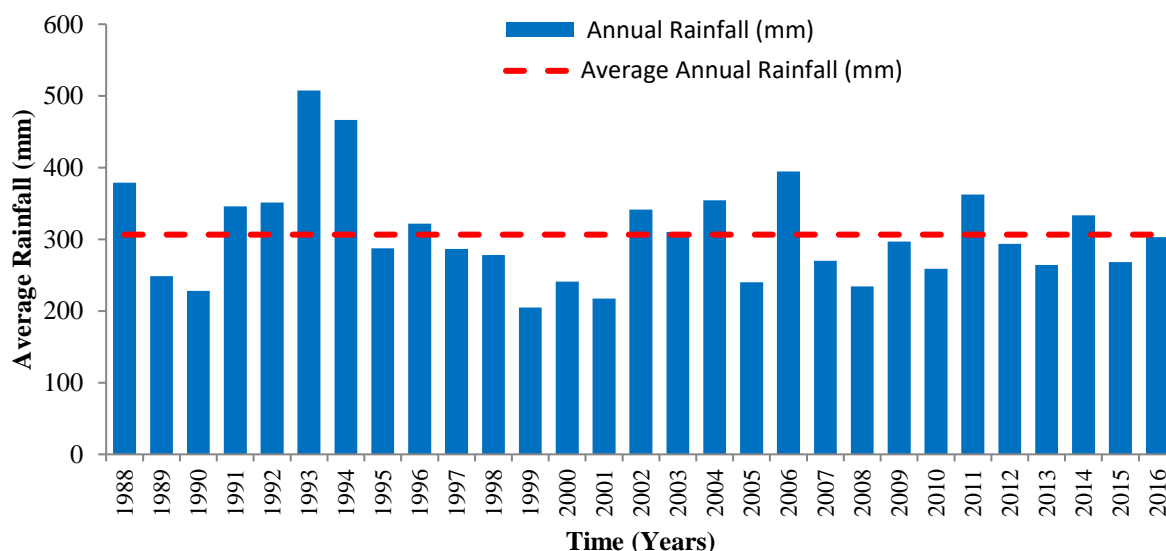


Figure 2- Annual and average rainfall distribution (mm) in The Urmia Lake basin

2.2. Meteorological drought index

Due to the vague and complex nature of droughts and the lack of identical definition of it, researchers often use drought indicators derived from hydrological variables to assess droughts and decide on drought management based on these indicators. So far, many indicators have been developed by researchers for drought monitoring. In this study, the SPEI was used, which is the multi-scale index comprising of precipitation and evapotranspiration variables, to analyse the danger of drought. Vicente-Serrano et al. (2010) proposed using the SPEI involving specifically the values of precipitation differences and evapotranspiration as expressed in equation 1, representing water balance value. In this equation, with a value for ET_{oi} , the difference between the precipitation (P) and reference evapotranspiration (ET_0) will be measured for i -th month.

$$D_i = P_i - ET_{oi} \quad (1)$$

Different methods have been proposed to calculate ET_{oi} . Some studies have compared different ET calculation methods (Sheffield et al. 2012) and it has been shown that the Penman-Monteith method gives more accurate results because the formula is more based on the atmospheric evaporation demand. In 1998, in its publication No. 56, the FAO introduced the Penman-Monteith method as the standard method for estimating the evapotranspiration of the reference plant (Allen et al. 1998):

$$ET_0 = \frac{0.408\Delta(R_n - G) + \gamma \left[\frac{890}{T + 273} \right] U_2 (e_a - e_d)}{\Delta + \gamma(1 + 0.34U_2)} \quad (2)$$

ET_0 Evapotranspiration - Reference plant (mm / day), R_n :Net radiation at the vegetation level (mega joules per square meter per day), T : average air temperature ($^{\circ}C$), U_2 wind speed at a height of 2 meters above the ground (meters per second), e_a ed Lack of steam pressure at a height of 2 meters (kPa), Δ : Slope of vapour pressure curve (kPa), γ : The coefficient of psychrometric (kilopascals per degree $^{\circ}C$), G : is the heat flux into the soil (mega joules per square meter-day).

Since the study area is semi-arid, SPEI index was preferred for drought analysis. SPEI also shows the effect of climate change on drought by considering precipitation and evaporation together. The advantage of SPEI over other multi-scalar drought indices (i.e., SPI) highlights the role of temperature on drought through potential evapotranspiration. In this case, SPEI is a reliable tool to assess global warming influences on drought events. Many studies have been done using the SPEI index, among the most recent of which Mehdizadeh et al. (2020), Inoubli et al. (2020), Danandeh Mehr & Fathollahzadeh Attar. (2021)'s articles can be mentioned.

2.3. Selecting inputs

Vicente-Serrano et al. (2011) found that drought prediction might be improved considering the lag impacts of ENSO events. In addition, other large scale atmospheric circulations (Sattari et al. 2020), namely SOI, NAO, the Mediterranean Oscillation Index of Algiers-Cairo (MOac), the Mediterranean Oscillation Index of Gibraltar-Israel (MOgi), and finally the Western Mediterranean Oscillation Index (WEMO). The last three indexes are all based on standardized pressure differences between the two preselected locations in the Mediterranean Sea. Following Sattari et al. (2020), we here included the following average sea surface temperature data observed in (i) Mediterranean Sea, (ii) Red Sea, (iii) Caspian Sea, (iii) Black Sea, and (iv) Persian Gulf. The Pearson correlation method was adopted to determine the lag times of each input variable in relation to SPEI index and a probable

predictor was chosen if it has the highest correlation with SPEI among various lag values. The combined effects of meteorological variables and large-scale atmospheric circulation indices on drought in the Urmia Lake basin are of primary interest in this research. Meteorological variables include lagged observations of SPEI index and Rainfall (R), Wind speed (W), mean temperature (Tmean), Evapotranspiration (ET), Average Relative Humidity (RH), minimum temperature (Tmin) and maximum temperature (Tmax).

2.4. Feature selection by RELIEF algorithm

A number of algorithms exists in the efforts of feature selection, along with processing speed problems. Due to the advent of fast computers and large storage capacities, a large data series of new issues have led to the continuing invention of the fast algorithm. The RELIEF method uses statistical solutions to select a feature as well as a weight-based method inspired by sample-based algorithms (Sattari et al. 2020). The RELIEF algorithm is known to be an effective tool for a dataset with a small number of training samples. Therefore, we preferred to adapt in identifying effective parameters in rainfall predictions due to the short span of our data.

2.5. Feature selection based on correlation (CFS)

Selection of feature based on correlation introduced by Hall (1999) is a commonly used method for selecting input variables and reducing problems in dimensions. The correlation method shows the subsets that have the properties with the highest correlation coefficient with the sample class, and the variables with the highest scores are considered as the main variables. This algorithm has a high ability to quickly detect irrelevant, additional, and error-free data, which generally results in the removal of half the data. This feature increases the production of the models by reducing the dimensions of the problem.

2.6. M5 tree predictions method

This model relies on a binary decision tree in which there are linear regression functions in the terminal node, revealing a relationship between independent and dependent variables. Tree-based models, which can be used for qualitative and quantitative data, resemble to a divide-and-conquer method in constructing a relationship between independent and dependent variables. The use of M5 tree model combined with neural networks gives more accurate result than decision trees like the CART method. The superiority of M5 tree model against regression trees is being smaller than regression trees. In comparison to neural networks, it results in easily understandable rules (Etemad-Shahidi & Mahjoobi 2009; Sattari et al. 2020). The advantage of M5 model tree over other previous linear models is that model trees are generally much smaller than regression trees and have proven more accurate in the tasks investigated. (Nourani et al. 2019). The M5 model tree can learn efficiently and can control tasks with very high dimensionality. This ability has developed the popularity of the M5 model tree and caused more usage in different fields of engineering. (Nourani et al. 2019). The fundamentals of the tree models are based on decision-making and problem solving. The structure of decision tree resembles to a tree whose body includes a system of leave, node, branch and root. Drawing the tree starts from top to bottom in which the root is placed as the first node on top and successively the chain of branches and nodes with the leaf. In the M5 tree model, the split criterion maximizes in reducing standard deviation in the child node (Sattari et al. 2020). In the case of reducing the standard deviation of the child node data impossible, the parent node do not branch out, instead reaching to final node or leaf. The first step in constructing a model tree is to calculate the standard deviation, which is expressed as in equation 3 (Quinlan. 1992).

$$SDR = SD(T) - \sum_{i=1}^N \frac{|T_i|}{T} SD(T_i) \quad (3)$$

Where; SD(T) is the standard deviation of the N input data points expressed as in equation 4.

$$SD(T) = \sqrt{\frac{1}{N} ((\sum_{i=1}^N Y_i^2) - \frac{1}{N} (\sum_{i=1}^N Y_i)^2)} \quad (4)$$

In these relations, T denotes a set of samples corresponding to each node as Ti does a subset of the subsample representing the sample. Our aim in this study is to evaluate the success of data mining methods which different from classical statistical methods. The M5 tree model offers practical, easier and more understandable solutions by generating linear relationships and if-then rules between target attribute and others. One of the major advantages of M5 model trees over normal regression trees is that normal regression trees can never predict the values outside the range of the trained model but the same is not the case with M5 model trees as they can extrapolate (Fayaz et al. 2022).

2.7. Association rules

Over the past years, among the methods of data mining, there has been a special interest in the algorithms of the discovery of patterns. As the name of these algorithms is known, we look for patterns existing in the dataset. In the meantime, the obtained algorithms of the repeated set of items have been discussed, which ultimately lead to the creation of Association Rules whose

purpose is to find the number of abundances in the series or a database, in which the events preceding and occurring take place together. Support (S) is a fraction of transactions that contains all of the objects in a set of specific objects (Eq. 5).
 $Support (X \rightarrow Y) = P(X \cap Y)$ (5)

Confidence (C) is the fraction of transactions containing all the objects of the conditional branch of the Association Rules that shows the accuracy of the rule. Unlike backup, an example for measuring the Confidence of a set of objects cannot be provided, because this criterion is only meaningful for associate rules (Eq. 6).

$$Confidence (X \rightarrow Y) = \frac{P(X \cap Y)}{P(X)}$$
 (6)

Rules, which have a low limit of both Support and Confidence, are called strong rules of the Association Rules, and all algorithms are aimed to be associated with such rules.

LIFT is a criterion, which shows the degree of independence between the objects A and B, which can be a numerical value from zero to infinity. Combining this benchmark with Support and Confidence is one of the best ways to explore associate rules. The LIFT criterion is obtained in accordance with equation 7.

$$Lift (X \rightarrow Y) = \frac{P(X \cup Y)}{P(X)P(Y)}$$
 (7)

All analytical steps in this study were processed using Weka, which is an open source tool collection of machine learning algorithms. Figure 3. illustrates analytical steps in our analysis.

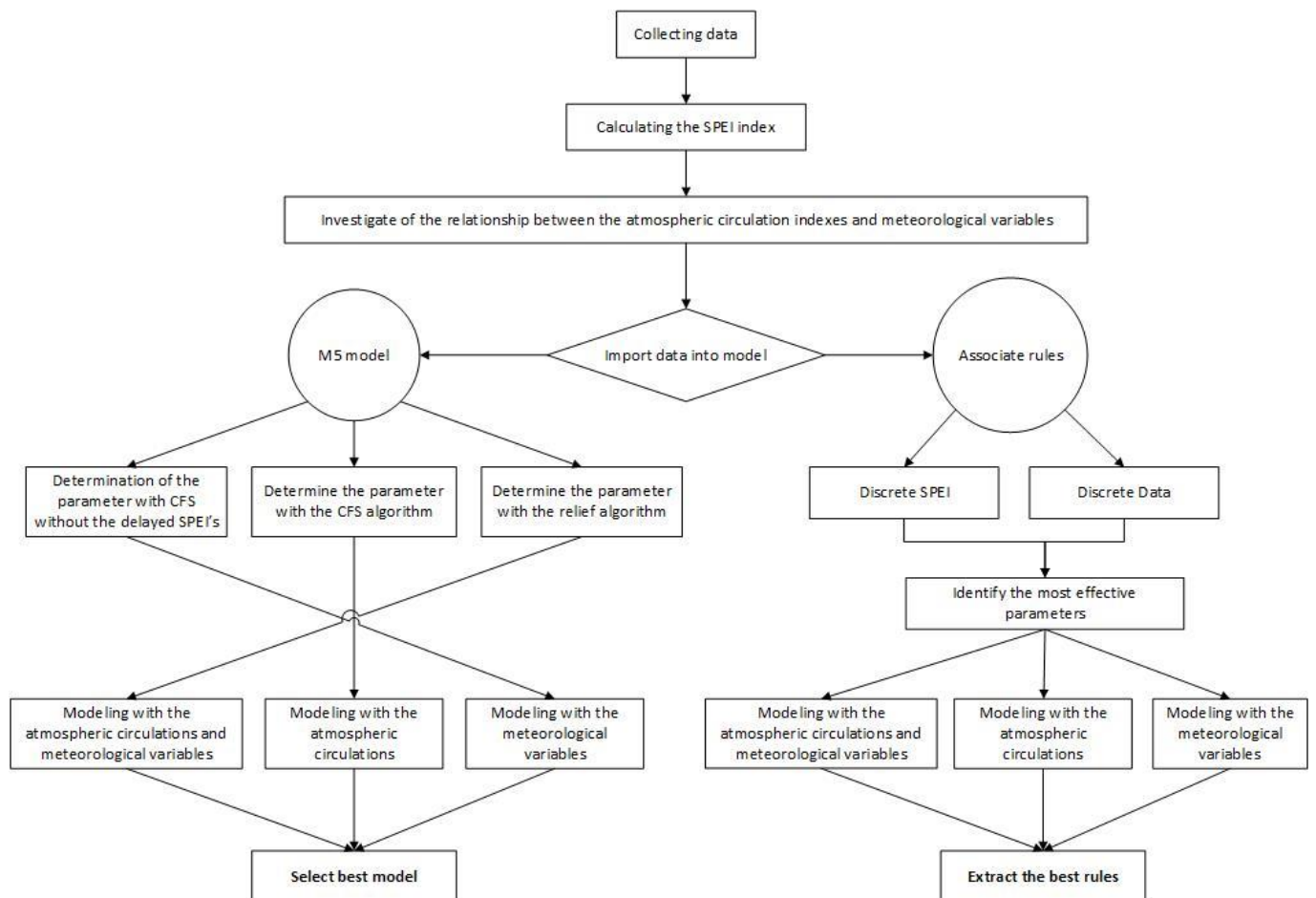


Figure 3- Analytical steps in drought predictions and forecasting

2.8. Model evaluation criteria

This criteria measures error rate and determines patterns and structures, exhibiting the least rainfall forecasting error. In this study, we used three model evaluation criteria, namely (i) correlation coefficient (R) (eq. 8), (ii) root mean square error (RMSE) (eq. 9) and (iii) mean absolute error (MAE) (eq. 10).

$$R = \frac{\sum_{i=1}^n (x_i - \bar{x})(y_i - \bar{y})}{\sqrt{\sum_{i=1}^n (x_i - \bar{x})^2 \sum_{i=1}^n (y_i - \bar{y})^2}} \quad (8)$$

$$RMSE = \sqrt{\frac{\sum_{i=0}^n (y_i - x_i)^2}{N}} \quad (9)$$

$$MAE = \frac{1}{n} \sum_{i=0}^n |X_i - y_i| \quad (10)$$

In these relations, x_i (y_i) are observational (computational) values. The higher (lower) the correlation coefficient (RMSE and MAE) values are the more accurate the model is. In addition, we used Taylor diagram, which is useful in evaluating complex models to study geophysical phenomena, as a model evaluation tool in this study. It provides a concise statistical summary of how well patterns match each other in terms of correlation, RMSE, and the ratio of variances. Readers are referred to Taylor (2001) for further information about theoretical basis for the diagram.

3. Results and Discussion

In this study, an index, which includes both the information of precipitation and evaporation was used to study the phenomenon of meteorological droughts in the Urmia Lake basin. The SPEI index is a preferable tool to analyse droughts in warm and relatively dry regions such as Iran due to evaporation. For this purpose, predictions procedures using new data mining methods such as a decision tree and Association Rules were carried out. We examined droughts in the Urmia Lake basin using the SPEI index, which was calculated in the following six steps: 3-, 6-, 9-, 12-, 24-, and 48-month (Figure 4). It is evident that drought events dominated after 1999, but much more after 2008 throughout all of the time scales. As the time scale gets higher, the spells of drought tend to unify in terms of the length of time but decrease in magnitude.

We obtained correlation coefficients between the SPEI and large-scale atmospheric circulation indices and climate variables at different points in time. Numerical values denote simultaneous and lagged correlations from 1- to 6-month at the 5% of significance level. In predicting, SPEI3 exhibits significant correlations with SOI, NAO, WeMO, MOgi, and MOac in the short term time scale. The SOI and WeMO have significant correlations with all the SPEI timescales, with the highest SOI correlation for SPEI9 with 5 steps of delay ($R = -0.440$) and the highest WeMO correlation for SPEI6 without a delay step ($R = 0.239$). Among the climate variables, the maximum temperature, mean humidity, mean rainfall and mean wind speed appeared to be significantly linked to the SPEI in short time lags. The remaining variables did not show a meaningful relationship with SPEI. Sattari et al. (2016) pointed out that drought index prediction works only in the short-term (i.e., time-scale 1) and the model accuracy decreases as the prediction time increases. Therefore, the SPEI index was predicted only for a single point in time in this research. In forecasting, SPEI3 with SOI, NAO, and WeMO, there is a significant correlation in the short-term scale. SOI and WeMO have a significant correlation with all SPEI time steps, with the highest correlation between SOI in SPEI9 with 4 steps of delay ($R = -0.440$) and the highest WeMO correlation in SPEI9 without a delay step ($R = 0.199$). Among the meteorological variables in the short-term scale, the maximum Temperature and average Relative Humidity and mean Rainfall and mean Wind speed are significantly correlated with 5% significance level.

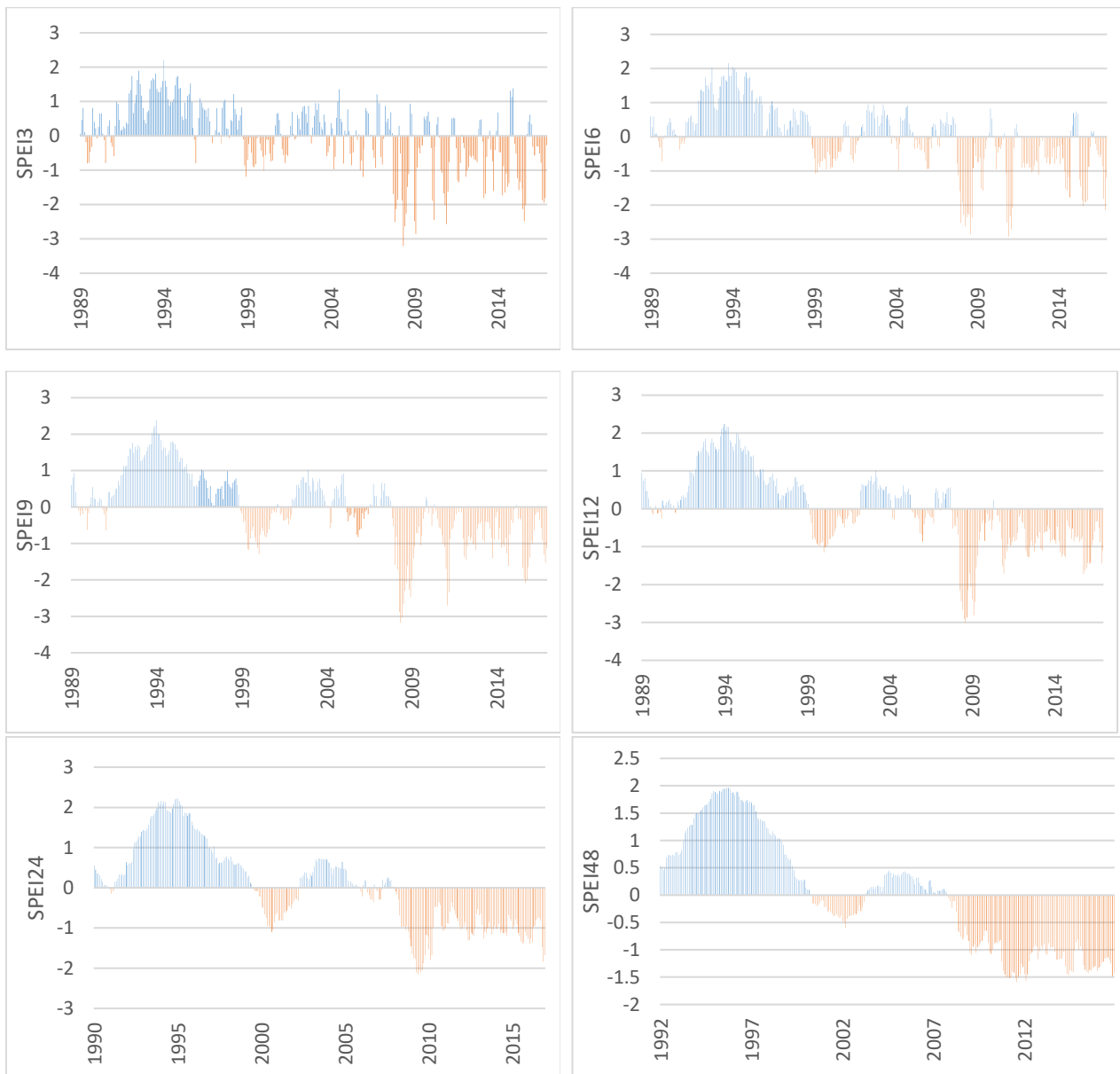


Figure 4- The SPEI index time series at time scales: 3, 6, 9, 12, 24, and 48 months in the Urmia Lake basin

In this research, after identifying the optimal combination by the RELIEF and correlation test, three input structures were determined to form an M5 tree model of possible combinations. In the first structure, the meteorological variables were used in addition to the SPEI with specific delays. In the second structure, atmospheric circulations were adopted in the model with the SPEI delays. In the third structure, a combination of these two groups of factors with the SPEI delays were considered.

In addition, each structure was given as three combinations in the model. In the first combination, the optimal combination of RELIEF tests with the SPEI delays were considered as the combination of the model. In the second combination, the correlation test for input parameters was used with considering the SPEI delays. In the third combination, the correlation test for input parameters was used without considering the SPEI delays. The optimal final composition of the three structures and three compounds was obtained according to these structures and combinations. The results of optimal combinations and structures are presented in Table 3. The optimal structures were entered into the M5 tree model. In Table 4, the results of the evaluation of the M5 tree model for assessing meteorological drought at the time scale of 3, 6, 9, 12, 24 and 48 months are presented in three structures with optimal combinations. In most situations, the third structure appears to be the best model performance when the input set is a combination of large-scale atmospheric circulation indices and climate variables. In general, the climate variables are more effective in the short-term analysis, whereas the atmospheric circulation indices are more effective in the long-term analysis (Miley et al. 2020; Dehghani et al. 2020).

Table 3- Best input structure for M5 tree model for drought predictions and forecasting

		<i>Structure</i>	<i>Input</i>
SPEI3	Predicting	Combinatorial	SPEI3t-1 , SOIt-2 , MOgit , Wt-1, Rt-2
	Forecasting	Combinatorial	SPEI3t-3, SPEI3t-2, SPEI3t-1, RHt, MOgit, Rt-1, ETt, Wt
SPEI6	Predicting	Meteorological variables	Tmaxt, Tmint, Tmeant, SPEI6t-1, SPEI6t-2, SPEI6t-3
	Forecasting	Atmospheric circulations	SPEI6t-3, SPEI6t-2, SPEI6t-1, WEMOt, SOIt-4, MOgit
SPEI9	Predicting	Meteorological variables	ETt, Tmeant, Tmint, SPEI9t-1, SPEI9t-2, SPEI9t-3
	Forecasting	Meteorological variables	RHt, Wt, SPEI9t-3, SPEI9t-2, SPEI9t-1
SPEI12	Predicting	Atmospheric circulations	WEMOt-4, MOact, MOgit , SPEI12t-1, SPEI12t-2, SPEI12t-3
	Forecasting	Combinatorial	Wt , SOIt-4, SPEI12t-1, SPEI12t-2, SPEI12t-3
SPEI24	Predicting	Combinatorial	SOIt-6, Wt-6, Rt-1, MOgi, MOac, Tmax, SPEI24t-1, SPEI24t-2, SPEI24t-3
	Forecasting	Meteorological variables	Wt , RHt , SPEI24t-1, SPEI24t-2, SPEI24t-3
SPEI48	Predicting	Atmospheric circulations	MOact , WEMOt , SPEI48 t-1, SPEI48t-2, SPEI48t-3
	Forecasting	Combinatorial	W t-6, Rt, RHt, Tmaxt, BSStt , MOact , WEMO t-6, SPEI48 t-1, SPEI48t-2, SPEI48t-3

Except the SPEI3 predictions (RELIEF + SPEI delays), in the rest, the second combination (SPEI delays+ cfs) was best input structure.

Table 4- Best results in the evaluation criteria for the M5 tree model for drought investigation and forecasting

		<i>SPEI3</i>	<i>SPEI6</i>	<i>SPEI9</i>	<i>SPEI12</i>	<i>SPEI24</i>	<i>SPEI48</i>
Predicting	Structure	Combinatorial	Meteorological variables	Meteorological variables	Atmospheric circulations	Combinatorial	Atmospheric circulations
	R	0.6745	0.7866	0.7953	0.7574	0.8084	0.85
	RMSE	0.6901	0.3485	0.3777	0.2931	0.1926	0.0843
	MAE	0.5421	0.5221	0.2809	0.2153	0.1427	0.118
Forecasting	Structure	Combinatorial	Atmospheric circulations	Meteorological variables	Combinatorial	Meteorological variables	Combinatorial
	R	0.7086	0.7856	0.7917	0.7561	0.8049	0.8538
	RMSE	0.6654	0.528	0.2809	0.2144	0.1985	0.1168
	MAE	0.4921	0.3667	0.3794	0.2896	0.1503	0.0859

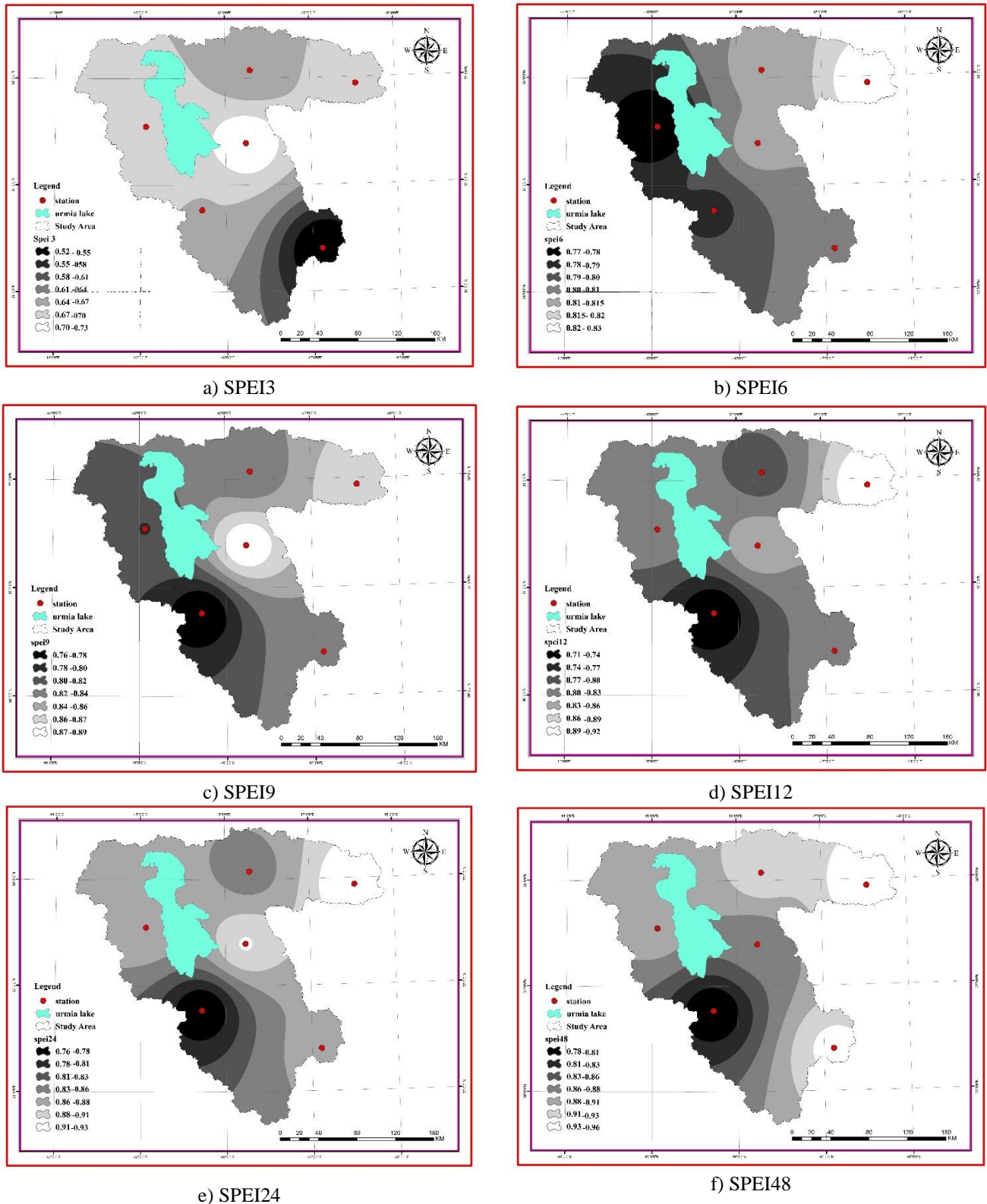


Figure 5- The correlation coefficients of M5 model for six stations between the years 1988–2016

The correlation coefficients are one of the criteria found in the evaluation in the M5 model and were calculated for six stations between the years 1988–2016. Figure 5 shows the results derived from the SPEI predictions for each station. If the model input is not the same for each time step of SPEI, comparisons cannot be made. The lighter colours in Figure 5 show higher correlation coefficients whereas the darker colours indicate lower correlation coefficients. Our results demonstrated that better information in most cases could be obtained from the combination of atmospheric circulations and meteorological variables. Moreover, the distribution charts display the best model for each SPEI time scale (Figures 6 and 7). As the time scale approaches the highest value (48-month), the accuracy of the resulting model increases. In other words, the SPEI48 model outperformed over the remaining models.

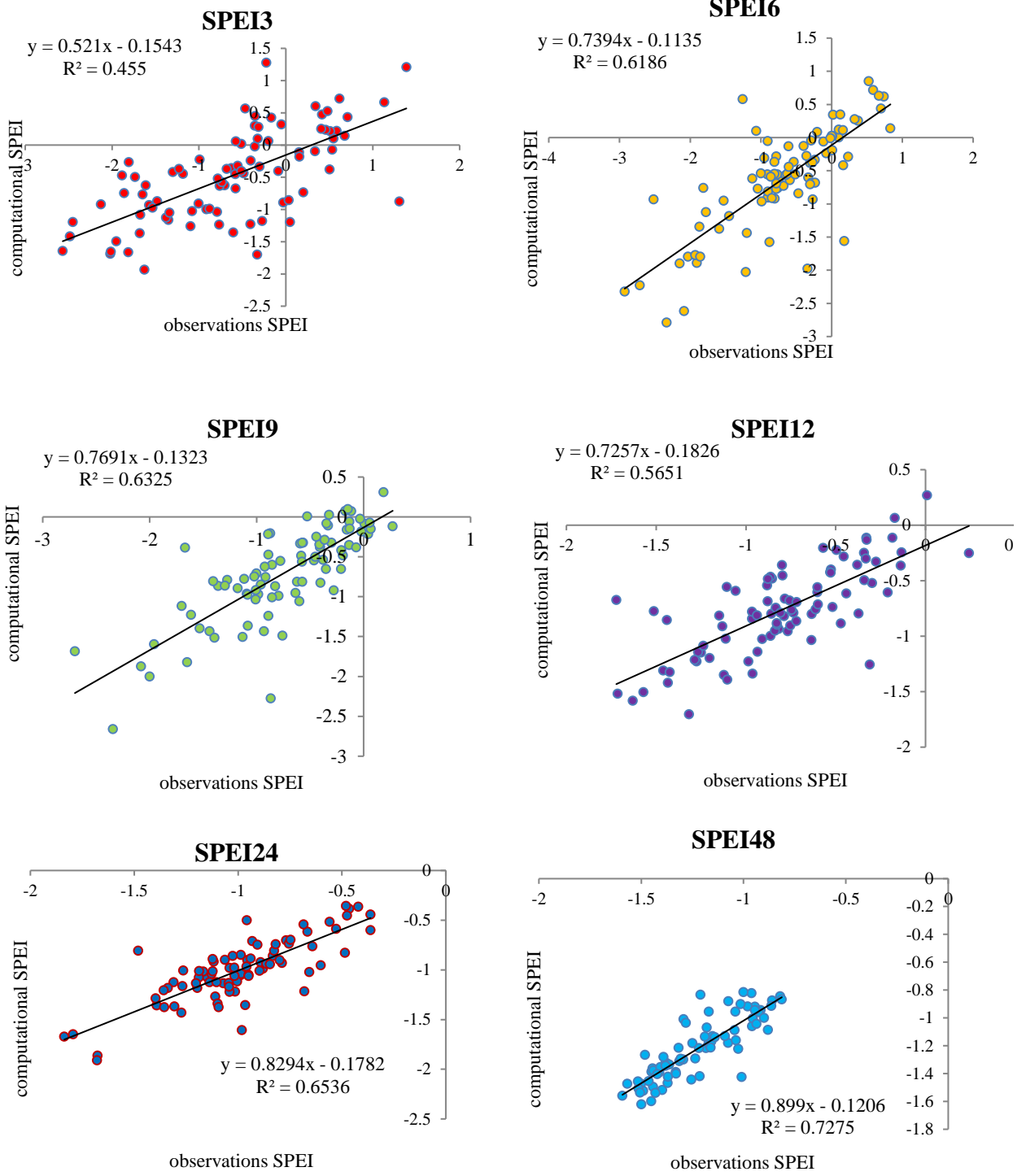


Figure 6- Distribution diagrams of actual and predicted SPEI for predictions of drought

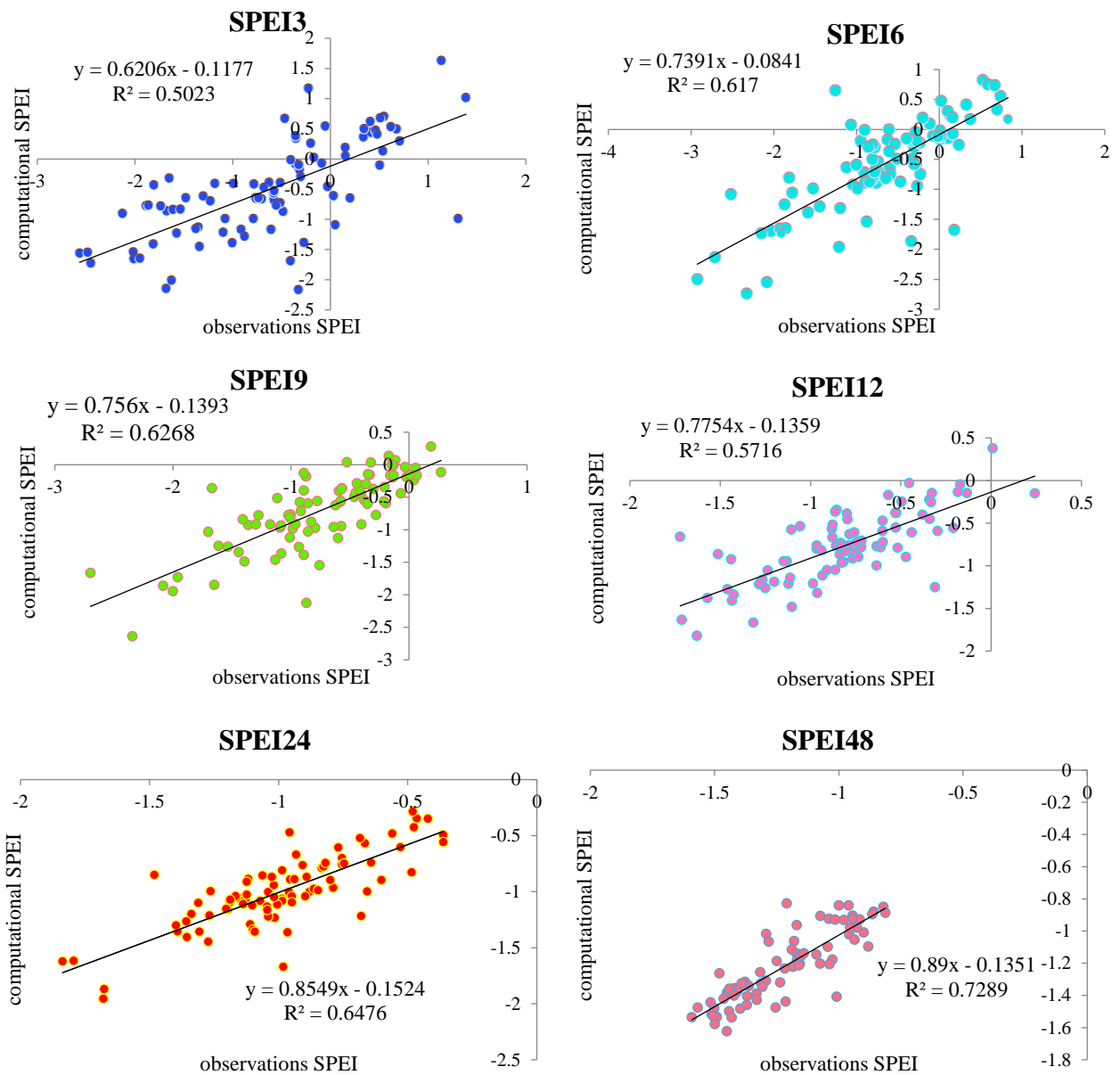


Figure 7- Distribution diagrams of actual and predicted SPEI for prediction of drought

Taylor diagrams are often applied to measure the predictions performance in hydrology and climatology. Information was plotted on Taylor's charts in identifying the best predictions and forecasting results for SPEI48 (Figure 8).

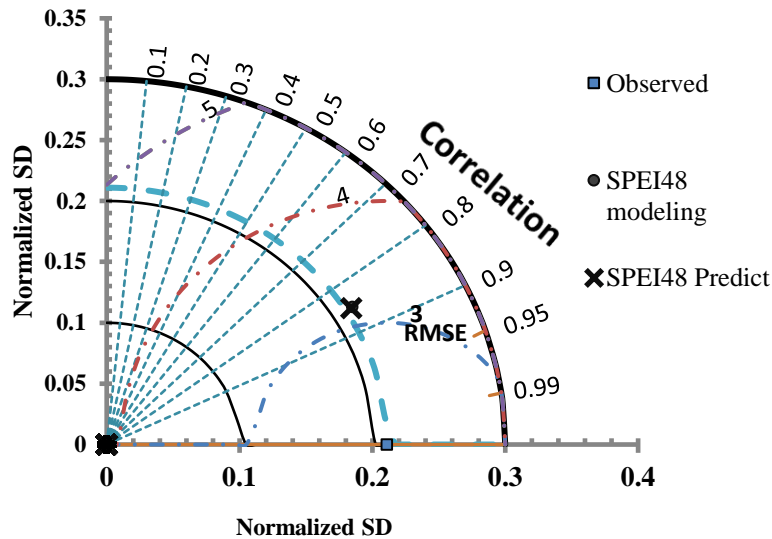


Figure 8- Taylor diagrams for SPEI48 predictions and prediction

Following to definition of drought index classification groups by the National Drought Reduction Center (Hayes 2003) we classified the monthly values of large-scale atmospheric circulation indices, climate variables and the drought index into seven discrete categories; namely, extremely dry (ED), severely dry (SD), moderately dry (MD), near normal (NN), moderately wet (MD), extremely wet (EW), and severely wet (SW). The classification threshold for drought indicators is shown in Figure 9. There is a lot of similarity between the SPI and SPEI indices. That is why many studies use the classification illustrated in Figure 9.

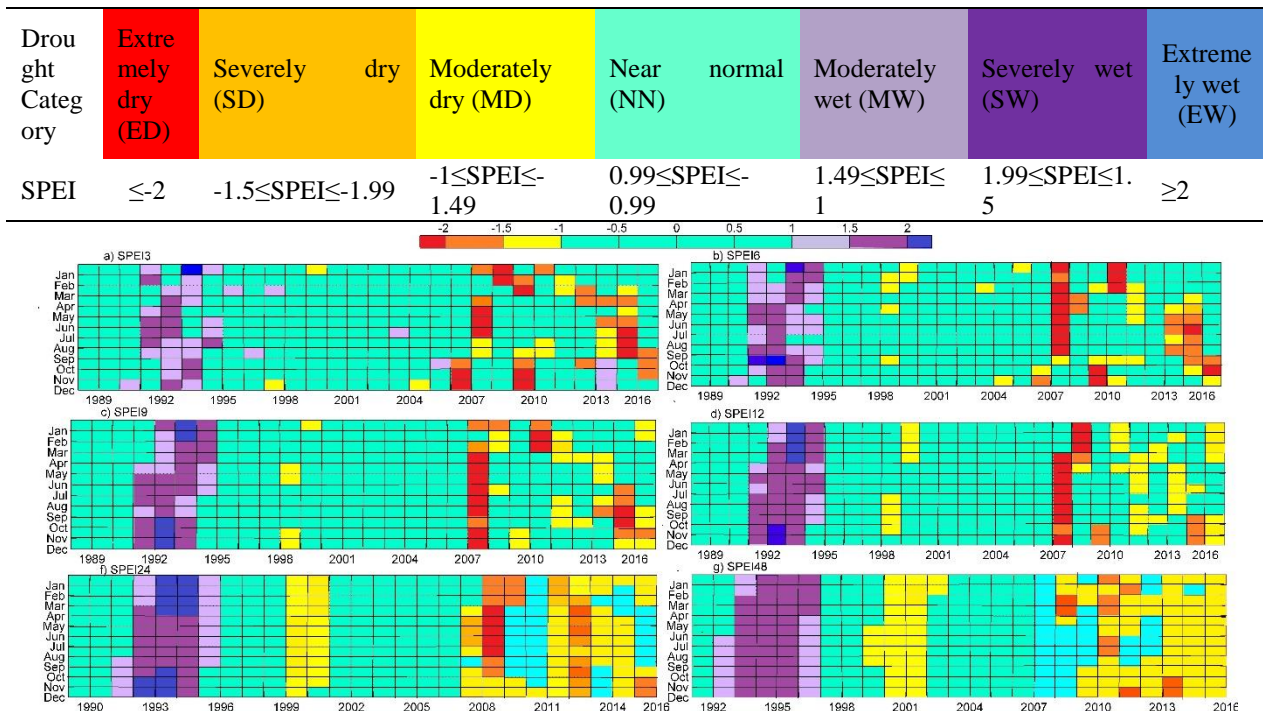


Figure 9- Drought index results in The Urmia Lake basin

Atmospheric circulation indices were further divided into seven categories with thresholds based on their frequency distribution. The data split is also shown in Figure 9, which presents the drought in recent years, from 2007 to 2016. It also indicates wetness from 1992 to 1997. This was ruled out in the case study. Assuming a normal distribution fit in to the period of 30-year observations, each circulation index and meteorological variable are divided with respect to magnitudes of 0.5, 1, and 1.5 times the standard deviation (SD). Table 5 shows the division of the data based on SD for the classification of each variable. For example, the SOI data were divided into seven groups as follows: SOI1 (group 1) corresponds to the SOI values more than 1.5 times its SD; SOI2 (group 2) for the range of 1 and 1.5 times its SD; SOI3 (group 3) for the range of 0.5 and 1 times its SD;

SOI4 (group 4) with internal values is 0.5 and -0.5 SD; SOI5 (group 5) for the range of -0.5 and -1 times its SD; SOI6 (group 6) for the range of -1 and -1.5 times its SD; and finally SOI7 (group 7) for the range of less than -1.5 times its SD. The similar rules apply for the classification of all meteorological variables and atmospheric circulation indices and this method was used by Tadesse et al. (2004).

Table 5- Classification of meteorological variables and atmospheric circulation indices

Variables	Extremely high (EH)	Very high (VH)	High (H)	Near Normal (NN)	Low (L)	Very low (VL)	Extremely low (EL)
Meteorological variables and sea surface temperature	$1.5 \leq$	$1.5 \leq X \leq 1$	$1 \leq X \leq 0.5$	$0.5 \leq X \leq -0.5$	$-1 \leq X \leq -0.5$	$-1 \leq X \leq -1.5$	$-1.5 \geq$
NAO	$3 \leq$	$3 \leq X \leq 2$	$2 \leq X \leq 1$	$1 \leq X \leq -1$	$-1 \leq X \leq -2$	$-2 \leq X \leq -3$	$-3 \geq$
SOI	$2 \leq$	$2 \leq X \leq 1$	$1 \leq X \leq 0.5$	$0.5 \leq X \leq -0.5$	$1 \leq X \leq 0.5$	$1 \leq X \leq 2$	$2 \geq$
MOac, MOgi	$0.6 \leq$	$0.6 \leq X \leq 0.4$	$0.4 \leq X \leq 0.2$	$0.2 \leq X \leq -0.2$	$-0.4 \leq X \leq -0.2$	$-0.6 \leq X \leq -0.4$	$-0.6 \geq$

After determining these rules, keeping the definition of three different scenarios in mind, the Association Rules between the SPEI and large-scale atmospheric circulation indices and climate variables were extracted in the Urmia Lake basin in the next step. At the first scenario, only the effects of meteorological variables on effective SPEI groups were examined to determine which meteorological variables will mostly affect the SPEI in the basin. In the second scenario for the effective SPEI, the influences of atmospheric circulations indexes were examined; and finally, the combined effects of atmospheric circulations indexes on all the SPEI timescales were analysed in the third scenario. The Association Rules algorithm was implemented for various SPEIs. In each case, an average of 100 community rules was obtained, including prefixes of one to five members of the indexes. The occurrence of drought could be verified based on the meteorological variables and atmospheric circulation indices. As stated earlier in the formation of the Association Rules, only sufficiently repeated rules are desired, that is to have the minimum amount of support (in this research 10%) and a high degree of certainty. In other words, the achieved rules, at least in 34 cases occurred during the research period. That is to say, at least 10 percent of support is based on trial and error, implying that an increase in the amount of support will reduce not only the number of rules produced but also the increase in the rules so that their analysis becomes difficult to achieve.

The selected patterns were then determined for the SPEI3, SPEI6, SPEI9, SPEI12, SPEI24, and SPEI48 time scales. An effective group for the SPEI was determined as NN by the Association Rules. Most influential variables in the predictions of SPEI timescales are specified in Table 6, which shows that the most effective clustering of meteorological variables (Structure 1) for the SPEI3, SPEI6, SPEI9, SPEI12, SPEI24, SPEI48 are NN, VL, H, H, H, and VH, respectively. The most effective clustering of atmospheric circulations indices (Structure 2) is the H, NN, H, H, VL, and H, respectively. The most effective classification combination of the atmospheric circulation indices and meteorological variables (Structure 3) on the SPEI time scales is NN, VH, VH, H, VL, and VH, respectively.

The most influential variables for the forecasting of SPEI timescales are specified in Table 6, which shows that the most effective classification of meteorological variables (Structure 1) for the SPEI3, SPEI6, SPEI9, SPEI12, SPEI24, SPEI48 are NN, VL, VH, VH, H, and VH, respectively. The most effective Classification of atmospheric circulation indices (Structure 2) is the (H, H, L, EL, VL, H), respectively. The most effective classification combination of atmospheric circulation indices and climate variables (Structure 3) on the SPEI time scales is NN, VH, VH, VL, NN, VH, respectively.

Table 6- Best rule of parameters with SPEI in Association Rules

<i>SPEI</i>	<i>Structure</i>	<i>Combination</i>
SPEI3t	Meteorological variables	TMIN=NN, RH=NN ==> SPEI3=near normal
	Atmospheric circulations	MOgi=H ==> SPEI3=near normal
	Combinatorial	W=NN, RSST=VH ==> SPEI3=near normal
SPEI6t	Meteorological variables	TMAX= VL, ET= VL ==> SPEI6=near normal
	Atmospheric circulations	NAO=NN, SOI =NN ==> SPEI6=near normal
	Combinatorial	TMAX=VH, CSST=VH, MOac=EH ==> SPEI6=near normal
SPEI9t	Meteorological variables	W=H ==> SPEI9=near normal
	Atmospheric circulations	SOI= L ==> SPEI9=near normal
	Combinatorial	TMAX=VH, MOac=EH 46 ==> SPEI9=near normal
SPEI12t	Meteorological variables	W=H ==> SPEI12=near normal
	Atmospheric circulations	SOI= L ==> SPEI12=near normal
	Combinatorial	TMAX=VH, CSST=VH, MOac=EH 40 ==> SPEI12=near normal
SPEI24t	Meteorological variables	W=H ==> SPEI24=near normal
	Atmospheric circulations	RSST= VL, MSST= VL ==> SPEI24=near normal
	Combinatorial	R=NN, BSST= VL ==> SPEI24=near normal
SPEI48t	Meteorological variables	Tmean=VH, ET=VH==> SPEI48=near normal
	Atmospheric circulations	MOac=H==> SPEI48=near normal
	Combinatorial	Tmax=VH, PSST=VH,RSST=VH==> SPEI48=near normal
SPEI3t+1	Meteorological variables	Tmax=NN,RH=NN, ET=NN==> SPEI3=near normal
	Atmospheric circulations	MOgi=H==> SPEI3=near normal
	Combinatorial	RH=NN,MOgi=NN==> SPEI3=near normal
SPEI6t+1	Meteorological variables	Tmax = VL, ET= VL==> SPEI6=near normal
	Atmospheric circulations	MOgi=H==> SPEI6=near normal
	Combinatorial	Tmax =VH, CSST=VH,MOac=EH==> SPEI6=near normal
SPEI9t+1	Meteorological variables	Tmean=VH, ET=VH==> SPEI9=near normal
	Atmospheric circulations	SOI= L ==> SPEI9=near normal
	Combinatorial	ET=VH, MOac=EH==> SPEI9=near normal
SPEI12t+1	Meteorological variables	Tmax =VH, RH= VL==> SPEI12=near normal
	Atmospheric circulations	WEMO=EL==> SPEI12=near normal
	Combinatorial	RH= VL, CSST=VH==> SPEI12=near normal
SPEI24t+1	Meteorological variables	RH=H==> SPEI24=near normal
	Atmospheric circulations	BSST= VL==> SPEI24=near normal
	Combinatorial	R=NN, MSST= VL==> SPEI24=near normal
SPEI48t+1	Meteorological variables	Tmean=VH, ET=VH==> SPEI48=near normal
	Atmospheric circulations	SOI=H==> SPEI48=near normal
	Combinatorial	Tmax =VH, PSST=VH==> SPEI48=near normal

For each of the three structures, the values of confidence and Lift indexes computed with respect to the Association Rules are given in Figure 10. The confidence indicator for a fixed limit on the threshold is used to compare the SPEI time scale results. As evident in Figure. 10, with an increase in the SPEI time increment, the index of ascending Association Rules increases between the third scenario and SPEI, which indicates the high efficiency of the combined method in this study for the drought assessment in terms of SPEI. For example, the value of Lift index for Association Rules based on the SPEI48 and combination of large-scale atmospheric circulation indices and climate variables. Came out to be 1.32 and 1.24 for the SPEI24 and 1.1 for the SPEI12, indicating that the first combination is more relevant than other two alternatives.

Atmospheric circulations can be also used solely as predictors without using meteorological variables – in longer horizons of SPEI (e.g.48-month). Due to Lake Urmia is close to the seas, it has been determined that the meteorological drought in this basin is more dependent on SOI and SST variables than other variables (Alizade Govarchin Ghale et al. 2018; Alizadeh-Chooari et al. 2016; Arkian et al. 2018). The Urmia Lake basin is one of the most important basins in Iran, facing many problems due to poor water management and rainfall reduction. Under current circumstances, it becomes critical to have an advanced understanding of rainfall patterns in the basin, setting the motivation of this study.

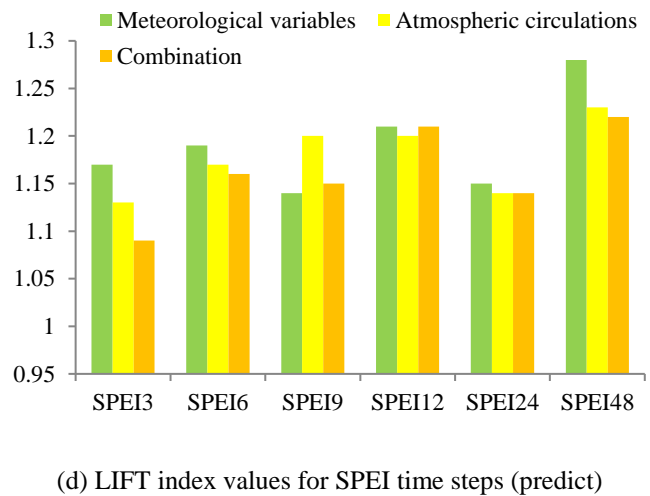
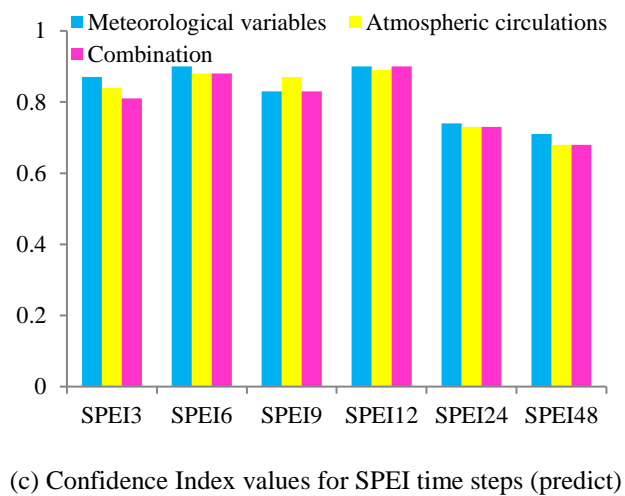
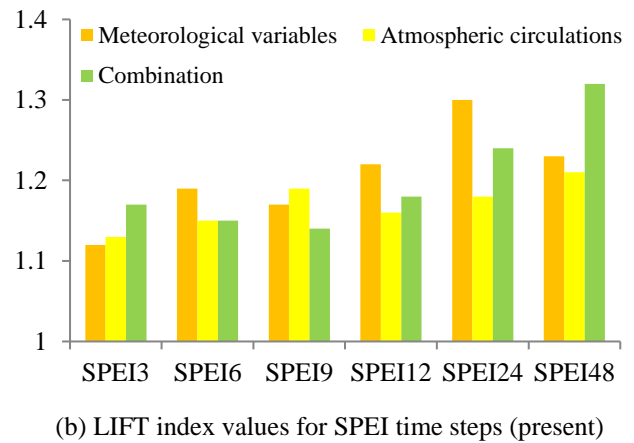
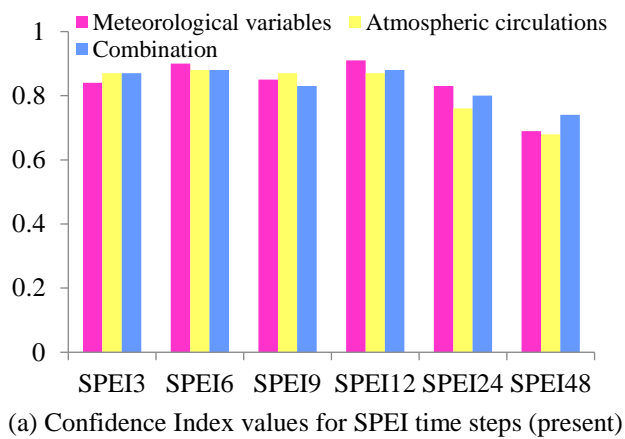


Figure 10- Confidence and Lift indicators of best rules

4. Conclusions

The drying of Lake Urmia and its socioeconomic side effects is one of Iran's major emerging environmental problems. This tragic phenomenon attracts the attention of many researchers in water resources and agricultural scientific communities. Many studies have used meteorological models to predict droughts in the Lake Urmia basin. However, the relationship between meteorological variables and atmospheric circulation and Lake Urmia's meteorological drought had never been determined. Therefore, this study focused on examining the droughts in this basin to develop predictive models in conjunction with large-scale atmospheric circulation indices and climate variables. The data mining algorithms were used to identify drought episodes associated with large-scale atmospheric circulation indices and climate variables. This study considered the meteorological drought in the Lake Urmia basin based on the SPEI index. SPEI index considers the effects of evapotranspiration with precipitation in drought. For the first time, in this study, a combination of meteorological variables, atmospheric circulations, and sea surface temperatures in the surrounding seas using data mining prediction methods provided a more comprehensive understanding of droughts. However, due to free access to the atmospheric circulations index data, the study area is limited to the Urmia basin. Our evaluation depends on three scenarios: the first included only the climate variables, the second with the atmospheric circulation indices, and finally, the third with a combination of both set variables. In the M5 tree model, forecasting was done for the next time step. The results showed that both methods are highly reliable and can be used for drought index modeling.

According to the results, atmospheric signals effectively forecast long-term drought. However, it was determined that the meteorological variables are more effective in forecasting short-term drought. Previous studies showed that atmospheric signals effectively forecast long-term precipitation and drought (Tadesse et al. 2004; Nikzad et al. 2013). Confidence and Lift indicators were computed to evaluate the rules extracted via the association rules method. A relationship was found between large-scale atmospheric circulation indices and climate variables and a combination of both with the SPEI index at different time steps. However, this relationship and efficiency vary regarding the delay time. The results revealed that regional atmospheric circulations have long-term impacts on weather patterns, and meteorological variables also play a significant role in short-term impacts. Therefore, it is plausible to use both sets of variables to reach acceptable results. Considering the recent droughts in the

catchment area of the Lake Urmia and the other lakes with similar climatic characteristics, the availability of data on regional atmospheric circulations via satellite imagery and the use of introduced methods, including Association Rules and M5 tree models facilitate providing simple and understandable rules and relationships; therefore, it may be suggested as a new approach in forecasting droughts with relatively high precision. The approach outlined in this paper can be used in any earth region with a relatively similar climatic characteristic to the Lake Urmia basin. It is suggested that other indicators be used to study drought in the region. Considering that in this research, the Thiessen averaging of the region has been used to study the drought, it is suggested that other methods be used in the research for averaging the stations in the region (such as is pluvial line) and the results obtained with the results. It is suggested that other data mining methods, such as support vector machines or gene expression, be used to study and predict drought indicators. The effect of meteorological data on rainfall and drought of each station can be examined one by one. Also, it is suggested to use more stations in similar studies.

Acknowledgments

We appreciate the kind efforts of Burhan Grtunca and Bediz eliker, who are English Language lecturers in the School of Foreign Languages of ITU North Cyprus, for improving the language quality of the manuscript.

Conflict of Interest: The authors have no conflicts of interest to declare that are relevant to the content of this article.

Funding Source: This research did not receive any specific grant from funding agencies in the public, commercial, or not-for-profit sectors.

Data availability: Data for this research are not publicly available due to governmental policies but available on request from the corresponding author.

References

- Alam N M, Sharma G C, Moreira E, Jana C, Mishra P K, Sharma N K & Mandal D (2017). Evaluation of drought using SPEI drought class transitions and log-linear models for different agro-ecological regions of India. *Physics and Chemistry of the Earth Parts A/B/C* 100: 31-43. <https://doi.org/10.1016/j.pce.2017.02.008>
- Alizade Govarchin Ghale Y, Altunkaynak A & Unal A (2018). Investigation anthropogenic impacts and climate factors on drying up of Urmia Lake using water budget and drought analysis. *Water resources management* 32: 325-337. <https://doi.org/10.1007/s11269-017-1812-5>
- Alizadeh-Choobari O, Ahmadi-Givi F, Mirzaei N & Oulad E (2016). Climate change and anthropogenic impacts on the rapid shrinkage of Lake Urmia. *International Journal of Climatology* 36(13): 4276-4286. <https://doi.org/10.1002/joc.4630>
- Arkian F, Nicholson S E & Ziaie B (2018). Meteorological factors affecting the sudden decline in Lake Urmia's water level. *Theoretical and Applied Climatology* 131: 641-651. <https://doi.org/10.1007/s00704-016-1992-6>
- Barlow M, Nigam S & Berbery E H (2001). ENSO Pacific decadal variability and US summertime precipitation drought and streamflow. *J Clim* 14: 2105-2128. [https://doi.org/10.1175/1520-0442\(2001\)014<2105:EPDVAU>2.0.CO;2](https://doi.org/10.1175/1520-0442(2001)014<2105:EPDVAU>2.0.CO;2)
- Buttafuoco G, Caloiero T, Ricca N & Guagliardi I (2018). Assessment of drought and its uncertainty in a southern Italy area (Calabria region). *Measurement* 113: 205-210. <https://doi.org/10.1016/j.measurement.2017.08.007>
- Danandeh Mehr A & Fathollahzadeh Attar N (2021). A gradient boosting tree approach for SPEI classification and prediction in Turkey. *Hydrological Sciences Journal* 66(11): 1653-1663. <https://doi.org/10.1080/02626667.2021.1962884>
- Dehghani M, Salehi S, Mosavi A, Nabipour N, Shamshirband S & Ghamisi P (2020). Spatial analysis of seasonal precipitation over Iran: Co-variation with climate indices. *ISPRS International Journal of Geo-Information* 9(2): 73. <https://doi.org/10.3390/ijgi9020073>
- Dracup J A & Kahya E (1994). the relationships between US streamflow and La Niña events. *Water Resources Research* 30(7): 2133-2141. <https://doi.org/10.1029/94WR00751>
- Etemad-Shahidi A & Mahjoobi J (2009). Comparison between M5 model tree and neural networks for prediction of significant wave height in Lake Superior. *Ocean Engineering* 36(15-16): 1175-1181. <https://doi.org/10.1016/j.oceaneng.2009.08.008>
- Fayaz S A, Zaman M & Butt M A (2022). Numerical and Experimental Investigation of Meteorological Data Using Adaptive Linear M5 Model Tree for the Prediction of Rainfall. *Review of Computer Engineering Research* 13: 9(1):1-2
- Hall M A (1999). Correlation-based Feature Selection for Machine Learning, Ph.D. thesis University of Waikato.
- Hayes M (2003). Drought indices. Available online at <http://www.drought.unl.edu/whatis/indices.html>
- Hosseini S M, Kashki A & Karami M (2022). Analysis of the North Atlantic Oscillation Index and rainfall in Iran. *Modeling Earth Systems and Environment* 1-10. <https://doi.org/10.1007/s40808-021-01309-y>
- Indurkha N & Weiss S M (1998). Estimating performance gains for voted decision trees. *Intelligent Data Analysis* 2(4):303-310. [https://doi.org/10.1016/s1088-467x\(98\)00028-6](https://doi.org/10.1016/s1088-467x(98)00028-6)
- Inoubli R, Abbes A B, Farah I R, Singh V, Tadesse T & Sattari M T (2020). A review of drought monitoring using remote sensing and data mining methods. In 2020 5th International Conference on Advanced Technologies for Signal and Image Processing (ATSIP) (pp. 1-6). IEEE. <https://doi.org/10.1109/atsip49331.2020.9231697>
- Kahya E & Karabrk M C (2001). The Analysis of El Nino and La Nina Signals in stream flows of Turkey. *International Journal of Climatology* 21:1231-1250. <https://doi.org/10.1002/joc.663>
- Kuzay M, Tuna M & Tombul M (2022). Determining the Relationship of Evapotranspiration with Precipitation and Temperature Over Turkey. *Journal of Agricultural Sciences* 28(3): 525-534. <https://doi.org/10.15832/ankutbd.952845>
- Le M H, Perez G C, Solomatine D & Nguyen L B (2016). Meteorological drought forecasting based on climate signals using artificial neural network—a case study in Khanhhoa Province Vietnam. *Procedia Engineering* 154:1169-1175. <https://doi.org/10.1016/j.proeng.2016.07.528>

- Lee J H & Julien P Y (2017). Influence of the El Niño/Southern Oscillation on South Korean Streamflow Variability: El Niño/Southern Oscillation on South Korean Streamflow Variability. *Hydrological Processes* 12:2162-2178. <https://doi.org/10.1002/hyp.11168>
- Masocha M, Murwira A, Magadza C H, Hirji R & Dube T (2017). Remote sensing of surface water quality in relation to catchment condition in Zimbabwe. *Physics and Chemistry of the Earth Parts A/B/C* 100:13-18. <https://doi.org/10.1016/j.pce.2017.02.013>
- McKee T B, Doesken N J & Kleist J (1993). The relationship of drought frequency and duration to time scales. In *Proceedings of the 8th Conference on Applied Climatology* AMS Boston MA 17(22):179-184
- Mehdizadeh S, Ahmadi F, Mehr A D & Safari M J S (2020). Drought modelling using classic time series and hybrid wavelet-gene expression programming models. *Journal of Hydrology* 587: 125017
- Miley K M, Downs J, Beeman S P & Unnasch T R (2020). Impact of the Southern Oscillation Index, temperature, and precipitation on Eastern equine encephalitis virus activity in Florida. *Journal of Medical Entomology* 57(5): 1604-1613. <https://doi.org/10.1093/jme/tjaa084>
- Moreira E E (2016). SPI drought class prediction using log-linear models applied to wet and dry seasons. *Physics and Chemistry of the Earth Parts A/B/C* 94:136-145. <https://doi.org/10.1016/j.pce.2015.10.019>
- Nam WH, Tadesse T, Wardlow BD, Hayes M J, Svoboda M D, Hong E M & Jang M W (2018). Developing the vegetation drought response index for South Korea (VegDRI-SKorea) to assess the vegetation condition during drought events. *International Journal of Remote Sensing* 39(5): 1548-1574. <https://doi.org/10.1080/01431161.2017.1407047>.
- Nikzad M, Behbahani M & Rahimi Good A (2013). Detection of dependencies between oceanic-wet and climatic parameters for drought monitoring by data mining method Case study Khuzestan province. *Iranian Journal of Water Research* (13)7: 183-175
- Nourani V, Davanlou Tajbakhsh A, Molajou A & Gokcekus H (2019). Hybrid wavelet-M5 model tree for rainfall-runoff modeling. *Journal of Hydrologic Engineering* 24(5): 04019012. [https://doi.org/10.1061/\(asce\)he.1943-5584.0001777](https://doi.org/10.1061/(asce)he.1943-5584.0001777)
- Nourani V, Sattari M T & Molajou A (2017). Threshold-based hybrid data mining method for long-term maximum precipitation forecasting. *Water Resources Management* 31(9): 2645-2658. <https://doi.org/10.1007/s11269-017-1649-y>
- Nourani V, Tajbakhsh A D & Molajou A (2019). Data mining based on wavelet and decision tree for rainfall-runoff simulation. *Hydrology Research* 50(1): 75-84. <https://doi.org/10.2166/nh.2018.049>
- Palmer W C (1965). *Meteorological Drought*. Research paper, n 45, U. S. Department of Commerce Weather Bureau, Washington, D. C: 58
- Quinlan J R (1992). Learning with Continuous Classes. *Proceedings of AI'92 World Scientific* 92: 343-348
- Sattari M, Mirabbai Najafabadi R, Alimohammadi, M (2016). Application of M5 Tree Model in Forecasting Drought (Case Study, Maragheh, Iran). *Hydrogeomorphology* 3(8): 73-92. <https://doi.org/10.1134/s0097807813030123>
- Sattari M T, Shaker Sureh F & Kahya E (2020). Monthly precipitation assessments in association with atmospheric circulation indices by using tree-based models. *Natural Hazards* 102: 1077-94. <https://doi.org/10.1007/s11069-020-03946-5>
- Sezen C & Partal T (2017). The relation of North Atlantic oscillation (NAO) and North Sea Caspian pattern (NCP) with climate variables in Mediterranean region of Turkey. *The Eurasia Proceedings of Science Technology Engineering and Mathematics* (1): 366-371. <https://doi.org/10.1007/s00703-019-00665-w>
- Sheffield J, Wood E F & Roderick M L (2012). Little change in global drought over the past 60 years. *Nature* 491: 435-438
- Stagge J H, Tallaksen L M, Gudmundsson L, Van Loon A F & Stahl K (2015). Candidate distributions for climatological drought indices (SPI and SPEI). *Int J Climatol* 35: 4027-4040. <https://doi.org/10.1002/joc.4267>
- Tadesse T, Wilhite D A, Harms S K, Hayes M J & Goddard S (2004). Drought Monitoring Using Data Mining Techniques: A Case Study for Nebraska USA. *Natural Hazards* 33(1): 137- 159. <https://doi.org/10.1023/B:NHAZ.0000035020.76733.0b>
- Taylor K E (2001) Summarizing multiple aspects of model performance in a single diagram. *J Geophys Res* 106:7183-7192. <https://doi.org/10.1029/2000JD900719>
- Uzun A & Ustaoglu B (2022). The effects of atmospheric oscillations on crop (olive, grape and cotton) yield in the eastern part of the Mediterranean region, Turkey. *International Journal of Environment and Geoinformatics* 9(1): 147-161. <https://doi.org/10.30897/ijegeo.1010181>
- Vicente-Serrano S M, Beguería S & Juan I A (2011). A multiscalar global evaluation of the impact of ENSO on droughts. *J Geophys Res Atm* 116 pp. <https://doi.org/10.1029/2011JD016039>
- Vicente-Serrano S M, Beguería S & López-Moreno J I (2010). A multiscale drought index sensitive to global warming: the standardized precipitation evapotranspiration index. *Journal of Climate* 23(7): 1696-1718. <https://doi.org/10.1175/2009JCLI2909.1>
- Wang W, Zhu Y, Xu R & Liu J (2015). Drought severity change in China during 1961-2012 indicated by SPI and SPEI. *Nat Hazards* 75: 2437-2451. <https://doi.org/10.1007/s11069-014-1436-5>



Copyright © 2024 The Author(s). This is an open-access article published by Faculty of Agriculture, Ankara University under the terms of the [Creative Commons Attribution License](https://creativecommons.org/licenses/by/4.0/) which permits unrestricted use, distribution, and reproduction in any medium or format, provided the original work is properly cited.



A Study on Recognizing the Value of Chestnut (*Castanea sativa*) Blossom Waste

Huseyin SAHIN^{a,*} , Sevgi KOLAYLI^b , Yakup KARA^b , Zehra CAN^c , Halil Ibrahim GULER^d ,
Asli OZKOK^e , Umit SERDAR^f 

^aGiresun University, Espiye Vocational School, Espiye, Giresun, TÜRKİYE

^bKaradeniz Technical University, Faculty of Sciences, Department of Chemistry, Trabzon, TÜRKİYE

^cBayburt University, Faculty of Applied Sciences, Department of Emergency Aid and Disaster Management, Bayburt, TÜRKİYE

^dKaradeniz Technical University, Faculty of Sciences, Department of Biology, Trabzon, TÜRKİYE

^eHacettepe University, Bee and Bee Products Application and Research Center (HARUM), Beytepe, Ankara, TÜRKİYE

^fOndokuz Mayıs University, Faculty of Agriculture, Department of Horticulture, Samsun, TÜRKİYE

ARTICLE INFO

Research Article

Corresponding Author: Huseyin SAHIN, E-mail: huseyin.sahin@giresun.edu.tr

Received: 08 September 2022 / Revised: 01 August 2023 / Accepted: 01 August 2023 / Online: 09 January 2024

Cite this article

Sahin H, Kolayli S, Kara Y, Can Z, Guler H I, Ozkok A, Serdar U (2024). A Study on Recognizing the Value of Chestnut (*Castanea sativa*) Blossom Waste. *Journal of Agricultural Sciences (Tarim Bilimleri Dergisi)*, 30(1):79-89. DOI: 10.15832/ankutbd.1172677

ABSTRACT

Chestnut (*Castanea sativa*) blossoms are natural resources that are not put to economic use. They are completely mixed with soil as waste. Thus, this extensive study was designed and remarkable results were found showing the potential usefulness of chestnut blossoms. In addition to the phenolic capacity and antioxidant capacity of the aqueous and ethanolic extracts of dried chestnut flowers, the anti-urease activity of these extracts was studied to demonstrate their therapeutic value. The binding interaction of phenolic substances present in chestnut blossom with urease was shown using molecular docking research. The aqueous extract, with most effect, had total phenolic content of 46.67 ± 0.37 mg GAE/g and total flavonoid content of 6.14 ± 0.40 mg QUE/g. The antioxidant activity was determined by FRAP (648.47 ± 5.27 μ mol FeSO₄.7H₂O/g for aqueous extract and 347.53 ± 2.09 μ mol

FeSO₄.7H₂O/g for ethanolic extract) and DPPH (0.05 ± 0.01 mg/mL for SC₅₀ of aqueous extract and 0.11 ± 0.01 mg/mL for SC₅₀ of ethanolic extract) assays, and rutin was found to be the dominant phenolic compound according to HPLC. IC₅₀ values for urease in aqueous and ethanolic extracts were 2.55 ± 0.09 mg/mL and 4.57 ± 0.24 mg/mL, respectively. According to the docking experiments, which were important to support the hypothesis of anti-urease activity, myricetin and luteolin showed different and effective bonding degrees to the target protein when compared with the reference molecule acetohydroxamic acid. In summary, chestnut flowers are rich in phenolic compounds which are responsible for a wide range of biological activities including antioxidant features and urease inhibition. These blossoms could be evaluated as potentially important raw materials for food.

Keywords: Chestnut, Blossom, Antioxidant, Phenolics, Molecular docking, Anti-urease

1. Introduction

Chestnut trees are highly valuable forest plants providing many benefits. In addition to wood and lumber, they also provide important non-wood products such as fruit and blossoms. Honeybees also directly benefit from these natural products (Carocho et al. 2015; Kolayli et al. 2016; Caleja et al. 2019; Rodrigues et al. 2020). The high antioxidant and other biologically active properties of chestnut honey, pollen, and propolis are due to high amounts of polyphenols in their composition (Comandini et al. 2014; Sahin et al. 2019; Karkar et al. 2021). Türkiye, a country rich in chestnut forests, is also the world's largest producer of chestnut honey. This type of honey, also known as medicinal honey, is one of the most valuable honeys in the world, with dark color, non-crystalline structure, and high antimicrobial and antiviral value. It is frequently used for asymptomatic treatments and wound healing therapies. Chestnut bee pollen and propolis are reported to be rich in polyphenols and tannins (Comandini et al. 2014; Carocho et al. 2015; Rodríguez-Flores et al. 2023). Tannins are complex polyphenols produced by a variety of plants, including chestnut trees (Aimone et al. 2023). Recent studies showed that chestnut blossoms should be evaluated as functional foods. The studies also indicated that in addition to chestnut honey and bee pollen, chestnut blossoms contain high levels of polyphenols (Barreira et al. 2008; Peng et al. 2022).

Comparisons of chestnut honey, blossoms, barks, leaves, and fruits showed that each product exhibits different antioxidant activities, with the highest levels being observed in blossoms (Barreira et al. 2008). Moreover, coumarins, flavonoids and their derivatives, proanthocyanidins, and sterols were found in horse chestnut seeds (Dudek-Makuch & Studzińska-Sroka 2015). Dried chestnut blossoms are also rich in oil, protein, sugar, antioxidants, polyphenols, and mineral and fiber substances, and they are used as natural ingredients in the bakery industry (Carocho et al. 2015).

Although there have been many studies about the chemical and biochemical properties of chestnut fruit, the studies involving chestnut blossoms are limited. The purpose of this study was to assess the usefulness of chestnut blossom extracts for the food industry, identify their biologically active properties, and describe their potential benefits to the economy. In brief, aqueous and ethanolic chestnut blossom extracts were tested for phenolic content, antioxidant activity, and anti-urease activity.

2. Material and Methods

2.1. Chemicals

Phenolic standards were obtained from Sigma-Aldrich (St. Louis, MO, USA). Daidzein was supplied by Cayman Chemical (Michigan, USA), and other chemicals required for current assays were purchased from Sigma-Aldrich (St. Louis, MO, USA) and Merck (Darmstadt, Germany).

2.2. Samples

Chestnut blossoms were collected from natural chestnut trees (*Castanea sativa*) on private land in Samsun, Türkiye, in June 2019. The fresh blossoms were collected, dried at room temperature, and powdered in a grinder. Then, the samples were extracted with distilled water and ethanol. For the aqueous extract, 6 g of dry sample was mixed with 60 mL of distilled water and brewed at 100 °C for 10 minutes. This extraction method is also known as infusion. The extract was filtered and stored at -20 °C until use. The second extract was prepared with 70% ethanol. For this purpose, 6 g of sample was added to 60 mL of 70% ethanol, shaken for 24 h, and filtered and evaporated under a vacuum evaporator (Heidolph, Schwabach, Germany) at 40 °C, after which the extract was finally dissolved in a small amount of 70% ethanol.

2.3. Determination of total phenolic content (TPC)

The TPC of the extracts was determined using the Folin-Ciocalteu method (Singleton & Rossi 1965) with gallic acid as the standard. TPC is expressed as mg gallic acid equivalent (GAE)/g dry sample using a standard curve.

2.4. Determination of total flavonoid content (TFC)

TFC of both extracts was measured using a spectrophotometric method with quercetin as standard (Fukumoto & Mazza 2000). TFC is expressed as mg quercetin equivalent (QUE)/g base on the curve.

2.5. Analysis of ferric reducing/antioxidant power (FRAP)

The ferric reducing/antioxidant power assay (FRAP) method described by Benzie & Strain (1999) was used to calculate the total antioxidant capacity of the extracts. For FRAP values, the results are given as $\mu\text{mol FeSO}_4 \cdot 7\text{H}_2\text{O}$ equivalents/ g dry matter.

2.6. DPPH•-free radical scavenging assay

The DPPH• assay was developed using a spectrophotometric method described previously by Brand-Williams *et al.* (1995). All DPPH• assay results are given with SC_{50} , which is the sample concentration that causes 50% radical scavenging.

2.7. Analyses of phenolic composition by HPLC-UV

To prepare the extract for chromatographic analysis, 10 mL of blossom extract was evaporated (Heidolph, Schwabach, Germany) at 40 °C to dryness. The residue was then dissolved in 10 mL distilled water (pH: 2), and the resulting aqueous solution was extracted three times with 5 mL diethyl ether (15 min, 200 rpm, room temperature). Following each extraction, the upper organic phase was collected. After that, the aqueous solution was extracted three times with 5 mL ethyl acetate (15 min, 200 rpm, room temperature). After these extractions, the organic phases were mixed and evaporated (Heidolph, Schwabach, Germany) at 30 °C to dryness. The residue was dissolved in 2 mL methanol, filtered through 0.45 μm filters, and analyzed using an HPLC device.

Calibrations were also performed for HPLC using 19 standard phenolic compounds at 280 and 340 nm (Elite La Chrome; Hitachi, Tokyo, Japan) on a device fitted with a reverse phase C_{18} column (150 mm, 4.6 mm, 5 μm ; Fortis). The R^2 values for each compound were between 0.998-1.000. The program employed was described in previous studies, with acetic acid, water, and acetonitrile being used as the mobile phase (Malkoç *et al.* 2019). The mobile phase was composed of (A) 2% acetic acid in water and (B) acetonitrile: water (70:30). Finally, 20 μL of the sample was injected individually at 25 °C, and the flow rate was set to 0.75 mL/min.

2.8. Anti-urease activity

The anti-urease activity test is based on urease inhibition of the indophenol method (Weatherburn 1967), and jack bean urease is used for the test. The absorbance was recorded at 625 nm (Thermo Scientific Spectrophotometer, Waltham, MA). The results for the samples and for acetohydroxamic acid (AA), which was used as a standard inhibitor compound, are expressed as IC₅₀, the level producing 50% inhibition of maximal activity.

2.9. In silico methods (Protocol for molecular docking study)

To analyze the interactions of four ligands, molecular docking experiments were performed using Autodock 4.2 software. The crystal structure of jack bean urease (*Canavalia ensiformis*) (PDB ID: 4GY7, Res: 1.49 Å) was downloaded from RCSB Protein Data Bank (<https://www.rcsb.org/>). In general, binding free energies (ΔG) for crystal structures and docking models are determined to assess the accuracy of binding affinity prediction between ligands and target proteins. The structures of the ligands were obtained from the Pubchem Database (pubchem.ncbi.nlm.nih.gov) and converted to a pdf file with BIOVIA Discovery Studio Visualizer 2018. The prepared ligands and proteins were used as input files for AutoDock 4.2 software (Morris et al. 2009). With the help of the software, a Lamarckian genetic algorithm technique was used. After minimizing the energy, the water molecules were removed, and a rigid protein and a flexible ligand were docked using the standard docking method with 100 independent runs for each ligand's torsion angle. In the catalytic site of the protein, Autodock 4.2 was used for all docking experiments. With a grid spacing of 0.375 Å, a grid was constructed with 126, 126, and 126 points in the x, y, and z directions. All other parameters were left at their default settings. The ligand-protein docked complexes were analyzed based on minimum binding energy values and ligand interaction (hydrogen/hydrophobic) patterns to predict the binding strength of four ligands. BIOVIA Discovery Studio Visualizer 2018 (Dassault Systèmes BIOVIA 2016) was used for the final visualization of the docked structures.

2.10. Statistical analyses

SPSS version 11.5 software was used for statistical analysis (IBM SPSS Statistics, Armonk, New York, USA). Mean and standard deviation are used to express descriptive statistics. Correlation analysis was performed using the Mann–Whitney U test. The significance level was set at $P < 0.05$.

3. Results and Discussion

3.1. TPC and TFC results for chestnut blossoms

The relevant values are shown in Table 1. The total amount of phenolic substance was 46.67 ± 0.37 mg GAE/g in the aqueous extract and 25.78 ± 0.15 mg GAE/g in the ethanolic extract. These data were statistically significantly different ($P < 0.05$). The higher amount of polyphenols in the aqueous phase indicates that the polyphenols found in chestnut blossom are rich in polar or hydrophilic compounds. Almost all phenolic acids are such compounds and are soluble in water. Flavonoids, the largest member of the polyphenol family, were determined at higher levels in the aqueous extract (6.14 ± 0.40 mg QE/g) than in the ethanolic extract (mg QE/g), although the statistical difference was significant ($P < 0.05$). Even though there was a statistically significant difference between the present values, the coefficient difference between the extracts was not as high as the difference for the total phenolic substance findings. The principal reason for this is that flavonoids are relatively non-polar in character, because ethanol has a lower polarity than water and, conversely, are more non-polar in character. Similar to the results of the present research, a previous study using the heat-assisted extraction method to extract total phenolic substances from chestnut blossoms reported rich water-soluble tannin (hydrolyzed tannin) and flavonoid contents (Caleja et al. 2019). When TPC and TFC values were compared with those of previous studies, this study clearly illustrates the bio-efficiency of chestnut blossoms. In a study using fresh chestnut flowers, TPC and TFC values were confirmed as 298 mg GAE/g and 160 mg catechin equivalent (CE)/g, respectively (Barreira et al. 2008). Another comprehensive study in the literature analyzed different parts of chestnut except the blossom in terms of some bioactivity assays (Silva et al. 2020). In this study, each part of the chestnut separately had value in terms of total phenolic substances. Although the study used a different unit than the current study, it was emphasized that the leaves (385.4 g of epicatechin equivalents per mg of residue) had higher total phenolic content than the inner and outer shells and burs of chestnut (Silva et al. 2020). In addition to this study, other indirect studies were carried out related to chestnut honey made from chestnut blossom nectar. Kolayli et al. (2016) determined the range of TPC and TFC in chestnut honey was 76.20-94.05 mg GAE/ 100 g and 4.20-6.50 mg QUE/ 100 g, and Can et al. (2015) found the mean value of TPC and TFC in chestnut honeys was 98.26 mg GAE/ 100 g and 8.10 mg QUE/100 g, respectively.

Table 1- Antioxidant properties of the chestnut blossom extracts

<i>Analysis Parameters</i>	<i>Aqueous Extract</i>	<i>Ethanollic Extract</i>
Total Phenolic Content (mg GAE/g)	46.67 ± 0.37 ^a	25.78 ± 0.15 ^b
Total Flavonoid Content (mg QE/g)	6.14 ± 0.40 ^a	5.02 ± 0.30 ^b
Total Antioxidant Capacity- FRAP (µmol FeSO ₄ .7H ₂ O/g)	648.47 ± 5.27 ^a	347.53 ± 2.09 ^b
DPPH Radical Scavenging-SC ₅₀ (mg/mL)	0.05 ± 0.01 ^b	0.11 ± 0.01 ^a

a, b: letters in the same lines are significantly different at the 5% level (P<0.05).

3.2. Antioxidant activity of chestnut blossoms

FRAP and DPPH• radical scavenging activities were utilized to evaluate the antioxidant properties of the chestnut blossoms. The FRAP method, which is based on the reduction of Fe (III)-complex in the presence of antioxidants, is used to calculate total antioxidant capacity. In general terms, a high FRAP value indicates high antioxidant capacity, and these values were approximately two times higher in aqueous extract than in ethanolic extract (648.47 ± 5.27 µmol FeSO₄.7H₂O/g for aqueous extract and 347.53 ± 2.09 µmol FeSO₄.7H₂O/g for ethanolic extract; P<0.005).

The DPPH• radical is an unnatural, synthetic radical, and the method based on it is a very sensitive, reliable, and simple test measuring the radical-scavenging ability of natural products. Any antioxidant scavenging this radical has high potential to eliminate dietary radicals, hydroxyl, superoxide, and nitric oxide formed by oxidative stress in the body. The amount of substance that cleanses half of this radical is defined as SC₅₀ (scavenging activity); the lower this value, the higher the activity. The DPPH• scavenging ability of the aqueous extract in the present study was approximately twice as high as for the ethanolic extract (0.05 ± 0.01 mg/mL SC₅₀ for aqueous extract and 0.11 ± 0.01 mg/mL SC₅₀ for ethanolic extract; P<0.005). In short, the results of both antioxidant tests showed that the aqueous extract had significant antioxidant capacity. This is mostly because the aqueous extract contains many phenolic compounds, which was also confirmed by HPLC-UV in this study. Some previous studies also confirmed that aqueous extracts of chestnut blossoms have high antioxidant value (Tuyen et al. 2017; Caleja et al. 2019).

3.3. Evaluation of the phenolic profile of chestnut blossoms

According to studies in the literature, the profusion of phenolic compounds present in the composition of chestnut flowers allows for combination of their remarkable bioactive properties. Moreover, these studies highlighted that the phenolic compounds in chestnut flowers are promising agents as natural food preservative in the food industry (Carocho et al. 2014; Caleja et al. 2019; Alaya et al. 2021).

The phenolic compositions of the current samples, extracted with two different extract polarities, are summarized in Table 2. The primary phenolic compounds in the aqueous extract, which analyzed 19 phenolic standards using HPLC-UV, were rutin, gallic acid, and myricetin, and the main phenolic compounds in the ethanolic extract were rutin, luteolin, and resveratrol. The ethanolic extract contained more rutin (1228.93 ± 2.76 µg/g) than the aqueous extract (1117.72 ± 2.92 µg/g) (P<0.005). Also, gallic acid values were approximately 10 times higher in the aqueous extract (979.47 ± 2.01 µg/g) than in the ethanolic extract (60.61 ± 0.88 µg/g) (P<0.005). A previous study also reported that chestnut blossoms are very rich in gallic acid (Tuyen et al. 2017). Luteolin, a flavonoid derivative and a flavone exhibiting wide biological activity, was detected at the highest level in the ethanolic extracts but not in the aqueous extracts. Rutin, also known as quercetin-3-O-rutinoside (α-L-rhamnopyranosyl- (1→6) -β-D-glucopyranose), is a product of glycosylation of the flavanol quercetin with a disaccharide and was detected at similar amounts in both extracts since it is amphipathic in character (Gullón et al. 2017).

Table 2- HPLC-UV analyses of the chestnut blossom extracts

<i>Phenolic Compounds (µg/g)</i>	<i>Aqueous Extract</i>	<i>Ethanolic Extract</i>
Gallic acid	979.47 ± 2.01 ^b	60.61 ± 0.88 ^a
Protocatechuic acid	77.60 ± 0.51 ^b	35.75 ± 0.44 ^a
<i>p</i>-OH benzoic acid	N.D.	4.85 ± 0.09
Catechin	104.22 ± 0.78 ^b	42.65 ± 0.31 ^a
Caffeic Acid	N.D.	N.D.
Syringic Acid	3.38 ± 0.07 ^b	2.03 ± 0.06 ^a
Epicatechin	N.D.	N.D.
<i>p</i>-coumaric acid	45.01 ± 0.39 ^b	37.86 ± 0.27 ^a
Ferulic acid	N.D.	N.D.
Rutin	1117.72 ± 2.92 ^a	1228.93 ± 2.76 ^b
Myricetin	334.59 ± 1.01 ^b	51.97 ± 0.56 ^a
Resveratrol	14.91 ± 0.16 ^a	104.42 ± 0.96 ^b
Daidzein	6.82 ± 0.17 ^b	2.42 ± 0.08 ^a
Luteolin	N.D.	918.24 ± 1.31
<i>t</i>-cinnamic acid	1.79 ± 0.09	N.D.
Hesperetin	N.D.	15.04 ± 0.38
Chrysin	N.D.	N.D.
Pinocembrin	N.D.	N.D.
CAPE	N.D.	N.D.

N.D. Not Detected; a, b letters in the same line are significantly different at the 5% level ($P < 0.05$)

3.4. Urease inhibition activity of chestnut blossoms

The other biological activity test for both samples was urease inhibition. Urease enzyme inhibitors are particularly important for *Helicobacter pylori* inhibition, and bacteria survive with this enzyme secreted into the extracellular environment. Both chestnut blossom extracts were found to inhibit the enzyme, but the aqueous extracts (IC_{50} : 2.55 ± 0.09 mg/mL) caused greater inhibition than the ethanolic extracts (IC_{50} : 4.57 ± 0.24 mg/mL). The statistical difference was confirmed at $P < 0.005$. (Table 3). Urease enzyme inhibition is thought to be caused by polyphenols; even so, it was shown that natural products with high phenolic acid and flavonoid contents exhibit higher activity in some urease inhibition studies (Al-Rooqi et al. 2023; Kataria & Khatkar 2019a). Aside from that, previous reports about natural compounds defended a close synergistic effect between urease inhibition activity and phenolic agents, which is similar to our claim (Uddin et al. 2011; Paun et al. 2014; Can et al. 2022). Moreover, in this study, the molecular docking properties of some compounds abundantly found in chestnut blossom extracts are presented to show the binding interaction of these compounds as a reason for urease inhibition.

Table 3- Urease inhibitions of the chestnut blossom extracts

<i>Samples</i>	<i>Inhibition IC_{50} (mg/mL)</i>
Aqueous Extract	2.55 ± 0.09^b
Ethanolic Extract	4.57 ± 0.24^a
Acetohydroxamic acid (AA) (µg/mL)	25.09 ± 0.02^c

a, b, c: letters in the same column are significantly different at the 5% level ($P < 0.05$)

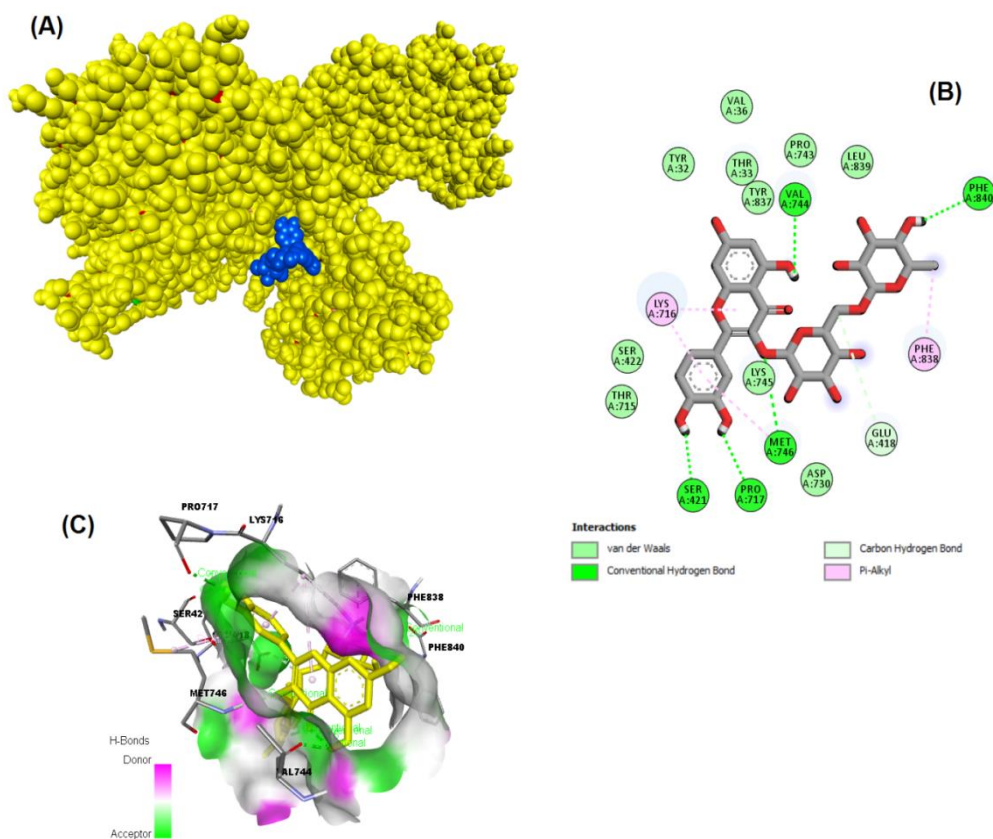
3.4. Molecular docking assessment of major phenolics found in chestnut blossoms

The results for successful docking of all ligands used in these docking experiments revealed significant interactions of the ligands with the target receptors. The target protein was more effectively bonded by four ligands (myricetin, gallic acid, rutin, and luteolin) than by the reference molecule. The ligand myricetin was strongly bound to jack bean urease with a binding energy of -7.30 kcal/mol. With a binding energy of -7.21 kcal/mol, the ligand luteolin also effectively docked with the target receptors. The ligands rutin and gallic acid were bound to the target protein with binding energies of -6.75 and -5.48 kcal/mol, respectively. Table 4 contains additional information. Figures 1-4 depict docked position in the target receptor for each ligand, as well as the residues with which each ligand interacts and the interactions. The molecular binding of some ligands, including phenolic compounds, with the urease enzyme was reported in the literature. In one study, some synthesized ligands showed significantly higher binding result to the active cavity of jack bean protein, and there was consistency between *in silico* and *in vitro* results (Kataria & Khatkar 2019a). Kataria & Khatkar (2019b) studied molecular docking with natural phenolic compounds as possible urease inhibitors. According to that study, five compounds -diosmin, morin, chlorogenic acid, capsaicin, and resveratrol- showed remarkable affinity towards the receptor.

Table 4- Summary of ligands against Urease enzyme from Jack Bean with binding energy, K_i and interacted residues in the binding site

No	Receptor Name	Receptor PDB ID	Ligand Name	Binding Energy (kcal/mol)	K_i	Interacted Residues with Ligand
1			Myricetin (3,3',4',5,5',7-Hexahydroxyflavone)	-7.30	4.44 μ M	Thr740, Val81, Ala80, Val36, Tyr32, Val744, Asp730, Glu718, Phe712, Lys716, Glu742
2			Luteolin (2-(3,4-Dihydroxyphenyl)-5,7-dihydroxy-4-chromenone)	-7.21	5.18 μ M	Arg835, Phe840, Glu34, Arg29
3	Urease from Jack bean (<i>Canavalia ensiformis</i>) EC: 3.5.1.5	4GY7	Rutin (Quercetin-3-rutinoside hydrate)	-6.75	11.28 μ M	Val744, Phe840, Phe838, Glu418, Lys745, Met746, Pro717, Ser421, Lys716
4			Gallic acid (3,4,5-trihydroxybenzoic acid)	-5.48	95.88 μ M	Lys709, Glu742, Gln82, Ala80, Leu77
5			*Acetohydroxamic acid (N-hydroxyacetamide)	-4.51	491.58 μ M	Leu833, Asn836, Val831, Ser834, Asp295

*: Reference compound

**Figure 1- Binding pose profile of Rutin (Quercetin-3-rutinoside hydrate) in the target protein (A), blue shaped molecule represents the ligand and yellow shaped molecule indicates the receptor. The two-dimension (2D) (B) and three-dimension (3D) (C) interactions analysis of Urease from Jack bean with compound Rutin. (Representation of docked structures with BIOVIA Discovery Studio Visualizer software)**

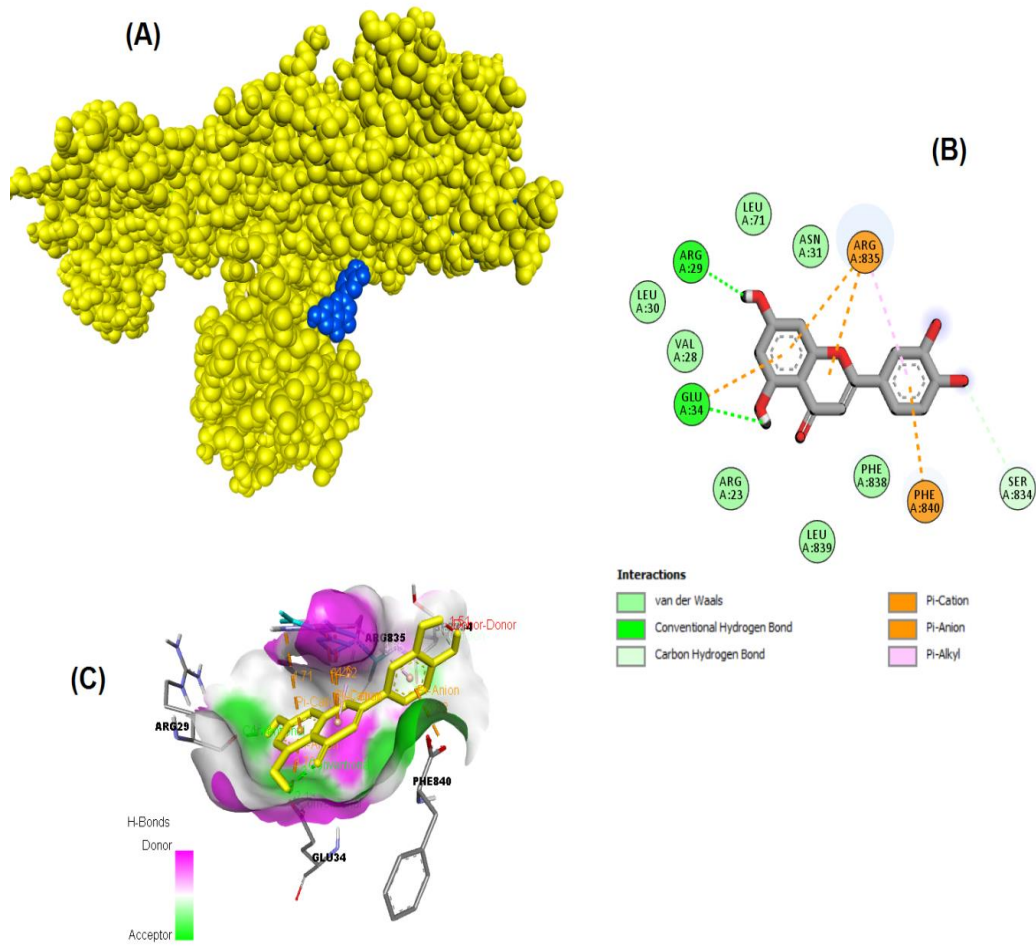


Figure 2- Binding pose profile of Luteolin (2-(3,4-Dihydroxyphenyl)- 5,7-dihydroxy-4-chromenone) in the target protein (A), blue shaped molecule represents the ligand and yellow shaped molecule indicates the receptor. The two-dimension (2D) (B) and three-dimension (3D) (C) interactions analysis of Urease from Jack bean with compound Luteolin. (Representation of docked structures with BIOVIA Discovery Studio Visualizer software)

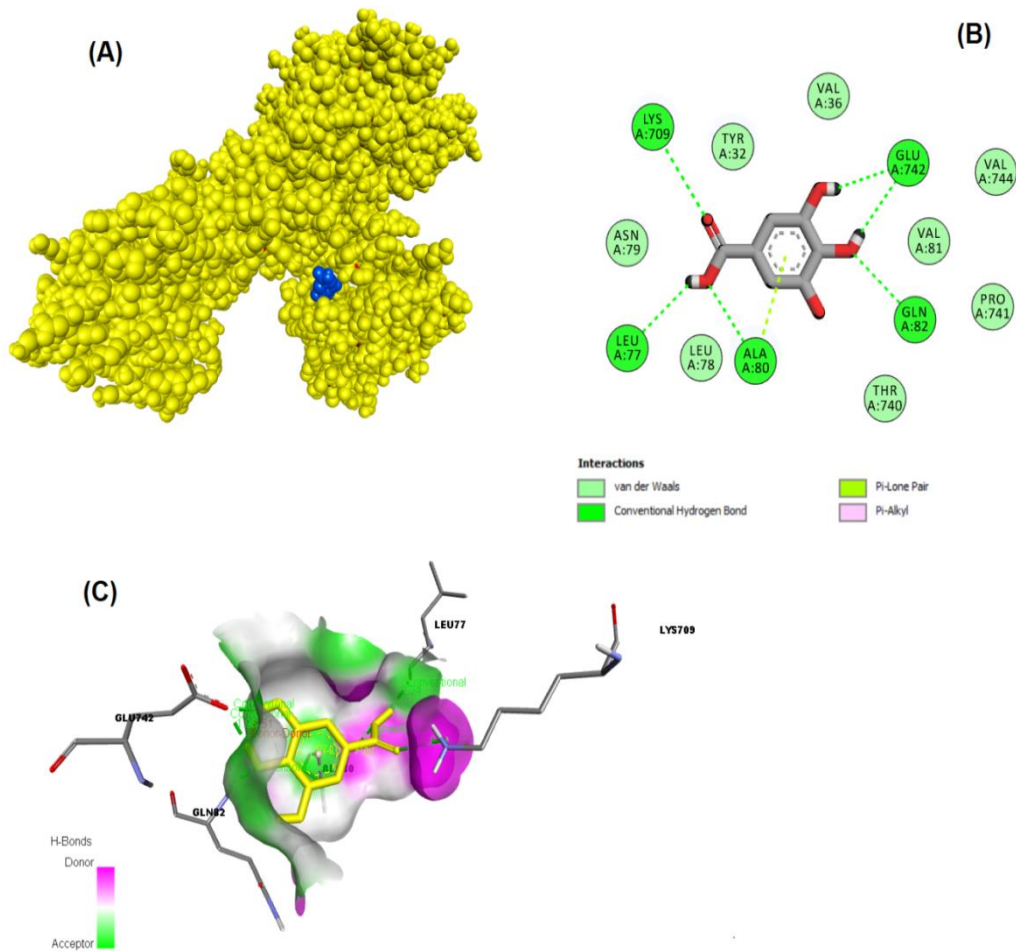


Figure 3- Binding pose profile of Gallic Acid (3,4,5-trihydroxybenzoic acid) in the target protein (A), blue shaped molecule represents the ligand and yellow shaped molecule indicates the receptor. The two-dimension (2D) (B) and three-dimension (3D) (C) interactions analysis of Urease from Jack bean with compound Gallic Acid. (Representation of docked structures with BIOVIA Discovery Studio Visualizer software)

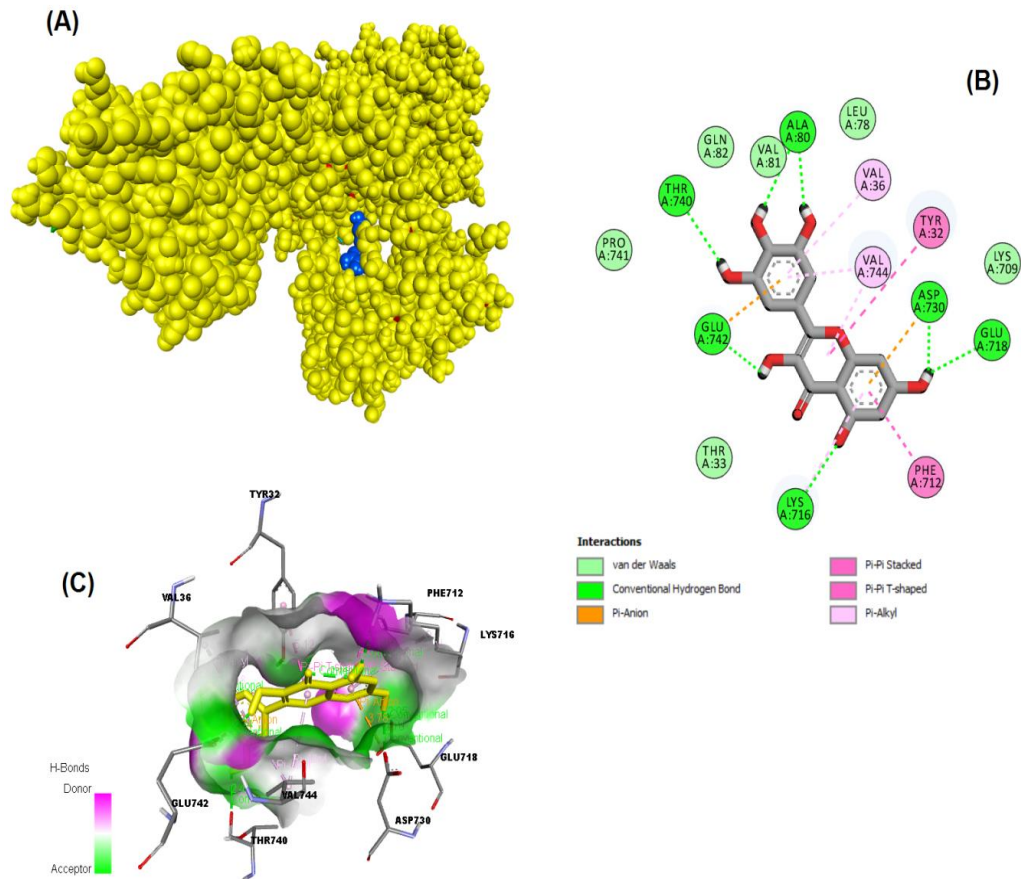


Figure 4- Binding pose profile of Myricetin (3,3',4',5,5',7-Hexahydroxyflavone) in the target protein (A), blue shaped molecule represents the ligand and yellow shaped molecule indicates the receptor. The two-dimension (2D) (B) and three-dimension (3D) (C) interactions analysis of Urease from Jack bean with compound Myricetin. (Representation of docked structures with BIOVIA Discovery Studio Visualizer software)

4. Conclusions

Thousands of tons of chestnut blossoms fall into the soil every year, and unfortunately, they rot spontaneously. However, it is well known that chestnut blossoms are a natural product with high biological activity that can be used as a natural food additive with numerous useful bio-properties. The current findings corroborate this assertion, especially the analysis of enzyme inhibition and antioxidant effects of the aqueous extract, which showed a nearly two-fold effect based on quantitative data. Furthermore, attempts were made to explain both antioxidants and urease inhibition by the phenolics found in each extract. Especially, rutin, which was the dominant phenolic in both chestnut blossom extract types, was a significant reason for the level of antioxidants; moreover, myricetin and luteolin were evaluated as excellent urease inhibitors due to having an effective response on molecular docking analysis at micromolar (μM) concentrations of 4.44 and 5.18, respectively. Even though this study explains some of the bioactive properties of chestnut blossoms, it is obvious that further research is needed to learn more about them.

Acknowledgments

We would like to thank Avni Haliloğlu (Fanus Gıda A.Ş., Türkiye) for the original idea for this study.

Data availability: Data are available on request due to privacy or other restrictions.

Authorship Contributions: Concept: H.S., S.K., U.S., Design: H.S., S.K., U.S., Data Collection or Processing: H.S., Y.K., Z.C., A.O., H.I.G., Analysis or Interpretation: H.S., Y.K., Z.C., H.I.G. Literature Search: H.S., S.K., A.O., Writing: H.S., S.K., H.I.G.

Conflict of Interest: All authors declare no conflict of interest.

Financial Disclosure: The author declared that this study received no financial support.

References

- Alaya Ib, Pereira E, Dias M I, Pinela J, Calhella R C, Soković M, Kostić M, Prieto M A, Essid F, Caleja C, Ferreira I C F R & Barros L (2021). Development of a natural preservative from chestnut flowers: Ultrasound-assisted extraction optimization and functionality assessment. *Chemosensors* 9(6): 141. doi.org/10.3390/chemosensors9060141
- Al-Rooqi M M, Mughal E U, Raja Q A, Hussein E M, Naeem N, Sadiq A, Asghar B H, Moussa Z & Ahmed S A (2023). Flavonoids and related privileged scaffolds as potential urease inhibitors: A review. *RSC Advances* 13: 3210-3233. doi.org/10.1039/D2RA08284E
- Aimone C, Grillo G, Boffa L, Giovando S & Cravotto G (2023). Tannin extraction from chestnut wood waste: From lab scale to semi-industrial plant. *Applied Sciences* 13(4): 2494. doi.org/10.3390/app13042494
- Barreira J C M, Ferreira I C F R, Oliveira M B P P & Pereira J A (2008). Antioxidant activities of the extracts from chestnut flower, leaf, skins and fruit. *Food Chemistry* 107(3): 1106–1113. doi.org/10.1016/j.foodchem.2007.09.030
- Benzie I F F & Strain J J (1999). Ferric reducing/antioxidant power assay: Direct measure of total antioxidant activity of biological fluids and modified version for simultaneous measurement of total antioxidant power and ascorbic acid concentration. *Methods in Enzymology* 299: 15–27. doi.org/10.1016/S0076-6879(99)99005-5
- Brand-Williams W, Cuvelier M E & Berset C (1995). Use of a free radical method to evaluate antioxidant activity. *LWT - Food Science and Technology* 28(1): 25–30. doi.org/10.1016/S0023-6438(95)80008-5
- Caleja C, Barros L, Prieto M A, Bento A, Oliveira M B P P & Ferreira I C F R (2019). Development of a natural preservative obtained from male chestnut flowers: Optimization of a heat-assisted extraction technique. *Food and Function* 10: 1352–1363. doi.org/10.1039/c8fo02234h
- Can Z, Yildiz O, Sahin H, Akyuz Turumtay E, Silici S & Kolayli S (2015). An investigation of Turkish honeys: Their physico-chemical properties, antioxidant capacities and phenolic profiles. *Food Chemistry* 180: 133–141. doi.org/10.1016/j.foodchem.2015.02.024
- Can Z, Kara Y, Kolayli S & Çakmak İ (2022). Determination of anti-urease activity of propolis from the Marmara Region of Turkey. *Uludağ Bee Journal* 22 (1): 25-30. doi.org/10.31467/uluarcilik.1068885
- Carocho M, Barros L, Bento A, Santos-Buelga C, Morales P & Ferreira I C F R (2014). *Castanea sativa* Mill. flowers amongst the most powerful antioxidant matrices: A phytochemical approach in decoctions and infusions. *BioMed Research International* 2014(Article ID 232956): 1–7. doi.org/10.1155/2014/232956
- Carocho M, Barreira J C M, Barros L, Bento A, Cámara M, Morales P & Ferreira I C F R (2015). Traditional pastry with chestnut flowers as natural ingredients: An approach of the effects on nutritional value and chemical composition. *Journal of Food Composition and Analysis* 44: 93–101. doi.org/10.1016/j.jfca.2015.08.003
- Comandini P, Lerma-García M J, Simó-Alfonso E F & Toschi T G (2014). Tannin analysis of chestnut bark samples (*Castanea sativa* Mill.) by HPLC-DAD-MS. *Food Chemistry* 157: 290–295. doi.org/10.1016/j.foodchem.2014.02.003
- Dudek-Makuch M & Studzińska-Sroka E (2015). Horse chestnut - efficacy and safety in chronic venous insufficiency: An overview. *Revista Brasileira de Farmacognosia* 25(5): 533–541. doi.org/10.1016/j.bjrp.2015.05.009
- Fukumoto L R & Mazza G (2000). Assessing antioxidant and prooxidant activities of phenolic compounds. *Journal of Agricultural and Food Chemistry* 48(8): 3597–3604. doi.org/10.1021/jf000220w
- Gullón B, Lú-Chau T A, Moreira M T, Lema J M & Eibes G (2017). Rutin: A review on extraction, identification and purification methods, biological activities and approaches to enhance its bioavailability. *Trends in Food Science & Technology* 67: 220–235. doi.org/10.1016/j.tifs.2017.07.008
- Karkar B, Şahin S & Güneş M E (2021). Evaluation of antioxidant properties and determination of phenolic and carotenoid profiles of chestnut bee pollen collected from Turkey. *Journal of Apicultural Research* 60(5): 765–774. doi.org/10.1080/00218839.2020.1844462
- Kataria R & Khatkar A (2019a). Molecular docking, synthesis, kinetics study, structure–activity relationship and ADMET analysis of morin analogous as *Helicobacter pylori* urease inhibitors. *BMC Chemistry* 13(1): 45. doi.org/10.1186/s13065-019-0562-2
- Kataria R & Khatkar A (2019b). Molecular docking of natural phenolic compounds for the screening of urease inhibitors. *Current Pharmaceutical Biotechnology* 20(5): 410–421. doi.org/10.2174/1389201020666190409110948
- Kolayli S, Can Z, Yildiz O, Sahin H & Karaoglu S A (2016). A comparative study of the antihyaluronidase, antiurease, antioxidant, antimicrobial and physicochemical properties of different unifloral degrees of chestnut (*Castanea sativa* Mill.) honeys. *Journal of Enzyme Inhibition and Medicinal Chemistry* 31(sup3): 96–104. doi.org/10.1080/14756366.2016.1209494
- Malkoç M, Çakır H, Kara Y, Can Z & Kolayli S (2019). Phenolic composition and antioxidant properties of Anzer honey from Black Sea Region of Turkey. *Uludağ Bee Journal* 19(2): 143–151. doi.org/10.31467/uluarcilik.602906
- Morris G M, Ruth H, Lindstrom W, Sanner M F, Belew R K, Goodsell D S & Olson A J (2009). AutoDock4 and AutoDockTools4: Automated docking with selective receptor flexibility. *Journal of Computational Chemistry* 30(16): 2785–2791. doi.org/10.1002/jcc.21256
- Paun G, Litescu S C, Neagu E, Tache A & Lucian Radu G (2014). Evaluation of *Geranium* spp., *Helleborus* spp. and *Hyssopus* spp. polyphenolic extracts inhibitory activity against urease and α -chymotrypsin. *Journal of Enzyme Inhibition and Medicinal Chemistry* 29(1): 28–34. doi.org/10.3109/14756366.2012.749399
- Peng F, Yin H, Du B, Niu K, Yang Y & Wang, S (2022). Anti-inflammatory effect of flavonoids from chestnut flowers in lipopolysaccharide-stimulated RAW 264.7 macrophages and acute lung injury in mice. *Journal of Ethnopharmacology* 290: 115086. doi.org/10.1016/j.jep.2022.115086
- Rodrigues P, Ferreira T, Nascimento-Gonçalves E, Seixas F, Gil da Costa R M, Martins T, Neuparth M J, Pires M J, Lanzarin G, Félix L, Venâncio C, Ferreira I C F R, Bastos M M S M, Medeiros R, Gaivão I, Rosa E & Oliveira P A (2020). Dietary supplementation with chestnut (*Castanea sativa*) reduces abdominal adiposity in FVB/n mice: A preliminary study. *Biomedicine* 8(4): 75. doi.org/10.3390/biomedicine8040075
- Rodríguez-Flores M S, Escuredo O, Seijo M C, Rojo S, Vilas-Boas M & Falcão S I (2023). Phenolic profile of castanea bee pollen from the Northwest of the Iberian Peninsula. *Separations* 10(4): 270. doi.org/10.3390/separations10040270
- Sahin H, Kaltalioglu K, Erisgin Z, Coskun-Cevher S & Kolayli S (2019). Protective effects of aqueous extracts of some honeys against HCl/ethanol-induced gastric ulceration in rats. *Journal of Food Biochemistry* 43(12): e13054. doi.org/10.1111/jfbc.13054
- Silva V, Falco V, Dias M I, Barros L, Silva A, Capita R, Alonso-Calleja C, Amaral J S, Igrejas G, C F R Ferreira I, Poeta P (2020). Evaluation of the phenolic profile of *Castanea sativa* Mill. by-products and their antioxidant and antimicrobial activity against multiresistant bacteria. *Antioxidants* 9(1): 87. doi.org/10.3390/antiox9010087

- Singleton V L & Rossi J A (1965). Colorimetry of total phenolics with phosphomolybdic-phosphotungstic acid reagents. *American Journal of Enology and Viticulture* 16: 144–158. doi.org/10.5344/ajev.1965.16.3.144
- Tuyen P T, Xuan T D, Khang D T, Ahmad A, Quan N V, Tu Anh T T, Anh H & Minh T N (2017). Phenolic compositions and antioxidant properties in bark, flower, inner skin, kernel and leaf extracts of *Castanea crenata* Sieb. et Zucc. *Antioxidants (Basel)* 6(2): 31. doi.org/10.3390/antiox6020031
- Uddin N, Siddiqui B S, Begum S, Bhatti H A, Khan A, Parveen S & Choudhary M I (2011). Bioactive flavonoids from the leaves of *Lawsonia alba* (Henna). *Phytochemistry Letters* 4(4): 454–458. doi.org/10.1016/j.phytol.2011.05.007
- Weatherburn M W (1967). Phenol-hypochlorite reaction for determination of ammonia. *Analytical Chemistry* 39(8): 971–974. doi.org/10.1021/ac60252a045



Copyright © 2024 The Author(s). This is an open-access article published by Faculty of Agriculture, Ankara University under the terms of the [Creative Commons Attribution License](#) which permits unrestricted use, distribution, and reproduction in any medium or format, provided the original work is properly cited.



Environmental Factors and Semiarid Plants Species on Eroded Marly Soils in Southwest Anatolia (Eskişehir/Türkiye)

Münevver ARSLAN^a, Neslihan BALPINAR^b, Mesrur Ümit BİNGÖL^{c*}, Nejat ÇELİK^a

^aResearch Institute for Forest, Soils & Ecology, 26160 Eskişehir, TÜRKİYE

^bBurdur Mehmet Akif Ersoy University, Faculty of Arts and Sciences, Department of Biology, 15030 Burdur, TÜRKİYE

^cAnkara University, Faculty of Science, Department of Biology, 06100 Ankara, TÜRKİYE

ARTICLE INFO

Research Article

Corresponding Author: Mesrur Ümit BİNGÖL, E-mail: mumit1111@hotmail.com

Received: 08 November 2022 / Revised: 31 July 2023 / Accepted: 02 August 2023 / Online: 09 January 2024

Cite this article

Arslan M, Balpinar N, Bingöl M Ü, Çelik N (2024). Environmental Factors and Semiarid Plants Species on Eroded Marly Soils in Southwest Anatolia (Eskişehir/Türkiye). *Journal of Agricultural Sciences (Tarım Bilimleri Dergisi)*, 30(1):90-98. DOI: 10.15832/ankutbd.1200867

ABSTRACT

The natural regeneration of vegetation in areas of marly soils is restricted due to drought and soil erosion. For the ecological restoration of eroded areas, the selection of suitable plant species is critical. The aim of this study is to assess specific plant species and their ecological characteristics for their ability to thrive under drought in eroded areas with marly soil. The study was conducted on 36 sampling locations in the marly areas of Eskişehir-Bozan, Türkiye, during the most drought-prone months, August and September, in 2011 and 2012. Vegetation sampling was conducted according to the Braun-Blanquet method. Fifteen plant taxa with the highest coverage and frequency were

identified. Relationships between plant species and environmental factors were determined using Spearman's correlation analysis. According to the results of numerical analysis, there were correlations between ecological parameters including nitrogen, phosphorus, organic matter, lime, slope, altitude and plant taxa. The resistance rate of fifteen plant taxa in marly areas is quite high even in the driest months. These plant taxa, possessing properties essential for soil protection, may be used for revegetation practices of marly areas exposed to soil erosion. This study's findings will provide useful guidance for vegetation programs.

Keywords: Eroded area, Growth form, Vegetation, Spearman's correlation

1. Introduction

Marl rocks are widespread in many countries and marl derived soil is a mixture of clay and calcium carbonate and is very susceptible to erosion (Bouma & Imeson 2000; Sokouti & Razaki 2015). It has been determined that the source of sediment yield in arid areas is marly soils with high erodibility (Thoms et al. 2004). Steep slopes and low vegetation lead to further erosion. Soil erosion affects all natural and cultivated areas around the world and causes significant soil loss (Burylo et al. 2011) and is known to be significant threat to sustainability in the context of ecosystem services. In particular, it is primarily responsible for land degradation in the cultivated areas located in fragile ecosystems (FAO & ITPS 2015). There is a consensus that ecosystem restoration should be scientifically reliable and reflect an accurate understanding of ecological principles (Stokes et al. 2014). Data regarding vegetation dynamics and some ecological characteristics of an area can help us assess the vulnerability of degraded soils due to soil erosion and the effectiveness of restoration activities (Burylo et al. 2011). In Türkiye, water erosion is a major problem and the predicted average soil loss rate is higher than 5 t ha⁻¹ y⁻¹ in the 26.4% of agricultural lands (Erpul et al. 2020). In particular in the wheat production areas, which constitute 67% of the agricultural areas in which field crops are cultivated, it leads to a significant reduction in production potentials at the national scale. But, wheat demand tends to increase due to rising population density (Anonymous 2019). Therefore, accurate estimation of land productivity under the accelerated soil erosion dynamics has great importance in terms of conservation natural resources (Saygın 2021).

The Central Anatolian Region of Türkiye is a mountainous Mediterranean climate, and semiarid climatic conditions prevail in this region (Akman 1999). The main anthropogenic pressures affecting the forest resources in this region are overexploitation and overgrazing (Kahveci 2017). Relict forests are essential for ecological restoration in such degraded semiarid regions (Kahveci 1998). The Anatolian black pine woodlands in the marl areas of Eskişehir on the eastern foot slopes of the Sündiken Mountains are one of the relict forests. In addition, plants in these areas can be evaluated as seed source reserves for plant species used in revegetation efforts. The plants in these areas can adapt to changing environmental conditions (Loreau et al. 2001).

Vegetation degradation leads to soil erosion that decline in vegetation cover and floristic composition (Guerrero-Campo & Montserrat-Martí 2000), and water erosion and drought conditions in marly fields prevent the regeneration of vegetation (Cerdeña 1999; Breton et al. 2016). The relationships between soil erosion on marly soils and the plant or vegetation characteristics have been widely studied (Cerdeña 1999; Guerrero-Campo & Montserrat-Martí 2000; Guerrero-Campo & Montserrat-Martí 2004; Guerrero-Campo et al. 2008; De Baets et al. 2007; Burylo et al. 2009; Varavipour et al. 2010; Burylo et al. 2011; Breton et al. 2016). Ecological studies have indicated that it is crucial to understand the environmental conditions and past rehabilitation projects to minimise erosion in marly soils. The selection of suitable species in studies of ecological restoration is also critical (Bochet & García-Fayos 2004; Bochet & García-Fayos 2015). Plant studies in the marly areas in Türkiye have to date generally focused on plant communities (Çetik 1985; Akman 1995). These vegetation studies are insufficient to reveal relevant site factors in detail. The aim of this study is to determine the plant species and some properties of eroded extremely limy soils in semiarid land, and to record growth forms of the plant species. This assessment will allow, for the first time, a determination of the plant species that can be used in the revegetation practices of highly limy and alkaline (marly) soils in semiarid areas.

2. Material and Methods

2.1. Site descriptions

This study was conducted in areas surrounding Bozan, Eskisehir, Türkiye (Table 1), in areas of degraded Anatolian black pine (*Pinus nigra* J.F.Arnold subsp. *pallasiana* (Lamb.) Holmboe) and anthropogenically degraded oak-juniper and steppe that developed after forest destruction in the eastern foot slopes of the Sündiken Mountains. It is in the Irano-Turanian phytogeographical region (Davis 1965). Vegetation cover has been destroyed due to long-term animal grazing pressure (Figure 1), which has resulted in soil and water erosion and the destruction of the areas vegetation. Marly soils are common and dominant in the research area. Generally, the upper soil layer in the area is lost because of erosion. As a result, surface erosion is generally observed in the area.

Table 1- Sampling areas, habitat and environmental variables

Sampling location	Date	Locality	Latitude (36S)	Longitude	Sampling location	Date	Locality	Latitude (36S)	Longitude
1	05.07.2011	Bozan-Circir	339327	4410312	19	10.07.2012	Circir-Agachisar V. road	339935	4412696
2	05.07.2011	Bozan-Circir	339328	4410226	20	10.07.2012	Circir-Agachisar V. road	339810	4412499
3	02.09.2011	Northern of Bugduz V.	337487	4418965	21	25.06.2015	4 km to Tasliburun wood storage	339589	4415712
4	02.09.2011	Southern of Ozdenk V.	329683	4417670	22	11.07.2012	Eastern of Bugduz V.	336555	4414325
5	02.09.2011	Southern of Ozdenk V.	329722	4417795	23	11.07.2012	Bugduz V.	337203	4415574
6	03.09.2011	Southern of Ozdenk V.	330057	4418877	24	11.07.2012	Bugduz V.	337030	4417567
7	03.09.2011	Southern of Ozdenk V.	330099	4417911	25	26.06.2015	Eastern of Derekoy V.	330126	4420066
8	03.09.2011	Bozan-Mihaliccik 4. km	340789	4409553	26	12.07.2012	Bozan-Mihaliccik road	346325	4410578
9	03.09.2011	Eastern part of Asagi Dudas V.	349093	4408892	27	12.07.2012	Asagi Dudas V.	348970	4408772
10	03.09.2011	Bozan-Circir	339904	4411838	28	12.07.2012	Asagi Dudas V.	348474	4408399
11	04.09.2011	Southeastern of A.Doganoglu V.	344636	4411530	29	12.07.2012	İlme farm	343095	4408100
12	04.09.2011	2 km east of Karageyikli V.	352529	4411977	30	12.07.2012	Southern of Asagi Doganoglu V.	346482	4408847
13	04.09.2011	2 km east of Karageyikli V.	352593	4411967	31	12.07.2012	Yukari Doganoglu V.	346888	4409057
14	04.09.2011	2 km east of Karageyikli V.	352593	4411967	32	13.07.2012	Between Ozdenk-Cukurhisar V.	330410	4416942
15	09.07.2012	Tasliburun wood storage	339876	4419335	33	13.07.2012	Between Agachisar-Ozdenk V.	330485	4417530
16	09.07.2012	Tasliburun	339664	4418684	34	13.07.2012	Circir	340901	4411107
17	09.07.2012	Between Circir-Tasliburun	339873	4414055	35	13.07.2012	Agachisar V. road	339540	4415828
18	09.07.2012	Tasliburun-Kalmagil	339469	4418790	36	20.05.2015	Ozdenk V.	330157	4418041

V: Village



Figure 1- Animal grazing pressure in the study area

2.2. Climate of the study area

We used climatic data from meteorological stations in the Eskişehir-Region (1960–2015) and Alpu-Region (1984–2002) taken from the Meteorology General Directorate which were the stations closest to the study area. The data were evaluated according to the Emberger method (Akman & Daget 1971; Akman 1999). Based on these data from the weather stations, the Eskişehir region is located in a semiarid and cold winter Mediterranean bioclimate and the Alpu region is located in a semiarid and extremely cold winter Mediterranean bioclimate (Table 2). The precipitation regime of the Alpu and Eskişehir stations is respectively spring, winter, autumn, and summer with the least precipitation in the summer season. According to the precipitation-temperature graph (Walter & Lieth 1967), there is a dry period from June to October in the study area (Figure 2).

Table 2- Bioclimatic classification of the research area

Meteorological station	P	M	m	PE	Q	S	Bioclimate type	
Locality	Alt. (m)							
Alpu-Region	765	376.8	30.4	-4.2	53.7	38.04	1.77	Semi-arid, extremely cold winter Mediterranean bioclimate
Eskişehir-Region	801	286.0	29.1	-3.0	44.0	31.13	1.51	Semi-arid, cold winter Mediterranean bioclimate

P: Average annual precipitation total (mm); M: Maximum temperature average of the warmest month (°C); m: Minimum temperature average of the coldest month (°C); PE: Sum of summer precipitation (mm); S: Drought index = $\frac{PE}{M}$; Q: Precipitation-temperature equal = $\frac{2000P}{(M + m + 546.4)(M - m)}$

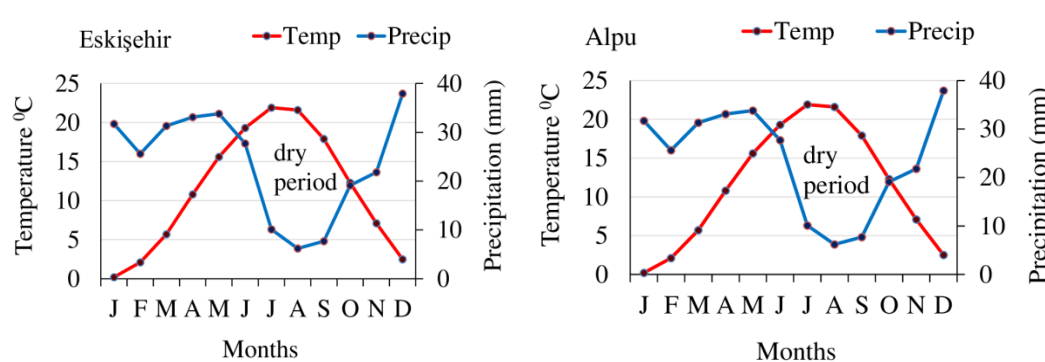


Figure 2- Climate diagrams of the nearest meteorological stations from the study area

2.2. Data collection and methods

The taxa studied were collected from 36 different locations where erosion had been observed. The sampling areas were within degraded forests, shrublands, and steppe areas (Figure 3). The size of the sampling areas is according to the smallest area method, which is 200 m² in wooded and bushy areas and 50 m² in steppe vegetation (Akman et al. 2001).



Figure 3- Degraded forest (a), shrublands (b), and steppe areas (c)

The study area is under intense anthropogenic pressure. However, the sampling areas were selected so that the vegetation was as representative as possible. The studies were carried out in August and September when the drought was most severe in 2011–2012, and all vascular plants were recorded on vegetation scorecards. The Braun-Blanquet (1932) method was used for vegetation measurements. Physiographic factors such as slope (degree), exposure (degree) and elevation (m) were determined. For the purpose of determine soil properties of each sampling area, 72 soil samples were taken from the depth of 0–10 cm and 10–30 cm. Growth forms of plant species were also recorded. The high-frequency species were determined by the vegetation table. Following this, plant species that formed bunches and colonies, shrubs and plants in tree form were identified.

2.3. Laboratory analyses

The collected plant specimens were identified according to Davis (1965–1985). Soil samples brought to the lab for analysis were air-dried, ground and sifted through a 2-mm sieve. Physical soil analyses included texture [sand (%), silt (%) and clay (%)], and chemical soil analyses included soil pH, organic matter (%) lime (CaCO_3 , %), total nitrogen (%) and available phosphorus (P, ppm). Soil pH was determined using an electrometric method in a solution ratio of 1:5 (soil/water) in distilled water (TS ISO 10390 2013). The texture was measured using the Bouyoucos hydrometer method (Kroetsch & Wang 2008). Total lime (CaCO_3) and nitrogen were determined by Scheibler calcimeter (Kacar 2009) and the Kjeldahl method (Jackson 1962), respectively. Organic matter content was determined using the Walkley–Black wet oxidation method (TS 8336 2008). Available phosphorus in alkaline soils was measured using the Olsen method (Kacar 2009).

2.4. Statistical analysis

In the statistical analysis, the presence/absence (1/0) data of plant species and numerical data of environmental variables were evaluated. Relationships between environmental factors and plant taxa were calculated using Spearman's correlation coefficient from non-parametric tests in SPSS program, because the data were not normally distributed.

3. Results and Discussion

In marly areas, different forms of soil erosion, are one of the prominent features (Thoms et al. 2004). Land erosion is clearly seen in the marl soils that are the subject of the study. For the purpose of reduce soil erosion, the soil loss preventive clonal and ligneous plant species could be used in planting studies in marl areas.

The plant taxa with the highest frequency and the growth forms were as follows (frequency of plant taxa are given in parentheses):

3.1. Bunched plants

Festuca valesiaca Schleich. ex Gaudin (26), *F. callieri* (Hack.) Markgr. subsp. *callieri* (14) and *Bromus tomentellus* Boiss. (29).

3.2. Batch plants (clonal plants)

Alyssum sibiricum Willd. (27), *Convolvulus phrygius* Bornm. (27, **endemic**), *Thymus leucostomus* Hausskn & Velen. (30, **endemic**), *Globularia orientalis* L. (22).

3.3. Chamaephyte and shrub

Salvia tchihatcheffii (Fisch. & C.A.Mey.) Boiss. (17, **endemic**), *Genista aucheri* Boiss. (16, **endemic**), *Jasminum fruticans* L. (11), *Rhamnus thymifolia* Bornm. (18, **endemic**), *Berberis crataegina* DC. (28), *Juniperus oxycedrus* L. subsp. *oxycedrus* (34) and *Quercus pubescens* Willd. (24).

3.4. Small tree and tree species

Quercus pubescens and *Pinus nigra* subsp. *pallasiana* (16).

The majority of these plant species, which are frequently seen in the study area, have a strong life energy even in the driest season. Notable among these species are: *Festuca* sp., *Convolvulus phrygius*, *Genista aucheri*, shrub and tree species. The results for some physiographic variables of the study area were presented in Table 3.

All identified plant taxa in this study were within the area formed by marly soil. All examined taxa demonstrated a natural distribution on both sunny and shady aspects. The altitude of the study area is between 860 and 1125 meters with steep slopes (Table 3).

Table 3- Environmental factors of the study area

Sampling location	Altitude (m)	Exposure (°)	Slope (°)	Bedrock	Sampling location	Altitude (m)	Exposure (°)	Slope (°)	Bedrock
1	870	270	30	Marl	19	927	270	45	Marl
2	898	270	47	Marl	20	928	90	37	Marl
3	996	115	55	Chlorite schist	21	1047	90	3	Marl
4	946	135	15	Marl	22	905	90	10	Marl
5	959	135	10	Marl	23	917	315	37	Limestone
6	1026	225	30	Limestone	24	965	90	25	Limestone
7	1023	315	30	Limestone	25	966	270	50	Claystone
8	863	180	30	Marl	26	902	270	30	Marl
9	932	20	22	Marl	27	936	45	23	Limestone
10	938	200	35	Marl	28	957	315	13	Marl
11	904	110	35	Limestone	29	901	200	28	Marl
12	979	20	3	Marl	30	940	90	16	Marl
13	980	270	20	Marl	31	925	135	28	Marl
14	976	90	22	Marl	32	968	200	37	Limestone
15	1123	270	40	Marble	33	987	270	25	Limestone
16	1086	270	8	Marl	34	880	270	30	Limestone
17	991	270	30	Marl	35	1030	70	4	Marl
18	1046	45	20	Claystone	36	1022	250	28	Marl

When considering the soil characteristics of the species, it can be seen that the soil texture of the study area is clay on the marl, on different bedrocks, is sometimes clayey loam and rarely sandy. All plants were generally distributed on soils that had high pH and lime levels. The soils were moderately and strongly alkaline (Table 4). The lime content in the soil is greater than 25%, except for areas with chlorite-schist and claystone bedrock. The plants can be grown in soils with extremely high lime conditions. The quantity of organic matter, N, and P were found to be 0.27–5.88 %, 0.04–0.31 % and 5–70 ppm, respectively (Table 4).

Table 4- The chemical properties of soils and soil texture

Sampling location	Lime_1	Lime_2	pH_1	pH_2	OM_1	OM_2	N_1	N_2	P_1	P_2	Soil texture (0-10 cm)	Soil texture (10-30 cm)
1	42.43	46.89	7.84	7.84	3.58	2.10	0.25	0.16	20	12	Clayey	Clayey
2	35.04	38.75	7.86	8.02	3.26	1.54	0.23	0.12	19	10	Clayey	Clayey
3	6.08	2.12	8.44	8.55	0.43	0.27	0.05	0.04	10	7	Clayey	Clayey
4	39.52	32.18	8.34	8.32	1.99	1.52	0.13	0.13	12	10	Clayey	Clayey
5	39.97	47.54	8.37	8.54	1.68	0.91	0.13	0.08	11	9	C. loam	Clayey
6	25.16	22.71	8.42	8.56	1.23	0.76	0.10	0.06	11	9	Clayey	Clayey
7	25.21	15.07	8.48	8.55	0.96	0.97	0.07	0.05	10	9	Clayey	Clayey
8	50.11	51.55	8.17	8.24	1.99	2.06	0.13	0.14	13	13	Clayey	Clayey
9	65.76	88.72	8.41	8.57	3.25	1.90	0.20	0.11	16	12	C. loam	C. loam
10	79.32	87.83	8.89	9.05	1.38	0.70	0.09	0.06	9	7	Clayey	Clayey
11	75.22	81.37	8.74	8.83	2.76	1.78	0.15	0.09	19	14	Loamy	Loamy
12	79.24	90.77	8.59	9.05	1.70	0.80	0.10	0.05	11	7	Clayey	Clayey
13	63.58	65.59	8.48	8.83	2.22	1.30	0.13	0.07	14	9	Clayey	Clayey
14	78.69	78.15	8.66	8.43	0.62	0.47	0.04	0.04	7	5	Clayey	Clayey
15	31.40	47.67	8.51	8.50	2.72	1.07	0.13	0.06	22	11	Clayey	Clayey
16	32.22	46.76	8.18	8.48	4.19	1.52	0.18	0.08	24	12	Clayey	Clayey
17	65.37	74.83	8.38	8.83	2.27	0.89	0.14	0.07	18	7	Clayey	Clayey
18	6.32	13.62	8.13	8.32	3.25	0.83	0.19	0.08	20	9	Clayey	Clayey
19	78.83	84.32	8.81	9.01	0.98	0.93	0.06	0.05	9	9	Clayey	Clayey
20	49.40	51.25	8.54	8.46	3.47	3.49	0.20	0.20	20	19	Clayey	Clayey
21	34.93	43.44	8.31	8.28	5.77	2.73	0.25	0.16	32	18	C. loam	C. loam
22	59.65	71.35	8.29	8.44	2.22	1.00	0.15	0.08	15	10	Clayey	Clayey
23	50.68	55.65	8.47	8.45	2.06	0.90	0.09	0.06	13	10	Clayey	Clayey
24	27.73	27.11	8.72	8.42	1.91	0.81	0.14	0.08	15	10	Clayey	Clayey
25	12.87	4.44	8.67	8.64	0.64	0.41	0.07	0.05	12	8	Clayey	Clayey
26	79.47	86.79	8.62	8.87	1.10	0.55	0.08	0.05	14	8	Clayey	Clayey
27	49.63	68.04	8.31	8.32	3.92	2.72	0.30	0.19	19	16	C. loam	Clayey
28	31.19	38.36	7.75	7.96	4.81	3.76	0.31	0.25	21	16	C. loam	Clayey
29	34.17	30.88	7.94	8.18	2.54	5.88	0.16	0.31	19	70	C. loam	S.C. loam
30	90.18	90.33	8.78	8.79	0.44	0.44	0.04	0.03	8	8	Clayey	Clayey
31	74.38	72.12	8.53	8.65	1.32	0.68	0.09	0.05	8	7	Clayey	Clayey
32	35.35	37.24	8.42	8.43	0.66	0.65	0.07	0.06	9	8	Clayey	Clayey
33	33.06	35.29	8.39	8.41	1.87	1.20	0.12	0.09	11	8	Clayey	Clayey
34	51.43	40.24	8.38	8.11	2.50	1.74	0.16	0.13	16	9	Clayey	Clayey
35	8.53	34.58	8.28	8.18	3.85	2.78	0.28	0.16	18	11	Clayey	Clayey
36	69.69	60.89	8.65	8.67	0.46	0.47	0.04	0.04	6	5	Clayey	Clayey

1: 0-10 cm; 2: 10-30 cm; Lime (%); pH: Potential of Hydrogen; OM: Organic matter (%); N: Nitrogen (%); P: Phosphorus (ppm); C: Clayey; S: Sandy

The statistical analysis revealed that N, P and soil organic matter were the significant environmental variables associated with the plant taxa (Table 5). There was no significant correlation between lime content at 0-10 cm soil depth, exposure, pH and plant species. *J. oxycedrus* and *F. valesiaca* were positively correlated with N, P and organic matter in soil ($P < 0.05$). *Quercus pubescens* preferred soil in which the phosphorus was higher. The positive variables were N and OM, and P at a depth of 10–30 cm for *G. orientalis*. While *J. fruticans* preferred steeper slopes, *G. orientalis* was located on the side with only a slight slope. Compared to the other species in this study, *G. aucheri* preferred relatively lower lime, P and OM. At depths of 0–10 cm, *C. phrygius* presence was negatively correlated with N, P, and organic matter. *R. thymifolia* was negatively correlated with the amount of lime at 10–30 cm soil dept and elevation. Compared to other taxa, *J. oxycedrus*, *G. orientalis* and *F. valesiaca* preferred soils containing more organic matter, and *J. oxycedrus*, *Q. pubescens*, *G. orientalis* and *F. valesiaca* preferred soils containing higher P. No correlation was found between the remaining 7 taxa (*P. nigra* subsp. *pallasiana*, *A. sibiricum*, *T. leucostomus*, *F. callieri*, *B. tomentellus*, *S. tchihatcheffii* and *B. crataegina*) and their site factors. It can be said that ecological tolerance of these taxa is slightly wider considering the ecological conditions of the study area.

Soil erosion control studies are very difficult to conduct in areas with high anthropogenic impact and extreme site conditions. Water deficiency is the most important factor affecting plant development in semiarid climates. The increase in rainfall and decrease in temperature that occurs with altitude increase in this region positively affects the water economy (Kahveci 1998; Güner et al. 2016). This elevation limit was determined to be 1000–1200 m in black pine plantations in the Central Anatolia region (Güner et al. 2016). The elevation of our study area is below 1150 m, and the summer season receives the least amount of precipitation in this region. For this reason, the summer season is quite dry in the region. Fifteen plant taxa in the study area have adapted to dry conditions and marly soils during the vegetation period when the water deficit reaches its maximum.

Table 5- Spearman's correlations between plant taxa and environmental variables

Species		N_1	N_2	Lime_2	P_1	P_2	OM_1	OM_2	Altitude	Slope
Junoxy	r _s	0.409*	0.385*	0.026	0.435**	0.429**	0.451**	0.408*	-0.213	0.017
	p	0.013	0.020	0.883	0.008	0.009	0.006	0.013	0.213	0.921
Quepub	r _s	0.225	0.188	-0.170	0.379*	0.354*	0.272	0.222	-0.082	0.259
	p	0.186	0.273	0.321	0.023	0.034	0.109	0.193	0.633	0.127
Gloori	r _s	0.465**	0.416*	0.099	0.294	0.373*	0.406*	0.379*	0.038	-0.482**
	p	0.004	0.012	0.567	0.082	0.025	0.014	0.023	0.824	0.003
Jasfru	r _s	0.105	0.105	0.030	0.102	0.078	0.078	0.030	-0.143	0.372*
	p	0.543	0.542	0.863	0.555	0.650	0.653	0.863	0.404	0.026
Fesval	r _s	0.540**	0.425**	-0.034	0.486**	0.254	0.573**	0.355*	0.170	-0.322
	p	0.001	0.010	0.844	0.003	0.134	0.000	0.034	0.321	0.056
Genauc	r _s	-0.337*	-0.222	-0.334*	-0.496**	-0.361*	-0.466**	-0.371*	0.124	0.065
	p	0.044	0.193	0.047	0.002	0.031	0.004	0.026	0.472	0.707
Conphr	r _s	-0.350*	-0.196	0.133	-0.415*	-0.296	-0.361*	-0.250	-0.275	0.292
	p	0.037	0.253	0.440	0.012	0.080	0.030	0.141	0.105	0.084
Rhathy	r _s	0.260	0.301	0.353*	0.102	0.240	0.195	0.289	-0.471**	0.032
	p	0.126	0.074	0.035	0.554	0.159	0.254	0.088	0.004	0.852

r_s: Spearman correlation coefficient; p: Significance level; 1: 0-10 cm; 2: 10-30 cm; OM: Organic matter; N: Total nitrogen; P: Available phosphorus; significant at the level of *p<0.05; **p<0.01; Junoxy: *Juniperus oxycedrus* subsp. *oxycedrus*; Quepub: *Quercus pubescens*; Gloori: *Globularia orientalis*; Jasfru: *Jasminum fruticans*; Fesval: *Festuca valesiaca*; Genauc: *Genista aucheri*; Conphr: *Convolvulus phrygius*; Rhathy: *Rhamnus thymifolia*

Much of the soils across the semiarid and arid forested regions of Türkiye commonly have high lime content (Çalışkan & Boydak 2017). In the study, the lime content in the soils was quite high, generally over 30%. Compared to other species, *G. aucheri* was found in the areas where the lime in the soil was lower. However, these taxa grow in soils where lime reaches 90%. The same results were also reported by Balpınar et al. (2019). The lime rate in the soil varied from 6.32% and 90.77%, (Table 4).

The decrease in soil organic matter reduces soil fertility and increases erosion in some soils (McCauley et al. 2009). In vegetation recovery, the major variable is organic substances in the soil (Romero-Díaz et al. 2017). The amount of organic matter in the soil of the study area varied between 0.27% and 5.88% (Table 4). The study area is generally poor in terms of organic matter in the soil. The plant taxa in this research are tolerant of soils poor in organic matter. However, according to numerical analysis, some of the plant species in our study area, *J. oxycedrus*, *G. orientalis* and *F. valesiaca* prefer soils in which organic matter is slightly higher. These species are also tolerant of poor soils.

Soil reaction (pH) strongly affects the chemical solubility and availability of essential plant nutrients (Çepel 1995; McCauley et al. 2009), and the greatest intake of plant nutrients is in the pH range of 6.5–7.5 (Güneş et al. 2007). According to the statistical analysis, no relationship was found between the soil pH and the plant species. The soil pH of the study area varied between 7.75 and 9.05 (moderate to strongly alkaline) (Table 4). The soil reaction of all plant taxa was generally medium alkaline, with an average soil reaction of approximately 8.50. However, it was determined that all plant taxa grow in soil with a pH of 9 at a depth of 10-30 cm. The development of woody species has been observed to decrease slightly as the reaction in soil increased.

Pinus nigra subsp. *pallasiana* showed deformed development (short form) in the study area. Although the study area soils were not shallow, it is possible to clearly see the lateral root system of *P. nigra* subsp. *pallasiana*. Similarly, Atalay & Efe (2012) stated that the lateral root systems developed well in hard and less weathered serpentines and marly deposits. This observation may be explained by the fact that the level of pH and lime in marl soils was slightly lower in the upper layers of the soil.

It has been observed that the first colonised plants after land restoration and environmental degradation are herbaceous species (Cammeraat et al. 2005; Burylo et al. 2007). In marly soils, the most suitable plant forms in terms of soil reinforcement are shrubs and herbaceous species (Burylo et al. 2011). In a study conducted in soils developing on different bedrock, woody sub-shrub, root-sprouts and clonal species were identified as suitable forms for eroded lands (Guerrero-Campo et al. 2008). Our study indicated that the identified fifteen taxa are clonal, bunch and woody species could retain their vitality in the driest conditions as well. In woody species, these taxa can be considered as having a significant role in preventing erosion in marly areas via their aboveground and underground organs. The grasses and shrubs with high root density have the highest potential to reduce soil erosion rates (De Baets et al. 2007). Grasses and shrubs show greater resistance to loss of the topsoil than tree seedlings. After the first growing season, the roots of tree seedlings can fix the upper layers of soil to the bedrock, and they can act as restraint piles firmly anchoring the root-permeated soil to the bedrock (Styzen & Morgan 2005; Burylo et al. 2011).

It is known that in the study region, with a decrease of soil depth in *Pinus nigra* subsp. *pallasiana* plantation areas, water and nutrient economy held in the soil are negatively affected (Güner et al. 2016). The eroded marly sites in this region have clay, alkaline and highly calcareous soils. Due to extreme conditions that limit plant growth in the marly areas, *Pinus nigra* subsp. *pallasiana*, *Quercus pubescens* and *Juniperus oxycedrus* subsp. *oxycedrus* do not grow normally, and therefore, grow to a shorter height than expected. Vegetation plays an essential role in the regulation of hydrological processes and soil

properties. Plant cover decreases the destructive forces of rainfall that cause soil erosion (Vásquez-Méndez et al. 2010). In our study, in the eroded marly areas where soil depth is sufficient, other plant forms should be considered in addition to tree species for revegetation. Clonal plant species are more advantageous than tree seedlings in highly eroded areas (Guerrero-Campo et al. 2008) and seed germination is more limited in the badlands (Guàrdia et al. 2000).

4. Conclusions

The rate of regeneration is very low or insufficient in studies of marly soil revegetation. The first issue in revegetating marly soils is selecting which plant species must be used in developing vegetation. The second issue is determining which plant species are best for preventing erosion. In this study, the plant species that survived the drought phase and their ecological requirements were determined. The species utilised on degraded marly soils must be able to adapt to soils with high pH and lime in semiarid climatic conditions subject to drought. In the eroded marly areas, vegetation cover can be supported by planting seedlings of groundcover and woody species adapted to marly field conditions. The best plant species are those grown with the least loss in the redevelopment of vegetation and erosion in the marly areas. In areas with excessive erosion and, consequently, shallow soil, bunching and clonal plants, as well as chamaephytes, are preferable for the development of vegetation.

Acknowledgements

This research was carried out using a portion of the data retrieved from the study, 'Examination of Erosion Fields in the Sundiken Mountains in terms of Plant Ecology and Determination of Plant Species that can be used in Erosion Control' by the Directorate of Research Institute for Forest Soil and Ecology (Eskişehir, Türkiye). It was presented orally as "Site factors and plant species of marly soils", and its abstract was published in the Proceedings of the "10th International Soil Congress 2019" (Arslan et al. 2019).

References

- Akman Y (1995). Türkiye Forest Vegetation. Ankara University Faculty of Science, Department of Botany, Ankara, Türkiye, 450 pp (In Turkish)
- Akman Y (1999). Climate and Bioclimate (Bioclimate Methods and Climates of Türkiye). Kariyer Printing, Ankara, Türkiye, 350 pp (In Turkish)
- Akman Y & Daget P H (1971). Quelques Aspects Synoptiques des Climats de la Turquie. Bulletin de Société Languedocienne de Géographie, Montpellier 5(3): 269-300
- Akman Y, Ketenoğlu O & Geven F (2001). Vegetation Ecology and Research Methods. ISBN: 975-97436-1-2, Ankara, Türkiye, 341 pp (In Turkish)
- Anonymous (2019). Turkey Grain and Feed Annual Report 2019. United States Department of Agriculture, Foreign Agriculture Service, Global Agricultural Information Network, GAIN Report Number: TR9008
- Arslan M, Balpınar N, Çelik N & Bingöl M Ü (2019). Site Factors and Plant Species of Marly Soils. 10th International Soil Congress 2019, 17-19 June 2019, Ankara, Turkey. Proceedings, (Eds: Prof. Dr. Ayten Namlı, Prof. Dr. Oğuz Can Turgay, MsC. Muhittin Onur Akça), oral presentation 306 pp
- Atalay İ & Efe R (2012). Ecological attributes and distribution of Anatolian black pine [*Pinus nigra* Arnold. subsp. *pallasiana* Lamb. Holmboe] in Turkey. *Journal of Environmental Biology* (Supplement Issue) 33(2): 509-519
- Balpınar N, Arslan M, Çelik N & Bingöl Ü (2019). Relationships between some endemic taxa and environmental factors in Alpu (Eskişehir), Turkey. *International Journal of Environmental Science and Technology* 16(9): 5065-5072. <https://doi.org/10.1007/s13762-018-1794-8>
- Bochet E & García-Fayos P (2004). Factors controlling vegetation establishment and water erosion on motorway slopes in Valencia, Spain. *Restoration Ecology* 12(2): 166-174. <https://doi.org/10.1111/j.1061-2971.2004.0325.x>
- Bochet E & García-Fayos P (2015). Identifying plant traits: a key aspect for species selection in restoration of eroded roadsides in semiarid environments. *Ecological Engineering* 83: 444-451. <https://doi.org/10.1016/j.ecoleng.2015.06.019>
- Bouma N A & Imeson A C (2000). Investigation of relationships between measured field indicators and erosion processes on badland surfaces at Petrer, Spain. *Catena* 40: 147-171. [https://doi.org/10.1016/S0341-8162\(99\)00046-6](https://doi.org/10.1016/S0341-8162(99)00046-6)
- Braun-Blanquet J (1932). Plant Sociology (Translated: Fuller, D. G. & Conard S. H. 1983). West Germany, 439 pp. <https://doi.org/10.5962/bhl.title.7161>
- Breton V, Crosaz Y & Rey F (2016). Effects of wood chip amendments on the revegetation performance of plant species on eroded marly terrains in a Mediterranean mountainous climate (Southern Alps, France). *Solid Earth* 7(2): 599-610. <https://doi.org/10.5194/se-7-599-2016>
- Burylo M, Rey F & Delcros P (2007). Abiotic and biotic factors influencing the early stages of vegetation colonization in restored marly gullies (Southern Alps, France). *Ecological Engineering* 30(3): 231-239. <https://doi.org/10.1016/j.ecoleng.2007.01.004>
- Burylo M, Rey F, Roumet C, Buisson E & Dutoit T (2009). Linking plant morphological traits to uprooting resistance in eroded marly lands (Southern Alps, France). *Plant and Soil* 324(1-2): 31-42. <https://doi.org/10.1007/s11104-009-9920-5>
- Burylo M, Hudek C & Rey F (2011). Soil reinforcement by the roots of six dominant species on eroded mountainous marly slopes (Southern Alps, France). *Catena* 84(1-2): 70-78. <https://doi.org/10.1016/j.catena.2010.09.007>
- Cammeraat E, Kooijman A & Van Beek R (2005). Vegetation succession and its consequences for slope stability in SE Spain. *Plant and Soil* 278(1-2): 135-147. <https://doi.org/10.1007/s11104-005-5893-1>
- Cerda A (1999). Parent material and vegetation affect soil erosion in eastern Spain. *Soil Science Society of American Journal* 63(2): 62-368. <https://doi.org/10.2136/sssaj1999.03615995006300020014x>

- Çalışkan S & Boydak M (2017). Afforestation of arid and semiarid ecosystems in Turkey. *Turkish Journal of Agriculture and Forestry* 41(5): 317-330. <https://doi.org/10.3906/tar-1702-39>
- Çepel N (1995). *Forest Ecology*. 4th Edition, Istanbul University Publication No: 3886, Istanbul University Press and Film Center, Istanbul, Türkiye, 536 pp (In Turkish)
- Çetik R (1985). *Vegetation and Ecology of Central Anatolia, Vegetation of Türkiye I*. Selçuk University Publications: 7, Faculty of Science and Letters Publications: 1, Konya, Türkiye, 496 pp (In Turkish)
- Davis P H (1965). *Flora of Turkey and East Aegean Islands*. Edinburg University Press, Volume 1, Edinburg, UK, 567 pp
- Davis P H (1965-1985). *Flora of Turkey and East Aegean Islands*. Edinburg University Press, Volume 1-9, Edinburg, UK
- De Baets S, Poesen J, Knapen A, Barberá G G & Navarro J A (2007). Root characteristics of representative Mediterranean plant species and their erosion-reducing potential during concentrated runoff. *Plant and Soil* 294(1-2): 169-183. <https://doi.org/10.1007/s11104-007-9244-2>
- Erpul G, Ince K, Demirhan A, Küçümen A, Akdağ M A, Demirtaş İ, Sarıhan B, Çetin E & Şahin S (2020). *Provincial Water Erosion Statistics – Soil Erosion Control Strategies (Sustainable Land/Soil Management Practices and Approaches)* General Directorate of Combating Desertification and Erosion Publications, Ankara. ISBN No: 978-605-7599-36-0 (In Turkish)
- FAO (Food and Agriculture Organization) & ITPS (Intergovernmental Technical Panel on Soils) (2015). *Status of the World's Soil Resources (SWSR) – Main Report*. Rome, Italy
- Guàrdia R, Gallart F & Ninot J M (2000). Soil seed bank and seedling dynamics in badlands of the Upper Llobregat basin (Pyrenees). *Catena* 40(2): 189-202. [https://doi.org/10.1016/S0341-8162\(99\)00054-5](https://doi.org/10.1016/S0341-8162(99)00054-5)
- Guerrero-Campo J & Montserrat-Martí G (2000). Effects of soil erosion on the floristic composition of plant communities on marl in northeast Spain. *Journal of Vegetation Science* 11(3): 329-336. <https://doi.org/10.2307/3236625>
- Guerrero-Campo J & Montserrat-Martí G (2004). Comparison of floristic changes on vegetation affected by different levels of soil erosion in Miocene clays and Eocene marls from Northeast Spain. *Plant Ecology* 173(1): 83-93. <https://doi.org/10.1023/B:VEGE.0000026331.85303.c8>
- Guerrero-Campo J, Palacio S & Montserrat-Martí G (2008). Plant traits enabling survival in Mediterranean badlands in northeastern Spain suffering from soil erosion. *Journal of Vegetation Science* 19(4): 457-464. <https://doi.org/10.3170/2008-8-18382>
- Güner Ş T, Çömez A, Özkan K, Karataş R & Çelik N (2016). Productivity modeling of larch plantations in Türkiye. *Istanbul University Faculty of Forestry Journal* 66(1): 159-172. <https://doi.org/10.17099/jffiu.18731> (In English)
- Güneş A, Alpaslan M & İnal A (2007). *Plant Nutrition and Fertilization*. Ankara University Faculty of Agriculture Textbook No: 504, Ankara University Publication, Ankara, Türkiye 576 pp (In Turkish)
- Jackson M L (1962). *Soil Chemical Analysis*, Constable and Company Ltd., London, UK. 498 pp
- Kacar B (2009). *Soil Analyzes*. 2nd Edition, Nobel Publishing, Ankara, Türkiye 467 pp (In Turkish)
- Kahveci G (1998). *Waldrelikte und natürliche Waldverbreitung in der zentralanatolischen Steppe: Grundlage für eine Waldrestauration*. Verlag Erich Goltze, Göttingen, Germany, 162 pp
- Kahveci G (2017). Distribution of *Quercus* spp. and *Pinus nigra* mixed stands in semiarid northern Central Anatolia. *Turkish Journal of Agriculture and Forestry* 41(2): 135-141. <https://doi.org/10.3906/tar-1609-14>.
- Kroetsch D & Wang C (2008). Particle Size Distribution, in section VI Soil Physical Analysis, Section Ed. By Angers D A, Larney F J, In: *Soil Sampling and Methods of Analysis 2*. Edition, Carter M R & Gregorich E G (eds.), CRC Press, Boca Raton, America, 1264 pp. <https://doi.org/10.1201/9781420005271.ch55>
- Loreau M, Naeem S, Inchausti P, Bengtsson J, Grime J P, Hector A, Hooper D U, Huston M A, Raffaelli D, Schmid B, Tilman D & Wardle D A (2001). Biodiversity and ecosystem functioning: current knowledge and future challenges. *Science* 294(5543): 804-808. <https://doi.org/10.1126/science.1064088>
- McCaughey A, Jones C & Jacobsen J (2009). Soil pH and organic matter. (Nutrient management modules 8, #4449-8). Montana State University Extension Service, Bozeman, Montana, USA, pp. 1-12
- Romero-Díaz A, Ruiz-Sinoga J D, Robledano-Aymerich F, Brevik E C & Cerdà A (2017). Ecosystem responses to land abandonment in Western Mediterranean Mountains. *Catena* 149(3): 824–835. <https://doi.org/10.1016/j.catena.2016.08.013>
- Saygın S (2021). Effects of Season and Phenology-based Changes on Soil Erodibility and Other Dynamic RUSLE Factors for Semi-arid Winter Wheat Fields. *Journal of Agricultural Sciences* 27(4): 526-535. <http://doi.org/10.15832/ankutbd.749181>
- Sokouti R & Razagi S (2015). Erodibility and loss of marly drived soils. *Eurasian Journal of Soil Science* 4(4): 279-286. <https://doi.org/10.18393/ejss.2015.4.279-286>
- Stokes A, Douglas G B, Fourcaud T, Giadrossich F, Gillies C, Hubble T, Kim J H, Kenneth W, Loades K W, Mao Z, Ian R, McIvor I R, Mickovski S B, Mitchell S, Osman N, Phillips C, Poesen J, Polster D, Preti F, Raymond P, Rey F, Schwarz M & Walker L R (2014). Ecological mitigation of hillslope instability: ten key issues facing researchers and practitioners. *Plant and Soil* 377: 1–23. <https://doi.org/10.1007/s11104-014-2044-6>
- Styrczen M E & Morgan R P C (2005). Engineering properties of vegetation. Chapter 2, In: Morgan, R.P.C. & Rickson R.J. (eds.), *Slope stabilization and erosion control: a bioengineering approach*. E and FN SPON, London, p. 288. <https://doi.org/10.4324/9780203362136>
- Thoms M, Hill S, Spry M, Chen X Y, Mount T & Sheldon F (2004). The geomorphology of the Barwon-Darling Basin. In: Breckwoldt R, Boden R, Andrew J (eds.) *The Darling*. Murray-Darling Basin Commission, pp. 68-103
- TS ISO 10390 (2013). *Soil quality - pH determination*. Turkish Standards Institution, Ankara, Türkiye, 11 pp (In Turkish)
- TS 8336 (2008). *Soils - Determination of Organic Matter*. Turkish Standards Institution, Ankara, Türkiye. 6 pp (In Turkish)
- Varavipour M, Asadi T & Arzjani Z (2010). Relationship between the physico-chemical properties and different types of erosion on marl soils south of Tehran, Iran. *Asian Journal of Chemistry* 22(7): 5201-5208
- Vásquez-Méndez R, Ventura-Ramos E, Oleschko K, Hernández-Sandoval L, Parrot J F & Nearing M A (2010). Soil erosion and runoff in different vegetation patches from semiarid Central Mexico. *Catena* 80(3): 162-169. <https://doi.org/10.1016/j.catena.2009.11.003>
- Walter H & Lieth H (1967). *Klimadiagramm-Weltatlas*. Gustav Fischer Verlag, Jena, East Germany





Enhancing Pest Detection: Assessing *Tuta absoluta* (Lepidoptera: Gelechiidae) Damage Intensity in Field Images through Advanced Machine Learning

Alperen Kaan BÜTÜNER^a , Yavuz Selim ŞAHİN^a , Atilla ERDİNÇ^b , Hilal ERDOĞAN^{c*} , Edwin LEWIS^d

^aBursa Uludağ University, Faculty of Agriculture, Department of Plant Protection, Görükle Campus, 16059 Bursa, TÜRKİYE

^bBursa Uludağ University, Faculty of Engineering, Department of Computer Engineering, Görükle Campus, 16059 Bursa, TÜRKİYE

^cBursa Uludağ University, Faculty of Agriculture, Department of Biosystems Engineering, Görükle Campus, 16059 Bursa, TÜRKİYE

^dDepartment of Entomology, Plant Pathology and Nematology, University of Idaho, USA

ARTICLE INFO

Research Article

Corresponding Author: Hilal ERDOĞAN, E-mail: hilalerdogan@uludag.edu.tr

Received: 01 June 2023 / Revised: 15 August 2023 / Accepted: 17 August 2023 / Online: 09 January 2024

Cite this article

Bütüner A K, Şahin Y S, Erdinç A, Erdoğan H, Lewis E (2024). Enhancing Pest Detection: Assessing *Tuta absoluta* (Lepidoptera: Gelechiidae) Damage Intensity in Field Images through Advanced Machine Learning. *Journal of Agricultural Sciences (Tarım Bilimleri Dergisi)*, 30(1):99-107. DOI: 10.15832/ankutbd.1308406

ABSTRACT

The tomato (*Solanum lycopersicum* (Solanaceae)) is particularly susceptible to *Tuta absoluta* (Meyrick) (Lepidoptera: Gelechiidae), a pest that directly and profoundly influences tomato yields. Consequently, the early detection of *T. absoluta* damage intensity on leaves using machine learning or artificial intelligence-based algorithms is crucial for effective pest control. In this ground-breaking study, the galleries generated by *T. absoluta* were examined via field images using the Decision Trees (DTs) algorithm, a machine learning method. The unique advantage of DTs over other algorithms is their inherent capacity to identify complex and vague shapes without the necessity of feature extraction, providing a more streamlined and effective approach. The DTs algorithm was meticulously trained using pixel values from the leaf images, leading to the

classification of pixels within regions with and without galleries on the leaves. Accordingly, the gallery intensity was determined to be 9.09% and 35.77% in the test pictures. The performance of the DTs algorithm, as evidenced by a high precision and an accuracy rate of 0.98 and 0.99 respectively, testifies to its robust predictive and classification abilities. This pioneering study has far-reaching implications for the future of precision agriculture, potentially informing the development of advanced algorithms that can be integrated into autonomous vehicles. The integration of DTs in such applications, due to their unique ability to handle complex and indistinct shapes without the need for feature extraction, sets the stage for a new era of efficient and effective pest control strategies.

Keywords: Convolutional neural networks, Decision trees, Image processing, Pest management, Precision agriculture

1. Introduction

The tomato (*Solanum lycopersicum*) is a plant belonging to the Solanaceae family, and is widely cultivated worldwide due to its high nutritional value. Production is significantly increased, especially in countries such as China, India, Türkiye, Italy, the United States, and Spain. Therefore, economically, the products obtained from the tomato plant are precious, and minimizing product loss is a primary objective (Viggiani et al. 2009; González-Cabrera et al. 2011; Urbaneja et al. 2012; Veres et al. 2020). Invasive insect pests of crops cause considerable losses in agriculture (Veres et al. 2020). *Tuta absoluta* (Meyrick) (Lepidoptera: Gelechiidae), commonly called the tomato leaf miner (Lietti et al. 2005), is one of the most widely invasive pest species and has been recorded on every continent except Antarctica (Cely et al. 2010). This pest is oligophagous but is best known for the damage it causes to tomatoes (*Solanum lycopersicum* (Solanaceae)), where it can cause yield losses of up to 100% (Biondi et al. 2018). *T. absoluta* damages the leaves, buds, branches, and stems, but the most important damage is the galleries formed between the two epidermis tissues (Viggiani et al. 2009). Chemical control is the most common method to manage this pest. The harmful effects of pesticides on non-target organisms have been identified by studies conducted in recent years (Urbaneja et al. 2012; Erdoğan et al. 2023). This research addresses machine learning-based *T. absoluta* gallery density as an aid to early-stage pest control. Thus, pesticides may be applied to the right location instead of the whole plant and prevent excessive use of pesticides. Early detection plays an essential role in successful pest management (Li et al. 2021). For example, yellow sticky traps are used for early detection, but this requires a lot of labour and time in the need to count the pests over the traps (Aliakbarpour & Rawi 2011). The increased use of technology in agriculture has provided new methods to acquire such data (Wolfert et al. 2017; Weersink et al. 2018; Şahin et al. 2023). In this context, the use of image processing techniques based on machine learning is an effective way to obtain agricultural data (Vibhute & Bodhe 2012; Singh et al. 2016). For instance, Ozguven & Adem (2019) employed deep learning algorithms to detect leaf spot disease in sugar beet with an accuracy rate of 95.48%. Similarly, Gerdan

et al. (2023) have achieved accuracy values of up to 99.82% by employing deep learning algorithms for the detection of certain diseases observed in tomato plants.

The objective of this study was to calculate the damage intensity caused by *T. absoluta* on the tomato plant through image processing techniques based on machine learning. This is because training machine learning-based algorithms that allow data to be classified and described can provide faster, more accurate and real-time pest detection than human observation (Finger et al. 2019). Allowing us to control pests at an early stage may also contribute to the development of algorithms that can be integrated into autonomous vehicles designed within the scope of precision agriculture. In summary, this study aims to provide a faster and more accurate solution for the early-stage detection of pests and prevention of excessive pesticide use by calculating the damage caused by *Tuta absoluta* using machine learning-based image processing techniques, specifically employing the Decision Trees (DTs) method.

2. Material and Methods

2.1. Image acquisition

The study was carried out on tomato plants produced in the farmland of Bursa Uludağ University, Faculty of Agriculture (Figure 1). Adults and larvae of *T. absoluta* were collected and identified using the morphological characters (size, scale pattern, shape, colour, etc.) determined by Nayana & Kallethwaraswamy (2015). Images of *T. absoluta* larvae damage on leaves (galleries) were recorded using a Canon EOS 700D camera with a resolution of 5184 x 3456 pixels. A total of 1000 infested leaf pictures were taken in 1 week to train the DT algorithm. Pictures were taken about 40 cm from the leaf surface. 20% of the images were allocated for training the DTs algorithm and the rest for testing.

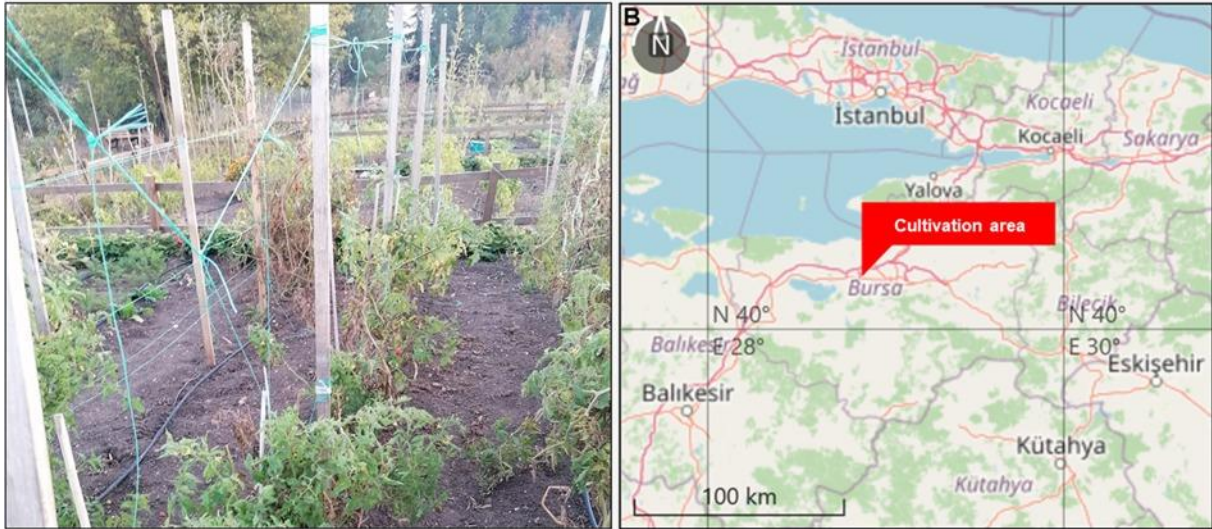


Figure 1- A: Tomato cultivation area. B: The location of the cultivation area.
Location: 40°13' 38.6" N, 28° 51' 55.8 "E, 50 m asl

2.2. Classification by decision trees (DTs)

DTs are a non-parametric supervised machine learning algorithm (Vishnoi et al. 2021). The Classification and Regression Tree (CART) decision tree algorithms that are commonly used for detecting plant pests and disease were utilized in this study (Bhatia et al. 2020; Daniya et al. 2020; Gallardo-Romero et al. 2023; Liu et al. 2023). The matrix values of the soil, galleries, healthy leaves, stems, and weeds in the original images were recorded to detect gallery intensity by DTs (Figure 2). These matrix values are made up of square pixels (image elements) arranged in columns and rows. Each digital image may contain pixel colors of different intensities. The combination of red, green, and blue creates the perception of color.



Figure 2- Matrix values of the healthy leaf (A), gallery (B), stems (C), soil (D), and weeds (E)

Matrix values were used to train and test the DTs. The classification was performed using the DTs algorithm and the precision and accuracy rate were calculated. The classification is started by creating a root node, after which the entropy value is calculated for all the data trained on the node (Adi et al. 2017; Liu et al. 2023). Galleries created by *T. absoluta* were visualized with a black tone in the test images, while a light grey tone was chosen for healthy leaf tissues. Grayscale values of the soil surface, weeds, healthy leaves, stems, and galleries from field pictures that are used for DTs training were set as in Table 1.

Table 1- Grey colours in RGB

Classifications	<i>R (Red)</i>	<i>G (Green)</i>	<i>B (Blue)</i>
Soil surface	90	90	90
Weeds	120	120	120
Stems	240	240	240
Healthy leaves	180	180	180
Galleries	0	0	0

2.3. Working diagram of decision trees algorithm

The process of using the Decision Trees (DTs) algorithm to classify matrix values in pictures of a tomato field infested by *T. absoluta*, to determine the intensity of damage caused by the pest, can be illustrated as follows:

- I. Collect a dataset of images from a tomato field infested by *T. absoluta* (Figure 3)
- II. Convert the images into matrix values representing the pixels in the image, including the values of the soil, galleries, healthy leaves, stems, and weeds.
- III. Use the matrix values to train a DTs algorithm, in which the algorithm learns to recognize patterns in the matrix values that correspond to the presence of galleries and healthy leaves in the images. The algorithm starts by using the matrix values of the soil, galleries, healthy leaves, stems, and weeds as input features.
- IV. The algorithm then builds a tree-like model by iteratively selecting the feature that best separates the data into different classes (in this case, the different matrix values of soil, galleries, healthy leaves, stems, and weeds) (Figure 4).
- V. At each node of the tree, the algorithm compares the matrix values of the input feature to a threshold value and makes a decision based on whether the values are greater or less than the threshold. This splits the data into two or more subsets, each represented by a child node.

- VI. The process is repeated for each child node until a stopping criterion is met, such as reaching a maximum depth or a minimum number of samples in a node.
- VII. The resulting tree can be used to predict the class of new samples by traversing the tree from the root node to a leaf node.



Figure 3- Collecting a dataset of images from a tomato field infested by *T. absoluta*. Regions with galleries are shown in a red circle

In the context of detecting gallery areas, the algorithm would use the matrix values as input features and the pixel values as the output. The algorithm would then build a tree-like model that uses the matrix values to predict the pixel values. Once the gallery areas are identified, the algorithm calculates the number of pixels in those areas, which would give you the total area of the galleries in pixels.

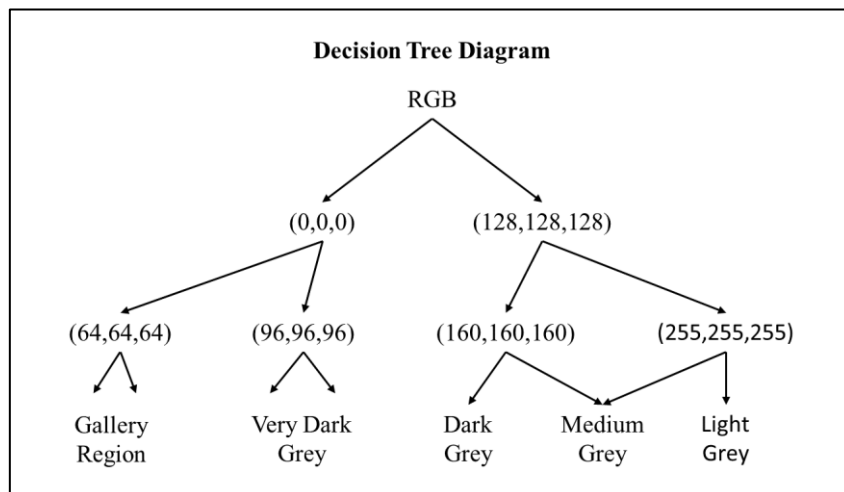


Figure 4- Selecting the feature that best separates the data into different classes

2.4. Determination of gallery intensity

T. absoluta damage intensity was determined using the DTs algorithm. The intensity was estimated by determining the pixel numbers of the areas with and without a gallery in the field images. It was calculated by the ratio of the total pigment number of the gallery-containing regions to the total pigment number of the healthy leaf regions (Goncalves et al. 2021). The intensity rate and precision are calculated by Equation (1) and Equation (2) respectively (G: Gallery area, H: healthy leaf area, I: Intensity rate (%), True Positive (TP): A True Positive is a correct identification of a positive instance in a classification task, where both the

actual and predicted classes are positive. False Positive (FP): A False Positive is an incorrect identification of a negative instance as positive, where the actual class is negative, but the predicted class is positive.

$$I = \left[\frac{G}{G+H} \times 100 \right] \quad (1)$$

$$\text{Precision} = \frac{TP}{TP+FP} \quad (2)$$

3. Results

The matrix values of the soil, stems, weeds, galleries, and healthy leaves taken from the original images in the field were used in the training of DTs, which is a non-parametric supervised machine learning algorithm. During the training process, these matrix values are clustered to make comparisons on the X, Y, and Z axes using the K-Nearest Neighbor (K-Nn) method (Hamdini et al. 2021). Clustering is visualized on the X, Y, and Z-axis (Figure 5).

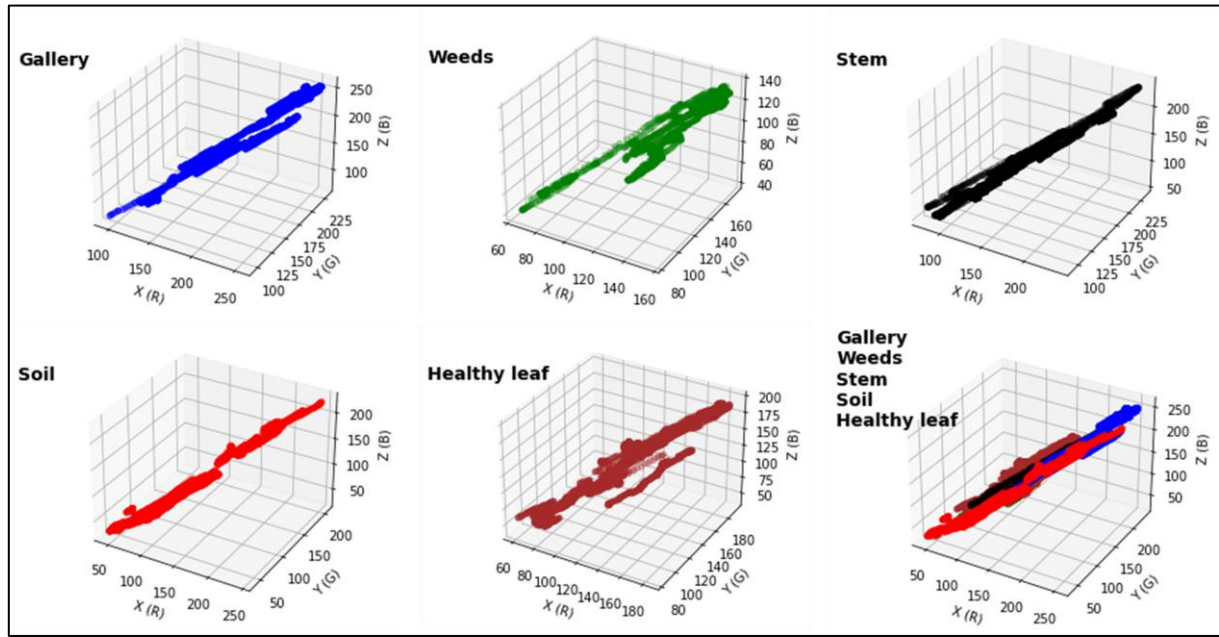


Figure 5- Clustering of RGB matrix values of healthy leaf, gallery, stems, soil, and weeds as in the original images from the field along the X, Y and Z-axes

The confusion matrix, representing the evaluation of a classification model on five distinct classes (galleries, weeds, stems, soil, and leaves), provides key insights into the model's performance. The galleries class is excellently classified with 282 577 correct predictions, while the weeds class is highly accurate but misclassified in some instances as stems (215) and soil (2,151). The stems and soil classes exhibit confusion with 239 557 and 215 108 correct predictions, respectively, and the leaves class shows high accuracy with 343 798 correct predictions. Some misclassification is observed, notably between stems and soil. The aggregate precision across these classes is 97.5%, reflecting the model's overall accuracy and highlighting areas for potential refinement in training and feature engineering (Figure 6).

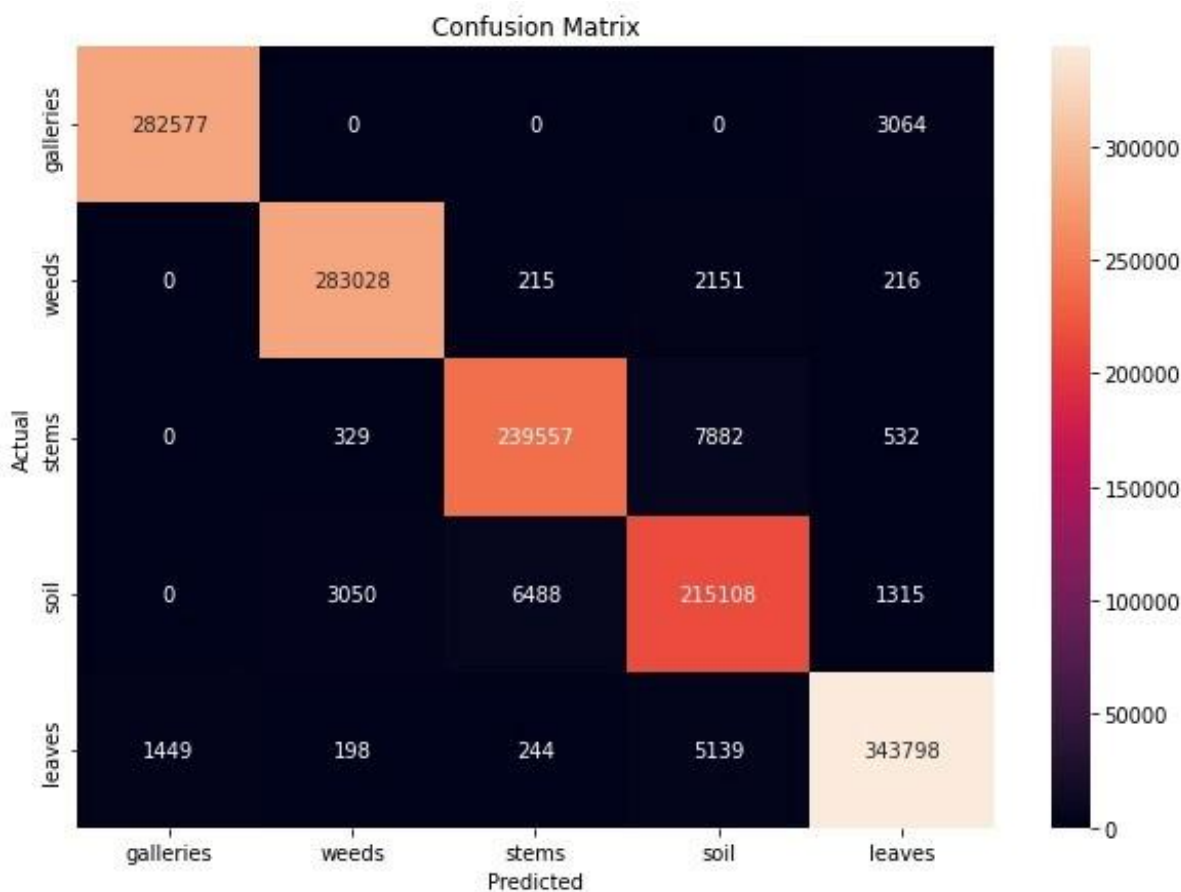


Figure 6- Confusion matrix of the classification model for the five classes (galleries, weeds, stems, soil, and leaves)

The classification model was trained and evaluated using a diverse dataset encompassing distinct classes. The evaluation metrics, including training accuracy, test accuracy, precision, recall, and F1-Score (Table 2), provide an essential understanding of the model's capability in predicting the correct classes. These metrics collectively affirm the model's robustness and predictive accuracy, reflecting a harmonious balance between the true positives and the overall number of actual positives and predictions. In this investigation, a DTs was utilized to classify various elements within an image, and the computational aspects of the methodology were assessed. The training process of the model was completed in a time of 3.08288 minutes, aligning with the theoretical time complexity of $O(n \cdot m \log m)$, where n represents the number of samples and m represents the number of features. The image prediction phase was executed in a remarkably brief span of 0.076231 seconds, corresponding to a time complexity of $O(p)$, with p denoting the total number of pixels in the image. These findings underscore the efficiency of the approach, highlighting its potential for real-time applications in the domain of image-based object recognition and categorization (Table 2).

Table 2- Evaluation metrics for the classification model, including training accuracy, test accuracy, precision, recall, and F1-Score

Training Accuracy	99%
Test Accuracy	98.7%
Precision	98%
Recall	97.54%
F1-Score	97.50%
Training Time for the Model	3.08288 minutes
Time Required for Test Image-Based Prediction	0.076231 seconds
Time Complexity for Prediction Based on Test Image	$O(p)$

Figure 7. shows the pictures used as test data in the training of the DTs algorithm; In "B", the grayscale of image "A", the total pixel values of Galleries and healthy leaves are 12101 and 121007, respectively. The precision and accuracy rate were determined as 0.98 and 0.99, respectively. In "D", the grayscale of image "C", the total pixel values of galleries and healthy leaves are 29764 and 53454, respectively. The precision and accuracy rate was determined as 0.98 and 0.98, respectively. According to the test results based on gallery intensity, 9.09% of tomato leaves were infested by *T. absoluta* in "A" while 35.77% of tomato leaves were infested by *T. absoluta* in "C".

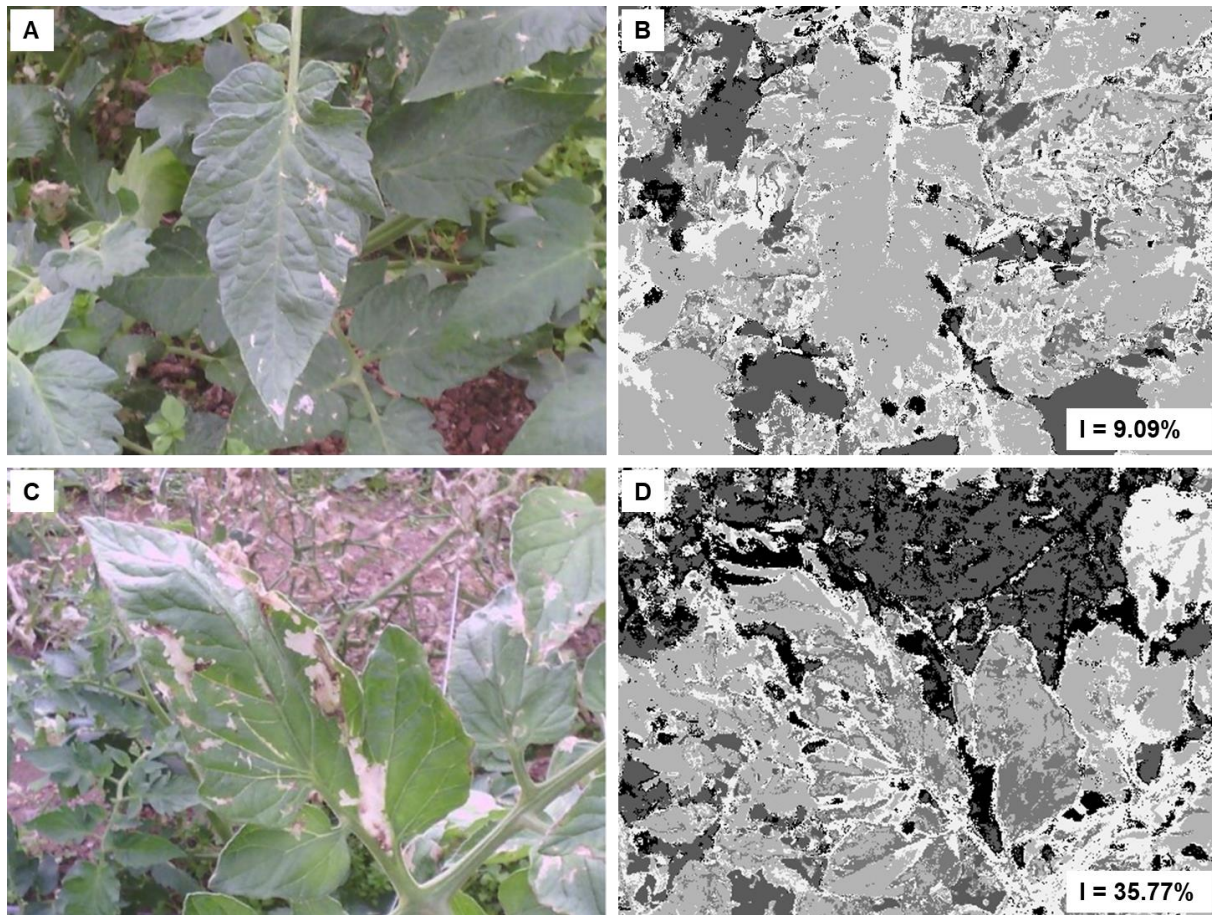


Figure 7- The test image changes to grayscale by clustering matrix values of soil, galleries, weeds, stems and healthy leaves (I = Intensity rate of galleries)

4. Discussion

Artificial Intelligence algorithms, specifically those based on Convolutional Neural Networks (CNNs), have a demonstrable effectiveness in various studies for identifying invasive pests. These methodologies offer rapid and accurate detection of agricultural pests, often surpassing the accuracy and speed of human observation (Li et al. 2022). Such algorithms facilitate the categorization and identification of data gleaned from images (Wolfert et al. 2017, Yan et al. 2021; Kiobia et al. 2023). However, the effectiveness of CNN-based models may be impeded by non-distinct object shapes in the images used for training. This complication could necessitate a larger data set for training and extend the training process (He et al. 2016; Lin et al. 2023). For instance, pests like *Cydia pomonella* and *Tuta absoluta* cause damage on leaves and fruits that may lack a distinct and stable structure. However, machine learning models like DTs are capable of classifying and learning from all the pixels of objects in images, even if those objects lack a clear shape. This property suggests that DTs might be able to discern complex shapes more effectively (Pedregosa et al. 2011; Collado & Tümbay 2023; Lin et al. 2023). Consequently, this study opted to employ the Decision Trees model, a supervised learning algorithm, instead of CNN-based models. Drawing from the work of Goncalves et al. (2021), CNN-based algorithms have shown promising results in the segmentation of necrotic leaf lesions caused by several plant disease agents, such as *Phakopsora pachyrhizi* (Soybean rust: SBR), *Pyrenophora tritici-repentis* (wheat tan spot: WTS), and *Leucoptera coffeina* (the coffee leaf miner: CLM). In the 2021 study of Goncalves et al., images were manually annotated and divided into three classes: injured leaf, healthy leaf, and leaf background. When comparing the annotated severity with the estimates, the concordance coefficients were found to be greater than 0.96, 0.98, and 0.95 for SBR, WTS, and CLM, respectively, after the leaf background was manually removed. The present study, however, approached this task from a different perspective. Rather than manually removing the background, the background elements (soil and weeds) in the field images were incorporated into the training of a Decision Trees (DTs) algorithm. This machine learning approach was employed to identify the gallery intensities created by *T. absoluta* larvae. Significantly, the algorithm was capable of detecting gallery intensities of 9.09% and 35.77% in the test images, eliminating the need for manual background removal. The precision was calculated as 0.98, indicating a high level of predictive accuracy. This suggests that machine learning models like DTs may offer a viable alternative to CNNs for pest detection, particularly in scenarios where manual background removal is impractical or undesirable. The relative strengths and weaknesses of these methods should be considered in future research and application in the field of precision agriculture. Diverse methodologies have been utilized in the context of image-based plant disease detection, as evinced by the studies conducted by Sabrol & Kumar (2016), Zou et al. (2021), and Sriwastwa et al. (2018). The approach taken by Sabrol &

Kumar (2016) enabled the determination of 78% of disease intensity in tomato plants using the Decision Trees (DTs) algorithm. The machine learning-based algorithm developed by Zou et al. (2021) facilitated the calculation of the wormhole areas ratio in broccoli seedling leaves, achieving a precision of 0.85 after manually separating the leaves from the background. Furthermore, Sriwastwa et al. (2018) deployed Otsu (1979) method's, a technique for automatic image thresholding, to perform insect detection via color-based segmentation. In contrast to these studies, the research currently under consideration embodies several distinguishing aspects. Firstly, a markedly higher precision of 0.98 was achieved, indicative of a superior predictive capability when compared to the performance reported by Zou et al. (2021). Secondly, an important deviation from prior research lies in the strategy of directly introducing background features, such as soil and weeds, into the DTs algorithm, thereby eliminating the need for manual background removal. This streamlined approach offers potential advantages over the methodologies employed by Zou et al. (2021) and Sriwastwa et al. (2018), which required manual pre-processing. In conclusion, the potency and utility of AI algorithms, notably those leveraging CNNs and DTs, have been corroborated through their crucial role in identifying and categorizing invasive pests. However, while CNNs have shown potential in similar studies, their dependence on distinct shapes within images can sometimes introduce limitations. This research spotlights the capability of DTs to tackle complex shapes more efficiently, removing the necessity for manual background elimination - an aspect that often hinders CNNs. A noteworthy achievement of this research, in comparison to previous studies, is the attainment of an exceptional precision of 0.98, indicating high predictive accuracy. This enhancement is made possible through the direct incorporation of background elements into the DTs algorithm, thereby eliminating the requirement for manual pre-processing and potentially streamlining the pest detection process. The current investigation provides an innovative viewpoint on the application of machine learning in pest detection, setting the groundwork for subsequent research. It reemphasizes the significance of choosing the most suitable algorithm, one that aptly addresses the unique challenges and requisites of each distinct case. As this exploration of varied methodologies progresses, it is expected to catalyze advancements in precision agriculture, ultimately encouraging the development of improved pest detection and disease control strategies.

5. Conclusions

This study sought an innovative method to address the problem of invasive pest detection in agriculture. Utilizing DTs as a supervised learning algorithm, the study diverged from conventional CNN-based methodologies, recognizing their limitations in handling non-distinct object shapes. By incorporating background elements, such as soil and weeds, directly into the training of the DTs algorithm, the research achieved a remarkable precision of 0.98. This indicated a high predictive accuracy, surpassing prior studies and eliminating the requirement for manual background removal, a step often essential in CNNs. The study's approach offered not only a viable alternative to CNNs for pest detection but also heralded potential advancements in precision agriculture. Significantly, this work contributes to the broader academic discourse by presenting an innovative method that aptly tackles unique challenges in pest detection. The success in utilizing DTs to detect complex shapes efficiently reemphasizes the need to consider diverse methodologies in pest detection. It sets a solid foundation for further research to develop more effective pest detection and disease control strategies.

References

- Adi K, Pujiyanto S, Dwi Nurhayati O & Pamungkas A (2017). Beef quality identification using thresholding method and decision tree classification based on android smartphone. *Journal of Food Quality* 9: 1-10. <https://doi.org/10.1155/2017/1674718>
- Aliakbarpour H & Rawi C S M (2011). Evaluation of yellow sticky traps for monitoring the population of thrips (Thysanoptera) in a mango orchard. *Environmental Entomology* 40(4): 873-879. <https://doi.org/10.1603/EN10201>
- Bhatia A, Chug A & Singh A P (2020). Plant disease detection for high dimensional imbalanced dataset using an enhanced decision tree approach. *International Journal of Future Generation Communication and Networking* 13(4): 71-78
- Biondi A, Guedes R N C, Wan F H & Desneux N (2018). Ecology, worldwide spread, and management of the invasive south American tomato pinworm, *Tuta absoluta*: past, present, and future. *Annual Review of Entomology* 63: 239-258. <https://doi.org/10.1146/annurev-ento-031616-034933>
- Cely P L, Cantor F & Rodríguez D (2010). Determination of levels of damage caused by different densities of *Tuta absoluta* populations (Lepidoptera: Gelechiidae) under greenhouse conditions. *Agronomía Colombiana* 28(3): 392-402
- Collado Jr M C & Tumibay G M (2023). Forecasting onion armyworm using tree-based machine learning models. *Global Journal of Engineering and Technology Advances* 15(3): 001-007. <https://doi.org/10.30574/gjeta.2023.15.3.0095>
- Daniya T, Geetha M & Kumar K S (2020). Classification and regression trees with gini index. *Advances in Mathematics: Scientific Journal* 9(10): 8237-8247. <https://doi.org/10.37418/amsj.9.10.53>
- Erdoğan H, Bütüner A K & Şahin Y S (2023). Detection of Cucurbit Powdery Mildew, *Sphaerotheca fuliginea* (Schlech.) Polacci by Thermal Imaging in Field Conditions. *Scientific Papers Series Management, Economic Engineering in Agriculture and Rural Development* 23(1): 189-192
- Finger R, Swinton S M, El Benni N & Walter A (2019). Precision farming at the nexus of agricultural production and the environment. *Annual Review of Resource Economics* 11(1): 313-335. <https://doi.org/10.1146/annurev-resource-100518-093929>
- Gallardo-Romero D J, Apolo-Apolo O E, Martínez-Guanter J & Pérez-Ruiz M (2023). Multilayer Data and Artificial Intelligence for the Delineation of Homogeneous Management Zones in Maize Cultivation. *Remote Sensing* 15(12): 3131-3148. <https://doi.org/10.3390/rs15123131>
- Gerdan D, Koç C & Vatandaş M (2023). Diagnosis of Tomato Plant Diseases Using Pre-trained Architectures and A Proposed Convolutional Neural Network Model. *Journal of Agricultural Sciences* 29(2): 618-629. <https://doi.org/10.15832/ankutbd.957265>

- Goncalves J P, Pinto F A, Queiroz D M, Villar F M, Barbedo J G & Del Ponte E M (2021). Deep learning architectures for semantic segmentation and automatic estimation of severity of foliar symptoms caused by diseases or pests. *Biosystems engineering* 210: 129-142. <https://doi.org/10.1016/j.biosystemseng.2021.08.011>
- González-Cabrera J, Mollá O, Montón H & Urbaneja A (2011). Efficacy of *Bacillus thuringiensis* (Berliner) in controlling the tomato borer, *Tuta absoluta* (Meyrick) (Lepidoptera: Gelechiidae). *BioControl* 56: 71-80. <https://doi.org/10.1007/s10526-010-9310-1>
- Hamdini R, Diffellah N & Namane A (2021). Color Based Object Categorization Using Histograms of Oriented Hue and Saturation. *Traitement du Signal* 38(5): 1293-1307. <https://doi.org/10.18280/ts.380504>
- He K, Zhang X, Ren S & Sun J (2016). Deep residual learning for image recognition. In: *Proceedings of the IEEE conference on computer vision and pattern recognition* pp. 770-778
- Kiobia D O, Mwitta C J, Fue K G, Schmidt J M, Riley D G & Rains G C (2023). A Review of Successes and Impeding Challenges of IoT-Based Insect Pest Detection Systems for Estimating Agroecosystem Health and Productivity of Cotton. *Sensors* 23(8): 4127-4147. <https://doi.org/10.3390/s23084127>
- Li W, Wang D, Li M, Gao Y, Wu J & Yang X (2021). Field detection of tiny pests from sticky trap images using deep learning in agricultural greenhouse. *Computers and Electronics in Agriculture* 183: 106048. <https://doi.org/10.1016/j.compag.2021.106048>
- Li W, Zhu T, Li X, Dong J & Liu J (2022). Recommending Advanced Deep Learning Models for Efficient Insect Pest Detection. *Agriculture* 12(7): 1065. <https://doi.org/10.3390/agriculture12071065>
- Lietti M M, Botto E & Alzogaray R A (2005). Insecticide resistance in argentine populations of *Tuta absoluta* (Meyrick) (Lepidoptera: Gelechiidae). *Neotropical Entomology* 34: 113-119. <https://doi.org/10.1590/S1519-566X2005000100016>
- Lin S, Xiu Y, Kong J, Yang C & Zhao C (2023). An Effective Pyramid Neural Network Based on Graph-Related Attentions Structure for Fine-Grained Disease and Pest Identification in Intelligent Agriculture. *Agriculture* 13(3): 567-587. <https://doi.org/10.3390/agriculture13030567>
- Liu Y, Zhang Y, Jiang D, Zhang Z & Chang Q (2023). Quantitative Assessment of Apple Mosaic Disease Severity Based on Hyperspectral Images and Chlorophyll Content. *Remote Sensing* 15(8): 2202-2020. <https://doi.org/10.3390/rs15082202>
- Nayana B P & Kallelshwaraswamy C M (2015). Biology and external morphology of invasive tomato leaf miner, *Tuta absoluta* (Meyrick) (Lepidoptera: Gelechiidae). *Pest Management in Horticultural Ecosystems* 21(2): 169-174
- Otsu N (1979). A threshold selection method from gray-level histograms. *IEEE Transactions on Systems, Man, and Cybernetics: Systems* 9(1): 62-66
- Ozguven M M & Adem K (2019): Automatic detection and classification of leaf spot disease in sugar beet using deep learning algorithms. *Physica A: Statistical Mechanics and its Applications* 535: 122537. <https://doi.org/10.1016/j.physa.2019.122537>
- Pedregosa F, Varoquaux G, Gramfort A, Michel V, Thirion B, Grisel O, Blondel M, Prettenhofer P, Weis R, Dubourg V, Vanderplas J, Passos A, Cournapeau D, Brucher M, Perrot M & Duchesnay E (2011). Scikit-learn: Machine learning in Python. *Journal of Machine Learning Research* 12(2011): 2825-2830
- Sabrol H & Kumar S (2016). Intensity based feature extraction for tomato plant disease recognition by classification using decision tree. *International Journal of Computer Network and Information Security* 14(9): 622
- Singh A, Ganapathysubramanian B, Singh A K & Sarkar S (2016). Machine learning for high-throughput stress phenotyping in plants. *Trends in Plant Science* 21(2): 110-124. <https://doi.org/10.1016/j.tplants.2015.10.015>
- Sriwastwa A, Prakash S, Swarit S, Kumari K & Sahu S S (2018). Detection of pests using color based image segmentation. *Second International Conference on Inventive Communication and Computational Technologies (ICICCT)*, 20-21 April, Coimbatore, India. <https://doi.org/10.1109/ICICCT.2018.8473166>
- Şahin Y S, Erdiñç A, Bütüner A K & Erdođan H (2023). Detection of *Tuta absoluta* larvae and their damages in tomatoes with deep learning-based algorithm. *International Journal of Next-Generation Computing* 14(3): 555-565. <https://doi.org/10.47164/ijnvc.v14i3.1287>
- Urbaneja A, González-Cabrera J, Arno J & Gabarra R (2012). Prospects for the biological control of *Tuta absoluta* in tomatoes of the Mediterranean basin. *Pest Management Science* 68(9): 1215-1222. <https://doi.org/10.1002/ps.3344>
- Veres A, Wyckhuys G A K, Kiss J, Tóth F, Burgio G, Pons X, Avilla C, Vidal S, Razinger J, Bazok R, Matyjaszczyk E, Milosavljević I, Vi Le X, Zhou W, Zhu R Z, Tarno H, Hadi B, Lundgren J, Bonmatin M J, van Lexmond B M, Aebi A, Rauf A & Furlan L (2020). An update of the worldwide integrated assessment (WIA) on systemic pesticides. Part 4: Alternatives in major cropping systems. *Environmental Science and Pollution Research* 27(24): 29867-29899. <https://doi.org/10.1007/s11356-020-09279-x>
- Vibhute A & Bodhe S K (2012). Applications of image processing in agriculture: a survey. *International Journal of Computer Application* 52(2): 34-40. <https://doi.org/10.5120/8176-1495>
- Viggiani G, Filella F, Delrio G, Ramassini W & Foxi C (2009). *Tuta absoluta*, nuovo lepidottero segnalato anche in Italia. *L'Informatore Agrario* 65(2): 66-68
- Vishnoi VK, Kumar K & Kumar B (2021). Plant disease detection using computational intelligence and image processing. *Journal of Plant Diseases and Protection* 128(1): 19-53. <https://doi.org/10.1007/s41348-020-00368-0>
- Weersink A, Fraser E, Pannell D, Duncan E & Rotz S (2018). Opportunities and challenges for big data in agricultural and environmental analysis. *Annual Review of Resource Economics* 10(1): 19-37. <https://doi.org/10.1146/annurev-resource-100516-053654>
- Wolfert S, Ge L, Verdouw C & Bogaardt M J (2017). Big data in smart farming—a review. *Agricultural Systems* 153: 69-80. <https://doi.org/10.1016/j.agsy.2017.01.023>
- Yan B, Fan P, Lei X, Liu Z & Yang F (2021). A real-time apple targets detection method for picking robot based on improved YOLOv5. *Remote Sensing* 13(9): 1619. <https://doi.org/10.3390/rs13091619>
- Zou K, Ge L, Zhou H, Zhang C & Li W (2021). Broccoli seedling pest damage degree evaluation based on machine learning combined with color and shape features. *Information Processing in Agriculture* 8(4): 505-514. <https://doi.org/10.1016/j.inpa.2020.12.003>





A Determination of the Change in Variance Components due to Heat Stress in Dairy Cattle Using a Random Regression Model

Ayşe PINARBAŞI^a , Kemal YAZGAN^{a*}

^aDepartment of Animal Science, Faculty of Agriculture, Harran University, 63300, Sanlıurfa, TÜRKİYE

ARTICLE INFO

Research Article

Corresponding Author: Kemal YAZGAN, E-mail: kemalyazgan@gmail.com, kyazgan@harran.edu.tr

Received: 16 May 2023 / Revised: 28 August 2023 / Accepted: 18 September 2023 / Online: 09 January 2024

Cite this article

Pinarbaşı A, Yazgan K (2024). A Determination of the Change in Variance Components due to Heat Stress in Dairy Cattle Using a Random Regression Model. *Journal of Agricultural Sciences (Tarım Bilimleri Dergisi)*, 30(1):108-117. DOI: 10.15832/ankutbd.1298051

ABSTRACT

The aim of this study is to evaluate changes in variance components for dairy cows under heat stress conditions using a random regression model. The daily milk yield and pedigree records used in the research were obtained from a dairy farm in Sanlıurfa, Türkiye. The records were from Holstein dairy cows registered between 2017 and 2019 at the farm. A total of 690 lactations from 690 healthy dairy cows were used in the study and the total number of cow-days was 207,003. In order to evaluate heat stress on animals meteorological data were used and collected from a public weather station located 15.04 km away from the farm. In the study, variance components were separately estimated for the comfort period (CP) and the heat stress period (HSP) using a random regression test-day model and six-knot linear spline function was used. In the study, it was observed that heat stress resulted in an increase in additive genetic,

permanent environmental, and consequently, phenotypic variance. During the lactation period, the average heritability was determined to be 0.13 ± 0.007 for CP, while it was found to be 0.18 ± 0.010 for HSP. According to the findings obtained from the study, it was concluded that the time periods for selection should coincide with the peak milk yield under heat stress conditions, while for the period without heat stress, it should be around the 120th day of lactation. These results indicate that climatic factors such as temperature and humidity should be included in the models used for genetic parameter and breeding value estimation. Thus, it may be possible to identify dairy cattle that are genetically more tolerant to hot conditions. In this way, more successful outcomes can be achieved in selection studies.

Keywords: Dairy cattle, Genetic analyses, Temperature-humidity index, Eigenfunction, Weather station

1. Introduction

It has been reported in many studies that heat stress negatively affects milk production and reproduction in dairy cattle (Bryant et al. 2007, Ravagnolo & Misztal 2002; Jordan 2003; Garcia-Ispierito et al. 2007; Polsky et al. 2017). Moreover, the adverse effects of global warming will only lead to more serious problems for dairy farmers.

According to Ravagnolo et al. (2000), since daily yields are impacted by weather conditions and reflect the effect of temperature and humidity, meteorological data obtained from public weather stations contain useful information for studies on heat stress in dairy cattle. This means that when weather conditions, such as temperature and humidity, prior to the test days are recorded, the effect of heat stress on animals can be predicted. Similarly, Freitas et al. (2006) reported that public weather data are reliable sources of information, as they have been found to be consistent with on-farm weather measurements. Misztal (1999) suggested a method for examining the genetic basis of heat stress in dairy cows, which involved utilizing performance records and publicly available weather data. In this method, unlike heat stress studies that rely on body temperature or respiration information (Gonzalez-Rivas et al 2018; Osei-Amponsah 2020), individual animal measurements are not required, allowing for the use of large datasets required for genetic evaluation. There is a significant genetic component to heat tolerance in first-lactation cows, particularly for milk, fat, and protein production, and the level of additive genetic variance at a high temperature-humidity index (THI) was observed to be comparable to the additive variance observed under non-stressful conditions (Ravagnolo & Misztal 2000). In addition to this, Aguilar et al. (2009) reported a substantial increase in the additive genetic effects associated with heat stress and yield traits from the first to third parity. Furthermore, female calves of bulls that possessed high genetic merit for heat tolerance exhibited lower milk yields, higher milk solids contents, more robust body types, better udders, longer productive lives, and higher pregnancy rates in comparison to the female calves of bulls with low genetic merit for heat tolerance. The heat tolerance of dairy cattle can be impacted upon by intensive sire selection, especially in temperate climates. If there is a negative genetic correlation between production and heat tolerance, ongoing selection for production will lead to a gradual decline in heat tolerance (Ravagnolo & Misztal 2000).

Random regression models (RRM) are frequently employed for the analysis of longitudinal data in animal breeding (Schaeffer 2004). These models can incorporate various functions to capture the (co)variance structures across days in milk (DIM). One common approach is to use splines to model the (co)variances in test-day models (White et al. 1999; Druet et al. 2003; Silvestre et al. 2005; Bohmanova et al. 2008). According to Misztal (2006), the numerical properties of linear splines are advantageous, and they exhibit localized effects, making them a favourable choice for modelling (co)variance structures in longitudinal data. Moreover, their ease of interpretability adds to their utility for data analysis.

Sanliurfa province is situated in the Southeastern Anatolia Region of Türkiye and is recognized as one of the country's hottest provinces. The weather in this area is characterized by hot and dry conditions between July and October, with temperatures occasionally soaring to 46.8 °C. The region experiences an annual average of 459.3 mm of precipitation and a relative humidity of 51% (Anonymous 2023a). For this reason, milk production in Sanliurfa, especially in summer, is adversely affected due to heat stress. This raises the possibility that, in addition to milk yield losses, the impact of the important environmental factor of temperature and humidity could lead to errors in estimating breeding values.

In previous studies on this region and nearby provinces (Yazgan 2017; Demir & Yazgan 2023) milk yield losses due to heat stress were detected, but no study was conducted on the effect of heat stress on variance components. The aim of this study is to evaluate changes in variance components for dairy cows under heat stress conditions using a random regression test-day model.

2. Material and Methods

2.1. Data

The daily milk yield and pedigree records used in the research were obtained from a dairy farm in Sanliurfa, affiliated with The General Directorate of Agricultural Enterprises (TIGEM), a public institution. The farm is located at 36°48'46" N latitude and 39°51'57" E longitude, with the altitude of 408 meters. Records were from Holstein dairy cows registered between 2017 and 2019 at the farm. The cows were housed in an open free-stall barn system, provided with ad libitum access to feed and water, and milked twice daily using an automated milking system that recorded their milk yield. In the dataset used for the study, each lactation record belongs to a different animal. There are no multiple lactation records for the same animal in the dataset. In other words, the number of lactations and the number of animals in the dataset are equal to each other. All lactation records were restricted to those between 5 and 305 DIM and number of minimum daily records for a lactation were 299. A total of 690 lactations from healthy 690 dairy cows were used in the study. Among these lactations, 278, 130, 135, and 147 were the first, second, third, and fourth or higher lactations, respectively. In addition to this, the total number of cow-days was 207,003 (The number of daily milk yield records in total lactations). The milk production data and pedigree information are summarized in Tables 1 and 2.

Table 1- Descriptive statistic of milk production data

OLP	N	n	Milk yield (kg)	
			\bar{X}	$S_{\bar{x}}$
1	278	83 400	17.65	± 0.015
2	130	39 004	17.44	± 0.022
3	135	40 497	17.01	± 0.024
≥ 4	147	44 102	16.09	± 0.025
Total	690	207 003	17.15	± 0.010

OLP: Order of lactation parity (Each animal has only one lactation record), N: Number of lactations (at the same time, the number of animals), n: The number of daily milk yield records in lactations

Table 2- Pedigree information of animals used in yield records

Item	n
The total number of animals in the pedigree file	1316
Number of animals with milk yield records;	
Animals	690
Sire	80
Dams	634
Animals with unknown sire	9
Animals with unknown dam	-
Animals with unknown parents	-

The daily maximum, minimum, and average temperature and humidity data were collected from a public weather station in Sanliurfa, which is operated by the Turkish State Meteorological Service authorized by the Ministry of Environment, Urbanization, and Climate Change of the Republic of Türkiye. The location of the meteorological station is 36°50'26.2" N latitude and 40°01'50.5" E longitude, with an altitude of 363 meters. While the distance between the public weather station and

the farm was 15.04 km as a straight line (crow flies), the altitude difference between the farm and the public weather station was only 45 m.

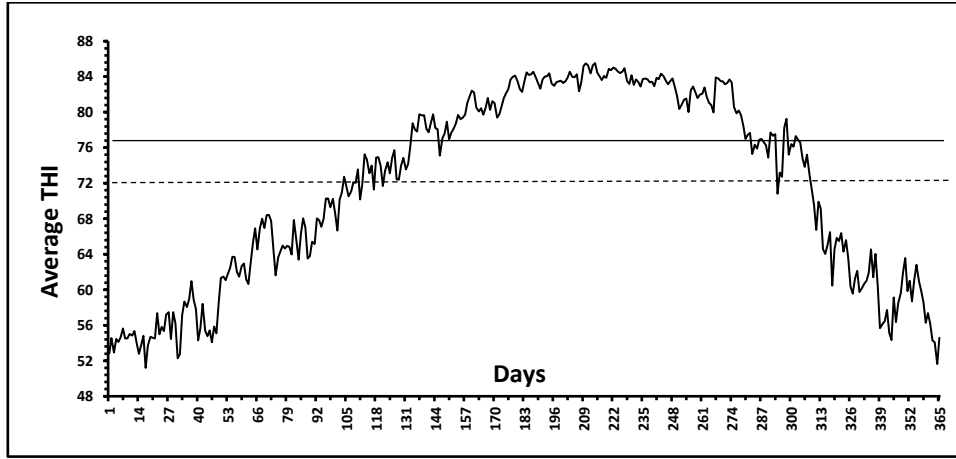


Figure 1- Three-year (2017-2019) average of THI values

According to a previous study (Demir & Yazgan 2023), using the maximum temperature and minimum humidity in the THI formula better represents the stress conditions that animals are exposed to as a result of temperature and humidity in the hot-dry Southeastern Anatolia Region of Türkiye. Similarly, Ravagnolo et al. (2000) stated that the most crucial variables for measuring heat stress were the maximum daily air temperature and minimum daily humidity for calculation of THI. For this reason, in our study, the THI formula proposed by Ravagnolo et al. (2000) was used to determine heat stress, which includes maximum temperature and minimum humidity values (Eq. 1):

$$THI = (1.8t + 32) - (0.55 - 0.0055 \times rh)(1.8t - 26.8) \quad (1)$$

Where; t is temperature in degrees Celsius and rh is relative humidity, expressed as a percentage. For this, heat stress in dairy cattle begins at a THI value of 72, which is equivalent to 22 °C at 100% humidity, 25 °C at 50% humidity, or 28 °C at 20% humidity. Figure 1 shows calculated THI values for each day of the year (averaged over 3 years) for the present data set. Each daily milk yield record was assigned the daily THI values of the previous days and put together with the daily milk production data.

2.2. Models and statistical analyses

The following model was used to calculate the least squares means for milk yield according to THI values (Eq. 2):

$$Y_{ijklmno} = cy_i + cs_j + ca_k + olp_l + dim_m + thi_n + e_{ijklmno} \quad (2)$$

Where; $Y_{ijklmno}$: least square mean of daily milk yield for calving year i , calving season j , calving age k , parity l , days in milk class m and THI class n , cy_i : effect of calving year ($i=2018, 2019$ and 2020), cs_j : effect of calving season ($j=$ spring, summer, autumn and winter), ca_k : effect of calving age ($k=1$ for ≤ 24 , $k=2$ for 25-30, $k=3$ for 31-36, $k=4$ for 37-42, $k=5$ for 43-48, $k=6$ for 49-54, $k=7$ for 55-60, $k=8$ for 61-66, $k=9$ for 67-72, $k=10$ for 73-78 and $k=11$ for ≥ 79 month), olp_l : effect of order of lactation parity (Each animal has only one lactation record and $l=1, 2, 3$ and ≥ 4), dim_m : effect of days in milk class ($m=1$ for ≤ 60 , $m=2$ for 61-120, $m=3$ for 121-180 and $m=4$ for 180-305 days), thi_n : effect of temperature humidity index ($n=48, 49, 50, 51, 52, \dots$ and 95) and $e_{ijklmno}$: random residual effect.

Following this stage, the dataset used in the study was divided into two parts based on the THI=77 values (The point where milk yield starts to decline continuously), including the period before the onset of heat stress, which is referred to as the comfort period (CP), and the term covering the heat stress period (HSP). In this case, the number of daily milk yield records for CP and HSP was 123,291 and 83,712, respectively. These data sets were analyzed with the RRM (Random Regression Model) for two thermal period (CP and HSP), and the six-knot linear spline function was used in the model. Linear spline parameters are calculated between 2 knots adjacent to the milk yield record and take the value 0 among all other knots. If T is a knot vector, the parameters of the line constructed for the milk yield record at time t between knots T_i and T_{i+1} can be calculated as given in Eq. 3 and 4 (Bohmanova et al. 2008):

$$Z_i(t) = \frac{t - T_i}{T_{i+1} - T_i} \quad (3)$$

$$Z_{i+1}(t) = \frac{T_{i+1}-t}{T_{i+1}-T_i} = 1 - Z_i(t) \quad (4)$$

However, the parameter value for yield records at the i^{th} knot is set to $Z_i=1$ and $Z_{1 \dots i-1, i+1 \dots q} = 0$. For example, in an instance with six knot points, there are at least two non-zero parameter values and their sum is always equal to 1. In this study knot points were selected at the 5th, 65th, 125th, 185th, 245th and 305th days of a 305-day lactation period based on milk yields, the vector containing the function parameters that for instance include the milk yield record at $t=36$ calculated as follows (Bohmanova et al. 2008):

$$Z(36) = \left\{ \frac{36-5}{65-5}, \frac{65-36}{65-5}, 0, 0, 0 \right\} = \{0.5166, 0.4833, 0, 0, 0\}$$

As seen above, the sum of parameter values is equal to 1. In addition to this, the following RRM model (Eq. 5) is provided for estimating daily additive genetic, permanent environmental, and error variances for CP and HSP in the study:

$$Y_{ijklmnr} = cy_i + cs_j + ca_k + olp_l + dim_m + \sum_{r=1}^6 b_r \phi_{ntr} + \sum_{r=1}^6 a_{nr} \phi_{ntr} + \sum_{r=1}^6 pe_{nr} \phi_{ntr} + e_{ijklmnr} \quad (5)$$

Where; $Y_{ijklmnr}$: milk yield record of cow n recorded on t within subclass calving year i , calving season j , calving age k , parity l , days in milk class m , b_r : fixed regression coefficients, a_{nr} and pe_{nr} : r^{th} (In this study, since a six-knot linear spline function was used, six random regression coefficients for additive genetic effect and six random regression coefficients for permanent environmental effect were calculated for each animal.) random regression for animal and permanent environment effects, respectively, for animal n : ϕ_{ntr} is the vector of the r^{th} spline function for the daily record of cow n recorded on day t , $e_{ijklmnr}$: random residual (which was heterogeneous in this study) was calculated separately for the intervals of 5, 6-30, 31-60, 61-90, 91-120, 121-180, 181-210, 211-240, 241-270, and 271-305 days. In matrix notation, the model (Eq. 5) can be written as below (Eq.6):

$$y = Xb + Za + Wpe + e \quad (6)$$

Where; y , vector of observations (records) and b , a , pe and e : vectors of fixed, additive genetic, permanent environmental and random residual effects, respectively. X , Z and W are incidence matrices which relate records to effects.

$$\text{var} \begin{bmatrix} a \\ pe \\ e \end{bmatrix} \cong \begin{bmatrix} G \otimes A & 0 & 0 \\ 0 & I \sigma_{pe}^2 & 0 \\ 0 & 0 & R \end{bmatrix} \quad (7)$$

The (co)variance matrices for the additive genetic and permanent environmental random regression coefficients, denoted as G and P , respectively (Eq. 7), are both 6×6 matrices (\otimes is the Kronecker product). Additionally, A represents the additive genetic relationship matrix, while I denotes the identity matrix and $R = I \sigma_e^2$. In addition, heritability (h^2) estimates were calculated based on the formula given in Eq. 8.

$$h^2 = \frac{\sigma_a^2}{\sigma_a^2 + \sigma_{pe}^2 + \sigma_e^2} \quad (8)$$

Where; σ_a^2 , σ_{pe}^2 and σ_e^2 are additive genetic, permanent environmental and random residual variances respectively. The following equation (Eq.9) was used in order to obtain eigenfunctions:

$$f_i = E \times S \quad (9)$$

Where; f_i represents the vector containing the values of i^{th} eigenfunctions, E is the matrix consisting of 6×6 eigenvector values obtained from the covariance matrix, and S is the 301×6 matrix containing the parameters of the linear spline function with six knots. In this study, to obtain least squares means using Eq. 2, SAS (2000) software was used, and for random regression analyses represented by Eq. 5 and to obtain eigenvectors of covariance matrix, WOMBAT software (Meyer 2007; Anonymous 2023b) was used.

3. Results and Discussion

3.1. Milk yield levels for THI values

The analysis conducted using the model given in Eq. 2 in the study found that the effect of all environmental factors was

significant ($P < 0.01$). The coefficient of determination (R^2) for the model was determined to be 0.4786, and the mean square error was 12.460. R^2 value, revealed that the model, which includes weather variables, explained almost half of the yield variation. Ravagnolo et al. (2000) indicated that while the moisture content in the air remained constant, the lowest humidity occurred when the temperature was at its highest. This corresponds with the findings of this study. In addition, the calculated R^2 value in this study is found to be higher than the values reported by Ravagnolo et al. (2000), West et al. (2003), and Freitas et al. (2006), while being very close to the values reported by Dikmen & Hansen (2009), Yazgan (2017), and Demir & Yazgan (2023).

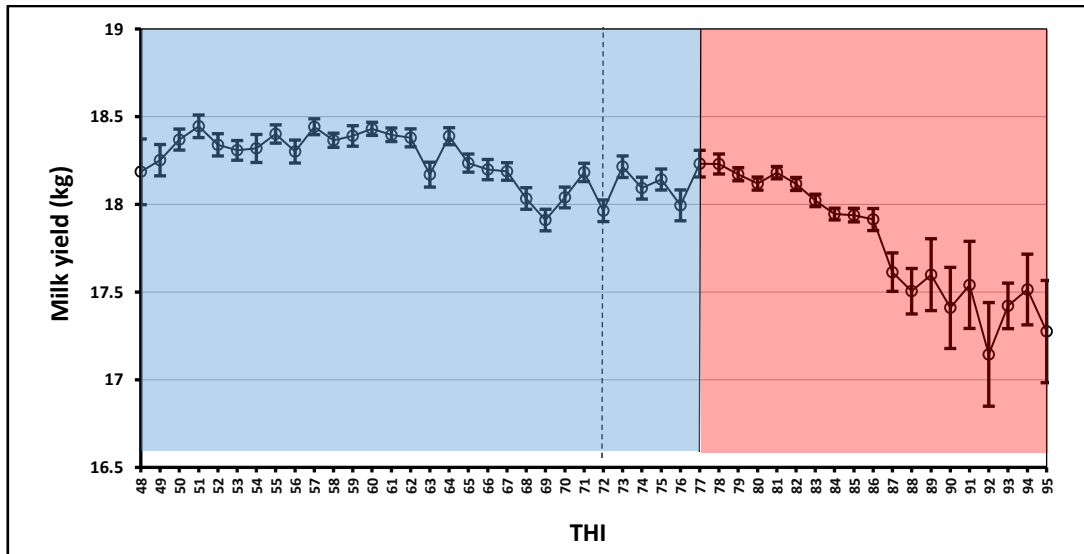


Figure 2 - Least square means of milk yields by THI values. Dashed vertical lines show the critical THI value (72). The blue area represents the comfort period (CP), while the red area indicates the heat stress period (HSP), during which milk yield starts to decrease continuously

Figure 2 illustrates the alteration of the least square means of milk yield based on THI values. THI values ranging from 48 to 95 were calculated by taking into account the daily maximum temperature and minimum humidity values. The threshold THI value at which the milk yield started to decrease continuously was identified as 77, which was 5 units higher than the critical value ($\text{THI}=72$). In the previous study (Demir & Yazgan 2023), the point at which milk yield began to continuously decrease was determined to be 69, which was below the critical value ($\text{THI}=72$) identified in this study. The lower average milk yield of the farm where the data was obtained in this study (17.15 ± 0.01) compared to the farm where the datasets used in the previous study (Demir & Yazgan 2023) were obtained (28.96 ± 8.89) may have caused this. This difference could potentially be attributed to the greater effect on high milk-yielding cows because high milk production requires more metabolic activity and leads to an increase in body temperature (Kadzere et al. 2002; Das et al. 2016). In addition, as the THI values ranged from 48 to 77, the milk yield remained relatively stable. However, beyond this point, it began to decrease rapidly, reaching a minimum at $\text{THI}=92$. At $\text{THI}=77$, the milk yield was 18.23 ± 0.07 kg, but when THI increased to 92, it decreased to 17.14 ± 0.295 kg, representing a difference of 1.09 kg. According to these findings, the period from the starting THI value (48) in Figure 2 to the vertical line (77) and the blue area shown can be considered as the comfort period (CP), while the period after the vertical line and shown in red represents the heat stress period (HSP). Additionally, as can be observed from Figure 2, minor fluctuations in milk yield are observed during the CP. The fluctuations observed during the CP period may be attributed to the utilization of fans, shading, and sprinkler equipment, which may reduce the heat stress at higher temperatures. This can cause the THI to exhibit not only a linear but also a zigzag pattern, as shown in Figure 2.

3.2. Variance components and heritability values for CP and HSP

The daily estimated additive genetic, permanent environmental, random residual error and phenotypic variances for CP and HSP are shown in Figure 3. According to this, all variance components except for random residual variance exhibited a fluctuating trend throughout lactation for both CP and HSP. The highest error variance values for both CP and HSP were determined to be 1.5284 kg^2 and 1.5228 kg^2 , respectively, between the 30th and 60th days. Afterwards, from day 121 until the end of lactation, the random error variance values for both CP and HSP tended to be close to each other and remained constant, and did not exceed the value of 0.35 kg^2 for either. When examining the daily changes of the additive genetic variance during lactation for both thermal periods (CP and HSP), intervals were observed where one was higher or lower than the other (Figure 3). Additive genetic variance values for HSP reached their highest value on the 66st day of lactation (8.57 kg^2). In contrast, the highest estimated additive genetic variance value for CP was reached on the 125st day of lactation and was only predicted as 3.06 kg^2 . In other words, additive genetic variance increased during the heat stress period, which is consistent with the findings of Armstrong (1994), Ravagnolo & Misztal (2000), Aguilar et al. (2009) and Bernabucci et al. (2014).

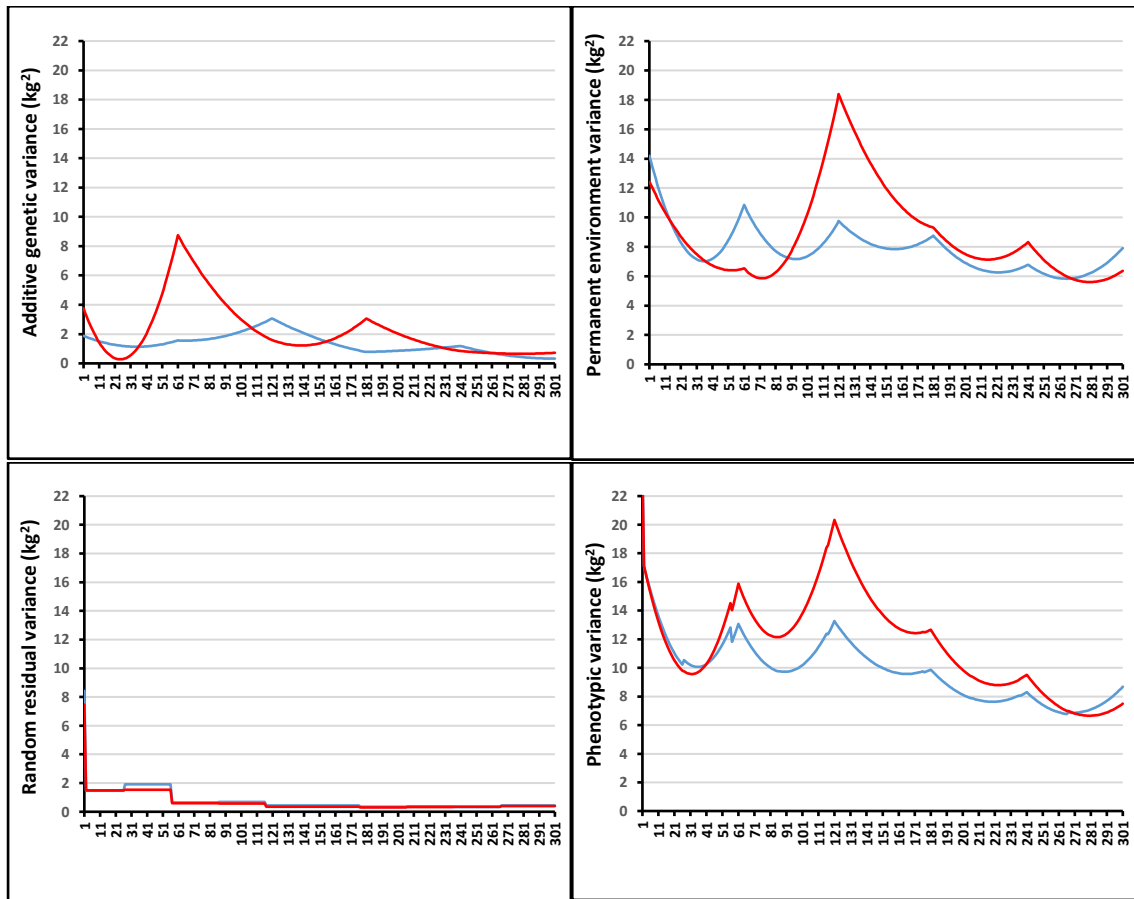


Figure 3 - The daily estimated additive genetic, permanent environmental, random residual error, and phenotypic variances for CP (—) and HSP (—)

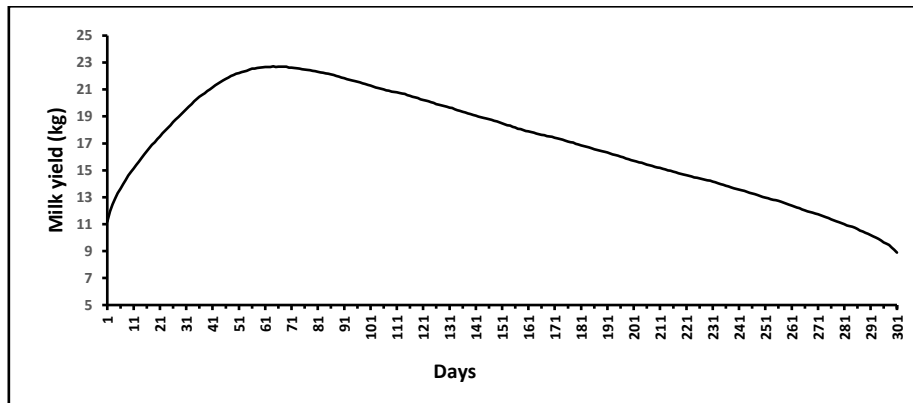


Figure 4- Lactation curve plotted from 207 003 daily milk yield records used in the study

As shown in Figure 3, the highest additive genetic variance value (8.57 kg^2) for HSP was obtained on the 66th day of lactation under heat stress conditions, whereas the value for CP was only 1.56 kg^2 on the same day. As can be observed from the lactation curve given in Figure 4, the highest additive genetic variance was obtained during the peak milk yield period. The difference in milk yield between genetically tolerant and sensitive cows to heat stress may have become more pronounced during this period, and this could have led to an increase in the additive genetic variance. The fact that the difference in additive genetic variance between CP and HSP during the lactation period is not as high as around the 66th day at any other period further confirms this result.

As can be observed from Figure 3, the highest permanent environment variance value (18.39 kg^2) for HSP was obtained on the 121th day of lactation under heat stress conditions, whereas the value for CP was only 9.75 kg^2 on the same day. While permanent environment variance values for HSP reached their highest value on the 121st day of lactation, the highest estimated permanent environment variance value for CP was reached on the 61st day of lactation and was only predicted as 10.86 kg^2 . The estimated permanent environmental variance for HSP was found to be consistently higher than the permanent environmental

variance estimated for CP throughout much of the lactation period. This suggests that, similar to additive genetic variance, permanent environmental variance also increases under heat stress conditions. These results are consistent with the findings of Ravagnolo & Misztal (2000) and Aguilar et al. (2009).

As previously stated, the permanent environmental variance for HSP reached its highest value on day 121th, which coincided with the end of the calving-to-conception interval (days open) at the farm where the study was conducted. Towards the end of this period, estrus continues in cows, and sudden drops in milk yield are observed (Rearte et al. 2018). In this case, the negative effect of heat stress may have also contributed to the increase in permanent environmental variance, in addition to the decrease in milk yield caused by estrus. This is because, as can be observed from Figure 3, on the days when the permanent environmental variance for HSP reached its highest value, the estimated permanent environmental variance for CP was only 9.75 kg² as previously mentioned. Abeni et al. (2007) demonstrated that the alterations in blood parameters associated with energy balance and enzyme activity during heat stress were most pronounced in cows in midlactation. Additionally, Perera et al. (1986) reported that the negative impact of summer heat stress on milk yield in cows was most significant during midlactation. These factors could provide another reason for why the permanent environmental variance increases towards the midlactation period during the heat stress period. Also, shown in Figure 3, on the days when permanent environment variance was highest, phenotypic variance also reached its highest value (19.88 kg²). Additionally, phenotypic variance is higher for HSP compared to CP, except for short periods that cover the beginning and end of lactation for HSP.

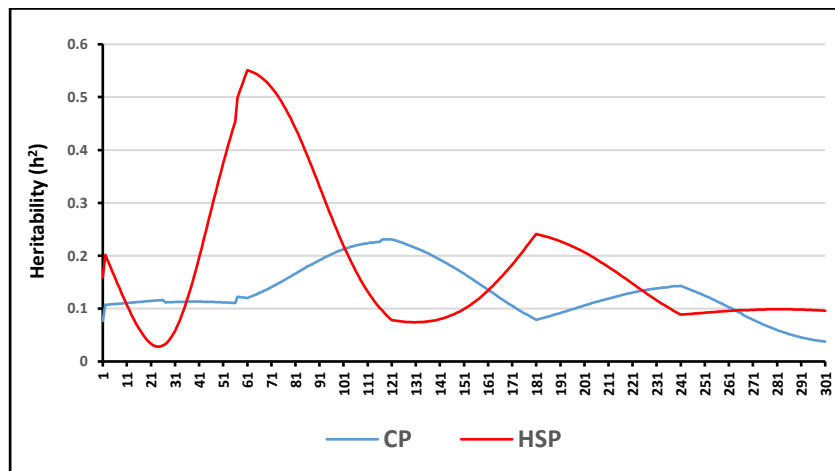


Figure 5 - The daily estimated heritability values for CP and HSP

Daily changes in the heritability estimates are presented in Figure 5. When considering changes in heritability in thermal zones, both CP and HSP exhibit fluctuating values. The daily course of heritability values for both HP and CP showed a significant similarity with the course of additive genetic variance values as expected (Figure 3 and 5). The heritability of HSP was found to increase above 50% on the 66th day in accordance with the trend of the additive genetic variance, with an average of 0.18 ± 0.010 throughout lactation. On the other hand, the average heritability estimate for CP was calculated as 0.13 ± 0.007 . However, the highest heritability for CP was reached around the 120th day (0.23). In other words, the highest heritability for CP was reached on the days when both permanent environmental variance and phenotypic variance were at their highest. On the other hand, Aguilar et al. (2009) reported that as THI values increased from 72 to 82, the heritability ranged from 0.10 to 0.24, which is slightly broader than the range observed in this study. Similarly, Ravagnolo & Misztal (2000) estimated heritability values between 0.16 and 0.21 when THI values ranged from 72 to 85. In our research, since multiple lactation records were not available for each animal, it was not possible to estimate how much the variance components changed by lactation order. This difference may explain the variation between the studies. Other factors that could contribute to the inconsistency include the use of daily milk yield records in this study versus monthly test-day milk yield records in the mentioned studies, as well as potential variations in the number of knots used in the linear spline models, differences in cooling applications such as fans and water spraying and other metrological factors.

3.3. Eigenfunctions for CP and HSP

Eigenfunctions, derived from the eigenvectors of the genetic (co)variance matrix (Kirkpatrick et al. 1990), can offer a perspective on the impacts of selection throughout the lactation period. Eigenvalues with their relative proportions (%) of coefficient matrix of the additive genetic covariance functions for CP and HSP are presented in Table 3. For CP and HSP, the first eigenvalues of the coefficient matrices of the additive genetic covariance functions accounted for approximately 63.76% and 69.93% of the total eigenvalues, respectively, in the six-knot linear spline model. The fourth, fifth, and sixth values can be neglected in contrast to the first three, which have negligible proportions of the total eigenvalues related to the variation in additive genetic variance. The eigenfunctions of the additive genetic coefficient matrix of the covariance functions for both CP and HSP in the six-knot linear spline model were plotted in Figures 6 and 7. Considering CP, the first eigenvalue of the coefficient matrix of the additive

genetic covariance function accounted for approximately 63.76% of the total eigenvalues. The large first eigenvalue implies that selecting based on the first eigenfunctions will lead to rapid changes in the lactation curve. This suggests that genetic selection for the 121st day would be successful. As previously mentioned, for CP, this period corresponds to the end of the estrous cycle, and it is the point where the eigenfunctions reaches its highest value, similar to the case of permanent environmental variance (Figure 3 and 6). However, when considering HSP, the first eigenvalue of the coefficient matrix of the additive genetic covariance function accounted for approximately 63.76% of the total eigenvalues. Similarly, the large first eigenvalue suggests that selection based on the first eigenfunctions will result in rapid changes in the lactation curve. Additionally, for HSP, the eigenfunctions value reaches its highest point on the 60th day. This implies that genetic selection around the 60th day would be successful. As discussed previously, it was the period around the 60th day when the peak milk yield is achieved, and for HSP, it coincides with the time when both the genetic variance and heritability were at their highest.

Table 3- Eigenvalues and their relative proportions (%) in the coefficient matrix of additive genetic covariances for CP and HSP.

<i>Thermal period</i>		<i>Order of eigenvalues</i>					
		<i>1.</i>	<i>2.</i>	<i>3.</i>	<i>4.</i>	<i>5.</i>	<i>6.</i>
CP	Eigenvalue	5.61	2.02	1.14	0.02	0.00	0.00
	(%)	63.76	23.03	12.93	0.27	0.02	0.01
HSP	Eigenvalue	13.08	4.66	0.77	0.20	0.00	0.00
	(%)	69.93	24.89	4.10	1.06	0.01	0.00

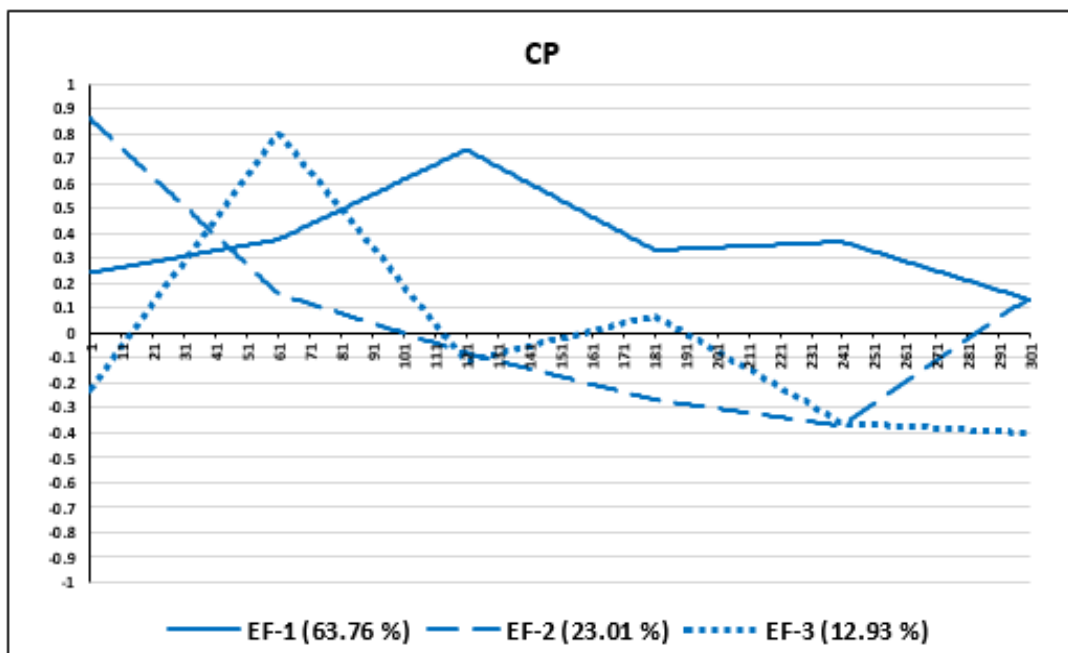


Figure 6- First three eigenfunctions (EF) of the random regression genetic covariance matrix of lactation for CP

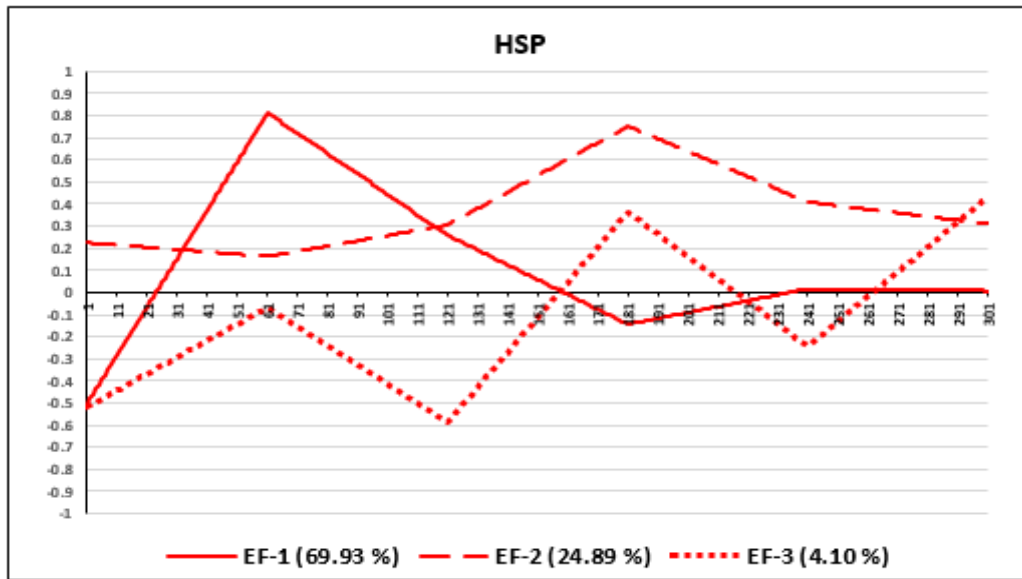


Figure 7- First three eigenfunctions (EF) of the random regression genetic covariance matrix of lactation for HSP.

In this study, due to the unavailability of multiple lactation records for each animal, the relationship between the lactation order and heat stress could not be examined. Similarly, the relatively low number of dairy cows with multiple offspring prevented the inclusion of maternal effects in the model. In the future, as global warming's negative effects on dairy animals' yields are expected to increase, the selection of genetically heat-tolerant dairy cattle may require the use of more complex models. It can be said that similar studies should continue using more complex models that include multiple genetic effects (such as direct and maternal genetic effects, genetic groups, etc.) with larger datasets containing more lactation records.

4. Conclusions

This study demonstrated the impact of heat stress specifically on additive genetic variance and permanent environmental variance as it differs from other studies by using daily milk yield records for estimating variance components. Heat stress resulted in an increase in additive genetic, permanent environmental, and consequently, phenotypic variance in this research. Although variance ratios may vary depending on the herd and region, it does not change the fact that heat stress will affect genetic parameters. According to the findings obtained from the research, it has been concluded that the time periods for selection should coincide with the period when peak milk yield is achieved under heat stress conditions, whereas for the period without heat stress, it should be around the 120th day of lactation. These results indicate that climatic factors such as temperature and humidity should be included in the models used for genetic parameter and breeding value estimation. Thus, it may be possible to identify dairy cattle that are genetically more tolerant to hot conditions. In this way, more successful outcomes can be achieved in selection studies. Additionally, similar studies should be replicated in hot-dry regions with different dairy cattle breeds and larger herds to obtain data that can further validate the findings of this study.

Acknowledgments

This study has been conducted as a summary of the first author's PhD study. Additionally, we would like to express our gratitude to the authorities of TIGEM-Ceylanpınar Agricultural Enterprise Directorate for their contributions in providing the necessary data for the realization of this study.

References

- Anonymous (2023a). <https://www.mgm.gov.tr/eng/forecast-cities.aspx?m=SANLIURFA> Access date: 08.05.2023
- Anonymous (2023b). <http://didgeridoo.une.edu.au/km/wombat.php> Access date: 12.02.2023
- Abeni F, Calamari L & Stefanini L (2007). Metabolic conditions of lactating Friesian cows during the hot season in the Po valley. 1. Blood indicators of heat stress. *International Journal of Biometeorology* 52(2):87-96. <https://doi.org/10.1007/s00484-007-0098-3>
- Aguilar I, Misztal I & Tsuruta S (2009). Genetic components of heat stress for dairy cattle with multiple lactations. *Journal of Dairy Science*. 92: 5702–5711. <https://doi.org/10.3168/jds.2008-1928>
- Armstrong D V (1994). Heat stress interaction with shade and cooling. *Journal of Dairy Science* 77: 2044–2050. [https://doi.org/10.3168/jds.S0022-0302\(94\)77149-6](https://doi.org/10.3168/jds.S0022-0302(94)77149-6)
- Bernabucci U, Biffani S, Buggiotti L, Vitali A, Lacetera N & Nardone A (2014) The effects of heat stress in Italian Holstein dairy cattle. *Journal of Dairy Science* 97(1):471-86. <https://doi.org/10.3168/jds.2013-6611>

- Bohmanova J, Miglior F, Jamrozik J, Misztal I & Sullivan P G (2008). Comparison of random regression models with legendre polynomials and linear splines for production traits and somatic cell score of Canadian Holstein cows. *Journal of Dairy Science* 91: 3627–3638 <https://doi.org/10.3168/jds.2007-0945>
- Bryant J R, Lopez-Villalobos N, Pryce J E, Holmes C W, Johnson D L & Garrick D J (2007). Environmental sensitivity in New Zealand dairy cattle. *Journal of Dairy Science* 90: 1538–1547. [https://doi.org/10.3168/jds.S0022-0302\(07\)71639-9](https://doi.org/10.3168/jds.S0022-0302(07)71639-9)
- Das R, Sailo L, Verma N, Bharti P, Saikia, J & Kumar R (2016). Impact of heat stress on health and performance of dairy animals: A review. *Veterinary World* 9(3): 260-268. <https://doi.org/10.14202/vetworld.2016.260-268>
- Demir O & Yazgan K (2023). Effects of air temperature and relative humidity on milk yield of Holstein dairy cattle raised in hot-dry Southeastern Anatolia Region of Türkiye. *Journal of Agricultural Sciences* 29(2): 710-720. <https://doi.org/10.15832/ankutbd.1159540>
- Dikmen S & Hansen P J (2009). Is the temperature-humidity index best indicator of heat stress in lactating dairy cows in a subtropical environment? *Journal of Dairy Science* 92(1): 109-116. <https://doi.org/10.3168/jds.2008-1370>
- Druet T, Jaffrézic F, Boichard D & Ducrocq V (2003). Modeling lactation curves and estimation of genetic parameters for first lactation test-day records of French Holstein cows. *Journal of Dairy Science* 86: 2480–2490. [https://doi.org/10.3168/jds.S0022-0302\(03\)73842-9](https://doi.org/10.3168/jds.S0022-0302(03)73842-9)
- Freitas M S, Misztal I, Bohmanova J & West J (2006). Utility of on- and off-farm weather records for studies in genetics of heat tolerance. *Livestock Science* 105: 223–228. <https://doi.org/10.1016/j.livsci.2006.06.011>
- Garcia-Ispuerto I, Lopez-Gatius F, Bech-Sabat G, Santolaria P, Yaniz J L, Nogareda C, De Rensis F & Lopez-Bejar M (2007). Climate factors affecting conception rate of high producing dairy cows in northeastern Spain. *Theriogenology* 67: 1379–1385. <https://doi.org/10.1016/j.theriogenology.2007.02.009>
- Gonzalez-Rivas P A, Sullivan M, Cottrell J J, Leury B J, Gaughan J B & Dunshea F R (2018). Effect of feeding slowly fermentable grains on productive variables and amelioration of heat stress in lactating dairy cows in a sub-tropical summer. *Tropical Animal Health and Production* 50: 1763–1769. <https://doi.org/10.1007/s11250-018-1616-5>
- Jordan E R (2003). Effects of heat stress on reproduction. *Journal of Dairy Science* 86 (E Suppl.):E104–E114. [https://doi.org/10.3168/jds.S0022-0302\(03\)74043-0](https://doi.org/10.3168/jds.S0022-0302(03)74043-0)
- Kadzer C T, Murphy M R, Silanikove N & Maltz E (2002). Heat stress in lactating dairy cows: a review. *Livestock Production Science* 77(1): 59-91. [https://doi.org/10.1016/S0301-6226\(01\)00330-X](https://doi.org/10.1016/S0301-6226(01)00330-X)
- Kirkpatrick M, Lofsvold D & Bulmer M (1990). Analysis of the inheritance, selection and evolution of growth trajectories. *Genetics* 124: 979–993. <https://doi.org/10.1093/genetics/124.4.979>
- Meyer (2007). WOMBAT—A tool for mixed model analyses in quantitative genetics by restricted maximum likelihood (REML). *Journal of Zhejiang University Science B* 8(11): 815-821. <https://doi.org/10.1631/jzus.2007.B0815>
- Misztal I (1999). Model to study genetic component of heat stress in dairy cattle using national data. *Journal of Dairy Science* 82(Suppl. 1):32.(Abstr.).(Cited by: Aguilar I, Misztal I & Tsuruta S (2009). Genetic components of heat stress for dairy cattle with multiple lactations. *Journal of Dairy Science*. 92: 5702–5711. <https://doi.org/10.3168/jds.2008-1928>)
- Misztal I (2006). Properties of random regression models using linear splines. *Journal Animal Breeding and Genetic* 123: 74–80. <https://doi.org/10.1111/j.1439-0388.2006.00582.x>
- Osei-Amponsah R, Dunshea F R, Leury B J, Cheng L, Cullen B, Joy A, Abhijith A, Zhang M H & Chauhan S S (2020). Heat Stress Impacts on lactating cows grazing Australian summer pastures on an automatic robotic dairy. *Animals* 10(5): 869. <https://doi.org/10.3390/ani10050869>
- Perera KS, Gwazdauskas FC, Pearson RE, Brumback TB (1986). Effect of Season and Stage of Lactation on Performance of Holsteins. *Journal of Dairy Science* 69 (1): 228-236. [https://doi.org/10.3168/jds.S0022-0302\(86\)80390-3](https://doi.org/10.3168/jds.S0022-0302(86)80390-3)
- Polsky L, Marina A G & Keyserlingk V (2017). Invited review: Effects of heat stress on dairy cattle welfare. *Journal of Dairy Science* 100: 8645-8657 <https://doi.org/10.3168/jds.2017-12651>
- Ravagnolo O & Misztal I (2000). Genetic component of heat stress in dairy cattle, parameter estimation. *Journal of Dairy Science* 83: 2126–2130. [https://doi.org/10.3168/jds.S0022-0302\(00\)75095-8](https://doi.org/10.3168/jds.S0022-0302(00)75095-8)
- Ravagnolo O, Misztal I & Hoogenboom G (2000). Genetic component of heat stress in dairy cattle, development of heat index function. *Journal of Dairy Science* 83(9): 2126–2130. [https://doi.org/10.3168/jds.s0022-0302\(00\)75094-6](https://doi.org/10.3168/jds.s0022-0302(00)75094-6)
- Ravagnolo O & Misztal I (2002). Effect of heat stress on nonreturn rate in Holsteins: Fixed-model analyses. *Journal of Dairy Science* 85: 3101–3106. [https://doi.org/10.3168/jds.S0022-0302\(02\)74397-X](https://doi.org/10.3168/jds.S0022-0302(02)74397-X)
- Rearte R, LeBlanc S J, Corva S G, De Da Sota R L, Lacau-Mengido I M & Giuliodori M J (2018). Effect of milk production on reproductive performance in dairy herds. *Journal of Dairy Science* 101(8): 7575-7584. <https://doi.org/10.3168/jds.2017-13796>
- SAS institute Inc. (2000). SAS User's guide statistics, version ed. SAS Institute, Gary, N.C. http://www2.sas.com/pdfs/s2k/v1_psm.pdf
- Schaeffer L R (2004). Application of random regression models in animal breeding. *Livestock Production Science* 86: 35–45. [https://doi.org/10.1016/S0301-6226\(03\)00151-9](https://doi.org/10.1016/S0301-6226(03)00151-9)
- Silvestre A M, Petim-Batista F & Colaco J (2005). Genetic parameter estimates of Portuguese dairy cows for milk, fat, and protein using a spline test-day model. *Journal of Dairy Science* 88: 1225–1230. [https://doi.org/10.3168/jds.S0022-0302\(05\)72789-2](https://doi.org/10.3168/jds.S0022-0302(05)72789-2)
- West J W, Mullinix B G & Bernard J K (2003). Effects of hot, humid weather on milk temperature, dry matter intake and milk yield of lactating dairy cows. *Journal of Dairy Science* 86(1): 232-242. [https://doi.org/10.3168/jds.s0022-0302\(03\)73602-9](https://doi.org/10.3168/jds.s0022-0302(03)73602-9)
- White I M S, Thompson R & Brotherstone S (1999). Genetic and environmental smoothing of lactation curves with cubic splines. *Journal of Dairy Science* 82: 632–638. [https://doi.org/10.3168/jds.S0022-0302\(99\)75277-X](https://doi.org/10.3168/jds.S0022-0302(99)75277-X)
- Yazgan K (2017). Determining heat stress effect in Holstein dairy cattle using daily milk yield and meteorological data obtained from public weather station in Sanliurfa province of Turkey. *Indian Journal of Animal Research* 51(6): 1002-1011. <https://doi.org/10.18805/ijar.v0i0f.3806>





A Meta-Heuristic Algorithm-Based Feature Selection Approach to Improve Prediction Success for *Salmonella* Occurrence in Agricultural Waters

Murat DEMİR^a , Murat CANAYAZ^b , Zeynal TOPALCENGİZ^{c, d*}

^aDepartment of Software Engineering, Faculty of Engineering and Architecture, Muş Alparslan University, 49250 Muş, TÜRKİYE

^bDepartment of Computer Engineering, Faculty of Engineering, Van Yüzüncü Yıl University, 65080 Van, TÜRKİYE

^cDepartment of Food Science, Center for Food Safety, University of Arkansas System Division of Agriculture, Fayetteville, AR 72704, USA

^dDepartment of Food Engineering, Faculty of Engineering and Architecture, Muş Alparslan University, 49250 Muş, TÜRKİYE

ARTICLE INFO

Research Article

Corresponding Author: Zeynal TOPALCENGİZ, E-mail: zeynalt@uark.edu; zeynaltopalcengiz@gmail.com

Received: 24 May 2023 / Revised: 20 September 2023 / Accepted: 21 September 2023 / Online: 09 January 2024

Cite this article

Demir M, Canayaz M, Topalcengiz Z (2024). A Meta-Heuristic Algorithm-Based Feature Selection Approach to Improve Prediction Success for *Salmonella* Occurrence in Agricultural Waters. *Journal of Agricultural Sciences (Tarım Bilimleri Dergisi)*, 30(1):118-130. DOI: 10.15832/ankutbd.1302050

ABSTRACT

The presence of *Salmonella* in agricultural waters may be a source of produce contamination. Recently, the performances of various algorithms have been tested for the prediction of indicator bacteria population and pathogen occurrence in agricultural water sources. The purpose of this study was to evaluate the performance of meta-heuristic optimization algorithms for feature selection to increase the *Salmonella* occurrence prediction success of commonly used algorithms in agricultural waters. Previously collected datasets from six agricultural ponds in Central Florida included the population of indicator microorganisms, physicochemical water attributes, and weather station measurements. *Salmonella* presence was also reported with PCR-confirmed method in data set. Features were selected by using binary meta-heuristic optimization methods including differential evolution optimization (DEO), grey wolf optimization (GWO), Harris hawks optimization (HHO) and particle swarm optimization (PSO). Each meta-heuristic method was run 100 times for the extraction of features before

classification analysis. Selected features after optimization were used in the K-nearest neighbor algorithm (kNN), support vector machine (SVM) and decision tree (DT) classification methods. Microbiological indicators were ranked as the first or second features by all optimization algorithms. Generic *Escherichia coli* was selected as the first feature 81 and 91 times out of 100 using GWO and DEO, respectively. The meta-heuristic optimization algorithms for the feature selection process followed by machine learning classification methods yielded a prediction accuracy between 93.57 and 95.55%. Meta-heuristic optimization algorithms had a positive effect on improving *Salmonella* prediction success in agricultural waters despite spatio-temporal variations. This study indicates that the development of computer-based tools with improved meta-heuristic optimization algorithms can help growers to assess risk of *Salmonella* occurrence in specific agricultural water sources with the increased prediction success.

Keywords: Optimization, Support Vector Machine, kNN, Decision tree, Water quality

1. Introduction

Agricultural waters can be the main source of microbiological contamination in produce fields (FDA 2015). Pathogens such as *Salmonella* and shiga toxin-producing *Escherichia coli* can survive at various temperatures in agricultural surface waters for prolonged periods of time (Topalcengiz & Danyluk 2019; Topalcengiz et al. 2019). Agricultural water sources have been implicated as the possible source of *Salmonella* contamination during produce related outbreaks (CDC 2007; Greene et al. 2008). Microbiological indicators including streptococci, enterococci, and total coliforms can be used to monitor the water quality (Steele et al. 2005). The measurement of a generic *Escherichia coli* population is commonly required or recommended to assess the risk of contamination from agricultural water sources around the world (Ashbolt 2001; FDA 2015). However, weather conditions and environmental factors may cause dramatic changes in agricultural surface water quality that may increase the risk of produce contamination.

Computer-based tools have been recently used to analyze the microbiological quality of agricultural water sources with various algorithms (Abimbola et al. 2020; Weller et al. 2020; Buyrukoğlu 2021; Buyrukoğlu et al. 2021). Artificial neural networks (ANN), K-Nearest neighbor algorithm (kNN), support vector machine (SVM), decision tree, random forest and AdaBoost can be listed as the most preferred algorithms to predict the presence of *Salmonella* based on measured environmental factors, the population of microbiological indicators, and the physicochemical attributes of agricultural waters (Polat et al. 2020; Weller et al. 2020; Buyrukoğlu 2021). In published studies, the performance of computer-based tools is mainly evaluated with the value of accuracy with or without feature selection.

Feature selection is considered a critical step towards improving the prediction success of machine learning tools by eliminating inappropriate, irrelevant, or unnecessary features (Agrawal et al. 2021). Meta-heuristic methods provide effective and acceptable solution methods for future selection-based optimization. Solutions are candidate values that can be a set of desired outputs for each method to get closer to better results depending on the structure of the algorithms. Meta-heuristic algorithms consist of two main components: intensification and diversification (Blum & Roli 2003). Intensification focuses on producing a solution in a local area with the best available solution. Diversification means creating a variety of solutions to explore the search space on a global scale. The combined selection of the best solutions ensures that the solutions converge towards the optimum (Yang 2011). Diversification also prevents solutions from being localized and increases the diversity of solutions to avoid stagnation in local optima or flat areas. Each algorithm uses different methods to achieve a balance between concentration and diversification.

The presence and concentration of pathogens in agricultural water have been predicted with artificial intelligence and machine learning tools with various classification techniques. In general, the success of classification techniques is evaluated with or without feature selection based on a researcher's preferences, experiences, data availability, and algorithm popularity. Feature selection can be performed with statistical and computer-based tools. In a recent survey and review, grey wolf optimization (GWO), Harris hawks optimization (HHO), differential evolution optimization (DEO), and particle swarm optimization (PSO) have been listed as the most studied conventional metaheuristic algorithms used on data sets produced in various fields (Akinola et al. 2022; Dokeroglu et al. 2022). In this study, the effectiveness of above-mentioned meta-heuristic optimization algorithms was evaluated for feature selection to improve the *Salmonella* occurrence prediction performance of commonly used algorithms in agricultural waters.

2. Material and Methods

2.1. Data set

A previously acquired data set for six agricultural ponds from Central Florida was obtained by Topalcengiz et al. (2017). The data set included the population of indicator microorganisms (total coliform, generic *Escherichia coli*, and enterococci), physicochemical attributes of water samples (air and water temperature, pH, oxidative reduction potential, conductivity, and turbidity), and weather station measurements as rain and solar radiation for 24 h before sampling, average solar radiation, 60 cm air temperature, relative humidity, ten-meter wind speed, wind direction, and 60 cm soil temperature in total of 540 samples (90 from each pond) for two growing seasons. In addition, the presence of *Salmonella* in water samples was confirmed through PCR after enrichment. In this study, adjustments were made on the data set at hand. In this context, a data set of 540 values * 17 features was obtained by combining all data from the six ponds. The class label for this dataset was determined as 1 for the presence of the *Salmonella* pathogen and 0 for its absence. Input and output values were normalized in the range of 0-1. Equation 1 was used for normalization.

$$y = (x_i - x_{min}) / (x_{max} - x_{min}) \quad (1)$$

Where; y is the normalized value of x_i . The x_{max} and the x_{min} are the maximum and minimum value of x_i , respectively.

2.2. Methods

Two process steps were applied. First, the feature selection was staged. After normalization, the data set was subjected to feature selection through four different meta-heuristic optimization algorithms. Metaheuristic algorithms including differential evolution optimization (DEO), grey wolf optimization (GWO), Harris hawks optimization (HHO) and particle swarm optimization (PSO) were assessed based on the nearest neighborhood algorithm (kNN) with 5 neighborhoods as a fitness function. The rate of error obtained from the kNN was checked each time after each run. When the error rate was lower than the previous value, the features providing this value were taken as the best values. The population size was standardized as 20 with 100 iterations for comparison of all tested meta-heuristic algorithms.

In the classification phase, the dataset was first segmented by using cross validation with k value of 5. One of these parts was used as test data for the part classification algorithm. The cross-validation method was used to confirm the reliability and accuracy of the results in the studies. The data sets obtained with k-fold are classified by support vector machines (SVM), kNN and decision tree algorithms based on successful classification as described in previous studies conducted on the same data set, respectively (Polat et al. 2020; Buyrukoğlu 2021; Buyrukoğlu et al. 2021). During the application, fitcsvm, fitcknn, fitctree functions in the Matlab program were used for classification. Default values were used for fitcsvm. NumNeighbors:5, Distance:minkowski parameters were used for fitcknn. Finally, MaxNumSplits: 7 value was applied for fitctree.

2.3. Feature selection

The multidimensionality of the data is considered as a challenge for classification techniques as well as for all data mining the methods. A reduction in the number of classified dimensions reduces computational demands and data collection requests with

increase in reliability of baseline results and data quality. In this study, binary versions of DEO, GWO, HHO, and PSO meta-heuristic methods were selected for feature selection to increase the accuracy success of classifiers. These meta-heuristic methods were determined based on previous successful applications by the authors (Canayaz 2021) and frequent use in the literature (Akinola et al. 2022; Dokeroglu et al. 2022). In this respect, it is also possible to evaluate our study as an ablation study.

2.3.1. Binary differential evolution optimization

The differential evolution (DEO) algorithm is a widely used as population-based stochastic direct search method for solving continuous-time optimization problems (Storn & Price 1997; Price et al. 2005; Das & Suganthan 2011). It uses real number coding and involves three basic operations: mutation, crossover, and selection. The initial population is randomly generated and covers the entire search space. While the traditional DEO algorithm is effective at solving continuous-time problems, it is unable to handle discrete problems and does not consider global or neighboring individual solution information. In contrast, the binary DEO incorporates information from neighboring solutions during the crossover phase to improve its performance on discrete problems (Liang et al. 2017). Binary DEO operates differently from the traditional DEO algorithm in the population initialization, mutation, and crossover phases.

Binary DEO creates the initial population with the formula in Equation 2 (Liang et al. 2017):

$$\begin{cases} 1, & \text{rand}_j(0,1) < 0.05 \\ 0, & \text{otherwise} \end{cases} \quad (2)$$

The mutation operator was performed with the formula in Equation 3:

$$V_{i,G}^j = \begin{cases} x_{p1,G}^j \oplus x_{p2,G}^j & x_{p1,G}^j = x_{p2,G}^j \\ x_{i,G}^j & \text{otherwise} \end{cases} \quad (3)$$

For the j th candidate node, if individuals $X_{p1,G}$, $X_{p2,G}$ have the same choice, the mutant individuals yields $x_{p1,G}^j$ or $x_{p2,G}^j$, otherwise it directly derives form $X_{i,G}$.

Crossover Operator was performed by the formula in Equation 4:

$$V_{i,G}^j = \begin{cases} v_{nbest,G}^j \text{ rand}_j[0,1] \leq CR \text{ or } j = \text{rand}(i) \\ v_{i,G}^j & \text{otherwise} \end{cases} \quad (4)$$

The crossover ratio CR was chosen by the designer in the range [0,1). Crossover ensures that $U_{i,G}$ has at least one value from the best neighbour. Neighborhood radius r depends on population size and complexity of the problem.

2.3.2. Binary grey wolf optimization

The binary version of grey wolf optimization (GWO) is an optimization algorithm inspired by the hunting and social behavior of grey wolves (Mirjalili et al. 2014). It involves a group of 5-12 wolves, divided into four categories: alpha, beta, delta, and omega. The alpha wolf is the leader and makes decisions concerning hunting, sleep times, and sleeping locations. The beta wolf assists the alpha wolf, while the delta wolf follows the alpha and beta wolves and only dominates the omega wolf, the lowest ranking member of the group. In this study, the binary version of GWO was used for feature selection, with the kNN error rate serving as the fitness function (Emary et al. 2016). The specific implementation of the algorithm is described by Too et al. (2018). The mathematical equations of the models developed for the hunting strategies of wolves are given in Equations 5 and 6:

$$X(t+1) = X_p(t) - A \cdot D \quad (5)$$

Where; X_p is the position of the prey, A is the coefficient vector, and D is defined as:

$$D = |C \cdot X_p(t) - X(t)| \quad (6)$$

Where; C is the coefficient vector, X is the position of the grey wolf.

The position updates of the grey wolves take place as in Equation 7:

$$X(t+1) = \frac{X_1 + X_2 + X_3}{3} \quad (7)$$

2.3.3. Binary harris hawks optimization

Harris hawks optimization (HHO) algorithm is a population-based algorithm. It is a new swarm intelligence optimization algorithm inspired by the behavior and hunting patterns of Harris hawks, referred to as “surprise attacks”. Harris hawks are one of the most intelligent hunting birds known. When a group of hawks get together and start the hunt, some of them make short tours one after the other and then descend into very high turnstiles. In this strategy, the hawks detect and attack their prey from different directions and approach simultaneously (Heidari 2019).

There are two different methods in the hunting process of HHO that decide which method will be used according to the randomly generated “q” value between [0-1]. In addition, a random number “r” is assigned between [0-1]. Different strategies are applied according to this “r” value and “E” escape energy. The “E” escape energy of the prey determines the attack on the prey. There are four different methods of producing solutions including soft besiege, hard besiege, developing attacks and soft besiege, and developing attacks and hard besiege (Çelik et al. 2019).

In Equation (8) and equation (10), the motion position equation and escape energy are defined for the new solution (Zhang et al. 2021):

$$x(t+1) = \begin{cases} x_r(t) - r_1 \cdot |x_r(t) - 2r_2x(t)|, & q \geq 0.5 \\ (x_{target}(t) - x_{average}(t)) - r_3 (r_4(UB - LB) + LB), & q < 0.5 \end{cases} \quad (8)$$

$X(t+1)$ and $X(t)$ are the position vectors of the search agents. q , r_1 , r_2 , r_3 , and r_4 are random values in each iteration and are randomly generated in the range 0-1. $X_r(t)$ represents the position vector of a random individual. $X_{target}(t)$ is the position vector of the prey. UB and LB show the lower and upper limits of the variables. $X_{average}(t)$ in Equation 3 is the average position vector of the available search agents, which can be calculated as (Zhang et al. 2021).

$$X_{average}(t) = \frac{1}{N} \sum_{i=1}^N X_i(t) \quad (9)$$

N is the population size of the hawks; $X_i(t)$ represents the position of an individual moving towards the prey (Zhang et al. 2021).

$$Escaping_energy = 2E_0(1 - \frac{t}{T}) \quad (10)$$

In Equation 10 escape energy is defined for the new solution where T is the maximum number of iterations, E_0 is the initial energy value (Zhang et al. 2021). kNN error rate was used as the fitness function of this algorithm.

2.3.4. Binary particle swarm optimization algorithm

Particle Swarm Optimization (PSO) is a meta-heuristic algorithm that was inspired by the movements of swarms of animals, such as birds and fish (Kennedy & Eberhart 1995). It uses two important parameters, known as $pbest$ and $gbest$, to update the velocity and position information of the candidate solutions in the swarm. The $pbest$ value represents the local best solution, while the $gbest$ value represents the global best solution.

The calculations of the algorithm are given in Equations 11-15 (Too et al. 2019):

$$v_i^d(t+1) = wv_i^d(t) + c_1r_1(pbest_i^d(t) - x_i^d(t)) + c_2r_2(gbest^d(t) - x_i^d(t)) \quad (11)$$

$$S(v_i^d(t+1)) = \frac{1}{1 + \exp(-v_i^d(t+1))} \quad (12)$$

$$x_i^d(t+1) = \begin{cases} 1, & \text{if } rand < S(v_i^d(t+1)) \\ 0, & \text{otherwise} \end{cases} \quad (13)$$

Where; $rand$ is a random number uniformly distributed between 0 and 1:

$$pbest_i^d(t+1) = \begin{cases} x_i(t+1), & \text{if } F(x_i(t+1)) < F(pbest_i(t)) \\ pbest_i(t), & \text{otherwise} \end{cases} \quad (14)$$

$$gbest(t+1) = \begin{cases} pbest_i(t+1), & \text{if } F(pbest_i(t+1)) < F(gbest(t)) \\ gbest(t), & \text{otherwise} \end{cases} \quad (15)$$

Where; x is the solution, $pbest$ is personal best and $gbest$ is global best solution. $F(.)$ is fitness function. t is number of iterations.

BPSO is the binary version of the PSO algorithm. In this study, the following parameter values were used: $c1=2$; $c2=2$; $V_{max}=6$; $W_{max}=0.9$; $W_{min}=0.4$.

2.4. Classification and evaluation of selected features

The classification process involves two phases: training (80% of the data) and testing (20% of the data). The dataset, consisting of features selected through the classification process, is divided into training and testing sets using cross-validation with a k value of 5. In the training phase, the parameters of the classification model are set and the resulting error is used to assess how well the model fits the training data. The testing phase demonstrates the model's ability to accurately predict labels for untested data. In this study, the kNN, SVM, and decision tree classification algorithms, which have previously been used to predict *Salmonella* in agricultural waters using the same dataset, were chosen to evaluate the performance of the meta-heuristic feature selection optimization (Polat et al. 2020; Buyrukoğlu 2021).

Figure 1 illustrates the four possible output states, representing the elements of a 2x2 confusion matrix or contingency table. The blue diagonal represents correct predictions, while the yellow diagonal indicates incorrect predictions. If a sample is positive and classified as positive, it is counted as a true positive (TP). If it is classified as negative, it is considered a false negative (FN). If a sample is negative and classified as negative, it is considered a true negative (TN). If it is classified as positive, it is considered a false positive (FP) (Tharwat 2018).

		True/Actual Class	
		Positive	Negative
Predicted Class	Positive	True Positive (TP)	False Positive (FP)
	Negative	False Negative (FN)	True Negative (TN)

Figure 1- An illustrative example of the 2X2 confusion matrix with two classes of Positive and Negative for classification. The output of the predicted class is defined as true or false

One of the most commonly used measures for evaluating classification performance is accuracy, which is calculated as the ratio of correctly classified samples to the total number of samples (Eq. 16). The precision, recall, and F-score metric values are given in Equations 17-19, respectively:

$$Accuracy = \frac{TP+TN}{TP+TN+FP+FN} \quad (16)$$

$$\text{Micro Average Precision} = \frac{\sum_{k=1}^K TP_k}{\sum_{k=1}^K FP_k} \quad (17)$$

$$\text{Micro Average Recall} = \frac{\sum_{k=1}^K TP_k}{\sum_{k=1}^K FN_k} \quad (18)$$

$$\text{Micro Average F - score} = \frac{\sum_{k=1}^K TN_k}{\sum_{k=1}^K FP_k} \quad (19)$$

The complement of the accuracy metric is the error rate or misclassification rate, which reflects the number of misclassified samples from both positive and negative classes (Bradley 1997). It is calculated as follows (Eq. 20):

$$Error = 1 - Accuracy = (FP + FN)/(TP + TN + FP + FN) \quad (20)$$

This metric can be expressed as a percentage by multiplying the result by 100.

The micro-average score was used when equal weighting was required for each sample or estimate. The micro-average sums the contributions of all classes to calculate the average metric. In general, 'micro' is preferred where greater emphasis is placed on accuracy. For this reason, the micro-average was preferred in this study.

2.4.1. *k*-Nearest-neighbours classification

The *k*-Nearest-Neighbors (*k*NN) classifier is a simple and effective non-parametric classification method (Hand et al. 2001). In the *k*NN algorithm, the first step is to determine the distance between the data points. Common methods for measuring distance include the Euclidean, Manhattan, and Minkowski methods.

The Euclidean distance method, most commonly used in practice, is defined between samples X_i and X_j as shown in Equation 21:

$$(X_i, X_j) = \sqrt{(X_{i1} - X_{j1})^2 + (X_{i2} - X_{j2})^2 + \dots + (X_{in} - X_{jn})^2} \quad (21)$$

Another important factor in the *k*NN algorithm is the *k* parameter, which determines the number of neighboring values to consider when classifying a point. Selecting an appropriate *k* value is crucial for the success of the classification (Guo et al. 2003). To determine the best *k* value, the algorithm is run with different values of *k* and the performance is evaluated. A small value of *k* may result in too many classes, while a large value may lead to fewer classes than necessary and higher error rates (Imandoust & Bolandraftar 2013). In this study, the *k* value was set to 5 for each variable (*k*=5). The *fitcknn* toolbox in Matlab uses the Euclidean distance as the default distance measure.

2.4.2. Support vector machine classification

Support Vector Machines (SVMs) are a type of algorithm used for pattern recognition and classification tasks (Cortes & Vapnik 1995). They are based on statistical learning theory and are known for their ability to achieve good generalization performance. SVMs are particularly useful for dealing with large data sets because they transform the classification problem into a squared optimization problem, which allows for faster solution times compared to other techniques (Osowski et al. 2004). Additionally, SVMs have been shown to have superior classification performance, computational complexity, and usability compared to other methods due to their optimization-based procedure (Nitze et al. 2012). The aim of SVMs is to find the optimal hyperplane that separates different classes by maximizing the distance between the support vectors of different classes (Ayhan & Erdoğmuş 2014).

In this study, the kernel, degree, and *C* parameters were used in the SVM algorithm. The kernel parameter determines the type of hyperplane used, with options including linear, rbf, sigmoid, and poly for nonlinear hyperplanes. The degree parameter controls the flexibility of the decision boundaries, with higher degrees allowing for more complex nonlinear relationships between the features.

Equations (22) and (23) represent formulas for a line or hyper plane, respectively. The SVM should find weights so that the data points are separated according to a decision rule.

$$wx+b=0 \quad (22)$$

$$y=mx+b \quad (23)$$

The *C* parameter controls the trade-off between minimizing misclassifications and maximizing the margin between the classes. Higher values of *C* result in a tighter margin and fewer misclassifications, while lower values allow for more overlap between the classes and prioritize maintaining a maximum margin. The Matlab *fitsvm* toolbox defaults to *C* values in the range of [0 1;1 0].

2.4.3. Decision tree classification

Decision trees are a type of machine learning algorithm used for building classifiers. They consist of decision nodes, which represent tests on a single attribute, and leaf nodes, which represent the resulting class. In binary decision trees, each decision node has two branches, one for each possible outcome of the attribute test. There are several decision tree algorithms, including ID3 (Iterative Dichotomiser 3), C4.5, CART (Classification and Regression Tree), CHAID (CHi-squared Automatic Interaction Detector), QUEST (Quick, Unbiased, Efficient, Statistical Tree), and MARS. In this study, the *fitctree* (binary decision trees) tool in Matlab was used.

The process of constructing a decision tree involves dividing the training data into smaller subsets and repeating this process until each subset belongs to a single class. The training data, represented by *T*, consists of *k* classes. If *T* consists of only one

class, it will be a leaf node. If T contains more than one class, it is divided into n subsets, where n is the number of outcomes for the attribute test a_i . This process is repeated iteratively on each subset T_j ($1 < j < n$) until each subset belongs to a single class (Buyrukoğlu et al. 2021). The default parameters of the Matlab fitctree toolbox used in this study were: MaxNumSplits = n-1, where n is the training sample size; MinLeafSize = 1; and MinParentSize = 10.

3. Results

3.1. Performance of meta-heuristic optimization algorithms for feature selection

Table 1 shows the feature distribution at each 100 steps for the binary version of DEO, GWO, HHO, and PSO optimization algorithms, respectively. The proposed feature selection approach was run 100 times for each meta-heuristic algorithm. The values in the Table 1 show how many times the relevant feature value is ranked among the first five features. However, when looking at the sum of some features, the total value appears below 100. This is because the algorithm discovers some parameters out of the first five features. Since there is an inherent randomness in heuristic algorithms, it is expected that such situations can occur.

All microbiological variables have been selected at least as the first, second, and third features. Total coliform was ranked as the first feature or non-feature among the selected first five features by all algorithms. HHO and PSO optimization chose total coliform 41 and 55 out of 100 times as the first feature for the prediction of *Salmonella* occurrences in agricultural water. Generic *E. coli* was selected as the first feature 81 and 91 times by GWO and DEO, respectively. However, HHO and PSO algorithms ranked generic *E. coli* 31 and 54 times as the first or second effective feature for prediction, respectively. *Enterococci* was chosen the highest 31 out of 100 times by all algorithms as the first or second feature. The GWO algorithm determined only microbiological indicators as the first feature followed by DEO (97 times), PSO (93 times), and HHO (69 times) for prediction of *Salmonella* in agricultural waters.

Air and water temperature were determined as the highest selected second and third features by all tested meta-heuristic algorithms with a selection range from 3 to 50 times. Conductivity, pH and oxidation-reduction potential of agricultural waters were ranked the highest as third, fourth and fifth features except for conductivity selected by the HHO algorithm. Turbidity and rain had the highest performance as fourth and fifth ranked features with the number of selections times below 19. The rest of the features were not consistently chosen as the successful feature for the prediction of *Salmonella* occurrence in agricultural waters. All meta-heuristic algorithms did not rank the rest of the features as the first or second feature, with the exception of 60 cm air temperature by the HHO algorithm.

Table 1- Numbers of selected first five features by tested meta-heuristic optimization algorithms for prediction of *Salmonella* occurrence in agricultural waters with classifiers

Feature	Meta-heuristic Optimization Algorithms																			
	Binary Differential Evolution Optimization					Binary Grey Wolf Optimization					Binary Harris Hawks Optimization					Binary Particle Swarm Optimization				
	1 st	2 nd	3 rd	4 th	5 th	1 st	2 nd	3 rd	4 th	5 th	1 st	2 nd	3 rd	4 th	5 th	1 st	2 nd	3 rd	4 th	5 th
Total Coliform	4	0	0	0	0	15	0	0	0	0	41	0	0	0	0	55	0	0	0	0
Generic <i>E. coli</i>	91	2	0	0	0	81	5	0	0	0	9	22	0	0	0	28	26	0	0	0
Enterococci	2	2	0	0	0	4	28	4	0	0	19	14	9	0	0	10	31	15	0	0
Air Temperature	0	50	3	0	0	0	42	21	3	0	14	19	10	6	0	3	19	19	5	0
Water Temperature	2	24	28	1	0	0	16	27	14	0	9	13	16	8	2	1	10	21	15	1
Conductivity	0	9	23	8	1	0	6	19	21	10	8	21	13	8	6	1	5	13	13	10
pH	1	8	15	30	3	0	1	18	19	13	0	2	15	15	5	1	2	12	20	15
Oxidation-Reduction Potential	0	3	11	17	24	0	2	2	22	24	0	1	11	11	11	1	2	8	14	17
Turbidity	0	2	8	15	19	0	0	8	9	18	0	2	2	9	8	0	4	2	9	11
Rain	0	0	4	10	11	0	0	1	5	15	0	0	2	3	12	0	1	5	9	10
Total Solar Radiation	0	0	7	9	21	0	0	0	7	9	0	0	1	3	6	0	0	0	4	7
Average Solar Radiation	0	0	0	3	8	0	0	0	0	6	0	0	14	9	4	0	0	1	4	9
60 cm Air Temperature	0	0	0	4	3	0	0	0	0	2	0	6	5	13	13	0	0	3	3	7
Relative humidity	0	0	1	1	2	0	0	0	0	0	0	0	1	5	9	0	0	1	2	5
Ten-meter Wind Direction	0	0	0	1	4	0	0	0	0	2	0	0	1	0	1	0	0	0	1	3
Ten-meter Wind Speed	0	0	0	1	2	0	0	0	0	1	0	0	0	6	7	0	0	0	1	3
60 cm Soil Temperature	0	0	0	0	1	0	0	0	0	0	0	0	0	3	3	0	0	0	0	0
Total Iteration	100	100	100	100	99	100	100	100	100	100	100	100	100	99	87	100	100	100	100	98

3.2. Frequency of meta-heuristic optimization algorithms for feature selection

Table 2 shows the feature selection frequency of meta-heuristic algorithms based on the first five ranked features. Generic *E. coli* was ranked as the most successful feature in the prediction of *Salmonella* presence in agricultural waters ranging from 31 to 93 times selected in the first five ranked features. Similar selection frequency was observed for total coliform and enterococci. DEO was the only algorithm to rank almost all physicochemical attributes and weather station measurement above microbiological indicators. Air and water temperature were ranked between 46 and 66 times in the first five features by all meta-heuristic algorithms. Similar to results for microbiological indicators, the distribution of feature selection was parallel between GWO and DEO and between PSO and HHO algorithms for air and water temperatures. 60 cm air temperature measurements from weather station was not selected as frequent feature as actual air and water temperatures measured in the field for prediction of *Salmonella* occurrence in agricultural waters. With the exception of HHO, conductivity, the pH and oxidation-reduction potential of agricultural were ranked from 41 to 57 times in the first five features based on all meta-heuristic algorithms. Turbidity was ranked in the first five features 21 to 44 times by all algorithms. The rest of the features including rain and solar radiation were ranked between none and 37 times in the first five algorithms. When the feature selections of all meta-heuristic algorithms were combined, generic *E. coli* (264 times) was selected almost twice as often as total coliform (115 times) and enterococci (138 times). The order of feature dominance was generic *E. coli* (264 times), air temperature (214 times), water temperatures (208 times), conductivity and pH (195 times).

Table 2- Total number of features selected as first and second feature by four tested meta-heuristic optimization algorithms for prediction of *Salmonella* occurrence in agricultural waters with classifiers

Feature	Frequency*				Total
	DEO	GWO	HHO	PSO	
Total Coliform	4	15	41	55	115
Generic <i>E. coli</i>	93	86	31	54	264
Enterococci	4	36	42	56	138
Air Temperature	53	66	49	46	214
Water Temperature	55	57	48	48	208
Conductivity	41	56	56	42	195
pH	57	51	37	50	195
Oxidation-Reduction Potential	55	50	34	42	181
Turbidity	44	35	21	26	126
Rain	25	21	17	25	88
Total Solar Radiation	37	16	10	11	74
Average Solar Radiation	11	6	27	14	58
60 cm Air Temperature	7	2	37	13	59
Relative humidity	4	0	15	8	27
Ten-meter Wind Direction	5	2	2	4	13
Ten-meter Wind Speed	3	1	13	4	21
60 cm Soil Temperature	1	0	6	0	7

*: Binary meta-heuristic optimization methods include differential evolution optimization (DEO), grey wolf optimization (GWO), Harris hawks optimization (HHO) and particle swarm optimization (PSO).

3.3. Performance of classifier based on selected meta-heuristic algorithm

Table 3 depicts the prediction accuracy results of kNN, SVM, and decision tree based on feature selection by tested meta-heuristic algorithms. Since each meta-heuristic method was run for 100 steps, the classification process was repeated each time to obtain the average and the highest prediction success as a percentage. All classification algorithms predicted the *Salmonella* occurrence based on selected features with accuracy values ranging from 93.70% to 95.18% on average. The highest accuracy rates based on feature selection by all meta-heuristic algorithms were 95.18% for kNN, 95.16% for SVM, and 95.55% for decision tree. The average accuracies predicted by SVM and KNN were 95.18% for all meta-heuristic algorithms. The average accuracy success rates of decision tree ranged from 93.70% to 95.55%.

Similar to accuracies, other evaluation parameters including precision, recall and f-score were calculated over 93.00% regardless of the feature selection and classification algorithm. The highest precision value was obtained from the kNN and SVM algorithms with 95.18%. The average precision value in the decision tree classification in all algorithms was lower than the other classifiers. The same results were observed in metrics such as recall, f-score that were between 93.57 and 95.18%. The kNN, SVM and DT accuracy results are shown in Figure 2 for each meta-heuristic algorithm (DEO, GWO, HHO and PSO).

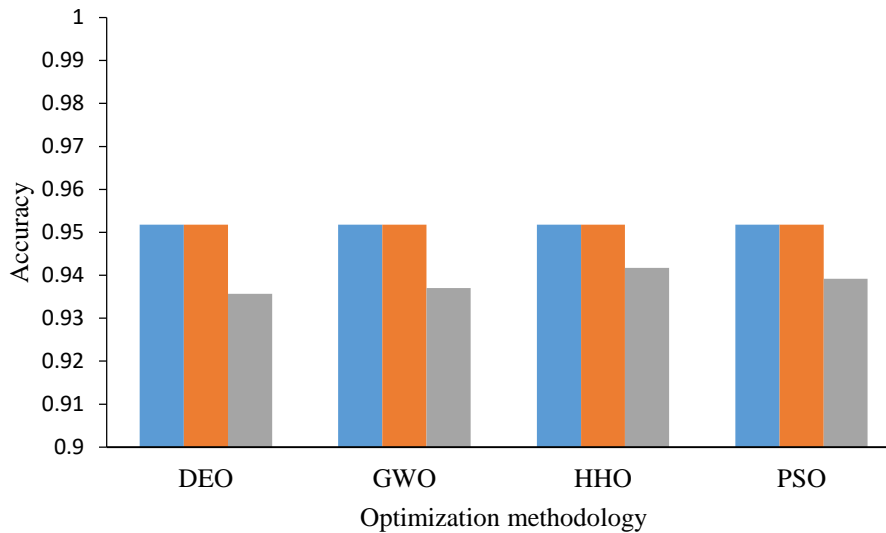


Figure 2- Accuracy results of kNN (■), SVM (■) and DT (■) classifiers after application of differential evolution optimization (DEO), grey wolf optimization (GWO), Harris hawks optimization (HHO) and particle swarm optimization (PSO) heuristics algorithms for feature selection

Table 3- Accuracy results of kNN, SVM, and decision tree (DT) classifications based on feature selection of meta-heuristic optimization algorithms

Algorithm	Classification	Accuracy (%)	Precision (%)	Recall (%)	F-Score (%)
DEO	kNN-Maximum	0.9518	0.9518	0.9518	0.9518
	kNN-Average	0.9518	0.9518	0.9518	0.9518
	SVM-Maximum	0.9518	0.9518	0.9518	0.9518
	SVM-Average	0.9518	0.9518	0.9518	0.9518
	DT-Maximum	0.9481	0.9481	0.9481	0.9481
	DT-Average	0.9357	0.9357	0.9357	0.9357
GWO	kNN-Maximum	0.9518	0.9518	0.9518	0.9518
	kNN-Average	0.9518	0.9518	0.9518	0.9518
	SVM-Maximum	0.9518	0.9518	0.9518	0.9518
	SVM-Average	0.9518	0.9518	0.9518	0.9518
	DT-Maximum	0.9555	0.9555	0.9555	0.9555
	DT-Average	0.9370	0.9370	0.9370	0.9370
HHO	kNN-Maximum	0.9518	0.9518	0.9518	0.9518
	kNN-Average	0.9518	0.9518	0.9518	0.9518
	SVM-Maximum	0.9518	0.9518	0.9518	0.9518
	SVM-Average	0.9518	0.9518	0.9518	0.9518
	DT-Maximum	0.9518	0.9518	0.9518	0.9518
	DT-Average	0.9417	0.9417	0.9417	0.9417
PSO	kNN-Maximum	0.9518	0.9518	0.9518	0.9518
	kNN-Average	0.9518	0.9518	0.9518	0.9518
	SVM-Maximum	0.9518	0.9518	0.9518	0.9518
	SVM-Average	0.9518	0.9518	0.9518	0.9518
	DT-Maximum	0.9499	0.9499	0.9499	0.9499
	DT-Average	0.9392	0.9392	0.9392	0.9392

*: Binary meta-heuristic optimization methods include differential evolution optimization (DEO), grey wolf optimization (GWO), Harris hawks optimization (HHO) and particle swarm optimization (PSO)

4. Discussion

The microbiological water quality via indicator microorganisms is monitored to reduce the pathogen contamination risk of produce. The detection of pathogens is also possible for agricultural water, but not preferred due to the high cost, length of time, advanced laboratory equipment and qualified personnel required to perform any analysis. To provide faster and easier risk assessment for growers, several statistical and computer-based approaches have been proposed for the prediction of pathogen occurrence in agricultural waters over the past (Benjamin et al. 2013; McEgan et al. 2013; Bradshaw et al. 2016; Havelaar et al. 2017; Truchado et al. 2018; Polat et al. 2020; Weller et al. 2020; Buyrukoğlu 2021;). The success of each model or algorithm varies depending on intrinsic and extrinsic parameters used for prediction. Several features including the population of microbiological indicators, physicochemical attributes, or environmental variables can be used for the prediction of a *Salmonella* population or occurrence in agricultural water sources (Buyrukoğlu 2021). However, unstable environmental conditions may dramatically affect variable changes used as features and, relatively, the performance of prediction tools. Preprocessing of parameter values can be a requirement for the success of prediction. In this study, since the intervals of the values in the data set contained various ranges and units, feature values were subjected to the normalization process before optimization.

The dataset used for the prediction of *Salmonella* presence in agricultural waters included 17 possible features with various ranges and units in this study. The order of feature dominance was generic *E. coli*, air temperature, water temperatures, conductivity and pH by tested meta-heuristic algorithms; however, 60 cm air temperature was determined as a weak predictor. This is because air and water temperatures were measured on-site while the 60 cm air temperature data was taken from the weather station (Topalcengiz et al. 2017). The meta-heuristic algorithms used for optimization ranked indicator microorganisms in the first and second place of the most selected features among the first five features. Particularly, the generic *E. coli* population was chosen as the first feature except for the HHO algorithm. Previously, the same dataset was evaluated for the best *Salmonella* prediction in agricultural waters with statistical and computer-based tools. Havelaar et al. (2017) developed a prediction model for the probability of the presence of *Salmonella* by using the *E. coli* population and turbidity based on the results of logistic regression analysis for feature selection. In another study with the same dataset, heterogeneous ensemble feature selection including information gain, ReliefF, analysis of variance, and Chi-square yielded the most successful *Salmonella* prediction with features including UV, turbidity, and the population of coliform and generic *E. coli* (Buyrukoğlu 2021). In the same study, microbiological indicators are noted as more effective features than physicochemical attributes and weather station measurements as meta-heuristic algorithms used in here.

Feature selection aims to find a subset of features for a learning operation that can describe data as well or better than the original dataset (Phyu & Oo 2016). In feature selection, there are three groups: filtering methods based on statistical information, spiral search methods, and embedded methods using the best divisor criterion. In filtering methods, feature selection is made before the selection algorithm works, while in spiral methods, the algorithm is used for the selection of the best features. In embedded methods, the data mining algorithm and feature selection algorithm work simultaneously (Budak 2018). In this study, four meta-heuristic methods were used for filtering before classification with kNN, SVM, and decision tree algorithms for the prediction of *Salmonella* occurrence in light of previous studies analyzing the same data set (Buyrukoğlu 2021; Buyrukoğlu et al. 2021; Polat et al. 2020). This study can be considered as the performance of an ablation study in the analysis of agricultural water quality.

Generic *E. coli* was ranked as the first feature (and dominant feature in total) over 80 out of 100 times by GWO and DEO for the prediction of *Salmonella* presence or absence in agricultural waters as previous studies conducted with the same data set (Buyrukoğlu 2021; Polat et al. 2020). However, HHO and PSO algorithms listed *E. coli* the highest 28 times as the first or second among the first five features. These differences show that swarm or population size-based optimization algorithms are not as successful as continuous optimization algorithms as GWO and DEO.

Previously, Polat et al. (2020) reported the highest accuracy around 76% with ANN, kNN and SVM classifiers by using the same dataset as individual or combined features. In their study, no feature selection was performed among microbiological indicators or physicochemical water attributes. In another study with the same dataset, Buyrukoğlu (2021) proposed a new hybrid data mining model for prediction of *Salmonella* occurrence. Ensemble models of ANN, SVM, random forest and Naïve Bayes using a heterogeneous feature selection approach (information gain, ReliefF, analysis of variance, and Chi-square) had a prediction accuracy ranging from 82.8 to 94.9% (Buyrukoğlu 2021). In this study, the accuracy success of kNN, SVM, and decision tree algorithms was determined between 93.70 and 95.55% on average after 100 iterations based on tested metaheuristic optimization algorithms. High accuracy calculations show that the feature selection obtained through the use of heuristic methods yields more successful results.

The method proposed in this study gave higher prediction accuracy results than previous studies using the same data set. Recently, Buyrukoğlu et al. (2022) managed to increase the prediction success of the deep feed-forward neural network (DFNN) for *Salmonella* occurrence up to an accuracy of 98.41% with determined correlation value based on the selected features in another study with the same dataset. In Buyrukoğlu's (2022) study, feature selection determined by gain ratio yielded the highest relationships between generic *E. coli* and rain, solar radiation, and turbidity. Then, predicted generic *E. coli* population by decision tree, SVM, and RF were combined with selected environmental and physicochemical features with and without

correlation value for the DFNN analysis (Buyrukoğlu et al. 2022). The generic *E. coli*, air temperature, water temperature, conductivity and pH selected by meta-heuristic methods appear to be more dominant in the prediction of *Salmonella* presence in agricultural waters. In addition, as a result of feature selection made with heuristic methods in here unlike previous studies using the same data set (Polat et al. 2020; Buyrukoğlu 2021; Buyrukoğlu et al. 2021; Buyrukoğlu et al. 2022), conductivity and pH stand out as advantageous and distinguishing features that can be measured with portable equipment in the field. The measured conductivity and pH values can be used with a computer-based tool or developed application to obtain immediate results.

A small number of positive *Salmonella* samples in our dataset can be considered as a limitation of this study due to imbalanced classifications. To overcome this limitation, the micro-average method (Grandini et al. 2020) was used to calculate the metrics in the classification process. The unique aspect of our study is that it is the first study in which feature selection was made using meta-heuristic algorithms on a dataset for the prediction of *Salmonella* in agricultural waters. At all combinations of feature selection and classification, prediction success was calculated higher than accuracies calculated with the same or similar datasets.

5. Conclusions

In this study, the data collected from six different agricultural ponds were analyzed. A classification study was conducted to predict the presence/absence of the *Salmonella* pathogen. In the first part of the proposed method, a feature selection was performed with four different meta-heuristic algorithms. Following this, a classification was made using the kNN, SVM and decision tree classification methods. Similar to previous studies using the same or similar data sets, generic *E. coli* was selected as the most prominent feature for the prediction of *Salmonella* occurrence in agricultural waters. This confirms the validity of the recommended microbiological indicator compared to water attributes and weather station measurements. The accuracy success of the classifiers was improved up to 95% after feature selection using the metaheuristic optimization algorithms. There has yet to be a study using heuristic optimization methods for feature selection on the same data set and performed classification with these features. In this respect, this study shows that the use of heuristic methods may improve results in future studies in this area, especially in cases where the data size and the number of parameters is high. In this study the main strength of the proposed model is the use of a hybrid approach that combines feature selection and machine learning.

Acknowledgements

The authors also thank Selim Buyrukoğlu for his support and advice.

Conflict of interest

The authors declare no conflict of interest.

Funding

This research was supported by Mus Alparslan University.

Author contributions

Data curation was obtained by Zeynal Topalcengiz. Conceptualization, formal analysis, and methodology were performed by Murat Demir and Murat Canayaz. Resources, software, supervision, writing – review & editing were organized by Zeynal Topalcengiz, Murat Demir and Murat Canayaz.

References

- Abimbola O P, Mittelstet A R, Messer T L, Berry E D, Bartelt-Hunt S L & Hansen S P (2020). Predicting Escherichia coli loads in cascading dams with machine learning: An integration of hydrometeorology, animal density and grazing pattern. *The Science of the Total Environment* 722: 137894. <https://doi.org/10.1016/j.scitotenv.2020.137894>
- Akinola O O, Ezugwu A E, Agushaka J O, Zitar R A & Abualigah L (2022). Multiclass feature selection with metaheuristic optimization algorithms: a review. *Neural Computing and Applications* 34: 19751-19790. <https://doi.org/10.1007/s00521-022-07705-4>
- Agrawal P, Abutarboush H F, Ganesh T & Mohamed A W (2021). Metaheuristic algorithms on feature selection: A survey of one decade of research (2009-2019). *IEEE Access* 9: 26766-26791. <https://doi.org/10.1109/ACCESS.2021.3056407>
- Ashbolt N, Grabow W O K & Snozzi M (2001). Indicators of microbial water quality. In: L Fewtrell & J Bartram (Eds.), *Water Quality: Guidelines, Standards and Health*, World Health Organization (WHO) IWA Publishing pp. 289-316
- Ayhan S & Erdoğan Ş (2014). Kernel function selection for the solution of classification problems via support vector machines. Destek vektör makineleriyle sınıflandırma problemlerinin çözümü için çekirdek fonksiyonu seçimi (In Turkish). *Eskişehir Osmangazi University Journal of Economics and Administrative Sciences* 9:175-201
- Benjamin L, Atwill E R, Jay-Russell M, Cooley M, Carychao D, Gorski L & Mandrell R E (2013). Occurrence of generic Escherichia coli, E. coli O157 and Salmonella spp. in water and sediment from leafy green produce farms and streams on the Central California coast. *International Journal of Food Microbiology* 165(1): 65-76. <https://doi.org/10.1016/j.ijfoodmicro.2013.04.003>
- Blum C & Roli A (2003). Metaheuristics in combinatorial optimization: Overview and conceptual comparison. *ACM Computing Surveys* 35: 268-308. <https://doi.org/10.1145/937503.937505>

- Bradley A P (1997). The use of the area under the roc curve in the evaluation of machine learning algorithms. *Pattern Recognition* 30: 1145-1159. [https://doi.org/10.1016/S0031-3203\(96\)00142-2](https://doi.org/10.1016/S0031-3203(96)00142-2)
- Bradshaw J K, Snyder B J, Oladeinde A, Spidle D, Berrang M E, Meinersmann R J, Oakley B, Sidle R C, Sullivan K & Molina M (2016). Characterizing relationships among fecal indicator bacteria, microbial source tracking markers, and associated waterborne pathogen occurrence in stream water and sediments in a mixed land use watershed. *Water Research* 101: 498-509. <https://doi.org/10.1016/j.watres.2016.05.014>
- Budak H (2018). Feature selection methods and a new approach. *Özellik seçim yöntemleri ve yeni bir yaklaşım* (In Turkish). Süleyman Demirel University Journal of Natural and Applied Sciences 22: 21-31. <https://doi.org/10.19113/sdufbed.01653>
- Buyrukoğlu S (2021). New hybrid data mining model for prediction of Salmonella presence in agricultural waters based on ensemble feature selection and machine learning algorithms. *Journal of Food Safety* 41: 12903. <https://doi.org/10.1111/jfs.12903>
- Buyrukoğlu G, Buyrukoğlu S & Topalcengiz Z (2021). Comparing regression models with count data to artificial neural network and ensemble models for prediction of generic Escherichia coli population in agricultural ponds based on weather station measurements. *Microbial Risk Analysis* 19: 100171. <https://doi.org/10.1016/j.mran.2021.100171>
- Buyrukoğlu S, Yılmaz Y & Topalcengiz Z (2022). Correlation value determined to increase Salmonella prediction success of deep neural network for agricultural waters. *Environmental Monitoring and Assessment* 194: 373. <https://doi.org/10.1007/s10661-022-10050-7>
- Canayaz M (2021). MH-COVIDNet: Diagnosis of COVID-19 using deep neural networks and meta-heuristic-based feature selection on X-ray images. *Biomedical Signal Processing and Control* 64: 102257. <https://doi.org/10.1016/j.bspc.2020.102257>
- Centers for Disease Control and Prevention (CDC) (2007). Multistate outbreaks of Salmonella infections associated with raw tomatoes eaten in restaurants--United States, 2005-2006. *MMWR. Morbidity and Mortality Weekly Report* 56(35): 909-911.
- Cortes C & Vapnik V (1995). Support-vector networks. *Machine Learning* 20: 273-297. <https://doi.org/10.1007/BF00994018>
- Çelik Y, Yıldız İ & Karadeniz A T (2019). A brief review of metaheuristic algorithms improved in the last three years. *European Journal of Science and Technology* pp. 463-477. <https://doi.org/10.31590/ejosat.638431>
- Das S & Suganthan P N (2011). Differential Evolution: A Survey of the State-of-the-Art. *IEEE Transactions on Evolutionary Computation* 15: 4-31. <https://doi.org/10.1109/TEVC.2010.2059031>
- Dokeroglu T, Deniz A & Kiziloz H E (2022). A comprehensive survey on recent metaheuristics for feature selection. *Neurocomputing* 494: 269-296. <https://doi.org/10.1016/j.neucom.2022.04.083>
- Emary E, Zawbaa H M & Hassanien A E (2016). Binary grey wolf optimization approaches for feature selection. *Neurocomputing* 172: 371-381. <https://doi.org/10.1016/j.neucom.2015.06.083>
- Food and Drug Administration (FDA) (2015). Federal Register Notice: Standards for the Growing, Harvesting, Packing, and Holding of Produce for Human Consumption; Final Rule. Available at: <https://www.gpo.gov/fdsys/pkg/FR-2015-11-27/pdf/2015-28159.pdf>. Accessed 12 July 2022
- Grandini M, Bagli E & Visani G (2020). Metrics for Multi-Class Classification: An Overview. *ArXiv*, <https://doi.org/10.48550/arXiv.2008.05756>
- Greene S K, Daly E R, Talbot E A, Demma L J, Holzbauer S, Patel N J, Hill T A, Walderhaug M O, Hoekstra R M, Lynch M F & Painter J A (2008). Recurrent multistate outbreak of Salmonella Newport associated with tomatoes from contaminated fields, 2005. *Epidemiology and Infection* 136(2): 157-165. <https://doi.org/10.1017/S095026880700859X>
- Guo G, Wang H, Bell D, Bi Y & Greer K (2003). KNN model-based approach in classification. In: R Meersman et al (Eds.), *On the move to meaningful internet systems 2003: CoopIS, DOA, and ODBASE. OTM 2003. Lecture Notes in Computer Science*, Springer, pp. 986-996. https://doi.org/10.1007/978-3-540-39964-3_62
- Hand D, Mannila H & Smyth P (2001). *Principles of data mining*. A Bradford Book the MIT Press.
- Havelaar A H, Vazquez K M, Topalcengiz Z, Muñoz-Carpena R & Danyluk M D (2017). Evaluating the U.S. Food Safety Modernization Act Produce Safety Rule standard for microbial quality of agricultural water for growing produce. *Journal of Food Protection* 80: 1832-1841. <https://doi.org/10.4315/0362-028X.JFP-17-122>
- Heidari A A, Mirjalili S, Faris H, Aljarah I, Mafarja M & Chen H (2019). Harris hawks optimization: Algorithm and applications. *Future Generation Computer Systems* 97: 849-872. <https://doi.org/10.1016/j.future.2019.02.028>
- Imandoust S B & Bolandraftar M (2013). Application of K-nearest neighbor (KNN) approach for predicting economic events: Theoretical background. *International Journal of Engineering Research and Applications* 3: 605-610.
- Kennedy J & Eberhart R (1995). Particle swarm optimization. *Proceedings of ICNN'95 - International Conference on Neural Networks*, 4: 1942-1948. <https://doi.org/10.1109/ICNN.1995.488968>
- Liang Y, Liao B & Zhu W. (2017). An improved binary differential evolution algorithm to infer tumor phylogenetic trees. *BioMed Research International* 2017: 5482750. <https://doi.org/10.1155/2017/5482750>
- McEgan R, Mootian G, Goodridge L D, Schaffner D W & Danyluk M D (2013). Predicting Salmonella populations from biological, chemical, and physical indicators in Florida surface waters. *Applied and Environmental Microbiology* 79(13): 4094-4105. <https://doi.org/10.1128/AEM.00777-13>
- Mirjalili S, Mirjalili S M & Lewis A. (2014). Grey wolf optimizer. *Advances in Engineering Software* 69: 46-61. <https://doi.org/10.1016/j.advengsoft.2013.12.007>
- Nitze I, Schulthess U & Asche H (2012). Comparison of machine learning algorithms random forest, artificial neural network and support vector machine to maximum likelihood for supervised crop type classification. *Proceedings of the 4th GEOBIA* 35-40.
- Osowski S, Siwek K & Markiewicz T (2004). MLP and SVM networks - a comparative study. *Proceedings of the 6th Nordic Signal Processing Symposium* pp. 37-40
- Phyu T Z & Oo N N (2016). Performance comparison of feature selection methods. *MATEC Web of Conferences* 42: 06002. <https://doi.org/10.1051/mateconf/20164206002>
- Polat H, Topalcengiz Z & Danyluk M D (2020). Prediction of Salmonella presence and absence in agricultural surface waters by artificial intelligence approaches. *Journal of Food Safety* 40: e12733. <https://doi.org/10.1111/jfs.12733>
- Price K V, Storn R M & Lampinen J A (2005). *Differential evolution: A practical approach to global optimization*, Springer <https://doi.org/10.1007/3-540->
- Steele M, Mahdi A & Odumeru J (2005). Microbial assessment of irrigation water used for production of fruit and vegetables in Ontario, Canada. *Journal of Food Protection* 68(7): 1388-1392. <https://doi.org/10.4315/0362-028X-68.7.1388>

- Storn R & Price K (1997). Differential evolution - A simple and efficient adaptive scheme for global optimization over continuous spaces. *Journal of Global Optimization* 11: 341-359. <https://doi.org/10.1023/A:1008202821328>
- Tharwat A (2018). Classification assessment methods. *Applied Computing and Informatics* 17: 168-192. <https://doi.org/10.1016/j.aci.2018.08.003>
- Too J, Abdullah A R, Mohd Saad N M, Ali N M & Tee W (2018). A new competitive binary grey wolf optimizer to solve the feature selection problem in EMG signals classification. *Computers* 7: 58. <https://doi.org/10.3390/computers7040058>
- Too J, Abdullah A R, Mohd Saad N M & Tee W (2019). EMG feature selection and classification using a Pbest-guide binary particle swarm optimization. *Computation* 7(1): 12. <https://doi.org/10.3390/computation7010012>
- Topalcengiz Z & Danyluk M D (2019). Fate of generic and Shiga toxin-producing *Escherichia coli* (STEC) in Central Florida surface waters and evaluation of EPA Worst Case water as standard medium. *Food Research International* 120: 322-329. <https://doi.org/10.1016/j.foodres.2019.02.045>
- Topalcengiz Z, McEgan R & Danyluk M D (2019). Fate of *Salmonella* in Central Florida surface waters and evaluation of EPA Worst Case Water as a standard medium. *Journal of Food Protection* 82(6): 916-925. <https://doi.org/10.4315/0362-028X.JFP-18-331>
- Topalcengiz Z, Strawn L K & Danyluk M D (2017). Microbial quality of agricultural water in Central Florida. *PLoS ONE* 12(4): e0174889. <https://doi.org/10.1371/journal.pone.0174889>.
- Truchado P, Hernandez N, Gil M I, Ivanek R & Allende A (2018). Correlation between *E. coli* levels and the presence of foodborne pathogens in surface irrigation water: Establishment of a sampling program. *Water Research* 128: 226-233. <https://doi.org/10.1016/j.watres.2017.10.041>
- Weller D L, Love T, Belias A & Wiedmann M (2020). Predictive Models may complement or provide an alternative to existing strategies for assessing the enteric pathogen contamination status of northeastern streams used to provide water for produce production. *Frontiers in Sustainable Food Systems* 4: 561517. <https://doi.org/10.3389/fsufs.2020.561517>
- Yang X S (2011). Review of metaheuristics and generalized evolutionary walk algorithm. *International Journal of Bio-Inspired Computation* 3: 77-84. <https://doi.org/10.1504/IJBIC.2011.039907>
- Zhang Y, Liu R, Wang X, Chen H & Li C (2021). Boosted binary Harris hawks optimizer and feature selection. *Engineering with Computers* 37: 3741-3770. <https://doi.org/10.1007/s00366-020-01028-5>



Copyright © 2024 The Author(s). This is an open-access article published by Faculty of Agriculture, Ankara University under the terms of the [Creative Commons Attribution License](https://creativecommons.org/licenses/by/4.0/) which permits unrestricted use, distribution, and reproduction in any medium or format, provided the original work is properly cited.



The Public Sector's Role Towards Sustainable Agricultural Economy and Rural Development: Techno-economic Feasibility Analysis of Hybrid Paddy Production

Sheer ABBAS^{a*} , Waqar AHMED^b , Rana Shahzad NOOR^{c,f*} , Sidra FATİMA^d , Muhammad Aali MİSAAL^e 

^aCollege of Law, University of Sharjah, UNITED ARAB EMIRATES

^bCollege of Agriculture, Northeast Agricultural University, Harbin 150030, CHINA

^cFaculty of Agricultural Engineering and Technology, PMAS-Arid Agriculture University, Rawalpindi 46000, PAKISTAN

^dCollege of Forestry Economic and Management, Beijing Forestry University BFU, Beijing, CHINA

^eFaculty of Agricultural Engineering and Technology, University of Agriculture, Faisalabad, PAKISTAN

^fDepartment of Agricultural, Biological, Environment and Energy Engineering, College of Engineering, Northeast Agricultural University, Harbin, 150030, CHINA

ARTICLE INFO

Research Article

Corresponding Author: Sheer ABBAS, Rana Shahzad NOOR, E-mail: sheer.abbas@sharjah.ac.ae, engr.rsnoor@uaar.edu.pk

Received: 17 May 2023 / Revised: 18 September 2023 / Accepted: 21 September 2023 / Online: 09 January 2024

Cite this article

Abbas S, Ahmed W, Noor R S, Fatima S, Misaal M A (2024). The Public Sector's Role Towards Sustainable Agricultural Economy and Rural Development: Techno-economic Feasibility Analysis of Hybrid Paddy Production. *Journal of Agricultural Sciences (Tarim Bilimleri Dergisi)*, 30(1):131-144. DOI: 10.15832/ankutbd.1298140

ABSTRACT

Rice is the major food crop and a significant source of foreign exchange of Pakistan. In order to meet food demands, high quality varieties of rice, including early and late maturing varieties, as well as hybrid and conventional rice varieties must be developed with the adoptability and suitability of different hybrid rice varieties in local soil. The hybrid varieties revealed supremacy regarding the growth characters over the inbred rice. The study results pretended that the highest plant height was recorded in hybrid variety ennpova-55 (106.5 cm) while inbred IRRI-9 produced the shortest height (65.5 cm) at reproduction stage. Whereas highest number of tillers was observed in Winner-55, Tahafuz-121, and Ashoka (24 m²) and have highest seedling number and lowest number of tillers were recorded in Komal 21 m². Highest plant dry matter per hill was found in Ennova-55 (95.9/cm and lowest observed in IRRI-9 (69.8

cm) as compared to all other rice varieties studied in this study. In chlorophyll studies, highest chlorophyll parameter was observed in Ennova-08 and Pukhraj and lowest was observed only in inbred varieties. Shoot and root length showed significant variation among the different rice varieties. The tallest shoot was found in Ennova-55 (82.3 cm) which was statistically identical with Thafuz-121 (78.1 cm), while shortest was found in IRRI-9 (54.1 cm) at harvest. However, the maximum Leaf area index was recorded from Komal (4.50) at the heading stage followed by Ennova-55 (4.20), but significantly lower in Shakar (2.70). Compared with inbred, hybrid rice produced a higher yield with BCR of 12.03. However, further research studies are obligatory to perform for adoptability of hybrid rice locally for sustainable rice production.

Keywords: Hybrid paddy rice, Physiological characteristics, Grain, Biological yield, Economic analysis

1. Introduction

Agriculture is the primary driver for global sustainability and socioeconomic improvement (Aslam et al. 2020) which aim to guarantee food security and economic diversification; therefore, appropriate attention must be taken to ensure the use of optimal crop production technologies. In 2018, agriculture contributed to 24% of Pakistan's GDP, playing a significant role in the country's economy. It is recorded that more than 40% of Pakistan's total land area is under cultivation over the last sixty years of cultivation (FAO 2017).

The most significant cereal crop in the world is rice (*Oryza sativa L.*), which is the main source of nutrition for about half of the world's population, especially in Asia, where around 90% of the world's rice is grown and consumed (Noora et al. 2020). For 2.7 billion people, rice provides 50–60% of their daily caloric intake (Metwally et al. 2010; Chukwu et al. 2019). In terms of acreage cultivated, rice is the second-largest crop in the world, accounting for around 11% of all agricultural land (Amanullah 2016). It is the most significant grain crop in the world and an annual semi-aquatic plant. According to estimates, in order to feed the anticipated increase in global population, farmers must produce 60% (Fageria 2010) and 21% (Uzzaman et al. 2015) more rice than they do now. High-yielding types are being developed more frequently recently for uses other than human consumption, like rice flour and animal feed (Yoshinaga et al. 2018). Breeders' top priorities now include developing and implementing rice cultivars with increased grain zinc content and high production potential.

Within a population, variability refers to the differences in individual genotypes (and corresponding traits) as well as the speed at which a particular genotype might vary in response to environmental or genetic variables (Zhang et al. 2011). The requirement for increasing the number of micronutrients in rice grains is influenced by both their inherent genetic diversity and cultural traditions. Therefore, to achieve the objectives of creating high yielding rice varieties as well as better grain micronutrients, a breeding program's performance will depend on the genetic diversity of a crop (Swamy et al. 2016). China has a significant role in the production and consumption of rice, but would struggle to increase the land area already used for rice cultivation considering recent economic growth and urbanization, in part due to the lack of agricultural water (Cui et al. 2014).

In general, hybrids are more robust and bigger than the parent stock. Young seedlings develop long roots and large leaves that allow them to absorb more nutrients and therefore produce more grains. According to Bhuiyan et al. (2014) hybrid rice has a high tiller capacity. In the early and middle growth stages of vegetative growth, hybrid rice collects more dry matter, leading to more spikelet per panicle. They have panicles that are larger and more spikelet per panicle. These elements lead to better yields, typically 15% or more, than regular rice, commonly known as inbred rice (Chakrabarti et al. 2010; Bhuiyan et al. 2014). Pakistan produces 6.95 million tons of rice annually on an area of 2.96 million hectares: with an average yield of 2.35 t ha⁻¹. In order to produce hybrid rice, two different types of seeds must be planted and cultivated side by side. Pollination can be done both naturally and artificially. The average rice production in Pakistan has increased by more than 2% annually as a result of numerous research initiatives. Despite this, it is still a lot less than the leading nations for rice production (Amanullah 2016; Amanullah & Inamullah 2016). Low temperatures with late sowing impact seed germination, which delays tillering, leaving less time for plants to grow properly (Noor et al. 2019.)

In Pakistan, unbalanced nutrient application is one of the main causes of low paddy output (Amanullah 2016). Thus, various characteristics such as the quantity of tillers per plant, panicle size, panicle count, number of fertile grains per panicle, number of spikelet per panicle, grain weight per 1000 grains, plant height, etc. combine to produce the yield. The genes and QTLs that influence the traits that contribute to yield have been found. The qTSN4 shown to be rice QTL increases the total number of spikelet produced per panicle and the area of the flag leaf, but depending on the environment, it may also decrease the number of panicles (Adriani et al. 2016). The Gn1 gene similarly regulates plant height and the quantity of grains per panicle. For the quality of the rice population and grain yield, tillering is a crucial agronomic feature (Wang et al. 2017a). This is because insufficient tiller production leads to insufficient panicles, while excessive tiller production creates a dense canopy that creates a damp microenvironment that is favorable for diseases and pests (Noor et al. 2020b). Since nitrogen (N) fertilizer raises the cytokinin content in tiller nodes and further promotes the germination of the tiller primordium, it is the most popular and efficient strategy to expand the tiller population under field settings (Liu et al. 2014). Unlike the lateral branching of dicotyledonous plants, gramineous plants contain a specific kind of side shoot known as a tiller. The sprouting of new tillers from the main stem occurs continuously, and these produce their own roots to grow independently, ensuring the survival of plants in a variety of environments (Wang et al. 2017b). Additionally, it has been noted that the quantity of tillers is positively correlated with plant biomass and rice yields (Xing et al. 2017). The most crucial traits to consider while selecting for improved yield in rice segregating generations are the number of panicles per plant and the quantity of grains per panicle. At the genotypic level, grain number per plant displayed a positive correlation with fertility percentage but a negative correlation with grain length, grain L/B ratio, and 1000 grain weight (Senapati & Semenov 2020)

A well-known measure of plant growth is the leaf area index LAI was first described by Zhao et al. (2012) and is the ratio of leaf area to a specified unit of land area. Spectral reflectance and the ratio are functionally connected (Yang et al. 2009). Modelling canopy interception, ET, and net photosynthesis depend on LAI, a significant structural element of vegetation canopies. Most land surface models also use LAI as a crucial biophysical parameter to control how energy, carbon, and water fluxes are distributed between the soil and canopy components of the land surface system (Zhao et al. 2012). Indicators of crop development dynamics, such as LAI or the amount of leaf area per unit ground area), can be used to assess the condition of paddy rice during the growing season (Wang et al. 2017a).

Studies on rice grains have shown that the grain's morphological characteristics vary greatly depending on where it is grown (Soe et al. 2019). Different rice hybrids' yields and yield components were also assessed by Ashraf & Akram (2009). Few hybrids have greater grain quality compared to checks, which is one of the most significant characteristics of hybrids, thus there is a need to work to increase quality traits (Riaz et al. 2017). The primary goal of the breeding program to create new rice varieties is to increase rice grain production. A complicated trait with numerous genes under control and a strong environmental influence is grain yield. Moreover, additional characteristics including the type of plant, the length of the development cycle, and the components of the yield also influence grain production (Uzzaman et al. 2015). Most of them are resistant to pests, illnesses, and extreme climatic conditions, and many have therapeutic benefits in addition to having great nutritional value. As natural resources are depleted, genetic material preservation has become more significant (Ranawake et al. 2013).

The main objective of study was to evaluate the adoptability and suitability of different hybrid rice varieties and inbred rice in local growing conditions. This study was performed to investigate the agronomic traits and yield variation among

the afore mentioned hybrid and inbred paddy varieties, and to recognize the higher yield contributing characters for hybrid rice varieties compared with inbred rice varieties. The rice varieties have not always been higher in yields due to vigour as well as physiological characters and environmental conditions. For this reason, our study mainly focused on the agronomical perspective in the environmental condition of Larkana Sindh, so that these varieties must be used in further research studies and to provide a good knowledge for the adoptability of these hybrid paddy. Finally, the economic analysis was carried out to test the feasibility of hybrid rice adoptability in the domestic growing environment producing higher yield and better source of revenue for farmers.

2. Material and Methods

The field tests for rice production were carried out across two cropping seasons in 2020-21 at the experimental field on the Dokri. 27.565° N Latitude and 68.771° E Longitude are the site's coordinates. The experimental area is level and has a drainage and irrigation system that is readily available. Table 1 provides an overview of the topsoil characteristics (0-15 cm) of the experimental plot. Extremely hot summers and mild winters characterized the climate over the whole crop period.

The highest temperature of study site was recorded as 50-53 °C and the lowest recorded temperature was below 20 °C. The annual rainfall was also recorded as 109-127.4 mm, higher in the monsoon season (July) while 41 mm rainfall was recorded in the crop period. At a weather station near to the experimental location, the average temperature, precipitation, and sunlight hours throughout the rice growing seasons of 2020-21 were measured. At the middle and late stages of growth, 2020 had higher temperatures, more sunlight hours, and less precipitation than 2021. The objective of this study is to evaluate the adoptability and suitability of different hybrid rice varieties in local conditions. However, the performance of hybrid rice varieties was evaluated with crop vegetative growth, yield, and their yield characteristics (Noor et al. 2020a). Prior to the commencement of field trails, the soil characteristics recorded were presented in Table 1.

Table 1- Physical and chemical properties of the initial soil of the experimental plots

<i>Characteristics</i>	<i>Value</i>
Textural class (% sand, silt, clay)	Silty clay loam (15.5, 36.3, 42)
Ph	7.6-8.3
% OM (organic matter)	<0.86)
Total N%	0.07
P (µ g/g soil)	3.67
S (µ g/g soil)	5.89
B (µ g/g soil)	0.10
CU (µ g/g soil)	0.11
Fe (µ g/g soil)	2.4
Mn (µ g/g soil)	0.57
Zn (µ g/g soil)	0.40
Available K (meq/100g)	0.09
Ca (meq/100g)	1.10
Mg (meq/100g)	0.025

2.1. Plant materials

There were twenty (20) hybrid and four inbred rice varieties were selected for the experimental study. The experiment was conducted in a rice-wheat cropping zone by applying traditional field preparation conditions. The hybrid varieties were selected based on market demand. The hybrid rice seed was purchased from different companies like as Guard seed company, AG pharma, Kanzo seeds, Greenlet group, Suncrop group, Chodri khair din group, Tara group, Afroz crop science, Comega group, Rachnna group, Soni dharti and Tahfuz, Haji sons' group, Sayban group corporations, while Inbred (local rice) seed was collected from Abdul Sattar Sons, Larkana, Sindh. In this experiment, the hybrid rice varieties were given different codes for the better understanding i.e. V1 (Ennova 08), V2 (Komal), V3 (Guard 53), V4 (Winner 40), V5 (Ennova 55), V6 (Winner 05), V7 (winner 55), V8 (Bakhtwar 121), V9 (Bakhtawar 275), V10 (Dimond121), V11 (Tara 786), V12 (Thafuz 121), V13 (Red star), V14 (Comrage), V15 (Karshma), V16 (Ashoka), V17 (Shakar), V18 (Anmol), V19 (Royal), V20 (Pukhraj) and Inbred (local rice) variety was V21 (Shua92), V22 (Shandar), V23 (sharshar), and V24 (Irri-9).

2.2. Nursery preparation

The nursery was prepared using the wet bed technique. Under the irrigated method of rice growing, saturated nurseries were preferred. The soil was prepared using local ploughings (2-4 pass). The nursery area was divided into small plots of 30 sq. meters. This makes it easier to perform irrigation, weeding, chemical spraying, and planting tasks. The drainage ditches (30 cm) were built between the seed beds and provided 500g of single super phosphate, 500 g of ammonium sulphate, or 225 g of urea evenly over 10 square meters. Rice seeds were evenly dispersed throughout following manure application and

puddling. For the first five days, the sowing plots were kept completely submerged in water; as the seedlings grew, the water level was gradually raised to a height of five centimeters. During instances of heavy rain during the first week of sowing, excess water was drained out. The appropriate disease and pest management methods were employed. In the event of symptoms of nitrogen deficiency, a top-dressing application of 50 g of urea per square meter was made. Additionally, two applications of zinc sulphate (5 kg zinc sulphate + 2.5 kg calcium hydroxide mixed in 1000 liters of water for one hectare) were made on soils that were lacking in zinc.

2.3. Field experiment layout

Three replications of each variety were used in the complete randomized design (CRD) studies. The field experiments were conducted at or around the beginning of August. The experimental field's total area was 9 hectares (2.25 acres), which was divided into 24 sub-fields (27×150 feet) for treatments. Each sub-field was further divided into three replication plots (27×50 feet). The traditional method was used to prepare the experimental field area, and each subplot had a 500 m² (25 m×20 m) space.

2.4. Soil preparation for field experiments

After harvesting the wheat crop, the sufficiently dried soil was cultivated to aerate the soil, lessen weeds and other pests, and mix organic elements into the soil. A four-wheel tractor mounted with a rotary or multiple discs plow was used for soil cultivation. The field soil was irrigated and puddled until saturation to soften and to spill rice seeds to germinate. Puddling of soil involves churning of soil in rice fields while it's flooded with water. This practice converts the soil into a semi-liquid state, resulting in puddled soil. This technique is particularly essential for lowland rice cultivation, where fields are flooded to create a waterlogged environment. The seedling/nursery was transplanted in the main field after 25 days.

2.5. Fertigation

The soil was in the best physical condition for crop growth before the rice was planted, and the soil surface was level. The land was prepped for rice farming, and chemical fertilizers such as urea, tri-superphosphate, muriate of potash, gypsum, and zinc sulphate were applied at rates of 270, 130, 120, 70, and 10 kg ha⁻¹, respectively. Equal amounts of fertilizer were administered to each crop. At the middle and late stages of growth, the temperature was recorded higher, less precipitation, and more sunny hours. However, throughout the field trial, adequate weed and pest management techniques were also used to maintain the crop.

2.6. Nursery transplantation

The prepared nursery was transplantations manually into the rice field July 25th and July 5th in 2018 and 2019 cropping seasons, respectively. The approximate plant to plant distance was measured as 15×15 cm.

3. Studied Characters

3.1. Morphological growth

The data were collected on the following characters of the crops i.e. Plant height (cm) (PH), no of tillers, shoot and root length, LAI and Chlorophyll. From the first flowering day until the harvest the plant's height was measured. From the level of the ground surface to the top of the plant, the height was measured and then averaged. From the first flowering to the harvest, the number of tillers was counted and then averaged on a per-hill basis. The leaf area index of rice plant was determined at the days from flowering to harvesting stage. The data recorded were then computed by multiplying with a factor (0.75) as discussed by Mariana & Hamdani (2016). The chlorophyll content was measured using a chlorophyll meter (SPAD-502, Minolta Camera Co. Ltd, Osaka) (SPAD value). The mean of five readings per plant was recorded, and a fully grown leaf from the top of the plant was chosen for recording the SPAD values. For the measurement of SPAD value, five plants were chosen randomly from each plot. Additionally, Duncan's multiple range tests was used to determine for the analysis of recorded data of various study parameters (Duncan 1955).

3.2. Yield characteristics

The parameters, days to harvesting, number of panicles (Per plant and meter square), panicle length, number of filled and empty grains per panicle, grain length (mm), 1000 grain weight (g), number of panicles (t/ha), straw yield (t/ha), biological yield (t/ha), and harvest index are some of the different yield characteristics (%).

The number of days required to harvest each plot was computed to determine the days to harvesting. Every plot's number of panicles per plant, panicle length, and grain length were noted from the start of blooming until harvest (Noor et al. 2020c). Additionally, the average value was determined for each plant. From randomly selected plot plants, the total number of

filled and empty grains was counted according to the presence of grain in spikelet and the absence of grain in spikelet. The average number of filled and empty grains in each panicle was then determined. Each plot's 1000 grains from seed were counted and weighed using any digital balance. Weighing and complete sun drying were done on the grains from each plot. The dried weight of the grains was considered for the plot in order to calculate the total grain yield per plot, which was then converted into tons/hectare. Each plot's straw was weighed and carefully dried in the sun. The dried weight of the straw was considered while calculating the plot's final straw output before being converted to tons per hectare. Biological yield was defined as both grain yield and straw yield combined. The formula below was used to compute the biology. The biological yield of rice production is equal to the grain yield obtained plus straw collected from the rice field. It stands for the ratio of economic yield (grain yield) to biological yield. The rice crop's grain and straw yield was also used to generate the harvesting index, which was displayed as a percentage. The following formula was used to calculate it (Mariana & Hamdani 2016):

$$\text{Harvest Index (\%)} = \frac{\text{grain yield}}{\text{biological yield}} \times 100 \quad (1)$$

3.3. Statistical analysis

The data of all parameters were statistically analyzed using the analysis of variance (ANOVA) and the significance of means among the treatments were compared using LSD (least significant difference) test at probability < 0.05.

3.4. Economic analysis

The production of hybrid and inbred rice was examined economically. The costs of chemicals, fuel, labor, seeds, fertilizers, and irrigation were among the variable costs. The gross, absolute, and relative profit metrics were calculated using the following formulas. In the conducted research, economic calculations were made according to the equations given below (Semerci 2020, 2021).

$$\text{Straw Income (PKR ha}^{-1}\text{)} = \text{Straw Yield (kg ha}^{-1}\text{)} \times \text{Straw Sales Price (PKR kg}^{-1}\text{)}$$

$$\text{Product Revenue (PKR ha}^{-1}\text{)} = \text{Product Yield (kg ha}^{-1}\text{)} \times \text{Product Sales Price (PKR kg}^{-1}\text{)}$$

$$\text{Total Revenue (PKR ha}^{-1}\text{)} = \text{Product Revenue (PKR ha}^{-1}\text{)} - \text{Straw Income (PKR ha}^{-1}\text{)}$$

$$\text{Production Cost (PKR ha}^{-1}\text{)} = \text{Variable Costs (PKR ha}^{-1}\text{)} + \text{Fixed Costs (PKR ha}^{-1}\text{)}$$

$$\text{Gross Profit (PKR ha}^{-1}\text{)} = \text{Total Revenue (PKR ha}^{-1}\text{)} - \text{Variable Costs (PKR ha}^{-1}\text{)}$$

$$\text{Net Profit (PKR ha}^{-1}\text{)} = \text{Total Revenue (PKR ha}^{-1}\text{)} - [\text{Variable Costs (PKR ha}^{-1}\text{)} + \text{Fixed Costs (PKR ha}^{-1}\text{)}]$$

$$\text{Benefit / Cost Ratio} = \text{Total Revenue (PKR ha}^{-1}\text{)} / \text{Production Cost (PKR ha}^{-1}\text{)}$$

4. Results and Discussion

4.1. Crop growth and development characteristics

Table 1 contains data on growth characteristics. The parameters under consideration were significantly influenced by both the hybrid and conventional varieties.

4.2. Tillers

The effective tillers/hill produced by the V₅ and V₂₂ were both high (16.0, 14) and statistically comparable. V₂₀ showed little variation, whilst V₂₄ had the lowest number (Table 2). Regarding non-effective rice tillers, inbred rice demonstrated the lowest number per hill (2), while the value (4) was higher for the hybrid V₁. An essential element of rice productivity is productive tillers in the transplanted rice culture, the variety or hybrid with a low tillering capacity is not desired. According to the statistics on mean values for productive tillers/hills, all hybrids generated the same number of productive tillers/hills, with the exception of V₁₉; hybrid V₁₉ generated substantially more tillers per hill (16). These findings are confirmed by Uzzaman et al. (2015), who claim that hybrid rice has a high tillering capacity. Together with V₂₄, which is second in producing the least number of productive tillers, V₁₂ generated the least productive tillers (13). Due to their great tillering capacity, high yielding varieties (HYVs) may be to blame for the noticeable variances (Uphoff 2006).

Table 2- Crop growth and development characteristics

<i>Rice variety</i>	<i>Seedling transplanted (No.) m⁻²</i>	<i>Tillers mortality (No.) at 15-DAT</i>	<i>Tillers (No.)</i>		<i>Plant DM (g)</i>
			<i>effective</i>	<i>un-effective</i>	
Hybrid rice					
Ennova 08 (V1)	22	2	13	2	84.6
Komal (V2)	21	3	15	2	92.1
Guard 53 (V3)	23	2	13	3	84.6
Winner 40 (V4)	22	1	14	2	92.1
Ennova 55 (V5)	23	2	16	3	95.9
Winner 05 (V6)	22	3	14	4	80.6
winner 55 (V7)	24	2	13	2	95
Bakhtwar 121 (V8)	22	0	13	3	91.6
Bakhtwar 275 (V9)	23	1	14	3	79.3
Dimond121 (V10)	22	3	14	3	92.1
Tara 786 (V11)	22	4	15	2	79.3
Thafuz 121 (V12)	24	1	13	2	80.6
Red star (V13)	23	2	14	3	87.6
Comrage (V14)	23	2	13	3	89.4
Karshma (V15)	22	1	15	1	90.3
Ashoka (V16)	24	3	14	1	93.1
Shakar (V17)	22	3	15	2	90.8
Anmol (V18)	23	4	15	3	78.3
Royal (V19)	22	2	12	1	78
Pukhraj (V20)	22	2	13	4	90.5
Mean	22.55	2.15	13.9	2.45	87.29
Inbred rice					
Shua 92 (V21)	22	2	12	3	72.3
Shandar (V22)	23	1	14	2	70.4
sharshar (V23)	23	2	14	2	72.7
Irri-9 (V24)	22	3	12	4	69.8
Mean	22.5	2	13	2.75	71.3

DM: dry matter, DAT: days after transplanting.

In this investigation, the vegetative phase of rice production took far longer. The tested hybrid varieties accumulated noticeably more dry matter at heading than the inbred due to robust vegetative growth at the intermediate growth stage. At the grain filling stage, a large amount of dry matter accumulated and remobilization of seed was activated. In terms of assimilate remobilization from shoot reserve in early planting, both the hybrids V5 and V16 significantly outperformed the elite inbred V24 (Table 1). Several other studies have reported a similar outcome (Wang et al. 2008; Ranawake & Amarasinghe 2014). Due to the prolonged vegetative lifetime caused by low temperature and the efficient source activity, dry matter accumulation was more in V5 at early planting. This indicates that the examined hybrid rice dry matter accumulation before heading was particularly thermo-sensitive. According to our study results, hybrids produce greater yields than modern inbred due to the accumulation of more dry matter before heading and its higher translocation into the growing grain during the filling stage. This outcome was comparable to that of (Ranawake et al. 2013).

4.3. Plant height

In terms of plant height, the examined cultivars varied statistically from one another. The inbred variety V22 generated plants that were statistically taller (96.4 cm) than all other treatment produced plants. However, as shown in figure 2, the hybrid V5 had a noticeable height (106.5 cm), which was far greater than V15 (81.2 cm), V13 (75.5 cm), and V20 (69.8 cm).

4.4. Root and shoot length

Significant differences in shoot and root length were observed among the production of inbred and hybrid rice. At harvest (Figure 2), the smallest shoot was identified in V24 (54.1 cm), whereas the tallest shoot was identified in V5 (82.3 cm), which was statistically identical with V12 (78.1cm). The longest root was identified in V12 (21.3), which was statistically similar to V5 (19.6 cm), whereas the shortest root was identified in V24 (13.3 cm) as given in Figure 2. This might be because the cultivars reached their full maturity at harvest, and as a result, the roots stopped growing and began to deteriorate, resulting in shorter roots. In conventional rice, the plant root growth noticeably increased (Uzzaman et al. 2015); additionally, SRI had deeper roots than SMP. The simplest technique to increase a crop's rooting depth and root distribution is to lengthen the vegetative stage (Qados 2011). This can be accomplished by either delaying flowering or seeding early.

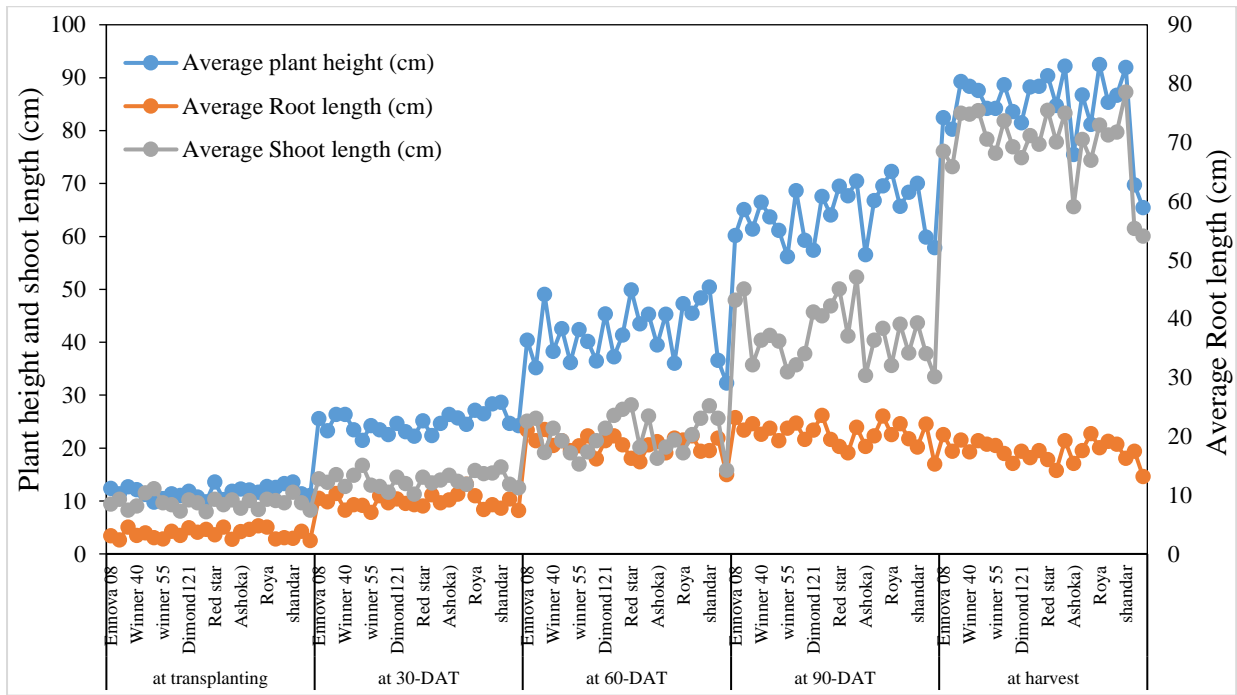


Figure 1- Plant Height, Root and shoot length of rice crop

4.5. Leaf area index

In comparison to inbred rice, hybrid rice has a much longer leaf area duration (LAD) and a quickly increasing LAI during vegetative growth. In all the examined rice seeds and planting dates up to heading, the LAI steadily rose, and for the most part, the differences are not statistically significant. However, at the heading stage, the highest LAI was obtained from V2 (4.50), followed by V5 (4.20), and was substantially reduced in V17 (2.70). The inbred rice varieties V22 and V23 had the highest LAI (3.40), while V24 had the lowest LAI (3.10). This outcome shows similar results to that of Qados (2011) and Howlader et al. (2017) (Figure 3).

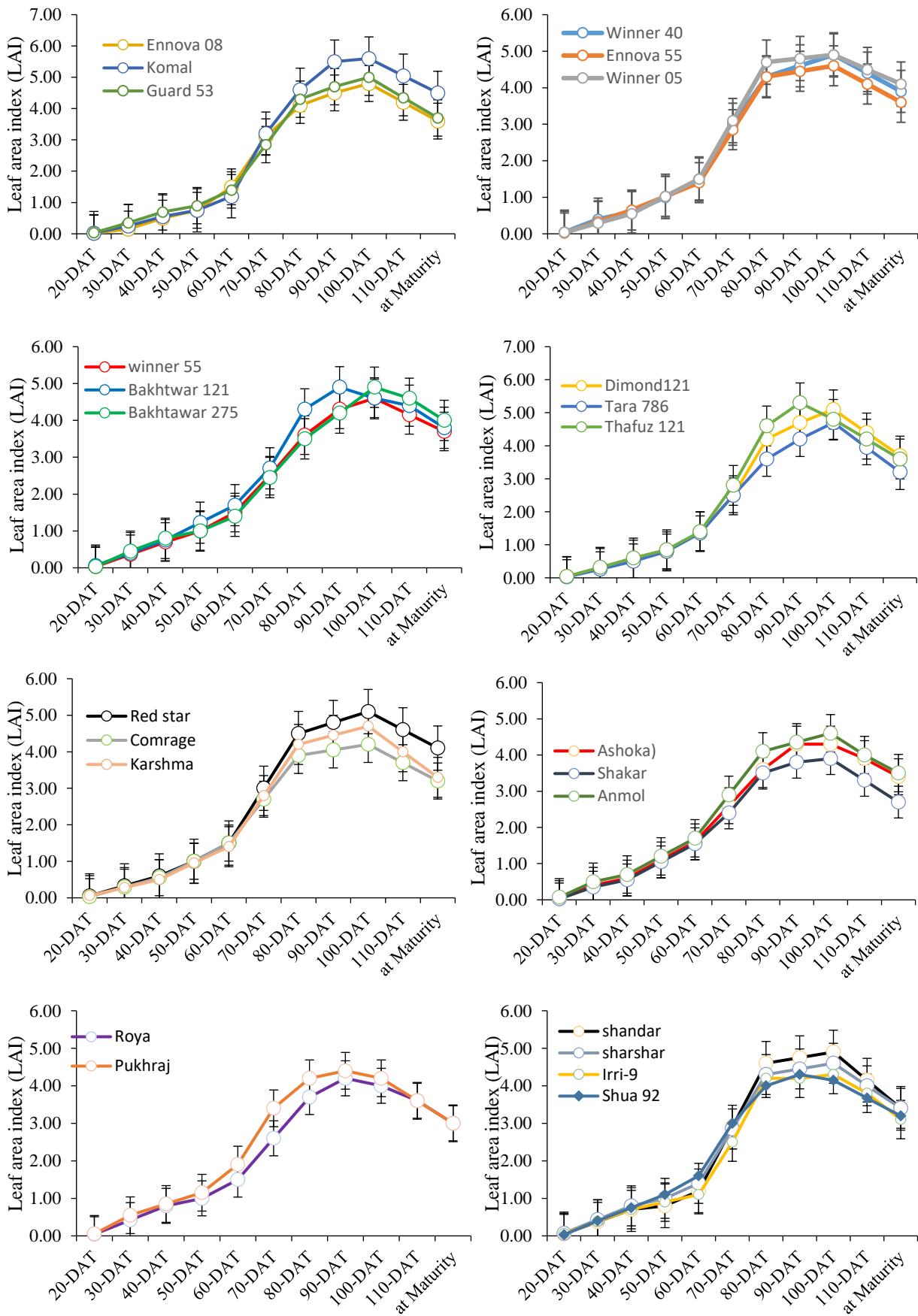


Figure 2- LAI of hybrid and inbred rice varieties at different DAT

4.6. Chlorophyll content

Rice grain output is primarily and actively photosynthesized by flag leaves (Uzzaman et al. 2015). Chlorophyll content reveals the leaves' capacity for photosynthetic activity (Swamy et al. 2016; Jagadish 2007). Hybrid rice, according to Chakrabarti et al. (2010), has more chlorophyll in its leaves. No distinction in leaf chlorophyll concentration was reported between hybrid and contemporary inbred types Haque et al. (2015). The amount of chlorophyll in flag leaves varied little between planting dates. It demonstrated that the hybrids under study possessed a higher flag leaf chlorophyll content as their distinctive traits. Flag leaf in hybrid rice has a better capacity for photosynthetic activity, according to Charkrabarti et al. (2010). In contrast to the inbred, the hybrid showed a decreased single-leaf photosynthetic rate at the grain filling phase, according to Cui et al. (2014).

The Flag leaf chlorophyll characters were studied based on twenty-four hybrid and conventional rice varieties in the naturally environmental system of Sindh province; however, significant results were identified in flag leaf chlorophyll. The hybrid and conventional rice varieties synthesized a higher amount of chlorophyll at 7, 15, 21 and 30th different DAT. The results obtained from both inbred and hybrid rice production were compared on 7th and 30th DAT. In hybrid rice, V19 at the 7th DAT showed least levels of chlorophyll (1.67 mg/g), whereas V1 showed higher levels of chlorophyll (2.87 mg g⁻¹). Whereas conventional rice Varieties at the 7th DAT showed the least level of chlorophyll in V24 (1.1mg/g), V22 showed higher chlorophyll levels (1.46 mg/g). However, at the 30th DAT, the V7 showed minimum levels of chlorophyll (0.70 mg/g) and V20 showed the maximum levels of chlorophyll (0.98 mg/g). Overall, V20 had high leaf chlorophyll as when compared to the other experimental treatments. While the conventional rice varieties (V21, V22) showed similar trends in Chlorophyll (0.72mg/g) at 30th DAT 7th DAT, which is less then hybrid Varieties. While V24 showed least significant results of leaf chlorophyll as compared to other conventional varieties. The total amount of chlorophyll in a flag leaf was largely unaffected by the environment. Additionally, there were variations between observations. According to some theories, the amount of chlorophyll in leaf tissues may vary depending on a plant's age, species, and growth season (Ramesh et al. 2002).

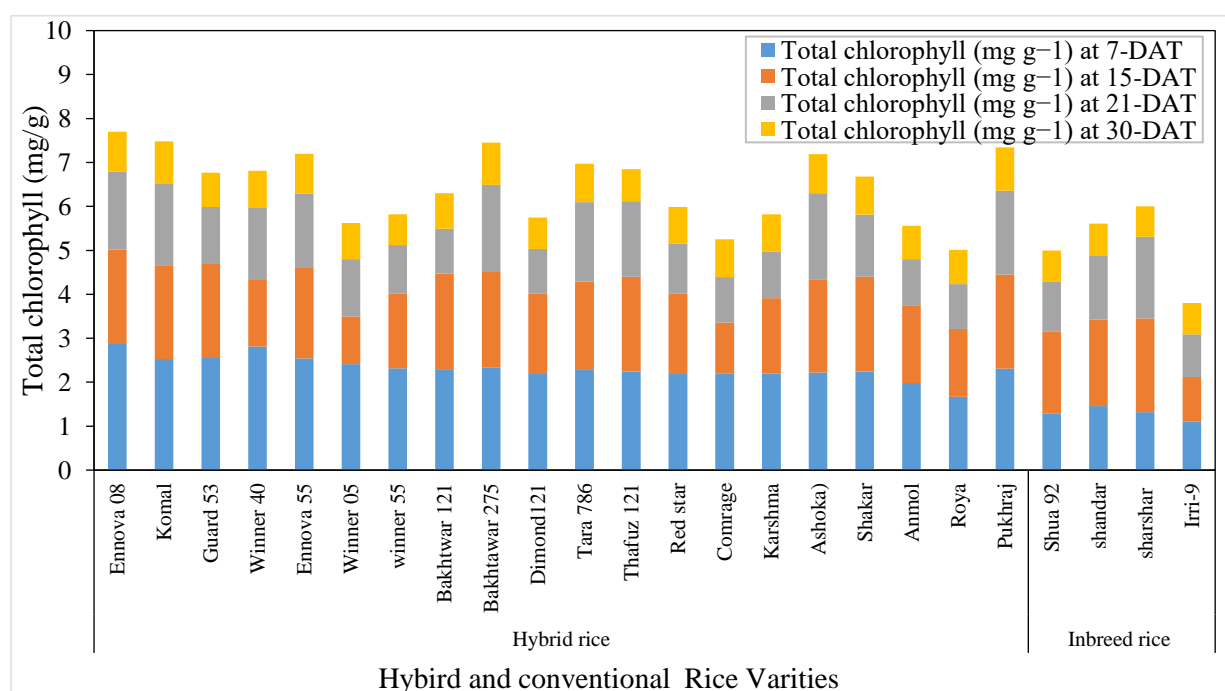


Figure 3- Comparison of total leaf chlorophyll (mg/g) among hybrid and inbred rice varieties

4.7. Yield attributing characters

Table 3 displayed the grain yield characteristics of the experimental cultivars at various planting dates. The number of days of rice flowers differs significantly. Hybrid varieties V10 and V18 showed early flowering (55 and 64 days, respectively), and V5 showed late flowering (60 and 65 days, respectively) (Table 3), while the inbred types of rice V21 (55 days and 60 days respectively). Regardless of the distance between transplants, the rice plant reached 50% flowering as the age of the transplanted seedling gradually decreased (Ram et al. 2014). The 8 days seedling transplantation showed early flowering (5-8 days) before 25-day old seedling transplanting. This might be the result of older seedlings taking longer than younger seedlings to initiate panicles due to slower growth in the main field (Uzzaman et al. 2015). This outcome is comparable to the research being discussed in this experiment.

In comparison to the predicted 105-day harvest period, the hybrid rice variety V4 matured and was ready for harvest at 90 days. Similar to V2, V3, V1, V5, V6, V7, V8, V9, V10, V11, V12, V13, V14, V15, V16, V17, V18, V19, and V20, which had a difference in maturity days of 11, 14, 13, 13, 8, 9, 6, 10, 8, 9, 8, 10, 11, 9, 8, and 7, while conventional rice varieties V21, V22, V23, and V24 had minimum days to maturity of 8, 8, 8, and 15, respectively. Under best management practices, traditional rice is harvested and ripe before the maturity period advised by the relevant released organization. Regarding paddy production, panicle length is also a crucial characteristic. In terms of panicle length, V4 and V10 had the longest panicles, measuring 27.2 cm, while V5 had the shortest panicles, measuring 26.5 cm. V24 and V20 were found to have the lowest value for panicle length among inbred and hybrid plants at 23.2 cm; V16 had the longest panicle length at 29 cm. The research study Idikut et al., (2009) identified various factors affecting the growth and the length of panicles under various crop production circumstances (Kim et al., 2012).

The highest number of filled grains per panicle (379) was identified in V5, while for the inbred the highest number of grains per panicle (285) was identified in V21, and the lowest number (190/panicle) was identified in V24 (Table 2). This outcome is consistent with that of Dutta et al. (1998), who found that the amount of grain per panicle affected yield. Maximum was discovered in V22 (33/panicle), which was statistically identical with V7 (26/panicle), while the minimum number of unfilled grains per panicle (12) was found in V14, which was statistically identical with V15 (15/panicle) and V16 (14/panicle) (Table 3). Similar findings were made by Dutta et al. (1998), who also noticed a wide range of changeability in the number of empty grains per panicle. The rice variety V14 had the longest seeds, measuring 9.2mm, while V24 had the shortest, measuring 6.21mm.

Table 3- Determination of yield characteristics of hybrid and inbred paddy varieties

Rice variety	Avg. Days to flowering	Average DAT to harvest	No. of panicle		Panicle length (cm)		Grains per panicle
			Per plant	Per m ²	Filled grains	Unfilled grains	
Hybrid rice							
Ennova 08	63	92	13	286	24.2	267	25
Komal	64	94	15	315	25.3	269	20
Guard 53	64	91	13	289	24.1	272	23
Winner 40	62	90	14	308	27.2	268	25
Ennova 55	65	92	12	276	26.5	379	24
Winner 05	61	97	14	310	25.5	274	22
Winner 55	59	96	13	312	24.3	312	26
Bakhtwar 121	63	99	13	290	25.2	305	24
Bakhtawar 275	62	95	14	310	25.3	260	17
Dimond121	64	96	14	318	27.2	270	19
Tara 786	57	97	16	319	24.5	265	18
Thafuz 121	60	96	13	312	25.3	270	20
Red star	57	97	14	320	24.2	281	18
Comrage	61	95	13	305	25.5	285	12
Karshma	58	95	17	320	26.3	280	15
Ashoka)	62	94	14	315	24.3	268	14
Shakar	63	96	15	317	24.3	272	25
Anmol	64	97	15	322	23.5	268	17
Roya	59	96	16	321	23.7	285	17
Pukhraj	60	98	13	286	23.2	285	20
Mean	61.4	95.15	14.05	307	24.98	281.75	20.05
Inbred rice							
Shua 92	60	97	12	264	27.1		285 20
Shandar	58	97	14	322	24.1		280 33
Sharshar	61	97	14	322	26.4		275 15
Irri-9	55	90	12	260	23.2		190 18
Mean	58.5	95.25	13	292	25.2		257.5 21.5

Among the traditional rice varieties, V22 produces maximum 1000-grain weight (20.6 g), which gave lower crop yield; the maximum 1000-grain weight (35.2 g) was observed in hybrid V5 (Table 4). The lowest amounts (12.7g) and (6.2g) were identified in V8 (hybrid) and V24 (inbred), respectively, which were statistically like V10's (16.4g) as given in Table 3. The thickness and length of rice were found to favorably correlate with the weight of 1000 grains (Coronel et al. 1984). The

variance in the weight of 1000 grains may be caused by the genic basis of rice strength. Table 3 showed that the V5 had the highest grain yield (4.51 t/ha), whereas V10 and V12 had the lowest (2.42 t/ha), while conventional rice yields the most grain (2.95 t/h). Compared with V22, the hybrid rice produced more grain yield per hectare than the conventional rice, as evidenced by the lowest (2.52t/h) grain yield also achieved from V24 (Howlader 2017). The rice variety V5 had the highest straw yield (7.1 t/ha), while the conventional rice variety V24 showed the lowest (5.2 t/ha). This outcome is consistent with that of Ndour et al. (2016), who found that plant height could influence straw yield. Maximum biological yield was discovered in V5 (11.61 t/ha), and minimum biological yield in V24 (7.92 t/ha). Compared to all conventional rice varieties, the biological yield of the V5 hybrid rice variety was 21.81% higher. The rice's grain yield and biological yield were favorably connected. Hybrid variety V15 had the highest harvest index (39.3%), while V24 had the lowest (35.5%). In comparison to V8, V9, and V24, hybrid rice variety V18 showed a higher harvest index. Amanullah and Inamullah, (2016) also noted that hybrid cultivars had greater harvest indices than inbred varieties.

Table 4- Performance of hybrid and inbred paddy varieties along with different parameters

<i>Rice variety</i>	<i>Grain length (mm)</i>	<i>1000 grain weight (g)</i>	<i>Grain yield (t ha⁻¹)</i>	<i>Straw yield (t ha⁻¹)</i>	<i>Biological yield (t ha⁻¹)</i>	<i>Harvest index (%)</i>
Hybrid rice						
Ennova 08	7.3	30.5	3.54	6.2	9.74	35.1
Komal	6.8	23.3	2.62	5.4	8.02	36.3
Guard 53	8.1	20.5	2.52	6.2	8.72	35.5
Winner 40	7.4	25.4	2.98	5.4	8.38	37.3
Ennova 55	8.3	35.2	4.51	7.1	11.61	36.8
Winner 05	7.76	25.4	3.15	6.2	9.35	37.2
Winner 55	8.24	22.8	2.57	5.4	7.97	35.6
Bakhtwar 121	8.97	25.8	3.05	5.4	8.45	38.3
Bakhtawar 275	6.9	12.7	2.48	6.5	8.98	36.5
Dimond121	8.5	16.4	2.42	6.2	8.62	36.8
Tara 786	8.11	19.5	2.52	5.4	7.92	38.6
Thafuz 121	7.76	18.3	2.42	6.3	8.72	35.5
Red star	7.87	23.5	2.73	6.2	8.93	37.8
Comrage	9.21	28.6	3.32	5.4	8.72	39.1
Karshma	7.89	29.3	3.45	6.3	9.75	39.3
Ashoka	8.32	13.7	2.62	6.5	9.12	38.3
Shakar	8.21	25.4	3.13	5.3	8.43	36.9
Anmol	9.15	25.1	2.98	6.5	9.48	38.6
Royal	7.91	25.5	2.88	5.3	8.18	38.5
Pukhraj	8.32	25.8	3.31	6.2	9.51	37.8
Mean	8.051	23.635	2.96	5.97	8.93	37.29
Inbred rice						
Shua 92	8.85	19.2	2.49	6.3	8.79	38.5
Shandar	9	20.6	2.95	6.2	9.15	38.6
Sharshar	9.2	19.3	2.84	6.3	9.14	37.4
Irri-9	6.21	12.7	2.52	5.4	7.92	35.5
Mean	8.315	17.95	2.7	6.05	8.75	37.5

4.8. Economic analysis

The economic analysis of production of hybrid and inbred paddy cultivars was carried out (Table 5). The overall fixed and variable costs served as the foundation for the economic inputs of different paddy cultivars. However, the costs of chemicals, gasoline, labor, fertilizer, seed, irrigation water, repair, energy, maintenance, and revolving interest are included in the variable costs. This does not include the fixed costs, which include general administrative costs, land value interest, irrigation machine and tool interest, depreciation value, facility cost amortization, and facility capital interest (Aslam et al., 2020).

Table 5- Economic analysis of hybrid and inbred rice varieties

<i>Cost indicators</i>	<i>PKR/quantity (inbred/hybrid)</i>	<i>Quantity</i>	<i>Inbred paddy (PKR)</i>	<i>Hybrid paddy (PKR)</i>
Nursery preparation				
Land ploughing (ha ⁻¹)	8000	4	32 000	32 000
Seed (Kg)	3000/4500	40	120 000	180 000
Fertilizers-organic (trolley)	2500	5	12 500	12 500
Irrigation (h ⁻¹)	1150	22	25 300	25 300
Fertilizers (Bags)	3000	1.5	4 500	4 500
Labor hours	300	42	12 600	12 600
Total			206 900	266 900
Field paddy transplantation				
Land ploughing (ha ⁻¹)	8000	5	40 000	40 000
Fertilizers (Bags)	18000	2.5	45 000	45 000
Irrigation	1150	16	18 400	18 400
Transplanted charges (h ⁻¹)	1800	7	12 600	12 600
Skilled labor hours	500	7	3 500	3500
Total			119 500	119 500
Spraying and chemicals application				
Sprays (liquid)	7500	4	30 000	30 000
Chemical (Powder/granular)	1500	3	4 500	4 500
Labor hours	500	60	30 000	30 000
Total			64 500	64 500
Irrigation and fertigation				
Irrigation charges	1150	85	97 750	97 750
Fertilizers (Bags)	18000	6	108 000	108 000
Labor hours	300	90	27 000	27 000
Total			232 750	232 750
Harvesting				
Combine harvester (h ⁻¹)	5500	3	16 500	16 500
Skilled labor hours	500	8	4 000	4000
Total			20 500	20 500
Total Variable Cost			694 150	754 150
Fixed Cost (land rent)			50 000	50 000
Total cost (ha ⁻¹)	744 150	804 150		
Crop yield				
Grain yield (kg h ⁻¹)			3 096	3 780
Grain Revenue			6 037 200	9 639 000
Straw yield (kg ha ⁻¹)			5 200	6 200
Straw revenue (PKR ha ⁻¹)			31 200	37 200
Total revenue			6 068 400	9 676 200
Total production cost (PKR ha ⁻¹)			744 150	804 150
Gross Profit			5 374 250	8 922 050
Net Profit			5 324 250	8 872 050
Benefit cost ratio (BCR)			8.15	12.03

The manual labor was engaged for planting, plant care, harvesting, and clean-up, while the tractor power or electric power was used to run agricultural machines for the manufacturing of rice. According to Noor et al. (2020e), the economic inputs to produce hybrid rice and inbred rice are largely based on total fixed and variable costs. The fixed costs included general administrative costs, interest on land value, interest on irrigation machine tool depreciation value, amortization of facility costs, and facility capital interest.

The variable costs included the costs of chemicals, fuel, human labor, seed, fertilizers, irrigation water, and electricity. For the purpose of calculating gross, absolute, and relative profit indicators, the following formulas were utilized (Noor et al. 2020f; Zhanbota et al. 2021). Hybrid rice production had a maximum BCR of 12.03 compared to inbred rice production's (8.15), which demonstrated that hybrid rice was more profitable to sow because it produced a higher yield, as well as other economic advantages. The highest total production costs were measured in inbred rice production at 744 150 PKR per hectare, while the hybrid rice production at 804 150 PKR per hectare (Zhanbota et al. 2022).

5. Conclusions

The development of high-quality varieties of rice, including early and late maturing varieties, hybrid and conventional rice varieties are needed to sustain global agricultural production. For this reason, the present study evaluated the different agronomical traits under the natural opening field at Larkana Sindh Pakistan. The tested hybrid and inbred rice varieties showed different responses toward adoptability, morphological growth, and yield characteristics. Broad variations have been found in these agronomic characters. Hybrid rice development has higher crop yield as compared to inbred varieties.

To meet the feeding requirement of the glowing global population there is need to produce new hybrids. From this study's results, it can be concluded that the Ennova-55, Winner-05 and Ennova-08 are at ensuring productive yields than inbred varieties. The results of our study indicate that the hybrid rice varieties can be adopted in Pakistan for sowing and increasing the productivity due to higher production. These hybrids rice varieties can be developed and further utilized in breeding programs. Further research work should be carried out to validate the results and adoptability of hybrid rice production. The economic analysis shows that hybrid rice production had a maximum BCR of 12.03 when compared with inbred rice production (8.15), which demonstrated that hybrid rice production is more profitable because it produces a higher yield and further economic advantages for rice growers.

Abbreviations

The abbreviations used in this study are listed below.

IRRI	International Rice Research Institute
BCR	Benefit Cost Ratio
FAO	Food and Agriculture Organization
QTL	Quantitative trait locus
LAI	Leaf area index
ET	Evapotranspiration
CRD	complete randomized design
LSD	Least significant difference
HYVs	High yielding varieties
DAT	Days after transplanting
LAD	Leaf area duration

References

- Adriani D E, Dingkuhn M & Dardou A (2016). Rice panicle plasticity in Near Isogenic Lines carrying a QTL for larger panicle is genotype and environment dependent. *Rice* 9:1–15
- Amanullah H (2016). Influence of organic and inorganic nitrogen on grain yield and yield components of hybrid rice in Northwestern Pakistan. *Rice Sci* 23: 326–333
- Amanullah I & Inamullah X (2016). Dry matter partitioning and harvest index differ in rice genotypes with variable rates of phosphorus and zinc nutrition. *Rice Sci* 23: 78–87
- Ashraf M & Akram NA (2009). Improving salinity tolerance of plants through conventional breeding and genetic engineering: an analytical comparison. *Biotechnol Adv* 27:744–752
- Aslam W, Noor R S & Hussain F (2020). Evaluating morphological growth, yield, and postharvest fruit quality of cucumber (*Cucumis sativus* L.) grafted on cucurbitaceous rootstocks. *Agriculture (Switzerland)* 10. <https://doi.org/10.3390/agriculture10040101>
- Bhuiyan M S H, Zahan A & Khatun H (2014). Yield performance of newly developed test crossed hybrid rice variety. *Intl J Agron Agril Res* 5:48–54
- Chakrabarti B, Aggarwal P K & Singh S D (2010) Impact of high temperature on pollen germination and spikelet sterility in rice: comparison between basmati and non-basmati varieties. *Crop Pasture Sci* 61:363–368
- Chukwu S C, Rafii M Y & Ramlee S I (2019). Bacterial leaf blight resistance in rice: a review of conventional breeding to molecular approach. *Mol Biol Rep* 46:1519–1532
- Cui Z, Dou Z & Chen X (2014). Managing agricultural nutrients for food security in China: past, present, and future. *Agron J* 106:191–198
- Duncan D B (1955). Multiple range and multiple F tests. *Biometrics* 11:1–42
- Fageria N K (2010). Optimal nitrogen fertilization timing for upland rice. In: World Congress of Soil Science, 19., 2010, Brisbane, Australia. Soil.
- Howlader M H K, Rasel M & Ahmed M S (2017). Growth and yield performance of local T Aman genotypes in southern region of Bangladesh. *Progressive Agriculture* 28:109–113
- Idikut L, Atalay A I, Kara S N & Kamalak A (2009). Effect of hybrid on starch, protein and yields of maize grain. *Journal of Animal and Veterinary Advances* 8:1945–1947
- Liu X, Beyrend-Dur D, Dur G & Ban S (2014). Effects of temperature on life history traits of *Eodiaptomus japonicus* (Copepoda: Calanoida) from Lake Biwa (Japan). *Limnology (Tokyo)* 15:85–97
- Mariana M & Hamdani J S (2016). Growth and yield of *Solanum tuberosum* at medium plain with application of paclobutrazol and paranet shade. *Agriculture and Agricultural Science Procedia* 9:26–30
- Metwally T F, Sedeek S E M & Abdelkhalik A F (2010). Genetic behaviour of some rice (*Oryza sativa* L.) genotypes under different treatments of nitrogen levels. *Electronic Journal of Plant Breeding* 1:1266–1278
- Noora R S, Hussain F, Saadb A & Umair M (2020). Maize (*Zea Mays*) production under different irrigation treatments: investigating the germination and early growth. *Science (1979)* 4:43–45
- Noor R S, Hussain F & Abbas I (2020a). Effect of compost and chemical fertilizer application on soil physical properties and productivity of sesame (*Sesamum Indicum* L.). *Biomass Convers Biorefin* pp. 1–11
- Noor R S, Hussain F & Umair M (2020b). Evaluating selected soil physical properties under different soil tillage systems in arid southeast rawalpindi, pakistan. *J Clean WAS* 4:41–45
- Noor R S, Hussain F, Umair M & Umar F M (2019). Silage Corn Production Under Different Planting Methods In Rainfed Agriculture System: An Energy Analysis. Education (Chula Vista)

- Noor R S, Wang Z & Umair M (2020c). Long-term application effects of organic and chemical fertilizers on soil health and productivity of taramira (*Eruca sativa* L.) under rainfed conditions. *JAPS: Journal of Animal & Plant Sciences*
- Qados A M S A (2011). Effect of salt stress on plant growth and metabolism of bean plant *Vicia faba* (L.). *Journal of the Saudi Society of Agricultural Sciences* 10:7–15
- Ranawake A, Amarasingha U & Dahanayake N (2013). Agronomic characters of some traditional rice (*Oryza sativa* L.) cultivars in Sri Lanka. *Journal of the University of Ruhuna*:
- Ranawake A L & Amarasinghe U G S (2014). Relationship of yield and yield related traits of some traditional rice cultivars in Sri Lanka as described by correlation analysis. *J Sci Res Rep* 3:2395–2403
- Riaz M, Iqbal M & Akhter M (2017). Assessment of genetic combinations for hybrid rice in the germplasm of Pakistan. *Asian J Agric Res* 4:1–8
- Semerci A (2020). Input usage and cost analysis in paddy production: a case study of Çanakkale City-Turkey. *Custos e @gronegocio on line* 16(2): 277-306
- Semerci A & Everest B (2021). The place and importance of paddy production in agricultural enterprises in Çanakkale province. *International Journal on Mathematic, Engineering and Natural Sciences* 5(19) 636-649.
- Senapati N & Semenov MA (2020). Large genetic yield potential and genetic yield gap estimated for wheat in Europe. *Glob Food Sec* 24:100340
- Soe I, Tamu A & d Asante M (2019). Genetic diversity analyses of rice germplasm using morphological traits. *J Plant Breed Crop Sci* 11:128–136
- Swamy B P M, Rahman M A & Inabangan-Asilo M A (2016). Advances in breeding for high grain zinc in rice. *Rice* 9:1–16
- Uphoff N (2006). The system of rice intensification (SRI) as a methodology for reducing water requirements in irrigated rice production. *International Dialogue on Rice and Water: Exploring Options for Food Security and Sustainable Environments* 1–23
- Uzzaman T, Sikder R K & Asif M I (2015). Growth and yield trial of sixteen rice varieties under System of Rice Intensification. *Scientia Agriculturae* 11:81–89
- Wang F, Huang J, Zhou Q & Wang X (2008). Optimal waveband identification for estimation of leaf area index of paddy rice. *J Zhejiang Univ Sci B* 9:953
- Wang Y, Lu J & Ren T (2017a). Effects of nitrogen and tiller type on grain yield and physiological responses in rice. *AoB Plants*
- Wang Y, Lu J & Ren T (2017b). Effects of nitrogen and tiller type on grain yield and physiological responses in rice. *AoB Plants*
- XING Z, Pei W U & Ming Z H U (2017). Temperature and solar radiation utilization of rice for yield formation with different mechanized planting methods in the lower reaches of the Yangtze River, China. *J Integr Agric* 16:1923–1935
- Yang Y, Timlin D J & Fleisher D H (2009). Simulating leaf area of corn plants at contrasting water status. *Agric For Meteorol* 149:1161–1167
- Yoshinaga S, Heinai H & Ohsumi A (2018) Characteristics of growth and quality, and factors contributing to high yield in newly developed rice variety 'Akidawara.' *Plant Prod Sci* 21:186–192
- Zhang J, Yang Y & Wang Y (2011). Identification of hub genes related to the recovery phase of irradiation injury by microarray and integrated gene network analysis. *PLoS One* 6:e24680
- Zhao D, Xie D & Zhou H (2012). Estimation of leaf area index and plant area index of a submerged macrophyte canopy using digital photography. *PLoS One* 7:e51034



Copyright © 2024 The Author(s). This is an open-access article published by Faculty of Agriculture, Ankara University under the terms of the [Creative Commons Attribution License](https://creativecommons.org/licenses/by/4.0/) which permits unrestricted use, distribution, and reproduction in any medium or format, provided the original work is properly cited.



Parasitism (*Flamingolepis liguloides* Gervais, 1847) with High Prevalence in Brine Shrimp Population from Çamaltı Saltworks

Edis KORU^a ^aEge University Fisheries Faculty Dept. of Aquaculture, Bornova-İzmir, TÜRKİYE

ARTICLE INFO

Research Article

Corresponding Author: Edis KORU, E-mail: edis.koru@ege.edu.tr

Received: 12 May 2023 / Revised: 21 September 2023 / Accepted: 22 September 2023 / Online: 09 January 2024

Cite this article

Koru E (2024). Parasitism (*Flamingolepis liguloides* Gervais, 1847) with High Prevalence in Brine Shrimp Population from Çamaltı Saltworks. *Journal of Agricultural Sciences (Tarım Bilimleri Dergisi)*, 30(1):145-152. DOI: 10.15832/ankutbd.1296270

ABSTRACT

Populations of the species *Artemia* (Brine shrimp) in saltworks have become a popularity popular field of study for aquaculture for its significance for aquatic ecosystems as being an important source of sustenance for water birds in hypersaline food webs. Besides, species in the genus *Artemia* are the intermediate host of severe cestode species which are associated with flamingos. This study reports on the prevalence of native *Artemia parthenogenetica* parasitism of *Flamingolepis liguloides* in the Çamaltı saltern ecosystem in the Gediz wetland between January and December 2022 in Türkiye. Infected *A. parthenogenetica* was sampled from April to September 2022 in salt pans where flamingo

birds and salt production are available for parasitological diagnosis. The parasites were determined in the abdomen, thorax and near the gut tract of *A. parthenogenetica*. The highest prevalence of parasite was found in juvenile individuals as 86.67±1.45% and adults as 76.06±1.16% in May. The main intensity was varied from 1.18±0.01 to 1.92±0.06 parasites per infected host depending on the sampling months and age of the brine shrimp. The most abundant parasite infestation was recorded as 1.44±0.02 parasites per investigated host in juvenile brine shrimp in June since seasonal conditions are favorable for such infestation.

Keywords: Aquaculture, Brine shrimp, Avian, Parasitism, Solar saltworks, Wetlands, İzmir, Türkiye

1. Introduction

The cosmopolitan brine shrimp *Artemia* (Branchiopoda, Anostraca) is one of the most studied aquatic organisms based on its broad use in ecotoxicology, ecology, developmental and evolutionary biology, feeding of aquatic organisms and the extensive use in the aquaculture industry (Büke 2002; Kırkağaç et al. 2017; Kaska 2019). Very saline waters, i.e. hypersaline waters, are unique extreme habitats where salinity limits species richness. There are major patterns of relationship between salinity and species richness of free-living aquatic animals in such ecosystems, but general regularities for parasitic organisms have yet to be established. All 85 species and forms of parasites found in hypersaline waters belong to five phylum: Platyhelminthes, Nematoda, Acanthocephala, Cnidaria and Arthropoda. Platyhelminthes is the most diverse and species-rich branch of the Cestoda class. Most species are found in hypersaline waters with salinities not exceeding 100 g/L. The total number of parasite species decreases exponentially with increasing salinity due to cellular osmotic stress in the organism. For this reason, the number of free living animal species living in waters with salinities between 35 and 210 g/L is approximately 12 times higher than that of parasites in all ranges of this salinity range. Salinity affects parasite richness and composition in two ways: directly and through the availability of hosts. Free-living crustaceans are the suitable hosts of most parasite species in hypersaline waters. The *Artemia* species, the most halotolerant, is a good intermediate host for 22 species and unidentified parasite forms (Kornychuk 2023). The *Artemia* species are reported as the keystone taxon in hypersaline food webs with different status; they are the main prey of aquatic birds, the intermediate host for several parasite species and the primary consumer of phytoplankton in the ecosystem (Georgiev et al. 2005; Sánchez et al. 2006; Vasileva et al. 2009; Rode et al. 2013 a,b). Specifically, brine shrimps are stated as the main prey of breeding flamingos (Britton & Johnson 1987; Bechet & Johnson 2008) and then brine shrimps are also reported as intermediate hosts of parasite cestodes.

In the scientific record, the first description of a cysticeroid in *Artemia* species was reported approximately 100 years ago (Heltdt 1929). There are now 22 cestode species from the genus *Artemia* (Redón et al. 2020). Five of these species belong to the genus *Flamingolepis* (Cyclophyllidea, Hymenolepididae) (Maksimova 1979) with *F. liguloides* (Gervais 1847) being the most common (Amarouayache et al. 2009). The first invasion of *Artemia* sp by larval forms of cestoda was reported from Tunisia (Heltdt 1929), then many other countries, such as Spain (Amat et al. 1991a,b; Sánchez et al. 2013), France (Gabrion & MacDonald 1980; Thierry et al. 1990), Italy (Mura 1995) and Türkiye (Koru 2022). The parasites spread to the birds with the

trophic transmission when feeding on infected *Artemia* species (Sánchez et al. 2013). It then develops into mature worms in the digestive tract of birds and the eggs of the adult parasite spread around the environment via the faeces of the main host (Amarouyache et al. 2009).

In this study, after the detection in 2018 (Koru 2022), the spread of the *Flamingolepis liguloides* (Gervais 1847) parasite in *A. parthenogenetica* (Barigozzi 1974) in the Çamaltı saltern ecosystem was investigated. The study aims to determine the temporal dynamics of bird parasites by means of *A. parthenogenetica* in the hypersaline saltworks ecological system, which is of great importance for wildlife. The area is also the breeding ground of flamingos and the results of this study reveal the presence of this parasitism in the Eastern Mediterranean.

2. Material and Methods

2.1. Study area

The study was performed in Çamaltı Saltern (Bird sanctuary biological area of İzmir), which is the largest sea-sourced saltworks in Türkiye, established in the Gediz River basin (Gediz wetland), 28 km away from İzmir. The size of the study area is 60 square kilometers, with a water depth of 1- 4 m and located at 38° 30' 18" N, 26° 54' 55" E district. The connection of the saltpan to the Aegean Sea is provided by pumps installed on the main channel. Thus, sea water can be gradually distributed to the sea salt crystallization pools and the wider area. Since the production and salt formation was finished in every October, the mechanical system that provides the water circulation was stopped. For this reason, there was no sea water inlet and outlet in the salt pans during the off season.

2.2. Sample collection and laboratory examinations

Brine shrimp (*A. parthenogenetica*) samples were collected monthly using a plankton net (125 µm mesh size) from three different salt pans of the Çamaltı Saltworks (38°30'12.73" N, 26°54'12.94" E) (Figure 1) from January to December 2022. The salinity parameters of the salt pans were measured using a refractometer (ATAGO Master-S28M, Tokyo, Japan), while the water temperature, oxygen and pH levels were measured using a multi-parameter probe (YSI ProQuatro, Ohio, USA) and recorded monthly during every sampling time at each sampling salt pans.

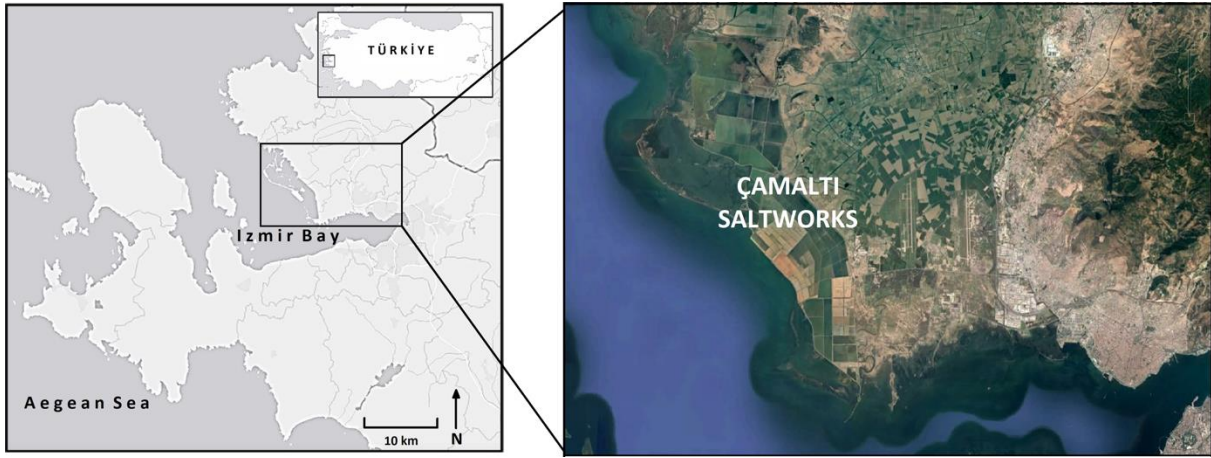


Figure 1- Geographical situation of the study area at Çamaltı saltern

The identification of the brine shrimps was carried out according to Brawne et al. (1991). The collected brine shrimp samples were washed with sterile physiological saline water and directly fixed in 3% formalin and preserved in 70% ethanol. The samples were mounted in temporary glycerol mounts and the mounted slides were examined under a light microscope (Olympus CX22RFS1) and parasites in the individual brine shrimp were counted. For each age group, 50 adults and 50 juvenile specimens were studied from each sampling station for every sampling month (a total of 150 brine shrimp specimens were studied for each age groups in every sampling months). Species identification of *F. liguloides* were performed according to Georgiev et al. (2005) and Redón et al. (2015) with oval cyst, elongated rostellar hooks and sucker hooklets, oval or round suckers. The prevalence, intensity and abundance of infection by month and host stages were calculated as follows (Bush et al. 1997):

$$Prevalence (\%) = \frac{\text{Number of infected hosts}}{\text{Number of examined hosts}} \times 100 \quad (1)$$

$$\text{Intensity (Number of parasites per infected host)} = \frac{\text{Total number of parasites recovered}}{\text{Total number of examined infected hosts}} \quad (2)$$

$$\text{Abundance (Number of parasites per examined host)} = \frac{\text{Total number of parasites recovered}}{\text{Total number of examined hosts}} \quad (3)$$

2.3. Statistical analysis

A comparison of the prevalence, intensity and abundance in juvenile and adult brine shrimp were performed using one-way ANOVA, followed by Duncan's multiple comparison post-hoc test to determine the significance of mean prevalence, intensity and abundance between age groups in monthly. Investigations in the study were repeated three times. An alpha level of 0.05 was used to determine the significance ($P < 0.05$). Data are expressed as means \pm standard error (SE). The statistical analysis was performed using SPSS (version 23.0) software.

3. Results

The physicochemical and biological characteristics of wetlands may differ depending on the seasonal climatic conditions of that year. These differences also affect the characteristics of the entire life cycle in the ecosystem. Some important water parameters, such as pH, oxygen, and water temperature and salinity were recorded monthly in the salt pans where brine shrimp specimens were collected. These can be seen in Figure 2. During the study, pH, oxygen, temperature, and salinity values varied between 6.30 ± 0.17 - 9.30 ± 0.06 , 3.90 ± 0.06 - 8.07 ± 0.07 ppm, 3.93 ± 0.07 - 34.33 ± 0.33 °C and 30.00 ± 1.15 - $265.00 \pm 2.89\%$, respectively. The highest water temperature was observed in July and the highest salinity in September. The salinity changed significantly in the off season due to seasonal rainfall, and the production time of salt changed due to the water pumping from the sea to salt pans as well as evaporation. This made it impossible to collect brine shrimps throughout the entire year.

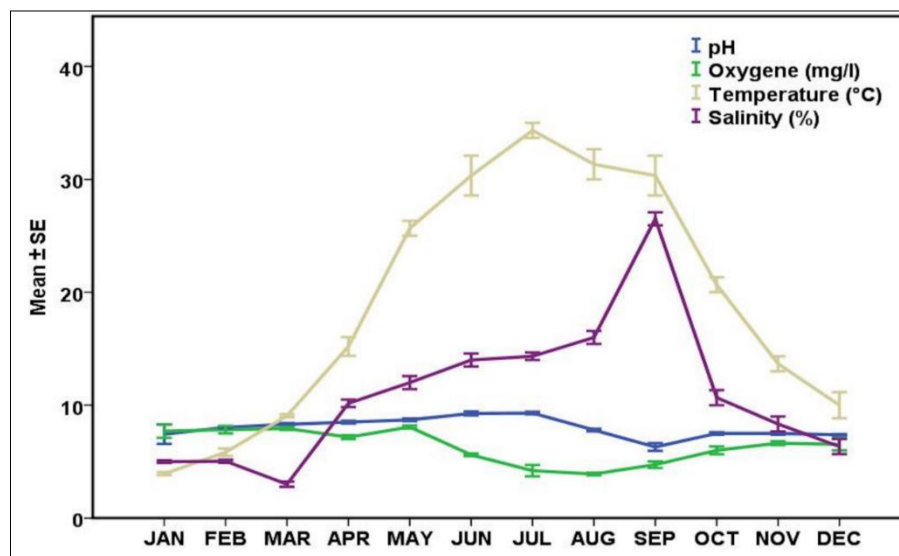


Figure 2- Detected annual water parameters from saltern area

The parasites were found in brine shrimp for five months, probably depending on abundance of great flamingos in wetland, the climate conditions and water regime. According to information received from ornithology experts, the number of migratory flamingo birds that came to the water in 2022 increased by 5×10^3 individuals in comparison to the previous year of 2021. This means an increase in the transmission rate of the parasite through migratory flamingos, according to the results in the literature reports (Amarouayache et al. 2009). This causes a high population in flamingos due to the suitability of positive climate conditions and due to the suitable for biological conditions in the water. It has been determined that this causes an increase in ecosystem compared to previous years. *F. liguloides* infection was recorded from both juvenile and adult *A. parthenogenetica* individuals between May-September 2022. Brine shrimps were sampled from January to December 2022. The first infestation was detected in May in both juveniles and adults' examples. The main prevalence was found to be higher in juveniles than adult brine shrimps ($df=9$, $F=494.35$ $p=0.00$) ($P < 0.05$) in May and June. The monthly prevalence of infestation is presented in Figure 3. The highest prevalence was detected as 86.67 ± 1.45 % for juveniles and 76.06 ± 1.16 % for adult brine shrimp specimens in May. A maximum of 7 and 4 cysticercoids were determined in infected adult and juvenile individuals, respectively. The mean intensity varied from 1.27 ± 0.01 to 1.73 ± 0.01 parasites per infected host in juveniles and from 1.18 ± 0.01 to 1.92 ± 0.06 parasites per infected host in adult brine shrimp. While the highest intensity value of juveniles was observed as 1.73 ± 0.01 parasite per infected host in August, the highest intensity of adult brine shrimp was detected as 1.92 ± 0.06 parasite per infected host in September. Differences in the intensity values of juveniles and adults are presented in Figure 4 ($df=9$, $F=35.1$, $P=0.00$). The mean abundance ranged between 0.82 ± 0.02 and 1.44 ± 0.02 parasite per investigated host in juveniles, 0.90 ± 0.01 and 1.24 ± 0.03

parasite per investigated host in adult brine shrimp. While the highest abundance of juveniles was detected in June, the highest abundance of adult brine shrimps was calculated in July. Differences between the mean abundance values of juveniles and adults were found to be statistically important ($P < 0.05$) in all parasitism observed months ($df=9$, $F=305.32$ $p=0,00$) (Figure 5).

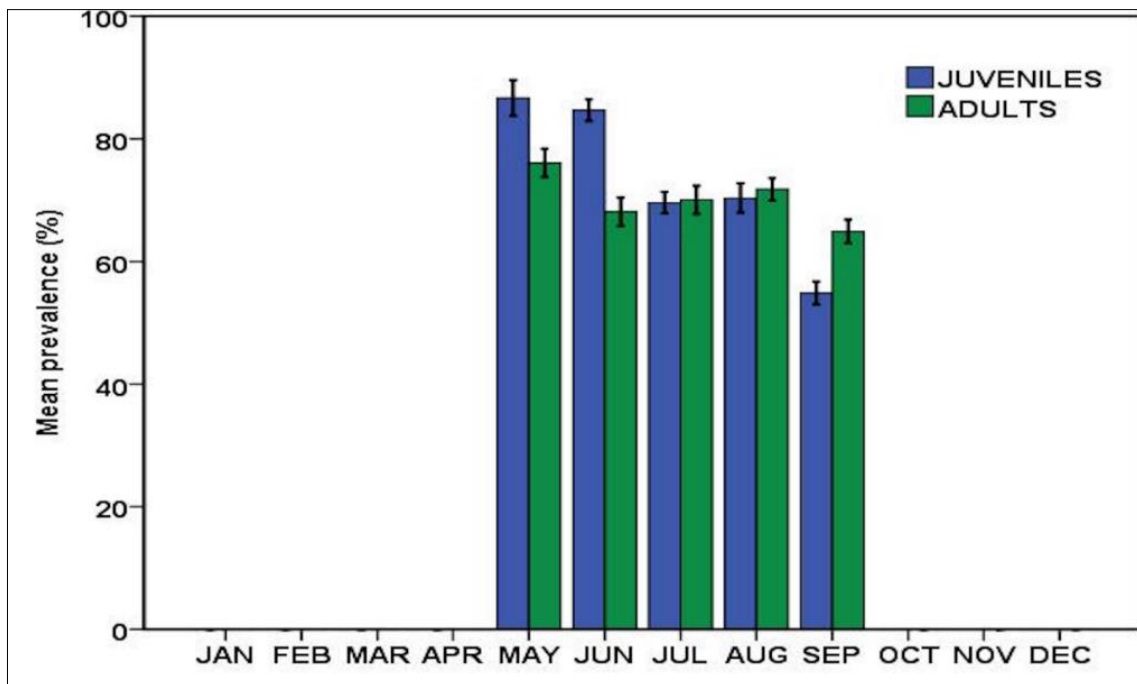


Figure 3- Monthly mean prevalence in juvenile and adult brine shrimps. (JAN, FEB, MAR, OCT, NOV, DEC) brine shrimp samples were not available. (MAY, JUN, JUL, AUG, SEP) in which the parasite was detected. Different letters indicate statistically differences at $P < 0.05$ and error bars represented.

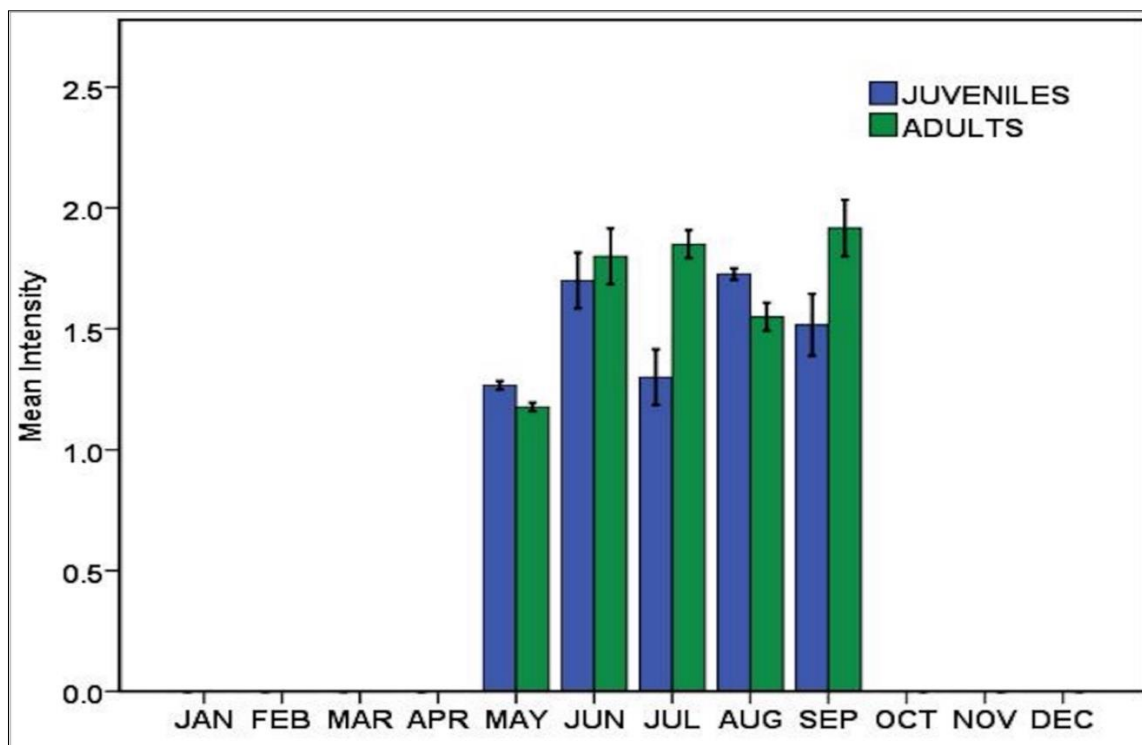


Figure 4- Monthly mean intensity in juvenile and adult brine shrimps. Egg&nauplii stage (JAN, FEB, MAR) brine shrimp samples were not available because of the end times of salt production. (OCT, NOV, DEC) parasitism was not detected (Salt production ponds were emptied because salt production ended. For this reason, there are no living things in the ecosystem). Different letters indicate statistically differences at $P < 0.05$ and error bars represented SE.

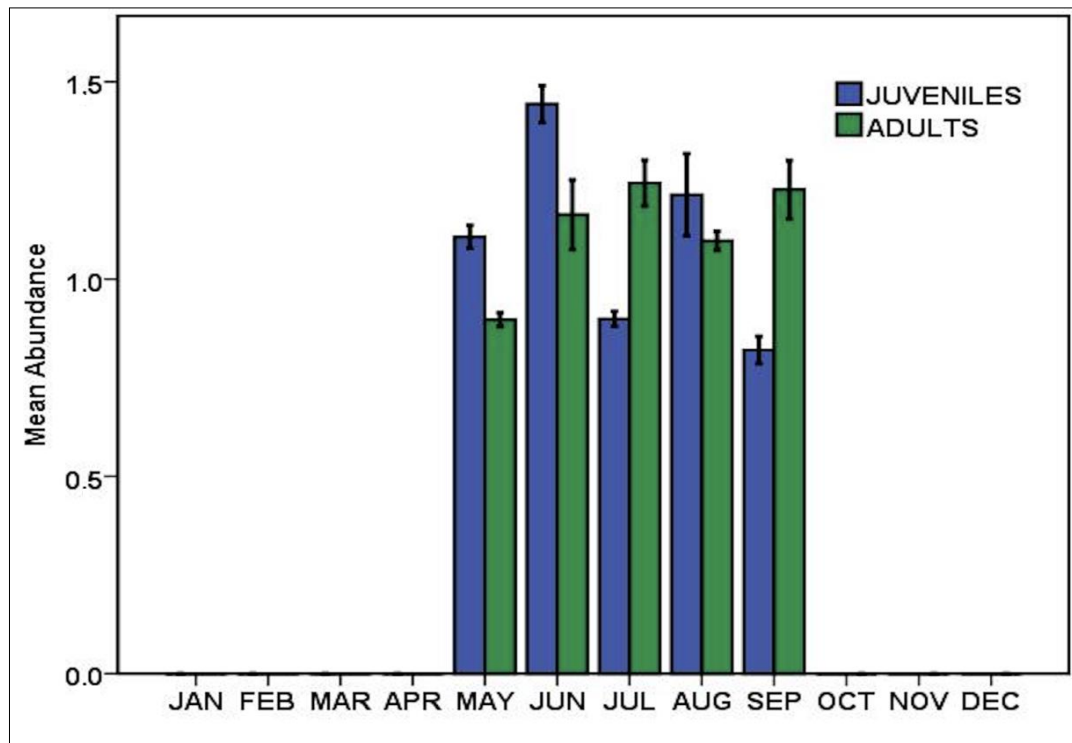


Figure 5– Monthly parasitism abundance in Çamaltı salt pans Brine shrimp samples were not available (JAN, FEB, MAR). Egg&nauplii stage; Monthly mean abundance in juvenile and adult brine shrimps (MAY, JUN, JUL, AUG). Parasitism was not detected (OCT, NOV, DEC). Different letters indicate statistically differences at $P < 0.05$ and error bars represented SE.

4. Discussion

The first reported parasitic infection of this species in *Artemia* from the Mediterranean region was recorded by Robert & Gabrion (1991). This study was carried out to determine the new status of the parasites of the *Artemia* species in the Çamaltı Region, Türkiye's largest sea salt ecosystem, compared to previous years. (Koru 2013; 2022). Field data were evaluated to determine the prevalence and seasonal effects of *F. liguloides*, which infects the *A. parthenogenetica* host brine shrimp. The brine shrimp *Artemia* has been reported to be a non-selective filter feeder (Sánchez et al. 2013). Thus, the *Artemia* species have been feeding on all kinds of microorganisms, including detritus in the water column (Sánchez et al. 2007; Savage & Knott 1998). The *Artemia* species engulf the cestode eggs, which are called oncosphere (20 μm) and become cysticeroid (larva with scolex), into the hemocoel (Amarouayache et al. 2009; Robert & Gabrion 1991; Sánchez et al. 2007). The parasitism of *Artemia* sp. could be related to the existence of flamingos and relationship with the ecosystem. Therefore, the *F. liguloides* parasitism period is varied according to the location of habitats. It was reported in *A. salina* from a wetland from Northeast Algeria at the end of winter (February/March), whereas the population of a second wetland area in Algeria was infected in spring (April/May) (Amarouayache et al. 2009). The parasite infection of *A. parthenogenetica* in Türkiye, was first recorded by Koru in 2022 (2022). This variation in the infection period was associated with the increase in the flamingo population density and the migratory behaviour of flamingos in wetland areas. Similarly, the parasitism of *F. liguloides* can be explained by the presence of flamingos at the same time in the Çamaltı Saltern area. The salt pans of Çamaltı are the breeding site of flamingos and the site has become a regular and important breeding region in Türkiye since 2000 (Balkız et al. 2015). The greater flamingos can be observed in this area between March and August. Egg-laying generally occurs between mid-April and early May. Flamingo populations consist of 45% of ringed birds in Türkiye. These birds migrate to 16 different countries along the western and eastern Mediterranean Basin and West Africa. It has been reported that most of the Çamaltı flamingo population consist of migratory flamingos from the Mediterranean basins (France, Italy, Spain) (Balkız et al. 2015). It may be that the migratory dynamics of the flamingo population make it possible to transport cestode parasites between these basins.

We observed high cestode infections with high prevalence (up to $86.67 \pm 1.45\%$) between the late spring and summer season in the Çamaltı Saltwork populations of *A. parthenogenetica*. The mean intensity and abundance were calculated up to 1.92 ± 0.06 parasite/per infected host and a mean abundance of 1.44 ± 0.02 parasite/per investigated host respectively. Some former studies reported a lower prevalence rate than this study; Mura (1995) reported a cestode parasitism (*F. liguloides*) in an *Artemia* sp. population from south-western Sardinia with 3% prevalence and 1.09 mean intensity. Sánchez et al. (2013) reported cestode parasitism with 43% prevalence, 1.39 intensity and a 0.6 abundance score in June from the Odiel Salt pans - Southwest Spain, and with 63% prevalence, 1.53 intensity and 0.97 abundance in April from Salinas de Cerrillos-Spain. On the other hand, Georgiev et al. (2007) reported a cestode parasitism with high prevalence (89%) from Salinas Portuguesas, Cádiz Province, Spain. The parasitism intensity was a reported variable; less than 3 cysticeroids per individual in Algeria (Amarouayache et al.

2009), 13 in the populations of Spain (Georgiev et al. 2005) and around 9-11 in France (Gabrion et al. 1990). Sánchez et al. (2013) reported multiple cysticercooid infections of around 2-4, with a maximum of fourteen. At the start of September, salt harvesting begins in the Çamaltı saltworks, which means that the use of circulation pumps that provide water circulation in the ecosystem are discontinued. This means the period when all water inflows and outflows from the wetland cease. Therefore, the circulation of *Artemia* and the aquatic parasite end. Due to physicochemical and biological changes such as increasing salinity and decreasing nutrient content in the water, the possibility of encountering parasites in salt pans is negligible.

In this study, as in the results obtained by Koru in his 2018 study, a total of 7 and 4 cysticercooids were detected at most in adult and juvenile individuals, respectively (Koru 2022). According to Thiery et al. (1990), the accumulation of the cysticercooids would be associated with the age and the body size. It is indicated that *Artemia* larval instar III-IV can feed 25-30 μm diameter particles; however, *F. liguloides* eggs which are 40-50 μm in size may only be ingested by adult *Artemia* individuals (Mura 1995). The location of the cysticercooids was, for the most part, found in the thorax and abdomen in this study. However, they were typically located in the abdomen of adults in the saltworks of Sardinia (Mura 1995). Thiery et al. (1990) remarked that, the location of the cysticercooids is related to the volume of the hemocoel and the distribution is relevant to the allometric changes during the growth stage of the *Artemia*. In nature, individuals of *A. parthenogenetica* make vertical migrations; generally, are found 75% in the bottom of the water columns during the day and in the other 25% at night, (Sánchez et al. 2007) and generally shows strong negative phototaxy and positive geotaxis (Sánchez et al. 2007). Nevertheless, this infection changes the proportion of time that is spent at different depths (Sánchez et al. 2007, 2013). In addition, parasites increase the buoyancy and make *Artemia* swim on the surface of the water which facilitates predation by water birds (Thomas et al. 1997; Helluy & Holmes 2005; Curio 1988; Amarouayache et al. 2009). Sánchez et al. (2007) studied the effects of cestode parasitism on the behaviour of *A. parthenogenetica* and reported that 86% of the uninfected *Artemia* showed positive geotaxis whereas 53% of infected *Artemia* showed surface-swimming behaviour (negative geotaxis). Infected brine shrimps become photophilous and their surface-swimming movement can be observed. This action facilitates to be realized by the final avian host and make parasite transmission easier. Infected brine shrimps become photophilous and their surface-swimming action can be observed (Figure 6). Cestodes that are known to alter the action of their *Artemia* in ways that give the parasite a better home, or provide more nutrients, or cause the host to move to a different environment, and in doing so improve its own transmission, are going to be favoured by natural selection. Behaviours such as these mentioned would contribute to increasing the chance of the infected brine shrimp being consumed by a flamingo. In this study, the *F. liguloides* infestation which was observed in *A. parthenogenetica* as a vector demonstrates a similar example. Parasitic castration and colour change from transparent to red is known to be observed in infected brine shrimp to benefit the parasite in addition to behavioural manipulation making *Artemia* more susceptible to predators also hypothesize that the parasitic infection increases the brine shrimps' lifespan, time spent at the water surface, and that the castration is to prevent the shrimps from spending time with sexual reproduction (Amat et al. 1991; Rode et al 2013; Sánchez et al. 2006).

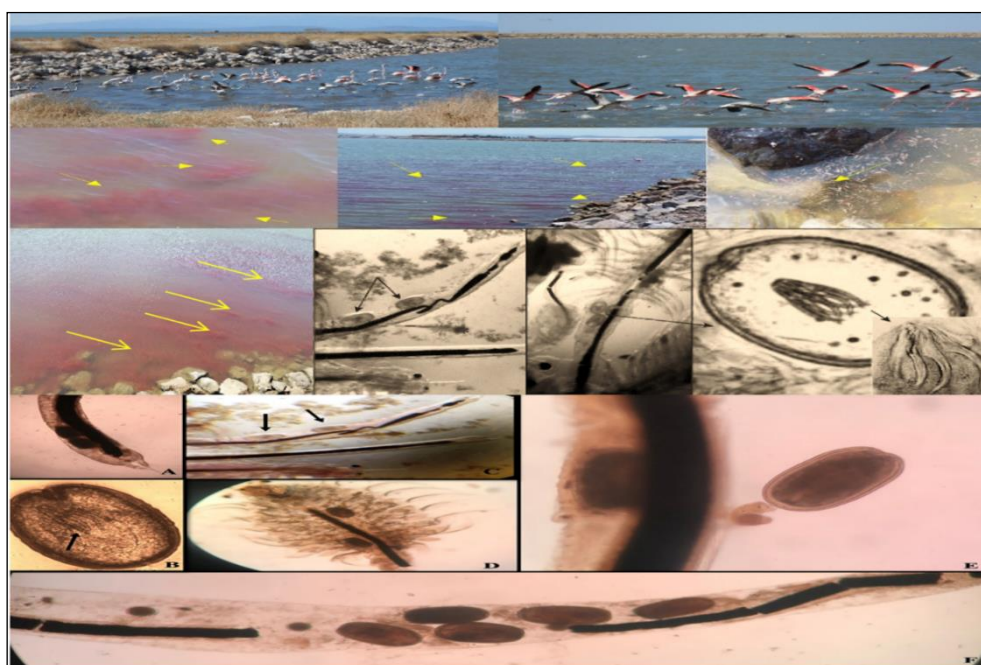


Figure 6- *Artemia parthenogenetica* individuals swimming towards the water surface infected with parasite carried by flamingo birds. (A-B-C-D-E-F). Cysticercooids of *Flamingolepis liguloides* (Gervais 1847) in the brine shrimp (*Artemia parthenogenetica*). A) Parasitic cyst in the *Artemia* caudal furca, B) Isolated parasitic cyst, C) Cysticercooid in the abdomen of the host, D) Cyts of *F. liguloides* in *Artemia* thorax, E) Cysticercooids of *F. liguloides* from *A. parthenogenetica* rectum, F) Parasitic cyts of *F. ligulepis* in *A. parthenogenetica* rectum (The photo was taken by Edis Koru in May-September)

5. Conclusions

Brine shrimp *Artemia* species are live food most commonly used in aquaculture production. It is the first nutrient in the larval stage of many aquaculture applications. Therefore, it is a zooplankton that should be used very carefully microbiologically. This species carries factors that can cause many aquaculture-related diseases. For this reason, it is necessary to know the factors that may cause pollution in the ecosystems in which *Artemia* grows. There is a strong link between parasitic parasitism in flamingos and *Artemia*. There is a noticeable connection based on nutrition between *Artemia*, at the bottom of the food pyramid, and the Flamingo, at the top. Through this relationship there is a risk of parasite contamination to fish with the relationship of *Artemia*, which is an important zooplankton in aquaculture nutrition. For this reason, biological events occurring in wetlands are and must continue to be researched and recorded. It is important to have data and records on all biological characteristics of a wetland that is the habitat of *Artemia*. The life cycle that takes place in wetlands every year depending on many natural factors shows us the situation of encountering different data. In addition, these data on the subject are among the first records of research findings on this geographical region of the Mediterranean (Çamaltı saltern). This is the first study on a *Flamingolepis* species infecting *A. parthenogenetica*, the parasite prevalence in Turkish wetland waters. In order to understand the effects of *F. liguloides* parasitism in the region, it is necessary to investigate the prey-predator relationships and their ecological effects. Saltworks are highly dynamic ecosystems in terms of biological and physicochemical properties. More multidisciplinary studies are needed to understand the parasitism cycle and the interaction between *Artemia* and flamingos in the Çamaltı wetland. Unfortunately, information regarding the population dynamics of *Artemia* in sampling areas in Türkiye is very limited. Comprehensive (such as salt production process, microalgae, zooplankton, benthic data, climate and atmospheric data) research over many years is needed to better understand the behavioral manipulation of this parasite and its effects on the interaction between *Artemia* and flamingos in the Çamaltı saltworks ecosystem.

Data availability: Data are available on request due to privacy or other restrictions

Conflict of Interest: No conflict of interest was declared by the author

Financial Disclosure: The author declares that this study has received no financial support. The work was carried out only with the logistical support of Çamaltı Tuzlası Binbir Gıda Tarım Tuz Ürünleri Sanayi ve Ticaret A.Ş.

References

- Amarouayache M F, Derbal F & Kara M H (2009). The Parasitism of *Flamingolepis liguloides* (Gervais, 1847) (Cestoda, Hymenolepididae) in *Artemia salina* (Crustacea, Branchiopoda) in Two Saline Lakes in Algeria. *Acta Parasitologica* 54(4): 330–34. <https://doi.org/10.2478/S11686-009-0049-8>
- Amat E, Illescas M E & Fernandez J (1991a). Brine Shrimp *Artemia* Parasitized by *Flamingolepis liguloides* (Cestoda, Hymenolepididae) Cysticercoids in Spanish Mediterranean Salterns. Quantitative Aspects. *Vie et Milieu/Life & Environment* 41(4): 237–244. hal-03039955
- Amat F, Gozalbo A, Navarro J C, Hontoria F & Varo I (1991b). Some Aspects of *Artemia* Biology Affected by Cestode Parasitism. *Hydrobiologia* 212: 39–44. <https://doi.org/10.1007/BF00025985>
- Büke E (2002). Sea Bass (*Dicentrarchus labrax* L., 1781) Seed Production. *Turkish of Fisheries and Aquatic Science* 2(1): 61–70
- Balkız Ö, Onmuş O, Sıkı M Ö, Döndürenc O G, Arnaud A & Germain C (2015). Zoology in the Middle East Turkey as a Crossroad for Greater Flamingos *Phoenicopterus roseus*: Evidence from Population Trends and Ring-Resightings (Aves: Phoenicopteridae). *J. Zoology in the Middle East* 61(3) 201–14. <https://doi.org/10.1080/09397140.2015.1058452>
- Bechet A & Johnson A R (2008). Anthropogenic and Environmental Determinants of Greater Flamingo *Phoenicopterus roseus* Breeding Numbers and Productivity in the Camargue (Rhône Delta, Southern France). *Ibis* 150(1): 69–79. <https://doi.org/10.1111/J.1474-919X.2007.00740.X>
- Brawne R, Sargeos P & Troman Clive N A (1991). *Artemia* Biology. CRC Press, Florida <https://doi.org/10.1201/9781351069892>
- Britton R H & Johnson A R (1987). An Ecological Account of a Mediterranean Salina: The Salin de Giraud, Camargue (S. France). *Biological Conservation* 42(3): 185–230. [https://doi.org/10.1016/0006-3207\(87\)90133-9](https://doi.org/10.1016/0006-3207(87)90133-9)
- Bush A O, Lafferty K D, Lotz J M & Shostak A W (1997). Parasitology Meets Ecology on Its Own Terms: Margolis et Al. Revisited. *Journal of Parasitology* 83(4): 575–83. <https://doi.org/10.2307/3284227>
- Curio E (1988). Parasitology in focus. Facts and trends. In E Curio & H Mehlhorn (Eds.), *Behavior and parasitism*, Springer-Verlag, Berlin, pp.149-160
- Gabrion C & MacDonald G (1980). *Artemia* sp. (Crustacea, Anostracea) as Intermediate Host of *Eurycestus Avoceti* Clark, 1954 (Cestoda, Cyclophyllidae). *Annales de Parasitologie Humaine et Comparée* 55: 327–31
- Georgiev B B, Sánchez M I A, Green J, Nikolov P N, Vasileva G P & Mavrodieva S R (2005). Cestodes from *Artemia parthenogenetica* (Crustacea, Branchiopoda) in the Odiel Marshes, Spain: A Systematic Survey of Cysticercoids. *Acta Parasitologica* 50: 105–17
- Georgiev B B, Sánchez M I, Vasileva G P, Nikolov P N & Green A J (2007). Cestode Parasitism in Invasive and Native Brine Shrimps (*Artemia* spp.) as a Possible Factor Promoting the Rapid Invasion of *A. franciscana* in the Mediterranean Region. *Parasitology Research* 101(6): 1647–55. <https://doi.org/10.1007/S00436-007-0708-3>
- Heldt H (1929). Sur La Présence d'un Cysticercocoe Chez *Artemia salina* L. Bull SOS.
- Helluy S & Holmes J C (2005). Parasitic Manipulation: Further Considerations. *Behavioural Processes* 68(3): 205–10. <https://doi.org/10.1016/J.BEPROC.2004.08.011>
- Kaska A (2019). Cytotoxic Activities on Selected Lamiaceae Species from Turkey by Brine Shrimp Lethality Bioassay. *Ordu University Journal of Science and Technology* 9(2):105-111. e-ISSN: 2146-6459

- Kırkağaç M, Gümüş E & Yokuş G (2017). The Effects of Environmental Factors on *Artemia* Population in Tuz Lake (Central Anatolia, Turkey). *Iğdır Univ. J. Inst. Sci. & Tech.* 7(2): 303-312. <https://doi.org/10.21597/jist.2017.143>
- Koru E (2013). The Potential of *Artemia* Population in Çamaltı Saltworks (Sasalı-İzmir) at Aquaculture. *Menba Journal of Fisheries Faculty* 2: 30–40
- Koru E (2022). Cestode Infection of the Native Brine Shrimp (*Artemia parthenogenetica*) in Çamaltı Saltpan (İzmir/Türkiye). *Çanakkale Onsekiz Mart University Journal of Marine Sciences and Fisheries* 5(1): 56–66. <https://doi.org/10.46384/JMSF.1084680>.
- Kornyychuk Y, Anufrieva E, & Shadrin N (2023). Diversity of Parasitic Animals in Hypersaline Waters: A Review. *Diversity* 15(409): 1-21. <https://doi.org/10.3390/d15030409>
- Maksimova A P (1979). Branchiopod Crustaceans as Intermediate Hosts of Cestodes of the Family Hymenolepididae. *Parazitologiya* 4: 349–53. <https://doi.org/10.7717/PEERJ.7395/SUPP-4>
- Mura G (1995). Cestode Parasitism (*Flamingolepis liguloides* Gervais, 1847 Spassky & Spasskaja 1954) in An *Artemia* Population from South-Western Sardinia. *International Journal of Salt Lake Research* 1995 3:2 3(2): 191–200. <https://doi.org/10.1007/BF01990494>
- Redón S, Green A J, Georgiev B B, Vasileva G P & Amat F (2015). Influence of Developmental Stage and Sex on Infection of the American Brine Shrimp *Artemia franciscana* Kellogg, 1906 by Avian Cestodes in Ebro Delta Salterns, Spain. *Aquatic Invasions* 10(4): 415–23. <https://doi.org/10.3391/AI.2015.10.4.05>
- Redón S, Vasileva G P, Georgiev B B & Gajardo G (2020). Exploring Parasites in Extreme Environments of High Conservational Importance: *Artemia franciscana* (Crustacea: Branchiopoda) as Intermediate Host of Avian Cestodes in Andean Hypersaline Lagoons from Salar de Atacama, Chile. *Parasitology Research* 119(10): 3377–90. <https://doi.org/10.1007/S00436-020-06768-3>
- Robert F & Gabrion C (1991). Cestodoses de l'avifaune Camarguaise. Rôle d'*Artemia* (Crustacea, Anostraca) et Stratégies de Rencontre Hôte-Parasite. *Annales de Parasitologie Humaine et Comparée* 66(5): 226–35. <https://doi.org/10.1051/PARASITE/1991665226>
- Rode N O, Lievens E J P, Flaven E, Segard A, Jabbour-Zahab R, Sanchez M I & Lenormand T (2013a). Why Join Groups? Lessons from Parasite-Manipulated *Artemia*. *Ecology Letters* 16(4): 493–501. <https://doi.org/10.1111/ELE.12074>
- Rode N O, Landes J, Landes E J P, Lievens E, Flaven A, Segard R Jabbour-Zahab, Michalakakis Y, Agnew P, Vivarès C P & Lenormand T (2013b). Cytological, Molecular and Life Cycle Characterization of Anostracospora Rigaudi n. g., n. sp. and Enterocytopora *Artemiae* n. g., n. sp., Two New Microsporidian Parasites Infecting Gut Tissues of the Brine Shrimp *Artemia*. *Parasitology* 140(9): 1168–85. <https://doi.org/10.1017/S0031182013000668>
- Sánchez M I, Green A J & Castellanos E M (2006). Temporal and Spatial Variation of an Aquatic Invertebrate Community Subjected to Avian Predation at the Odiel Salt Pans (SW Spain). *Archiv Für Hydrobiologie* 166(2): 199–223. <https://doi.org/10.1127/0003-9136/2006/0166-0199>
- Sánchez M I, Georgiev B B & Green A J (2007). Avian Cestodes Affect the Behaviour of Their Intermediate Host *Artemia parthenogenetica*: An Experimental Study. *Behavioural Processes* 74(3): 293–99. <https://doi.org/10.1016/J.BEPROC.2006.11.002>
- Sánchez M I, Nikolov P N, Georgieva D D, Georgiev B B, Vasileva G P, Pankov P, Paracuellos, Lafferty D K & Green A J (2013). High Prevalence of Cestodes in *Artemia* spp. throughout the Annual Cycle: Relationship with Abundance of Avian Final Hosts. *Parasitology Research* 112(5): 1913–23. <https://doi.org/10.1007/S00436-013-3347-X>
- Sánchez M I, Varo N, Matesanz C, Ramo C, Amat J A & Green A J (2013). Cestodes Change the Isotopic Signature of Brine Shrimp, *Artemia*, Hosts: Implications for Aquatic Food Webs. *International Journal for Parasitology* 43(1): 73–80. <https://doi.org/10.1016/J.IJPARA.2012.11.003>
- Savage A & Knott B (1998). *Artemia parthenogenetica* in Lake Hayward, Western Australia. II. Feeding Biology in a Shallow, Seasonally Stratified, Hypersaline Lake. *International Journal of Salt Lake Research* 1998 7:1 7(1): 13–24. <https://doi.org/10.1023/A:1009084902677>.
- Thiery A, Robert F & Gabrion C (1990). Distribution Des Populations d'*Artemia* et de Leur Parasite *Flamingolepis liguloides* (Cestode, Cyclophyllidea), Dans Les Salins Du Littoral Méditerranéen Français. *Canadian Journal of Zoology* 68(10): 2199–2204. <https://doi.org/10.1139/Z90-305>
- Thomas F, Cezilly F, De Meeüs T, Crivelli A & Renaud F (1997). Parasitism and Ecology of Wetlands: A Review. *Estuaries* 20:3 20(3): 646–54. <https://doi.org/10.2307/1352622>
- Vasileva G P, Redón S, Amat S F, Nikolov P N, Sánchez, M I, Lenormand T & Georgiev B B (2009). Records of Cysticercoids of *Fimbriarioides tadornae* Maksimova, 1976 and *Branchiopodataenia gvozdevi* (Maksimova 1988) (Cyclophyllidea, Hymenolepididae) from Brine Shrimps at the Mediterranean Coasts of Spain and France, with a Key to Cestodes from *Artemia*. *Acta Parasitologica* 54(2): 143–50. <https://doi.org/10.2478/S11686-009-0025-3>



Copyright © 2024 The Author(s). This is an open-access article published by Faculty of Agriculture, Ankara University under the terms of the [Creative Commons Attribution License](https://creativecommons.org/licenses/by/4.0/) which permits unrestricted use, distribution, and reproduction in any medium or format, provided the original work is properly cited.



Potato Plant Leaf Disease Detection Using Deep Learning Method

Cemal Ihsan SOFUOGLU^a , Derya BIRANT^{b*} 

^aDokuz Eylul University, Graduate School of Natural and Applied Sciences, Izmir, TURKEY

^bDokuz Eylul University, Department of Computer Engineering, Izmir, TURKEY

ARTICLE INFO

Research Article

Corresponding Author: Derya BIRANT, E-mail: derya@cs.deu.edu.tr

Received: 04 April 2023 / Revised: 23 September 2023 / Accepted: 25 September 2023 / Online: 09 January 2024

Cite this article

Sofuoglu C I, Birant D (2023). Potato Plant Leaf Disease Detection Using Deep Learning Method. *Journal of Agricultural Sciences (Tarim Bilimleri Dergisi)*, 30(1):153-165. DOI: 10.15832/ankutbd.1276722

ABSTRACT

In agriculture, plant disease detection and cures for those diseases are crucial for high crop production and yield sustainably. Improvements in the automated disease detection and analysis areas may provide important benefits for early action that would allow intervention at earlier stages for cure and preventing spread of the disease. As a result, damages on crop yield could be minimized. This study proposes a new deep-learning model that correctly classifies plant leaf diseases for the agriculture and food sectors. It focuses on the detection of plant diseases for potato leaves from images by designing a new convolutional neural network (CNN)

architecture. The CNN methodology applies filters to input images, extracts key features, reduces dimensions while preserving important characteristics in images, and finally, performs classification. The experimental results conducted on a real-world dataset showed that a significant improvement (8.6%) in accuracy was achieved on average by the proposed model (98.28%) compared to the state-of-the-art models (89.67%) in the literature. The weighted averages of recall, precision, and f-score metrics were obtained around 0.978, meaning that the method was highly successful in disease diagnosis.

Keywords: Agriculture, Disease diagnosis, PlantVillage, Smart farming, Image classification, Deep learning, Convolutional neural networks

1. Introduction

Due to making better predictions and reliability, the development of digitalized systems has been popular in implementing applications for agriculture production areas and fields, such as the identification of crop varieties (Çınar & Koklu 2022; Bayram & Yıldız 2023), detection of weeds (Sabzi et al. 2018), and grading crops (Sabzi et al. 2015); the expansion and development of this technological area also seeks to investigate or detect plant diseases. As a result of unstable environmental conditions and climate change, plant diseases have increased rapidly, which may result in food shortages in places around the world in the near future.

The primary causes of plant diseases and their biotic and abiotic factors are represented in Figure 1, i.e. microorganisms and variables that result in environmental stress, respectively. Fungi, viral and bacterial pathogens differ in type of diseases they cause. They infect the crops by killing the cells of plants. The cause of fungal infection may be the result of infected seeds, crop rubbish, inappropriate soil, weeds, and other nearby crops. Plants may be infected by bacteria internally, which may not show any internal or external symptoms during the development of a disease. Viral infections are also difficult to detect which means that diagnosis can be challenging. The virus spreads through carriers of different bugs such as leafhoppers, whiteflies, cucumber beetles, and insects. Due to the presence of these factors (i.e., bacteria, fungi, viruses) and environmental changes (i.e., drought, frost), farmers are face numerous plant diseases that decrease the quality and yield of their crops. Additionally, the bacteria-infected plant spreads the infection to nearby plants and increases the rate of spreading. For these reasons, early-stage detection is crucial in order to protect plants from infection. It is reported that 80-90% of plant diseases occur on the plant leaves (Salih et al. 2020). With this in mind, this study focuses on the plant leaf, rather than the whole plant.

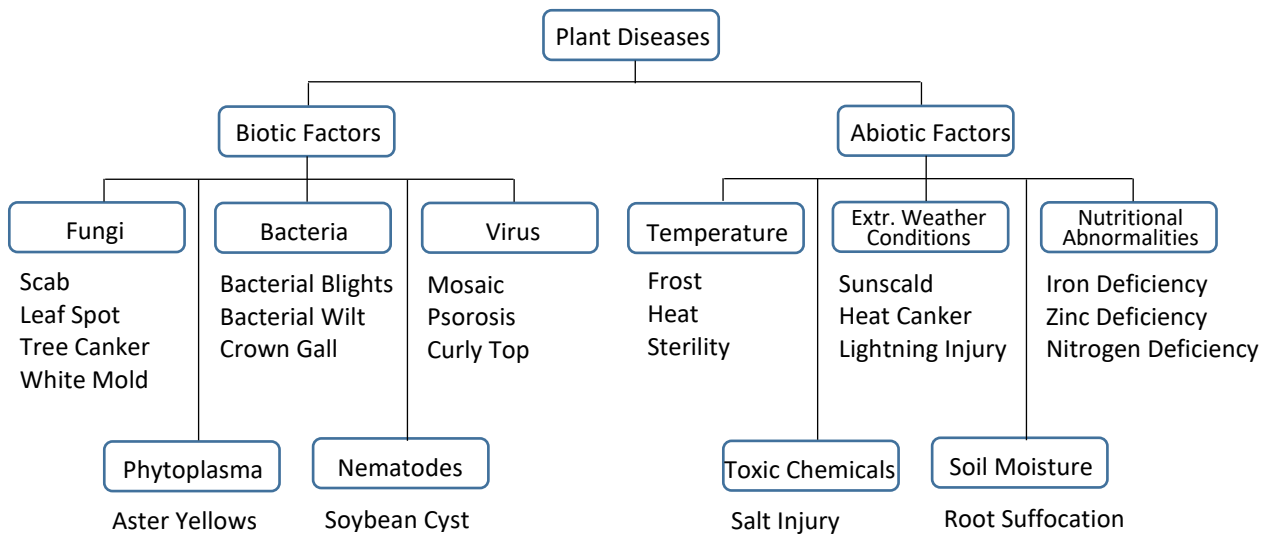


Figure 1- Factors & effects of diseases on plants

Visual identification of diseases by humans in plants of a large area is costly and time-consuming, depending on their ability which may not be accurate (Prajna 2021). The diseases could be very diverse because of the variety of plants and microorganisms. In addition, variations in the types of plant leaf diseases and the meteorological conditions due to climate change and global warming could increase the disease spread rate to the regions where they have not been seen before, in which even experts may be unfamiliar with (Sladojevic et al. 2016). Therefore, it is important to design a smart system that will help diagnose plant disease accurately and automatically (Gerdan Koc et al. 2022). A mobile application will further help non-expert farmers and farmers who do not have phytopathological and agronomic support infrastructure (Ferentinos 2018).

Plant diseases can have enormous impact on farming lands and forests, which threaten production and overall food quality and safety. Early stage and accurate detection of such diseases play a crucial role in prevention, guidance or management strategies. In recent years, artificial intelligence (AI) has expanded and developed and improved disease detection in agriculture. AI-based solutions provide alternative ways for automated disease diagnosis. These methods have the ability to work with large image datasets to create and train models, and diagnose and classify diseases using patterns with a high success prediction probability. The progress in such areas create capabilities that enhance disease detection, early-stage intervention, diagnosis, and suggestions for further-steps including cures.

The significant developments in machine learning (ML) technologies can result in the design and implement of an architecture for automated systems which could help to attain fast and accurate results to detect plant diseases. For example, Mathew et al. (2022) proposed a machine-learning-based automated system with a combination of support vector machine (SVM), k-nearest neighbors (KNN), and decision tree (DT) methods for classifying the diseases on potato leaves. Some studies worked with commonly-used approaches; for example, Sharma et al. (2021) compared the prediction success rates between SVM, DT, and KNN. Moreover, Iqbal & Talukder (2020) investigated the performances of logistic regression (LR), random forest (RF), naive Bayes (NB), linear discriminant analysis (LDA), KNN, SVM, and DT. Ismail et al. (2020) compared linear, quadratic, and cubic SVMs for the plant disease detection task and reported that cubic SVM obtained higher accuracy than others. Pardede et al. (2018) compared different kernels (linear, radial basis function, and polynomial) for SVM and stated that the linear kernel achieved the best accuracy. Some studies proposed a hybrid methodology like Singh & Kaur (2020) by combining the k-means algorithm with SVM and Mukherjee (2020) by creating the architecture using SVM and fuzzy logic.

Deep learning (DL) is a developed sub-category of machine learning that computes more complex problems with a variety of data types like videos and images. DL techniques received a great deal of attention because of their capability to achieve higher prediction accuracy than traditional ML algorithms. Recently, some efforts (Moharekar et al. 2022; Shwetha & Sneha 2022; Ahmed & Yadav 2023) have been made that focused on DL algorithms to improve prediction accuracies in the detection of plant diseases. Several research papers (Sarker et al. 2022; Kumar & Patel 2023) compared various DL architectures such as convolutional neural network (CNN), residual network (ResNet), and visual geometry group (VGG). Nanekaran et al. 2023 used pre-trained model architectures like GoogleNet, Zeiler and Fergus Network (ZFNet), and AlexNet, which were trained by a high variety of data and capability of working with different tasks. Atik (2022); Ertem & Özbay (2022) investigated the performances of different architectures like AlexNet, GoogleNet, ShuffleNet, and ResNet with tomato leaves. Contributions in DL in the agriculture area have been made by the works of Monowar et al. (2022), He et al. (2022), Tiwari et al. (2020), Oppenheim & Shani (2017), and Patil et al. (2017). One deep learning technique, CNN, is fast becoming a popular classification method due to its ability to overcome challenges encountered in complex problems (Ghosh & Roy 2021; Saeed et al. 2021; Jasim & Al-Tuwajjari 2020; Chaitanya & Yasudha 2020). Therefore, this study employed the CNN technique for disease detection and classification on potato leaves.

In the literature, different ML and DL algorithms have been tested for plant leaf disease classification in different countries, under different environmental conditions, and for different plants such as rice (Nanehkaran et al. 2023), tomatoes (He et al. 2022), peppers (Bhagat & Kumar 2023), apples (He et al. 2022), maize (Nanehkaran et al. 2023), peaches (Wagle & Harikrishnan 2021), cherries (Kurmi & Gangwar 2022), corn (Ciran & Özbay 2022; Pardede et al. 2018), cucumbers (Nanehkaran et al. 2023), apricots (Türkoğlu et al. 2020), olive (Dikici et al. 2022), lemons (Saygılı 2023), and strawberries (Wagle & Harikrishnan 2021). This study focuses on the detection of diseases for potato crops due to their large scale and varied uses.

The main contributions of this paper can be summarized as follows. (i) It proposes a new deep-learning model that correctly classifies plant diseases for the agriculture sector. (ii) This study is original in that it especially focuses on the detection of plant diseases for potato leaves by designing a CNN architecture.

2. Material and Methods

2.1. Dataset description

The PlantVillage dataset (Hughes & Salathe 2015) is a resource in the agriculture area and plant pathology. The dataset contains a collection of labeled images with various plant types such as tomato, potato, pepper, and more. The dataset contains the collected and reported diseases for each plant and is used as an open-source dataset to develop and evaluate machine learning, deep learning, or any other models to design and detect diseases through classification. In our study, we used potato plant diseases from the PlantVillage dataset. It contains 2152 images of potato leaves divided into 3 categories: healthy, early blight, and late blight. Figure 2 shows example leaf images that belong to potato plants.

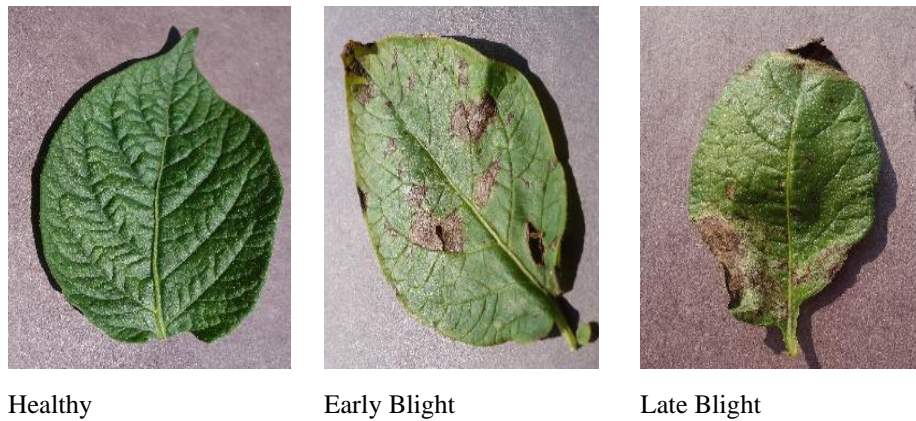


Figure 2- Sample images of potato leaf diseases

The PlantVillage dataset is a well-known and popular dataset for crop disease with a significant number of public records available. All images in the dataset were captured by Land Grant Universities in the USA (Penn State, Cornell, Florida State, and others). They aimed to diagnose plant diseases by using advanced technologies to support farmers around the globe, by providing the knowledge they need to protect and improve crop health. The diseases of plants were identified and labeled by plant pathology experts. These experts directly worked in the field with two technicians providing the diagnosis and used standard phenotyping approaches in plant pathology. The dataset only contains the images of expertly identified leaves, and, therefore, these images are sufficient for each disease to be used in classification. The details about the technical validation of the dataset can be found in the related article (Hughes & Salathe 2015).

To classify images correctly, it is important to perform a pre-processing stage which includes resizing and rescaling operations. These processes help the algorithm to minimize the possible errors by capturing the characteristic features of diseases while preparing to feed the algorithm. The input image size is 256 x 256 pixels, which was obtained with a resizing stage for efficiency. After that, a rescale operation was performed to scale the image related to the given ratio (1/255) to preserve the same distribution throughout the image by protecting the key features in the images. In this way, the pre-processing operation converted each pixel value in the range 0-255 to values in the range 0-1.

2.2. Proposed method

This section describes and explains the proposed methodology for the classification of potato leaf diseases. The idea of detecting such diseases in plants is to identify unordinary or sick parts of the leaves which are used as images to feed the method.

The proposed deep-learning-based model has numerous advantages. Firstly, since the detection of leaf disease systems could have a significantly important role in the early stages. If the disease is quickly diagnosed, it can help to prevent the disease from

spreading. In addition, such a system could provide benefits to farmers who do not have any information, or knowledge about such diseases and their possible impact on plants. The proposed model could be used to detect the disease and learn how to act, preserve, and improve crop health conditions.

The proposed model was designed specifically to perform accurate classification of plant leaf diseases related to potato leaves and to execute operations sufficiently and accurately. The CNN architecture can automatically characterize the local features. With the architecture, patterns and relationships in images can be captured effectively through the algorithm. Furthermore, CNNs can extract unique patterns and features from each image and learn by improving every cycle round using mathematical operations and features like convolutional and pooling layers. These allow CNN architecture to gain the ability to recognize patterns and features, and execute complex issues efficiently. Such capabilities in CNN architecture allows models to execute prediction operations with high accuracies and produce better results than conational models in most cases.

The general structure of the proposed approach is illustrated in Figure 3. The initial step is to prepare a dataset to feed the deep learning algorithm as input. The plant leaf disease dataset includes different disease images and their labels as directories. Pre-processing is performed to improve the quality of extracting the needed segments or features from the input images. Different operations can be performed for images like rescaling and resizing. Pre-processing operations are important since they can affect the model's classification performance directly. Afterward, the dataset is divided into training, validation, and testing sets. The next step is the training process in which the inputs are fed to the CNN architecture and trained to evaluate a set of weights that will result in a prediction with the trained labels. After that, the performance of the model is evaluated according to various criteria such as accuracy, precision, recall, and f-score. Finally, the class label of the given test image is obtained as an output from the deep learning model which is evaluated with the achieved probability scores for each label.

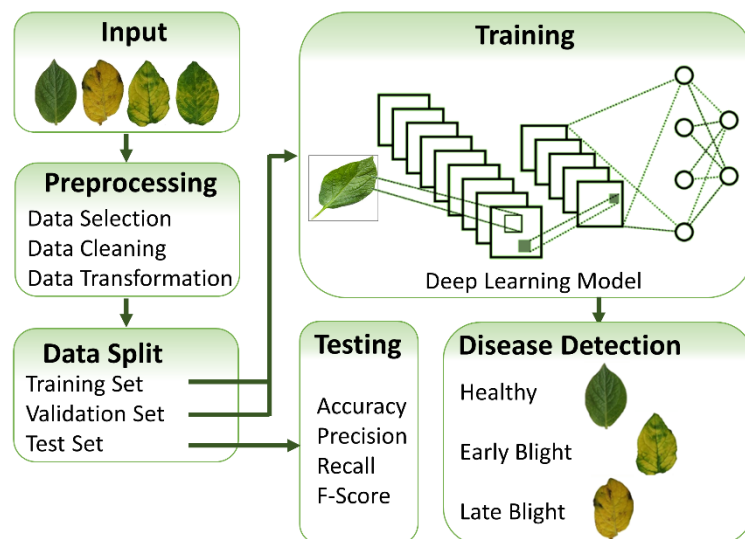


Figure 3- The proposed method: an overview of the general structure

Figure 4 represents the architecture of the proposed model based on the CNN structure. CNN is a type of deep neural network, mostly used to analyze images and videos. The convolution layer uses filters that perform convolution operations which is the dot product of two matrices. One of the matrices is the kernel which is a set of parameters, whereas another matrix is the input that is converted to an array. The pooling operation is simple in that there is a two-dimensional filter over each feature by sliding on them and creating an array with a smaller portion that contains the features extracted from the Conv2D layer. Pooling layers are useful in reducing the number of parameters to be learned and simultaneously decrease the computational complexity of the network. The fully connected input layer, called flatten, takes the output from the last layer and performs a flattening operation to turn it into a single vector. After the flattening operation is completed, the output is fed to the neural network and applies weights to predict the class label. In the end, it gives the final probabilities for each label.

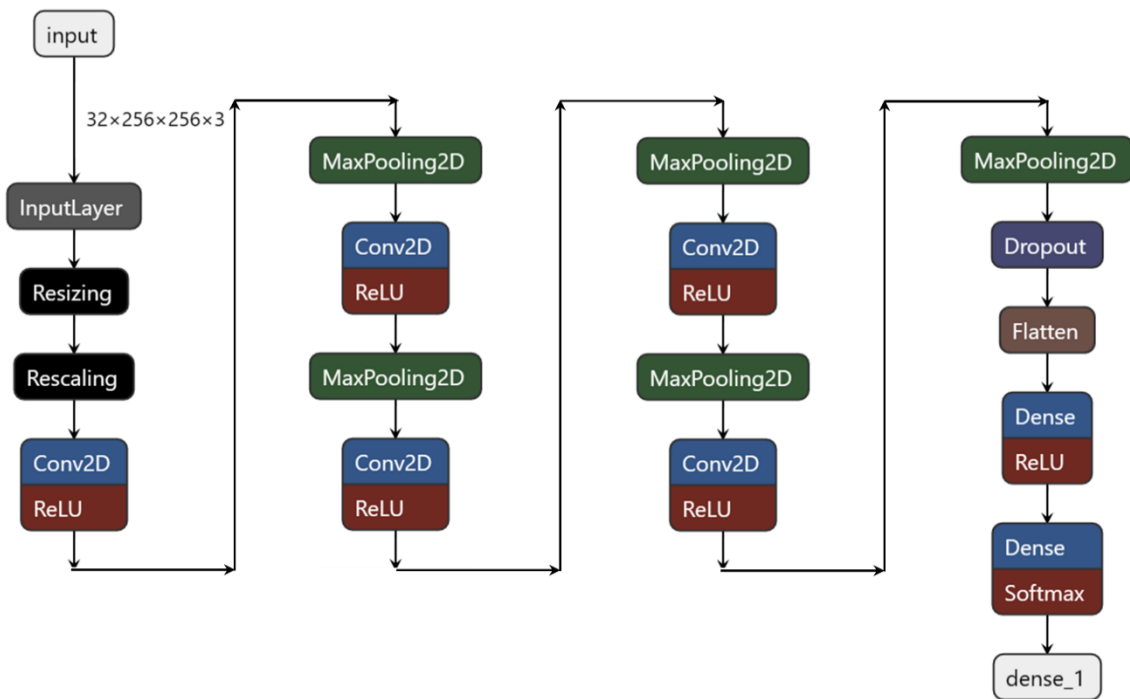


Figure 4- Proposed CNN architecture for potato plant leaf disease detection and classification

The proposed method includes the steps described below.

1. Reading input images from the dataset.
2. Pre-processing images using resize and rescale operations to preserve standards between images.
3. Dividing the data into a training dataset, a testing dataset, and a validation dataset.
4. Applying filters to input images, extracting key features through convolution operations which are performed with Conv2D and Rectified Linear Unit (ReLU) in Figure 4.
5. Reducing the computational complexity of the network while preserving important features which is represented as MaxPooling2D in Figure 4.
6. After convolution and pooling operations are performed, dropout functionality is executed to prevent overfitting to force the model to learn independent features by setting randomly a portion of the input units to zero.
7. After the dropout operation, the feature maps are flattened and transformed into one-dimensional vectors. Then, those vectors are connected to fully connected layers. These layers classify the learned features by mapping the extracted features to the labeled outputs.
8. The final step involves performing classification based on the outputs from the fully connected layers with the usage of the softmax activation function at the end of the proposed model as a layer. This function calculates the probabilities for each class. The sum of the predicted probabilities needs to be in the range of 0 to 1. The class that has the highest probability is labeled as the predicted result which is done using dense_1 in Figure 4.
9. After the model is created, with the usage of testing and validation datasets, performance metrics are calculated to identify the effectiveness and reliability of the proposed model. The classification metrics could be accuracy, precision, recall, and f-score.

Accuracy is the proportion of correct results (either true positive or true negative) in a testing set. It is calculated using the following equation:

$$Accuracy = \frac{(TP + TN)}{(TP + FP + FN + TN)}$$

Where; the parameters TP (True Positives), TN (True Negatives), FP (False Positives), and FN (False Negatives) are the metrics to calculate specificity, sensitivity, and accuracy in performance measurement. TP is used to present the number of correctly predicted positive classes. TN is the result of correctly predicted negative classes. FP is the number of cases predicted positive when they are negative. Finally, FN represents the number of cases predicted as negative when the results should be positive.

Precision is the accuracy of positive predictions with the proportion of correctly predicted positive classes out of the total classes positively predicted. The calculation formula is as follows:

$$Precision = \frac{TP}{(TP + FP)}$$

Recall (sensitivity) represents correctly predicted positive classes divided by the total actual positive classes. It is calculated using the following equation:

$$Recall = \frac{TP}{(TP + FN)}$$

The f-score is a metric that is used in classification problems that measure the model performance using correctly predicted positive classes (recall) with the accuracy of positive predictions (precision). The calculation formula is as follows:

$$Fscore = \frac{2 * (Precision * Recall)}{(Precision + Recall)}$$

Macro-averages represent the average across all classes. The performance metric (e.g., precision, recall, or f-score) take place separately for each class. For weighted-averages, the metric is also calculated separately for each class and weighted by the class usage frequencies.

3. Results and Discussion

In this section, the overall achieved prediction accuracies are presented. The proposed CNN model was trained and tested using the potato leaf images dataset. The data is divided into three groups: training, validation, and testing. The training set with 0.8, the testing set with 0.1, and the validation set with 0.1 split ratio are evaluated.

The proposed model obtained 96.82% accuracy and 8.76% loss in training, and 99.48% accuracy and 4.55% loss in the validation dataset. In the testing dataset, the model achieved 98.28% accuracy and 6.44% loss for potato leaf disease classification. Figure 5 and Figure 6 show the ranges of the model indicator that emphasize the effectiveness of the proposed model. Figure 5 represents the accuracy of the proposed model on both the training and testing datasets throughout 15 epochs. It is clear that the model performance increases as the number of epochs increases. Figure 6 shows the loss plot for the proposed model on the training and testing sets for 15 epochs. In general, the model provides low-loss values with increasing epochs.

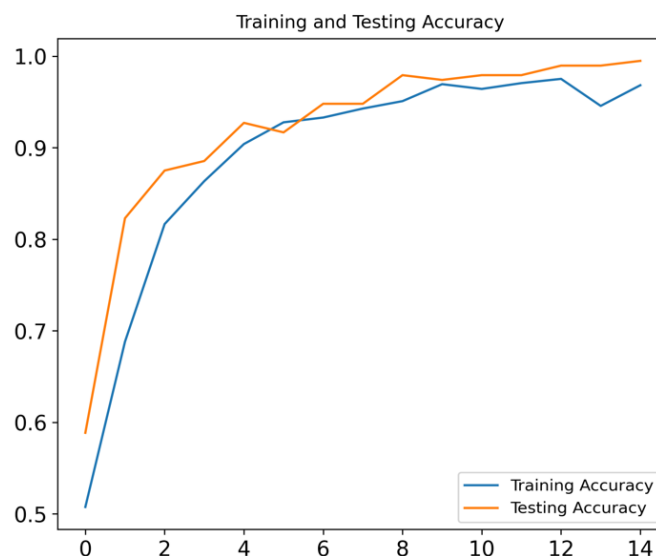


Figure 5- Training & testing accuracy graph of the proposed model



Figure 6- Training & testing loss graph of the proposed model

Table 1 shows the performance of the proposed model using precision, recall, and f-score results for potato diseases. The macro-averages and weighted-averages range between 0.946 and 0.985, which are very close to 1, meaning that the method does return few errors.

Table 1- The performance of the proposed model for each class in terms of precision, recall, and f-score metrics

<i>Potato Leaf Disease</i>	<i>Precision</i>	<i>Recall</i>	<i>F-score</i>
Early Blight	1.000000	0.972727	0.986175
Late Blight	0.955357	1.000000	0.977169
Healthy	1.000000	0.866667	0.928571
Macro Average	0.985119	0.946465	0.963972
Weighted Average	0.979410	0.978448	0.978297

Table 2 represents the confusion matrix of potato diseases which represents the proposed CNN algorithm performance over the validation dataset. It visualizes the predicted true positive, false negative, false positive, and true negative values for each class label. High diagonal elements of the confusion matrix (102, 115, and 12) for each class, with low non-diagonal elements, confirmed the high performance and robustness of the machine learning model for predicting plant leaf diseases. According to the matrix, the proposed model produced only 3 incorrect outputs out of 232 predictions.

Table 2- Confusion matrix of the proposed model for all potato diseases

	<i>Early Blight</i>	<i>Late Blight</i>	<i>Healthy</i>
Early Blight	102	0	0
Late Blight	1	115	2
Healthy	0	0	12

Figure 7 shows samples that were taken from the dataset randomly and labeled with actual and predicted labels using the proposed model for potato leaves. As can be seen, the constructed model usually had no difficulty in identifying potato leaf diseases. For example, the first sample leaf image was labeled correctly with a 99.96% probability.

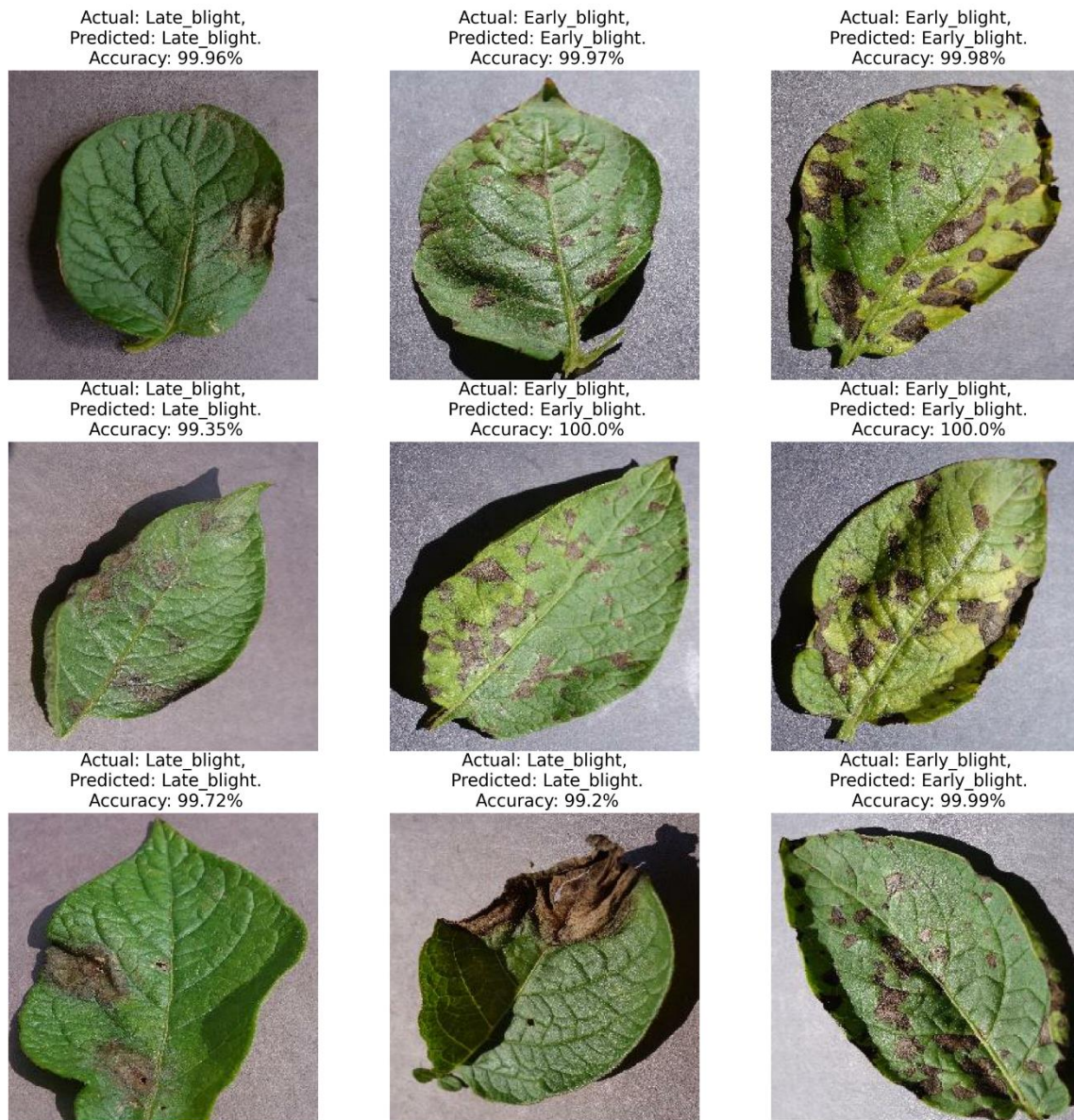


Figure 7- Sample prediction results for potato leaf images

Table 3 shows the results of previously designed models for the detection of potato plant leaf diseases. Based on the table, it is clear that the proposed model achieved a higher performance (98.28%) than the state-of-the-art models (89.67%) on the same dataset and same plant type on average. Consequently, the model demonstrated its superiority over the other models with an average of 8.6% improvement. For example, it performed better than RF (92%) (Swetha & Jayaram 2019), DT (91%) (Iqbal & Talukder 2020), KNN (86.40%) (Sharma et al. 2021), and LR (74.80%) (Kurmi & Gangwar 2022). As observed in Table 3, SVM is the most frequently used methodology. As seen in Table 3, the proposed model outperformed SVM-based models. Compared to the deep learning models such as Google Network (GoogleNet) (92.33%) (Nanehkaran et al. 2023), dense network (DenseNet-121) (95.00%) (Ahmed & Yadav 2023), efficient DenseNet (97.20%) (Mahum et al. 2023), VGG (91.60%) (Kumar & Patel 2023), AlexNet (90.00%) (Wagle & Harikrishnan 2021), and ResNet-18 (95.81%) (He et al. 2022), the proposed model achieved the highest accuracy.

In addition to the accuracy indicator, the precision, recall, and f-score values were also compared. Sharma et al. (2021) obtained the results of approximately 0.899 for all the metrics using the SVM method. Islam et al. (2017) achieved 0.9500 for all these metrics using the SVM method. Mathew et al. (2022) achieved values of 0.9205 and 0.9200 for precision and recall, respectively, from their model. In another study (Aurangzeb et al. 2020), the results of these measures were obtained using Cubic SVM with precision (0.9433) and recall (0.8530) values. The precision value was recorded as 0.9160 by Sanjeev et al. (2020). Jeyalakshmi & Radha (2020) recorded precision (0.9679), recall (0.9702), and f-score (0.9689) values using the SVM method. Mukherjee (2020) measured and obtained precision, recall, and f-score as 0.5655, 0.4562, and 0.5050, respectively. When precision, recall, and f-score metrics are considered, the proposed model in this study performed better than the previous studies by obtaining 0.9794, 0.9784, and 0.9783, respectively.

Table 3- Comparison of the proposed model compared to the state-of-the-art models on the potato leaf image dataset

<i>Reference</i>	<i>Year</i>	<i>Method</i>	<i>Accuracy (%)</i>
Ahmed & Yadav	2023	DenseNet-121	95.00
Mahum et al.	2023	DenseNet-201	96.03
		Efficient DenseNet	97.20
Nanehkaran et al.	2023	AlexNet	90.00
		GoogleNet	92.33
		ZFNet	89.33
		CNN	91.33
		Le Network (LeNet)	91.00
Bhagat & Kumar	2023	SVM	97.00
Kumar & Patel	2023	VGG	91.60
		RF	73.80
		Deep CNN	92.90
		First Scalable Neuromorphic Fault-Tolerant Context-Dependent Learning	94.00
		Dendritic Event-Based Processing	93.00
		Entropy-based Local Binary Pattern	90.00
		Hierarchical Deep Learning CNN	95.77
		Tree-CNN	86.50
Mathew et al.	2022	Radial Basis Function Neural Network	86.50
		SVM	83.00
Sarker et al.	2022	Voting (SVM + KNN + DT)	92.00
		CNN	93.00
Shwetha & Sneha	2022	ResNet50	97.00
		VGG19	84.00
		Backpropagation Neural Network	92.00
Moharekar et al.	2022	SVM	95.00
He et al.	2022	VGG19 + LR	97.80
		CNN	94.60
Monowar et al.	2022	ResNet-18	95.81
		Disease Image Recognition based on Bilinear Residual Networks	96.05
		Bootstrap Your Own Latent	88.30
		Simple Siamese	86.10
Kurmi & Gangwar	2022	Cross Iterative Kernel K-means enhanced with Image Classification and Similarity Measurements	82.50
		Deep CNN	89.90
		Bag-of-visual-words (BoW) + Fisher Vectors (FV) + Hand-Crafted Feature (HCF) + SVM	91.90
Rozaqi et al.	2021	BoW + FV + HCF + LR	89.60
		BoW + FV + HCF + Multi-Layer Perceptron	87.10
		VGG16	95.00
		CNN - Sederhana	80.00
Wagle & Harikrishnan	2021	Inception-V3	78.00
		ResNet-50	78.00
Ghosh & Roy	2021	SVM	95.83
		AlexNet	90.00
Kaur & Devendran	2021	CNN	87.47
		Scale-Invariant Feature Transform (SIFT) + Ensemble	88.23
		Law's Mask + Gabor + Ensemble	95.66
		Law's Mask + SIFT + Gabor + Ensemble	93.16
Saeed et al.	2021	Gabor + Ensemble	84.23
		CNN	91.67
Sharma et al.	2021	SVM	92.90
		KNN	86.40
		DT	78.70
Guo et al.	2021	GhostNet	97.17
Ismail et al.	2020	Linear SVM	90.00
		Quadratic SVM	88.00
		Cubic SVM	91.30
		Boosted Tree	94.70
		Deep Learning	90.40
Tiwari et al.	2020	VGG19	97.80
Aurangzeb et al.	2020	Cubic SVM	94.50
		LDA	92.70
		Ensemble Tree	92.60

Table 3 (Continue) - Comparison of the proposed model compared to the state-of-the-art models on the potato leaf image dataset

<i>Reference</i>	<i>Year</i>	<i>Method</i>	<i>Accuracy (%)</i>
Singh & Kaur	2020	K-Means + SVM	95.99
Mukherjee	2020	SVM + Fuzzy Logic	91.59
Iqbal & Talukder	2020	LR	94.00
		RF	97.00
		KNN	91.00
		NB	84.00
		DT	91.00
		LDA	78.00
Jeyalakshmi & Radha	2020	NB	88.67
		KNN	94.00
		SVM	96.83
Chaitanya & Yasudha	2020	CNN	94.84
Ahmad et al.	2020	Local Binary Pattern	92.50
		Directional Local Quinary Patterns	96.20
		Local Ternary Patterns	90.60
Jasim & Al-Tuwaijari	2020	CNN	97.20
Sanjeev et al.	2020	Feed Forward Neural Network	96.50
Singh & Kaur	2019	Gray-Level Co-Occurrence Matrix + KNN	97.00
Swetha & Jayaram	2019	RF	92.00
		SVM	94.00
		DT	91.00
		KNN	89.00
		LR	16.00
		NB	85.00
Pardede et al.	2018	SVM - Linear	87.01
		SVM - Radial Basis Function	83.99
		SVM - Polynomial (Order 2)	83.06
		SVM - Polynomial (Order 3)	79.58
Islam et al.	2017	SVM	95.00
Oppenheim & Shani	2017	VGG16	96.00
Patil et al.	2017	Neural Networks	92.00
		RF	79.00
		SVM	84.00
Aparajita et al.	2017	Segmentation Methodology	96.00
<i>Average</i>			89.67
Proposed Model	Convolutional Neural Network		98.28

In a deep learning study, there are two main types of uncertainty: model uncertainty and data uncertainty. Model uncertainty (MU) includes the uncertainty in network architecture design that could yield a high performance. Data uncertainty (DU)

typically refers to incorrect, incomplete, or unknown samples in input data that cause uncertainty in the corresponding output. In this study, the MU was assessed by using various metrics, including accuracy, precision, recall, and f-score; the MU was measured using the Wilcoxon statistical test. The differences between the results of various CNN architectures given in Table 3 and the result of the proposed CNN architecture were evaluated in a pairwise comparison manner. The p-value ($0.03781e-4$) obtained by the Wilcoxon test indicates that the proposed CNN architecture is proper for making an accurate prediction since the p-value is smaller than the significance threshold (0.05). In the point of data uncertainty, the proposed model was tested on a public and widely-used dataset in the literature. The information on data collection and its technical validation can be found in (Hughes & Salathe 2015).

4. Conclusions

The development of detection systems is crucial for achieving and performing stable, precise, and reliable predictions in agriculture. The detection of plant diseases can be achieved through the use of general image processing methods and with a deep learning algorithm that can be integrated at various stages of a plant's life cycle. The effort performed to analyze and identify diseases could be reduced and simplified with the usage of automation technologies in agriculture which, could provide a healthy and sustainable environment for plants and it could limit significant threats like extinction of various plant species.

The main findings of this study can be summarized as follows:

- The results of the experiments showed that the proposed model achieved 98.28% accuracy in potato leaves.
- On the testing dataset, the model obtained a 6.44% loss for potato leaf disease classification.
- The model presented in this study performed very well by achieving precision (0.9794), recall (0.9784), and f-score (0.9783) values.
- The CNN model reached a high accuracy in a number of epochs (15 iterations).
- According to the confusion matrix, the proposed model produced only 3 incorrect outputs out of 232 predictions over the validation dataset.
- When the results of the studies (89.67%) in the literature were compared, the performance was approximately 8.6% improved on average.

One limitation of this study is that it is capable of detecting only diseases that are labeled in the dataset used for the proposed model training which are named as healthy, early and late blight. Future studies could focus on gathering well-designed and easily processed datasets that include other diseases, and in this way, improve the performance of previously found methods. Another possible future study may also be the use of detection algorithms in mobile devices to assist people who do not have an opportunity to access such applications for their plants for early-stage support.

References

- Ahmad W, Shah S M A & Irtaza A (2020). Plants disease phenotyping using quinary patterns as texture descriptor. *KSII Transactions on Internet and Information Systems* 14(8): 3312-3327. doi.org/10.3837/tiis.2020.08.009
- Ahmed I & Yadav P K (2023). A systematic analysis of machine learning and deep learning based approaches for identifying and diagnosing plant diseases. *Sustainable Operations and Computers* 4: 96-104. doi.org/10.1016/j.susoc.2023.03.001
- Aparajita A, Sharma R, Singh A, Dutta M K, Riha K & Kriz P (2017). Image processing based automated identification of late blight disease from leaf images of potato crops. In: *Proceedings of the 40th International Conference on Telecommunications and Signal Processing (TSP)*, 05-07 July, Barcelona, Spain, pp. 758-762. doi.org/10.1109/tsp.2017.8076090
- Atik I (2022). Classification of plant leaf diseases using deep learning methods. *Kahramanmaraş Sutcu Imam University Journal of Engineering Sciences* 25(2): 126-137. (In Turkish) doi.org/10.17780/ksujes.1096541
- Aurangzeb K, Akmal F, Khan M A, Sharif M & Javed M Y (2020). Advanced machine learning algorithm based system for crops leaf diseases recognition. In: *Proceedings of the 6th Conference on Data Science and Machine Learning Applications (CDMA)*, 4-5 March, Riyadh, Saudi Arabia, pp. 146-151. doi.org/10.1109/cdma47397.2020.00031
- Bayram F & Yıldız M (2023). Classification of some barley cultivars with deep convolutional neural networks. *Journal of Agricultural Sciences (Tarim Bilimleri Dergisi)* 29(1): 262-271. doi.org/10.15832/ankutbd.815230
- Bhagat M & Kumar D (2023). Efficient feature selection using BoWs and SURF method for leaf disease identification. *Multimedia Tools and Applications* 82: 28187-28211. doi.org/10.1007/s11042-023-14625-5
- Chaitanya P K & Yasudha K (2020). Image based plant disease detection using convolution neural networks algorithm. *International Journal of Innovative Science and Research Technology* 5(5): 331-334
- Ciran A & Özbay E (2022). Classification of maize leaf diseases by fusion of pre-trained CNN architectures. *European Journal of Science and Technology* 44: 74-83. (In Turkish) doi.org/10.31590/ejosat.1216356
- Çınar İ & Koklu M (2022). Identification of rice varieties using machine learning algorithms. *Journal of Agricultural Sciences (Tarim Bilimleri Dergisi)* 28(2): 307-325. doi.org/10.15832/ankutbd.862482
- Dikici B, Bekçioğulları M F, Açıkgöz H & Korkmaz D (2022). Performance investigation of pre-trained convolutional neural networks in olive leaf disease classification. *Konya Journal of Engineering Sciences* 10(3): 535-547. (In Turkish) doi.org/10.36306/konjes.1078358
- Ertem S & Özbay E (2022). Disease detection in tomato leaf images by deep feature combination approach in classification problem. *European Journal of Science and Technology* 44: 84-92. (In Turkish) doi.org/10.31590/ejosat.1216380
- Ferentinos K P (2018). Deep learning models for plant disease detection and diagnosis. *Computers and Electronics in Agriculture* 145: 311-318. doi.org/10.1016/j.compag.2018.01.009

- Gerdan Koc D, Koc C & Vatandas M (2022). Diagnosis of tomato plant diseases using pre-trained architectures and a proposed convolutional neural network model. *Journal of Agricultural Sciences (Tarim Bilimleri Dergisi)* 29(2): 627-638. doi.org/10.15832/ankutbd.957265
- Ghosh A & Roy P (2021). AI Based automated model for plant disease detection, a deep learning approach. *Communications in Computer and Information Science* 1406: 199-213. doi.org/10.1007/978-3-030-75529-4_16
- Guo Y, Fang Z, Zhang S & Dong H (2021). Classification of potato early blight with unbalanced data based on GhostNet. In: *Proceedings of the 3rd International Academic Exchange Conference on Science and Technology Innovation (IAECST)*, 10-12 December, Guangzhou, China, pp. 559-563. doi.org/10.1109/iaecst54258.2021.9695532
- He Y, Gao Q & Ma Z (2022). A crop leaf disease image recognition method based on bilinear residual networks. *Mathematical Problems in Engineering*, 2022: 1-15. doi.org/10.1155/2022/2948506
- Hughes D P & Salathe M (2015). An open access repository of images on plant health to enable the development of mobile disease diagnostics. *ArXiv*, arXiv:1511.08060. https://arxiv.org/pdf/1511.08060
- Islam M, Dinh A, Wahid K A & Bhowmik P K (2017). Detection of potato diseases using image segmentation and multiclass support vector machine. In: *Proceedings of the Canadian Conference on Electrical and Computer Engineering*, 30 April-3 May, Windsor, ON, Canada, pp. 1-4. doi.org/10.1109/ccece.2017.7946594
- Ismail W, Khan M A, Shah S A, Javed M Y, Rehman A & Saba T (2020). An adaptive image processing model of plant disease diagnosis and quantification based on color and texture histogram. In: *Proceedings of the 2nd International Conference on Computer and Information Sciences (ICCIS)*, 13-15 October, Sakaka, Saudi Arabia, pp. 1-6. doi.org/10.1109/iccis49240.2020.9257650
- Iqbal M A & Talukder K H (2020). Detection of potato disease using image segmentation and machine learning. In: *Proceedings of the International Conference on Wireless Communications Signal Processing and Networking (WiSPNET)*, 4-6 August, Chennai, India, pp. 43-47. doi.org/10.1109/wispnet48689.2020.9198563
- Jasim M A & Al-Tuwaijari J M (2020). Plant leaf diseases detection and classification using image processing and deep learning techniques. In: *Proceedings of the International Conference on Computer Science and Software Engineering (CSASE)*, 16-18 April, Duhok, Iraq, pp. 259-265. doi.org/10.1109/csase48920.2020.9142097
- Jeyalakshmi S & Radha R (2020). An effective approach to feature extraction for classification of plant diseases using machine learning. *Indian Journal of Science and Technology* 13(32): 3295-3314. doi.org/10.17485/ijst/v13i32.827
- Kaur N & Devendran Dr V (2021). Plant leaf disease detection using ensemble classification and feature extraction. *Turkish Journal of Computer and Mathematics Education* 12(11): 2339-2352.
- Kumar A & Patel V K (2023). Classification and identification of disease in potato leaf using hierarchical based deep learning convolutional neural network. *Multimedia Tools and Applications* 82: 31101-31127. doi.org/10.1007/s11042-023-14663-z
- Kurmi Y & Gangwar S (2022). A leaf image localization based algorithm for different crops disease classification. *Information Processing in Agriculture* 9(3): 456-474. doi.org/10.1016/j.inpa.2021.03.001
- Mathew A, Antony A, Mahadeshwar Y, Khan T & Kulkarni A (2022). Plant disease detection using GLCM feature extractor and voting classification approach. *Materials Today: Proceedings* 58(1): 407-415. doi.org/10.1016/j.matpr.2022.02.350
- Mahum R, Munir H, Mughal Z, Awais M, Khan F S, Saqlain M, Mahamad S & Tlili I (2023). A novel framework for potato leaf disease detection using an efficient deep learning model. *Human and Ecological Risk Assessment* 29(2): 303-326. doi.org/10.1080/10807039.2022.2064814
- Moharekar D T T, Pol D U R, Ombase R & Moharekar T J (2022). Detection and classification of plant leaf diseases using convolution neural networks and streamlit. *International Research Journal of Modernization in Engineering Technology and Science* 4(7): 4305-4309.
- Monowar M M, Hamid A, Kateb F, Ohi A Q & Mridha M F (2022). Self-supervised clustering for leaf disease identification. *Agriculture* 12(6): 1-14. doi.org/10.3390/agriculture12060814
- Mukherjee A (2020). Analysis of diseased leaf images using digital image processing techniques and SVM classifier and disease severity measurements using fuzzy logic. *International Journal of Scientific & Engineering Research* 11(9): 1905-1912. doi.org/10.14299/ijser.2020.08.12
- Nanekaran Y A, Zhang D, Chen J, Tian Y & Al-Nabhan N (2023). Recognition of plant leaf diseases based on computer vision. *Journal of Ambient Intelligence and Humanized Computing*, in press. doi.org/10.1007/s12652-020-02505-x
- Oppenheim D & Shani G (2017). Potato disease classification using convolution neural networks. *Advances in Animal Biosciences* 8(2): 244-249. doi.org/10.1017/s2040470017001376
- Pardede H F, Suryawati E, Sustika R & Zilvan V (2018). Unsupervised convolutional autoencoder-based feature learning for automatic detection of plant diseases. In: *Proceedings of the International Conference on Computer, Control, Informatics and Its Applications (IC3INA)*, 1-2 November, Tangerang, Indonesia, pp. 158-162. doi.org/10.1109/ic3ina.2018.8629518
- Patil P, Yaligar N & Meena S (2017). Comparison of performance of classifiers - SVM, RF and ANN in potato blight disease detection using leaf images. In: *Proceedings of the IEEE International Conference on Computational Intelligence and Computing Research (ICCIC)*, 14-16 December, Coimbatore, India, pp. 1-5. doi.org/10.1109/iccic.2017.8524301
- Prajna U (2021). Detection and classification of grain crops and legumes disease: a survey. *Sparklinglight Transactions on Artificial Intelligence and Quantum Computing* 1(1): 41-55. doi.org/10.55011/staiqc.2021.1105
- Rozaqi A J, Arief M R & Sunyoto A (2021). Implementation of transfer learning in the convolutional neural network algorithm for identification of potato leaf disease. *Procedia of Engineering and Life Science* 1(1): 1-9. doi.org/10.21070/pels.v1i1.820
- Sabzi S, Abbaspour-gilandeh Y, Abbaspour-gilandeh Y, Javadikia H, Javadikia H, Havaskhan H & Havaskhan H (2015). Automatic grading of emperor apples based on image processing and ANFIS. *Journal of Agricultural Sciences* 21(3): 326-336. doi.org/10.1501/tarimbil_0000001335
- Sabzi S, Abbaspour Gilandeh Y & Javadikia H (2018). Developing a machine vision system to detect weeds from potato plant. *Journal of Agricultural Sciences* 24(1): 105-118. doi.org/10.15832/ankutbd.446402
- Saeed F, Khan M A, Sharif M, Mittal M, Goyal L M & Roy S (2021). Deep neural network features fusion and selection based on PLS regression with an application for crops diseases classification. *Applied Soft Computing* 103: 1-15. doi.org/10.1016/j.asoc.2021.107164
- Salih T A, Ali A J & Ahmed M N (2020). Deep learning convolution neural network to detect and classify tomato plant leaf diseases. *Open Access Library Journal* 7(5): 1-12. doi.org/10.4236/oalib.1106296
- Sanjeev K, Gupta N K, Jeberson W J & Paswan S (2021). Early prediction of potato leaf diseases using ANN classifier. *Oriental Journal of Computer Science and Technology* 13(2): 129-134. doi.org/10.13005/ojct13.0203.11

- Sarker M R K R, Borsha N A, Sefatullah M, Khan A R, Jannat S & Ali H (2022). A deep transfer learning-based approach to detect potato leaf disease at an earlier stage. In: Proceedings of the Second International Conference on Advances in Electrical, Computing, Communication and Sustainable Technologies (ICAECT), 21-22 April, Bhilai, India, pp. 1-5. doi.org/10.1109/icaect54875.2022.9807963
- Saygılı A (2023). The efficiency of transfer learning and data augmentation in lemon leaf image classification. *European Journal of Engineering and Applied Sciences* 6(1): 32-40. doi.org/10.55581/ejeas.1321042
- Sharma S, Anand V & Singh S (2021). Classification of diseased potato leaves using machine learning. In: Proceedings of the 10th IEEE International Conference on Communication Systems and Network Technologies (CSNT), 18-19 June, Bhopal, India, pp. 554-559. doi.org/10.1109/csnt51715.2021.9509702
- Shwetha K S & Sneha S P (2022). Machine learning techniques for potato leaf disease. *International Research Journal of Modernization in Engineering Technology and Science* 4(7): 434-441.
- Singh A & Kaur H (2021). Potato plant leaves disease detection and classification using machine learning methodologies. IOP Conference Series: Materials Science and Engineering 1022(1): 1-9. doi.org/10.1088/1757-899x/1022/1/012121
- Singh J & Kaur H (2019). Plant disease detection based on region-based segmentation and KNN classifier. *Lecture Notes in Computational Vision and Biomechanics* 30: 1667-1675. doi.org/10.1007/978-3-030-00665-5_154
- Sladojevic S, Arsenovic M, Anderla A, Culibrk D & Stefanovic D (2016). Deep neural networks based recognition of plant diseases by leaf image classification. *Computational Intelligence and Neuroscience* 2016: 1-11. doi.org/10.1155/2016/3289801
- Swetha V & Jayaram R (2019). A novel method for plant leaf malady recognition using machine learning classifiers. In: Proceedings of the 3rd International Conference on Electronics, Communication and Aerospace Technology (ICECA), 12-14 June, Coimbatore, India, pp. 1360-1365. doi.org/10.1109/iceca.2019.8822094
- Tiwari D, Ashish M, Gangwar N, Sharma A, Patel S & Bhardwaj S (2020). Potato leaf diseases detection using deep learning. In: Proceedings of the 4th International Conference on Intelligent Computing and Control Systems (ICICCS), 13-15 May, Madurai, India, pp. 461-466. doi.org/10.1109/iciccs48265.2020.9121067
- Türkoğlu M, Hanbay K, Saraç Sivrikaya I. & Hanbay D (2020). Classification of apricot diseases by using deep convolution neural network. *Bitlis Eren University Journal of Science* 9(1): 334-345. (In Turkish) doi.org/10.17798/bitlisfen.562101
- Wagle S A & Harikrishnan R (2021). Comparison of plant leaf classification using modified AlexNet and support vector machine. *Traitement Du Signal* 38(1): 79-87. doi.org/10.18280/ts.380108



Copyright © 2024 The Author(s). This is an open-access article published by Faculty of Agriculture, Ankara University under the terms of the [Creative Commons Attribution License](https://creativecommons.org/licenses/by/4.0/) which permits unrestricted use, distribution, and reproduction in any medium or format, provided the original work is properly cited.



Optimization of Inulin Extraction from Chicory Roots and an Ultrafiltration Application to Obtain Purified Inulin and Hydrolyzed Fructooligosaccharides

Nihan SAGCAN^a , Hasan SAGCAN^b , Fatih BOZKURT^c , Ayşe Nur BULUT GÜNEŞ^d , Hüseyin FAKİR^e ,
Enes DERTLİ^c , Osman SAGDIÇ^{c*}

^aTekirdağ Namik Kemal University, Corlu Vocational School, Food Technology Department, TR-59850 Tekirdağ, TURKEY

^bIstanbul Medipol University, Vocational School of Health Services, TR-34810 Istanbul, TURKEY

^cYıldız Technical University, Chemical and Metallurgical Engineering Faculty, Food Engineering Department, TR-34210 Istanbul, TURKEY

^dÖzyeğin University, School of Applied Sciences, Gastronomy and Culinary Arts, TR-34794 Istanbul, TURKEY

^eApplied Sciences University of Isparta, Faculty of Forest, Forest Engineering Department, TR-32200 Isparta, TURKEY

ARTICLE INFO

Research Article

Corresponding Author: Osman SAGDIÇ, E-mail: osagdic@yildiz.edu.tr

Received: 09 August 2023 / Revised: 25 September 2023 / Accepted: 27 September 2023 / Online: 09 January 2024

Cite this article

Sagcan N, Sagcan H, Bozkurt F, Bulut Güneş A N, Fakir H, Dertli E, Sagdic O(2024). Optimization of Inulin Extraction from Chicory Roots and an Ultrafiltration Application to Obtain Purified Inulin and Hydrolyzed Fructooligosaccharides. *Journal of Agricultural Sciences (Tarım Bilimleri Dergisi)*, 30(1):166-178. DOI: 10.15832/ankutbd.1338572

ABSTRACT

Inulin and fructooligosaccharides (FOS) are prominent functional components in the food industry due to prebiotic and other pharmaceutical properties. Inulin is a storage polysaccharide in various plants. FOS are naturally present in various plants and can be obtained by partial hydrolysis of inulin. In this study, ground and sieved chicory roots (*Cichorium intybus* L.) were used as starting material for inulin extraction under optimized conditions determined by Response Surface Methodology (RSM) with a Box-Behnken design. Optimum inulin

extraction conditions from chicory roots were; temperature of 90 °C, extraction time of 30 min., and liquid-to-solid (LS) ratio of 10:1 mL/g. Inulin extract was further hydrolyzed to FOS by enzymatic or acid treatment, separately. Purification of inulin extract and FOS hydrolysate was performed by ultrafiltration with a 10 kDa membrane under the pressure of 2 bar with continuous stirring. As a result, inulin and FOS were obtained at 90% and 76% purity, respectively.

Keywords: *Cichorium intybus*; fructooligosaccharides, Response surface methodology, HPLC-RID analysis, Acid-enzyme hydrolysis, Membrane filtration

1. Introduction

The chicory plant (*Cichorium intybus* L.) is a natural source of inulin from the fresh roots and can grow in many different climates (Chandra et al. 2016; El-Kholy et al. 2020). Inulin is a biological macromolecule composed of a linear polymer of D-fructose with β -(2-1) glycosidic linkages, and a terminal glucose moiety which is linked to fructosyl unit via α -(1-4) linkage (Öztürk 2016; Fu et al. 2018; Singh et al. 2020a). The polymerization degree (DP) of inulin varies between 2-60 according to species, harvest time, and time of storage. Fructooligosaccharides (FOS) are fructans with DP<10 that naturally exist in various plants such as chicory, Jerusalem artichoke, yacon, and burdock (Li et al. 2013; Singh et al. 2020c; Redondo-Cuenca et al. 2021; Stökle et al. 2023). Additionally, FOS can be obtained by transfructosylation of sucrose by β -fructofuranosidases or by partial enzymatic hydrolysis of inulin using endoinulinases acting on internal β -(2, 1) glycosidic linkages (Beirão-Da-Costa et al. 2009; Li et al. 2013; Khuenpet et al. 2017). Transfructosylation by β -fructofuranosidases forms small chain length (2-4 fructosyl units) FOSs, whereas hydrolysis of inulin using endoinulinases forms long chain length (1-9 fructosyl units) FOSs (Singh et al. 2020a).

In the food industry, chicory stands out due to its content of inulin and derivative FOS and is a natural food ingredient. Both inulin and fructooligosaccharides have prebiotic activity that can promote probiotic growth, especially *Bifidobacteria*. Inulin also has pharmaceutical effects such as modulation of intestinal microbiota, anti-cancer and antioxidant activity, immunological enhancement, antidiabetic effect, hepatoprotective activity, and many others (Li et al. 2013; Dominguez et al. 2014; Fu et al. 2018; Perović et al. 2021). In addition to its serum cholesterol reducing and pathogenic bacteria inhibitory effects, FOS has cerebral protective activity and improves cognition (Li et al. 2013; Dominguez et al. 2014; Fu et al. 2018; Perović et al. 2021). Inulin and FOS are used as sugar and fat replacers in low-calorie foods to decrease obesity and diabetes risks (Dominguez et al. 2014; Khuenpet et al. 2017; Beirão-Da-Costa et al. 2009). Mostly they are preferred in desserts, infant formula, baked products, and fermented dairy products (Lopes et al. 2017; Kralj et al. 2018; Redondo-Cuenca et al. 2021). Inulin is used as dietary fiber,

gel-forming, and viscosity regulator agent in the food industry (El-Kholy et al. 2020). Due to these properties, food and pharmaceutical industries have utilized inulin and FOS for functional foods, nutritional composites, and drugs (Singh et al. 2020a; Perović et al. 2021; Singh & Singh 2022a).

Inulin can be obtained by extraction of plant materials such as chicory, Jerusalem artichoke, salsify, and dahlia, and by biosynthesis pathways (Beirão-Da-Costa et al. 2009; Apolinário et al. 2014; Kralj et al. 2018). According to Barclay et al. (2014), inulin is synthesized from sucrose by a polymerization reaction that transfers fructose from another sucrose molecule with catalytic enzymes in plants. Differing from this pathway, Apolinario et al. (2014) proposed distinctive biosynthetic pathway models in detail. FOS was obtained from various plants by partial enzymatic hydrolysis of inulin or sucrose transfructosylation by using fungal fructosyltransferases (Ávila-Fernández et al. 2011; Dominguez et al. 2014; Muñoz-Márquez et al. 2019). Also, FOS production from inulin by acidic hydrolysis was demonstrated in a previous study with an alternative methodology (Grzybowski et al. 2014).

Extraction is an important step for inulin production and hot water extraction is the method of choice due to the water-soluble property of inulin (Khuenpet et al. 2017). Extraction time and temperature are critical factors as they can cause either transfer of inulin from plant to water or degradation of inulin to reducing sugars. For this reason, extraction parameters should be selected properly. In the conventional method, to observe the effect of each experimental factor, one variable at a time is changed but this approach is time consuming and labor intensive (Singh et al. 2020c). To deal with these problems, the response surface methodology (RSM) technique is used for optimization processes. The Box Behnken experimental design (BBD) in RSM was used in this study for the optimization of process variables for inulin extraction from chicory roots.

In addition to extraction procedures, a further purification step is necessary to obtain high-purity ingredients for the food and pharmaceutical industries. To remove the impurities such as reducing sugars, high molecular weight carbohydrates, proteins, and fibers from crude inulin and FOS extracts, some physicochemical methods and chromatographic techniques were described previously (Li et al. 2004; 2013; Apolinário et al. 2014). However, recent studies focused on alternative membrane technology for the purification of these components. The membrane separation technique stands out with advantages of high productivity, low operation costs, and high product quality (Barclay et al. 2014; Muñoz-Márquez et al. 2019). In previous studies of inulin purification using membrane filtration, membranes with 5-50 kDa pore size were used with continuous stirring under 1-2.6 bar pressure to prevent membrane clogging (Zhu et al. 2018; Murtiningrum et al. 2020). In the studies of FOS purification, 1-10 kDa membrane filters were used (Qing et al. 2013). More studies are required to determine the effect of different separation applications during the extraction of inulin from its plant source. From this perspective, this study aimed to discover the most efficient and easiest way of obtaining inulin and FOS from chicory roots. This study explains how to obtain two different end products step by step in detail, starting from the chicory plant. At first, the inulin extraction conditions from chicory roots were optimized by the BBD in RSM. Inulin extract was obtained with these optimized conditions and then hydrolyzed to FOS by acid or enzyme treatment. A membrane filtration system was used to maximize the purity of inulin and FOS separately. Also, total carbohydrate and total protein content were investigated before and after filtration to calculate the purity and efficiency of the filtration system. At the end of the study, two different end products with relatively high purity were obtained from chicory. Considering that there is no extensive information about the purification of inulin and FOS using a membrane filtration system in the literature, and that this purification is generally performed by chromatographic techniques, this study is an example of the feasibility of a membrane filtration system for inulin and FOS purification and will be a pioneer for more detailed studies.

2. Material and Methods

2.1. Chicory root samples

The chicory roots were collected from Isparta province (located in the western Mediterranean region) in Türkiye during the flowering stage. The chicory roots were identified by Prof. Dr. Huseyin Fakir, Director of the Herbarium Section, Applied Sciences University of Isparta, Türkiye. The roots were conventionally dried (final moisture content was 7.5%), cleaned of soil, and ground, sieved (1 mm), and stored at 4 °C until use.

2.2. Chemicals

The endo-inulinase enzyme from *Aspergillus niger* (300 U/mL, 60 °C, 4.5 pH) was purchased from Megazyme, USA. Commercial inulin from chicory, that was kindly provided by Artisan Gıda (Türkiye), was a product of Orafiti (Belgium). Glucose, fructose, sucrose, 1-kestose (GF₂), and nystose (GF₃) standards of analytical grade were purchased from Sigma-Aldrich (St. Louis, MO, USA). 1^F-fructofuranosylnystose (GF₄) analytical standard was purchased from Novagentek (England). All other reagents and solvents were of analytical reagent grade. All aqueous solutions were prepared using deionized water.

2.3. Experimental design

Design Expert-13 was used to optimize the extraction conditions of inulin from chicory roots. In RSM, a 3-factor BBD was used. Independent variables were temperature (°C, A), time (min, B), and liquid-to-solid ratio (mL/g, C). The dependent variable was

inulin content (g/100 g dry weight). Independent variables were defined according to our preliminary trials and optimum extraction conditions in the literature (Dobre et al. 2008; Beirão-Da-Costa et al. 2009; Apolinário et al. 2014; Tewari et al. 2015; Balzarini et al. 2018; Başaran et al. 2018).

The complete design consisted of 18 experimental points (including six replicates of the center point), and the experiments were performed randomly. Experimental data were fitted to a quadratic polynomial model (1) to obtain regression coefficients.

$$Z = \beta_0 + \sum_{i=1}^3 \beta_i x_i + \sum_{i=1}^3 \beta_{ii} x_i^2 + \sum_{i=1}^2 \sum_{j=1}^3 \beta_{ij} x_i x_j \quad (1)$$

Where; Z was the dependent variable to be modeled, x_i and x_j were the independent variables, β_0 was the constant coefficient, β_i was the coefficient of linear effect, β_{ii} was the coefficient of quadratic effect, and β_{ij} was the coefficient of interaction effect.

2.4. Extraction of chicory roots

Inulin extractions were performed by using 2 g chicory root samples (described above). The calculated ratio of hot water was added to each sample. Water temperature of 60-90 °C, extraction time of 30-90 min, and liquid-to-solid ratio (water: root sample) of 10:1-30:1 v/w were used as extraction conditions. Extractions were carried out in a water bath running at the extraction temperature with 100 rpm shaking. After extraction, chicory root extract was filtered firstly through cotton cheesecloth and then centrifuged at 1400 rpm for 10 min. Supernatants of each extract were stored at -20 °C until analysis.

2.5. HPLC-RID analysis of inulin and FOS

Inulin and FOS content determination was performed with an HPLC (High Pressure Liquid Chromatography) Shimadzu (Kyoto, Japan) system (LC-20A pump, SIL-20A HT autosampler) combined with a refractive index detector (RID-20A). Inulin separation was performed on an Inertsil-NH₂ column (5µm, 4.6 × 250 mm). The measurements were performed at a column temperature of 80 °C and detector temperature of 60 °C, using deionized water as mobile phase at flow rate of 1 mL/min and injection volume of 20 µL (Başaran et al. 2018).

FOS determination on HPLC was performed according to the methods of Nobre et al. (2018) and Muñoz-Márquez et al. (2019). 1-kestose (GF₂), 1-nystose (GF₃), and 1^F-fructofuranosylnystose (GF₄) were used as FOS standards, and glucose, fructose, and sucrose were also analyzed as residual sugars. Total FOS content was calculated as the sum of GF₂, GF₃, and GF₄. For the quantification of FOS and sugars, calibration curves were obtained with known concentrations of each compound. Samples were analyzed with a ReproSil Carbohydrate-Plus column (5µm, 4.6 × 250 mm) at 30 °C. The operating temperature of the refractive index detector (RID) was 35 °C. A mixture of acetonitrile/water 80:20 (v/v) was used as the mobile phase at flow rate of 1 mL/min. Before analyses, all samples were filtered through a 0.45 µm polytetrafluoroethylene (PTFE) filter.

2.6. Hydrolysis of inulin to FOS

The enzymatic hydrolysis of inulin was carried out following the methods of Ricca et al. (2009), Yi et al. (2010) and Sarchami & Rehmann (2014) with slight modifications. Inulin extract, obtained in optimum extraction conditions according to our experimental design, was used as substrate for hydrolysis. Enzymatic hydrolysis was performed for FOS production in different experimental conditions according to the literature. These experimental conditions are given in Table 1. The appropriate enzyme concentration that gives the highest FOS yield was selected through our preliminary studies.

Table 1- Conditions for acid (A) and enzymatic (E) hydrolysis

<i>Sample Name</i>	<i>Temperature (°C)</i>	<i>Time (min)</i>	<i>Buffer volume (mL)*</i>	<i>pH**</i>
A-1	85	15	-	2.5
A-2	85	25	-	2.5
E-1	40	60	-	5.28
E-2	40	60	4	4.50
E-3	40	30	4	4.50
E-4	60	60	-	5.28
E-5	60	60	4	4.50
E-6	60	30	4	4.50

*: 0.05M sodium acetate was used as a buffer; **: 0.5 M citric acid was used in pH adjustment

For enzyme hydrolysis, 0.2 mL of the endo-inulinase enzyme (60 U) was added to 10 mL of inulin extract at room temperature and incubated in a water bath at the temperature and time in Table 1 with 100 rpm shaking. The hydrolysates were left at 100 °C for 15 min to inactivate the enzyme and cooled immediately for later study.

To compare the results, acid hydrolysis was also carried out following the method of Grzybowski et al. (2014). For acid hydrolysis, 10 mL of inulin extract, obtained in optimum conditions, was used. The pH value of each extract was adjusted to 2.5 with 0.5 M citric acid solution. Acid hydrolysis was performed in a 100 rpm shaking water bath at temperatures and times given in Table 1. At the end of the relevant period, the hydrolysates were cooled rapidly and stored at -20 °C.

2.7. Purification by membrane filtration

To separate high molecular weight sugars, proteins, and other impurities from inulin and FOS extracts and to obtain high-purity products, the ultrafiltration technique was used. Dead-end ultra-filtration runs were carried out in a filtration module that was manufactured for this aim (maximal volume 200 mL) (Fig. 1). The membrane filtration system was manually installed and operated under high-purity nitrogen gas, accompanied by a magnetic stirrer. Polyethersulfone ultrafiltration membranes (Sartorius Stedim Biotech GmbH, Germany) with 1, 5, and 10 kDa pore sizes were used individually.

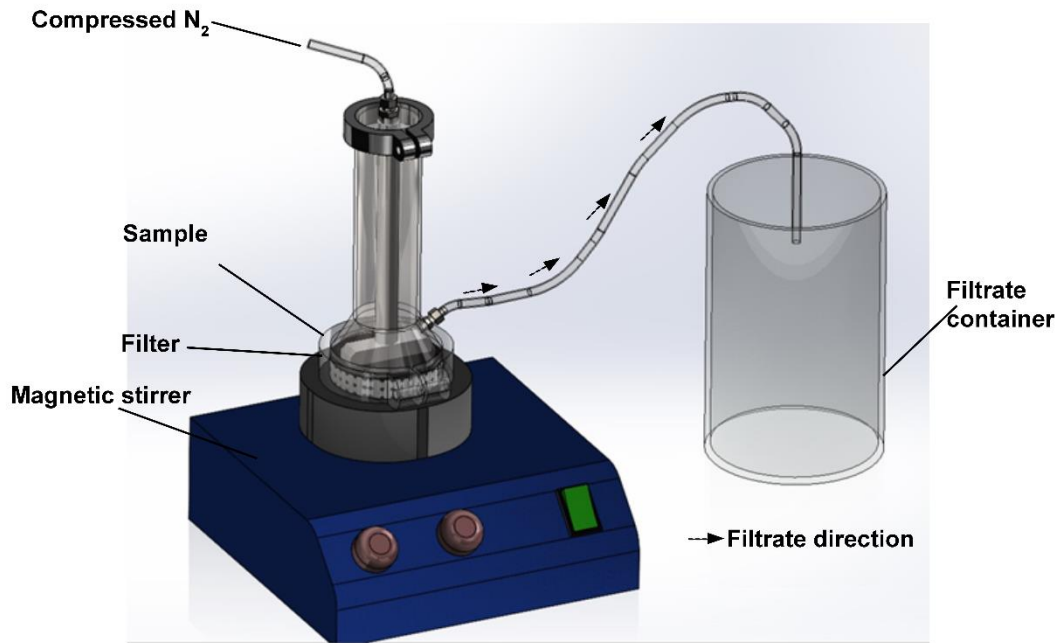


Figure 1- Filtration module

For the inulin filtration step, inulin extract was prepared under the previously determined optimum inulin extraction conditions (90 °C-30 min-10 mL/g). The volume of the extract was determined as 40 mL for effective filtration and a 4g chicory root sample was studied for each trial. A membrane filtration system was installed using a membrane filter and loading the inulin extract into the system. 1, 5, and 10 kDa membranes were used in different trials. Nitrogen gas was operated at a pressure of 2 bar and the magnetic stirrer placed under the filtration system was operated at 400 rpm. The filtrate was collected in a test tube placed at the outlet of the filtration system. The inulin contents of the extract and final filtrate were determined by HPLC analysis. Filtration of FOS was carried out with hydrolyzed inulin extract (FOS hydrolysate). Hydrolysis conditions were 40 °C, 60 min and 60 U enzyme concentration. The membrane filtration system was set up as for the inulin purification. FOS contents of the hydrolysate and final filtrate were determined by HPLC analysis. Experiments were carried out as two replicates, using a new membrane for each experiment.

Purities of inulin and FOS were calculated according to Zhu et al. (2018).

$$\text{Inulin or FOS purity (\%)} = \frac{\text{inulin or fos content}}{\text{total carbohydrate content} + \text{protein content}} \times 100 \quad (2)$$

2.8. Total carbohydrate analysis

Total carbohydrate quantities of samples were measured by the phenol-sulfuric acid technique using D-glucose as standard (Albalasmeh et al. 2013). Briefly, 1 mL of phenol (5%) was added to 1 mL of the sample in a test tube. Afterwards, 5 mL of sulfuric acid (98%) was rapidly added and the tube was left standing for 10 minutes. After stirring, the tubes were placed in a water bath at room temperature for 20 minutes. Color development was measured at 490 nm on a spectrophotometer (Biotek-Synergy/HTX). The calibration curve was prepared with 0.01-0.75 mg/mL concentrations of standard glucose.

2.9. Total protein analysis

The protein concentration of samples was measured by the bicinchoninic acid (BCA) protein assay kit (Pierce, Thermo Fisher Scientific, USA). The calibration curve was prepared with between 20-2000 $\mu\text{g}/\text{mL}$ of bovine serum albumin (BSA) standard that was supplied with the kit. Then, 0.1 mL of each standard and sample were transferred into test tubes. After this, 2 mL of working reagent (WR), that was prepared with supplied reagents, was added to each tube and mixed. Tubes were covered and incubated at 37 °C for 30 minutes. Color development was measured at 562 nm on a spectrophotometer.

2.10. Statistical analysis

The responses obtained from experimental designs underwent regression analysis by using the Design Expert Software (version 13). As a result, the determination coefficient (R^2), regression constants, and analysis of variance (ANOVA) were determined. The significance of the regression coefficient was verified by F-test and p-value. The statistical analyses were performed using JMP 9 (SAS, NC, USA). In the 0.95 confidence interval, the data were analyzed using one-way analysis of variance followed by Tukey's test.

3. Results and Discussion

3.1. Effects of temperature, time, and LS ratio on the inulin concentration

Effects of temperature (2A), time (2B), and LS ratio (2C) on the inulin content are presented in the Figure 2. As shown in Fig. 2A, increasing the extraction temperature from 60 to 90 °C resulted in the increase in inulin content when the other extraction parameters were fixed to 60 min (time) and 20:1 LS (ratio). This result is compatible with other studies about the extraction of inulin either from chicory roots or other plant materials (Lingyun et al. 2007; Tewari et al. 2015; Fu et al. 2018). Many of the previous studies extracted inulin at the temperature range of 80–90 °C from chicory roots as the water solubility of inulin increases with temperature (Apolinário et al. 2014). Although high temperatures positively affect inulin extraction, temperatures close to boiling point may increase undesired co-extract materials and cause release of simple sugars by hydrolysis (Redondo-Cuenca et al. 2021).

As can be seen in Fig. 2B, when extraction time increased from 30 to 90 min, the inulin content decreased significantly ($P < 0.05$), while the other extraction parameters were fixed to 75 °C (temperature) and 20:1 LS (ratio). In the study by Fu et al., with *Codonopsis pilosula* roots (Fu et al. 2018), inulin yield increased until 120 min and then started to decrease. Tewari et al. (2014) indicated that inulin yield reduced as the time increased from 30 min to 50 min with microwave-assisted extraction. They also obtained maximum inulin yield at 30 min, similar to our finding. According to previous reports, mostly extraction periods of 30-60 min were used for inulin extractions from various plants (Apolinário et al. 2014). Since inulin is a polydisperse carbohydrate, prolonging the extraction time may lead to hydrolysis of inulin to monosaccharides.

The effect of LS ratio on inulin content is presented in Fig. 2C. Different LS ratios (10:1 to 30:1 mL/g) were examined, while other parameters were kept constant at temperature of 75 °C and time of 60 min. The inulin content was found to decrease as the LS ratio increased. At a higher LS ratio, the problem of insufficient solute (dilute solution) may occur and intermolecular forces between the inulin and the solvent become unable to provide sufficient solubility (Noori 2014; Esmaeili et al. 2021). The lower LS ratio (10:1) resulted in the highest inulin yield in this study. In contrast to our results, Tewari et al. (2015) found that a higher volume of solvent led to a higher response with microwave-assisted extraction. Another study, that focused on LS ratios of 5 to 12, found that inulin yield increased up to an LS ratio of 10, and then decreased (Lingyun et al. 2007). This result also showed that solvent ratios less than 10:1 v/w were insufficient to ensure immersion of the entire sample. From an economic point of view, the use of less solvent for the extraction process is preferable for large-scale production.

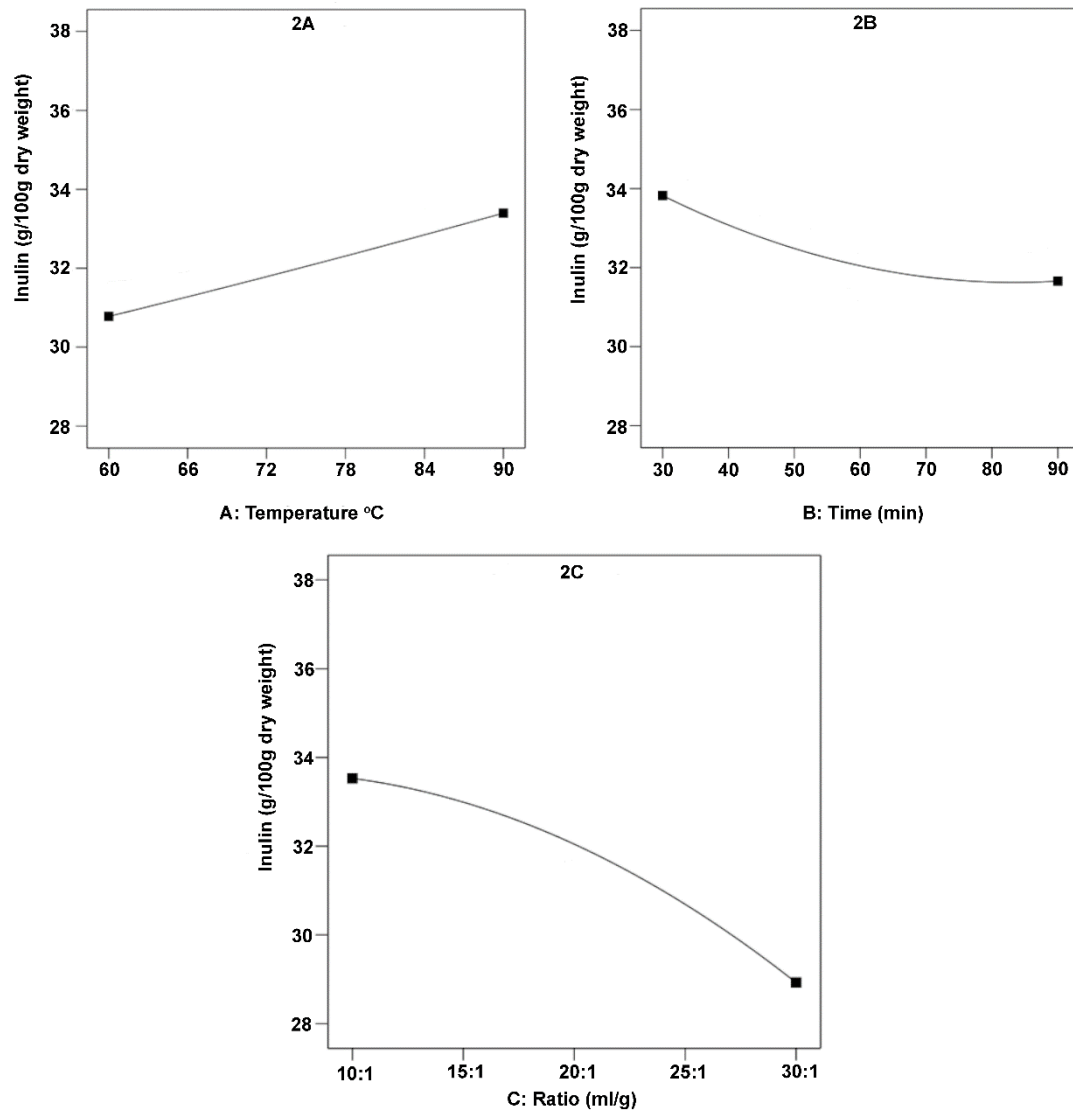


Figure 2- Effects of extraction parameters on inulin content

3.2. Optimization of inulin extraction conditions by BBD

Extraction results according to BBD are shown in Table 2. Inulin contents of extracts varied between 28.45-36.26 g/100 g dry weight (dw). In the literature, inulin contents of chicory extract were reported to be between 11.67% to 65.60% (Figueira et al. 2004; Dobre et al. 2008; Beirão-Da-Costa et al. 2009; Tewari et al. 2015; Redondo-Cuenca et al. 2021). Although our results are in this range, different inulin contents obtained in different studies may be due to the variety of plant, geographic location, harvest time, and length of storage. Different physiological processes that occur in each plant tissue might also affect inulin content (Apolinário et al. 2014; Redondo-Cuenca et al. 2021).

Table 2- Box-Behnken experimental design with coded and uncoded factors and results for inulin content*

Run	Factor 1	Factor 2	Factor 3	Experimental Values	Predicted Values
	A: Temperature (°C)	B: Time (min)	C: Ratio (mL/g)	Inulin (g/100g)**	Inulin (g/100g)
1	60(-1)	60(0)	10:1(-1)	31.83±1.02	31.16
2	60(-1)	60(0)	30:1(1)	28.45±0.95	28.76
3	90(1)	90(1)	20:1(0)	33.25±1.32	32.85
4	75(0)	60(0)	20:1(0)	32.50±0.84	32.05
5	90(1)	30(-1)	20:1(0)	35.29±1.05	35.34
6	75(0)	60(0)	20:1(0)	31.31±1.27	32.05
7	75(0)	90(1)	30:1(1)	28.61±0.92	28.36
8	75(0)	60(0)	20:1(0)	32.57±1.08	32.05
9	75(0)	30(-1)	30:1(1)	31.61±1.10	30.89
10	90(1)	60(0)	30:1(1)	28.51±1.52	29.18
11	75(0)	60(0)	20:1(0)	32.80±1.23	32.05
12	75(0)	30(-1)	10:1(-1)	34.86±0.89	35.11
13	60(-1)	90(1)	20:1(0)	30.61±1.05	30.23
14	60(-1)	30(-1)	20:1(0)	31.98±1.16	32.39
15	75 (0)	60(0)	20:1(0)	31.55±1.12	32.05
16	90(1)	60(0)	10:1(-1)	36.29±1.02	35.98
17	75(0)	90(1)	10:1(-1)	32.61±1.45	33.33
18	75(0)	60(0)	20:1(0)	31.55±1.53	32.05

*: Mean of triplicate determinations;** Inulin content presented on dry weight basis

Table 3- Analysis of variance for the fitted quadratic polynomial model of extraction of inulin

Source	<i>p</i> -value Prob>F	DF	Mean Square	Sum of Squares
Model	0.000	9	8.35	75.15
A-Temperature	0.001	1	13.70	13.70
B-Time	0.004	1	9.37	9.37
C-Ratio	< 0.0001	1	42.37	42.37
AB	0.673	1	0.11	0.11
AC	0.021	1	4.84	4.84
BC	0.637	1	0.14	0.14
A ²	0.912	1	0.01	0.01
B ²	0.094	1	2.10	2.10
C ²	0.056	1	2.92	2.92
Residual	0.223	8	0.58	4.67
Lack of Fit		3	0.86	2.59
Pure Error		5	0.42	2.08
Cor Total		17		79.82
R²	0.942			
R²_{adj}	0.876			
Adeq. precision	13.39			

The *p*-value (Prob > F) serves as an important tool in ANOVA and it is used to check the significance of the model and variables (Karadag et al. 2019; Singh & Singh 2022a). A value of *p* less than 0.05 shows a significant coefficient of model terms (Singh et al. 2021). According to Table 3, the *p*-value for the model and independent variable of C-Ratio was found to be < 0.0001, which confirms the fitness of the designated model (Singh & Singh 2022a). Model terms A, B, and AC had *p* value of < 0.05, which justifies their significance (*P*<0.05). Lack of fit value is essential to define the authenticity of the model and the fitness of the model is represented by insignificant (*P*>0.05) 'lack of fit' (Singh et al. 2021). A low lack of fit (0.223) confirms that the model is adequate for predicting inulin concentration. Degree of freedom (DF), which is an important interpretation of ANOVA, is found by the number of times a specific run with similar values for all selected independent variables is repeated in the designed model (Singh & Singh 2022b). In the current study, DF 5 for pure error confirms the fitness of the selected model, which was further confirmed by the coefficient of determination (*R*²) of 0.942, indicating that only 5.8% of total variation cannot be explained by our model. Adequate precision that measures the signal to noise (S/N) ratio of the designed model also authenticates the model fitness (Singh & Singh 2022b). An adequate precision value greater than 4 is desirable for a fitted model. In this model, an adequate precision value of 13.392 indicates a sufficient signal.

The final equation obtained in terms of coded factors (A: temperature (°C), B: time (min), C: liquid-to-solid (LS) ratio (mL/g)) is:

$$\text{Inulin (g/100g)} = 32.050 + 1.310A - 1.080B - 2.300C - 0.167AB - 1.100AC - 0.187BC + 0.042A^2 + 0.694B^2 - 0.818C^2 \quad (3)$$

3D response surface plots of the graphical representations of regression equations are presented in Fig. 3. They show the relationship between responses and experimental levels and the type of interactions between two test variables. Each figure represents the effect of two factors on the inulin content, while the other factor was kept at zero level (center value of the testing range). The interactive effects of extraction temperature (°C) and time (min), extraction temperature (°C) and liquid: solid ratio (mL/g) and time (min) and liquid: solid ratio (mL/g) are given in Figure 3A, 3B and 3C, respectively. In the 3D plots, the navy-blue color represents lower and the raspberry red color represents upper range variables, whereas light green color, yellow color, and sky blue color represent the intermediate range of the selected variables. In our model, only the interaction between the LS ratio and the temperature was significant ($p=0.021$). These figures show that an increase in the inulin content was observed when temperature increased and other factors (time and LS ratio) decreased.

The plots showed that inulin extraction reached its maximum at a combination of temperature of 90 °C, extraction time of 30 min and LS ratio of 10:1 mL/g. Maximum inulin content of 37.62 g/100 g dw was obtained under these parameters. Redondo-Cuenca et al. (2021) examined optimal conditions for the extraction of inulin plus FOS from chicory root and found optimal parameters were 77.4 °C, 59.4 min, and 27.8 mL/g LS ratio. Tewari et al. (2015) investigated optimum conditions for microwave-assisted extraction of inulin from chicory roots and found 90 °C, 30 min, and 40 mL/g LS ratio were the optimum parameters. Lingyun et al. (2007) also reported optimum conditions for inulin from Jerusalem artichoke tubers as 76.65 °C, 20 min, and 10:1 mL/g LS ratio.

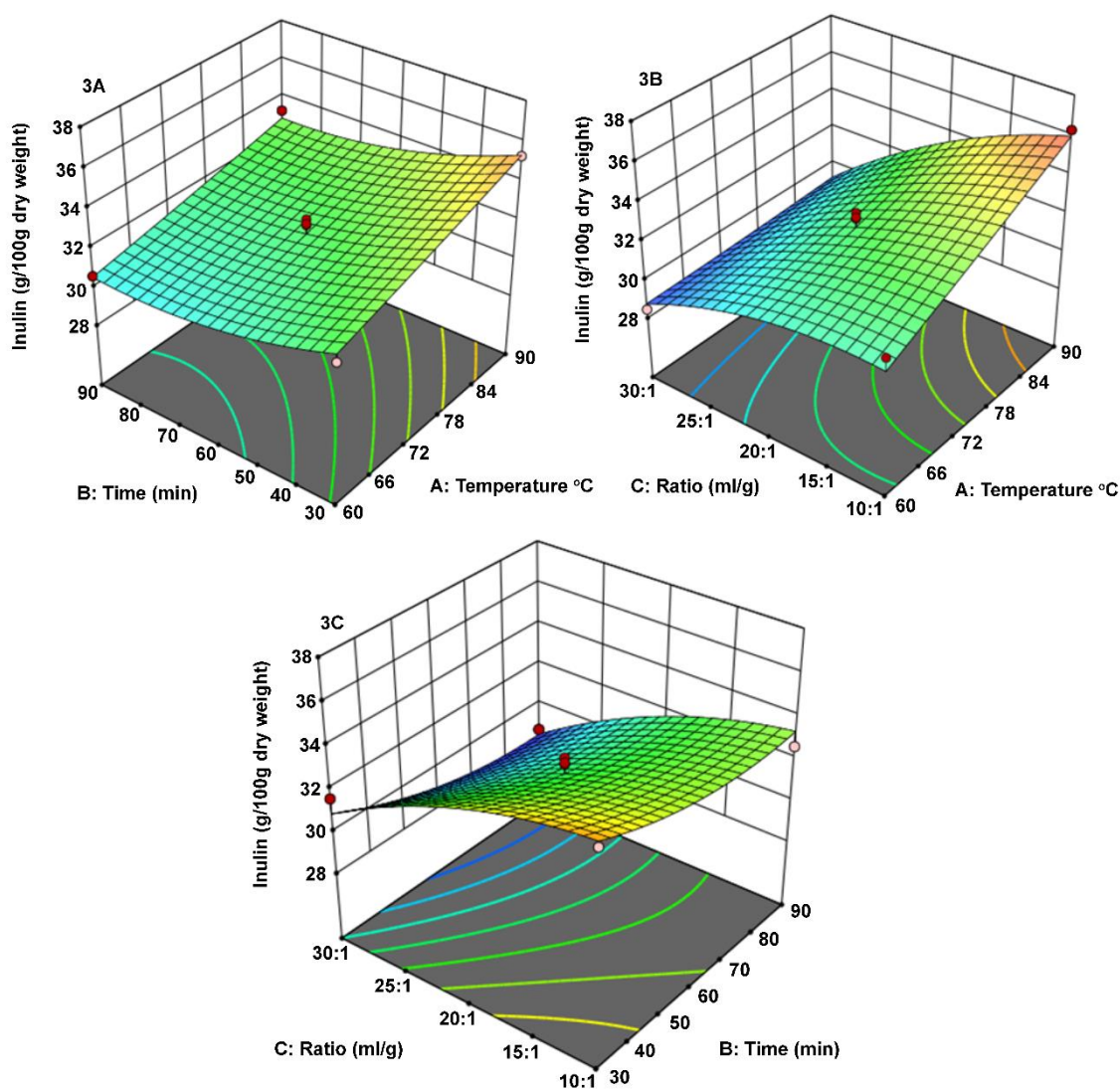


Figure 3- 3D response surface plots

3.3. FOS content of hydrolysates

FOS hydrolysates were analyzed for inulin, FOS, and residual sugar content. Also, the inulin extract used as the substrate was analyzed. Total FOS content was calculated as the sum of GF₂, GF₃, and GF₄. HPLC chromatograms of FOS and residual sugars are shown in Figure 4. FOS, inulin, residual sugar contents of hydrolysates, and inulin extracts are given in Table 4.

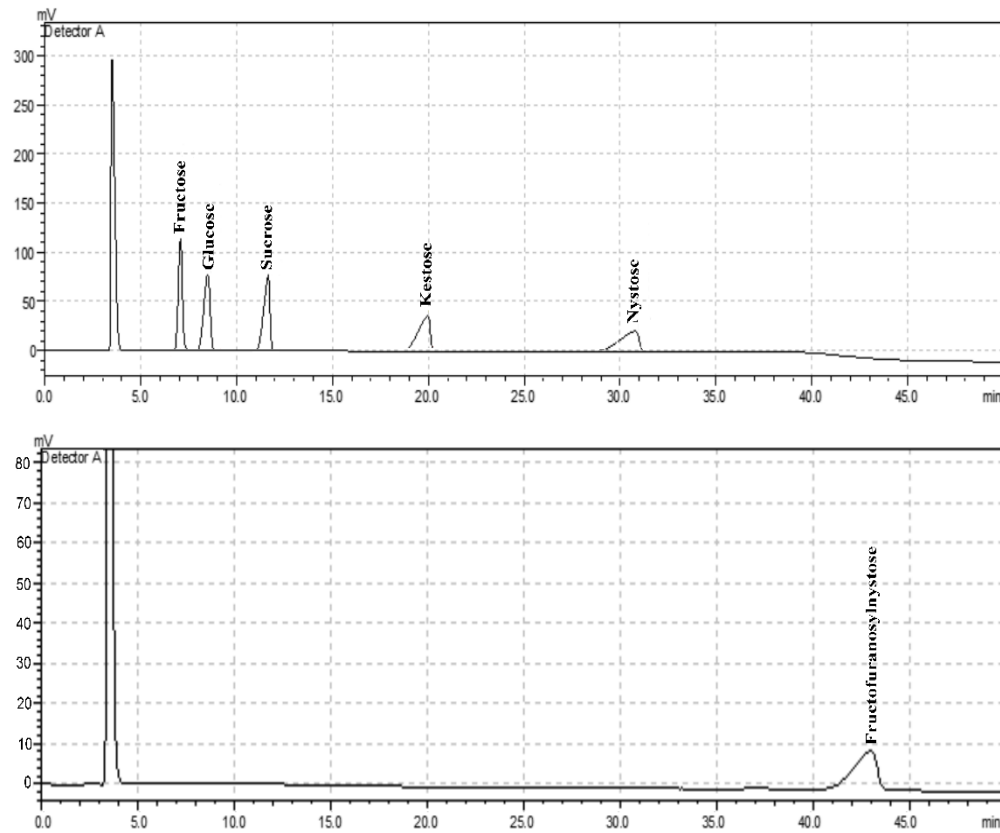


Figure 4- HPLC chromatograms of FOS and residual sugars

Table 4- FOS, inulin and residual sugar contents of hydrolysates and inulin extract

Contents (mg/mL)	Samples*								
	Inulin extract	E-1	E-2	E-3	E-4	E-5	E-6	A-1	A-2
Inulin	16.97±1.22 ^A	10.82±0.75 ^{AB}	7.53±0.63 ^C	8.32±1.18 ^{BC}	10.94±0.31 ^{ABC}	8.33±0.51 ^{BC}	9.36±0.58 ^{ABC}	11.14±1.20 ^{ABC}	12.84±0.95 ^{ABC}
Fructose	6.40±0.39 ^C	6.47±0.89 ^C	3.88±0.15 ^D	3.77±0.36 ^D	6.99±0.28 ^C	3.72±0.52 ^D	4.02±0.51 ^D	8.83±0.37 ^B	15.06±0.19 ^A
Glucose	1.95±0.32 ^{ABC}	2.22±0.57 ^A	1.17±0.17 ^{BC}	1.07±0.13 ^{BC}	2.02±0.22 ^{AB}	0.99±0.40 ^C	1.07±0.24 ^{BC}	1.59±0.30 ^{ABC}	2.25±0.45 ^A
Sucrose	1.95±0.49 ^A	2.21±0.29 ^A	1.31±0.24 ^A	1.15±0.31 ^A	1.96±0.96 ^A	1.05±0.24 ^A	1.15±0.23 ^A	1.61±0.30 ^A	1.73±0.24 ^A
1-kestose(GF ₂)	0.78±0.14 ^{ABC}	1.16±0.31 ^A	0.55±0.13 ^{BC}	0.44±0.16 ^C	1.12±0.34 ^{AB}	0.48±0.28 ^C	0.53±0.15 ^{BC}	0.32±0.09 ^C	0.38±0.14 ^C
1-nystose (GF ₃)	0.82±0.10 ^{CDE}	2.35±0.27 ^A	1.23±0.39 ^{BCD}	1.41±0.20 ^{BC}	1.69±0.17 ^{AB}	0.93±0.22 ^{CD}	1.02±0.22 ^{BCD}	0.64±0.27 ^{DE}	0.23±0.20 ^E
1 ^F -fructofuranosylnystose (GF ₄)	1.22±0.19 ^{BCD}	2.60±0.49 ^A	1.83±0.43 ^{ABC}	1.98±0.29 ^{AB}	0.00±0.01 ^E	1.12±0.26 ^{CD}	1.28±0.24 ^{BCD}	1.03±0.24 ^{CD}	0.99±0.22 ^D
Total FOS	2.82±0.35^{CD}	6.11±0.38^A	3.61±0.29^{BC}	3.83±0.37^B	2.81±0.18^{CD}	2.53±0.27^D	2.83±0.20^{CD}	1.99±0.20^{DE}	1.60±0.52^E

*: Sample names were coded as defined in Table 1. Inulin extract refers to unhydrolyzed extract obtained in the optimum conditions. All results are mean of triplicate determinations. Different uppercase letters represent statistical difference between different samples for each component.

According to Table 4, the highest amount of FOS (statistically significant ($P < 0.05$)) was obtained from sample E-1 (40 °C-60 min-enzyme hydrolysis-without buffer and acid). Although the inulin content was lower in hydrolysates using acid and buffer solution (E-2, 3, 5, and 6), no statistically significant increase in FOS content was observed in hydrolysates E-5 and E-6.

Acid hydrolysis results showed not only the lowest FOS formation but also the highest fructose content. This implies that acid hydrolysis might cause full hydrolysis of inulin to fructose units. The degradation of inulin to its monosaccharides was not targeted in this study since the functional properties are lost with degradation. Stökle et al. (2023) tested the acid hydrolysis of inulin to obtain fructose-enriched extracts but observed the formation of undesirable components, especially hydroxymethylfurfural (HMF), indicating that acid hydrolysis was not suitable to obtain FOS. Another methodology to obtain FOS is the transfructosylation of sucrose but previous studies reported that FOS produced from inulin hydrolysis might contain longer fructo-oligomer chains (DP 5-9) than the ones produced by the sucrose transfructosylation process (DP 2-4) (Dominguez et al. 2014; Singh et al. 2020b). Additionally, in the trans-fructosylation process, a considerable amount of by-products (unreacted sucrose, generated fructose and glucose) were produced, which decreases the amount of product and increases the purification cost (Singh et al. 2020b).

Han et al. (2017) found temperature of 35 °C and pH value of 4.5 were appropriate conditions for FOS production from inulin, verifying the hydrolyzation at low temperatures. In contrast to our study, a lower pH value was found to be optimum for hydrolyzation of inulin treated with recombinant endo-inulinase enzyme-engineered *Yarrowia lipolytica* strain in the aforementioned study.

3.4. Inulin purification

The extraction method for inulin usually results in solutions comprising a mixture of inulin, other polysaccharides, and non-carbohydrate compounds, mainly proteins, which should be further purified for industrial purposes (Apolinário et al. 2014; Perović et al. 2021). For this reason, inulin, total carbohydrate, and total protein contents of both inulin extract (before filtration) and inulin filtrate (after filtration) were analyzed to determine the yield of purification.

Ultrafiltration tests with 1 and 5 kDa membranes resulted in lower inulin recovery than with 10 kDa. For this reason, only 10 kDa membrane results are presented in this study (Table 5).

Table 5- Purification* of inulin and FOS****

Sample	Inulin or FOS content (mg/mL)	Total carbohydrate (mg/mL)	Total protein (mg/mL)	Purity (%)
Inulin extract (before filtration)	23.72±1.21 ^{***}	41.74±3.05 ^a	1.36±0.40 ^a	55.04
Inulin filtrate (after filtration)	17.15±1.25 ^{b**}	18.17±1.77 ^b	0.77±0.21 ^a	90.54
FOS hydrolysate (before filtration)	13.70±1.22 ^{A***}	45.38±3.86 ^A	1.77±0.49 ^A	29.06
FOS filtrate (after filtration)	13.41±0.77 ^{A***}	17.35±2.27 ^B	0.68±0.18 ^B	76.02

*: All results are mean of triplicate determinations. Different lowercase letters indicate statistical difference between inulin samples in the same column, different uppercase letters show statistical difference between FOS samples in the same column

According to Table 5, purification by ultrafiltration resulted in a statistically significant ($P<0.05$) reduction in the total carbohydrate content of inulin extract. After filtration, 94% of the total carbohydrate content was composed of inulin, proving that other polysaccharides were mostly removed. In the filtrate, total carbohydrate content decreased by 56.47% and protein content decreased by 43.39%. The purity of inulin reached 90.54% in the filtrate.

There are several studies related to purification of chicory inulin by chromatographic techniques (Mavumengwana 2004), ion exchange resins (Zhang et al. 2022), and ultrafiltration for Jerusalem artichoke (Zhu et al. 2018), and red fruit (*Pandanus conoideus*) (Murtiningrum et al. 2020) inulin extracts. Mavumengwana et al. (2004) investigated the purification of inulin suspension by chromatographic techniques for color removal and tannin elimination. Zhu et al. (2018) studied ultrafiltration of Jerusalem artichoke extract, using a 50-kDa membrane with trans-membrane pressure of 0.3 MPa and a rotation speed of 800 rpm. The researchers were able to obtain a filtrate with 98% inulin purity, and showed that membrane type, pressure, and rotation speed were factors affecting the purity.

3.5. FOS purification

FOS hydrolysate was purified for the removal of residual enzymes, polysaccharides, and proteins. FOS purity (%) was calculated as for inulin purity. Purification with the 10 kDa membrane filter resulted in the highest recovery of FOS. As can be seen in Table 5, FOS purification with 10 kDa membrane resulted in 97.88% FOS recovery, a decrease of 61.77% of total carbohydrate content, and 61.59% of protein content in the filtrate. The reduction in the total carbohydrate and protein content was statistically significant ($P<0.05$). The final purity of FOS reached 76.02%.

A fast protein liquid chromatography method was used by Li et al. (2013) to purify FOS from burdock and 75-95% FOS purity was found at different conditions. Kuhn et al. (2014) purified FOS by column chromatography to 94% purity. In the literature, most of the purification studies about inulin and FOS were performed using chromatographic techniques such as size exclusion chromatography, ion exchange chromatography, and gel permeation chromatography (Muñiz-Márquez et al. 2019). Although higher purity levels were reported in studies with chromatographic techniques, the main disadvantage of chromatographic techniques for the purification of inulin and FOS is their relatively high installation cost, energy requirement, and resin requirement (Muñiz-Márquez et al. 2019). Purification by membrane techniques is simpler, and easily adaptable to large-scale processes, and although it involves installation costs, membrane filtration technique is more cost-effective than chromatographic techniques (Barclay et al. 2010; Muñiz-Márquez et al. 2019).

4. Conclusions

The process conditions for the extraction of inulin from chicory roots were optimized by using RSM design. The results verified that the RSM model was suitable and reliable for actualizing the expected optimization. Hydrolyzation of inulin to FOS was carried out by using acid and enzyme treatments in different trials. Acid hydrolysis resulted in the degradation of inulin to fructose. To obtain a high-quality product, purification is necessary. In this study, the membrane filtration technique was preferred because of its advantages such as easy scale-up and easily manipulated critical operational variables. However, membrane applications to purify inulin and FOS are limited in the literature. Mostly, chromatographic separation techniques that require high installation and operational costs and qualified employees were used for the purification of these components. In contrast to complex techniques, the membrane filtration method offers a simpler, more rapid, and economical way to obtain both inulin and FOS from chicory roots.

Acknowledgements

This study is part of a project funded by Yildiz Technical University BAP (Project code: FCD-2021-4573) department. We are grateful to Artisan Gıda for providing commercial inulin samples. The authors declare that they have no conflicts of interest.

References

- Albalasmeh A A, Berhe A A & Ghezzehei T A (2013). A new method for rapid determination of carbohydrate and total carbon concentrations using UV spectrophotometry. *Carbohydrate Polymers* 97(2): 253–261. <https://doi.org/10.1016/j.carbpol.2013.04.072>
- Apolinário A C, Lima Damasceno B P G, Macêdo Beltrão N E, Pessoa A, Converti A & Silva J A (2014). Inulin-type fructans: A review on different aspects of biochemical and pharmaceutical technology. *Carbohydrate Polymers* 101(1): 368–378. <https://doi.org/10.1016/j.carbpol.2013.09.081>
- Ávila-Fernández Á, Galicia-Lagunas N, Rodríguez-Alegría M E, Olvera C & López-Munguía A (2011). Production of functional oligosaccharides through limited acid hydrolysis of agave fructans. *Food Chemistry* 129(2): 380–386. <https://doi.org/10.1016/j.foodchem.2011.04.088>
- Balzarini M F, Reinheimer M A, Ciappini M C & Scenna N J (2018). Mathematical model, validation and analysis of the drying treatment on quality attributes of chicory root cubes considering variable properties and shrinkage. *Food and Bioprocess Processing* 111: 114–128. <https://doi.org/10.1016/j.fbp.2018.07.005>
- Barclay T G, Ginic-Markovic M, Cooper P D & Petrovsky N (2014). Inulin-A versatile polysaccharide with multiple pharmaceutical and food chemical uses. *Journal of Excipients and Food Chemicals* 1(3): 27–50. <https://www.researchgate.net/publication/49597010>
- Başaran U, Akkbik M, Mut H, Gülümser E, Doğrusöz M Ç & Koçoğlu S (2018). High-Performance liquid chromatography with refractive index detection for the determination of inulin in chicory roots. *Analytical Letters* 51(1–2): 83–95. <https://doi.org/10.1080/00032719.2017.1304952>
- Beirão-Da-Costa M L, Januario I & Leitão A (2009). Characterisation of inulin from chicory and salsify cultivated in Portugal. *Alim. Nutr. Araraquara* 16(3): 221–225. <https://www.researchgate.net/publication/49599872>
- Chandra S, Kumar M, Dwivedi P & Arti K (2016). Studies on industrial importance and medicinal value of chicory plant (*Cichorium intybus* L.). *International Journal of Advanced Research* 4(1): 1060–1071.
- Dobre T, Bull C, Stroescu M, Stoica A, Draghici E & Antohe N (2008). Inulin extraction and encapsulation. *Buletinul Științific al Universității "Politehnica" Din Timisoara* 53: 215–217. <http://mt.pub.ro>
- Dominguez A L, Rodrigues L R, Lima N M & Teixeira J A (2014). An overview of the recent developments on fructooligosaccharide production and applications. *Food and Bioprocess Technology* 7: 324–337. <https://doi.org/10.1007/s11947-013-1221-6>
- El-Kholy W M, Aamer R A & Ali A N A (2020). Utilization of inulin extracted from chicory (*Cichorium intybus* L.) roots to improve the properties of low-fat synbiotic yoghurt. *Annals of Agricultural Sciences*, 65(1): 59–67. <https://doi.org/10.1016/j.aoas.2020.02.002>
- Esmacili F, Hashemiravan M, Eshaghi M R & Gandomi H (2021). Optimization of aqueous extraction conditions of inulin from the arctium lappa l. roots using ultrasonic irradiation frequency. *Journal of Food Quality*. <https://doi.org/10.1155/2021/5520996>
- Figueira G M, Park K J, Brod F P R & Honório S L (2004). Evaluation of desorption isotherms, drying rates and inulin concentration of chicory roots (*Cichorium intybus* L.) with and without enzymatic inactivation. *Journal of Food Engineering*, 63(3): 273–280. <https://doi.org/10.1016/j.jfoodeng.2003.06.001>
- Fu Y P, Li L X, Zhang B Z, Paulsen B S, Yin Z Q, Huang C, Feng B, Chen X F, Jia R R, Song X, Ni X Q, Jing B, Wu F & Zou Y F (2018). Characterization and prebiotic activity in vitro of inulin-type fructan from *Codonopsis pilosula* roots. *Carbohydrate Polymers*, 193: 212–220. <https://doi.org/10.1016/j.carbpol.2018.03.065>
- Grzybowski A, Tiboni M, Passos M, Baldo G R & Fontana D J (2014). Production of fructo-oligosaccharides (FOS) from inulin and applications. In: Fontana D J, Tiboni M & Grzybowski A (Eds.), *Cellulose and Other Naturally Occurring Polymers, Brazil*, pp. 49–54.

- Han Y Z, Zhou C C, Xu Y Y, Yao J X, Chi Z, Chi Z M & Liu G L (2017). High-efficient production of fructo-oligosaccharides from inulin by a two-stage bioprocess using an engineered *Yarrowia lipolytica* strain. *Carbohydrate Polymers* 173: 592–599. <https://doi.org/10.1016/j.carbpol.2017.06.043>
- Karadag A, Pelvan E, Dogan K, Celik N, Ozturk D, Akalin K & Alasalvar C (2019). Optimisation of green tea polysaccharides by ultrasound-assisted extraction and their in vitro antidiabetic activities. *Quality Assurance and Safety of Crops and Foods* 11(5): 479–490. <https://doi.org/10.3920/QAS2019.1579>
- Khuenpet K, Fukuoka M, Jittanit W & Sirisansaneeyakul S (2017). Spray drying of inulin component extracted from Jerusalem artichoke tuber powder using conventional and ohmic-ultrasonic heating for extraction process. *Journal of Food Engineering* 194: 67–78. <https://doi.org/10.1016/j.jfoodeng.2016.09.009>
- Kralj S, Leeftang C, Sierra E I, Kempniński B, Alkan V & Kolkman M (2018). Synthesis of fructooligosaccharides (FosA) and inulin (InuO) by GH68 fructosyltransferases from *Bacillus agaradhaerens* strain WDG185. *Carbohydrate Polymers* 179: 350–359. <https://doi.org/10.1016/j.carbpol.2017.09.069>
- Kuhn R C, Mazutti M A, Albertini L B & Filho F M (2014). Evaluation of fructooligosaccharides separation using a fixed-bed column packed with activated charcoal. *New Biotechnology* 31(3): 237–241. <https://doi.org/10.1016/j.nbt.2014.02.005>
- Li J, Cheong K L, Zhao J, Hu D J, Chen X Q, Qiao C F, Zhang Q W, Chen Y W & Li S P (2013). Preparation of inulin-type fructooligosaccharides using fast protein liquid chromatography coupled with refractive index detection. *Journal of Chromatography A* 1308: 52–57. <https://doi.org/10.1016/j.chroma.2013.08.012>
- Li W, Li J, Chen, T & Chen C (2004). Study on nanofiltration for purifying fructo-oligosaccharides I. Operation modes. *Journal of Membrane Science* 245(1–2): 123–129. <https://doi.org/10.1016/j.memsci.2004.07.021>
- Lingyun W, Jianhua W, Xiaodong Z, Da T, Yalin Y, Chenggang C, Tianhua F & Fan Z (2007). Studies on the extracting technical conditions of inulin from Jerusalem artichoke tubers. *Journal of Food Engineering* 79(3): 1087–1093. <https://doi.org/10.1016/j.jfoodeng.2006.03.028>
- Lopes S M S, Krausová G, Carneiro J W P, Gonçalves J E, Gonçalves R A C & Oliveira A J B (2017). A new natural source for obtainment of inulin and fructo-oligosaccharides from industrial waste of *Stevia rebaudiana* Bertoni. *Food Chemistry* 225: 154–161. <https://doi.org/10.1016/j.foodchem.2016.12.100>
- Mavumengwana V B (2004). Isolation, purification and characterization of inulin and fructooligosaccharides from chicorium intybus and inulinase from *aspergillus niger*. M.Sc. Thesis, Rhodes University, South Africa
- Muñiz-Márquez D B, Teixeira J A, Mussatto S I, Contreras-Esquivel J C, Rodríguez-Herrera R & Aguilar C N (2019). Fructo-oligosaccharides (FOS) production by fungal submerged culture using aguamiel as a low-cost by-product. *LWT* 102: 75–79. <https://doi.org/10.1016/j.lwt.2018.12.020>
- Murtiningrum S P, Suryani A & Manguwidjaja D (2020). Determination of ultrafiltration resistance using series resistance model in inulin purification from red fruit (*Pandanus conoideus* L.) pedicel extract. *IOP Conference Series: Earth and Environmental Science* 443: 1. <https://doi.org/10.1088/1755-1315/443/1/012086>
- Nobre C, Filho E G A, Fernandes F A N, Brito E S, Rodrigues S, Teixeira J A & Rodrigues L R (2018). Production of fructo-oligosaccharides by *Aspergillus ibericus* and their chemical characterization. *LWT* 89: 58–64. <https://doi.org/10.1016/j.lwt.2017.10.015>
- Noori W O (2014). Selection of Optimal Conditions of Inulin Extraction from Jerusalem Artichoke (*Helianthus Tuberosus* L.) Tubers by using Ultrasonic Water Bath. *Journal of Engineering* 20: 110–119. <https://www.researchgate.net/publication/328278566>
- Öztürk B (2016). A rising star prebiotic dietary fiber: inulin and recent applications in meat products. *Journal of Food and Health Science* 3(1): 12–20. <https://doi.org/10.3153/jfhs17002>
- Perović J, Tumbas Šaponjac V, Kojić J, Krulj J, Moreno D A, García-Viguera C, Bodroža-Solarov M & Ilić N (2021). Chicory (*Cichorium intybus* L.) as a food ingredient – Nutritional composition, bioactivity, safety, and health claims: A review. *Food Chemistry* 336. <https://doi.org/10.1016/j.foodchem.2020.127676>
- Qing Q, Li H, Kumar R & Wyman C E (2013). Xylooligosaccharides production, quantification, and characterization in context of lignocellulosic biomass pretreatment. In: *Aqueous Pretreatment of Plant Biomass for Biological and Chemical Conversion to Fuels and Chemicals*, John Wiley and Sons, pp. 391–415. <https://doi.org/10.1002/9780470975831.ch19>
- Redondo-Cuenca A, Herrera-Vázquez S E, Condezo-Hoyos L, Gómez-Ordóñez E & Rupérez P (2021). Inulin extraction from common inulin-containing plant sources. *Industrial Crops and Products* 170. <https://doi.org/10.1016/j.indcrop.2021.113726>
- Ricca E, Calabrò V, Curcio S & Iorio G. (2009). Optimization of inulin hydrolysis by inulinase accounting for enzyme time- and temperature-dependent deactivation. *Biochemical Engineering Journal* 48(1): 81–86. <https://doi.org/10.1016/j.bej.2009.08.009>
- Sarchami T & Rehm L (2014). Optimizing enzymatic hydrolysis of inulin from Jerusalem artichoke tubers for fermentative butanol production. *Biomass and Bioenergy* 69: 175–182. <https://doi.org/10.1016/j.biombioe.2014.07.018>
- Singh R S & Singh T (2022a). Fructooligosaccharides production from inulin by immobilized endoinulinase on 3-aminopropyltriethoxysilane functionalized halloysite nanoclay. *Catalysis Letters* 152(7): 1927–1949. <https://doi.org/10.1007/s10562-021-03803-5>
- Singh R S & Singh T (2022b). Glutaraldehyde functionalization of halloysite nanoclay enhances immobilization efficacy of endoinulinase for fructooligosaccharides production from inulin. *Food Chemistry* 381. <https://doi.org/10.1016/j.foodchem.2022.132253>
- Singh R S, Singh T, Hassan M & Kennedy J F (2020). Updates on inulinases: Structural aspects and biotechnological applications. *International Journal of Biological Macromolecules* 164: 193–210. <https://doi.org/10.1016/j.ijbiomac.2020.07.078>
- Singh R S, Singh T & Kennedy J F (2020). Enzymatic synthesis of fructooligosaccharides from inulin in a batch system. *Carbohydrate Polymer Technologies and Applications* 1. <https://doi.org/10.1016/j.carpta.2020.100009>
- Singh R S, Singh T & Kennedy J F (2021). Understanding the interactive influence of hydrolytic conditions on biocatalytic production of fructooligosaccharides from inulin. *International Journal of Biological Macromolecules* 166: 9–17. <https://doi.org/10.1016/j.ijbiomac.2020.11.171>
- Singh R S, Singh T & Pandey A (2020). Fungal endoinulinase production from raw *Asparagus inulin* for the production of fructooligosaccharides. *Bioresource Technology Reports* 10. <https://doi.org/10.1016/j.biteb.2020.100417>
- Stökle K, Jung D & Kruse A (2023). Acid-assisted extraction and hydrolysis of inulin from chicory roots to obtain fructose-enriched extracts. *Biomass Conversion and Biorefinery* 13(1): 159–170. <https://doi.org/10.1007/s13399-020-01108-y>
- Tewari S, Ramalakshmi K, Methre L & Rao L J M (2014). Microwave-assisted extraction of inulin from chicory roots using response surface methodology. *Journal of Nutrition & Food Sciences*, 05(01). <https://doi.org/10.4172/2155-9600.1000342>
- Yi H, Zhang L, Hua C, Sun K & Zhang L (2010). Extraction and enzymatic hydrolysis of inulin from Jerusalem artichoke and their effects on textural and sensorial characteristics of yogurt. *Food and Bioprocess Technology* 3(2): 315–319. <https://doi.org/10.1007/s11947-009-0247-2>

Zhang X, Zhu X, Shi X, Hou Y & Yi Y (2022). extraction and purification of inulin from jerusalem artichoke with response surface method and ion exchange resins. *ACS Omega* 7(14): 12048–12055. <https://doi.org/10.1021/acsomega.2c00302>

Zhu Z, Luo X, Yin F, Li S & He J (2018). Clarification of jerusalem artichoke extract using ultra-filtration: effect of membrane pore size and operation conditions. *Food and Bioprocess Technology* 11(4): 864–873. <https://doi.org/10.1007/s11947-018-2054-0>



Copyright © 2024 The Author(s). This is an open-access article published by Faculty of Agriculture, Ankara University under the terms of the [Creative Commons Attribution License](https://creativecommons.org/licenses/by/4.0/) which permits unrestricted use, distribution, and reproduction in any medium or format, provided the original work is properly cited.



Organic Water-Soluble Fertilizers Enhance Pesticide Degradation: Towards Reduced Residues

Dongsheng LIU^a, Weizhen LI^b, Haixiang GAO^{b*}, Changsheng HUANG^a, Shihong XU^a,
Wenqi LIU^c

^aGuangxi Panshibao Co., Ltd. CHINA

^bChina Agricultural University. CHINA

^cSoil Fertilizer Work Station of Guangxi Zhuang Autonomous Region. CHINA

ARTICLE INFO

Research Article

Corresponding Author: Haixiang GAO, E-mail: hxgao@cau.edu.cn

Received: 15 June 2023 / Revised: 09 October 2023 / Accepted: 13 October 2023 / Online: 09 January 2024

Cite this article

Liu, D, Li W, Gao H, Huang C, Xu S, Liu W (2024). Organic Water-Soluble Fertilizers Enhance Pesticide Degradation: Towards Reduced Residues. *Journal of Agricultural Sciences (Tarim Bilimleri Dergisi)*, 30(1):179-192. DOI: 10.15832/ankutbd.1315200

ABSTRACT

This scientific undertaking meticulously inspected chlorpyrifos degradation kinetics when interacts with assorted organic water-soluble fertilizer formulations. Through rigorous field experimentation, we evaluated the modulatory effects of organic water-soluble fertilizers on the kinetics of pesticide degradation. Under specific conditions, organic water-soluble fertilizers can promote the degradation of pesticides. The integration of distinct fertilizer dilutions conspicuously enhanced degradation, alluding to intricate concentration-dependent mechanisms. In our quest to decipher the underlying mechanisms, we delved into both the biochemical and physicochemical facets. Notably, we monitored plant peroxidase activity across varying concentrations of these fertilizers throughout the investigative period. Temporal tracking displayed escalated plant peroxidase activity, mirroring bolstered detoxification. The results of the UV degradation experiment showed no significant difference in the acaricide degradation rate, regardless of the presence or

absence of organic water-soluble fertilizers. However, illumination-induced degradation remained unperturbed by fertilization. Simulated rainwater cleansing was enacted on farmer's market produce, spanning crucifers, asters, chenopods, and amaranths. Our assays pertaining to washing elucidated the capability of organic water-soluble fertilizers to curtail pesticide residues across representative vegetable taxa. Fertilizer supplementation substantially reduced chlorpyrifos residuals, especially in crucifers. This inquiry underscores the inherent botanical mechanisms of detoxification, which, when augmented by judicious fertilizer supplementation, culminate in the diminution of chlorpyrifos pesticide residues. While promising, extensive multi-crop trials are required to optimize assimilation strategies. Harnessing the intrinsic synergy between agricultural enrichment and pest mitigation, as expounded in this study, heralds a paradigm shift towards sustainable agriculture, ensuring both food security and ecological stewardship.

Keywords: Chlorpyrifos degradation, Peroxidase-mediated detoxification, Pesticidal residue diminution, Photolysis and UV effects, Agricultural sustainability

1. Introduction

Plants possess the ability to synthesize carbohydrates via photosynthesis; however, essential elements such as nitrogen, phosphorus, and potassium, which are integral for the formation of vital biomolecules like proteins, must be procured through mineral elements present in the soil. Continuous harvesting of plants inevitably leads to a decline in these mineral elements, resulting in soil impoverishment. Fertilizers, serving as a crucial constituent of agricultural chemicals, assume the responsibility of providing plant nutrition. Fertilizers play a pivotal role in fortifying soils with mineral elements that are inherently deficient, a step that ensures plant growth remains unhindered by elements such as nitrogen, phosphorus, and potassium (Savci 2012). It is imperative to acknowledge that while these inorganic compounds are vital in compensating for nutrient scarcities, their excessive application may culminate in deleterious consequences such as soil acidification and aquatic pollution (Medel et al. 2022). Fertilizers derived from organic, water-soluble sources present a viable alternative, addressing these detriments via a mechanism characterized by the gradual release of nutrients.

Pesticides arise as indispensable constituents within the anthology of agricultural amalgamations, their cardinal purpose being the protection of harvests from pernicious pestilent organisms. Despite its utility, the pronounced toxic attributes of chlorpyrifos residues, coupled with their persistent manifestation within both plant structures and aquatic domains, invite substantial trepidation. The precipitous accrual of such chemical vestiges upon agricultural yields, antithetical to rigorous safety prerequisites, spotlights an imperative for expeditious diminution (Medel et al. 2022; Senthilkumar et al. 2022). Though efficacious in pest control, the implications encompass potential degradation of soil matrices, contamination of aquatic conduits,

threats to human health, and the fiscal implications of their synthesis and administration (Bonmatin et al. 2021; R. Ramadevi et al. 2022; Senthilkumar et al. 2022). Although the protective role of pesticides in plant health is indisputable, a lack of knowledge among farmers often leads to over-application of pesticides, and in some instances, products are sold within the safety interval of the pesticide, potentially jeopardizing consumer health (Philippe et al. 2021) As a consequence, there is a pressing need for the development of scientifically sound methodologies to reduce pesticide residues and curtail the safety interval of pesticides (Adhikari 2017).

The organophosphorus pesticide, chlorpyrifos, known for its role in obstructing nerve impulse transmission through the inhibition of acetylcholinesterase enzymatic functions, has been corroborated for its efficacy against a diverse spectrum of pests plaguing various crops. However, abundant trepidations pervade surrounding chlorpyrifos' overt toxicity and persistence within botanical and aqueous environments, underscoring the necessity of minimizing accumulations on consumable crops to uphold exacting safety standards. Given the concerns, we explored how organic water-soluble fertilizers might enhance microbial and enzymatic activities, thereby reducing chlorpyrifos residues and shortening pre-harvest intervals. This study unveils new insights into the synergistic interactions between fertilizers and pesticides, enriching current knowledge. Rigorous experimentation verified that synergistic co-applications can effectively diminish pesticide accumulations, consequently abbreviating pre-harvest intervals. Our experiments confirmed that using organic water-soluble fertilizers with pesticides effectively reduces pesticide residues and safety intervals (Niu et al. 2021). The outcomes elucidate that the synergistic application of organic water-soluble fertilizers in conjunction with pesticides paves the way for diminished pesticide residues, consequently abbreviating the safety interlude necessary before the harvested yield can be adjudicated as fit for intake. In charting the intricate coordinates of this scholarly passage, the undertaken empirical maneuvers have unfurled illuminating glimpses into a cardinal quandary that lies firmly ingrained within the expansive realm of agricultural sustainability.

2. Material and Methods

2.1. Experimental reagents and materials

The reagents and materials were obtained from commercial sources:

Acetamiprid emulsion concentrate (480g/L, Jiatong, Jiangsu Baoling Chemical Co., Ltd.) for its pesticidal properties, and acetamiprid (Aladdin Reagent Co., Ltd., Shanghai, China) as a reference standard for comparison purposes. Organic water-soluble fertilizer (water-based) (Guangxi Panshibao Co., Ltd.) for its plant nutrient content. (Detailed Information on the Fertilizer: (1) Composition: The fertilizer is an organic multi-element compound water-soluble type, abundant in essential crop nutrients such as nitrogen, phosphorus, potassium, boron, zinc, manganese, and other minerals. Moreover, it encompasses organic nutrients like fulvic acid, amino acids, vitamins, and polysaccharides. (2) Product Features: This fertilizer grants crops with thorough and balanced nutrition throughout their growth cycle. It aids in tissue repair, growth promotion, and product quality enhancement. It's known to elevate crop immunity, catalyze enzymatic activity, bolster resistance against environmental adversities, augment chlorophyll content, enhance photosynthesis efficiency, and promote fruiting and flowering. (3) Chemical Properties: Organic Matter: $\geq 125\text{g/L}$; Nitrogen (N): $\geq 100\text{g/L}$; Phosphorus (P₂O₅): $\geq 50\text{g/L}$; Potassium (K): $\geq 20\text{g/L}$; Zinc (Zn): $\geq 20\text{g/L}$; Boron (B): $\geq 8\text{g/L}$; Manganese (Mn): $\geq 2\text{g/L}$; (4) Safety and Quality Standards: The fertilizer adheres to stringent safety standards, with specific thresholds set for insoluble matter, heavy metals, microbial contamination, among other potential contaminants. The pH for a 1:250 dilution resides between 3.0 to 5.0.)

Acetonitrile, methanol, and acetone (chromatographically pure, Beijing Dimachem Technology Co., Ltd.) as organic solvents for extraction and analytical processes. Sodium chloride, sodium dihydrogen phosphate, and sodium phosphate monobasic (analytical grade, China National Pharmaceutical Group Chemical Reagent Co., Ltd., China) as reagents in the analytical process. Cleanert SC18-SPE (Bonna-Agela Technologies Co., Ltd.) as a sorbent material in sample preparation. Guaiacol (Tokyo Chemical Industry Co., Ltd., Japan) and 30% hydrogen peroxide (China National Pharmaceutical Group Chemical Reagent Co., Ltd., China) as reagents in the analytical process. A ceramic small grinding bowl (Guangda Hengyi Co., Ltd., China) for grinding and homogenizing samples, and a 2 mL centrifuge tube (Guangda Hengyi Co., Ltd., China) for sample storage and processing.

The vegetables used in the experimental procedure, including rapeseed, lettuce, Chinese kale, spinach, and amaranth (Meili Meijia Supermarket, Beijing, China), were procured for use as samples. All of the aforementioned reagents and materials were used in the described experimental procedure, and their properties and sources have been accurately reported for transparency and repeatability purposes.

2.2. Experimental Instruments

The Agilent 1200 infinity series high-performance liquid chromatography instrument with a UV-visible light detector (Agilent Technologies, Palo Alto, California, USA) was used for detection, separation, and quantitative analysis. The chromatographic column used was the Spursil C18 column (5 μm , 4.6 \times 250mm) and the Spursil C18 guard column (5 μm , 2.1 \times 10mm).

Other instruments included an analytical balance, a circulating multi-functional water pump, a rotary evaporator, a freezer, an organic membrane, latex gloves, sterile disposable syringes, a nitrogen concentrator, a manual adjustable pipette, an ultrapure water system, a CNC ultrasonic cleaner, a high-speed centrifuge, a micro-injector, an electric heating blast drying oven, a vortex mixer, a homogenizer, a UV lamp, a homemade UV box, a UV-visible spectrophotometer, a temperature-controlled high-speed centrifuge, an automatic tension meter, and a CNC ultrasonic cleaner.

2.3. Field trial

2.3.1. Overview of the trial site

The trial field for this field experiment is located in Houzhang Village, Shangzhuang Town, Haidian District, Beijing. It is surrounded by many villages, such as Qianzhang Village, Bajia Village, Shuangta Village, and Xixinlitun Village, and is located in the northwest corner of Shangzhuang. The soil in this area is fertile and belongs to the good quality loam soil of the North China Plain. The area has a temperate monsoon climate with little water and strong winds in spring, rainy and humid in summer, short and dry in autumn, and cold and frozen in winter. The average annual temperature is 12 °C, the annual precipitation is 630 mm, with 60-70% concentrated in July and August, the annual evaporation is 1500mm, and the average annual wind speed is 2.4 m/s.

2.3.2. Experimental method

The land was divided into 10 plots, each plot measuring 6 m² with a safety zone between each plot. Plots 1, 2, and 3 were recommended for high doses of Chlorpyrifos, with 900 mL of Chlorpyrifos diluted 1000 times applied. Plots 3, 4, and 5 were also recommended for high doses of Chlorpyrifos, with 900 mL of diluted Chlorpyrifos and 900µL of 1000-fold diluted organic water-soluble fertilizer added (Chang et al. 2020; Sun et al. 2018). Plots 5, 6, and 7 were recommended for high doses of Chlorpyrifos, with 900 mL of diluted Chlorpyrifos and 600 µL of 1500-fold diluted organic water-soluble fertilizer (Penshibao) added. Plot 10 was left as a blank control group without any Chlorpyrifos application. When the rapeseed plants were approximately 10 cm tall, the spraying was carried out on a windless morning. Samples were collected 3, 5, and 7 days after spraying.

The pesticide detection method referred to GBT 20769-2008 (Pang 2018) (Determination of 450 Pesticides and Related Chemical Residues in Fruits and Vegetables).

According to the experimental needs and the prediction of sample content, a standard substrate solution of Chlorpyrifos with five concentrations of 1mg/L, 0.8mg/L, 0.5mg/L, 0.1mg/L, and 0.05mg/L were prepared with small rapeseed as the substrate. The chromatographic peak area of each concentration was detected and the standard quantification curve of Chlorpyrifos was plotted, with the concentration of the Chlorpyrifos standard substance on the x-axis and the chromatographic detection integral area on the y-axis.

The linear regression equation for the standard substrate solution of *Brassica rapa* subsp. *chinensis* is:

Chlorpyrifos, $y = 116.16x + 28.673$, $R^2 = 0.9971$ (Figure 1).

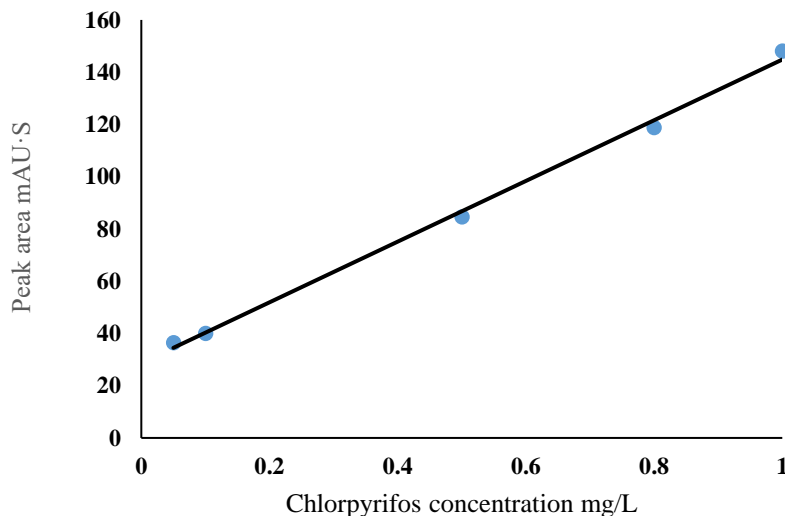


Figure 1- Calibration Curve of Chlorpyrifos in Real Sample *Brassica rapa* subsp. *chinensis*

Table 1- The recovery and RSD of added analytes in real vegetable sample

Samples	Added concentration (mg/kg)	Recovery rate (%)				Average recovery rate (%)	RSD (%)	
		88.7	94.8	101.4	93.2			
<i>Brassica rapa subsp. chinensis</i>	0.005	88.7	94.8	101.4	93.2	95.3	94.7	4.8
	0.1	94.0	89.3	94.6	91.1	88.7	91.5	2.9
	0.5	97.7	94.1	95.5	86.6	93.2	93.4	4.5

2.4. Biological factor - peroxidase activity

The experimental area was partitioned into ten distinct plots, each encompassing 6 m² and separated by safety zones (Andreu & Picó 2004; Hossain et al. 2022; Pal et al. 2010; Pavlidis et al. 2020; Shalaby & Abdou 2010). Plots 1-3 were subjected to elevated concentrations of Chlorpyrifos, achieved by administering 900 mL of 1000-fold diluted Chlorpyrifos. Plots 4-6 received a similar treatment, with the addition of 900 µL of at a 1000-fold dilution. In plots 7-9, 900 mL of diluted Chlorpyrifos was supplemented with 600 µL of at a 1500-fold dilution. Plot 10 served as an untreated control group. When the rapeseed plants reached approximately 10 cm in height, the spraying was conducted on a calm morning. Samples were procured on days 3, 5, 7, and 14 post-spraying, with experiments executed immediately following sample collection.

Initially, a mortar, phosphate buffer solution, and rapeseed samples were precooled, with the mortar situated in an ice bath to maintain a low temperature, thereby preserving enzyme activity. A rapid weighing balance was employed to measure 0.200 g of fresh rapeseed leaf samples, which were subsequently added to the mortar in the ice bath for grinding. Peroxidase extraction was achieved using a 50 mmol/L precooled phosphate buffer solution (pH 6.0). A pipette was used to extract 600 µL of the phosphate buffer solution, which was then transferred to a 2 mL centrifuge tube. Following this, 500 µL of enzyme solution was extracted twice, ultimately combining with the initial extract. The resulting mixture was subjected to temperature-controlled high-speed centrifugation at 4°C and 12,000 g for 20 minutes. The supernatant was then aspirated and stored in a refrigerator.

The instrument was zeroed using a blank phosphate buffer solution. A 3 mL aliquot of the reaction solution was withdrawn using a pipette, and 40 µL of the test enzyme solution was introduced. The solution was promptly mixed with a pipette and positioned within a UV-visible spectrophotometer. The enzyme-catalyzed reaction ensued, yielding a colored product quantifiable by the UV-visible spectrophotometer. The OD470 alteration curve within 15 minutes was constructed using the spectrophotometer, with the curve's slope signifying the reaction rate. Peroxidase activity can be denoted as the change in OD470 per minute multiplied by 100, with the unit being U. Lastly, enzyme activity was converted to the per gram of fresh weight of rapeseed enzyme activity value (Singh et al. 2004).

2.5. Non-biological factor - light exposure

2.5.1. Experimental design

A 175 W UV mercury lamp served as the light source for the investigation (Hossain et al. 2013), Plots 1-3 comprised a 5 ppm solution of Chlorpyrifos (water: methanol = 1:1), while plots 4-6 contained a 5 ppm solution of Chlorpyrifos combined with a 1000-fold diluted organic water-soluble fertilizer. Plots 7-9 were treated with a 5 ppm solution of Chlorpyrifos and a 1500-fold diluted organic water-soluble fertilizer. Plots 10-12, which housed a 5 ppm solution of Chlorpyrifos, were maintained in darkness as a control group. Following 0, 10, 25, and 45 minutes of exposure, samples were collected and analyzed using high-performance liquid chromatography (HPLC).

2.5.2. Standard curve

An external standard method was employed, with Chlorpyrifos concentration plotted on the x-axis and chromatographic peak area on the y-axis to construct a standard curve for subsequent quantitative analysis.

$$\text{Standard Curve: } y = 9.8016x + 0.0478 \quad R^2 = 0.9999 \text{ (Figure 2)}$$

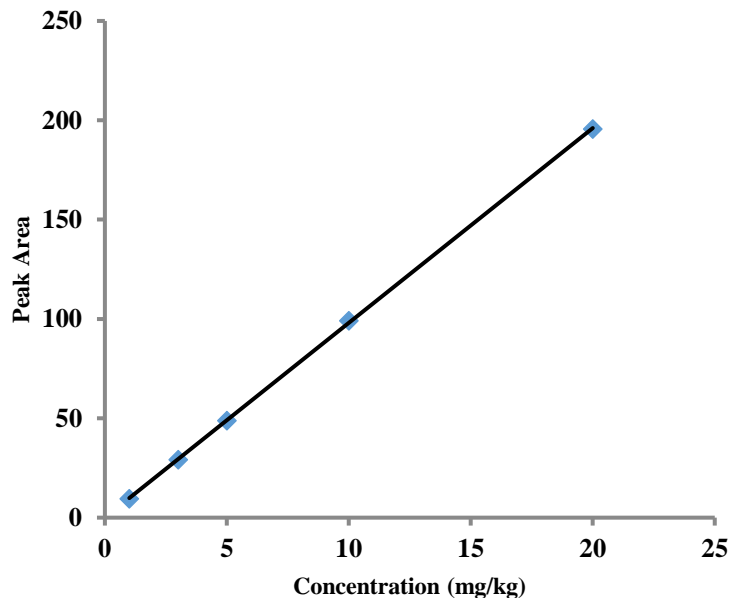


Figure 2- Calibration Curve of Chlorpyrifos

2.6. Surface activity verification experiment

2.6.1. Instrumentation

A JK99B automatic tensiometer (brand: POWEREACH, Shanghai Zhongchen Digital Technology Equipment Co., Ltd.) was utilized for the experiments.

2.6.2. Experiment

The gradient dilution method was implemented: The organic water-soluble fertilizer, sourced from Guangxi Panshibao Co., Ltd., was chosen for its specific nutrient composition, which plays a pivotal role in its properties and efficacy. A 2% organic water-soluble fertilizer solution was prepared and successively diluted by 2-fold to generate a series of gradient solutions, specifically 2%, 1%, 0.5%, 0.25%, and 0.125%. The platinum plate method was employed to measure surface tension values, with three parallel measurements executed for each group (a platinum plate is immersed in the test solution and subsequently lifted, with the surface tension value recorded upon detachment from the liquid surface). The surface tension of pure water at room temperature is 72 mN/m.

2.7. Non-biological factor - facilitates pesticide dissolution experiment

2.7.1. Experimental method

Experimental Design

Four experimental groups were established using four stainless steel pans, each containing 2 L of deionized water and 2 mL of Chlorpyrifos emulsion (formulated as a 1000-fold diluted solution of Chlorpyrifos). Groups 1 and 2 did not incorporate organic water-soluble fertilizer. Group 3 introduced 2 mL of a 1000-fold diluted solution of organic water-soluble fertilizer, while Group 4 added 665 μ L of a 1500-fold diluted solution of organic water-soluble fertilizer, administered twice. Equal quantities of oilseed rape were submerged in the pesticide solution in each stainless-steel pan, stirred thrice, and subsequently removed and dried.

Upon drying, the samples were cleansed. Group 1 remained unwashed, whereas the other groups were rinsed with 2 L of deionized water, employing the same soaking and stirring protocol, and then dried. Ultrasonic extraction was utilized for analysis (Balkan & Yılmaz 2022; Ikeura et al. 2011). The oilseed rape plants chosen for the experiments were specifically in the vegetative growth stage, at the rosette phase, ensuring uniform developmental progression among all specimens. Each plant consistently presented an average of 8-10 leaves. Three oilseed rape plants were randomly chosen for each group as parallel samples. Each plant was accurately weighed to 0.800 g in a centrifuge tube, and 8.00 mL of methanol was introduced to extract the Chlorpyrifos residue on the leaf surface. The solution was sonicated for 20 min and analyzed via liquid chromatography.

Solvent optimization

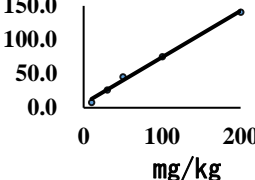
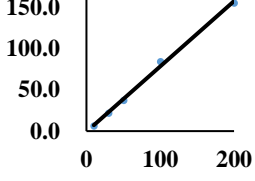
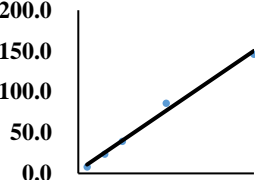
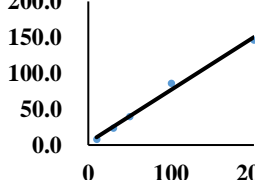
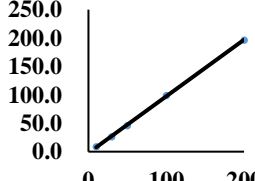
Table 2- The influence of different solvents on extraction recovery of chlorpyrifos

Vegetables (Family)	Vegetables (Species)	Solvent optimization	Optimization result								
Brassicaceae	<i>Brassica rapa subsp. Chinensis</i>	<table border="1"> <tr> <th>Solvent</th> <th>Recovery (%)</th> </tr> <tr> <td>Methanol</td> <td>75.1</td> </tr> <tr> <td>Acetonitrile</td> <td>56.0</td> </tr> <tr> <td>Acetone</td> <td>67.4</td> </tr> </table>	Solvent	Recovery (%)	Methanol	75.1	Acetonitrile	56.0	Acetone	67.4	Methanol
Solvent	Recovery (%)										
Methanol	75.1										
Acetonitrile	56.0										
Acetone	67.4										
Asteraceae	<i>Brassica napus subsp. oleifera</i>	<table border="1"> <tr> <th>Solvent</th> <th>Recovery (%)</th> </tr> <tr> <td>Methanol</td> <td>48.8</td> </tr> <tr> <td>Acetonitrile</td> <td>66.7</td> </tr> <tr> <td>Acetone</td> <td>84.7</td> </tr> </table>	Solvent	Recovery (%)	Methanol	48.8	Acetonitrile	66.7	Acetone	84.7	Acetone
	Solvent	Recovery (%)									
Methanol	48.8										
Acetonitrile	66.7										
Acetone	84.7										
	<i>Lactuca sativa</i>	<table border="1"> <tr> <th>Solvent</th> <th>Recovery (%)</th> </tr> <tr> <td>Methanol</td> <td>64.2</td> </tr> <tr> <td>Acetonitrile</td> <td>74.8</td> </tr> <tr> <td>Acetone</td> <td>71.3</td> </tr> </table>	Solvent	Recovery (%)	Methanol	64.2	Acetonitrile	74.8	Acetone	71.3	Acetonitrile
Solvent	Recovery (%)										
Methanol	64.2										
Acetonitrile	74.8										
Acetone	71.3										
Amaranthaceae	<i>Spinacia oleracea</i>	<table border="1"> <tr> <th>Solvent</th> <th>Recovery (%)</th> </tr> <tr> <td>Methanol</td> <td>81.1</td> </tr> <tr> <td>Acetonitrile</td> <td>77.4</td> </tr> <tr> <td>Acetone</td> <td>61.3</td> </tr> </table>	Solvent	Recovery (%)	Methanol	81.1	Acetonitrile	77.4	Acetone	61.3	Methanol
Solvent	Recovery (%)										
Methanol	81.1										
Acetonitrile	77.4										
Acetone	61.3										
Amaranthus tricolor	<i>Amaranthus spp.</i>	<table border="1"> <tr> <th>Solvent</th> <th>Recovery (%)</th> </tr> <tr> <td>Methanol</td> <td>89.8</td> </tr> <tr> <td>Acetonitrile</td> <td>96.0</td> </tr> <tr> <td>Acetone</td> <td>101.5</td> </tr> </table>	Solvent	Recovery (%)	Methanol	89.8	Acetonitrile	96.0	Acetone	101.5	Acetone
Solvent	Recovery (%)										
Methanol	89.8										
Acetonitrile	96.0										
Acetone	101.5										

Precisely weigh 0.800 g of intact vegetable leaves and use a microsyringe to draw up 80 μL of a 1000 mg/kg stock solution of chlorpyrifos in methanol, achieving a concentration of 100 mg/kg. Gradually dispense one drop in 40 steps, with each drop approximately 2 μL , lightly touching the leaf surface to establish contact with the droplet. Repeat this process 40 times to uniformly coat the leaf surface with 40 small droplets. Allow the leaves to rest for 20 minutes for methanol evaporation before placing the pesticide-treated leaves in a 10 mL centrifuge tube. Add 8 mL of ultrasonic extraction solvent (methanol, acetonitrile, or acetone, with three replicates for each solvent) and sonicate for 20 minutes. Analyze the methanol extract using high-performance liquid chromatography to calculate the recovery rate. The solvent exhibiting the highest recovery rate is selected as the optimal solvent for subsequent experiments.

Calibration Curve

Table 3- Calibration curve of chlorpyrifos on different vegetables

Vegetables (Family)	Vegetables (Species)	Calibration Curve*	R ²
Brassicaceae	<i>Brassica rapa subsp. Chinensis</i>	$y=0.6831x+6.0689$ 	0.9946
Asteraceae	<i>Brassica napus subsp. oleifera</i>	$y=0.7885x-0.6840$ 	0.9969
	<i>Lactuca sativa</i>	$y=0.7338x+0.3889$ 	0.9911
Chenopodiaceae	<i>Spinacia oleracea</i>	$y=0.7143x+0.3889$ 	0.9985
Amaranthaceae	<i>Amaranthus spp.</i>	$y=0.9970x-2.3032$ 	0.9996

*: The adding concentrations are 10mg/kg, 30mg/kg, 50mg/kg, 100mg/kg, 200mg/kg

The specific experimental procedure entails the following steps: accurately weigh 0.800 g of vegetable leaves and utilize a micro-syringe to draw the appropriate volume of the stock solution for each desired concentration. Gradually dispense a droplet multiple times, with each droplet measuring approximately 2 μ L, gently touching the leaf surface such that the droplet merely contacts the surface and is adsorbed onto the leaf due to surface interactions. This process is repeated numerous times to uniformly coat the leaf surface with small droplets. Allow the leaves to rest for 20 minutes for methanol evaporation before

placing the treated leaves in a 10 mL centrifuge tube. Add 8 mL of ultrasonic extraction solvent, sonicate for 20 minutes, and analyze the solvent extract using high-performance liquid chromatography to calculate the recovery rate and construct the standard curve.

3-Results and Discussion

3.1. Results of field control trials

The empirical outcomes suggest that subsequent to the administration of the organic water-soluble fertilizer, there was a marked diminution in the remnants of pesticides. Specifically, pesticide residue levels after adding 1500-fold diluted organic water-soluble fertilizer for 3 and 7 days were approximately half of those without its addition. In contrast, the concentration of 1000-fold diluted organic water-soluble fertilizer did not exhibit any noticeable change in pesticide residue in comparison to samples without the fertilizer (Figure 3). This intimates a potential dependency on concentration. Subsequent experimental designs might explore the precise interplay between the promotion of degradation and the gradations of organic fertilizer dilution, aiming to discern the ideal dilution for optimal efficacy. The meticulous calibration of such dilution models is of utmost importance for the articulation of efficacious application protocols.

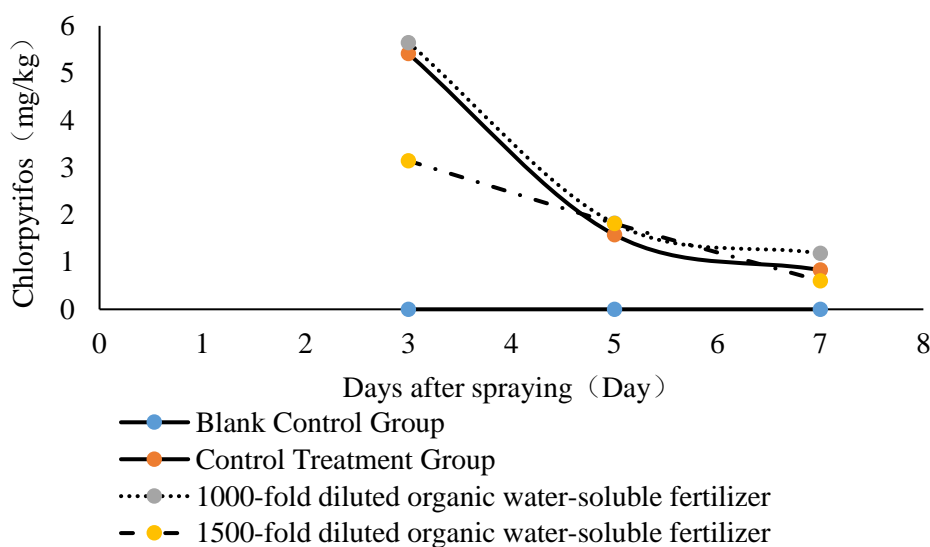


Figure 3- The influence of organic water-soluble fertilizer on degradation curve of chlorpyrifos

3.2. Biological factor - peroxidase activity results

The experimental data underscore that during the initial 7-day period, the peroxidase activity remained relatively constant across all vegetable samples, irrespective of the application of organic water-soluble fertilizers. (Figure 4) However, as the days progressed, a noticeable difference emerged. Particularly after the 7-day mark, vegetables that received the organic water-soluble fertilizer treatment showed a surge in peroxidase activity. The peak difference was observed at 14 days, suggesting that the organic water-soluble fertilizer might be playing a more pronounced role in influencing enzyme activity over extended periods. This could potentially be attributed to the gradual absorption and utilization of the nutrients present in the fertilizer by the plants.

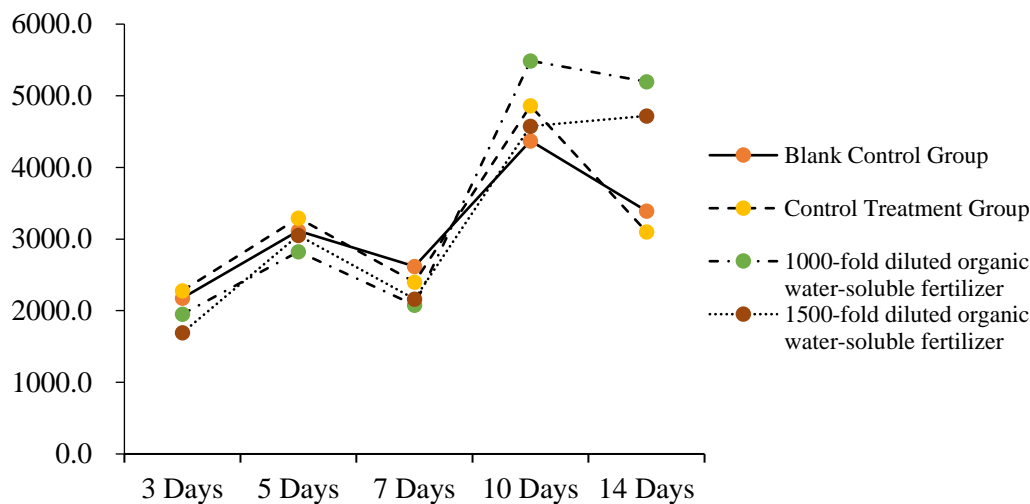


Figure 4- The influence of organic water-soluble fertilizer on the activity of peroxidase

The meticulous calibration of such dilution models is of utmost importance for the articulation of efficacious application protocols. Enzymes of the peroxidase family are instrumental in plant detoxification endeavors. The surge in their activity suggests an augmented detoxification apparatus, aligning seamlessly with the documented diminution in pesticide residues.

The organic water-soluble fertilizer may be catalyzing this detoxification process in the oilseed rape leaves, thereby ensuring a healthier vegetable yield with reduced pesticide content. The specific mechanisms could involve upregulation of certain detoxification enzymes or metabolic pathways by active ingredients in the fertilizer.

Advanced transcriptomic or proteomic analyses could potentially elucidate the genetic underpinnings bolstering detoxification in the presence of fertilizer supplementation. This insight aligns coherently with prior scholarly endeavors highlighting the versatile roles of peroxidases in plant defense mechanisms. These enzymes, besides their role in detoxification, are integral to the reinforcement of plant cellular architectures and enhancing adaptability to a plethora of stress conditions. It becomes compelling to theorize that organic water-soluble fertilizers may be magnifying these intrinsic vegetal defense systems, thus furnishing an augmented barrier against pesticide accrual.

In synthesizing the observations, the evident amplification in peroxidase activity, modulated by the presence of organic water-soluble fertilizers, necessitates additional academic exploration. A profound exploration of the constituents within these fertilizers and their nexus with plant biochemistry could illuminate pioneering tactics for sustainable agronomy. Through judicious tailoring of fertilizer compositions, we might envision a scenario wherein flora not merely assimilate vital growth nutrients but concurrently fortify their innate defensive armamentarium against extrinsic contaminants, including pesticides (Saparrat et al. 2010).

3.3. Non-biological factors - light exposure experiment results

As demonstrated in the Figure 5, the chlorpyrifos concentration stored in the dark remained stable throughout the experiment, indicating that pesticide hydrolysis during this period was markedly slower than photolysis, which underscores the difference between hydrolytic and photolytic degradation processes. Specifically, hydrolysis, which occurs in the absence of light, is often a slower process when compared to photolysis, where light serves as a catalyst to promote degradation. Nonetheless, the addition of various concentrations of organic water-soluble fertilizer did not significantly accelerate the photolysis reaction compared to the chlorpyrifos solution without organic water-soluble fertilizer. While these constituents might have a role in nourishing the soil or promoting plant health, their interaction with pesticides, in this case chlorpyrifos, seems minimal with respect to photodegradation. A plausible conclusion here is that the organic matter present in the fertilizer does not engage in any significant interactions leading to the indirect photolysis of chlorpyrifos, as supported by references (Graça et al. 2017; Wang et al. 2000). Thus, the overarching degradation effect of the organic water-soluble fertilizer on chlorpyrifos might be facilitated through other mechanisms, potentially biological or chemical, rather than the promotion of photolysis. Ensuing investigations might navigate these ancillary routes, facilitating a comprehensive comprehension of the dynamic interplay between organic fertilizing agents and pesticidal compounds.

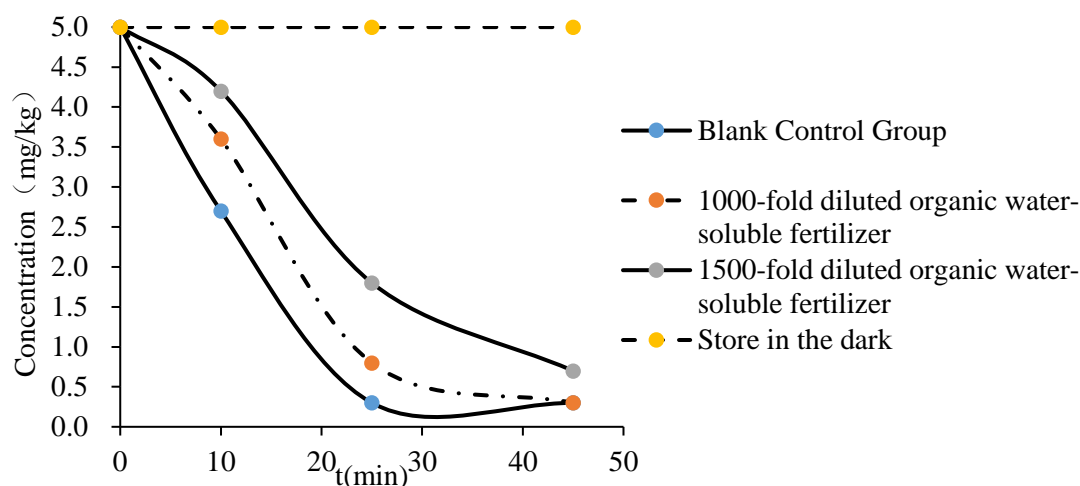


Figure 5- The influence of organic water-soluble fertilizer on photodegradation curves of chlorpyrifos

3.4. Surface Activity of Organic Water-soluble Fertilizer

Figure 6 delineates the intricate interplay of surface tension dynamics associated with organic water-soluble fertilizers, accentuating a pronounced surfactant-like behavior. Upon systematic escalation of the fertilizer's mass fraction, an unequivocal attenuation in surface tension becomes manifest, culminating in a stabilization plateau at a 2% threshold. Such observations not only attest to the inherent amphiphilic nature of the fertilizer but also insinuate a labyrinthine compositional matrix. Predominantly, specific molecular entities, perhaps surfactants or analogous amphiphilic moieties within the fertilizer, emerge as the plausible catalysts orchestrating this surfactant-like behavior.

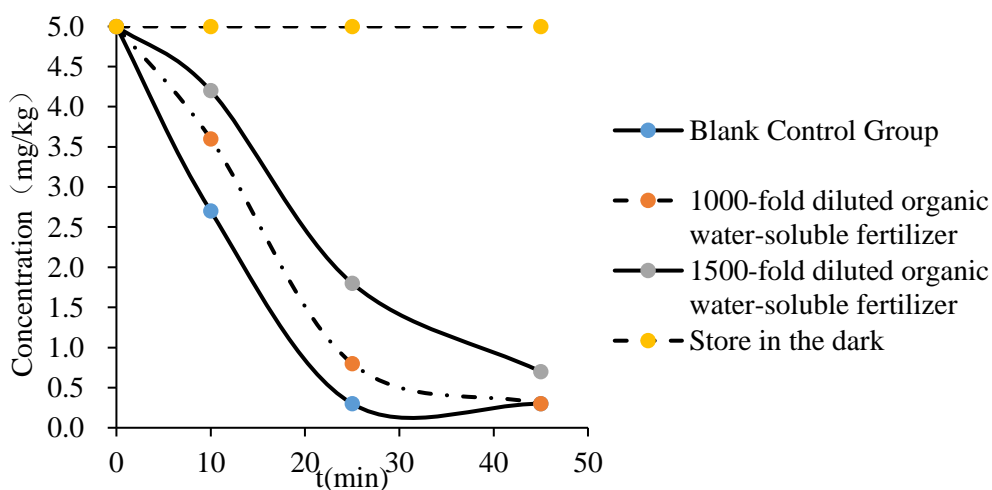


Figure 6- surface tension curves of organic water-soluble fertilizer

This amphiphilic characteristic, intrinsically embedded within the fertilizer, fosters a propitious milieu for synergistic interactions with hydrophobic pesticidal agents, epitomized by chlorpyrifos. Envisage an intricate dance where the lipophilic factions of the fertilizer entwine with the non-polar pesticide moieties, concurrently, the polar factions are immersed in an aqueous continuum. This orchestrated interplay precipitates a marked diminution in pesticide residues, accentuated post-aqueous events such as precipitation or intentional irrigation, thereby truncating the requisite safety interludes preceding vegetable ingestion. Such a mechanism proffers an avant-garde stratagem to efficaciously modulate pesticide residues.

Contemporary scholarly treatises, as corroborated by references (Sundaram & Sundaram, 1994; Pinto et al.2015), resonate with this narrative, spotlighting the synergistic interplay of humic acid vis-à-vis chlorpyrifos. These molecular dalliances can be adeptly leveraged to further mitigate pesticidal residues on flora, particularly subsequent to ablation in the presence of organic water-soluble fertilizers.

3.5. Non-biological factors - Effects of Spraying Organic Water-soluble Fertilizer on Pesticide Dissolution

3.5.1. Results and analysis of cruciferous vegetables (rapeseed)

In this study, rapeseed specimens imbued with pesticides underwent aqueous ablution to quantify residual pesticide levels. Comparing the experimental group treated with organic water-soluble fertilizer to the group without it, a decrease in residual pesticide concentration was observed with the addition of Organic water-soluble fertilizer. The residual rate after washing was 76%, a 28% reduction compared to the group without Organic water-soluble fertilizer.

The notable decrement in persistent pesticidal contaminants accentuates the formidable potential of organic water-soluble fertilizers, positing them as an efficacious paradigm in the pursuit of agricultural products of heightened purity and security. Concurrently, this underscores an emergent trajectory toward the attenuation of an entrenched reliance upon synthetic chemical agents in pest deterrence.

An examination of the experimental groups with different concentrations of Organic water-soluble fertilizer revealed that the group with a higher 1000-fold concentration exhibited the least pesticide residue, with a residue rate decrease of 41%.

The postulated mechanism responsible for this discernment is predominantly anchored in the surfactants that are intrinsic to the composition of organic water-soluble fertilizers. These surfactants, esteemed for their amphiphilic characteristics, are posited to augment the dissolution of pesticides, particularly in the context of natural rainfall or controlled irrigation techniques. Such a supposition aligns seamlessly with the venerated role of surfactants in augmenting the solubility of hydrophobic entities within aqueous mediums.

Consequently, it can be concluded that adding Organic water-soluble fertilizer organic water-soluble fertilizer to rapeseed reduces pesticide residues. The reduction mechanism may involve surfactants in organic water-soluble fertilizer dissolving more pesticides into water during natural rainfall or artificial cleaning. Organic water-soluble fertilizer, a water-soluble organic fertilizer, contains organic matter such as humic acid. Evidence indicates that humic acid can increase the apparent solubility of pesticides, with a linear correlation between the apparent solubility of pesticides and humic acid concentration. Empirical data indicates that humic acid demonstrates an aptitude for elevating the ostensible solubility of pesticides, with linear correlation observed between pesticide ostensible solubility and humic acid concentration. Thus, it can be inferred that organic water-soluble fertilizer organic water-soluble fertilizer reduces pesticide residues and decreases the safety interval for rapeseed.

3.5.2. Results and analysis of asteraceae vegetables (lettuce)

Amaranth, a member of the Asteraceae family, is relatively easy to wash, exhibiting a residue rate of 78% after washing with water. The inherent ease of washing Amaranth might be attributed to its leaf structure or the nature of its epidermal layer, which might be less adhesive to pesticide residues compared to other vegetables.

Upon the addition of a 1500-fold concentration of organic water-soluble fertilizer, the pesticide residue rate decreased by 11%. Whereas a modest decrement in residual concentrations suggests that even at augmented concentrations, the organic hydrophilic nourishment manifests a non-trivial influence upon the dissolution dynamics of pesticidal residues. More strikingly, with a 1000-fold concentration of the organic water-soluble fertilizer, the residue rate decreased by 32%. This substantial drop at a lower concentration might hint at an optimal concentration range where the fertilizer exhibits maximal efficiency in aiding pesticide dissolution.

Among the four vegetable types examined, organic water-soluble fertilizer demonstrated a significant effect in reducing pesticide residues on Amaranthaceae vegetables such as amaranth, second only to cruciferous vegetables.

Such specificity in action suggests that different vegetable families, due to their unique anatomical and biochemical traits, might interact differently with the organic water-soluble fertilizer. For instance, the waxy cuticle of cruciferous crops could facilitate surfactant interactions, while certain secondary metabolites in Asteraceae vegetables may preferentially bind with humic acids. Discerning attributes idiosyncratic to discrete categories could pave the way for a more tailored formulation of nutriment. The paramount inference drawn from these rigorous experiments is the revelation that organic water-soluble fertilizers precipitate a substantive diminution in pesticide residues. This is most salient in the context of cruciferous vegetables and those of the Amaranthaceae family. The empirical evidence presented furnishes a persuasive justification for prudently incorporating organic hydrophilic supplements within established agricultural frameworks, particularly for botanical varieties exhibiting a pronounced susceptibility to pesticidal treatments.

As for the underlying mechanism, it's postulated that surfactants and humic acid present in the organic water-soluble fertilizer play pivotal roles in promoting pesticide dissolution in water. Surfactants, by their nature, reduce the surface tension of water, potentially allowing for better penetration and removal of pesticide residues from the vegetable surfaces. Humic acid, on the other hand, might be binding to the pesticide molecules, enhancing their solubility and consequently their ease of removal. For a holistic epistemological panorama, it stands to reason that the orchestration of further investigative undertakings, plumbing the depths of these postulated mechanistic underpinnings, will either vindicate or challenge these suppositions, thereby amplifying our grasp of the cardinal function of organic water-soluble fertilizers in residue diminishment.

3.5.3. Summary of vegetable experiments

The results shown in Figure 7 demonstrate that the utilization of water soluble fertilizer has an effect, on decreasing the levels of pesticide residue in different kinds of vegetables belonging to the Cruciferae, Asteraceae, Chenopodiaceae and Amaranthaceae families. This corresponds with the pattern we observed in our research, where organic water soluble fertilizers successfully lower pesticide residues, across plant groups. Cruciferous vegetables represent the most abundant and diverse edible vegetable group. For a holistic epistemological panorama, it stands to reason that the orchestration of further investigative undertakings, plumbing the depths of these postulated mechanistic underpinnings, will either vindicate or challenge these suppositions, thereby amplifying our grasp of the cardinal function of organic water-soluble fertilizers in residue diminishment. This could explain the pronounced pesticide residue reduction observed in crucifers. Organic water-soluble fertilizer organic water-soluble fertilizer exhibited the strongest effect in reducing pesticide residues on cruciferous vegetables, indicating potential applicability in agricultural production for residue reduction.

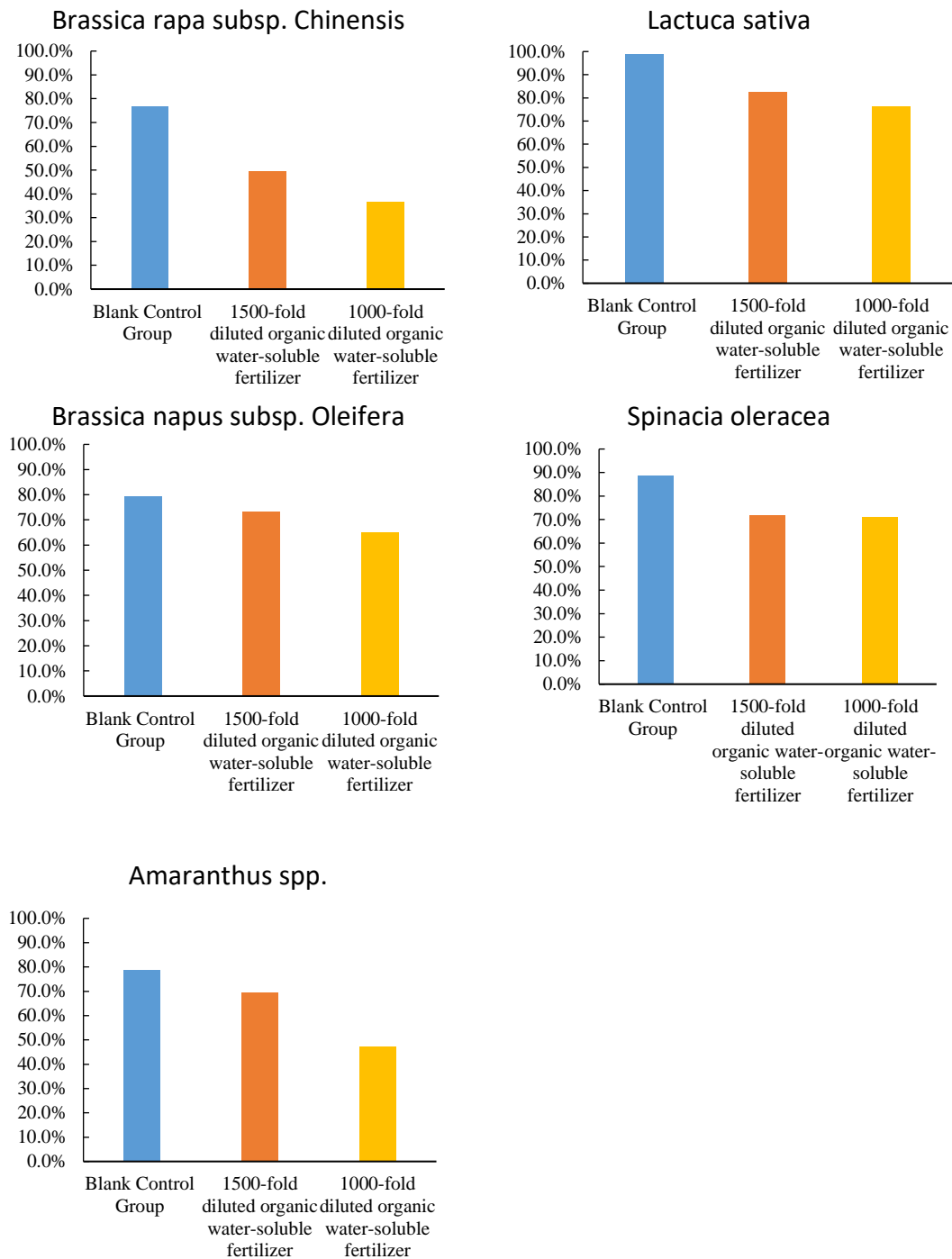


Figure 7- The influence of organic water-soluble fertilizer on the quantity of pesticide residue on Cruciferae vegetables, Asteraceae vegetables, Chenopodiaceae vegetables, Amaranthaceae vegetables

Additionally, the organic hydrophilic nourishment delineates a salient influence in attenuating pesticidal remnants on verdant consumables hailing from the taxonomies of Asteraceae and Amaranthaceae, as well as other taxonomic groupings. These discernments evoke the nuanced versatility of this approach across a diverse spectrum of botanical classifications, signifying a pivotal evolution in approaches to ameliorating challenges associated with pesticide residues. The broad efficacy across botanically diverse vegetables implies that the mechanisms of pesticide dissolution promoted by organic water-soluble fertilizers are not strictly limited to specific plant taxa. The phenomena of surfactant-mediated effects coupled with humic acid complexations seem to be ubiquitously exhibited across an array of foliaceous vegetables. However, fine-tuning fertilizer compositions to match the properties of certain vegetable groups could further maximize pesticide residue removal.

4. Conclusions and Outlook

Traditionally, agricultural chemicals have been distinctly categorized into two groups: pesticides for plant protection and fertilizers for plant nutrition. With advancing research, the scientific community has proposed the novel concept of integrating fertilizers and pesticides. A growing body of evidence suggests that the combined application of pesticides and fertilizers can yield higher crop productivity or improved quality compared to the sole use of fertilizers. This study explores the integration of fertilizers and pesticides to reduce pesticide residues, thus enriching the theory of fertilizer and pesticide integration. This erudite inquiry delves into the intricate confluence between nutrient supplements and pesticidal entities, aiming to diminish the persistence of pesticidal traces, thus rejuvenating the theoretical underpinnings of their symbiotic orchestration.

Initially, this study confirmed through field experiments that organic water-soluble fertilizer promotes the degradation of the insecticide imidacloprid. Subsequently, the underlying mechanism of this promoting effect was examined, focusing on two primary factors - biological and non-biological factors. Biological factors were primarily illustrated through field experiments demonstrating that, after a certain period, organic water-soluble fertilizer can enhance peroxidase activity, thereby augmenting its detoxification effect and reducing pesticide residues. Non-biological environmental factors are divided into photolysis and rainwater washing. Photolysis experiments indicated that the addition and concentration of organic water-soluble fertilizer did not significantly influence pesticide degradation. Washing experiments, simulating rainwater washing, were conducted on five common vegetables from four families - cruciferous, Asteraceae, Chenopodiaceae, and Amaranthaceae - and demonstrated that the residue rate of imidacloprid in vegetables with added organic water-soluble fertilizer decreased.

This decremental phenomenon was conspicuously manifest in cruciferous species, insinuating singular interplays between their ceraceous exteriors and the active moieties of the nourishment. In summation, this investigative endeavor, wielding a quintessential organic hydrophilic nourishment in tandem with a conventional insect deterrent, riveted its focus upon its prowess to catalyze pesticide degradation. The empiricism affirms that such nourishments can be instrumental in attenuating imidacloprid remnants, thus fortifying the theoretical edifice of nourishment and pesticidal integration. While this scholarly pursuit bequeaths seminal empirical foundations, the clarion call for additional investigative depth remains, aimed at unraveling the intricate tapestry underpinning pesticidal residue diminution via organic nourishments. Nuances encompassing optimal nourishment matrices, dosage interplays, and temporally calibrated applications warrant exploration across an expansive spectrum of pesticidal-crop dyads. The symbiotic deployment of pesticidal agents and nourishments, especially those of the hydrophilic foliar ilk, looms as an indomitable fulcrum in the odyssey toward agronomic modernization.

The seamless integration of plant nutrition, plant protection, health concerns arising from pesticide use, and soil issues caused by fertilizers theoretically aligns with the developmental requirements of modern agriculture and supports the exploration and advancement of innovative agricultural technologies in the future.

References

- Adhikari P R (2017). An overview of pesticide management in Nepal. *Journal of Agriculture and Environment* 18: 95-105. <https://doi.org/10.3126/aej.v18i0.19894>
- Andreu V & Picó Y (2004). Determination of pesticides and their degradation products in soil: critical review and comparison of methods. *TrAC Trends in Analytical Chemistry* 23(10-11): 772-789. <https://doi.org/10.1016/j.trac.2004.07.008>
- Balkan T & Yılmaz Ö (2022). Method validation, residue and risk assessment of 260 pesticides in some leafy vegetables using liquid chromatography coupled to tandem mass spectrometry. *Food Chemistry* 384, 132516. <https://doi.org/10.1016/j.foodchem.2022.132516>
- Bonmatin J-M, Giorio C, Sánchez-Bayo F & Bijleveld van Lexmond M (2021). An update of the Worldwide Integrated Assessment (WIA) on systemic insecticides. *Environmental Science and Pollution Research* 28(10): 11709-11715. <https://doi.org/10.1007/s11356-021-12853-6>
- Chang X, Liang J, Sun Y, Zhao L, Zhou B, Li X & Li Y (2020). Isolation, Degradation Performance and Field Application of the Metolachlor-Degrading Fungus *Penicillium oxalicum* MET-F-1. *Applied Sciences* 10(23): 8556. <https://doi.org/10.3390/app10238556>
- Graça C A, de Velosa A C & Teixeira A C S (2017). Amicarbazone degradation by UVA-activated persulfate in the presence of hydrogen peroxide or Fe²⁺. *Catalysis Today* 280: 80-85. <https://doi.org/10.1016/j.cattod.2016.06.044>

- Hossain M E, Shahrukh S & Hossain S A (2022). Chemical Fertilizers and Pesticides: Impacts on Soil Degradation, Groundwater, and Human Health in Bangladesh. In *Environmental Degradation: Challenges and Strategies for Mitigation*. Springer, Cham https://doi.org/10.1007/978-3-030-95542-7_4
- Hossain M S, Fakhruddin A, Chowdhury M A Z & Alam M K (2013). Degradation of chlorpyrifos, an organophosphorus insecticide in aqueous solution with gamma irradiation and natural sunlight. *Journal of Environmental Chemical Engineering* 1(3): 270-274. <https://doi.org/10.1016/j.jece.2013.05.006>
- Ikeura H, Kobayashi F & Tamaki M (2011). Removal of residual pesticides in vegetables using ozone microbubbles. *Journal of Hazardous Materials* 186(1): 956-959. <https://doi.org/10.1016/j.jhazmat.2010.11.094>
- Medel I D, Gabriel M W, Wengert G M, Filigenzi M S & Clifford D L (2022). Passive monitoring of soluble pesticides linked to cannabis cultivation: a multi-scale analysis. *Water Quality Research Journal*. <https://doi.org/10.2166/wqrj.2022.101>
- Niu H, Pang Z, Fallah N, Zhou Y, Zhang C, Hu C, Lin W & Yuan Z (2021). Diversity of microbial communities and soil nutrients in sugarcane rhizosphere soil under water soluble fertilizer. *PLoS One* 16(1): e0245626. <https://doi.org/10.1371/journal.pone.0245626>
- Pal R, Chakrabarti K, Chakraborty A & Chowdhury A (2010). Degradation and effects of pesticides on soil microbiological parameters-a review. *International journal of agricultural research* 5(8): 625-643. <https://doi.org/10.3923/ijar.2010.625.643>
- Pang G-F (2018). Chapter 4 - Determination of 450 Pesticides and Related Chemical Residues in Drinking Water: LC-MS-MS Method (GB/T 23214-2008). In G.-F. Pang (Ed.), *Analytical Methods for Food Safety by Mass Spectrometry*. Academic Press. <https://doi.org/10.1016/B978-0-12-814167-0.00004-1>
- Pavlidis G, Karasali H & Tsihrintzis V A (2020). Pesticide and fertilizer pollution reduction in two alley cropping agroforestry cultivating systems. *Water, Air, & Soil Pollution* 231: 1-23. <https://doi.org/10.1007/s11270-020-04590-2>
- Philippe V, Neveen A, Marwa A & Basel A-Y A (2021). Occurrence of pesticide residues in fruits and vegetables for the Eastern Mediterranean Region and potential impact on public health. *Food Control* 119: 107457. <https://doi.org/10.1007/s11356-021-12853-6>
- Pinto M I, Salgado R, Cottrell B A, Cooper W J, Burrows H D, Vale C, Sontag G & Noronha J P (2015). Influence of dissolved organic matter on the photodegradation and volatilization kinetics of chlorpyrifos in coastal waters. *Journal of Photochemistry and Photobiology A: Chemistry* 310: 189-196. <https://doi.org/10.1016/j.jphotochem.2015.05.024>
- R. Ramadevi R R, C. Ramachandraiah, C. R., & Reddy, G. V. S. (2022). A Review on Contamination of Soil and Water by Neonicotinoid Pesticides and Trends it's in Soil and Water Samples with Chromatographic Analytical Techniques. *Oriental Journal Of Chemistry* <https://doi.org/10.13005/ojc/380205>
- Saparrat M C, Jurado M, Díaz R, Romera I G & Martínez M J (2010). Transformation of the water soluble fraction from "alpeorajo" by *Coriopsis rigida*: the role of laccase in the process and its impact on *Azospirillum brasiliense* survival. *Chemosphere*, 78(1): 72-76. <https://doi.org/10.1016/j.chemosphere.2009.09.050>
- Savci S (2012). Investigation of effect of chemical fertilizers on environment. *Apcbee Procedia* 1: 287-292. <https://doi.org/10.1016/j.apcbee.2012.03.047>
- Senthilkumar V S, Pandya H M, Vijayageetha V, Pandiyarajan A & Janakarajan V N (2022). A study on the continuous usage of organic, inorganic persistent pesticides in the agricultural fields in and around sirumalai area with a special reference to the impact on ground water and soil. *Pollution Research* <https://doi.org/10.53550/pr.2022.v4i102.027>
- Shalaby S & Abdou G (2010). The Influence of Soil Microorganisms and Bio- or -Organic Fertilizers on Dissipation of Some Pesticides in Soil and Potato Tubers. *Journal of Plant Protection Research* 50, 86-92. <https://doi.org/10.2478/v10045-010-0015-3>
- Singh S B, Foster G D & Khan S U (2004). Microwave-assisted extraction for the simultaneous determination of thiamethoxam, imidacloprid, and carbendazim residues in fresh and cooked vegetable samples. *Journal of Agricultural and Food Chemistry* 52(1): 105-109. <https://doi.org/10.1021/jf030358p>
- Sun S, Sidhu V, Rong Y & Zheng Y (2018). Pesticide Pollution in Agricultural Soils and Sustainable Remediation Methods: a Review. *Current Pollution Reports* 4(3): 240-250. <https://doi.org/10.1007/s40726-018-0092-x>
- Sundaram K M S & Sundaram A (1994). Rain-washing of foliar deposits of Dimilin®WP-25 formulated in four different carrier liquids. *Journal of Environmental Science and Health, Part B* 29(4): 757-783. <https://doi.org/10.1080/03601239409372903>
- Wang G-S, Hsieh S-T & Hong C-S (2000). Destruction of humic acid in water by UV light—catalyzed oxidation with hydrogen peroxide. *Water Research* 34(15): 3882-3887. [https://doi.org/10.1016/s0043-1354\(00\)00120-2](https://doi.org/10.1016/s0043-1354(00)00120-2)



Copyright © 2024 The Author(s). This is an open-access article published by Faculty of Agriculture, Ankara University under the terms of the [Creative Commons Attribution License](https://creativecommons.org/licenses/by/4.0/) which permits unrestricted use, distribution, and reproduction in any medium or format, provided the original work is properly cited.



An Analysis of Factors Influencing African Indigenous Vegetable Farmers' Bargaining Power: A Case Study from Zambia

Zhigang YU^{a,b} , Huiping XU^b , Ramu GOVINDASAMY^{b,*} , Emmanuel Van WYK^c , Burhan OZKAN^d ,
James E. SIMON^e

^aCollege of Economics and Management, Northeast Agricultural University, Harbin, 150030, CHINA

^bDepartment of Agricultural, Food and Resource Economics, Rutgers – The State University of New Jersey, New Brunswick, NJ, 08901, USA

^cAgriSmart, Lusaka, ZAMBIA

^dDepartment of Agricultural Economics, Faculty of Agriculture, Akdeniz University, Antalya 07070, TURKEY

^eDepartment of Plant Biology, Rutgers – The State University of New Jersey, New Brunswick, NJ, 08901, USA

ARTICLE INFO

Research Article

Corresponding Author: Ramu GOVINDASAMY, E-mail: ramuphd@hotmail.com

Received: 19 January 2023 / Revised: 20 September 2023 / Accepted: 22 October 2023 / Online: 09 January 2024

Cite this article

Yu Z, Xu H, Govindasamy R, Wyk E V, Ozkan B, Simon J E (2024). An Analysis of Factors Influencing African Indigenous Vegetable Farmers' Bargaining Power: A Case Study from Zambia. *Journal of Agricultural Sciences (Tarim Bilimleri Dergisi)*, 30(1):193-204. DOI: 10.15832/ankutbd.1239590

ABSTRACT

Growing African Indigenous Vegetables (AIVs) is an innovative way to address poverty and malnutrition problems in Zambia. Farmers' bargaining power plays an important role in increasing AIV production and farmers' income. Based on 300 responses from Zambian AIV farmers, we defined AIV farmers' bargaining power and analyzed its benefits to farmers and the AIV industry. We used the ordered logistic regression model (OLRM) to analyze the influence of several factors that contribute to farmers' bargaining power, and then used the interpretative structural modeling (ISM) to analyze the relationship and hierarchical structure between the effects. Four key results and innovations arose from the analysis of the data. First, we defined farmers' bargaining power through their self-reported bargaining power. Second, we found that the respondents' bargaining power was significantly influenced by seven

variables: age, gender, education, main trading partners, awareness of AIV prices, and distance to the market from the farm. Third, the main trading partners and awareness of AIV prices are surface direct factors, gender, education and distance to the market from the farm are middle indirect relationships, and age, belong to any community are deep root factors. Last, farmers' bargaining power can be improved through education, especially women's education level, strengthening farmers' organization construction, altering some of the farmers' trading methods, and developing infrastructure. Overall, we found that bargaining power has played an important role in obtaining higher prices, getting faster payment, getting more income from AIV sales, and expanding AIV planting areas for farmers.

Keywords: AIVs, Negotiating prices, Selling prices, Influencing factor analysis, Profitability

1. Introduction

Sub-Saharan Africa is the only region in the world where hunger is prevalent in over one-third of the population, and people have been threatened by low income and malnutrition for decades (Cumani & Rojas 2016). In Zambia, 60% of the population lives below the poverty line, and 42% are considered in extreme poverty (World Bank 2017). Because of poverty, many children suffer from micronutrient deficiency, and Zambia is one of the most nutritionally deficient countries in the world (Nkobole et al. 2016).

Increased production and consumption of African Indigenous Vegetables (AIVs) would help address problems related to nutrition and increase food supply and income for rural households (Mwadingeni et al. 2021). In 2019, Africa produced 192.1 million tons of cassava, which feeds nearly 800 million people in West Africa. Yam production of 72.4 million tons is an important component of the region's economic development (Arumugam et al. 2022). Moreover, the AIVs such as amaranth, nightshade, African eggplant, jute mallow, and okra, can provide African people with nutrients (Yang et al. 2009; Byrnes et al. 2017; Gogo et al. 2017; Hoffman et al. 2018) and help reduce the number of nutrition-related diseases in Africa (Kamga et al. 2013; Weller et al. 2015). Additionally, except for the contributions made to food security, as a commercial product, AIVs have immense potential for creating employment opportunities and increasing household income in rural as well as peri-urban areas (Gido et al. 2016), which is becoming a source of income for smallholder farmers in some regions such as Arumeru, Tanzania and Kiambu, and Kenya (Shackleton et al. 2010).

Despite AIVs' vital role in improving health and nutrition, their popularity in production is much lower than staple crops such as maize and even far less than European-introduced vegetables (Ayua et al. 2017; Weller et al. 2015; Chepkoech et al. 2023). Due to various restrictions, AIVs are in short supply, primarily neglected, and have in the past been considered "poor people's" plants (Muhanji et al. 2011). Some researchers conclude that the main reasons are that AIVs are prone to deterioration (Gogo et al. 2017) and the non-availability of improved seeds (Adebooye et al. 2005). While those factors contribute to current constraints, others argue that the most important constraint relates to market factors (Shackleton et al. 2010). By strengthening the value chain, the potential of AIVs as food can be unleashed and become a significant way to address Africa's food security and nutrition problems (Weller et al. 2015; Kansime et al. 2018).

In many Sub-Saharan African countries, farmers' uncertainty about market prices is usually high, and traders may take advantage of farmers' ignorance of the market price and extract rent from them by offering very low prices for their products (Courtois & Subervie 2015). Bargaining power, as the ability of farmers to negotiate better conditions for the sale of their produce (including such factors as price, timing, quantity, and quality) (Gebert 2010), plays an important role in promoting farmers' market status (Falkowski et al. 2017). If a farmer has more bargaining power, she/he may earn more in the AIVs' selling market through improved farmers' selling prices, leading to increased farmers' income and market participation enthusiasm.

Previous studies have discussed the factors affecting bargaining power from different angles. Some works refer to production factors, such as farm size (Dries et al. 2009), the distance between a farm and its contractor (Falkowski 2012), farmers outside options (Vandeplas et al. 2013), and even the development and introduction of irrigation (Mwangi & Crewett 2019). Other studies have reported on power relations within the food supply chain and farmers' marketing decisions (Hingley 2005; Fischer et al. 2007; Leat & Revoredo-Giha 2008). Momanyi et al. (2015) thoroughly studied group marketing and concluded that group marketing can make full use of the advantages of production and sales clusters to improve bargaining power and obtain better sale prices. Handschuch and Wollni (2016) studied gender factors in price-fixing in western Kenya, and results show that female farmers may obtain higher selling prices when participating in a group. Additionally, other studies have focused on Market Information Services (MIS) (Courtois & Subervie 2015) and a streamlined and effective sales system (Bauhardt et al. 2015), finding that MIS can improve farmers' bargaining power and then increase their profits.

However, although there are many related studies, systematic research on the bargaining power of AIV farmers has not yet been reported. Therefore, in this paper, we address the following three questions: (1) Do Zambian farmers have enough bargaining power to sell AIVs? (2) If they obtain more bargaining power, what benefits would accompany that new position? (3) What are the factors that influence their bargaining power? What is the structure of the influencing factors?

2. Material and Methods

2.1. Sample selection

The analysis is based on the survey data gathered in Zambia, a landlocked country in south-central Africa where agriculture is predominantly dependent on rain-fed subsistence farming. The survey, which included 300 participating respondents, each involved in AIV small-scale production, was conducted in October and November of 2015. There were a total of five districts interviewed: Lusaka province (including Lusaka and Chongwe) and Chipata, Lundazi, Katete, and Petauke districts from Eastern Province (including 50 producers from Lusaka, 50 from Katete, 50 from Chipata, 75 from Lundazi, and 75 from Petauke). The interviewees were mostly farmers who belonged to ready-made cooperatives.

A structured questionnaire was used to collect information about the respondents' household demographics, land ownership, assets, labor allocation, vegetable production, marketing, access to financial capital, and constraints in AIV farming. The survey was conducted in English and the native provincial language. Along with the sixteen interviewers trained in questionnaire handling and the local languages (Bemba, Nyanja, etc.), data associates, district managers, and technology transfer officers in the eastern province conducted the survey. Enumerators were trained to be engaged in such surveys; each completed the CITI (Collaborative Institutional Training Initiative) certificate, and each respondent agreed to be interviewed following proper protocols. The survey was designed to specifically collect data about nine AIVs, namely: amaranth, nightshade, spider plants, cowpea, jute mallow, kale, sweet potato leaves, orange sweet potato, and okra. These were the most popular AIVs reported in an earlier focus group and prior studies in these same geographical regions.

2.2. Extraction of influencing factors

Many factors influenced AIV farmers' bargaining power, including individual and family characteristics, production and organizational characteristics, and market characteristics (Shackleton et al. 2010; Muhanji et al. 2011; Krause et al. 2019; Vivas et al. 2022). The results of Arumugam et al. (2022) showed that older people have more bargaining power, men have more bargaining power, and more educated farmers have more bargaining power. Moreover, production and organization characteristics also play an important role in influencing farmers' bargaining power. Some studies find that farmers who contact the market frequently and have benefited from the MIS program usually have more bargaining power (Courtois & Subervie 2015). Therefore, based on the above study, we selected three aspects of individual and family characteristics, production and

organizational characteristics, and market characteristics to measure the factors influencing the bargaining power of AIV farmers. Among them, individual and family characteristics include age, gender, and education. Production and organizational characteristics include AIVs planting proportion, changing production costs, belong to any community. Market characteristics include main trading partners, nearest market meet frequency, awareness of AIVs prices, and distance to market from the farm (Table 1).

Table 1 – Variables definition and description

Category	Variables	Symbol	Definition	Mean	SD
Dependent variable	bargaining power	BP	1=full bargaining power 1/2=half bargaining power 1/3=one-third bargaining power 0=no bargaining power	0.702	0.342
	age	age	Actual age	45.370	13.025
Individual and family characteristics	gender	gender	1=male; 0=female	0.790	0.408
	education	edu2	1=primary and below; 0=others	0.620	0.501
		edu3	1=secondary; 0=others	0.200	0.401
		edu4	1=college; 0=others	0.160	0.370
		edu5	1=university; 0=others	0.020	0.140
Production and organizational characteristics	AIVs planting proportion	planting	AIVs planting area/total planting area	29.278	25.643
	changing production costs	cost_in	1=increased; 0=others	0.560	0.497
		cost_de	1=decreased; 0=others	0.110	0.318
	belong to any community	community	1=belong; 0=not	0.970	0.171
	main trading partners	partner_con	1=Direct to consumers or roadside stands; 0=others	0.080	0.272
		partner_mar	1=Direct to supermarkets or retailers; 0=others	0.740	0.439
	Market characteristics		market_daily	1=daily; 0=others	0.200
nearest market meet frequency		market_twice	1=twice a week; 0=others	0.110	0.318
		market_thrice	1=thrice a week; 0=others	0.020	0.140
		market_weekly	1=weekly; 0=others	0.660	0.473
awareness of AIVs prices		price	1=aware of AIVs prices before sale; 0=not	0.830	0.373
distance to market from the farm	distance	Average distance of all AIVs	5.387	14.866	

2.3. Method

This study is based on the ordinal logistic regression model (OLRM), which is typically used to solve cumulative approach problems. Generally, when the outcome represents an underlying continuous scale subdivided into several categories, the most adequate modeling framework is a cumulative approach (Fullerton 2009). The OLRM can be written as follows (Williams 2006):

$$P(Y_i > j) = g(X_i > \beta_j) = \left\{ \frac{\exp(\alpha_j + X_i\beta_j)}{1 + [\exp(\alpha_j + X_i\beta_j)]} \right\} \tag{1}$$

In formula (1), j=1, 2,..., M-1, where M is the number of categories of the ordinal dependent variable. From the above, it can be determined that the probabilities that Y will take on each of the values 1, ..., M are equal to

$$P(Y_i = 1) = 1 - g(X_i\beta_j) \tag{2}$$

$$P(Y_i = j) = g(X_i\beta_{j-1}) - g(X_i\beta_j) \tag{3}$$

$$P(Y_i = M) = g(X_i\beta_{M-1}) \tag{4}$$

When M=2, the model is equivalent to the logistic regression model. And, in this study, M=4. The identification of significant variables for each logit of Y is carried out by using a stepwise selection procedure. The decision to include a variable is based

on the significance of the log-likelihood ratio of the estimation and the χ^2 statistical test of the variables. After a variable is included, it is tested to see whether the exclusion of a variable included at an earlier stage causes a significant decline in the log-likelihood. This process is terminated when the inclusion of an extra variable does not lead to a significant improvement in the model. The level of significance for acceptance and rejection in the stepwise selection is 0.01, 0.05, and 0.1, respectively.

3. Results and Discussion

3.1. Results of the survey

3.1.1. Bargaining power of the sample

In our research, in order to measure farmers' bargaining power more accurately, we used self-reported strength with one question: "Who fixed the price of AIVs?". As shown in Figure 1, about 55% of respondents stated that they fixed the sale price on their own; 22% stated that the prices were fixed after negotiation; 4% stated that the price was fixed by the buyer; and 18% stated that the prices were fixed by a middleman or broker.

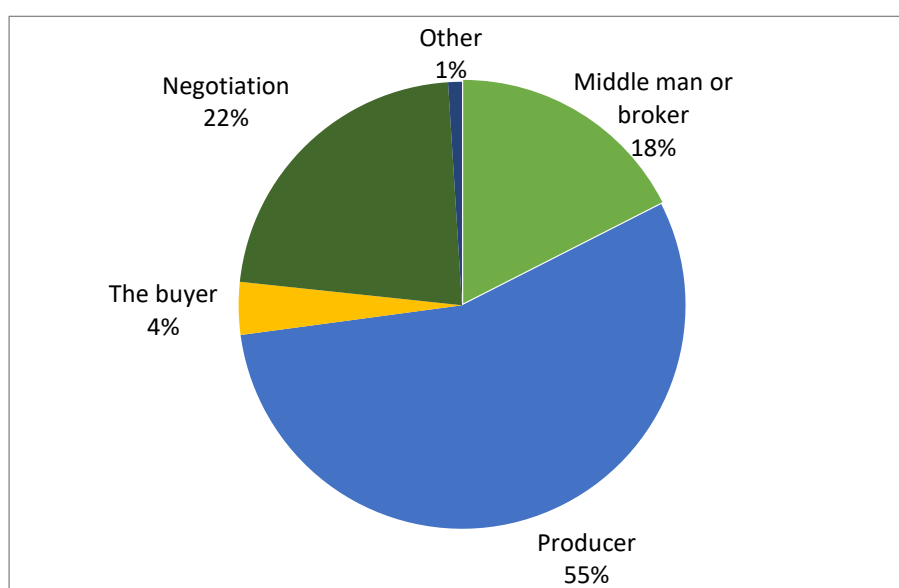


Figure 1 – Determination of sales prices for indigenous African vegetables (AIVs) by Zambian growers

Drawing on the studies of Ngenoh et al. (2019) and Arumugam et al. (2022), we categorized every respondent's bargaining power into four levels (Table 2). If the price was fixed by oneself, we considered he/she to have full bargaining power; if the price was fixed after negotiation, we thought she/he had half bargaining power; if it was fixed by a middleman or broker, we defined it as having one-third bargaining power; or if the price was fixed by the buyer or another, we thought he/she had no bargaining power.

Table 2 – Definition of different levels or categories of bargaining power

Level	The price was fixed by?	Definition	Numerical value
1	Oneself	full bargaining power	1
2	Negotiation	half bargaining power	1/2
3	Middleman or broker	one-third bargaining power	1/3
4	The buyer or another	no bargaining power	0

Second, if one's bargaining power belongs to levels 1 to 3, we asked her/him another question: "Have you had the opportunity to bargain for higher producer prices?" If the respondent replied "yes", we did not change her/his level; if her/his reply was "no", we marked it as the next level. Eventually, about 47% of respondents (141 respondents) had full bargaining power, 21% (63 respondents) had half bargaining power, 20% (60 respondents) had one-third bargaining power, and 12% (36 respondents) had no bargaining power.

3.1.2. Advantages of having bargaining power

For the farmers that grow AIVs, the more bargaining power one has, the higher the price she/he may obtain. For farmers with different bargaining powers, the AIVs prices' changing ratios in the past five years are different (Figure 2). About 67% of respondents with full bargaining power stated that their AIVs prices have increased in the past five years. The ratios for half-

bargaining power, one-third bargaining power, and no bargaining power were 46.15%, 41.18%, and 36.36%, respectively. The decreased AIV price ratios for different bargaining power farmers were 5.59%, 10.77%, 15.69%, and 18.18%, respectively.

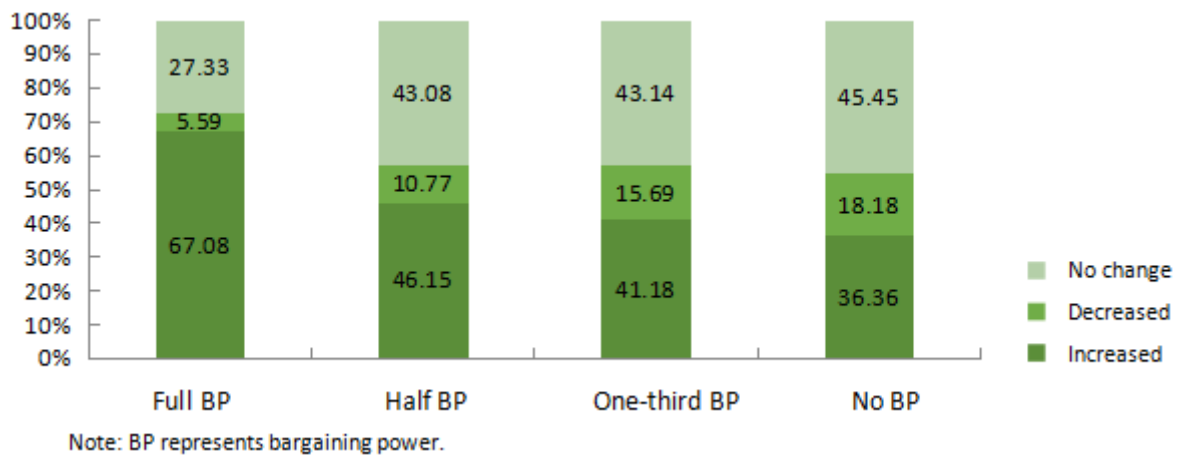


Figure 2 – AIVs prices’ changing ratio of the last five years according to different bargaining power (%)

For farmers that grow African indigenous vegetables, the more bargaining power one has, the faster she/he can get the payment. As shown in Figure 3, about 85% of respondents stated that they got paid at the time of selling the AIVs. The average ratios for half bargaining power farmers were 85%, while one-third bargaining power, and no bargaining power for farmers were 78%, and 57%, respectively.

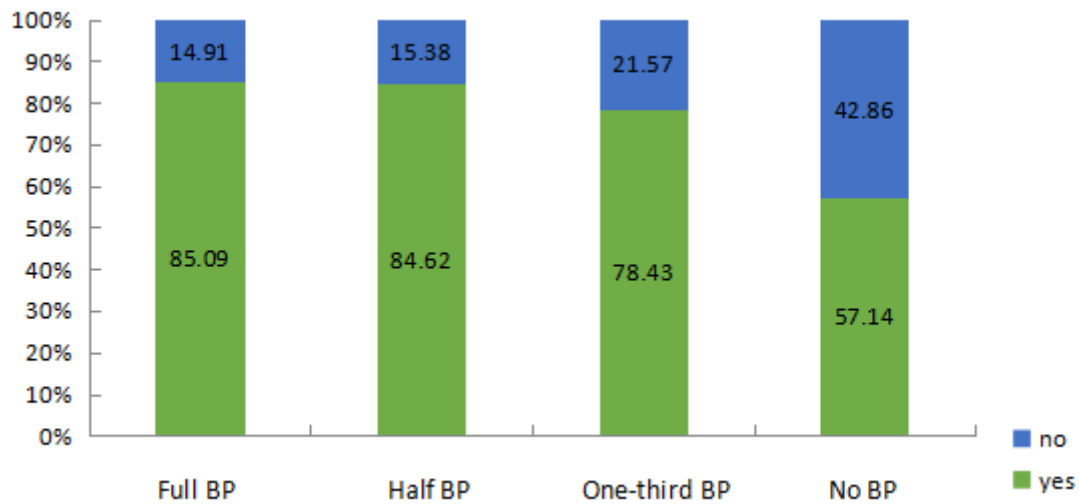


Figure 3 – The ratio of “whether you get paid at the time of selling the AIVs” (%)

For farmers that grow African indigenous vegetables, the more bargaining power one has, the more income one gets from the sale of African indigenous vegetables. About 24% of respondents with full bargaining power (39 respondents) selected “sale of AIVs” as the main source of household income (Figure 4) and the ratios of respondents with half bargaining power, one-third bargaining power, and no bargaining power who selected “sale of AIVs” as the main source of household income were only 21%, 5%, and 13%, respectively.

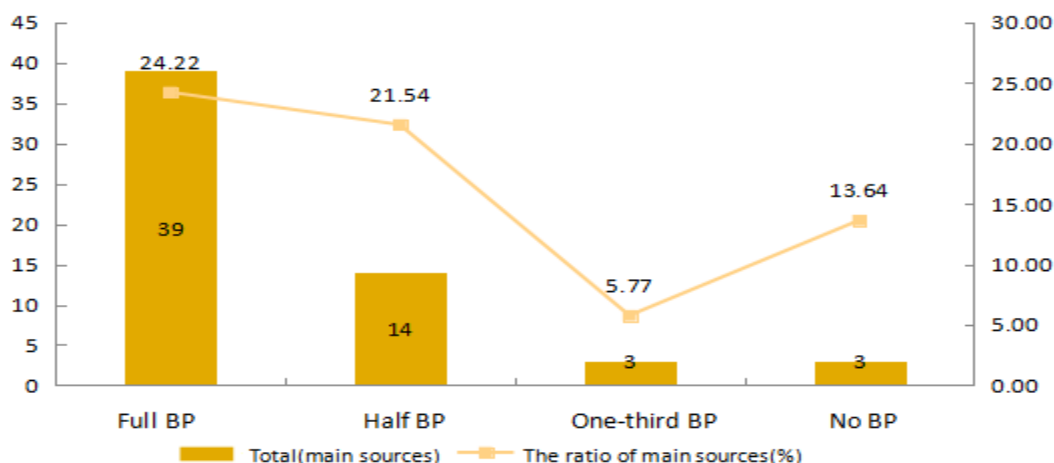


Figure 4 – The number and ratio that select “Sale of AIVs” as the main source of household income

We next analyzed the ratio of one respondent’s AIV income to her/his total income. The average ratio of the respondents with full bargaining power was 27%, which meant 27% of their income was from the sales of AIVs. The figures for half bargaining power, one-third bargaining power, and no bargaining power were only 10%, 14%, and 9%, much lower than 27% (Figure 5).

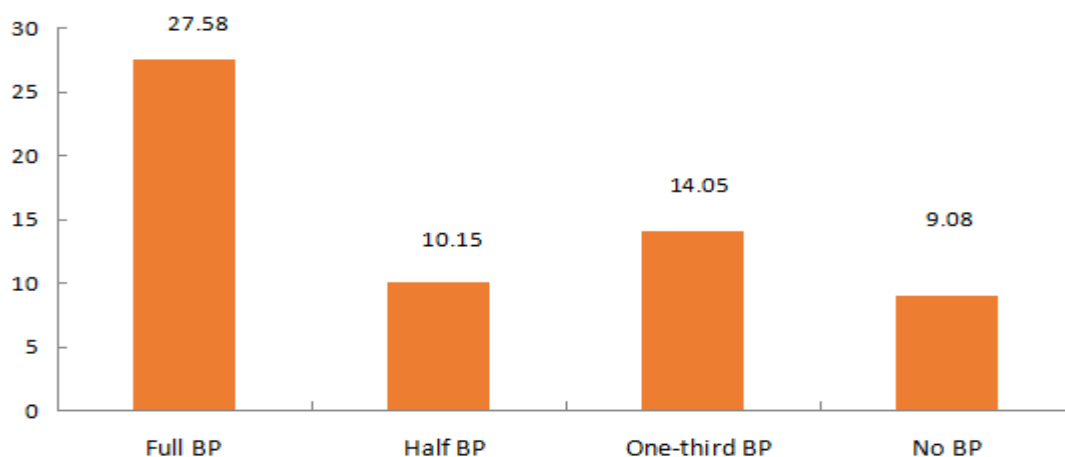


Figure 5 – The ratio of AIVs income to total income (%)

For the African indigenous vegetable industry, once farmers have higher bargaining power, they are willing to grow more African indigenous vegetables, which will further promote the African indigenous vegetable market’s development. Researchers who analyzed the relationship between bargaining power proxies and coffee output found that with coffee, there was a significant negative correlation (Lim et al. 2007). In contrast, with our survey on AIVs, we found that the average planting area of farmers who had full bargaining power was greater than those who had partial bargaining power or no bargaining power (Figure 6).

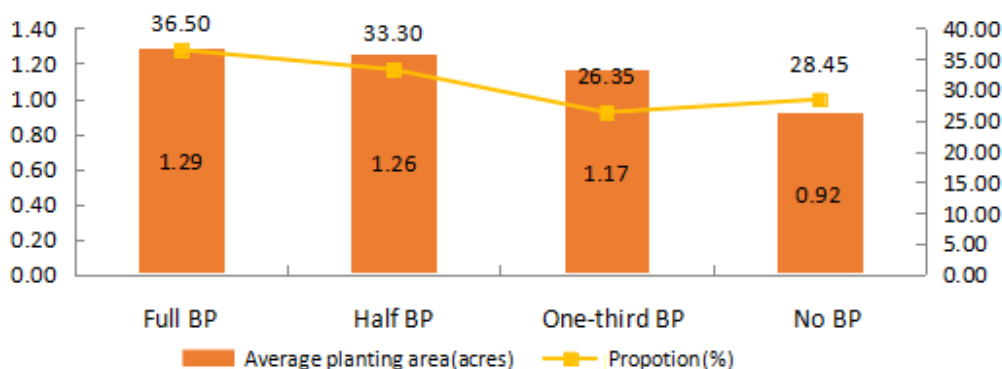


Figure 6 – Average AIVs planting area and its proportion according to different bargaining powers

Overall, the analysis indicates that bargaining power plays an important role in raising agricultural product prices, increasing farmers' income, and promoting industrial development. We further analyze the empirical results.

3.2. Results of empirical analysis

3.2.1. Model fitting information and parallel lines test

The statistical package SPSS 23.0 is used for carrying out the OLRM analysis. First, we performed a multi-collinearity test. We found that the variable “nearest market meet frequency” failed the multi-collinearity test and therefore dropped that variable and then performed the same test on other variables. Then, we ran the model again. The model fitting information shows the significant value of the model is less than 0.01 through the chi-square test, indicating that it passed the test at 1% significance (Table 3). That is, the results indicate that all the independent variables collectively significantly contribute to the change in the dependent variable. The χ^2 in parallel lines test is 18.520, $p=0.231>0.05$, so it passes the test of the parallel line and can be analyzed by OLRM.

Table 3 – Model fitting information and parallel lines test

Type of test	Model	-2 Log Likelihood	χ^2	Df	Sig.
Model fitting information	Intercept only	696.452			
	Final	648.127	48.325	14	0.000
Parallel lines test	Null Hypothesis	648.127			
	General	466.607	18.520	28	0.231

The regression results are reported in Table 4. B is the coefficient of variables, and Exp(B) is the odds ratio (OR). The results show that seven variables pass the test of significance. They are age, gender, education, main trading partners, being aware of AIVs prices, belonging to a group/community, and distance to market from the farm.

Table 4 – Regression results of OLRM

Variable	B	S.E.	95% Confidence Interval		Wald χ^2	Exp(B)	95% Confidence Interval of Exp(B)	
			lower limit	Upper limit			lower limit	Upper limit
[BP=.00]	4.08	1.86	0.45	7.72	4.84	59.14	1.56	22 41.31
[BP=.33]	5.60	1.86	1.96	9.24	9.09	270.62	7.10	10 311.77
[BP=.50]	6.73	1.87	3.07	10.39	12.97	837.89	21.50	32 660.85
Gender	-0.68**	0.28	-1.23	-0.13	5.85	0.51	0.29	0.88
Age	0.04***	0.01	0.02	0.06	12.66	1.04	1.02	1.06
Edu1	1.43***	0.43	0.59	2.27	11.18	4.19	1.81	9.70
Edu2	1.11**	0.47	0.18	2.03	5.48	3.02	1.20	7.62
Edu3	1.41***	0.49	0.45	2.38	8.19	4.11	1.56	10.82
Edu4	1.45	1.01	-0.54	3.43	2.04	4.25	0.58	30.97
Cost_in	-0.09	0.26	-0.59	0.42	0.12	0.92	0.55	1.51
Cost_de	-0.12	0.40	-0.91	0.67	0.09	0.89	0.41	1.95
Community	-0.70**	0.67	-2.00	0.61	1.10	0.50	0.14	1.83
Partner_con	1.22***	0.39	0.45	1.98	9.78	3.38	1.58	7.24
Partner_mar	1.61***	0.52	0.59	2.63	9.49	4.99	1.80	13.89
Price	-0.66**	0.33	-1.30	-0.02	4.08	0.52	0.27	0.98
Planting	-0.01	0.01	-0.02	0.01	1.66	0.99	0.98	1.00
Distance	-0.02**	0.01	-0.03	-0.01	5.77	0.98	0.97	1.00
Cox & Snell R ²	0.15							
Nagelkerke R ²	0.17							

Notes: ** and *** are statistically significant at 5% and 1%, respectively

(1) Individual and family characteristics influence

A farmer’s age has a significant influence on their bargaining power. Its OR is 1.036, indicating that if one farmer’s age increases by one year, the odds of having more bargaining power will increase by a factor of 1.036. For a female, the odds of having more bargaining power are 0.507 times as large as the odds for a male. This is consistent with many previous studies (Breda, 2015; Lenjiso et al. 2016; Lim et al. 2007). In comparison with no education, primary education, secondary education, and college education are significant at 0.05 levels, which means good education is helpful to improve farmers’ bargaining power, and their odds of having more bargaining power are about 4.2 times, 3.0 times, and 4.1 times, respectively, that of farmers who have no education. This is a key finding to use in capacity training, education, and awareness programs for growers.

(2) Production and organizational characteristics' influences

There are three variables in production and organizational characteristics, including AIVs planting proportion, changing production costs, and belonging to any community. For a farmer who did not take part in a community, the odds of having more bargaining power are only 0.497 times higher than for farmers who participated in a community.

(3) Market characteristics' influences

Awareness of AIVs' prices and distance to market from the farm do have significant influences on farmers' bargaining power (Table 4). Information was found to play a vital role in increasing farmers' bargaining power. The farmers who knew the AIV price before the sale created a psychological expectation of the price and were reluctant to bargain. The odds of it are about twice that of the farmers who are not. This is also in line with the findings that were previously reported (Draganska et al. 2010). The distance to the market from the farm is significant at the 0.05 level. This can explain why there are large differences in bargaining power among the five districts (Table 5). Differences between the reported bargaining powers between districts as observed may in part be due to growers having a shorter distance from farm to market. Delayed infrastructure construction may also lead to lower prices for rural households (Bumbangi et al. 2016; Sinyangwe et al. 2016). There are three main trading partners for farmers: direct to consumers or roadside stands; direct to supermarkets or retailers; or direct to brokers or wholesalers. Take the last as a reference; the other two main trading partners are significant in influencing farmers' bargaining power. The farmers who sell their products direct to consumers, roadside stands, supermarkets, or retailers are more likely to have high bargaining power; the odds of this are about 3.4 and 4.9 times higher than those who sell directly to brokers or wholesalers.

Table 5 – Bargaining power and distance to market in each of the five districts in Zambia

<i>Districts</i>	<i>Lusaka</i>	<i>Lundazi</i>	<i>Chipata</i>	<i>Petauke</i>	<i>Katete</i>
Respondents with Full BP	35	25	6	35	45
Respondents with Half BP	11	0	42	8	3
Respondents with One-third BP	2	24	1	0	0
Respondents with No BP	2	1	1	7	2
Average BP	0.82	0.55	0.55	0.73	0.93
Distance to market from the farm	2.11	12.49	6.98	2.59	0.62

3.3. Prediction success of the model

We use the cross-tabulation of bargaining power and predicted response category to test the prediction success of the model (Table 6). The correct predictions of no bargaining power, 1/3 bargaining power, 1/2 bargaining power, and full bargaining power are 5, 32, 33, and 143, respectively. So, the prediction success of the model is $(5+32+33+143)/300=71\%$.

Table 6 – Bargaining power and predicted response category cross-tabulation

<i>Variable</i>		<i>Predicted response category</i>				<i>Total</i>
		<i>No BP</i>	<i>1/3 BP</i>	<i>1/2 BP</i>	<i>Full BP</i>	
No BP	Count	5	1	0	16	22
	% within BP	22.7%	4.5%	0.0%	72.8%	100.0%
1/3 BP	Count	0	32	7	13	52
	% within BP	0.0%	61.5%	13.4%	25.0%	100.0%
1/2 BP	Count	0	6	33	26	65
	% within BP	0.0%	9.2%	50.8%	40%	100.0%
Full BP	Count	1	7	10	143	161
	% within BP	0.6%	4.3%	6.2%	88.8%	100.0%
Total	Count	6	46	50	198	300
	% within BP	2.0%	15.3%	16.7%	66.0%	100.0%

3.4. Further analysis

Although the OLRM can be used to calculate and identify the factors influencing the bargaining power of AIVs and their degree of influence, it cannot effectively reflect the underlying and process elements of the model. Therefore, the next step of this paper is to use the ISM model to analyze the correlation and hierarchy among the factors influencing the bargaining power of AIVs in order to identify the root factors affecting the quality of employment. Drawing on Roson et al. (2015), the specific steps of the analysis are as follows :

3.4.1. Determine the relevant factors

According to the estimated results of OLRM, seven factors affect the bargaining power of AIVs. Through the integration of the above factors, the influence of African indigenous vegetable farmers bargaining power ISM (interpretative structural modeling) has seven factors: F_1 on behalf of gender, F_2 on behalf of age, F_3 on behalf of education, F_4 on behalf of community, F_5 on behalf of the main trading partners, F_6 on behalf of farmers price, F_7 on behalf of the distance to market from the farm.

3.4.2. Establish adjacency matrix

After consulting five African experts engaged in agriculture-related research to conduct simple inferential statistics on the data in this paper, and after in-depth discussions and judgments based on relevant literature, the logical relationships between variables were determined and the adjacency matrix A was established. The adjacency matrix in Table 7 describes the relationships between the elements in the system, where "1" indicates row factors have direct or indirect influence on column factors, and "0" means no influence.

Table 7 – Adjacency matrix A

	F_1	F_2	F_3	F_4	F_5	F_6	F_7
F_1	1	0	0	0	1	1	0
F_2	0	1	1	0	0	0	0
F_3	0	0	1	0	1	1	0
F_4	0	0	0	1	1	0	1
F_5	0	0	0	0	1	1	0
F_6	0	0	0	0	1	1	0
F_7	0	0	0	0	1	0	1

3.4.3. Establish achievable matrix

As shown in Table 8, we use Matlab 7.0 to obtain the achievable matrix M of the adjacency matrix A by using formula (5), where I denotes the unit matrix and the Boolean operator is used for the power operation of the matrix.

$$M = (A + I)^{+1} = (A + I) \neq (A + I)^{-1} \neq (A + I)^2 \neq (A + I) \tag{5}$$

Table 8 – Achievable matrix M

	F_1	F_2	F_3	F_4	F_5	F_6	F_7
F_1	1	0	0	0	1	1	0
F_2	0	1	1	0	1	1	0
F_3	0	0	1	0	1	1	0
F_4	0	0	0	1	1	1	1
F_5	0	0	0	0	1	1	0
F_6	0	0	0	0	1	1	0
F_7	0	0	0	0	1	1	1

3.4.4. Determine the hierarchy between factors

$M(F_i) \cap N(F_i) = M(F_i)$ is the hierarchical decomposition of factors and extraction based on conditions. $M(F_i)$ represents the set of all factors in the accessible matrix M that can be reached from factor F_i . $N(F_i)$ represents the set of factors in the accessible matrix M of accessible factor F_i . According to the accessible matrix M and the above conditions, the accessible sets and advance sets of the factors are shown in Table 8. In this study, by calculation, the $L_1 = \{F_5, F_6\}$. The elements of F_5 and F_6 in the original accessible matrix M are extracted to obtain a new matrix, then and so on, and finally, $L_2 = \{F_1, F_3, F_7\}$ and $L_3 = \{F_2, F_4\}$. Thus, the goal of performing a hierarchical decomposition of the accessible matrix M is achieved (Table 9).

Table 9 – Reachable set, antecedent set and its intersection

	$M(F_i)$	$N(F_i)$	$M(F_i) \cap N(F_i)$
F_1	1, 5, 6	1	1
F_2	2, 3, 5, 6	2	2
F_3	3, 5, 6	2, 3	3
F_4	4, 5, 6, 7	4	4
F_5	5, 6	1, 2, 3, 4, 5, 6, 7	5, 6
F_6	5, 6	1, 2, 3, 4, 5, 6, 7	5, 6
F_7	5, 6, 7	4, 7	7

3.4.5. Establish an explanatory structural model

According to the hierarchical structure among the factors, the factors at the same level are represented by boxes in the same position. Based on the logical relationship between the factors, each factor was connected with a directed line segment to obtain the correlation and hierarchy among the factors influencing the bargaining power of AIVs farmers. As shown in Table 7, age and community play a deep-rooted role in the bargaining power of AIVs farmers. Gender, education and distance to market are key connecting variables at the intermediate level. Awareness of AIVs prices and marketing partners are direct causes at the superficial level such as influencing the bargaining power of AIVs farmers.

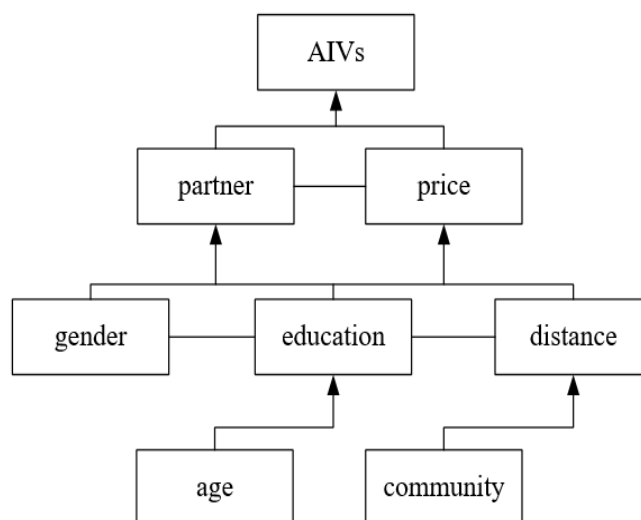


Figure 7 – The correlation relationship and the hierarchical structure of the influencing factors

4. Conclusions

Based on data obtained from a field study in Zambia, a landlocked country in south-central Africa, this paper investigates the bargaining power of 300 vegetable farmers in five states of Zambia. The bargaining power of AIV farmers and the factors influencing them were studied through a Logistic-ISM model and the following conclusions were drawn:

First, we defined farmers' bargaining power through their self-reported bargaining power. We found that bargaining power has played an important role in obtaining higher prices, getting faster payment, getting more income from AIV sales, and expanding AIV planting areas for farmers. The promotion production and power expand the scope of higher interests, enhances vegetable farmers' ability to manage risks, unleashes the potential of vegetable production, and facilitates the transformation and upgrading of the vegetable industry. This, in turn, increases the income of AIVs farmers.

Second, we used OLRM to analyze the influence of several factors that contribute to farmers' bargaining power. Results indicated that respondents' bargaining power is significantly influenced by seven variables: age, gender, education, main trading partners, awareness of AIVs prices, belonging to a group/community, and distance to the market from the farm. Among them, education, age, and major trading partners had a positive effect on the bargaining power of farmers. Gender, community, awareness of AIVs prices, and distance to market from the farm had a negative effect on the bargaining power of farmers. Further analysis of interactions of the seven significant influencing factors using ISM revealed that the age and community attributes of farmers are the deep root factors that affect the bargaining power of AIVs farmers. Gender, education and distance to market from the farm were the three intermediate level factors. Awareness of AIVs prices and marketing partners were the direct factors influencing the bargaining power of AIV farmers.

Finally, it is important to note that the farmers' bargaining power can be improved by improving farmers' education, strengthening farmers' organization construction, altering some of the farmers' trading methods, and developing infrastructure. To improve the bargaining power of AIVs farmers in the market, several measures can be taken. Firstly, by improving their education and training, farmers can better utilize various policies and negotiate more effectively. Secondly, strengthening their organizational structure can reduce costs and increase bargaining power. Thirdly, changing their trading methods and increasing sales concentration can lead to long-term benefits. Finally, developing infrastructure can expand their trading range and improve their bargaining power. Moreover, this provides a clear path for future studies to incorporate such training and education for smallholder farmers as part of a larger best practices approach. These findings should be considered by international and national public policy programs that continually seek to reduce poverty and strengthen market access for smallholder farmers.

Acknowledgments

This research was supported by the Horticulture Innovation Lab with funding from the U.S. Agency for International Development (USAID EPA-A-00-09-00004), as part of the U.S. Government's global hunger and food security initiative, Feed the Future, for a project titled "Improving nutrition with African indigenous vegetables" in eastern Africa. We also thank the New Jersey Agriculture Experiment Station (HATCH project 12131); Himoonga Moonga, Mebelo Mataa, and John Shindano, University of Zambia; and Kenneth Chali and Lupiya Sakala, AgriSmart, Zambia; John Bowman, USAID- Washington and Beth Mitcham, UC-Davis. This work was also supported by the National Social Science Fund of China (21BJY249), and the MOE Project of Humanities and Social Sciences of China (Project No. 18YJA790100).

References

- Adebooye O C, Ajayi S A, Baidu-Forson J J & Opabode J T (2005). Seed constraint to cultivation and productivity of African indigenous leafy vegetables. *African Journal of Biotechnology* 4(13): 1480-1484
- Arumugam S, Govindasamy R, Simon J E, Van Wyk E & Ozkan B (2022). Market outlet choices for African Indigenous Vegetables (AIVs): a socio-economic analysis of farmers in Zambia. *Agricultural and Food Economics* 10(1): 28
- Ayua E, Mugalavai V, Simon J, Weller S, Obura P & Nyabinda N (2017). Comparison of a mixed modes solar dryer to a direct mode solar dryer for African indigenous vegetable and chili processing. *Journal of Food Processing and Preservation* 41(6): 7
- Bauhardt C, Brückner M & Caglar G (2015). *Understanding consumer behaviour: the social embeddedness of food practices*. Paper presented at the 143rd Joint EAAE/AEA Seminar, March 25-27, 2015, Naples, Italy
- Breda T (2015). Firms' rents, workers' bargaining power and the union wage premium. *Economic Journal* 125(589): 1616-1652
- Bumbangi N F, Muma J B, Choongo K, Mukanga M, Velu M R, Veldman F, Hatloy A & Mapatano M A (2016). Occurrence and factors associated with aflatoxin contamination of raw peanuts from Lusaka district's markets, Zambia. *Food Control* 68: 291-296
- Byrnes D R, Dinssa F F, Weller S C & Simon J E (2017). Elemental micronutrient content and horticultural performance of various vegetable Amaranth genotypes. *Journal of the American Society for Horticultural* 142(4): 265-271
- Chepkoech W, Stoeber S, Kurgat B K, Bett H K, Mungai N W & Lotze-Campen H (2023). What drives diversity in climate change adaptation strategies for African indigenous vegetable production in Kenya? *Economic Analysis and Policy* 77: 716-728
- Courtois P & Subervie J (2015). Farmer Bargaining Power and Market Information Services. *American Journal of Agricultural Economics*, 97(3): 953-977
- Cumani M & Rojas O (2016). Characterization of the agricultural drought prone areas on a global scale. *Food and Agriculture Organization of the United Nations*. <http://www.fao.org/3/a-i5764e.pdf>
- Dries L, Germejenji E, Noev N & Swinnen J F M (2009). Farmers, Vertical Coordination, and the Restructuring of Dairy Supply Chains in Central and Eastern Europe. *World Development* 37(11): 1742-1758
- Falkowski J (2012). Dairy supply chain modernisation in Poland: what about those not keeping pace? *European Review of Agricultural Economics* 39(3): 397-415
- Falkowski J, Malak-Rawlikowska A & Milczarek-Andrzejewska D (2017). Farmers' self-reported bargaining power and price heterogeneity Evidence from the dairy supply chain. *British Food Journal* 119(8): 1672-1686
- Fischer C, Gonzalez M A, Henchion M & Leat P (2007). Trust and economic relationships in selected European agrifood chains. *Acta Agriculturae Scandinavica, Section C — Food Economics* 4(1): 40-48
- Fullerton, A. S. (2009). A Conceptual Framework for Ordered Logistic Regression Models. *Sociological Methods & Research* 38(2): 306-347
- Gebert R (2010). Farmer Bargaining Power in the Lao PDR: Possibilities and Pitfalls. *Joint Sub-Working Group on Farmers and Agribusiness & Helvetas*
- Gido E O, Bett H K & Bokelmann W (2016). Importance of African Indigenous Vegetables in Food Systems. *African Journal of Horticultural Science* 10: 7-7
- Gogo E, Opiyo A, Ulrichs C & Huyskens-Keil S (2017). Nutritional and economic postharvest loss analysis of African indigenous leafy vegetables along the supply chain in Kenya. *Postharvest Biology and Technology*, 130: 39-47
- Handschuh, C. and M. Wollni (2016). Traditional Food Crop Marketing in Sub-Saharan Africa: Does Gender Matter? *Journal of Development Studies* 52(3): 343-359
- Hingley M K (2005). Power imbalanced relationships: cases from UK fresh food supply. *International Journal of Retail & Distribution Management* 33(8): 551-569
- Hoffman D, Merchant E, Byrnes D & Simon J E (2018). Preventing micronutrient deficiencies using African Indigenous vegetables in Kenya and Zambia. *Sight and Life* 32(2): 177-181
- Kamga R T, Kouamé C, Atangana A, Chagomoka T & Ndango R (2013). Nutritional evaluation of five African indigenous vegetables. *Journal of Horticultural Research* 21(1): 99-106
- Kansiime M K, Karanja D K, Aloit C & Ochieng J (2018). Derived demand for African indigenous vegetable seed: implications for farmer-seed entrepreneurship development. *International Food and Agribusiness Management Review* 21(6): 723-739
- Krause H, Fasse A & Grote U (2019). Welfare and food security effects of commercializing African indigenous vegetables in Kenya. *Cogent Food & Agriculture* 5(1)
- Leat P & Revoredo-Giha C (2008). Building collaborative agri-food supply chains. *British Food Journal* 110(4-5): 395-411
- Lenjiso B M, Smits J & Ruben R (2016). Transforming Gender Relations through the Market: Smallholder Milk Market Participation and Women's Intra-household Bargaining Power in Ethiopia. *Journal of Development Studies* 52(7): 1002-1018
- Lim S S, Winter-Nelson A & Arends-Kuenning M (2007). Household bargaining power and agricultural supply response: Evidence from Ethiopian coffee growers. *World Development* 35(7): 1204-1220
- Momanyi D, Lagat K & Ayuya O I (2015). Determinants of smallholder African indigenous leafy vegetables farmers' market participation behaviour in Nyamira County, Kenya. *J. Econ. Sustain* 16: 212-217
- Muhanji G, Roothaert R L, Webo C & Stanley M (2011). African indigenous vegetable enterprises and market access for small-scale farmers in East Africa. *International Journal of Agricultural Sustainability* 9(1): 194-202

- Mwadzingeni L, Afari-Sefa V, Shimelis H, N'Danikou S, Figlan S, Depenbusch L, Derera J (2021). Unpacking the value of traditional African vegetables for food and nutrition security. *Food Security* 13(5): 1215-1226
- Mwangi J K & Crewett W (2019). The impact of irrigation on small-scale African indigenous vegetable growers' market access in peri-urban Kenya. *Agricultural Water Management* 212: 295-305
- Ngenoh E, Kurgat B K, Bett H K, Kebede S W & Bokelmann W (2019). Determinants of the competitiveness of smallholder African indigenous vegetable farmers in high-value agro-food chains in Kenya: A multivariate profit regression analysis. *Agricultural and Food Economics* 7(1): 2
- Nkobole N, Hussein A & Prinsloo G (2016). Metabolomics profile of wild versus cultivated South African indigenous/traditional African leafy vegetables. *South African Journal of Botany* 103(339)
- Roson R & Hubert F (2015). Bargaining Power and Value Sharing in Distribution Networks: A Cooperative Game Theory Approach. *Networks & Spatial Economics* 15(1): 71-87
- Shackleton C, Paumgarten F, Mthembu T, Ernst L, Pasquini M & Pichop G (2010). Production of and trade in African indigenous vegetables in the urban and peri-urban areas of Durban, South Africa. *Development Southern Africa* 27(3): 291-308
- Sinyangwe D M, Mbewe B & Sijumbila G (2016). Determination of dichlorvos residue levels in vegetables sold in Lusaka, Zambia. *The Pan African Medical Journal* 23(113)
- Vandeplass A, Minten B & Swinnen J (2013). Multinationals vs. Cooperatives: The Income and Efficiency Effects of Supply Chain Governance in India. *Journal of Agricultural Economics* 64(1): 217-244
- Vivas J, Kim M K, Takagi C & Kirimi L (2022). Adopting African Indigenous Vegetables: A Dynamic Panel Analysis of Smallholders in Kenya. *Journal of Agricultural and Resource Economics*, 48(1)
- Weller S C, Van Wyk E & Simon J E (2015). Sustainable production for more resilient food production systems: case study of African indigenous vegetables in eastern Africa. *Acta Horticulture* 1102(1102): 289-298
- Williams R (2006). Generalized ordered logit/partial proportional odds models for ordinal dependent variables. *Stata Journal* 6(1): 58-82
- World Bank (2017). The World Bank in Zambia. <http://www.worldbank.org/en/country/zambia/overview>.
- Yang R Y, Wu W J & Oluoch M (2009). Are African Indigenous vegetables nutritious? evaluation and comparison of nutritional values among indigenous, adapted, and exotic vegetables in tropical Africa. *Annals of Nutrition and Metabolism* 55: 170-171



Copyright © 2024 The Author(s). This is an open-access article published by Faculty of Agriculture, Ankara University under the terms of the [Creative Commons Attribution License](https://creativecommons.org/licenses/by/4.0/) which permits unrestricted use, distribution, and reproduction in any medium or format, provided the original work is properly cited.